Universidad de Valladolid

Escuela de Doctorado Universidad de Valladolid

PROGRAMA DE DOCTORADO EN QUÍMICA

TESIS DOCTORAL:

RESIDUOS DE CLORPROMAZINA, INDOMETACINA, CELECOXIB, ALPRAZOLAM Y OXICANES EN AGUA DE RÍO SEGÚN ENSAYOS DE LABORATORIO: PERSISTENCIA, PRODUCTOS DE DEGRADACIÓN Y ADSORCIÓN A SEDIMENTO. MÉTODO DE ANÁLISIS.

Presentada por Beatriz Estíbaliz Muñoz González
para optar al grado de
Doctora por la Universidad de Valladolid

Dirigida por:
Dr. Juan José Jiménez Sevilla
Dr. Rafael Pardo Almudí

AGRADECIMIENTOS

Quiero comenzar agradeciendo al Dr. Juan José Jiménez, director y tutor de esta Tesis, sus valiosas enseñanzas, su estrecha colaboración y sobre todo su infinita paciencia; al Dr. Rafael Pardo, la oportunidad brindada para la realización de este trabajo y los ánimos recibidos.

No puedo dejar de mencionar a la Dra. María Isabel Sánchez; aunque no haya podido ver este trabajo finalizado, su amistad, consejo y colaboración han sido fundamentales para mí.

Deseo expresar mi gratitud al Laboratorio de Técnicas Instrumentales de la Universidad de Valladolid por las facilidades ofrecidas para la realización del trabajo experimental desarrollado en esta Tesis.

Asimismo quiero agradecer el apoyo de Viki y Miguel Ángel, amigos y compañeros en la Escuela de Ingenierías Industriales, ya que sin ellos no me hubiera embarcado en este proyecto. Gracias por aconsejarme siempre tan bien.

Por último, pero no menos importante, cómo no dar las gracias a mi familia: a Hernán, por alegrar mi vida, y a Héctor, por estar siempre a mi lado; a mis padres, mi hermana y hermano por confiar siempre en mí y a mis sobrinas y sobrino por su cariño.

A todos, muchas gracias.

ÍNDICE

INTRODUCCIÓN

Desde finales de los años 90 muchos artículos científicos han puesto de manifiesto la presencia de drogas de uso farmacéutico y veterinario, a nivel de trazas, en aguas superficiales y en aguas residuales de las grandes ciudades, denominándose a este tipo de compuestos como contaminantes emergentes.

Hoy en día, existe cierta preocupación por la persistencia, movilidad y toxicidad de estos residuos en los ecosistemas acuáticos porque los tratamientos efectuados en las plantas de depuración de aguas residuales, principal ruta de introducción de estos microcontaminantes, no eliminan completamente estos compuestos en los efluentes sometidos a depuración. Paralelamente, las plantas de potabilización de agua destinada para consumo humano tampoco son capaces de eliminar totalmente muchos de estos compuestos.

En la bibliografía existen datos sobre la incidencia en agua superficial de muchas drogas de uso farmacéutico, especialmente de aquellas de mayor prescripción o consumo, pero la información sobre su persistencia y/o degradación en condiciones medioambientales es escasa; a este respecto la mayoría de datos disponibles se han obtenido principalmente en estudios destinados a conocer la estabilidad de medicamentos comerciales, y manteniendo las drogas bajo condiciones de stress. Del mismo modo, también existen trabajos que intentan predecir el comportamiento de las drogas en masas de agua naturales a partir de su comportamiento en condiciones forzadas durante cortos periodos de tiempo.

En este contexto, este trabajo evalúa la persistencia y transformación en agua de río, a escala de laboratorio, de 7 drogas prescritas para el tratamiento de diferentes enfermedades, y para las cuales la información existente sobre su incidencia y degradación en aguas superficiales es nula o escasa. Estos compuestos son clorpromazina, alprazolam, indometacina, celecoxib, tenoxicam, piroxicam y meloxicam. También se proponen métodos de análisis de estos principios activos y de los productos de degradación mayoritarios caracterizados en este trabajo en agua de río, evaluándose determinadas características analíticas básicas después de una extracción en fase sólida.

Para ello, muestras de agua de río dopadas individualmente con cada compuesto a nivel de trazas han sido sometidas a diversos estudios de degradación para discernir la importancia de los procesos químicos, fotoquímicos y biológicos en la degradación del microcontaminante. Además de ensayos en condiciones forzadas se han planteado también ensayos en condiciones no forzadas para simular el comportamiento de la droga en una masa de agua. Los residuos han sido extraídos de alícuotas de las muestras de agua mediante una extracción en fase sólida con cartuchos poliméricos y los extractos han sido analizados mediante cromatografía de líquidos de ultra-alta resolución con detección de espectrometría de masas, empleando como analizador una combinación Q-ToF. Las estructuras de los productos de degradación detectados en los extractos han sido tentativamente elucidadas a partir de las fórmulas moleculares de los iones y la fragmentación observada en espectros masas-masas de alta resolución. Al mismo tiempo, se ha estimado también la capacidad

de adsorción de las drogas y sus productos de degradación sobre un sedimento acuático, calculando los correspondientes coeficientes de adsorción.

ANTECEDENTES

El desarrollo humano está ligado a la utilización constante de compuestos químicos en diferentes ámbitos de nuestra sociedad y a la búsqueda de nuevos compuestos, naturales o sintéticos, que mejoren las características perseguidas con su uso, lo cual, indudablemente, ha tenido, y tendrá, un efecto notable en la mejora de nuestro nivel de vida.

Se considera que esta "revolución química" se intensificó entre los años 1920 y 1930, y durante muchas décadas se puso énfasis únicamente en los aspectos positivos de esos productos, principalmente a nivel económico, tecnológico, sanitario y alimentario. Sin embargo, ciertas personas comenzaron a mostrar su preocupación por los posibles efectos no deseados de la revolución industrial y tecnológica en el medio ambiente y la alimentación. En 1962 se publicó el libro de Rachel Carson "Primavera Silenciosa" en el que se advertía del peligro que entrañaba el uso de pesticidas en el medio ambiente, y que es considerado el primer texto divulgativo sobre el impacto ambiental que genera la actividad humana [1]. Fue precisamente a partir de los años 60-70 cuando se dispuso de pruebas fehacientes de estos efectos indeseados: en 1966 Jensen detecta DDT y otros compuestos sintéticos organoclorados en animales marinos del mar del Norte [2] y en 1974 se detecta la presencia de trihalometanos en aguas potables de consumo humano en Estados Unidos de América [3].

Actualmente, nuestro estilo de vida está generando un número cada vez mayor de compuestos químicos extraños al medio ambiente y, en consecuencia, el interés de la sociedad por los efectos imprevistos de la utilización de los mismos, sobre todo aquellos compuestos sintéticos, su incorporación a los compartimentos medioambientales y a la cadena alimentaria no ha dejado de incrementarse paulatinamente.

Durante décadas la investigación estuvo centrada en los contaminantes "peligrosos o prioritarios", como metales pesados, pesticidas o hidrocarburos aromáticos policíclicos, de los que se conocía su toxicidad y se sabía que eran persistentes y bioacumulables en el medio ambiente. De hecho, muchos de estos compuestos están considerados como sustancias prioritarias a controlar dentro de la Directiva Marco del Agua, norma del Parlamento Europeo que surge con el fin de unificar actuaciones para garantizar la calidad de las aguas [4]. Sin embargo, en las últimas décadas, se viene hablando de los llamados "contaminantes emergentes", entendiéndose éstos como contaminantes previamente desconocidos o no reconocidos como tales, cuya presencia en el medio ambiente no es necesariamente nueva, pero sí lo es la preocupación por las posibles consecuencias de la misma [5]. Son sustancias no incluidas en marcos regulatorios de control y prevención de contaminación ambiental, y es precisamente esta falta de legislación respecto a su uso la que crea una falsa sensación de seguridad; estos compuestos no necesitan ser persistentes, ni estar presentes en elevadas concentraciones para causar efectos negativos, ya que sus velocidades de transformación y/o eliminación son compensadas por su continua introducción en el medio ambiente.

Efectivamente, la expresión contaminante emergente no es nueva. Éstos han existido desde el momento en que se descubre la presencia de moléculas inesperadas en esferas diferentes a las de su uso habitual. Lo que se ha ido modificando con el tiempo es la naturaleza de los mismos. En la actualidad existen diferentes acepciones para los denominados contaminantes emergentes, siendo alguna de las clases más relevantes los retardantes de llama, compuestos perfluorados, drogas de abuso, productos farmacéuticos y de cuidado personal (englobados bajo el nombre PPCPs por sus siglas en inglés), disruptores endocrinos (EDCs), nanomateriales y nanoplásticos.

En lo que respecta a la contaminación ambiental con compuestos farmacéuticos, a pesar de encontrar las primeras referencias a la presencia de estos contaminantes en aguas en la década de los años 1970 en los EE.UU. [6, 7] y en la de los años 1980 en Europa [8-10], su inclusión en la lista de contaminantes emergentes es relativamente reciente debido a los muy bajos niveles de concentración presentes habitualmente (partes por trillón) y a la complejidad de las matrices medioambientales. Fue a raíz del artículo de revisión llevado a cabo por Daugthon y Ternes [11] cuando el interés por estos contaminantes se generalizó e incluso atrajo la atención de instituciones gubernamentales [8]; a partir de este momento, la investigación al respecto ha ido aumentando progresivamente, convirtiéndose en un tema de estudio muy frecuente en estos últimos años. A este hecho ha contribuido la mayor disponibilidad de técnicas instrumentales de análisis progresivamente más sensibles y selectivas, y entre ellas la combinación de técnicas de separación cromatográficas con la espectrometría de masas es la herramienta más indicada y poderosa para el análisis de compuestos de naturaleza polar o semipolar a nivel traza en los diferentes compartimentos medioambientales.

Poco se conoce acerca de los efectos de los productos farmacéuticos a bajos niveles de concentración sobre el medio ambiente, pero existen motivos de preocupación, ya que éstos se desarrollan con el fin de llevar a cabo una actividad biológica, y por lo tanto también pueden actuar sobre especies para las que no han sido ideados, como por ejemplo microorganismos y fauna acuática con receptores similares a los humanos [12, 13]. Estos compuestos se encuentran en el medio ambiente en concentraciones de varios órdenes de magnitud inferiores a las necesarias para producir un efecto farmacológico, lo que hace muy improbable que se observen efectos debidos a una exposición aguda, pero no se puede descartar que la exposición continua y prologada tenga efectos crónicos negativos [12, 14]. Además deben tenerse en cuenta las posibles interacciones entre compuestos, que pueden hacer aumentar su toxicidad, así como el hecho de que los fármacos pueden liberarse al medio, no sólo en su forma original, sino también como metabolitos, que en ocasiones pueden ser más peligrosos que el compuesto original [14].

Así por ejemplo los antibióticos han sido uno de los grupos de fármacos más analizados debido a su amplia utilización como droga farmacéutica humana y veterinaria [11]. Sus residuos afectan en muchas ocasiones a organismos acuáticos, a la actividad microbiana en suelos y se relacionan con la aparición de resistencias bacterianas a los mismos [15, 16], afectando también en gran medida a los microorganismos beneficiosos presentes en las estaciones depuradoras de aguas residuales

(EDARs) [17]. También se ha estudiado ampliamente la presencia de actividad estrogénica en los efluentes de aguas residuales y se ha demostrado la contribución del anticonceptivo 17 α-etinilestradiol a la feminización de los peces, fenómeno que ya fue observado a mediados de los años 80 [18], y que también puede ser provocado por el antiinflamatorio diclofenaco, mismo fármaco que se relaciona con el descenso de la población de buitres en Pakistán [19]. De hecho, en informe del 2012, sobre el resultado de la revisión de la Directiva 2000/60/CE del Parlamento Europeo y del Consejo, en relación con las sustancias prioritarias en el ámbito de la política de aguas, se propone por primera vez identificar estas dos sustancias, junto con el 17 β-estradiol, ya no como emergentes, sino como prioritarias [20]; en la lista de compuestos en observación decidida en el año 2018 por la CE, continúa el 17 α-etinilestradiol, si bien el diclofenaco ha sido retirado [21].

1. ORIGEN DE LOS PRODUCTOS FARMACEÚTICOS EN EL MEDIO AMBIENTE

Existen diferentes vías de introducción de compuestos farmacéuticos en el medio ambiente, como son los lixiviados de vertederos, la escorrentía en tierras urbanas o agrícolas o los fármacos veterinarios desechados junto a los purines en granjas, pero se considera que la principal vía de acceso es a través de los vertidos de las depuradoras de aguas residuales urbanas [22, 23]. Ya en 1977 investigadores de la Universidad de Kansas publicaron el primer informe conocido sobre la descarga de fármacos (ácido salicílico y ácido clofíbrico) desde una planta de tratamiento de aguas residuales hacia las aguas superficiales [7] y este tipo de estudios que analizan los efluentes de las depuradoras y las corrientes receptoras de los mismos no deja de incrementarse, habiéndose encontrado restos de fármacos (antidepresivos por ejemplo) no sólo en el agua, sino incluso en tejidos de los peces que las habitan, en Texas o Canadá [24, 25].

La Figura 1 muestra las vías de entrada de estos compuestos en el medio ambiente y en el ciclo del agua. Las plantas de tratamiento de aguas residuales reciben restos de medicamentos bien a través de excreciones de los usuarios (en su forma original o como metabolitos) o bien a través de eliminaciones directas de fármacos no utilizados, además de los vertidos procedentes de hospitales e industrias de manufactura de fármacos. Estos compuestos se han convertido en una familia de contaminantes que son detectados habitualmente, no sólo en los influentes de entrada a estas plantas de tratamiento, sino también en los efluentes depurados, los cuales se vierten en las aguas superficiales (ríos, mares) y llegan a alcanzar las aguas subterráneas, no sólo mediante procesos de infiltración, sino también por la aplicación de lodos de las depuradoras como abono de las tierras agrícolas. Asimismo el estiércol procedente de granjas ganaderas es utilizado como una fuente de nutrientes en agricultura y en los últimos años han aumentado las referencias que confirman esta vía de entrada de este tipo de microcontaminantes hacia el medio ambiente. Así, se han detectado tetraciclinas, por ejemplo, en suelos que han sido tratados con abono animal, o irrigados con aguas residuales domésticas y aguas procedentes de acuicultura en China [26-29], en suelos abonados en Brasil [30] o en aguas subterráneas de zonas agrícolas en Holanda [31]. Incluso se ha comprobado que las plantas cultivadas en estos suelos o que han sido regadas con aguas reutilizadas, absorben

los fármacos presentes, llegando así éstos a la cadena alimentaria [11, 26, 32]. En estudios hechos en invernaderos, bajo condiciones controladas y con diferentes especies vegetales, se han encontrado residuos de distintos fármacos como clortetraciclina, salbutamol, carbamazepina o cloranfenicol en los tejidos de diferentes cultivos, aunque otros como tilosina, sulfametacina o eritromicina no fueron absorbidos [29, 33, 34]. Teniendo en cuenta las concentraciones encontradas no parece que puedan suponer un peligro para la salud humana, pero aun así no está claro el riesgo que puede conllevar la ingesta diaria de estos productos, lo que hace necesario continuar las investigaciones al respecto [35, 36].

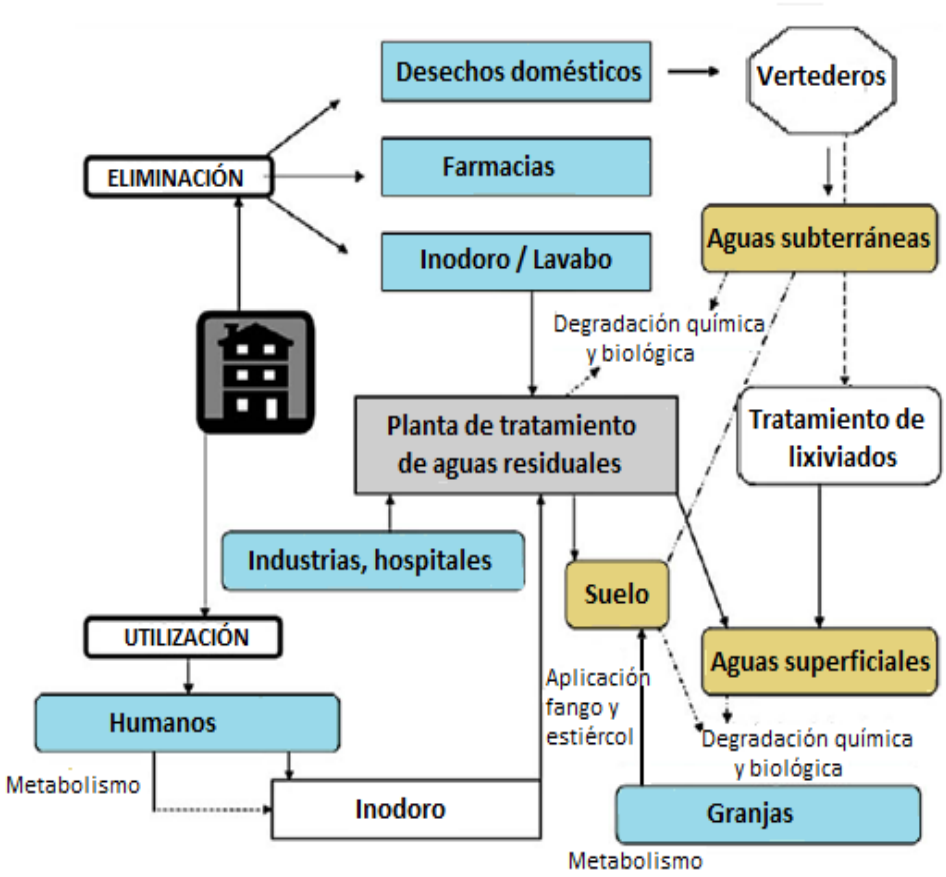

Figura 1: Rutas de entrada de los principios activos farmacéuticos en el medio ambiente [37].

La presencia de fármacos en todos estos compartimentos medioambientales pone de manifiesto la escasa eficacia de depuración de este tipo de compuestos, y es que actualmente las plantas de tratamiento de aguas residuales no están diseñadas para la eliminación de este tipo de residuos, sino que de forma convencional están proyectadas para disminuir el contenido de materia orgánica, nitrógeno, fósforo y patógenos.

En la Tabla 1 se muestran algunos ejemplos de concentraciones halladas en influentes y efluentes de estaciones depuradoras de aguas residuales para alguno de los fármacos más comúnmente estudiados. Las tasas de eliminación mostradas se calculan basándose en las concentraciones encontradas en la fase acuosa, como $(c_{Influente} - c_{Efluente})\cdot 100/c_{Influente}$, y la eliminación

se atribuye a un conjunto de mecanismos, principalmente la biodegradación y la adsorción a sólidos, entre los que no se suele diferenciar a efectos de cálculo [13, 38, 39].

Como puede apreciarse, las concentraciones a la entrada de las EDARs varían desde las decenas de $ng \cdot L^{-1}$ hasta las centenas de $\mu g \cdot L^{-1}$, encontrándose las más elevadas para fármacos de consumo libre y habitual como acetaminofeno e ibuprofeno, cuyas concentraciones son superiores a 600 de $\mu g \cdot L^{-1}$ para el primero en Portugal, y a 100 $\mu g \cdot L^{-1}$ en EDARs de Singapur o Inglaterra. Los antiinflamatorios no esteroideos (AINEs) son medicamentos frecuentemente detectados en los influentes de las plantas de tratamiento, con concentraciones para ibuprofeno y naproxeno un orden de magnitud inferiores en Japón e Italia en comparación con las que se pueden encontrar en otros países como Portugal, Inglaterra, España, Suecia, EE.UU. o Singapur. Las concentraciones de diclofenaco son generalmente menores que las de ibuprofeno, naproxeno o acetaminofeno, dato que en Singapur puede deberse al hecho de que en este país el primero requiere prescripción médica mientras que los otros pueden adquirirse libremente [40]. La carbamazepina es uno de los fármacos más habituales, encontrándose en la gran mayoría de las muestras analizadas, tanto en influentes como en efluentes. Entre los reguladores lipídicos, los más frecuentes son bezafibrato y gemfibrozil, con concentraciones para éste un orden de magnitud superior en depuradoras españolas que en otros países. Los antibióticos también son comúnmente detectados y por ejemplo el sulfametoxazol es detectado en la totalidad de muestras de efluente en Inglaterra [39].

Tabla 1: Concentraciones ($ng \cdot L^{-1}$) de entrada y salida en algunas EDARs y porcentaje de eliminación de drogas farmacéuticas

Fármaco	Concentración influente	Concentración efluente	Porcentajes de eliminación	Lugar	Cita
Carbamazepina	174 - 1330	69 - 889	17 ; 79	Roma (4 EDARs)	[41][a]
	47 - 226	62.7 -245	NE ; 57	Portugal (2 EDARs)	[42][a]
	14.9 -270	10.8 – 90.8	-122 ; 78	Tokyo (5 EDARs)	[43][a]
	1680	1180	30	Suecia	[44][b]
	2593	3117	-20	Gales	[45][d]
	650	316	51	Inglaterra	[46][d]
	129	117	10	Madrid	[47][c,f]
	< 15.8 – 355	nd – 293	-35 ; 82	Grecia (8 EDARs)	[50][c]
	210- 710	220 - 730	-12	República Checa	[51][a]
	323 – 339	298 – 320	2 ; 8	Singapur	[40][e]
Diclofenaco	514 - 2230	339 - 1424	22 ; 53	Roma (4 EDARs)	[41][a]
	nd - 972	nd - 724	83	Portugal (2 EDARs)	[42][a]
	160	120	22	Suecia	[44][b]
	70	123	-75	Gales	[45][d]
	549	436	21	Inglaterra	[46][d]
	232	220	5	Madrid	[47][c,f]
	110	90	18	EE.UU.	[48]
	1200	240	80	Cádiz	[49]
	nd – 5164	nd – 382	- 34 ; 80	Grecia (8 EDARs)	[50][c]
	318 – 390	210 – 363	- 5 ; 44	Singapur	[40][e]
Ibuprofeno	77 – 564	41 - 184	22 ; 93	Roma (4 EDARs)	[41][a]
	3877 - 24505	< 27.8 - 3304	81 ; 100	Portugal (2 EDARs)	[42][a]
	381 - 1130	1.41 - 177	84 ; 99	Tokyo (5 EDARs)	[43][a]
	3590	150	96	Suecia	[44][b]
	3742	227	94	Gales	[45][d]
	12907	1290	90	Inglaterra	[46][d]
	2687	135	95	Madrid	[47][c,f]
	1900	250	87	EE.UU.	[48]
	6620	150	98	Cádiz	[49]
	2740- 5700	910 - 2100	63 ; 67	Galicia	[38][a]
	nd – 8890	nd – 301	63 ; 97	Grecia (8 EDARs)	[50][c]
	29075 - 58975	573 - 1135	97 ; 98	Singapur	[40][e]
Naproxeno	20 – 231	13 - 80	24 ; 65	Roma (4 EDARs)	[41][a]
	< 0.10 - 3245	nd - 270	NE ; 100	Portugal (2 EDARs)	[42][a]
	38 - 230	12 - 139	-2 ; 83	Tokyo (5 EDARs)	[43][a]
	3650	250	93	Suecia	[44][b]
	1082	400	63	Gales	[45][d]
	13660	3516	74	Inglaterra	[46][d]
	2363	923	61	Madrid	[47][c,f]
	3200	380	88	EE.UU.	[48]
	8600	3100	64	Cádiz	[49]
	1790 - 4700	800 - 2600	43 ; 55	Galicia	[38][a]
	nd – 5900	nd – 1076	25 ; 98	Grecia (8 EDARs)	[50][c]
	3560 – 7762	1840 – 2161	48 ; 72	Singapur	[40][e]

Tabla 1: continuación

Fármaco	Concentración influente	Concentración efluente	Porcentaje de eliminación	Lugar	Cita
Ketoprofeno	< 3.70 - 147	< 0.50 - 233	NE ; 100	Portugal (2 EDARs)	[42][a]
	108 – 369	68 – 219	14 ; 68	Tokyo (5 EDARs)	[43][a]
	940	330	65	Suecia	[44][b]
	102	23	77	Gales	[45][d]
	1200	280	77	EE.UU.	[48]
	460	100	78	Cádiz	[49]
Acetaminofeno	2024 - 615135	45.9 - 4909	90 ; 100	Portugal (2 EDARs)	[42][a]
	138164	1454	99	Inglaterra	[46][d]
	23202	< 33	100	Madrid	[47][c,f]
	960	n.d.	> 99	EE.UU.	[48]
	nd – 65403	nd – 1060	64 ; 100	Grecia (8 EDARs)	[50][c]
	79178 – 105817	1002 – 2568	97 ; 99	Singapur	[40][e]
Sulfametoxazol	nd - 343	nd -73.4	67 ; 100	Portugal (2 EDARs)	[42][a]
	20	70	- 250	Suecia	[44][b]
	113	47.5	58	Inglaterra	[46][d]
	279	231	17	Madrid	[47][c,f]
	580	250	57	Galicia	[38][a]
	nd – 2626	nd – 481	58 ; 99	Grecia (8 EDARs)	[50][c]
	43- 490	31 - 260	58	República Checa	[51][a]
Trimetoprima	80	40	49	Suecia	[44][b]
	1879	1004	46	Gales	[45][d]
	672	769	- 15	Inglaterra	[46][d]
	104	99	5	Madrid	[47][c,f]
	nd – 1866	nd – 533	23 ; 91	Grecia (8 EDARs)	[50][c]
	120 - 530	83 - 440	20	República Checa	[51][a]
Gemfibrozil	113 – 1489	56 - 1032	19 ; 78	Roma (4 EDARs)	[41][a]
	710	180	75	Suecia	[44][b]
	3525	845	76	Madrid	[47][c,f]
	410	130	68	EE.UU.	[48]
	3900	1600	59	Cádiz	[49]
	nd – 899	nd – 356	57 ; 80	Grecia (8 EDARs)	[50][c]
	282.5 – 378.5	14.6 – 81.3	79 ; 96	Singapur	[40][e]
Bezafibrato	971	418	57	Gales	[45][d]
	1540	892	42	Inglaterra	[46][d]
	141	128	9	Madrid	[47][c,f]
	nd – 946	nd – 278	26 ; 90	Grecia (8 EDARs)	[50][c]

[a] Fangos activos; [b] fangos activos + eliminación química de P; [c] fangos activos con eliminación de N y P; [d] filtros goteo biológicos; [e] Biorreactores de membrana; [f] valores medios ; nd – no detectado

Las diferencias en las concentraciones halladas en las muestras de influentes pueden ser debidas a diferentes pautas de consumo según los países, por ejemplo en países desarrollados los fármacos más consumidos son los analgésicos, mientras que en los países en vías de desarrollo son más comunes los antibióticos [52], también a factores demográficos como el rango de edad o densidad de población, presencia de hospitales y/o industrias, a factores meteorológicos o incluso a los diferentes sistemas de alcantarillado [40].

La tasa de eliminación de los contaminantes emergentes es dependiente tanto de las propiedades físico-químicas y de la biodegradabilidad del compuesto en concreto, como de los procesos llevados a cabo en cada estación depuradora para la eliminación o transformación de estos contaminantes, cuyas condiciones operacionales (cantidad de biomasa, pH, temperatura, tiempo de retención hidráulico y otras) no son constantes en el tiempo [42, 53, 54]. De hecho en la Tabla 1 pueden apreciarse datos muy dispares.

En ocasiones se observa que las concentraciones encontradas en los efluentes de las plantas de tratamiento son superiores a las de los influentes, obteniéndose tasas de eliminación negativas. Esto se atribuye a diferentes causas. Así, puede explicarse por la presencia de fármacos conjugados en las excreciones humanas y animales que son incorporadas a las aguas residuales, los cuales pueden posteriormente hidrolizarse en las EDARs para liberar el compuesto original que no sería eliminado en ella. Por otra parte, existen equilibrios de adsorción entre los fangos, y sólidos en general, de las EDARs y las aguas en contacto, pudiéndose dar el caso de que el sólido libere residuos hacia la fase acuosa. Otro motivo argumentado es que los fármacos podrían estar adsorbidos en las heces sólidas y liberarse durante el tratamiento en la depuradora. Asimismo hay que tener también en cuenta la técnica de muestreo, ya que en ocasiones no se considera el tiempo de retención hidráulico, por lo que la comparación entre la concentración de influente y efluente debería hacerse con cautela [40, 43, 44, 55, 56].

Los procesos de degradación se ven afectados por factores tales como la radiación solar, la temperatura y la actividad microbiana, por lo que las concentraciones de salida, incluso dentro de una misma planta, son dependientes de variaciones estacionales [12, 57]. Mohapatra et al. encuentran mejores tasas de eliminación en verano que en invierno, tanto en estaciones depuradoras de la India como de EE.UU., debido a una mayor actividad de los microorganismos a temperaturas más cálidas [52]. En Italia se ha observado una eliminación más eficaz en primavera para carbamazepina, naproxeno e ibuprofeno, al contrario que para otros fármacos como diclofeno o gemfibrozil, pudiendo ser debido a que eliminación de éstos se lleve a cabo predominantemente por procesos de adsorción que son más eficaces al disminuir la temperatura [41]. En otros casos las diferencias estacionales son prácticamente nulas [50]. Los factores estacionales no sólo afectan a los procesos llevados a cabo en las EDARs, sino que también influyen en las concentraciones de fármacos que llegan a las mismas; por ejemplo las concentraciones más elevadas de fármacos como antibióticos, analgésicos y antitérmicos se encuentran en invierno, ya que éstos son utilizados para tratar dolencias que se dan principalmente en estos meses. En esta época del año el nivel de lípidos

en sangre aumenta lo que se ve reflejado en el aumento de la concentración de fármacos utilizados para regularlo, como el gemfibrozil. También se aprecia en los influentes un mayor consumo de antihistamínicos en primavera, mientras que la carbamazepina presenta niveles similares durante todo el año ya que se trata de un fármaco utilizado en el tratamiento de enfermedades crónicas [51, 52, 58].

Las plantas de depuración convencionales efectúan los denominados tratamientos primario y secundario de las aguas residuales previamente a su vertido. Las separaciones físicas para la eliminación de sólidos proporcionan limitadas reducciones en las concentraciones de estos microcontaminantes. Procesos como la coagulación-floculación y precipitación se muestran inefectivos habitualmente para la eliminación de una mayoría de contaminantes [38, 57, 59]. Así, por ejemplo, no se observa una disminución significativa durante la sedimentación para ibuprofeno, naproxeno y sulfametoxazol, compuestos con tendencia a permanecer en la fase acuosa, estableciéndose que su eliminación tiene lugar durante el tratamiento secundario mediante fangos activos [38]. La eliminación durante la sedimentación es mayor cuando la droga es lipofílica [60].

El proceso biológico más ampliamente utilizado en el tratamiento secundario de las estaciones depuradoras de todo el mundo es el de fangos activos. Habiendo sido diseñado para eliminar materia orgánica y sólidos en suspensión no resulta eficaz, por lo general, para eliminar compuestos farmacéuticos a nivel de trazas [61], aunque en algún caso puede ser muy efectivo según las condiciones de operación. Una de las opciones más consideradas son los biorreactores de membrana, que combinan el tratamiento biológico con membranas de microfiltración o ultrafiltración, siendo generalmente el primero el mecanismo responsable de la degradación de los fármacos [57, 62]. Esta tecnología parece mejorar el rendimiento de eliminación de los contaminantes al operar con mayor concentración de biomasa y tiempos de retención de sólidos más elevados que en los procesos convencionales permitiendo a las bacterias de lento crecimiento adaptarse a las sustancias resistentes y viéndose obligadas a mineralizar compuestos poco biodegradables para la obtención de energía [40, 62-64]. Varios estudios se han centrado en comparar las eliminaciones obtenidas utilizando el habitual procedimiento convencional de fangos activos con las obtenidas al emplear biorreactores de membrana. Así, en Barcelona se concluyó que este último resultaba más eficaz en el caso de diclofenaco, enalapril y trimetoprima aunque ambos sistemas eran comparables para el caso de aceclofenaco y carbamazepina [65]. En Singapur se encontraron mejores eliminaciones para ácido salicílico, naproxeno, gemfibrozil y diclofenaco, no viendo diferencias para ibuprofeno y fenoprofeno [40]. En ocasiones los resultados son contradictorios, como para el caso del diclofenaco, siendo corroborada una mejora en la eliminación con reactores de membrana por unos investigadores [40, 62, 63, 66, 67] mientras que otros estudios no lo constatan [59, 68, 69]. Estas discrepancias en los resultados pueden ser debidas a diferencias en la edad del fango y en la composición de éste y del agua residual [40]. Las membranas de microfiltración y ultrafiltración por si solas no resultan eficaces en la eliminación de este tipo de contaminantes, y son normalmente utilizadas para la eliminación de sólidos en suspensión,

microorganismos y macromoléculas. Para eliminar microcontaminantes orgánicos, de menor tamaño, con procesos físicos de este tipo, han de aplicarse membranas con menor tamaño de poro, hablándose entonces de etapas de nanofiltración u ósmosis inversa, pudiéndose aplicar las primeras como pretratamiento antes de las segundas [70].

En las EDARs las mejores eliminaciones de drogas de uso farmacéutico y veterinario, y microcontaminantes orgánicos en general, se consiguen mediante la implementación de procesos de oxidación avanzada. Sin embargo estos procesos no son de aplicación generalizada ya que suponen unos costes de operación mucho mayores y son quizá más frecuentes en instalaciones industriales de determinados sectores concretos. Existen varias alternativas para efectuar una oxidación avanzada, como por ejemplo la fotocatálisis, electroxidación, reacción de Fenton, ozonización o posibles combinaciones entre ellas [71]. A título de ejemplo, con dosis moderadas de ozono se ha conseguido eliminar compuestos como diclofenaco, indometacina, carbamazepina, atenolol, metopropol y propanolol, cuya eliminación era menor del 20 % con tratamiento biológico [47]. Diferentes artículos de revisión sobre sus posibilidades, condiciones de operación, capacidad de eliminar materia orgánica y microcontaminantes orgánicos, cinéticas de reacción y otros aspectos han sido publicados [72-78].

Sin embargo, los vertidos de aguas residuales desde las estaciones depuradoras no son la única fuente de contaminación con productos farmacéuticos. Por ejemplo en Kenia se encuentran concentraciones elevadas en un punto del río cercano a un vertedero por lo que es propenso a contaminación por lixiviados [79] y en China la zona más contaminada, además de estar influida por la descarga de una depuradora, fluye por una zona con intensa actividad agrícola y ganadera [80]. El origen de la contaminación no siempre es conocido. En Méjico, aun consiguiéndose una buena depuración mediante tratamiento terciario, las concentraciones aguas abajo del río Apatlaco, aun habiendo disminuido siguen siendo relevantes [81], al igual que ocurre en el río Lis (Portugal) donde se detectan fármacos incluso en su nacimiento [42], o en el río Turia donde el perfil de compuestos encontrados en agua superficial está más de acuerdo con el encontrado en los influentes que con el de los efluentes [82], por lo que apuntan a fuentes adicionales de contaminación como la descarga de aguas residuales no tratadas por edificios no conectados al sistema de alcantarillado o por desbordamientos [83].

2. INCIDENCIA EN LAS AGUAS SUPERFICIALES

Son múltiples los estudios que analizan la presencia de contaminantes farmacéuticos en las aguas superficiales (ríos, lagos y mares). Su presencia no sólo se limita al agua superficial sino que se detectan también en aguas subterráneas e incluso en agua de grifo potabilizada y embotellada destinada al consumo humano, lo que evidencia que varios fármacos resisten no sólo los procesos llevados a cabo en las EDARs, sino también los llevados a cabo en las plantas potabilizadoras de agua. El agua superficial es la principal captación para el suministro de agua potable, y las mismas

corrientes de agua que reciben los efluentes de las estaciones depuradoras son empleadas después en diferentes actividades de agricultura y ganadería, por lo que es recomendable conocer la presencia de contaminantes, entre ellos las drogas farmacéuticas, y el riesgo que conlleva la exposición a los mismos [84, 85].

Una vez que los fármacos alcanzan las masas de agua superficial, las concentraciones encontradas en las mismas son, generalmente, al menos un orden de magnitud inferior que las detectadas en los efluentes de los que proceden debido principalmente al efecto de la dilución, aunque también influyen otros factores como los fenómenos de adsorción a sólidos suspendidos y sedimentos, la fotodegradación y la biodegradación que tienen lugar en las aguas naturales [41, 42, 86]. Así, los rangos de concentración varían de decenas a centenas de $ng \cdot L^{-1}$, aunque en ocasiones pueden llegar a detectarse valores en el orden de $\mu g \cdot L^{-1}$ para algún fármaco en puntos concretos. La Tabla 2 muestra concentraciones encontradas en distintos países para algunos de los fármacos más frecuentemente detectados en aguas superficiales, donde se puede apreciar que, al igual que en los influentes de las EDARs, los AINEs son una de las familias de compuestos farmacéuticos más habitualmente detectadas y con mayores concentraciones en disolución. Nótense los 85 $\mu g \cdot L^{-1}$ de ibuprofeno detectados en Sudáfrica o los 37 $\mu g \cdot L^{-1}$ en Costa Rica, donde también se detectan cantidades elevadas de otros AINEs y analgésicos como 10 $\mu g \cdot L^{-1}$ de ketoprofeno ó 13 $\mu g \cdot L^{-1}$ de acetaminofeno, compuestos fácilmente accesibles por parte del consumidor y relativamente baratos [81, 87, 88]. En Kenia los fármacos más frecuentemente detectados son antiretrovirales (no mostrados en tabla) y antibióticos como sulfametoxazol y trimetoprima, comunes en tratamientos para VIH y malaria, con concentraciones mucho más elevadas que en cualquier otro país y destacando asimismo la concentración de acetaminofeno, que supera los 100 $\mu g \cdot L^{-1}$ [79]. También en Korea se encuentran entre los compuestos más detectados el acetaminofeno, naproxeno e ibuprofeno junto con la carbamazepina (frecuencia de detección > 80 %) aunque aquí las concentraciones no llegan a las centenas de $ng \cdot L^{-1}$, siendo menores que en ríos europeos [59]. Los ríos españoles de la cuenca mediterránea (Llobregat, Turia) se encuentran entre los más contaminados, en términos generales, a nivel europeo, lo que podría aplicarse a los niveles de residuos farmacológicos, ya que son ríos muy afectados por periodos de sequía y con múltiples puntos de vertido de EDARs que hacen que ocasiones prácticamente la totalidad del flujo del río sea debido a estas descargas [82, 86]. En el río Lis, al igual que en el Llobregat, los AINEs vuelven a estar entren los compuestos más frecuentemente detectados junto con los fármacos psiquiátricos [42]. En China, debido al limitado uso en la región estudiada del bezafibrato, gemfibrozil y diclofenaco, éstos sólo fueron detectados en un único punto de muestreo de los analizados, siendo compuestos habituales en otros países. Aquí, también es frecuente encontrar antibióticos en el agua superficial a lo que contribuye probablemente el abuso que se realiza de los mismos [80]. En Japón, carbamazepina y bezafibrato son habituales, pero sulfametoxazol y ketoprofeno se detectan de manera ocasional [85].

Tabla 2: Concentraciones ($ng \cdot L^{-1}$) de diversos fármacos en aguas superficiales.

	ACT	DCF	IBU	KET	NAP	CBZ	GFZ	BZF	SMX	TMP	Cita
Río Mszunduzi (Sudáfrica)	1740	----	84600	----	----	3240	----	----	5320	290	[87][a]
Sudáfrica	64	1461	312	330	1113	279	---	234	1013	899	[89]
Kenia	106970	530	17440	----	----	430	----	----	33100	6950	[79][a]
Costa RIca	13612	266	36788	9808	----	82	17036	----	56	9	[88][a]
Río Apatlaco (Méjico)	354 - 4460	258 - 1398	247 - 1106	----	732 - 4880	36 – 276	15 - 368	286 - 2100	222 - 722	44 - 120	[81]
Korea del Sur	4.1 - 73	1.1 – 6.8	11 - 38	----	1.8 - 18	4.5 - 61	1.8 – 9.1	----	1.7 - 36	3.2 – 5.3	[59]
China	0.36 - 446	nd – 1.5	0.86 – 116	----	----	0.41 – 30	nd – 1.4	nd – 31	0.44 – 115	0.35 - 20	[80]
Río Beiyun (China)	----	7.8 – 170	----	nd - 509	----	nd – 189	nd – 63	nd – 71	---	----	[90]
Río Tone (Japón)	52	3.3	< 30	24	nd	12	nd	77	7.2	< 6	[85][a]
Río Llobregat (España)	20 - 755	66 – 443	11 - 503	14 – 285	56 – 633	31 – 2667	9.3 – 152	----	97 -1500	2.7 - 36	[86]
Río Turia (España)	----	865	16482	----	1797	----	934	21	----	----	[82][a]
Río Tajo (España)	80	145	500	18	262	56	966	145	74	29	[91][a]
Río Lis (Portugal)	527	38	1317	73	260	214	----	----	43	----	[42][a]
Río Taff (Gales)	62 – 388	9 - 28	13 - 29	2 - 3	12 - 50	7 - 251	----	41 - 60	----	< 1.5 - 108	[45]
Inglaterra	163	21	27	< 3.1	127	76	----	42	1.8	22	[46][b]
Cuenca Tíber (Italia)	----	132	112	90	155	102	65	----	----	----	[41][a]
Suecia	----	120	220	70	250	500	170	----	10	20	[44][a]
Cuenca Danubio	----	166	----	58	22	40	----	----	30	12	[92][a]
Cuenca Hérault (Francia)	11 -72	1.4 - 33	nd – 4.5	nd - 14	nd – 9.1	nd - 56	nd – 2.3	----	----	----	[84]
(Francia) Río Doubs US	120	nd	nd	39	nd	1.1	----	----	nd	62	[83][b]
(Francia) Río Doubs DS	274	300		45		149				1338	

[a]valores máximos; [b] valores medios; US upstream (aguas arriba); DS downstream (aguas abajo); nd-no detectado; ACT acetaminofeno; DCF diclofenaco; IBU ibuprofeno; KET ketoprofeno; NAP naproxeno; CBZ carbamazepina; GFZ gemfibrozil; BZF bezafibrato; SMX sulfametoxazol, TMP trimetoprima

Todas las investigaciones coindicen en que las corrientes receptoras están fuertemente influidas por los efluentes de las estaciones depuradoras, y como ya se ha indicado, éstos son los mayores contribuyentes de la contaminación del medio acuático, hecho que concluyen los autores de los estudios que analizan la corriente de agua superficial en puntos anteriores y posteriores a la descarga. Así, está claro que la concentración de contaminante depende del punto de muestreo y se encuentran valores más elevados en puntos cercanos a las estaciones depuradoras y que atraviesan zonas densamente pobladas [93-95]. Así, en Costa Rica, las concentraciones más elevadas se detectan en zonas cercanas a hospitales o con uso intensivo de agua [88]. En el río Taff, en Gales, las mayores concentraciones se encuentran 2 km aguas abajo de la descarga de una depuradora con tratamiento biológico, pasando por ejemplo de 435 a 5970 $ng \cdot L^{-1}$ para tramadol, de 17 a 487 $ng \cdot L^{-1}$ para atenolol, de 7 a 137 $ng \cdot L^{-1}$ para carbamazepina o de no detectarse a encontrar 108 $ng \cdot L^{-1}$ para trimetoprima [45]. También en el río francés Doubs se constata un aumento notable de diclofenaco, carbamazepina, sulfametoxazol y trimetoprima despúes de recibir el efluente de la depuradora [83]. A lo largo del río Llobregat, no sólo no se observa una atenuación natural de los contaminantes, sino que éstos se detectan en concentración creciente al mismo tiempo que aumentan el número de depuradoras que realizan sus vertidos al río [86] y en el río Lis el punto más contaminado se localiza cercano a la desembocadura del río, siendo ésta una zona más poblada y por tanto más susceptible a actividades antropogénicas [42].

Algunos estudios han puesto de manifiesto que la atenuación de los contaminantes farmacéuticos en los ríos tiene lugar lejos de las fuentes de descarga gracias a la dilución y a través de diversos procesos de degradación. En el río Iguazú, en Brasil, el nacimiento del río es la zona más afectada por las actividades humanas, pero a medida que el río discurre hacía su desembocadura las concentraciones son menores, debido al efecto de la dilución y a la propia capacidad de autorrecuperación del río [96]. A lo largo del río Höje, en Suecia, se observa una tendencia decreciente en las concentraciones de ibuprofeno, ketoprofeno, naproxeno, diclofenaco y gemfibrozil, que los autores atribuyen a reacciones de transformación bióticas o abióticas, volatilidad o adsorción, mientras que trimetoprima, sulfametoxazol, metoprolol y propanolol se muestran persistentes [44]. En estos procesos las variaciones estacionales en la temperatura e intensidad de la luz resultan ser dos factores determinantes. Los climas fríos y con pocas horas de luz solar tienden a disminuir la fotodegradación y biodegradación en los meses de invierno cuando se comparan con los meses de verano, y no sólo en las aguas superficiales sino que como ya se ha indicado en el apartado anterior, también afecta a la eficiencia de las estaciones depuradoras. Así, por ejemplo, en el río Fyris (Suecia) se han observado concentraciones mayores de β-bloqueantes y carbamazepina en invierno, cuando la temperatura es menor y la radiación solar menos intensa [97]. En el río Tajo en España se han encontrado variaciones estacionales estadísticamente significativas para trimetoprima, gemfibrozil, bezafibrato y β-bloqueantes, hallándose mayores concentraciones en invierno que en verano. Asimismo, el número de sustancias encontradas también ha sido superior en los meses fríos [91]. También en las aguas, suelos y sedimentos cerca de una instalación de compostaje de estiércol en Korea, se han encontrado mayores concentraciones de tetraciclinas

y sulfonamidas en septiembre que en junio, atribuido a una menor degradación a menor temperatura y una mayor dilución en junio cuando las lluvias son mayores [98]. Sin embargo en Portugal, después de llevar a cabo un análisis y posterior estudio estadístico no fue posible establecer una correlación entre las concentraciones de distintos fármacos encontradas en el río Lis y las distintas épocas del año [42]. El flujo de agua de la corriente también influye en la concentración detectada, y podría esperarse que en las estaciones más lluviosas los contaminantes se encuentren en menor concentración por efecto de la dilución, como han observado en el río Iguazú (Brasil), donde las menores concentraciones se detectaron en un muestreo posterior a días de intensa lluvia [96], o en el río Tone (Japón), donde el flujo en verano es 2.7 veces mayor que en invierno [85]. Sin embargo esto no siempre es así; por ejemplo en el río Beiyun y sus afluentes (China), aunque ciertos fármacos como trimetoprima, metoprolol, ketoprofeno, carbamazepina, bezafibrato, gemfibrozil y cloranfenicol sí se encuentran con mayor frecuencia y más concentrados en la estación más seca y con menor temperatura del agua, otros como ácido mefenámico, indometacina y diclofenaco siguen la tendencia contraria [90]. Asimismo se han encontrado mayores concentraciones para ciertos fármacos en épocas con mayor flujo, lo que se achaca a la desorción o lixiviación de fármacos desde los sedimentos [86]. Como ya se ha comentado no sólo los factores meteorológicos afectan a la variación estacional sino que hay que tener en cuenta factores sociales, como por ejemplo la prevalencia de enfermedades en determinadas estaciones del año y hábitos de la población, habiendo por ejemplo un mayor consumo de antibióticos en invierno o psicoactivos en primavera y otoño [91]. También hay zonas que en verano ven incrementada su población debido al turismo, lo que puede repercutir en los datos encontrados o se pueden encontrar variaciones según la edad de los habitantes de la zona de muestreo.

A la hora de evaluar la movilidad los fármacos y su distribución en el medio ambiente, los estudios se centran mayoritariamente en la fase acuosa, y sólo ocasionalmente se incluye el análisis de sedimentos o partículas en suspensión [87, 94, 98, 99]. La distribución de los contaminantes entre la fase acuosa y los sólidos es un aspecto a tener en cuenta en el estudio de la compleja dinámica del transporte de contaminantes, ya que en ocasiones, a la vista de los datos obtenidos en fase acuosa se podría pensar que está teniendo lugar una atenuación del fármaco cuando en realidad podrían estar adsorbiéndose a los sólidos suspendidos o sedimentos, proceso en el que influirán las características de los mismos además de las características propias del medicamento en cuestión [100]. El coeficiente de adsorción sedimento-agua (K_d), que relaciona la cantidad de un compuesto en la fase sólida con la presente en solución en equilibrio, es clave para entender el comportamiento de los contaminantes en el medio. Asimismo se utiliza el coeficiente K_{oc}, que expresa el coeficiente de adsorción normalizado al contenido de carbono orgánico, ya que la distribución entre sedimento y agua está fuertemente influida por la cantidad de materia orgánica del sedimento [57].

La movilidad de los microcontaminantes orgánicos, y los principios activos farmacéuticos en particular, en agua superficial está regida no sólo por la capacidad de adsorción a sedimentos acuáticos sino también por otros factores: sus propiedades ácido-base; su solubilidad en agua que

suele ser relativamente elevada dada su polaridad; sus valores de la constante de Henry que informa de su distribución entre la fase acuosa y la fase gas, debiéndose observar aquí que las drogas farmacéuticas y veterinarias no son proclives a la volatilización; y el coeficiente de reparto octanol-agua que se relaciona con la lipofilicidad del compuesto, habiéndose descritos casos de bioacumulación en la fauna piscícola. A partir de estos datos se pueden elaborar estudios de modelización del comportamiento de las drogas en los ecosistemas acuáticos [101, 102].

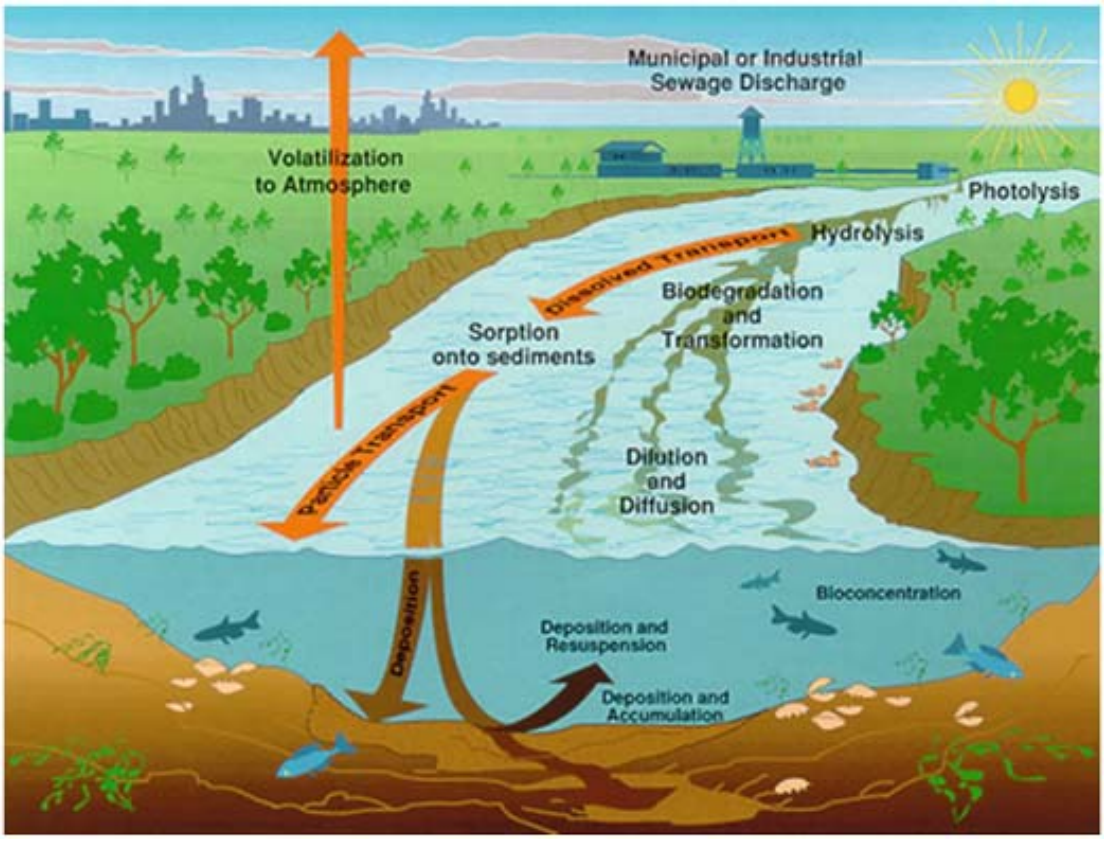

Figura 2: Destino de los contaminantes en el medio ambiente acuático [103].

En la Figura 2 se esquematiza la movilidad de estos compuestos en agua y se considera de forma implícita otro factor relacionado con ella: la persistencia de estos compuestos, que está íntimamente ligada a los procesos de degradación que suceden de manera natural en una masa de agua. Estos procesos de degradación son básicamente de 3 tipos: degradación química, degradación fotoquímica y degradación bioquímica [103-105], como ya se ha comentado. Existen publicaciones en las que se estudia la degradación de principios activos en agua purificada, y menos frecuentemente en aguas superficiales, casi siempre en estudios temporales a corto plazo bajo condiciones de stress: temperatura elevada, exposición a la radiación de una lámpara UV, pHs extremos, condiciones oxidantes,…. En estos ensayos se siguen en mayor o menor medida las condiciones recomendadas por la "International Conference on Harmonisation of Technical Requirements for Registration of Pharmaceuticals for Human Use" [106-108], que están descritas

principalmente para conocer la estabilidad de las drogas en los fármacos que se comercializan con el fin de mejorar la salud.

3. MÉTODOS DE ANÁLISIS

Como se ha mencionado anteriormente la detección de nuevos microcontaminantes en el medio ambiente ha estado íntimamente ligada al desarrollo de técnicas instrumentales de análisis progresivamente más sensibles y selectivas, y capaces de detectar compuestos a niveles traza en muestras complejas como las que se encuentran en el medio ambiente.

Tradicionalmente, el análisis de contaminantes en este tipo de muestras estaba enfocado a la búsqueda de compuestos hidrofóbicos, como PCBs (bifenilos policlorados) y PAHs (hidrocarburos aromáticos policíclicos) por lo que la técnica de elección era la cromatografía de gases acoplada a espectrometría de masas (GC/MS) debido a su alta sensibilidad unido al hecho de la existencia de amplias bases de datos de espectros que ayudan a identificar compuestos no objetivo [13]. Actualmente el interés está centrado en un universo de compuestos mucho más polares, como lo son los productos farmacéuticos, por lo que para llevar a cabo su análisis por GC se hace necesario un proceso previo de derivatización que mejore la estabilidad térmica y la volatilidad de los analitos, tarea no siempre sencilla y que resulta muy laboriosa, además de incrementar la posibilidad de introducción de errores y contaminación. Es por ello que el desarrollo de los acoplamientos de la cromatografía líquida de alta resolución (HPLC) con la espectrometría de masas ha sido crucial para mejorar la detección de este tipo de compuestos y a día de hoy es la técnica de elección en la gran mayoría de los estudios sobre el tema. La tendencia actual es la utilización de columnas con una menor longitud y rellenos con partículas de menor diámetro (< 2 µm) en lo que se conoce como cromatografía líquida de ultra-alta resolución (UHPLC ó UPLC); la reducción del tamaño de partícula mejora la eficacia de la columna pero aumenta la resistencia al flujo y por lo tanto es necesario trabajar a mayores presiones y diseñar equipos que las soporten, al tiempo que las bajas velocidades de flujo deben ser reproducibles. Esta técnica ha permitido perfeccionar las separaciones en matrices complejas, obteniendo picos cromatográficos más estrechos, con anchuras entre 5 y 10 s que mejoran notablemente la resolución, reduciendo la co-elución de interferentes y disminuyendo tanto los tiempos de análisis como el consumo de disolventes [109-113]. Así, por ejemplo, Petrović et al. consiguen la separación de 29 fármacos pertenecientes a diversas clases en muestras de agua residual en tan sólo 10 minutos [114].

Aun así, la cromatografía de gases sigue siendo utilizada debido a una mayor disponibilidad de la técnica por su menor coste e incluso obteniendo menores límites de detección en ciertos casos [115, 116]. De este modo, se encuentran artículos científicos que utilizan la cromatografía de gases para determinar fármacos ácidos, con grupos carboxílicos, después de llevar a cabo una alquilación con sulfato de dimetilo [117], clorometanoato de metilo [118], trifluoruro de boro en metanol [119, 120], bromuro de pentafluorobencilo [48, 121,122] o sales de tetrabutilamonio [123]. No obstante,

los agentes sililantes son los reactivos más utilizados en las reacciones de derivatización previas a la determinación por cromatografía de gases, siendo útiles para transformar grupos hidroxilo, aminas y tioles, además del grupo carboxilo, ampliando así el rango de fármacos susceptibles de ser analizados. Se utilizan para ello MSTFA (N-metil-N-(trimetilsilil) trifluoroacetamida), BSTFA (N,O-bis-(trimetilsilil) trifluoroacetamida) o MTBSTFA (N-metil-N-terc-butildimetilsilil) trifluoroacetamida) [14, 23, 84, 99, 124-133].

La mayor sencillez de la preparación de muestra para el análisis mediante cromatografía de líquidos, donde se evita el tedioso proceso de derivatización que en algunos casos incluso puede llegar a no ser completa para compuestos extremadamente polares [37], y la mayor versatilidad de la técnica, hace que actualmente la mayoría de los investigadores opten por la misma para llevar a cabo la etapa de separación en el análisis de residuos de drogas, en combinación con un detector de espectrometría de masas.

Tanto si la técnica de separación elegida es la cromatografía líquida o la gaseosa, la etapa de preparación de muestra es uno de los aspectos cruciales en la metodología de análisis de compuestos orgánicos en matrices medioambientales. Los procedimientos de extracción, limpieza y preconcentración (y en su caso derivatización) deben ser adecuada y laboriosamente combinados para cuantificar los compuestos a los niveles de concentración comúnmente presentes en las muestras de agua. Para llevar a cabo esta tarea la técnica más comúnmente empleada es la extracción en fase sólida (SPE), basada en la retención de los analitos sobre una fase sólida y la posterior elución de los mismos con disolventes adecuados, para lo cual se emplean cartuchos con distintos tipos de relleno, siendo los más habituales los poliméricos frente a los ODS (octadecilsilano), y entre ellos Oasis HLB (copolímero de divinilbenceno y vinilpirrolidona) es el más ampliamente utilizado ya que este adsorbente presenta características tanto hidrofílicas como hidrofóbicas, lo que permite su uso para una gran cantidad de compuestos en un amplio rango de pH, lo que hace que sea la primera opción en el análisis multirresiduo de fármacos [38, 39, 46, 58, 59, 67, 79, 81, 85-87, 89, 90, 94, 95, 97, 111, 113, 114, 125, 129, 134-142]. Se ha comparado la eficacia de éste y otros rellenos (principalmente basados en poliestireno-divinilbenceno) para la extracción de fármacos ácidos, básicos y neutros de muestras de aguas, observando diferencias en el caso de las recuperaciones obtenidas para los primeros, donde los mejores datos se obtenían en el caso de Oasis HLB, superando el 80 % (excepto para acetaminofeno) [118], lo que también se ha observado al compararlo con ODS [127]. Asimismo es una buena opción para la extracción de sulfonamidas y tetraciclinas después de compararlo con cartuchos ENV+ y ODS [143]. Otro relleno polimérico no tan ampliamente aplicado es el Strata-X (copolímero de estireno y divinilbenceno modificado con piperidinona) que ha sido utilizado para análisis de AINEs y de analgésicos, entre otros PPCPs, en aguas residuales y superficiales, incluyendo agua de mar [14, 19, 41, 42, 48, 55, 88, 92, 110]. Cartuchos empleados en menor medida son los Oasis MCX y Oasis MAX, cuyos sorbentes presentan en su estructura posiciones de intercambio iónico (catiónico para el primero y aniónico para el segundo) sobre la base del copolímero del Oasis HLB, por lo que también puede llevar a cabo

interacciones de fase reversa [116, 144, 145]. Han sido utilizados para extraer PPCPs y drogas en agua superficial y residual, siendo más habitual el primero [45, 62, 84, 112, 124, 146, 147], aunque al comparar las recuperaciones obtenidas al analizar fármacos utilizando Oasis MCX o HLB, este último vuelve a arrojar datos más satisfactorios [50, 113]. Stumpf et al. utilizan cartuchos Strata-XC, relleno que también combina interacciones con intercambio catiónico, en el análisis de fármacos psicoactivos, drogas y productos de degradación, obteniendo recuperaciones superiores al 80 % para 56 de los 68 compuestos analizados [148].

Con el objetivo de disminuir la cantidad de disolventes utilizados tanto con la técnica SPE como con la tradicional extracción líquido-líquido, ya en desuso, se tiende hoy en día a una adaptación de estas técnicas basada en la miniaturización [149], y así varios estudios utilizan técnicas de microextracción en fase líquida o de microextracción en fase sólida (SPME), con distintas fibras y diversas configuraciones; también se desarrolló en su día la extracción por adsorción en barra magnética (SBSE). La SPME se utiliza habitualmente en combinación con GC y consiste en una fibra recubierta de una pequeña cantidad de material adsorbente que se pone en contacto con la muestra por inmersión directa o en el espacio de cabeza durante un tiempo determinado, para posteriormente desorberlo en el cromatógrafo para su análisis. Se ha utilizado SPME para determinar sulfonamidas [150, 151], macrólidos y trimetoprima [151] en aguas residuales, y a pesar de la rapidez, el ahorro de disolventes y una disminución del efecto matriz, se obtiene peor sensibilidad y mayores límites de detección que cuando se lleva a cabo SPE. Esta técnica presenta una serie de inconvenientes como falta de robustez y reproducibilidad y baja eficacia de extracción debido a la pequeña cantidad de fase estacionaria que se puede depositar sobre la fibra. La técnica SBSE utiliza el mismo principio que SPME pero se cuenta con una mayor cantidad de material adsorbente al disponerlo sobre una barra agitadora, superando así la principal limitación de SPME. El polidimetilsiloxano usado como recubrimiento en SBSE ha mostrado buenos resultados sólo para analitos no polares [152], aunque se desarrollan nuevos materiales [153-155]. Al comparar SBSE frente a SPE se han obtenido mejores recuperaciones con menores desviaciones estándar con esta última en el análisis de ciertos PPCPs (carbamazepina e ibuprofeno entre otros) por GC [156] o en la determinación de estatinas por HPLC-qTOF-MS, aunque los autores también señalan menor efecto matriz mediante el procedimiento SBSE [157].

La microextracción en fase líquida dispersiva se ha descrito para la extracción de antiinflamatorios en aguas de grifo y de río seguida de análisis por LC-MS llegándose a límites de cuantificación comprendidos entre 0.5 y 10 $ng \cdot L^{-1}$ [158]. En esta técnica el extractante se mezcla con un compuesto orgánico, que ayuda a que al inyectar la muestra acuosa se forme una dispersión mediante sacudidas, lo que hace que aumente la superficie de contacto entre muestra y extractante. Cuando se ha comparado con SPE, la primera ha mostrado peores resultados en términos de recuperación de estatinas [157].

Aún con estas técnicas, la extracción en fase sólida sigue siendo la técnica más ampliamente utilizada para el análisis de fármacos en aguas naturales y aguas residuales, y de hecho se están

implementando cada vez más los acoplamientos "on-line" de la SPE con los sistemas UPLC-MS [159-161].

La técnica de detección empleada para alcanzar límites de detección del orden de $ng \cdot L^{-1}$, habituales en las muestras medioambientales, y con buena selectividad, es la espectrometría de masas (MS) y especialmente la espectrometría de masas en tándem (MS/MS), utilizando distintos analizadores. Así, las técnicas LC-MS y LC-MS/MS son las mayoritariamente elegidas para el análisis de microcontaminantes orgánicos polares como son los compuestos farmacéuticos. Debido a la complejidad de las muestras medioambientales no siempre se consigue una resolución cromatográfica completa de los analitos de interés y la utilización en la detección de técnicas de masas en tándem ayuda en estos casos. La interfase utilizada mayoritariamente en el acoplamiento con cromatografía de líquidos es la ionización electrospray (ESI), técnica de ionización suave utilizada para el análisis de compuestos de polaridad media a alta, aplicable también a compuestos iónicos y a compuestos termolábiles con grupos funcionales ionizables en disolución. Se puede trabajar en modo de ionización positivo o negativo, mostrando el espectro de masas comúnmente un pseudoion molecular $[M-H]^+$ o $[M-H]^-$ según el caso. Al ser una técnica que presenta poca fragmentación se obtiene buena sensibilidad y selectividad pero con la desventaja de que la información estructural obtenida es menor. En los experimentos en tándem se obtiene el espectro de iones-fragmento de un ion previamente seleccionado, habitualmente el pseudoion molecular, mediante disociación inducida por colisión (CID) con gas nitrógeno y obteniéndose distinta fragmentación según la energía de colisión seleccionada. La velocidad de adquisición de datos en los equipos de espectrometría de masas actuales es suficientemente rápida para definir con precisión los picos cromatográficos obtenidos mediante UPLC y poder, así, cuantificarlos de forma precisa.

Respecto a los analizadores, el triple quadrupolo (QqQ) es ampliamente utilizado para la cuantificación de trazas. Utilizando el modo SRM (selected-reaction monitoring) se monitorizan dos o incluso tres fragmentos característicos del pseudoion molecular del analito objetivo, utilizando la transición más abundante para la cuantificación y las otras transiciones con propósitos de identificación, consiguiendo selectividad y sensibilidad. Tiene la desventaja de que las transiciones deben ser pre-seleccionadas con lo que la información cualitativa para elucidación estructural se pierde y no es posible detectar la presencia de otros posibles contaminantes presentes en la muestra. En el modo "scan" este analizador resulta menos sensible que el de trampa de iones (IT) o el de tiempo de vuelo (ToF) [148, 162]. Quintana et al. realizan estudios de laboratorio con el fin de conocer la degradación microbiológica de 5 AINEs utilizando para el análisis un analizador de triple cuadrupolo con el que detectan los metabolitos realizando un barrido (scan) e interpretan la estructura mediante el registro de espectros de iones producto a distintas energías de colisión [163]; sin embargo este enfoque no es el habitual para la identificación de desconocidos y el triple cuadrupolo es normalmente utilizado en métodos de cuantificación [39, 40, 45, 67, 80, 83].

El analizador de trampa de iones está formado por electrodos que forman una cavidad donde los iones se retienen y se pueden manipular en diversos ciclos de aislamiento y fragmentación mediante CID, obteniendo espectros MS^n, lo que lo hace útil para identificar nuevos compuestos, aunque la cuantificación es menos fiable que en el modo SRM con triple cuadrupolo [164]. La combinación cuadrupolo-cuadrupolo-trampa de iones lineal (QqLIT) resulta un método apropiado para la confirmación y cuantificación de fármacos [162]; se ha utilizado en métodos multirresiduo de fármacos en aguas naturales y residuales, utilizando para la identificación y confirmación de los mismos dos transiciones SRM, en un método selectivo y sensible con límites de detección de pocos $ng \cdot L^{-1}$ [83, 113, 165].

El analizador de tiempo de vuelvo proporciona medidas de masa exacta gracias a su alto poder de resolución, al contrario que en los cuadrupolos, siendo posible determinar la fórmula molecular. Para ello es necesario realizar una calibración del eje de masas, en continuo o discontinuo, con una disolución de un compuesto cuyas masas exactas sean bien conocidas. Ofrece la ventaja de que se puede investigar la presencia de compuestos que no hayan sido previamente seleccionados, en otros términos, es posible realizar análisis dirigidos y no dirigidos [166]. El sistema hibrido entre un cuadrupolo y un tiempo de vuelo (QToF) se muestra como una técnica muy potente para la identificación de compuestos, incluidos compuestos no objetivo, ya que se obtienen masas exactas tanto para el ion padre como para los iones producto y es posible obtener espectros de masas y de masas-masas simultáneamente [147]. La posibilidad de llevar a cabo un análisis retrospectivo resulta muy interesante en el análisis medioambiental ya que permite incorporar la búsqueda de nuevos compuestos y productos de transformación que originariamente no formaran parte del alcance del método.

Los espectrómetros de masas de alta resolución, como el mencionado QToF y también el denominado Orbitrap, resultan adecuados para la identificación de compuestos de naturaleza desconocida en un cromatograma. Además de estimar la fórmula molecular del ion pseudomolecular, y de sus iones-fragmento, proporcionan su perfil isotópico y el número de dobles enlaces y anillos de la estructura que ayudan tanto a la confirmación de la fórmula molecular como a la interpretación de la estructura. Por otra parte, es cada vez más frecuente la existencia de librerías de espectros masas-masas del pseudoion molecular, tanto aquellas comercializadas por las casas comerciales como aquellas accesibles vía internet. Entre estas últimas deben mencionarse las bases de datos METLIN y Chemspider que recopilan estructuras y espectros de una multitud de fuentes de datos.

Existen productos de transformación de las drogas farmacéuticas y veterinarias que son conocidos, tanto de origen metabólico (en seres vivos) y de origen natural (medio ambiente), como fruto de la inestabilidad del producto puro a lo largo del tiempo, y es usual que éstos puedan ser identificados a partir de librerías de espectros o de consultas bibliográficas. La identificación, o al menos la proposición de estructuras tentativas, para compuestos desconocidos es una tarea ardua que requiere la combinación de todos los datos posibles, no sólo de aquellos proporcionados por

un analizador QToF, sino también de los datos de retención cromatográficos y de software predictivo de productos de degradación [167-173]. Evidentemente, la disponibilidad de datos suministrados mediante técnicas de resonancia magnética nuclear y otras como la espectroscopia infrarroja sería de ayuda en esta tarea.

Debe tenerse en cuenta que estos productos de degradación son de especial interés para el medio ambiente si son biológicamente activos, resistentes a la degradación, o presentan riesgos de toxicidad; algunos de ellos son incluso más tóxicos que su precursor en los ecosistemas acuáticos. Sin embargo, la información disponible sobre su comportamiento en el medio ambiente es limitada y muchos de ellos ni siquiera son conocidos [174]. Se desconocen incluso los mecanismos de actuación de la mezcla droga/productos de degradación en los compartimentos ambientales y su inclusión en los modelos de evaluación de riesgos es recomendada [94, 175, 176].

Como se puede inferir de todo lo comentado los procesos involucrados en el transporte y destino final de las drogas en una masa de agua son tremendamente complejos, viéndose influidos por las características físico-químicas del compuesto y del medio receptor. Por ello, es aconsejable aportar información que ayude a predecir el comportamiento de dichas drogas.

En consecuencia, esta memoria presenta el trabajo realizado para estimar la degradación química, fotoquímica y biológica de 7 drogas farmacéuticas en agua de río. Los ensayos de degradación se realizan bajo condiciones forzadas durante cortos períodos de tiempo, y bajo condiciones ambientales durante cierto número de meses simulando, en este último caso, el comportamiento de las drogas en el interior de una masa de agua. La influencia de la presencia de un sedimento acuático es también contemplada al tiempo que se evalúan las constantes de adsorción de los principios activos y de los productos de degradación. La estructura de los productos de degradación es propuesta a partir de los datos obtenidos mediante espectrometría de masas de alta resolución, después de una separación de los analitos mediante UPLC en las condiciones usuales de análisis de las drogas, y verificándose la posibilidad de analizar conjuntamente la droga y sus productos de degradación en una muestra de agua de río después de una extracción en fase sólida. Finalmente, la toxicidad de los residuos hacia determinados biomarcadores indicativos de la calidad de un ecosistema acuático es también predicha mediante el uso de software predictivo.

Las drogas seleccionadas para realizar este trabajo son: clorpromazima, indometacina, alprazolam, celecoxib, tenoxicam, piroxicam y meloxicam. Se trata de drogas que no se monitorizan habitualmente en los métodos de análisis multirresiduo de aguas superficiales y residuales por lo que los datos disponibles sobre su incidencia son mínimos. Tampoco se dispone de información sobre su comportamiento a largo plazo en una masa de agua. Así, la

clorpromazina, compuesto tóxico para determinados microorganismos, sólo ha sido monitorizada en efluentes de varias EDARS según los datos de una publicación [148], al igual que el celecoxib, antiinflamatorio con actividad anticancerígena cuyo efecto terapéutico se está considerando, y que se ha comprobado que no es eliminado en las EDARs [177]. El alprazolam es un compuesto del que se logra una disminución del orden del 30-35 % en las estaciones depuradoras si bien hay pocos datos de concentración en aguas superficiales [136, 178]. La indometacina es un compuesto que sí ha sido más considerado en la bibliografía, detectándose en efluentes en concentraciones del orden de 20 y 100 $ng \cdot L^{-1}$, aunque se ha informado incuso de la presencia de concentraciones en el rango de $\mu g \cdot L^{-1}$ [67, 179]. En el caso de los oxicanes, la información es igualmente escasa [180, 181]. Salvo datos puntuales, no hay en la bibliografía información fiable que revele la posible degradación de estas drogas en las condiciones ambientales de una masa de agua natural.

OBJETIVOS

Los objetivos que se pretenden alcanzar en el desarrollo de la presente tesis doctoral son los siguientes:

- Estimar la estabilidad de clorpromazima, indometacina, alprazolam, celecoxib, tenoxicam, piroxicam y meloxicam en agua de río mediante ensayos de degradación forzada y no forzada en el laboratorio.

- Identificar los productos de degradación de las siete drogas farmacéuticas que presumiblemente podrían ser encontradas en las aguas superficiales, proponiendo una estructura tentativa y estableciendo la ruta de degradación del principio activo.

- Conocer la capacidad de adsorción de los principios activos y sus productos de degradación a un sedimento acuático.

- Verificar las posibilidades de un método de análisis para la determinación de residuos (principio activo y productos de transformación) de clorpromazima, indometacina, alprazolam, celecoxib, tenoxicam, piroxicam y meloxicam en agua de río a nivel de trazas, para lo que es necesario establecer sus características analíticas básicas.

PARTE EXPERIMENTAL

1. MATERIALES Y REACTIVOS

- Patrones sólidos de pureza cromatográfica (99%) de alprazolam, celecoxib, hidrocloruro de clorpromazina, indometacina, tenoxicam, piroxicam y meloxicam suministrados por Sigma-Aldrich (St. Louis, MO, USA). Se prepararon disoluciones individuales de cada principio activo en metanol (70-100 $mg \cdot L^{-1}$) y una disolución multipatrón a partir de éstas para obtener las líneas de calibrado y dopar las muestras en diferentes ensayos. Todas las diluciones se hicieron con metanol.
- Metanol, acetonitrilo y ácido fórmico de calidad LC-MS (Panreac, Barcelona, España).
- Hidróxido de sodio, ácido clorhídrico, dihidrógenofosfato de potasio, azida de sodio de calidad para análisis (Panreac).
- Muestras de agua recogidas en el río Pisuerga (pH 7.8, DQO 4.6 $mg \cdot L^{-1}$) a su paso por la ciudad de Valladolid y en el río Tuerto (pH 7.4, DQO 3.9 $mg \cdot L^{-1}$) en el área rural de La Bañeza (León).
- Muestra de sedimento recogido en el río Pisuerga (carbono orgánico total 1.2 %; 11 % arcilla, 44 % limo, 45 % arena).
- Equipo de cromatografía UPLC Acquity de Waters (Milford, MA, USA), con bomba binaria, cuatro depósitos de disolvente, sistema de desgasificación y muestreador automático.
- Equipo de espectrometría de masas de alta resolución Maxis Impact con analizadores de cuadrupolo y tiempo de vuelo en serie (QToF) y fuente de ionización electrospray suministrado por Bruker Daltonics (Bremen, Alemania).
- Generador continuo de nitrógeno de alta pureza (99.999 %), modelo Zefiro 35 (Vigonza, Italia).
- Bomba de jeringa para la infusión directa de calibrante en el espectrómetro de masas (KDS).
- Columna EBH C18 (Waters, Milford, MA, USA), de 5 cm de longitud, 2.1 mm de diámetro interno y un tamaño de partículas de 1.7 µm
- Equipo de purificación de agua Milli-Q plus (Millipore, Milford, MA, USA)
- Balanza analítica de precisión Mettler E240 (Mettler Toledo, Darmstadt, Alemania).
- Evaporadora centrífuga modular acoplada a sistema de vacío, Myvac (Genevac, Ipswich, UK).
- Centrífuga de alta velocidad PK120 (ALC, Winchester, VA, USA).
- Agitador de movimiento recíproco, Promax 2020 (Heidolph, Alemania).
- Cubeta para la extracción en fase sólida simultánea de múltiples muestras acoplada a sistema de vacío (Sharlab, Barcelona, España).
- Cartuchos de extracción en fase sólida Oasis HLB (Waters) y EBH (Scharlab) con 60 mg de fase estacionaria cada uno de ellos.

- Filtros de PTFE, con tamaño de poro de 0.20 µm, para la preparación de muestras (Sartorius, Barcelona, España) y discos de nitrato de celulosa con tamaño de poro de 0.20 µm, 3 µm y 0.45 µm para filtrar las muestras de agua (Sartorius, Barcelona, España).
- Material de vidrio de uso general.
- El paquete estadístico "Statgraphics Plus for Windows, version5.0" (Manugustics Inc., Rockville, MD, USA), fue empleado en las pruebas de significación.

2. PREPARACION DE MUESTRA PARA EL ANÁLISIS DE RESIDUOS

Para la determinación de residuos de alprazolam, celecoxib, clorpromazina, indometacina, tenoxicam, piroxicam y meloxicam en muestras de agua dopadas, tanto agua ultrapura como agua de río, se ha recurrido a la extracción en fase sólida. Las muestras de agua de río se filtraban previamente a vacío a través de discos de nitrato de celulosa, de 0.45 µm de tamaño de poro.

Se ha estudiado la eficacia de dos tipos de fases estacionarias para la extracción en fase sólida de los compuestos estudiados. Los cartuchos utilizados fueron Oasis HLB (Waters) y EBH (Scharlab), ambos con 60 mg de relleno.

Los cartuchos de extracción eran primeramente activados mediante la elución sucesiva de 6 mL de metanol y 6 mL de agua por gravedad. A continuación se llevaba a cabo la elución del volumen de muestra de agua y la fase estacionaria se lavaba con 3 mL de una mezcla agua-metanol 80:20 (v/v).

Posteriormente el cartucho se secaba mediante la circulación forzada de aire durante 3 minutos y finalmente se eluía por gravedad, utilizando para ello 4 mL de metanol.

El extracto en metanol, recogido en viales, era llevado a sequedad en un sistema de evaporación centrífuga, calentando a 40 °C durante 30 minutos. Dicho extracto se redisolvía en 0.5 mL de metanol, se filtraba sobre un filtro de PTFE de 0.20 µm de tamaño de poro y se emplazaba en viales de inyección para el correspondiente análisis cromatográfico.

3. DETERMINACIÓN MEDIANTE CROMATOGRAFÍA DE LÍQUIDOS ACOPLADA A ESPECTROMETRÍA DE MASAS

Para el análisis de las drogas y productos de degradación se utilizó un cromatógrafo de líquidos de ultra-alta presión (UPLC) Acquity de Waters, acoplado a un espectrómetro de masas de alta resolución equipado con analizadores cuadrupolo y tiempo de vuelo en serie (QToF) (Bruker Daltonics).

En cuanto a los principios activos los análisis fueron realizados mediante ionización electrospray en modo positivo (ESI+) para el caso de alprazolam, clorpromazina, tenoxicam, piroxicam y meloxicam y en modo negativo (ESI-) para el caso de celecoxib e indometacina. La presencia de

productos de transformación en los ensayos de degradación fue verificada en los modos positivo y negativo. Para la determinación de los productos de degradación en los experimentos de recuperación y precisión se usó el mismo modo de ionización que había sido empleado para los compuestos precursores.

Para el análisis conjunto de los principios activos, la separación se realizó en fase inversa utilizando una columna BEH C18 (Waters), de 5 cm de longitud, 2.1 mm de diámetro interno y un tamaño de partículas de 1.7 µm, empleando un gradiente de fase móvil agua/acetonitrilo, conteniendo ambos un 0.1 % (v/v) de ácido fórmico. El porcentaje de acetonitrilo aumentaba de un 30 % inicial hasta el 60 % en 4.5 minutos, volviendo al 30% en 1 minuto, a un flujo de 0.5 mL/min. La columna se mantenía a temperatura ambiente. Se inyectaba un volumen de 5 µL para las determinaciones el modo ESI+ y de 7 µL para las determinaciones en modo ESI-, en el modo de inyección denominado PLNO (partial loop needle overfill).

Para conocer la capacidad de detección de los productos de degradación, y también para su búsqueda y caracterización como se comentará más adelante, se trabajó asimismo en condiciones de gradiente de fase móvil, diferente en cada caso. Igualmente la fase móvil utilizada consistía en agua conteniendo un 0.1 % de ácido fórmico y acetonitrilo conteniendo 0.1 % de ácido fórmico; la Tabla 3 muestra los gradientes utilizados para cada una de las drogas estudiadas.

Tabla 3: Porcentaje de acetonitrilo (0.1% ácido fórmico) en la fase móvil para el análisis de los productos de degradación de cada droga.

Tiempo (min)	0	4.5	5.5
Clorpromazina	5	50	80
Indometacina	20	55	60
Alprazolam	10	44	60
Celecoxib	25	80	90
Tiempo (min)	0	1	4.5
Tenoxicam	0	2	28
Tiempo (min)	0	2.5	4.5
Piroxicam	0.5	10	44
Meloxicam	0.5	18	46

El tiempo de reequilibrio en todos los casos era de 1 minuto. El resto de parámetros de operación era similar.

La determinación de las drogas y sus productos de degradación se realizó mediante espectrometría de masas. La adquisición de espectros se realizó mediante el software Microtof de

Bruker; la medida de masas exactas y asignación de fórmulas moleculares a los iones se llevó a cabo mediante el software de análisis de datos incorporado en el instrumento.

En la Tabla 4 se muestran las condiciones de trabajo de la cámara de ionización electrospray (Figura 3); el gas nitrógeno era usado como gas de secado y de nebulización.

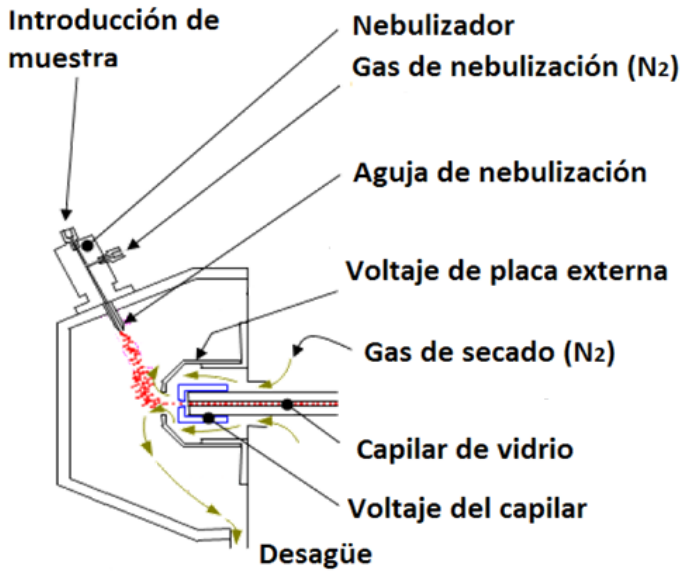

Figura 3: Esquema de la fuente de ionización electrospray.

Tabla 4: Condiciones de trabajo de la cámara de ionización.

Compuesto	Modo	Presión nebulizador (bar)	Voltaje del capilar (V)	Voltaje placa protección externa (V)	Temperatura gas secado (°C)	Flujo gas secado (L/min)
Tenoxicam	ESI+	0.4	-3500	-2500	200	8
Piroxicam	ESI+	0.4	-3500	-2500	200	8
Alprazolam	ESI+	0.4	-3500	-2500	200	8
Clorpromazina	ESI+	0.4	-3500	-2500	200	8
Meloxicam	ESI+	0.4	-3500	-2500	200	8
Indometacina	ESI-	2	4500	1000	200	6
Celecoxib	ESI-	2	4000	1000	200	6

Las condiciones utilizadas para la detección inicial y posterior análisis de los correspondientes productos de degradación eran similares a las del principio activo del que proceden, excepto para aquellos derivados de los oxicanes detectados con mayor intensidad en modo ESI-, en los que la presión de nebulizador era de 2 bar, el voltaje del capilar de 2900 V, el voltaje de la placa de protección externa 1000 V, con un flujo de gas de secado de 6 L/min y manteniendo la misma temperatura de gas de secado.

La identificación de las drogas estudiadas en los cromatogramas (Figura 4) obtenidos puede realizarse de tres formas en orden creciente de fiabilidad:

a) Comparación de tiempos de retención frente a los patrones disponibles;

b) Observación de los espectros de masas obtenidos en los que se observa el pseudoion molecular del compuesto (ion $[M+H]^+$ o ion $[M-H]^-$) y;

c) Determinación de la masa exacta del pseudoion molecular, lo que es posible ya que se dispone de un espectrómetro de masas de alta resolución.

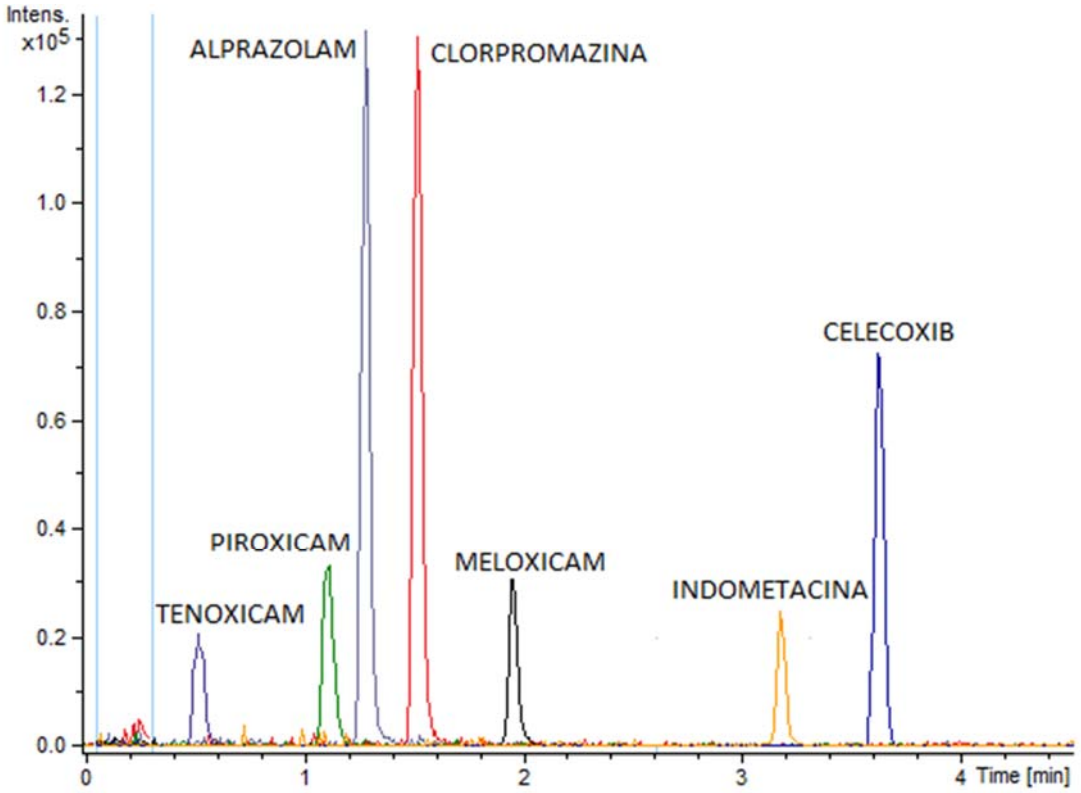

Figura 4: Superposición de cromatogramas de iones extraídos (EIC) para la masa de cada pseudoion molecular ±0.01 Da. Concentración de cada compuesto 20 $ng \cdot L^{-1}$ aproximadamente.

Para la medida de masas exactas el equipo era calibrado diariamente mediante la infusión directa (180 µL/h) de una disolución de formiato sódico 10 mM disuelto en isopropanol-agua 1:1 (v/v), conteniendo 0.05 % (v/v) de ácido fórmico. Dado que la calibración del eje de masas es muy sensible a la temperatura ambiental, el compuesto de calibración se inyectaba también al principio de cada cromatograma para recalibrar el eje de masas en cada caso.

La Tabla 5 muestra la masa exacta del pseudoion molecular para cada droga estudiada, la fórmula molecular calculada a partir del correspondiente ion, así como su tiempo de retención en las condiciones descritas. Los datos relativos a los productos de degradación se exponen en apartados posteriores de esta memoria.

Tabla 5: Tiempos de retención (t_r), fórmulas moleculares de los pseudoiones moleculares y masas exactas de dichos iones.

Compuesto	t_r (min)	Pseudoion molecular	Fórmula molecular	Masa exacta (Da)
Tenoxicam	0.51	$[M+H]^+$	$C_{13}H_{12}N_3O_4S_2^+$	338.0264
Piroxicam	1.11	$[M+H]^+$	$C_{15}H_{14}N_3O_4S^+$	332.0700
Alprazolam	1.27	$[M+H]^+$	$C_{17}H_{14}ClN_4^+$	309.0902
Clorpromazina	1.52	$[M+H]^+$	$C_{17}H_{20}ClN_2S^+$	319.1030
Meloxicam	1.93	$[M+H]^+$	$C_{14}H_{14}N_3O_4S_2^+$	352.0420
Indometacina	3.16	$[M-H-CO_2]^-$	$C_{18}H_{15}ClNO_2^-$	312.0791
Celecoxib	3.61	$[M-H]^-$	$C_{17}H_{13}F_3N_3O_2S^-$	380.0686

Para la cuantificación de alprazolam, piroxicam**,** tenoxicam, meloxicam, celecoxib, indometacina y clorpromazina se obtuvieron líneas de calibrado basadas en la medida de áreas de pico en los cromatogramas de iones extraídos para el ion pseudomolecular. De forma similar, las áreas de pico de los productos de degradación fueron medidas y usadas para verificar los métodos de análisis.

4. ESTUDIO DE DEGRADACIÓN

Los ensayos de degradación para evaluar la persistencia de las 7 drogas farmacéuticas en agua de río y detectar sus productos de degradación se exponen de forma resumida a continuación. En las publicaciones adjuntas se pueden consultar con detalle los experimentos de degradación y la consiguiente preparación de muestra previa a su análisis cromatográfico.

4.1. DEGRADACIÓN BIOLÓGICA

Se han realizado ensayos de degradación biológica a temperatura ambiente en condiciones tanto aeróbicas como anaeróbicas, y en ciertos casos en presencia de un medio de cultivo a 35°C para favorecer el crecimiento de microorganismos. Para ello se usó agua de río a pH 7.8 dopada individualmente con cada droga a una concentración de 2 ó 100 $\mu g \cdot L^{-1}$. La clorpromazina no se incluyó en este estudio dado que ya se conocía que es un compuesto no biodegradable [182]. Se prepararon también blancos y disoluciones de control, en paralelo a las muestras de estudio, recogiendo alícuotas de muestra periódicamente, que eran inyectadas en el sistema cromatográfico después de una extracción en fase sólida similar a la descrita.

4.2. DEGRADACIÓN EN CONDICIONES FORZADAS

Se ha estudiado la degradación térmica y fotoquímica (sin ninguna restricción a la radiación) de los 7 principios activos en agua dopada (2-100 $\mu g \cdot L^{-1}$). Los experimentos de degradación térmica se

han llevado a cabo en una estufa a temperatura de 70 °C con la finalidad de evaluar la importancia de las reacciones químicas en disolución en el proceso de degradación.

Para los experimentos de degradación fotoquímica se introducía la muestra dopada en cubetas de cuarzo cerradas que se exponían directamente a la luz solar situándolas en la repisa exterior de una ventana, con orientación sur. Las muestras dopadas con alprazolam y celecoxib, emplazadas en cubetas de cuarzo, fueron también expuestas a la radiación de una lámpara (8 W) cuya emisión estaba centrada en 254 nm. Se prepararon también blancos y disoluciones de control protegidas con papel de aluminio. Alícuotas de las disoluciones sometidas a la degradación forzada fueron recogidas de forma periódica y analizadas mediante UPLC-MS.

4.3. DEGRADACIÓN EN CONDICIONES NO FORZADAS

Los procesos naturales que suceden en una masa de agua a lo largo del tiempo han sido simulados en el laboratorio para estimar la persistencia de las siete drogas estudiadas. Para ello se ha considerado una estrategia sencilla consistente en depositar un volumen de agua de río (2.5 L) dopado con los compuestos en un contenedor de vidrio (4 L) transparente, con cierre hermético, el cual era abierto semanalmente para muestrear una alícuota de agua y renovar el aire en contacto con la superficie del agua; el recipiente se mantenía en condiciones ambientales dentro del laboratorio (18-21 °C) expuesto directamente a la radiación solar y al ciclo natural día-noche. El experimento se realizó con agua de dos ríos diferentes (ríos Pisuerga y Tuerto) y también en presencia de un sedimento acuático para estimar su posible influencia; el sedimento se añadía en una proporción conocida, y deliberada, con el fin de que se produjera una cierta adsorción de la droga sobre él.

En las condiciones de experimentación, la radiación solar debe pasar a través de la ventana de vidrio del laboratorio y a través del vidrio del recipiente, los cuales absorben radiación UV y el comportamiento de las drogas en la disolución del recipiente simula su comportamiento en una masa de agua ya que en ella la transmisión de la radiación solar disminuye con la profundidad.

La atenuación de la radiación a través del vidrio de la ventana y del recipiente fue estimada a partir de medidas de transmitancia del vidrio en un espectrofotómetro UV-visible. Así se verificó que la radiación transmitida hacia la masa de agua era un 40 % de la radiación incidente a una longitud de onda de 350 nm, un 1.3 % a 320 nm, un 0.02 % a 310 nm, un $8 \cdot 10^{-4}$ % a 305 nm y $8 \cdot 10^{-5}$ % a 290 nm.

La experimentación se mantuvo durante varios meses muestreando semanalmente 25 mL de agua; después de una extracción en fase sólida el extracto era inyectado en el sistema cromatográfico. Las condiciones experimentales detalladas de todos los experimentos de degradación se muestran en apartados posteriores de esta memoria, individualmente para cada compuesto.

En los diferentes ensayos reseñados se detectaron diversos productos de degradación en el análisis de las muestras mediante UPLC-QToF-MS; la mayoría de los cuales han sido tentativamente

identificados en este trabajo a partir de la medida de la masa exacta del pseudoion molecular y de la información estructural obtenida en los espectros masas-masas de alta resolución registrados mediante disociación inducida por colisión del mismo.

5. CÁLCULO DE COEFICIENTES DE ADSORCIÓN

La capacidad de adsorción a un sedimento acuático de los 7 principios activos y diversos productos de degradación ha sido estimada mediante el cálculo de los correspondientes coeficientes de adsorción (K_d). En el caso de los principios activos se obtuvieron las isotermas de adsorción calculando sus K_d a partir de estos experimentos.

Volúmenes de agua río (100 mL) depositados en matraces y dopados con cantidades crecientes de la droga eran puestos en contacto con una cierta cantidad de sedimento, constante para cada disolución, para conseguir una determinada relación masa/volumen (R). El pH de la disolución (7.8) se controlaba con una disolución reguladora de fosfato y se evitaba su exposición a la luz solar recubriendo el matraz con papel de aluminio. La disolución en contacto con el sedimento se dejaba reposar durante 24 horas para permitir que se estableciera el equilibrio de adsorción, a temperatura ambiente, y después se recogía una alícuota para determinar la cantidad de droga que permanecía en disolución; a partir de aquí se puede calcular la cantidad de droga adsorbida al sedimento mediante un balance de materia.

En lo que respecta al cálculo de los coeficientes en el caso de los productos de degradación, debe tenerse en cuenta que no existen patrones disponibles para realizar su cuantificación mediante líneas de calibrado. Por este motivo, se ha supuesto que existe una relación lineal entre el área de pico medida en el cromatograma y su concentración, lo cual es principio lógico dado que se trabaja con pequeñas cantidades.

De esta forma se planteó una experimentación similar a la descrita para las drogas usando disoluciones degradadas del principio activo para dopar el agua de río. El porcentaje de disminución del área de pico medida en el extracto de agua en contacto con el sedimento, con respecto al área de pico en ausencia de éste, se asume que es debido a su adsorción sobre el mismo, por lo que el porcentaje de compuesto adsorbido sobre el sedimento (A %) debe corresponderse con ese porcentaje de disminución estimado experimentalmente. Así, el valor de K_d del producto de degradación se puede estimar mediante la ecuación (1) [183], la cual es válida si la isoterma de adsorción es lineal.

$$\log K_d = \log\left[\frac{A\%/_{100}}{1-A\%/_{100}}\right] - \log R \qquad \text{Ecuación (1)}$$

RESULTADOS Y DISCUSIÓN

1. LINEAS DE CALIBRADO

Previamente a la obtención de las líneas de calibrado se estimaron los límites de detección (LOD) y de cuantificación (LOQ) mediante la inyección de patrones disueltos en metanol, en concentraciones decrecientes, usando como criterio la relación señal/ruido (3 ó 10, respectivamente). La Tabla 6 muestra los LOD y LOQ obtenidos en cada caso, expresados en $\mu g \cdot L^{-1}$.

Tabla 6: Límites de detección y cuantificación

Compuesto	LOD ($\mu g \cdot L^{-1}$)	LOQ ($\mu g \cdot L^{-1}$)
Tenoxicam	0.2	0.4
Piroxicam	0.2	0.4
Alprazolam	0.2	0.5
Clorpromazina	0.2	0.4
Meloxicam	0.2	0.4
Indometacina	0.7	1.3
Celecoxib	0.5	1.2

Se realizó un calibrado por el método del patrón externo para cada uno de los compuestos. Para ello se inyectaron los patrones en un intervalo de concentración comprendido entre el LOQ, y una concentración aproximadamente 30 veces superior, y cuantificando el área del pseudoion molecular de cada compuesto en el cromatograma de iones extraídos (Tabla 5).

Las Figuras 5-11 muestran las líneas de calibrado obtenidas en cada caso; en dicha figura se muestra la media de las áreas de pico integradas en 3 inyecciones de cada uno de los patrones de concentración conocida.

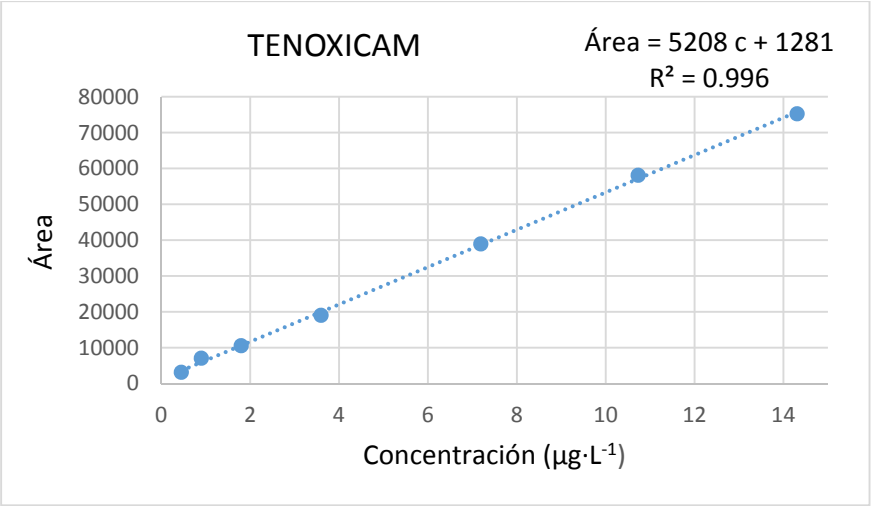

Figura 5: Línea de calibrado para tenoxicam (n=3)

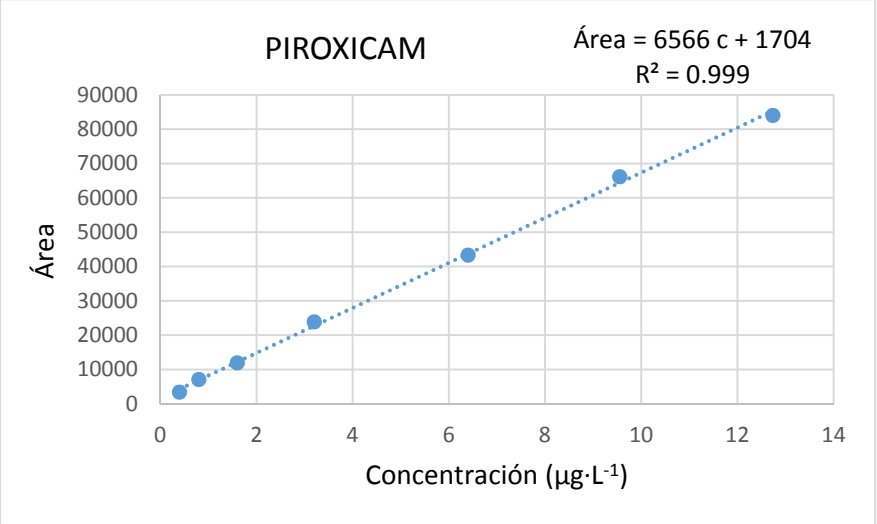

Figura 6: Línea de calibrado para piroxicam (n=3)

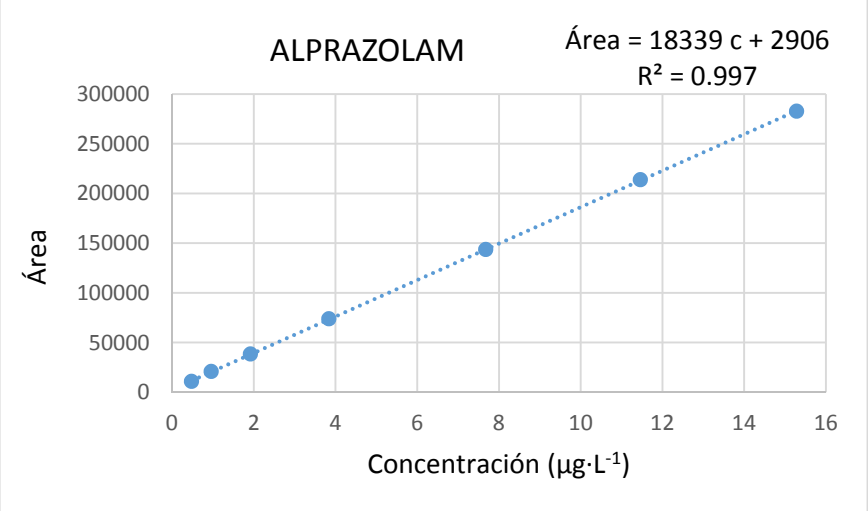

Figura 7: Línea de calibrado para alprazolam (n=3)

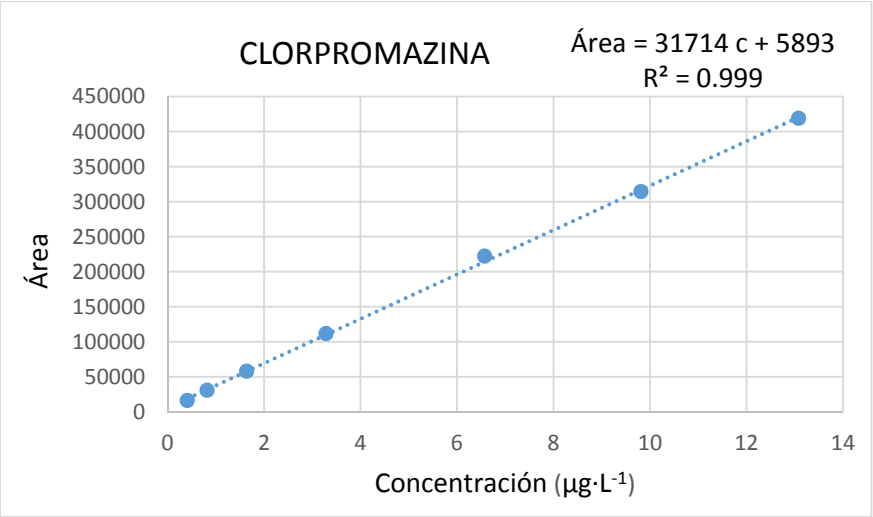

Figura 8: Línea de calibrado para clorpromazina (n=3)

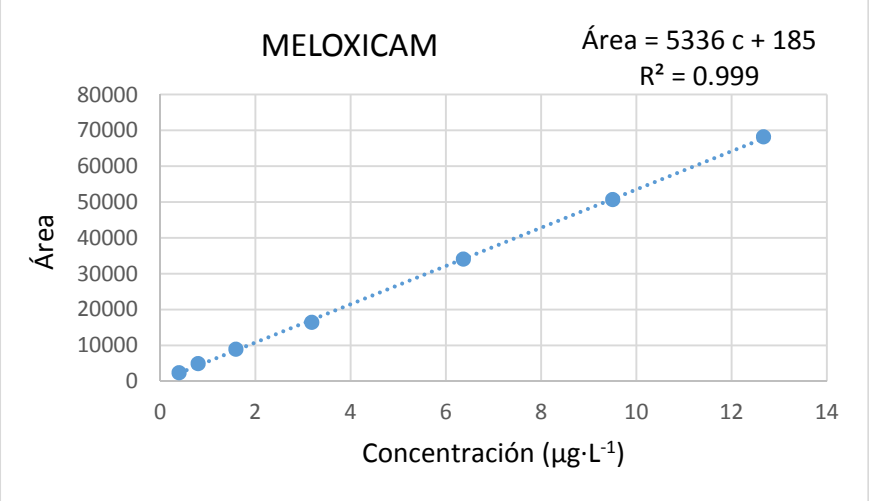

Figura 9: Línea de calibrado para meloxicam (n=3)

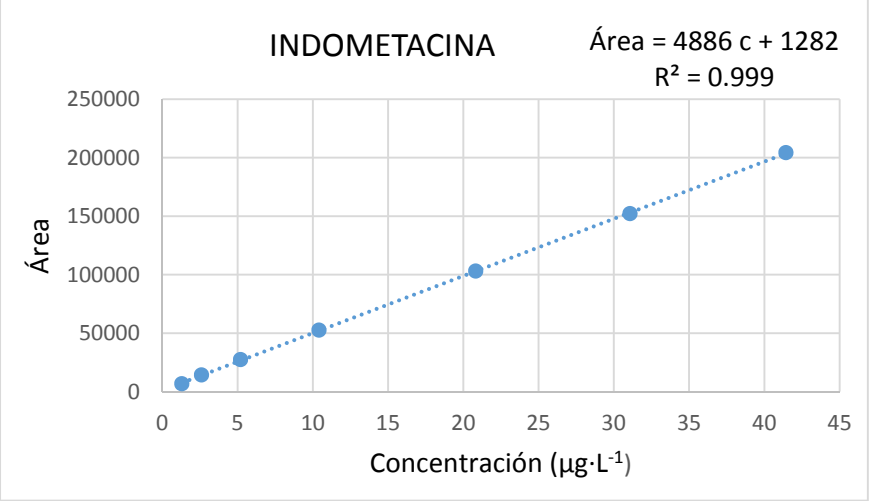

Figura 10: Línea de calibrado para indometacina (n=3)

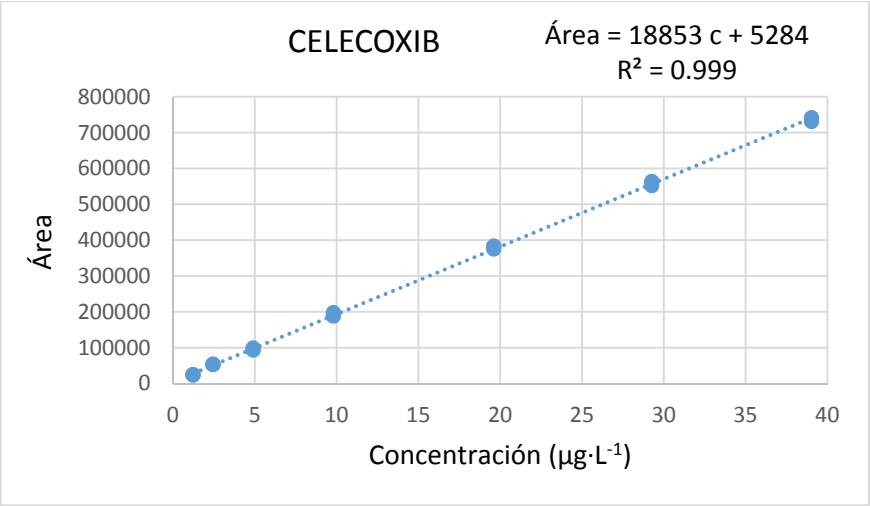

Figura 11: Línea de calibrado para celecoxib (n=3)

Se verificó el modelo de calibración lineal en el intervalo de concentración considerado mediante un análisis de varianza que evalúa la posible falta de ajuste. Esta prueba consiste en una prueba F de una cola donde se compara la varianza explicada por la falta de ajuste con la varianza explicada por el puro error experimental. Para llevarla a cabo se necesitan medidas replicadas de las experiencias (n=3 en este caso), ya que son estas réplicas las que estiman el error experimental que puede causar diferencias entre los valores observados. El mantenimiento de la hipótesis nula, según la cual ambas varianzas son comparables, significa que el modelo de calibración elegido es adecuado.

Tabla 7: Valores de F en la prueba de falta de ajuste (p=0.05)

Compuesto	F experimental	F crítico
Tenoxicam	0.58	2.96
Piroxicam	0.53	
Alprazolam	0.03	
Clorpromazina	1.39	
Meloxicam	0.09	
Indometacina	0.81	
Celecoxib	2.20	

La Tabla 7 muestra el valor de F experimental obtenido en el análisis de varianza que verifica el modelo de regresión lineal para cada compuesto y lo compara con el valor de F crítico tabulado (p=0.05). Como puede observarse, el valor de F experimental es en todos los casos inferior al valor de F crítico, manteniéndose por tanto la hipótesis nula planteada, lo que indica que en ninguno de

los casos existe una falta de ajuste, concluyendo que el modelo lineal es adecuado en el rango de concentración estudiado.

2. RECUPERACIÓN Y PRECISIÓN MEDIANTE DIFERENTES FASES ESTACIONARIAS.

A continuación se presentan los resultados de los experimentos de recuperación de los compuestos farmacéuticos después de aplicar el procedimiento de extracción en fase sólida a un volumen de 1 L de muestras de agua del río Pisuerga y agua ultrapura, las cuales fueron eluídas sobre dos rellenos poliméricos: Oasis HLB y EBH (Figura 12), ambos en cantidad de 60 mg. Estos experimentos se han realizado sobre muestras de agua dopadas a dos niveles de concentración: una concentración próxima al límite de cuantificación reseñado de cada compuesto, y una cercana a la máxima del intervalo de calibración considerado. La Figura 13 muestra dos cromatogramas de estos experimentos.

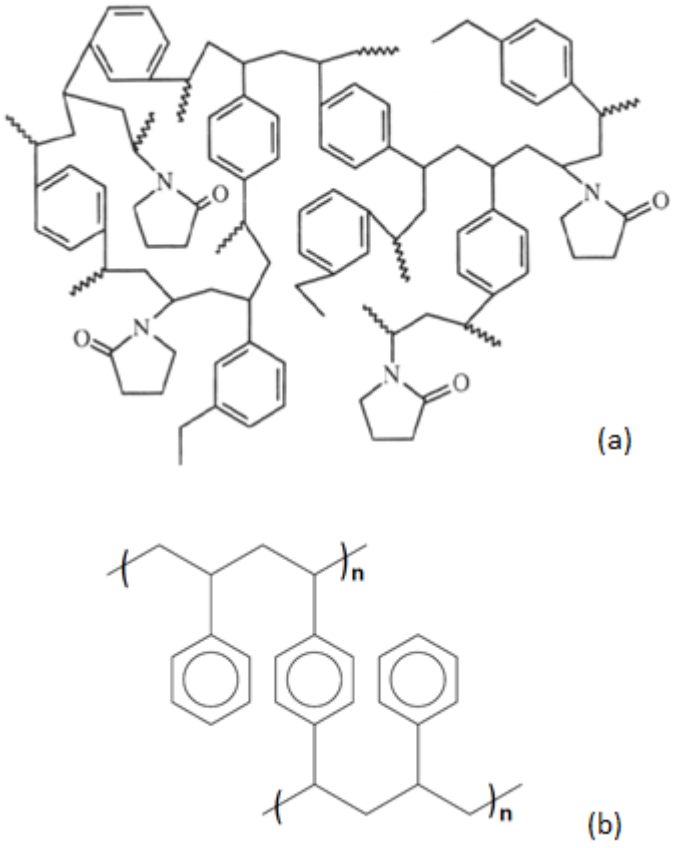

Figura 12: Estructura de los rellenos poliméricos ensayados (a) Oasis HLB [poli(divinilbenceno-o-N-vinilpirrolidona)], (b) EBH (poliestireno-divinilbenceno)

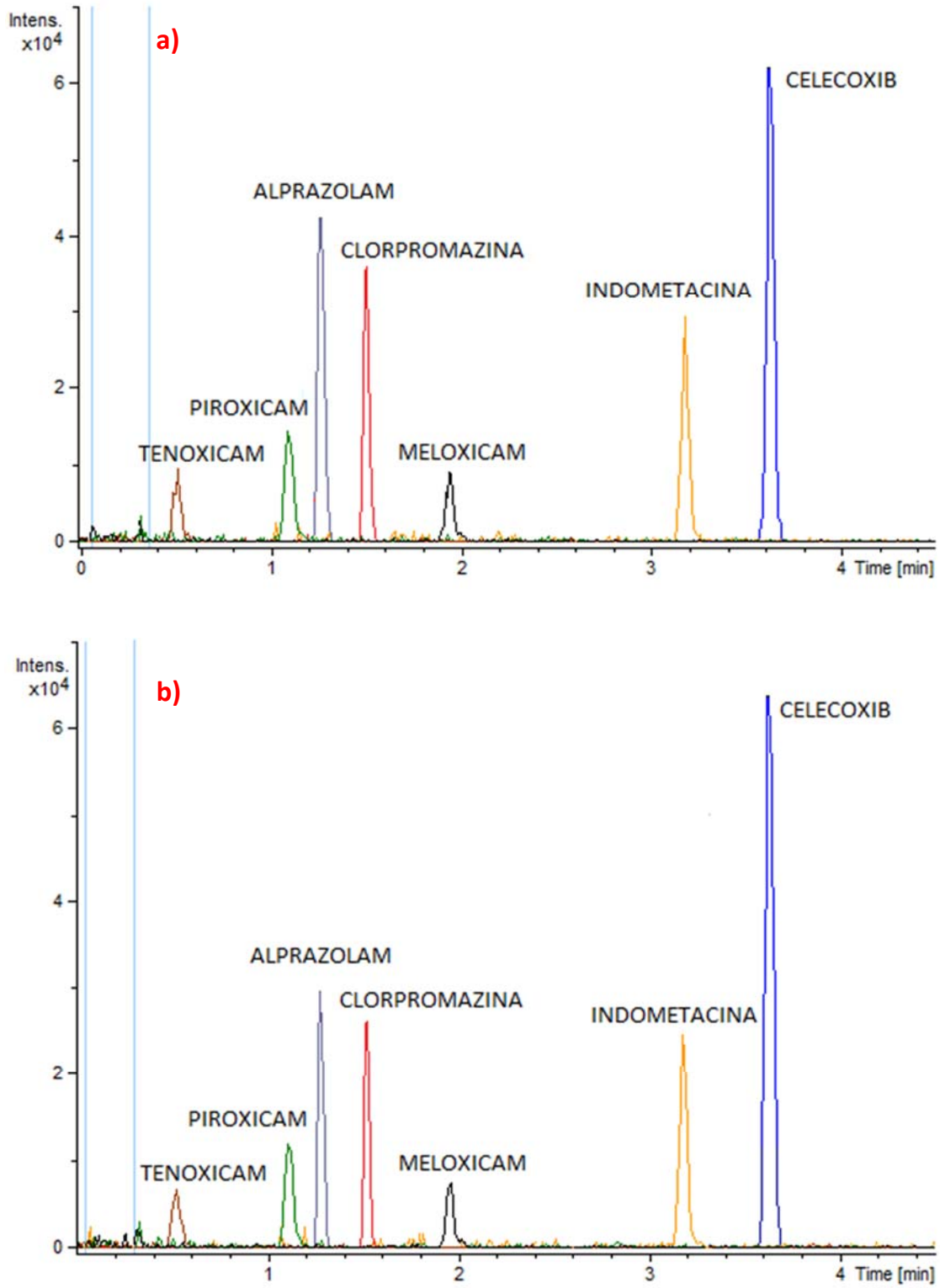

Figura 13: Cromatogramas de iones extraídos, superpuestos, de un extracto de agua de río dopada. (a) cartuchos Oasis HLB; (b) cartuchos EBH

Para interpretar los resultados se aplicó a los datos obtenidos para cada compuesto un análisis de varianza de tres vías con réplicas (n=5) con el fin de comprobar si existían diferencias significativas, con un nivel de confianza del 95 %, en las recuperaciones según tres parámetros: el

nivel de concentración, el tipo de cartucho utilizado, y el tipo de agua en el que se llevaba a cabo la extracción. Los resultados se detallan seguidamente e individualmente para cada compuesto.

2.1. TENOXICAM

En la Tabla 8 se presentan las recuperaciones y precisiones obtenidas al llevar a cabo el análisis para tenoxicam, utilizando ambos tipos de cartucho, tanto en agua de río como ultrapura. En este caso las muestras de agua fueron dopadas con concentraciones de 0.7 $ng \cdot L^{-1}$ y 6.7 $ng \cdot L^{-1}$. La tabla 9 muestra el análisis de varianza de 3 vías aplicado para detectar los factores que afectan significativamente a estos resultados.

Tabla 8: Recuperaciones y precisiones obtenidas en la determinación de tenoxicam en muestras de agua ultrapura y de río a dos niveles de concentración (n=5).

Cartucho	Oasis HLB				EBH			
Agua	Ultrapura		Río		Ultrapura		Río	
Concentración ($ng \cdot L^{-1}$)	0.7	6.7	0.7	6.7	0.7	6.7	0.7	6.7
Recuperación (%)	90	90	69	68	94	83	69	65
	83	90	74	66	84	73	59	59
	76	80	86	76	81	70	64	61
	87	88	65	84	78	84	72	53
	72	74	71	66	73	73	76	69
Recuperación media (%)	82	84	73	72	82	77	68	61
RSD (%)	9.2	8.4	10.9	10.9	9.6	8.4	9.8	9.9

Tabla 9: Resultados del ANOVA de 3 vías aplicado a las recuperaciones obtenidas para tenoxicam.

Fuente	g.d.l.	Suma de Cuadrados	Cuadrados Medios	F	p
Agua	1	1575	1575	30.69	<0.001
Concentración	1	65.02	65.02	1.27	0.268
Cartucho	1	330.6	330.6	6.44	0.016
Total error (residual)	36	1848	51.32		
Total (corr.)	39	3818			

Según se puede observar en la Tabla 9, los resultados en las recuperaciones obtenidas difieren significativamente según la naturaleza del agua y al variar el cartucho utilizado para llevar a cabo la extracción, ya que son estos factores los que muestran estadísticos p inferiores a 0.05. Como se aprecia en la Tabla 8, las recuperaciones en agua de río son inferiores a las obtenidas en agua ultrapura. Con los cartuchos Oasis HLB se obtienen recuperaciones superiores, siendo éstas del 73 y 72 % a nivel de concentración bajo y alto respectivamente en agua de río, frente al 68 y 61 %

obtenidas con los cartuchos EBH. En el agua ultrapura a nivel alto la media de recuperación es 82 % con ambos cartuchos, mientras que a nivel bajo se obtiene un 84 % para Oasis HLB y un 74 % para EBH. La precisión de los análisis, expresada como desviación típica relativa (RSD) está comprendida entre el 8 y el 11% (n=5).

2.2. PIROXICAM

La Tabla 10 muestra las recuperaciones y precisiones obtenidas al aplicar el procedimiento de extracción con cada uno de los 2 tipos de cartuchos a muestras de agua ultrapura y de agua de río dopadas con piroxicam en concentraciones de 0.8 $ng \cdot L^{-1}$ y 6.8 $ng \cdot L^{-1}$. Los resultados del ANOVA se muestran en la Tabla 11.

Tabla 10: Recuperaciones y precisiones obtenidas en la determinación de piroxicam en muestras de agua ultrapura y de río a dos niveles de concentración (n=5).

Cartucho	Oasis HLB				EBH			
Agua	Ultrapura		Río		Ultrapura		Río	
Concentración ($ng \cdot L^{-1}$)	0.8	6.8	0.8	6.8	0.8	6.8	0.8	6.8
Recuperación (%)	92	83	81	80	94	83	79	75
	89	80	93	68	80	93	76	68
	80	93	79	74	91	85	85	76
	91	82	76	85	95	79	72	64
	95	97	71	79	93	82	69	62
Recuperación media (%)	89	87	80	77	89	84	76	69
RSD (%)	6.4	8.6	10.2	8.4	7.6	6.2	8.2	9.2

Tabla 11: Resultados del ANOVA de 3 vías aplicado a las recuperaciones obtenidas para piroxicam.

Fuente	g.d.l.	Suma de Cuadrados	Cuadrados Medios	F	p
Agua	1	1500	1500	36.5	<0.001
Concentración	1	216.2	216.2	5.26	0.028
Cartucho	1	112.2	112.2	2.73	0.107
Total error (residual)	36	1479	41.08		
Total (corr.)	39	3180			

Como se observa en la Tabla 11, las recuperaciones obtenidas no dependen, del relleno del cartucho utilizado pero sí son significativamente diferentes atendiendo al tipo de agua ($p<0.001$) y al nivel de concentración presente ($p=0.028$). En la Tabla 10 se observa que, como en el caso del tenoxicam, las recuperaciones obtenidas para el agua ultrapura son mayores, tanto a nivel de concentración bajo como nivel alto, que las obtenidas con agua de río en ambos cartuchos, siendo

en los cartuchos Oasis del 89-87 % las primeras y del 80-77 % las segundas, y en los EBH 89-84 % y 76-69 % respectivamente. La precisión de los análisis es del orden del 6-10 % (n=5). En cuanto a la influencia de la concentración se observa que la recuperación media es un 5-7 % inferior al nivel de concentración alto para los cartuchos EBH, mientras que para los cartuchos Oasis es un 2-3 % inferior.

2.3. ALPRAZOLAM

La Tabla 12 muestra los datos de recuperación y precisión obtenidos al llevar a cabo el análisis de alprazolam, variando los tres parámetros estudiados: tipo de agua, tipo de cartucho y concentración de analito en el agua: 0.7 y 7.2 $ng \cdot L^{-1}$. Las desviaciones típicas relativas variaban en este caso entre el 4 y el 10 % (n=5).

Tabla 12: Recuperaciones y precisiones obtenidas en la determinación de alprazolam en muestras de agua ultrapura y de río a dos niveles de concentración (n=5).

Cartucho	Oasis HLB				EBH			
Agua	Ultrapura		Río		Ultrapura		Río	
Concentración ($ng \cdot L^{-1}$)	0.7	7.2	0.7	7.2	0.7	7.2	0.7	7.2
Recuperación (%)	91	95	93	90	106	97	98	82
	88	107	108	82	108	96	96	78
	96	88	96	89	115	100	87	85
	86	96	110	87	102	86	91	83
	90	95	93	98	98	94	103	101
Recuperación media (%)	90	96	100	89	106	95	95	86
RSD (%)	4.2	7.1	8.3	6.5	6.1	5.6	6.5	10.3

Tabla 13: Resultados del ANOVA de 3 vías aplicado a las recuperaciones obtenidas para alprazolam.

Fuente	g.d.l.	Suma de Cuadrados	Cuadrados Medios	F	p
Agua	1	176.4	176.4	2.85	0.100
Concentración	1	396.9	396.9	6.42	0.016
Cartucho	1	19.6	19.6	0.32	0.577
Total error (residual)	36	2225	61.79		
Total (corr.)	39	2818			

Los resultados del ANOVA de tres vías (Tabla 13) indican que sólo existe diferencia significativa entre las recuperaciones (p=0.016) cuando se modifica la concentración de alprazolam en agua; la recuperación media de alprazolam en agua de río es un 9 y un 11 % mayor a baja concentración con respecto al nivel alto de concentración para los cartuchos EBH y Oasis, respectivamente.

2.4. CLORPROMAZINA

Para el caso de la clorpromazina, los resultados obtenidos se muestran en la Tabla 14. Las concentraciones con que se dopó la muestras de agua eran 0.7 $ng \cdot L^{-1}$ y 6.2 $ng \cdot L^{-1}$. La desviación típica relativa de los experimentos variaba entre el 5 y 13 % (n=5) aproximadamente, siendo ligeramente más elevada que en los ensayos anteriores. Los factores significativos en la extracción de la clorpromazina se muestran en la Tabla 15.

Tabla 14: Recuperaciones y precisiones obtenidas en la determinación de clorpromazina en muestras de agua ultrapura y de río a dos niveles de concentración (n=5).

Cartucho	Oasis HLB				EBH			
Agua	Ultrapura		Río		Ultrapura		Río	
Concentración ($ng \cdot L^{-1}$)	0.7	6.2	0.7	6.2	0.7	6.2	0.7	6.2
Recuperación (%)	51	75	53	85	62	75	73	83
	53	84	64	89	55	72	64	75
	65	79	69	88	68	64	75	72
	68	82	62	78	75	77	65	76
	57	76	54	68	76	66	74	81
Recuperación media (%)	59	79	60	82	67	71	71	77
RSD (%)	13.0	4.8	11.0	11.0	13.0	8.0	7.5	5.8

Tabla 15: Resultados del ANOVA de 3 vías aplicado a las recuperaciones obtenidas para clorpromazina.

Fuente	g.d.l.	Suma de Cuadrados	Cuadrados Medios	F	p
Agua	1	115.6	115.6	2.05	0.161
Concentración	1	1716	1716	30.4	<0.001
Cartucho	1	19.6	19.6	0.35	0.559
Total error (residual)	36	2033	56.47		
Total (corr.)	39	3884			

No se observaron diferencias significativas (p=0.05) en las recuperaciones obtenidas para los factores “tipo de cartucho” y “tipo de agua”, por lo que en estos casos se mantendría la hipótesis nula al comparar las varianzas. Las recuperaciones difieren significativamente al variar la concentración del analito (p<0.001), como para las dos drogas anteriores, pero con una diferencia: en este caso la recuperación de clorpromazina aumenta al aumentar la concentración, y no al disminuirla como en el caso del piroxicam y alprazolam. Se deduce de la Tabla 14 que el incremento de la recuperación con la concentración es del 20 % para el agua ultrapura y del 22 % para el agua

de río con los cartuchos Oasis; para los cartuchos EBH el incremento es menos acusado, del orden del 4-6 %.

2.5. MELOXICAM

El procedimiento se aplicó a muestras de agua ultrapura y agua de río dopadas en este caso con 0.7 $ng \cdot L^{-1}$ y 5.9 $ng \cdot L^{-1}$ de meloxicam, obteniéndose las recuperaciones y precisiones mostradas en la Tabla 16 para los dos cartuchos ensayados, donde se observan precisiones comprendidas entre el 4 y el 11 %. Un análisis de varianza de 3 vías fue aplicado a estos datos obteniendo los resultados indicados en la Tabla 17.

Tabla 16: Recuperaciones y precisiones obtenidas en la determinación de meloxicam en muestras de agua ultrapura y de río a dos niveles de concentración (n=5).

Cartucho	Oasis HLB				EBH			
Agua	Ultrapura		Río		Ultrapura		Río	
Concentración ($ng \cdot L^{-1}$)	0.7	5.9	0.7	5.9	0.7	5.9	0.7	5.9
Recuperación (%)	83 90 73 86 91	80 96 88 94 83	73 91 79 82 94	77 79 81 89 85	85 99 93 77 79	76 79 85 82 78	65 82 77 72 80	77 83 79 73 69
Recuperación media (%)	85	88	84	82	87	80	75	76
RSD (%)	8.5	7.8	10.3	5.9	10.8	4.4	9.1	7.1

Tabla 17: Resultados del ANOVA de 3 vías aplicado a las recuperaciones obtenidas para meloxicam.

Fuente	g.d.l.	Suma de Cuadrados	Cuadrados Medios	F	p
Agua	1	302.5	302.5	6.50	0.015
Concentración	1	8.1	8.1	0.17	0.679
Cartucho	1	270.4	270.4	5.81	0.021
Total error (residual)	36	1677	46.57		
Total (corr.)	39	2258			

Al igual que ocurría para tenoxicam, se observan diferencias significativas en las recuperaciones obtenidas para el tipo de agua y el cartucho utilizado, no siendo así para el nivel de concentración. Nuevamente las recuperaciones son superiores al utilizar cartuchos Oasis HLB y en agua ultrapura, con valores de 85 y 88 % para el nivel bajo y alto de concentración respectivamente, frente al 87 y 80 % obtenidos cuando se utilizan cartuchos EBH. Para el agua de río las recuperaciones son

aproximadamente un 3 % inferiores de media respecto a agua ultrapura para los cartuchos Oasis HLB y la disminución es de aproximadamente 10 % cuando se trata de los EBH.

2.6. INDOMETACINA

Las recuperaciones y precisiones obtenidas para la indometacina a los niveles de concentración de 1.6 $ng \cdot L^{-1}$ y de 19.4 $ng \cdot L^{-1}$ se muestran en la Tabla 18. La interpretación estadística de los resultados se muestra en la Tabla 19. La precisión de los análisis no alcanza en ninguna de las experiencias el 10 % (RSD, n=5).

Tabla 18: Recuperaciones y precisiones obtenidas en la determinación de indometacina en muestras de agua ultrapura y de río a dos niveles de concentración (n=5).

Cartucho	Oasis HLB				EBH			
Agua	Ultrapura		Río		Ultrapura		Río	
Concentración ($ng \cdot L^{-1}$)	1.6	19.4	1.6	19.4	1.6	19.4	1.6	19.4
Recuperación (%)	93	94	94	73	106	89	86	74
	92	87	94	74	108	83	77	75
	90	89	88	71	97	93	89	64
	98	85	74	80	106	93	84	77
	96	91	87	76	99	85	79	77
Recuperación media (%)	94	89	87	75	103	89	83	73
RSD (%)	3.4	3.9	9.4	4.6	4.7	5.1	6.0	7.4

Tabla 19: Resultados del ANOVA de 3 vías aplicado a las recuperaciones obtenidas para indometacina.

Fuente	g.d.l.	Suma de Cuadrados	Cuadrados Medios	F	p
Agua	1	1974	1974	66.3	<0.001
Concentración	1	1071	1071	36.0	<0.001
Cartucho	1	5.625	5.625	0.19	0.666
Total error (residual)	36	1072	29.77		
Total (corr.)	39	4123			

De acuerdo con los niveles de significación (p) calculados en la Tabla 19, se puede afirmar con una probabilidad de al menos un 95 % que las recuperaciones de indometacina son significativamente diferentes al variar la concentración ($p<0.001$) y cuando se modifica la matriz de la muestra de agua ($p<0.001$).

Con respecto a la influencia de la concentración se deduce de la Tabla 18 que la recuperación media de indometacina en agua de río es un 10 % y un 12 % mayor a baja concentración para los

cartuchos EBH y Oasis, respectivamente, mientras que con agua ultrapura los incrementos de recuperación a baja concentración son del 14 % y 5 %, respectivamente. Respecto al tipo de agua muestreada, al igual que sucedía para los tres oxicanes, se observa que las recuperaciones son mayores en agua ultrapura que en agua de río; para el cartucho EBH la recuperación media en agua de río era un 16 y 20 % menor para el nivel de concentración alto y bajo, respectivamente, y para el cartucho Oasis HLB la recuperación media era un 14 % y 7 % menor respectivamente.

2.7. CELECOXIB

Finalmente se muestran los resultados para el celecoxib en las Tablas 20 y 21, después de dopar el agua de río y agua ultrapura con concentraciones de 1.5 $ng \cdot L^{-1}$ y 18.3 $ng \cdot L^{-1}$, y de extraer el analito sobre los cartuchos EBH y Oasis. De acuerdo con los resultados del ANOVA de 3 vías el único factor significativo es el tipo de agua analizado (p=0.003), no existiendo diferencias significativas (p=0.05) cuando se estudia la influencia de la concentración y del tipo de relleno.

Tabla 20: Recuperaciones y precisiones obtenidas en la determinación de celecoxib en muestras de agua ultrapura y de río a dos niveles de concentración (n=5)

Cartucho	Oasis HLB				EBH			
Agua	Ultrapura		Río		Ultrapura		Río	
Concentración ($ng \cdot L^{-1}$)	1.5	18.3	1.5	18.3	1.5	18.3	1.5	18.3
Recuperación (%)	97	110	90	80	99	96	89	95
	94	102	100	72	98	87	89	81
	100	95	98	84	92	94	91	86
	86	92	83	93	97	98	105	84
	84	89	80	86	85	109	83	77
Recuperación media (%)	92	98	90	83	94	97	91	85
RSD (%)	7.5	8.4	9.8	9.3	6.2	8.2	8.9	8.0

Tabla 21: Resultados del ANOVA de 3 vías aplicado a las recuperciones obtenidas para celecoxib

Fuente	g.d.l.	Suma de Cuadrados	Cuadrados Medios	F	p
Agua	1	624.1	624.1	10.29	0.003
Concentración	1	22.5	22.5	0.37	0.546
Cartucho	1	10.0	10.0	0.16	0.687
Total error (residual)	36	2183	60.63		
Total (corr.)	39	624.1			

Como en el caso de oxicanes e indometacina la recuperación media obtenida sobre agua de río es menor que sobre agua ultrapura para los dos tipos de cartuchos. Así, para el agua de río y

cartuchos Oasis se obtienen recuperaciones medias del 90 y 83 % a concentración baja y alta, respectivamente, y recuperaciones del 92 y 98 % para el agua ultrapura. Las diferencias de recuperación son del orden del 2-5 %.

En el caso de los cartuchos EBH, las recuperaciones son 91 y 85 % en el agua de río y del orden de 94 y 97 % en ultrapura, para los niveles de concentración bajo y alto, respectivamente; para el nivel de concentración elevado la diferencia de recuperación media alcanza el 12 %. Las precisiones de estos análisis están comprendidas entre el 6 y el 10 %.

2.8. SELECCIÓN DE UN RELLENO PARA CADA ANALITO. LÍMITES DE DETECCIÓN

La experimentación que se muestra en los siguientes apartados de esta memoria se ha realizado exclusivamente sobre uno de los dos tipos de cartuchos ensayados. De acuerdo con la interpretación estadística de los ensayos de recuperaciones, para tenoxicam y meloxicam existen diferencias significativas según el relleno utilizado, ofreciendo mejores resultados el cartucho Oasis HLB por lo que éste fue el seleccionado para estos dos compuestos; sin embargo, para las 5 drogas restantes, no existe diferencia estadísticamente significativa entre los dos tipos de rellenos, por lo que cualquiera de ellos sería válido para la determinación de esos fármacos en concentraciones traza en agua de río.

No obstante, si se comparan visualmente las recuperaciones obtenidas con los dos rellenos sobre la muestra de agua de río se comprueba que las recuperaciones de piroxicam y alprazolam son mayores cuando se emplean los cartuchos Oasis HLB, motivo por el que se seleccionó esta fase estacionaria para estos dos compuestos. Mediante una prueba de t sólo se confirmaba que los cartuchos Oasis eran más adecuados que los EBH para la extracción de piroxicam a concentración baja.

En el caso de la clorpromazina la elección de un cartucho sobre el otro atendiendo a la recuperación media no es fácil porque según el nivel de concentración es preferible un cartucho u otro: finalmente se utilizaron igualmente los cartuchos Oasis HLB (Tabla 22).

Las recuperaciones medias de indometacina y celecoxib sobre agua de río eran muy similares con ambos cartuchos, y también a ambas concentraciones; para estos compuestos se ha usado el cartucho EBH para llevar a cabo la experimentación que se describe seguidamente en esta memoria, relativa a la robustez del método para determinar residuos a nivel de trazas y estimar la degradación y persistencia de las drogas.

Por otra parte, para cada combinación compuesto-cartucho se ha estimado experimentalmente el límite de detección del método de análisis. A tal fin se doparon muestras de 1 L de agua de río con cantidades muy pequeñas de los analitos y se les aplicó el procedimiento de preparación de muestra. La Tabla 22 muestra los límites de detección estimados a partir de una relación señal/ruido de 3, expresados como concentración en agua de río ($ng \cdot L^{-1}$); éstos son inferiores a 1 $ng \cdot L^{-1}$ y varían entre 0.2 $ng \cdot L^{-1}$ para clorpromazina y 0.6 $ng \cdot L^{-1}$ para la indometacina.

Los límites de detección teóricos se podrían calcular a partir de los LOD estimados en la inyección de patrones disueltos en metanol teniendo en cuenta el factor de concentración del método de análisis (2000 veces). Si éstos límites teóricos se comparan con los límites de detección estimados experimentalmente se comprueba que los últimos son aproximadamente 2-4 veces mayores que los teóricos.

Tabla 22: Cartuchos empleados para cada compuesto en las siguientes experiencias recogidas en la memoria. Estimación de los límites de detección alcanzables mediante el método de análisis de residuos ($ng \cdot L^{-1}$).

Compuesto	Cartucho	LOD ($ng \cdot L^{-1}$)
Tenoxicam	Oasis HLB	0.4
Piroxicam	Oasis HLB	0.4
Alprazolam	Oasis HLB	0.3
Clorpromazina	Oasis HLB	0.2
Meloxicam	Oasis HLB	0.4
Indometacina	EBH	0.6
Celecoxib	EBH	0.5

3. ROBUSTEZ, PRINCIPIOS ACTIVOS

La robustez de un método de análisis evalúa la capacidad del mismo para permanecer inalterado cuando se introducen pequeñas variaciones en los parámetros de operación. La robustez proporciona una estimación de la fiabilidad del método y de la influencia de ciertos parámetros durante la operación de rutina.

Se identificaron cuatro parámetros de operación de la preparación de muestra que podrían afectar a las áreas de pico y consecuentemente a la concentración medida en el extracto. Éstos eran el pH de la muestra de agua, el volumen de metanol usado para eluir los cartuchos, el volumen de disolución de lavado de los cartuchos y el tiempo de evaporación a 40°C. La variación del pH se incluyó en este estudio para tener en cuenta la posible modificación de éste, en un rango estrecho, en el agua de río. Respecto al tiempo de evaporación, se ha considerado el aumento del mismo en la evaporadora centrífuga para verificar la estabilidad térmica de los analitos.

La robustez se ha evaluado mediante un diseño de Plackett-Burman. Éste es un diseño factorial fraccional a dos niveles, donde se estudian n-1 variables, en n ensayos, siendo n un múltiplo de 4. En este caso, se han planteado 8 ensayos para estudiar 7 factores de los cuales 3 son factores simulados (dummys) [184, 185]. La Tabla 23 muestra el valor nominal de las 4 variables estudiadas y su valor para los niveles alto y bajo del diseño de experimentos.

Tabla 23: Factores y niveles seleccionados para evaluar la robustez mediante un diseño de experimentos Plackett-Burman.

Factor	Valor nominal	Nivel alto	Nivel bajo
F1: pH	7.8	9.0	7.0
F2: Volumen de metanol (mL)	4.0	4.1	3.9
F3: Volumen de lavado (mL)	3.0	3.3	2.7
F4:Tiempo de evaporación (min)	30	40	30

La matriz de experimentos del diseño Plackett-Burman se muestra en la Tabla 24. También se muestran las áreas de pico obtenidas en cada experimento para cada uno de los analitos. Para la realización de los experimentos se ha eluído 1 L de agua de río (al pH adecuado) dopado con los 7 compuestos sobre un determinado tipo de cartucho según la asignación cartucho-analito de la Tabla 22. Las concentraciones de los analitos en la muestra de agua dopada eran las siguientes: tenoxicam 6.0 $ng{\cdot}L^{-1}$, piroxicam 6.0 $ng{\cdot}L^{-1}$, alprazolam 7.3 $ng{\cdot}L^{-1}$, clorpromazina 7.0 $ng{\cdot}L^{-1}$, meloxican 6.0 $ng{\cdot}L^{-1}$, indometacina 15.6 $ng{\cdot}L^{-1}$ y celecoxib 16.2 $ng{\cdot}L^{-1}$. El orden de los ensayos fue aleatorizado.

El efecto que tiene cada factor, se estima como la diferencia entre el valor medio de la respuesta al nivel alto (+) y el valor medio a nivel bajo (-). Por lo tanto, el efecto E de cada uno de los factores, real o simulado, se evalúa con la Ecuación 2, donde A (+) representa las áreas de pico obtenidas en las experiencias a nivel alto y A (-) las obtenidas en aquellas realizadas a nivel bajo

$$E = \frac{\sum A\,(+)}{4} - \frac{\sum A\,(-)}{4} \qquad (2)$$

El efecto de un factor simulado se considera que es debido al error experimental. El error estándar, *SE*, de los efectos, se estima a través de la raíz cuadrada de la varianza de los factores simulados como se aprecia en la Ecuación 3, donde n es el número de efectos simulados.

$$SE = \sqrt{\frac{\sum (E_d)^2}{n}} \qquad (3)$$

La existencia de diferencias significativas se comprueba mediante la comparación del efecto de cada una de las variables, con un efecto crítico, E_C, que se calcula multiplicando el valor del error estándar, *SE*, por un valor de t crítico (Ecuación 4). El valor de t crítico se encuentra tabulado; para un nivel de significación de 0.05 y con un número de grados de libertad de 3 (coincide con el número de factores simulados) su valor es 3.182.

$$E_C = t_{crítico}\ x\ SE = 3.182\ x\ SE \qquad (4)$$

Tabla 24: Matriz de experimentos del diseño Plackett-Burman y áreas de pico obtenidas en la experimentación. Nivel alto (+), nivel bajo (-)

	Factores							Áreas de pico						
	F1	F2	F3	F4	Dummy	Dummy	Dummy	Tenoxicam	Piroxicam	Alprazolam	Clorpromazina	Meloxicam	Indometacina	Celecoxib
1	+	+	+	+	+	+	+	18805	27792	82091	109604	19433	31365	221914
2	-	-	+	+	-	+	-	13547	21424	60319	118991	13379	22843	188768
3	+	-	-	+	-	-	+	13942	19592	70367	92502	15558	33666	144067
4	-	+	-	+	-	-	+	17573	29423	76098	107780	22937	38142	177469
5	+	+	+	-	-	-	-	16365	27238	95391	91103	22300	35469	165067
6	-	-	+	-	+	-	+	15165	28135	90332	131060	21403	38097	264795
7	+	-	-	-	-	+	+	19831	34509	145811	132162	28968	40094	208755
8	-	+	-	-	+	+	-	17532	24567	83417	112513	18094	36001	216154

En la Tabla 25 se muestran los valores de los efectos críticos (E_c) y de cada una de las cuatro variables (E_v) estudiadas, para los 7 analitos.

Tabla 25: Efectos de las variables y efecto crítico.

Compuesto	E_c	E (F1)	E (F2)	E (F3)	E (F4)
Tenoxicam	5583	1281.5	1947.5	- 1249	- 1256.5
Piroxicam	13801	1395.5	1340	-875	-4054
Alprazolam	49051	20863	- 7468	- 11900	- 31509
Clorpromazina	38134	- 11243	- 13429	1450	- 9490
Meloxicam	12368	2611.5	864	- 2260.5	- 4864.5
Indometacina	11462	1378	1569	- 5032	- 5911
Celecoxib	96081	- 26846	- 6445	23525	-30638

Al comparar los efectos de cada uno de los cuatro factores, en valor absoluto, con el efecto crítico para cada compuesto, se observa que los efectos de los factores son siempre menores que el efecto crítico, lo que indica que no existen diferencias significativas cuando se introducen pequeñas variaciones en las condiciones de operación de la preparación de la muestra.

4. ESTUDIOS DE DEGRADACIÓN E INDENTIFICACIÓN DE PRODUCTOS DE DEGRADACIÓN

Los resultados se presentan y discuten para cada compuesto, y en el caso de los oxicanes conjuntamente, en los artículos de investigación que se presentan a continuación.

4.1. CLORPROMAZINA

Chemosphere 162 (2016) 285–292

Contents lists available at ScienceDirect

Chemosphere

journal homepage: www.elsevier.com/locate/chemosphere

Fate of the drug chlorpromazine in river water according to laboratory assays. Identification and evolution over time of degradation products. Sorption to sediment

Juan J. Jiménez [a, b, *], Beatriz E. Muñoz [c], María I. Sánchez [c], Rafael Pardo [a], María S. Vega [a]

[a] Department of Analytical Chemistry, Faculty of Sciences, Campus Miguel Delibes, University of Valladolid, Paseo de Belén 7, 47011 Valladolid, Spain
[b] I.U. CINQUIMA, Campus Miguel Delibes, University of Valladolid, Paseo de Belén 5, 47011 Valladolid, Spain
[c] Department of Analytical Chemistry, School of Industrial Engineers, University of Valladolid, Francisco Mendizábal 1, 47014 Valladolid, Spain

HIGHLIGHTS

- Chlorpromazine is detected during 4 weeks when exposure to sunlight is limited.
- 16 degradation products tentatively identified from high-resolution MS/MS spectra.
- Oxidation, hydroxylation and breakdown of the promazine are degradation ways.
- Benzo[1,4]thiazin-6-ol derivatives are the main residues after 20 weeks.
- Sorption coefficient of chlorpromazine onto aquatic sediment is very high.

GRAPHICAL ABSTRACT

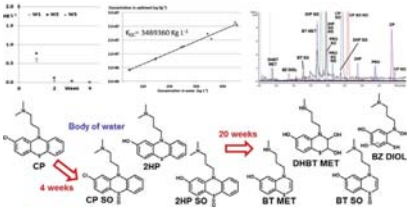

ARTICLE INFO

Article history:
Received 6 May 2016
Received in revised form
25 July 2016
Accepted 29 July 2016
Available online 16 August 2016

Handling Editor: Klaus Kümmerer

Keywords:
Chlorpromazine
Degradation products
River water
Sorption coefficients
High-resolution mass spectrometry

ABSTRACT

Toxic effects of the non-biodegradable drug chlorpromazine and its degradation products have been reported on microorganisms in aqueous media. Here, chlorpromazine degradation assays in forced and non-forced conditions have been done to know its persistence and degradation products in river water. Sunlight irradiation promotes the complete degradation of chlorpromazine (2 μg L^{-1}) in less than 4 h, but if the exposure to sunlight is limited chlorpromazine is detected during 4 weeks in river water. Sixteen degradation products in surface water are described for first time after solid-phase extraction and analysis by ultra-pressure liquid chromatography/quadrupole time-of-flight/mass spectrometry; their structures are proposed from the molecular formulae of the fragment-ions observed in high-resolution tandem mass spectra. Hydroxylation and oxidation products such as chlorpromazine sulfoxide, 2-hydroxypromazine and 2-hydroxypromazine sulfoxide were predominant degradation products in the early stages; some benzo[1,4]thiazin-6-ol derivatives resulting from the breakdown of the phenothiazine core were the major and relatively stable products after 20 weeks under non-forced conditions. A degradation pathway of chlorpromazine in water is outlined. Moreover, it is shown that chlorpromazine is very strongly adsorbed on sediment while the degradation products that kept the promazine core have a notable capacity of sorption, too; sorption coefficients are calculated. Finally, a prediction about the

* Corresponding author. Department of Analytical Chemistry, Faculty of Sciences, Campus Miguel Delibes, University of Valladolid, Paseo de Belén 7, 47011 Valladolid, Spain.
E-mail address: jjimenez@qa.uva.es (J.J. Jiménez).

http://dx.doi.org/10.1016/j.chemosphere.2016.07.107

toxicity of the degradation products in aquatic ecosystems suggests that some of them have toxicities similar, or even higher, than chlorpromazine.

1. Introduction

Chlorpromazine (CP) is a lipophilic phenothiazine drug with antipsychotic and neuroleptic activity prescribed for the treatment of mental and behavioral disorders. It was introduced into psychiatry in the early 1950s, and nowadays, it is included in the World Health Organization's List of Essential Medicines which compiles the drugs needed in a basic health system. It has some veterinary uses, too.

There is some concern for the influence of the CP residues in the environment. Toxic and allergic effects on biomolecules, bacteria and protozoans have been observed in presence of CP residues and attributed to photochemical reactions involving the parent compound and its transformation products, whose composition is generally not well known (Nalecz et al., 2008; Viola and Dall'Acqua, 2006; Chignell et al., 1985; Trautwein and Kümmerer, 2012). Harmful effects on *Daphnia magna*, a biomarker of the health of the aquatic ecosystems, have also been reported (Oliveira et al., 2015) while the alteration of the microbial function of soil has been described (Gielen et al., 2011), too. Furthermore, a study of biological degradation of CP in water concluded that CP had to be classified as a non-biodegradable compound (Trautwein and Kümmerer, 2012).

Pharmaceutical compounds can reach the surface waters by different ways although the discharges from the wastewater treatment plants are usually the main introduction way. As regards CP only a manuscript has considered its analysis in wastewater effluents, it was not detected after the monitoring of effluents from five treatment plants (Borova et al., 2014). There are not data about its occurrence in surface waters.

In this context, some experiments have been conducted to estimate the degradation-rate of CP in river water and know its degradation products over time. Solutions of CP in river water were subjected to high temperature, and sunlight irradiation without any limitation, to force the degradation. Non-forced degradation involved the monitoring of residues in river water kept in glass container at room temperature, with or without added aquatic sediment; since glass absorbs partially UV radiation, the behavior of CP is thus comparable to that in a mass of water where the penetration of solar UV radiation is diminished with depth. Extracts of water samples were injected in an ultra-pressure liquid chromatographic system and the structure of the detected degradation products was tentatively elucidated from the molecular formulae estimated by high-resolution mass spectrometry (MS) and the interpretation of the fragments observed in high-resolution tandem mass spectrometry (MS/MS), proposing a degradation pathway. Furthermore, since a strong capacity of sorption of CP on sediment was observed, a sorption isotherm is presented while sorption coefficients for degradation products are calculated on the supposition that peak areas vary linearly with concentration. Finally, the possible toxicity of the identified degradation products is predicted by the TEST software (Toxicity Estimation Software Tool) developed by the US Environmental Protection Agency (EPA).

2. Experimental

2.1. Material and reagents

Water samples were collected from the rivers Pisuerga (pH value 7.8, chemical oxygen demand value 4.6 mg L^{-1}), in the urban area of the city of Valladolid, and Tuerto (pH value 7.4, chemical oxygen demand value 3.9 mg L^{-1}), in the rural area of the La Bañeza (León). A sediment sample (total organic carbon 1.2%; clay 11%, silt 44%, sand 45%) was collected from the river Pisuerga.

Cellulose nitrate disks, 0.20 and 0.45 μm pore size, to filter water samples were obtained from Sartorious (Barcelona, Spain). Chlorpromazine hydrochloride (99% purity) was obtained from Sigma-Aldrich. LC-MS grade methanol, acetonitrile and formic acid were supplied by Panreac (Barcelona, Spain) and ultrapure water was obtained from a Milli-Q plus apparatus (Millipore, Milford, MA, USA).

Sodium hydroxide, potassium dihydrogen phosphate and sodium azide were purchased from Panreac. Oasis HLB cartridges (60 mg) were obtained from Waters and nitrogen for the LC-MS system was supplied by a gas generator from Zefiro (Vigonza, Italy). A vacuum centrifuge evaporator, Myvac model, was provided by Genevac (Ipswich, UK) and PK120 centrifuge by ALC (Winchester, VA, USA).

2.2. Degradation assays

Forced conditions are commonly applied to aqueous solutions to estimate the stability of environmental contaminants and foresee their degradation products in aquatic ecosystems. In addition to this strategy a simpler, although slower, approach was also adopted in this work to simulate the concurrent natural processes in a body of water. So, river water filtered through a 0.45 μm pore-size cellulose nitrate disk was placed in a transparent and sodium calcium silicate glass container with air-tight seal, which was weekly open to collect a sample aliquot and replace the air inside in contact with the water surface. The container was placed within the laboratory at 18–21 °C and exposed to sunlight under the natural day-night cycle for 20 weeks, at which time the non-forced degradation assay was ended.

A volume of 2500 mL of river water placed in glass container was spiked with CP to achieve an initial concentration of 2 μg L^{-1} in each degradation assay; aliquots of 25 mL were periodically collected, subjected to SPE and injected in the chromatographic system to follow the degradation of CP, look for degradation products and monitor them. Degradation experiments were made between the months of November and March with waters from the rivers Pisuerga (W1 sample) and Tuerto (W2 sample), and between January and May with water from the Pisuerga river (W3 sample). Simultaneously, the degradation on W1 sample was also studied in presence of sediment (SED sample), by adding river sediment to the container in a sediment to solution ratio of 0.03 g mL^{-1}, and in absence of sunlight (DARK sample) by coating the container with aluminum foil.

Furthermore, some degradation assays were done on W1

sample at high temperature, 70 °C (HT sample), and under direct sunlight irradiation (UV sample), in order to ascertain the origin of the degradation products. Irradiation assay was carried out in the month of January with CP solutions placed in quartz cuvettes. Additional information about degradation studies is given as supplementary material.

2.3. Sorption to river sediment

Experiments to investigate the capacity of sorption of CP and degradation products were conducted. The sorption coefficient (K_d) of CP into sediment (sieved through a 0.5 mm mesh) was determined using a batch approach. River water filtered through 0.20 μm pore-size cellulose nitrate and spiked with CP was added to sediment (2 g) to achieve a sediment to solution ratio of 0.000025 g mL^{-1}; CP concentrations were 200, 400, 600, 800 and 1000 ng L^{-1}. Control solutions without sediment were also prepared. River water contained 0.02% sodium azide as a biocide to minimize a possible microbial activity and pH (7.8) was controlled with phosphate buffer (0.02 M). Flasks, protected from sunlight with aluminum foil, were manually shaken for 1 min and left standing at 20±1 °C for a period of 24 h. Afterwards, an aliquot of 10 mL, previously centrifuged to remove solids, was analyzed to determine the concentration in equilibrium. Concentration adsorbed on the sediment was not directly measured.

Analytical standards were unavailable for most of the degradation products of CP, however an estimation of their K_d was carried out for some of them on the assumption that there is a linear relationship between peak area and concentration for each compound. Experiments similar to the above-described were devised by spiking water with a degraded CP solution containing the degradation products and selecting an appropriate sediment to solution ratio. So, the decrease percentage of peak area in water was supposed to be the percentage of compound adsorbed onto sediment (A%) and K_d was calculated by Eq. (1), which is valid if adsorption equation is linear (OECD, 2000). Peak areas measured in the sorption experiments were compared with those of control solutions by a *t*-test (n = 5) to confirm the existence of differences before applying the equation.

$$\log K_d = \log\left[\frac{\frac{A\%}{100}}{1-\frac{A\%}{100}}\right] - \log R \quad (1)$$

2.4. Extraction of chlorpromazine residues from water

Water aliquots (10 or 25 mL) were eluted through Oasis cartridges, previously conditioned by successive elution of methanol (6 mL) and water (6 mL). Cartridges were washed with 3 mL of water-methanol (80:20, v/v) mixture after sample elution. Stationary phase was dried with air for 3 min and extract was eluted with methanol (4 mL) by gravity. Then, extract was evaporated in 30 min by a vacuum centrifuge evaporator heated at 40 °C and the dry residue was collected in 0.5 mL of methanol, which was filtered through a 0.20 μm pore-size PTFE filter for its chromatographic analysis.

2.5. Analysis by liquid chromatography – mass spectrometry

An Acquity ultra-pressure liquid chromatograph from Waters coupled to a Maxis Impact quadrupole time-of-flight tandem mass spectrometer from Bruker Daltonics was used to monitor CP and degradation products in the extracts. Analyses were done with electrospray ionization in positive mode.

The chromatograph was fitted with a Waters BEH ODS column (50 mm × 2.1 mm, particle size 1.7 μm). The column was at room temperature and the mobile phase flow rate was 0.5 mL min^{-1}. The mobile phase consisted of 0.1% formic acid in water (A) and 0.1% formic acid in acetonitrile (B); a linear gradient was applied: from 5% B to 50% B in 4.5 min, and then 80% B in 1 min. Injection volume was 5 μL.

Mass spectrometer can record simple mass spectra (MS mode) or be operated in the tandem mass spectrometry mode (MS/MS mode) to acquire MS^2 spectra. The operation parameters of the electrospray ionization source for MS and MS/MS experiments were as follows: nebulizing gas pressure 0.4 bar, end plate offset voltage −2500 V, capillary voltage − 3500 V, drying gas temperature 200 °C, dry gas flow 8 L min^{-1}. Nitrogen was used as drying and nebulizing gas. Mass calibration adjustments were performed by using a 10 mM sodium formate solution in 2-propanol/water. Spectra acquisition was done via the Microtof software from Bruker, the accurate masses and elemental compositions of the precursor and product ions were calculated by using the data analysis software incorporated in the instrument.

Quantitation of CP was done by linear calibration graphs based on the measure of peak areas in the MS chromatograms extracted for the protonated molecular ion $[M+H]^+$, with a mass range of ±0.01 Da. Similarly, peak areas of degradation products were integrated in the chromatograms extracted for the corresponding $[M+H]^+$ ions.

As regards the performance of the analytical method, mean recovery of CP (2 μg L^{-1}) was 95 and 96% with repeatabilities of 3.0 and 3.5% for W1 and W3 samples, respectively (n = 5). Repeatabilities in the determination of the degradation products varied from 2.8 to 5.5% (n = 5).

2.6. Software to predict ecotoxicity

The TEST software, version 4.1 (EPA, 2008), was applied in order to estimate the possible toxicity of the degradation products. This software estimates the toxicity of an organic compound for an ecotoxicological endpoint using quantitative structure activity relationships (QSARs) methodologies; QSARs are mathematical models used to predict measures of toxicity from the physical and chemical characteristics of a target-compound. The software only requires the introduction of the chemical structure of the compound. In this study the toxicity estimation was calculated by the consensus method, which provides the average value of different calculation approaches, and after activating the fragment constraint relaxation option. Three endpoints of concern for fresh waters were selected: the 48-h *Daphnia magna* and 96-h fathead minnow 50% lethal concentrations (LC_{50}) and the *Tetrahymena pyriformis* 50% growth inhibition concentration (IGC_{50}).

3. Results and discussion

3.1. Degradation of chlorpromazine

Fig. 1 shows the variation of the CP concentration over time in water samples, data are the average of two or three independent experiments for each water matrix; individual data are shown in supplementary material. CP exposed to sunlight without any restriction was completely degraded in less of 4 h while the degradation at 70 °C in darkness was relatively slow. Degradation data were fitted to first-order kinetics with half-lives of 53.7 min (R^2 = 0.94) and 4.55 weeks (R^2 = 0.98) for UV and HT samples, respectively. Moreover, the degradation of CP in darkness at room temperature (DARK sample) was almost negligible: half-life was estimated at 87.3 weeks (R^2 = 0.98). These assays indicate a notable

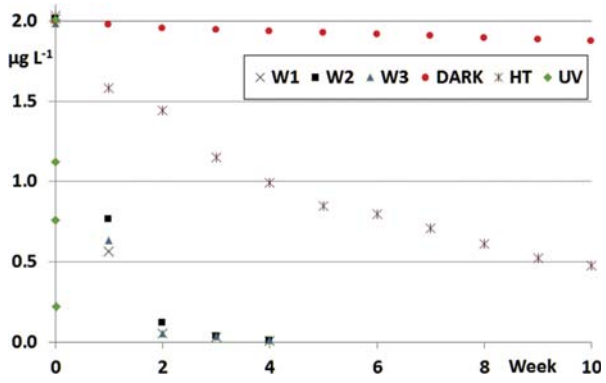

Fig. 1. Degradation of chlorpromazine in river water. Mean of two (W3, DARK, HT, UV) or three (W1, W2) experiments.

importance of the photochemical reactions and a limited significance of the non-photochemical reactions in the transformation of CP in surface water.

CP was detected during 4 weeks in river water exposed to sunlight under non-forced conditions, which are useful to assess experimentally the fate of CP in a body of surface water. Its concentration decreased gradually until it reached the detection limit of the method, which was estimated in 4 ng L^{-1}. Half-lives calculated from the fitting to first-order kinetics were now 0.44 ($R^2 = 0.97$), 0.46 ($R^2 = 0.99$) and 0.49 ($R^2 = 0.95$) weeks for W1, W2 and W3 samples, respectively. The half-life of CP in these conditions is very much higher, about 200 times, than that achieved after direct exposure to sunlight. On the other hand, CP was not detected when experimentation was done in presence of sediment, suggesting a possible sorption to sediment.

3.2. Detection and identification of degradation products

The presence of compounds related to degradation of CP was noted by the observation of new chromatographic peaks in the MS chromatograms, which were present neither in the previous chromatograms nor in blanks, and the gradual variation of their peak areas throughout time. Sixteen degradation products were detected in the degradation studies during the time period under research. The $[M+H]^+$ ion of each degradation product, besides of CP, was isolated and fragmented by collision induced dissociation to obtain structural information. MS/MS spectra, commentaries about the fragmentation patterns, the interpretation of the fragment-ions and an explanation about the assignation of tentative structures to the degradation products can be consulted in the supplementary material. Table 1 shows the established molecular formulae, the proposed identifications and abbreviations of the compounds. In summary, CP can undergo oxidation of amine and sulfur groups, dechlorination and hydroxylation of the benzene ring to form some degradation products in which the promazine structure is kept. In more advanced stages of degradation, the promazine structure is broken and benzo[1,4]thiazin-6-ol derivatives are formed, being also observed the demethylation of the terminal amine and some hydroxylations. Well-defined structures are proposed for 13 out of 16 degradation products. The structures for DHBT MET, BZDIOL and DHP SO were not unequivocally assigned because the position of some substituents could not be delimited from the fragmentation data.

Many degradation products of CP found in river water have not been described till now; in particular, there is not any reference to degradation products in which the rings of phenothiazine (characteristic of the promazine-based drugs) are opened. The occurrence of CP NO and CP SO had already been reported in aqueous solution after irradiation with UV light (Huang and Sands, 1964, 1967) and in biological matrixes (Yeung et al., 1993; Zhang et al., 1996). In a previous work, the origin of CP SO, 2HP and 2HP SO was attributed to the photolysis of CP in aqueous solution while PRO was found in anaerobic conditions (Trautwein and Kümmerer, 2012).

3.3. Occurrence of degradation products in river water

Peak areas of the degradation products were monitored during the degradation studies; a value of 100 was assigned to the initial peak area of CP (week 0) in each experiment, all other peak areas were referred to this value. Fig. 2 resumes the evolution in non-forced conditions. Data for all compounds and experiments are provided as supplementary material. In the initial stages the main degradation products resulted from the substitution of the chlorine atom by a hydroxyl group, and from N-oxidation and S-oxidation processes: so, the major degradation products found in W1, W2, and W3 samples after 4 weeks were 2HP, 2HP SO, CP SO, PRO SO NO, 2HP SO NO, PRO SO and CP SO NO. The occurrence of these compounds decreased in the following weeks while the presence of compounds in which the phenothiazine structure is broken increased gradually. Many degradation products can be found when CP was not already detected. After 20 weeks 9 degradation products were still detected in W1 and W2 samples, and 8 compounds in W3; the major products were BT MET, BT SO, DHBT MET and BZDIOL, whereas the compounds detected in lower amount were BT NH2, CP SO, CP SO NO, PRO SO and PRO SO NO.

The evolution profile of the compounds was similar in waters from two rivers (W1 and W2). The profile for W3 was obtained in other time period and it exhibited some differences, which mainly affected the amount ratios between the degradation products. The modification of the profile in W3 is mainly ascribed to radiation intensity differences between the experimentation periods, although the influence of the water composition cannot be discarded. Anyway, it must be noted that the evolution profile of the compounds in these water samples roughly resembles the evolution pattern observed in the UV sample regardless of the time scale.

The photochemical reactions induce the degradation of CP in surface water and the formation of degradation products. In fact, all degradation products found in the UV sample were also detected in W1, W2 and W3 samples, excepting BT NH2, which was only observed in the latter samples. Small amounts of CP SO, CP SO NO, CP NO and PRO SO were found in DARK sample after 20 weeks, in agreement with the study at 70 °C for 10 weeks, which showed the thermal formation of CP SO and CP SO NO as major compounds and of CP NO, PRO, PRO SO and PRO SO NO as minor compounds.

3.4. Degradation pathway

A main degradation pathway of CP in river water has been outlined taking into account the evolution of the compounds over time and the tentative structural elucidation. The bond lines in Fig. 3 show the formation of the major compounds and their corresponding precursors. Obviously, other transformation routes between different compounds are possible; for instance, PRO SO could also come from the dechlorination of CP SO, which is more abundant than PRO.

It is though that BT MET, the most prominent benzo[1,4]thiazine, derives from 2HP because 2HP is the most abundant, and analogous structurally, degradation product in the first degradation points of the UV sample, when BT MET begins to be detected. For

Table 1
Retention times (RT), masses measured in the MS spectra for the $[M+H]^+$ ion, error in the determination of the exact masses, molecular formulae and number of rings and double bonds (RDB) of the corresponding structure for the detected degradation products.

RT (min)	Molecular formula	Exact mass (Da)	Measured mass (Da)	Error (ppm)	RDB	Compound	Abbreviation
0.41	$C_{12}H_{19}N_2O_3S$	271.1111	271.1110	0.3	4.5	3,4-dihydro-N-(3-methylaminopropyl)-S-oxide-benzo[1,4]thiazine-x,6-diol	DHBT MET
0.88	$C_{11}H_{19}N_2O_3S$	259.1111	259.1111	0.1	3.5	3-(N-(3-(dimethylamino)propyl-N-hydroxyamino)-4-mercaptobenzene-1,x-diol	BZDIOL
1.32	$C_{13}H_{19}N_2O_2S$	267.1162	267.1162	0.0	5.5	N-(3-dimethylaminopropyl)-S-oxide-benzo[1,4]thiazin-6-ol	BT SO
1.68	$C_{11}H_{15}N_2OS$	223.0900	223.0900	−0.3	5.5	N-(3-aminopropyl)-benzo[1,4]thiazin-6-ol	BT NH2
1.71	$C_{12}H_{17}N_2OS$	237.1056	237.1054	0.7	5.5	N-(3-methylaminopropyl)-benzo[1,4]thiazin-6-ol	BT MET
1.81	$C_{17}H_{21}N_2O_2S$	317.1318	317.1316	0.7	8.5	2-Hydroxypromazine sulfoxide	2HP SO
1.96	$C_{17}H_{21}N_2O_3S$	333.1267	333.1270	−0.7	8.5	2-Hydroxypromazine sulfoxide N-oxide	2HP SO NO
1.97	$C_{17}H_{21}N_2OS$	301.1369	301.1367	0.5	8.5	Promazine sulfoxide	PRO SO
2.16	$C_{17}H_{21}N_2O_2S$	317.1318	317.1319	−0.3	8.5	Promazine sulfoxide N-oxide	PRO SO NO
2.40	$C_{17}H_{21}N_2O_3S$	333.1267	333.1266	0.3	8.5	2,x-Dihydroxypromazine sulfoxide	DHP SO
2.43	$C_{17}H_{20}ClN_2OS$	335.0979	335.0981	−0.5	8.5	Chlorpromazine sulfoxide	CP SO
2.58	$C_{17}H_{20}ClN_2O_2S$	351.0929	351.0927	0.6	8.5	Chlorpromazine sulfoxide N-oxide	CP SO NO
2.89	$C_{17}H_{21}N_2OS$	301.1369	301.1369	0.1	8.5	2-Hydroxypromazine	2HP
2.98	$C_{17}H_{21}N_2O_2S$	317.1318	317.1314	0.7	8.5	2-Hydroxypromazine N-oxide	2HP NO
3.38	$C_{17}H_{21}N_2S$	285.1420	285.1419	0.4	8.5	Promazine	PRO
3.85	$C_{17}H_{20}ClN_2S$	319.1030	319.1035	−1.4	8.5	Chlorpromazine	CP
3.93	$C_{17}H_{20}ClN_2OS$	335.0979	335.0972	2.1	8.5	Chlorpromazine N-oxide	CP NO

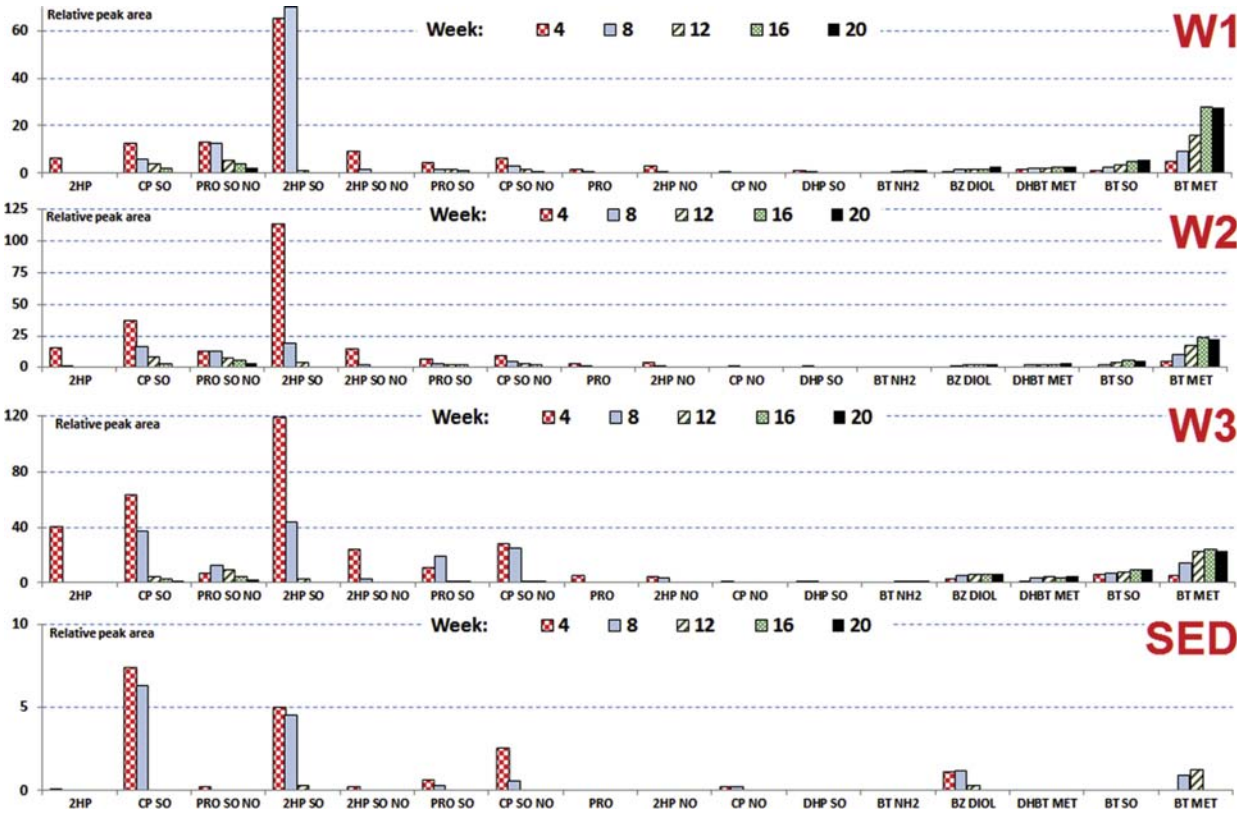

Fig. 2. Variation of peak areas of the degradation products in river water under non-forced conditions. Mean of two experiments.

similar reasons, BT SO could be formed from 2HP SO.

3.5. Degradation in presence of sediment. Sorption coefficients

CP SO, 2HP SO and CP SO NO were the most abundant degradation products for SED sample in the first weeks, 2HP, 2HP SO NO, PRO SO and PRO SO NO were now less abundant than in the experiments without sediment; the proportion of the other compounds was also different with respect to previous assays (Fig. 2). Moreover, a sharp decay in the peak areas of the degradation products was observed since the 9th and 10th weeks at the same time that a smelly odor began to be perceived in the glass container,

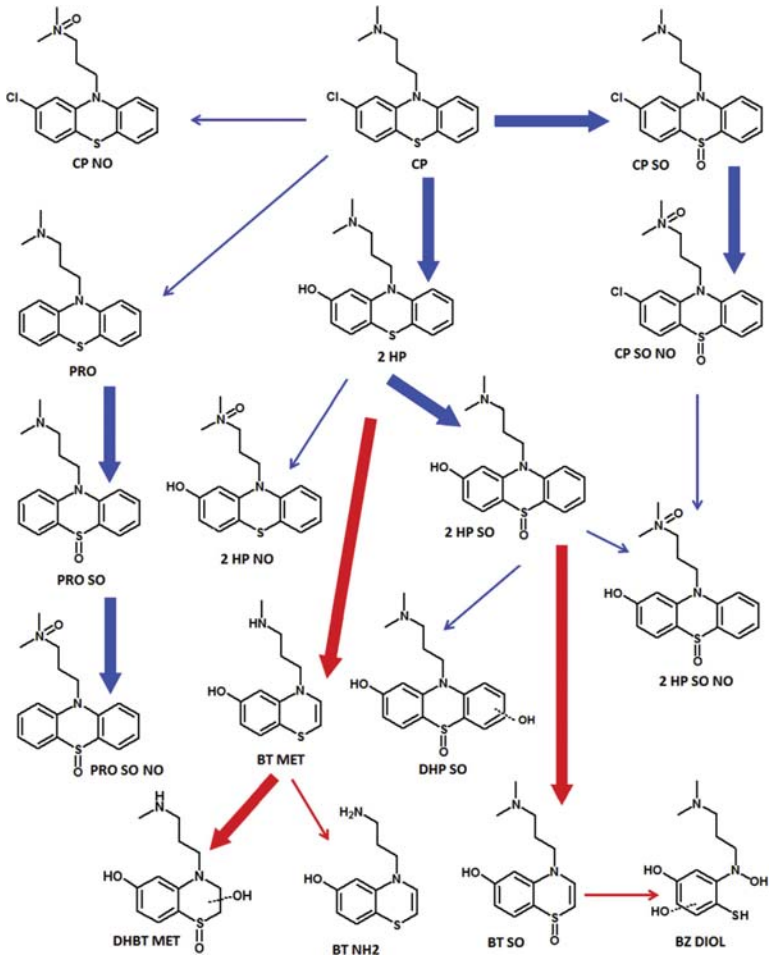

Fig. 3. Main degradation pathway of chlorpromazine in river water. Bold lines are related to the possible predominance of the transformation process.

which suggests a possible growth of microorganisms in presence of sediment and the subsequent biodegradation of the degradation products by them. No compound was detected from the 14th week. CP related compounds different from those already described were not seen in these assays.

It was verified that CP is strongly adsorbed to sediment. Fig. 4 shows the sorption isotherm obtained for CP in the batch experiments; K_d and K_{oc} (organic carbon normalized sorption coefficient) values resulted to be 41 632 and 3 469 360 kg L^{-1} (RSD 4.3%, n = 10), respectively. They are very high, comparable for instance to those for benzo(*a*)pyrene and other high molecular weight polycyclic aromatic hydrocarbons (Delle-Site, 2001).

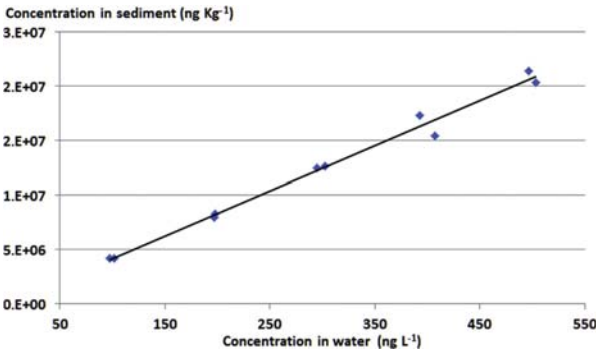

Fig. 4. Sorption isotherm of chlorpromazine (n = 2).

Sorption coefficients were also calculated for most of the degradation products; their K_d and K_{oc} values can be consulted in Table 2 (n = 5). Sorption coefficient of CP was also calculated by this method and it was similar to the previous value. As it is shown in Table 2, sorption coefficient of PRO was also relatively high, ten-fold lower than that of CP, while the N and S-oxidations and the presence of hydroxyl in C2 decrease the capacity of sorption of the corresponding compound. The lowest sorption coefficients correspond to DHBT MET, BTSO and BZDIOL, in fact only an estimation of K_d is given for the two latter compounds since their low sorption capacity.

The calculated sorption coefficients are coherent with the observed experimental behavior. So, PRO SO and PRO SO NO, less prone to be adsorbed, were commonly detected in SED sample while PRO was never detected. In the same way, 2HP SO NO was found in the first week of degradation of SED sample but 2HP and 2HP SO were not detected. However, BT SO (low K_d) was commonly detected in W1, W2 and W3, but not in SED sample.

Table 2
K_d and K_{oc} mean values (RSDs in parenthesis). Mean adsorption percentages (A%) onto sediment and experimental sediment to water ratios (R), n = 5.

Compound	K_d (Kg L^{-1})	K_{oc} (Kg L^{-1})	A%	R (Kg L^{-1})	Experimental t-value[a]
DHBT MET	0.24	20.5 (16.3%)	10.9	0.509	5.3
BZDIOL	<0.22	<18	<10	0.509	0.3
BT SO	<0.22	<18	<10	0.509	0.5
BT MET	6.4	530 (5.9%)	66.1	0.307	23.0
2HP SO	6.6	551 (8.1%)	46.4	0.131	22.1
2HP SO NO	2.5	205 (4.3%)	33.0	0.201	20.9
PRO SO	40.8	3401 (2.3%)	51.8	0.0263	17.6
PRO SO NO	3.4	287 (7.3%)	31.1	0.132	16.4
CP SO	46.2	3853 (9.9%)	54.8	0.0263	18.6
CP SO NO	35.4	2947 (6.5%)	46.4	0.123	19.0
2HP	89.9	7495 (6.4%)	69.4	0.0253	25.4
2HP NO	13.7	1142 (7.4%)	64.2	0.131	31.8
PRO	38 502	317 084 (10.2)	56.9	0.000349	14.6
CP	40 451	3 370 906 (7.5%)	50.2	0.000025	17.1

[a] Critical t-value: 2.3.

3.6. Prediction of ecotoxicity

The ecotoxicity of CP and those degradation products with a defined tentative structure has been predicted. Table 3 presents the results for three endpoints. The LC_{50} for *Daphnia magna* of many degradation products was similar, and even lower, than that of CP; for instance, CP NO and 2HP are presumably more toxic that its precursor CP, they had LC_{50} values of 0.7, 1.3 and 1.5 μM, respectively. As regards the ecotoxicity towards fathead minnow three major degradation products in the first weeks: 2HP, 2HP SO and CP SO, besides other three compounds, are at least four-fold more toxic than CP; in particular CP SO NO is 125-fold more toxic than CP. Finally, growth inhibition concentrations instead of lethal concentrations were calculated for *Tetrahymena pyriformis,* for which the degradation products were less toxic, excepting CP NO whose IGC_{50} was the same that for CP.

The ecotoxicity values predicted by the software for some degradation products of CP in surface water seems to confirm the previously reported findings that describe undesirable effects of the degradation products in certain biological systems; theoretically, toxicity would be higher for fathead minnow. However, it must be remarked that the toxicity of a mixture of degradation products has not been assessed and it is well known that the toxicity of a mixture is different.

4. Conclusions

Chlorpromazine in water is degraded by exposure to UV irradiation. The degradation rate decreases notably when the direct exposure to sunlight is avoided. Non-photochemical reactions affect scarcely to chlorpromazine at alkaline pH (7.8) and ambient temperature. A relatively high number of degradation products can be detected when chlorpromazine has been completely degraded in non-forced conditions and some of them are detected after 20 weeks. The evolution pattern of the compounds over time is essentially similar to that obtained under direct sunlight irradiation, varying the transformation rate.

Degradation products, many of them not described before in water, have been characterized by quadrupole/time-of-flight tandem mass spectrometry, proposing their structures. The breakdown of the phenothiazine moiety in an environmental sample is reported. N-oxidation and S-oxidation processes, substitution of the chorine atom of the aromatic ring for a hydroxyl group or a hydrogen atom, removing of the non-substituted benzene ring, demethylation of the terminal amine and hydroxylation reactions are the transformation routes of chlorpromazine.

Chlorpromazine is strongly adsorbed onto sediment, and so do some of its degradation products. Adsorbed chlorpromazine is also degraded; degradation products are less persistent in river water kept in contact with sediment, likely as consequence of a biological degradation. Harmful effects observed in diverse studies could be ascribed to chlorpromazine or some degradation products according to the ecotoxicities predicted from the elucidated chemical structures.

Table 3
Predicted 50% lethal concentrations (LC_{50}, μM) and 50% growth inhibition concentrations (IGC_{50}, μM) of chlorpromazine and degradation products for different tests.

	Daphnia magna LC_{50} (48 h)	*Tetrahymena pyriformis* IGC_{50}	Fathead minnow LC_{50} (96 h)
BT SO	2.6	398	40
BT NH2	1.0	100	79
BT MET	7.6	63	7.9
2 HP SO	5.0	132	6.3
2HP SO NO	1.6	25	6.3
PRO SO	6.3	49	13
PRO SO NO	1.3	25	10
CP SO	2.0	32	6.3
CP SO NO	1.9	7.8	0.2
2 HP	1.3	20	3.2
2 HP NO	1.3	13	25
PRO	1.9	63	16
CP	1.5	4.0	25
CP NO	0.7	4.0	1.3

Acknowledgements

Authors acknowledge the facilities given by the Laboratorio de Técnicas Instrumentales of the University of Valladolid to perform the experimental work.

Appendix A. Supplementary data

Supplementary data related to this article can be found at http://dx.doi.org/10.1016/j.chemosphere.2016.07.107.

References

Borova, V.L., Maragou, N.C., Gago, P., Pistos, C., Thomaidis, N.S., 2014. Highly sensitive determination of 68 psychoactive pharmaceuticals, illicit drugs, and related human metabolites in wastewater by liquid chromatography-tandem mass spectrometry. Anal. Bioanal. Chem. 406, 4273–4285.
Chignell, C.F., Motten, A.G., Buettner, G.R., 1985. Photoinduced free radicals from chlorpromazine and related phenothiazines: relationship to phenothiazine-induced photosensitization. Environ. Health Perspect. 64, 103–110.
Delle-Site, A., 2001. Factors affecting sorption of organic compounds in natural sorbent water systems and sorption coefficients for selected pollutants. A

review. J. Phys. Chem. Ref. Data 30, 187–439.
EPA Toxicity Estimation Software Tool (TEST), 2008. http://www2.epa.gov/chemical-research/toxicity-estimation-software-tool-test. (accessed 04.01.16.).
Gielen, G.J.H.P., Clinton, P.W., Van den Heuvel, M.R., Kimberley, M.O., Greenfiled, L.G., 2011. Influence of sewage and pharmaceuticals on soil microbial function. Environ. Toxicol. Chem. 30, 1086–1095.
Huang, C.L., Sands, F.L., 1964. The effect of ultraviolet irradiation on chlorpromazine. I. Aerobic condition. J. Chromatgr. 13, 246–249.
Huang, C.L., Sands, F.L., 1967. The effect of ultraviolet irradiation on chlorpromazine. II. Anaerobic condition. J. Pharm. Sci. 56, 259–264.
Nalecz, G., Hajnas, A., Sawickij, J., 2008. Photodegradation and phototoxicity of thioridazine and chlorpromazine evaluated with chemical analysis and aquatic organisms. Ecotoxicology 17, 13–20.
OECD guideline for the testing of chemicals No 106, 2000. Adsorption – Desorption Using a Batch Equilibrium Method, p. 8.
Oliveira, L.L., Antunes, S.C., Goncalves, F., Rocha, O., Nunes, B., 2015. Evaluation of ecotoxicological effects of drugs on Daphnia magna using different enzymatic biomarkers. Ecotoxicol. Environ. Saf. 119, 123–131.
Trautwein, C., Kümmerer, K., 2012. Degradation of the tricyclic antipsychotic drug chlorpromazine under environmental conditions, identification of its main aquatic biotic and abiotic transformation products by LC-MS^n and their effects on environmental bacteria. J. Chromatogr. B 889–890, 24–38.
Viola, G., Dall'Acqua, F., 2006. Photosensitization of biomolecules by phenothiazine derivatives. Curr. Drug Targets 7, 1135–1154.
Yeung, P.K.E., Hubbard, J.W., Korchinski, E.D., Midha, K.K., 1993. Pharmacokinetics of chlorpromazine and key metabolites. Eur. J. Clin. Pharmacol. 45, 563–569.
Zhang, D., Freeman, J.P., Sutherland, J.B., Walker, A.E., Yang, Y., Cerniglia, C.E., 1996. Biotransformation of chlorpromazine and methdilazine by Cunninghamella elegans. Appl. Environ. Microbiol. 62, 798–803.

Supplementary data

Fate of the drug chlorpromazine in river water according to laboratory assays. Identification and evolution over time of degradation products. Sorption to sediment.

Chemosphere, 2016

Contents

2.2. Degradation assays

Attenuation of UV radiation in non-forced experiments

Non-forced degradation experiments involved the monitoring of residues in river water kept in a glass cylindrical container (20.5 cm length x 14.0 cm inner diameter). The containers were placed near a window of the laboratory. The solar radiation must pass through the laboratory window glass and the glass of the container to reach the body of water. As the two glasses absorb UV radiation the behavior of CP in the container can simulate, in a greater or lesser extent, that inside a mass of water because the penetration of solar UV radiation inside a mass of water is diminished with depth. Radiation is partially reflected away when it reaches the surface of a natural body of water, and once within the water, radiation may be scattered or absorbed by solid particles: higher amounts of solid particles in water will decrease the depth of radiation penetration.

The attenuation of radiation through the two glasses (container and window, together) has been estimated in this work by transmittance measurements. Thus, the transmittance of radiation through the glasses has been estimated at five wavelengths with the help an UV-visible spectrophotometer, by placing pieces of the two types of glass in the sample holder. The percentages of radiation transmitted through the two types of glass resulted to be:

Wavelength	Measured transmittance
350 nm	40%
320 nm	1.3%
310 nm	0.02%
305 nm	0.0008%
290 nm	0.00008%

As it can be seen, the attenuation of incidental radiation is more pronounced at the shortest wavelengths as it is expected to happen in a mass of water.

Forced photochemical degradation in quartz cuvettes

River water was placed in quartz parallelepiped cuvettes (inner dimensions: 44 x 10 x 10 mm), which were closed and put on a window ledge, outside the laboratory and south-facing, to allow the direct exposure of the water sample to sunlight. Aliquots of 0.3 mL were withdrawn at regular time intervals for its analysis. Assay was done in the city of Valladolid, in one day, in the month of January (between 9 and 13 h approximately, true solar time). Solar radiation data for the city of Valladolid and the day in which the assay was carried out are shown below; they were achieved from the AEMET (Spanish meteorological agency; Ministry of Agriculture, Food and Environment).

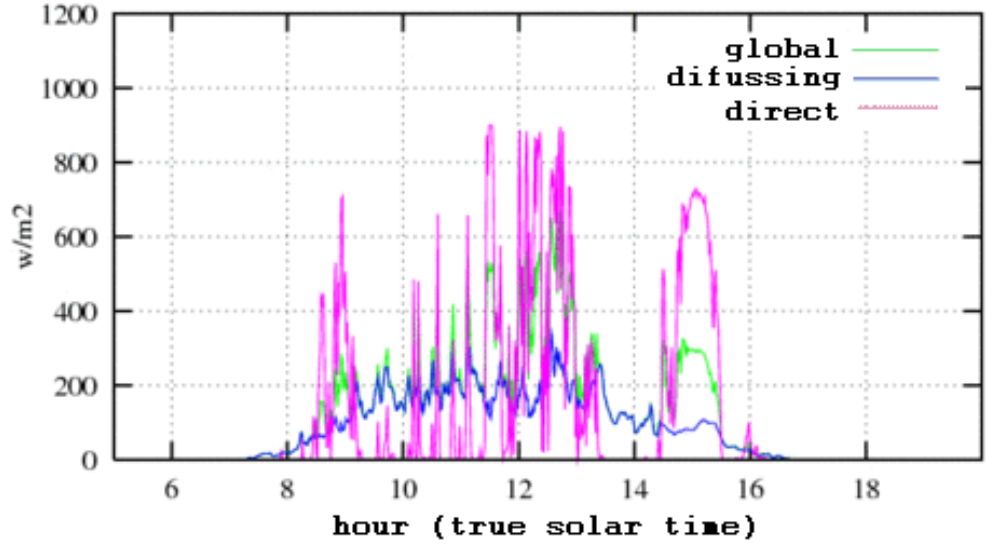

2.5. Analysis by liquid chromatography – mass spectrometry.

Table: Repeatabilities (expressed as RSDs) achieved in the determination of chlorpromazine degradation products in two different river water samples by the applied analytical method (n=5). See section 3.2 for compound identification.

	Sample 1 RSD (%)	Sample 2 RSD (%)
DHBT MET	5.4	5.0
BZDIOL	4.8	4.2
BT SO	3.1	4.0
BT NH2	3.5	3.7
BT MET	4.0	4.5
2HP SO	4.1	3.8
2HP SO NO	3.6	3.2
PRO SO	4.2	4.2
PRO SO NO	3.6	2.8
DHP SO	4.6	5.0
CP SO	3.3	3.7
CP SO NO	3.7	2.8
2HP	4.1	4.2
2HP NO	5.3	4.8
PRO	4.6	4.2
CP NO	5.3	5.5

3.1. Degradation of chlorpromazine.

Table: Degradation of chlorpromazine in water (W1, W2, W3 samples) under non-forced conditions. Individual data of each assay.

	W1 Concentrations (μg L^{-1})			W2 Concentrations (μg L^{-1})			W3 Concentrations (μg L^{-1})	
Week	Assay 1	Assay 2	Assay 3	Assay 1	Assay 2	Assay 3	Assay 1	Assay 2
0	2.00	2.01	2.03	2.00	2.03	2.04	1.98	1.99
1	0.51	0.58	0.60	0.75	0.78	0.93	0.65	0.62
2	0.048	0.048	0.062	0.11	0.13	0.015	0.056	0.054
3	0.025	0.033	0.031	0.033	0.040	0.072	0.032	0.040
4	0.005	0.007	0.008	0.009	0.010	0.013	0.015	0.011
R^2	0.96	0.96	0.98	0.99	0.99	0.98	0.94	0.95
k ($week^{-1}$)	1.48	1.43	1.40	1.39	1.37	1.27	1.28	1.31
$t_{1/2}$ (weeks)	0.43	0.45	0.46	0.46	0.47	0.50	0.50	0.49

R^2: Coefficient of regression of the fitting; kinetics of first-order reactions.
$t_{1/2}$: half-life time.
k: kinetic constant.

Table: Degradation of chlorpromazine in water samples at room (DARK) or 70 °C (HT) temperature without sunlight irradiation, and in quartz cuvettes under sunlight irradiation (UV sample). Individual data of each assay.

	DARK Concentrations (µg L^{-1})		HT Concentrations (µg L^{-1})			UV Concentrations (µg L^{-1})	
Week	Assay 1	Assay 2	Assay 1	Assay 2	min	Assay 1	Assay 2
0	1.99	2.01	2.04	2.02	0	2.01	2.01
1	1.97	1.98	1.58	1.58	60	1.12	1.11
2	1.96	1.95	1.51	1.42	115	0.76	0.77
3	1.95	1.94	1.20	1.10	180	0.22	0.20
4	1.94	1.93	1.10	0.88			
5	1.93	1.92	0.88	0.81			
6	1.92	1.91	0.81	0.78			
7	1.91	1.90	0.72	0.70			
8	1.90	1.89	0.59	0.62			
9	1.89	1.88	0.53	0.52			
10	1.88	1.87	0.49	0.47			
11	1.86	1.85	--	--			
12	1.85	1.83	--	--			
13	1.84	1.81	--	--			
14	1.83	1.80	--	--			
15	1.81	1.79	--	--			
16	1.79	1.78	--	--			
17	1.77	1.76	--	--			
18	1.75	1.74	--	--			
19	1.72	1.73	--	--			
20	1.70	1.71	--	--			
R^2	0.97	0.99	0.99	0.97	R^2	0.95	0.94
k ($week^{-1}$)	0.0072	0.0074	0.14	0.14	k (min^{-1})	0.012	0.012
$t_{1/2}$ (weeks)	88.5	86.0	4.49	4.60	$t_{1/2}$ (min)	53.7	53.3

R^2: Coefficient of regression of the fitting; kinetics of first-order reactions.
$t_{1/2}$: half-life time.
k: kinetic constant.
-- : without data.

3.2. Detection and identification of degradation products.

3.2.1 MS/MS spectra: General commentaries and fragmentation patterns.

MS spectra were simple, the corresponding protonated molecular ion $[M+H]^+$ was the base peak and fragmentation was not observed. Structural information about the detected chlorpromazine-related compounds was obtained by MS/MS experiments. The corresponding $[M+H]^+$ ion was isolated and then fragmented by collision induced dissociation with nitrogen gas at different collision energies. The molecular formulae of the most abundant fragment-ions in each MS/MS spectrum, and some of the lesser abundant ones, were established and the composition differences with respect to the precursor ion were obtained in order to propose a tentative structure for the unknown compound.

Many fragmentations affected to the amine alkyl chain bonded to the phenothiazine; the neutral losses C_2H_7N, $C_4H_{11}N$, $C_5H_{12}N$ and others were frequent. The generally abundant fragment ion at m/z 86 ($C_5H_{12}N^+$) was characteristic of the amine alkyl chain, too. The presence of an N-oxide group in the triaalkylamine moiety of the structure was easily distinguished in the MS/MS spectra by the formation of an ion at m/z 102 ($C_5H_{12}NO^+$) instead of the $C_5H_{12}N^+$ ion, characteristic of the promazine (phenothiazine bonded to the amine alkyl chain).

However, the fragment $C_5H_{12}NO^+$ could also be assigned to another possible moiety; it is usual that the methyl group in terminal position is oxidized, microbial way, to a primary alcohol. In order to discard this last possibility a water aliquot with chlorpromazine residues was treated with H_2O_2 and extracted. The formation of sulfoxides was relatively fast whereas the production of N-oxides was slower, after two days it was verified that peak area of the degradation products identified as N-oxides increased. As the retention times of these compounds were not modified and any more susceptible chromatographic peak was found it was deduced that the assignment was likely correct.

The electron configuration of the molecule can be deduced from the number of rings and double bonds (RDB) calculated with the ion formula. So, some radical ions were also ascertained in the spectra. Many times, these radical ions were due to the presence of a sulfoxide group in the structure in whose case these fragment ions were generated by the loss of oxygen and a terminal methyl group or hydrogen atom from the amine. The simultaneous losses of oxygen from the sulfoxide group and alkyl amines from the amine alkyl chain were often, too. The loss of SO together with other cleavages was also observed, the exclusive loss of SO generated fragment ions of low abundance, below 1%. Furthermore, the loss of Cl or OH in the structures of many degradation products also provided radical ions.

In advanced stages of fragmentation the MS/MS spectra of the transformation products that kept the phenothiazine structure showed several ions related to the aromatic ring, such as m/z 117 ($C_9H_9^+$), 133 ($C_9H_9O^+$), 149 ($C_9H_9O_2^+$) and 167 ($C_9H_8ClO^+$), which were presumably formed by rearrangement reactions and indicated the presence of oxygen.

The elemental composition and number of RDB of diverse structures suggest the formation of benzo[1,4]thiazin-6-ol derivatives. As in previous cases, the positions of the hydroxyl substituent and alkyl chain cannot be known exactly from the spectrum but it is assumed that the initial configuration of the phenothiazine is kept.

On the other hand, some rules can be inferred as regards the chromatographic behaviour of the compounds that kept the phenothiazine structure. The introduction of a sulfoxide group in the molecule implies a decrease of the retention time with respect to the non-oxidized compound whereas the n-oxides have a retention time slightly higher in comparison with those compounds for which the tertiary amine was preserved.

3.2.2 Identification of degradation products. Detailed discussion and MS/MS spectra.

The fragment-ions in the MS/MS spectrum of CP ($C_{17}H_{20}ClN_2S^+$, Fig. SM1) arise mainly from the cleavage of the amine alkyl chain bonded to the phenothiazine due to losses of alkylamines such as C_2H_7N, $C_4H_{11}N$ or $C_5H_{12}N$. The most intense ion at m/z 86 ($C_5H_{12}N^+$) was characteristic of the amine alkyl chain. Some radical ions were also ascertained in the spectrum and attributed to the loss of chlorine.

CP SO ($C_{17}H_{20}ClN_2OS^+$) was identified as the sulfoxide derivative of CP (Fig. SM2). The alkyl chain was intact as deduced from the observation of the $C_5H_{12}N^+$ ion and some alkylamines were lost, too. Fragments involving the loss of SO ($C_{13}H_9ClN^+$, $C_{15}H_{13}N^{\bullet+}$, $C_{15}H_{12}ClN_2^+$) confirmed the identification. Radical ions attributed to the loss of oxygen and a terminal methyl group ($C_{16}H_{17}ClN_2S^{\bullet+}$), or hydrogen ($C_{17}H_{19}ClN_2S^{\bullet+}$), from the amine were associated to the existence of a sulfoxide group in the molecule. It is required to point out that in various degradation products the structure postulated for some fragments could be slightly modified and match properly the elemental composition of the ion. For instance, in the fragments at m/z 273 and 290 of the CP SO MS/MS spectrum the position of the double bond in the alkyl chain could be different; in these cases, when a comparison is feasible, the criterion followed in the reference "Trautwein and Kummerer, 2012" has been adopted to allow a better comparison with the reported spectra.

The elemental composition of 2HP ($C_{17}H_{20}N_2OS^+$, Fig. SM3) differed from that of CP in the loss of chlorine and the addition of hydroxyl. 2HP was identified as 2-hydroxypromazine, a primary degradation product of CP in which the chlorine atom from the aromatic ring is substituted for a hydroxyl group. The interpretation of the fragments agrees with this assumption, and the general fragmentation pattern exposed for the above-mentioned promazine derivatives is repeated: loss of alkylamines and notable $C_5H_{12}N^+$ ion.

2HP SO ($C_{17}H_{21}N_2O_2S^+$, Fig. SM4) was identified as 2-hydroxypromazine sulfoxide owing to the formation of radical ions similar to those observed for CP SO. The molecular formula of PRO ($C_{17}H_{20}N_2S^+$, Fig. SM5) indicated the substitution of the chlorine atom of CP for a hydrogen atom while PRO SO ($C_{17}H_{21}N_2O_2S^+$, Fig. SM6) was identified as the corresponding S-oxidation product of PRO. The fragmentation patterns for all these compounds are similar to those exposed. It must be noted that the introduction of oxygen in the molecule gives MS/MS spectra with more profuse fragmentation although this aspect is also depending on the intensity of the chromatographic peaks. Otherwise, in advanced stages of fragmentation, the MS/MS spectra of the oxygenated transformation products show several ions related to the aromatic ring, such as 117 ($C_9H_9^+$), 133 ($C_9H_9O^+$), 149 ($C_9H_9O_2^+$) and 167 ($C_9H_8ClO^+$), which are presumably formed by rearrangement reactions that involve the oxygen atom.

As regards the elucidation of DHP SO ($C_{17}H_{21}N_2O_3S^+$, Fig. SM7), the molecular formula and the interpreted fragment-ions suggest that it was a dihydroxylated compound. In addition, the number of RDB of the protonated molecular ion was kept unchanged as happens for the above-described compounds in which the phenothiazine moiety is unaltered. As it can be seen in the

spectrum the elemental composition of the fragment at m/z 244 differs in CO with respect to ion at m/z 216, and the composition of this later also varies in CO in relation to ion at m/z 188; the loss of CO from a phenolic group is frequent. Assuming that this compound derives from 2HP SO the position of the new hydroxyl group in the structure could not be reliably assigned. Nevertheless, it is supposed that each hydroxyl is bonded in different benzene rings because the loss of H_2O, usual for adjacent diols, has not been observed. Moreover, assuming that DHP SO is originated from a photochemistry process involving free hydroxyl radicals, the ortho (C1 and C8) and para (C3 and C6) positions related to the phenylamine group are more prone to hydroxylation.

The structure of CP SO NO ($C_{17}H_{20}ClN_2O_2S^+$, Fig. SM8) maintained the chlorine atom and had two additional oxygens compared with the CP composition; it has been postulated as chlorpromazine sulfoxide N-oxide. The ion at m/z 86 ($C_5H_{12}N^+$) is not present in the spectra where is now detected an ion at m/z 102 ($C_5H_{12}NO^+$), which was attributed to a cleavage in the alkyl chain bonded to the N-oxide, similar to the former. The presence of a sulfoxide group in the molecule was denoted by the loss of oxygen or SO in some fragmentations.

The structures of the N-oxides 2HP SO NO ($C_{17}H_{21}N_2O_3S^+$, Fig. SM9), PRO SO NO ($C_{17}H_{21}N_2O_2S^+$, Fig. SM10), 2HP NO ($C_{17}H_{21}N_2O_2S^+$, Fig. SM11) and CP NO ($C_{17}H_{20}ClN_2OS^+$, Fig. SM12) were assigned according to the stated fragmentation patterns.

The number of RDB, the observation of $C_5H_{12}N^+$ and the loss of alkylamines suggest that BT SO ($C_{13}H_{19}N_2O_2S^+$, Fig. SM13) is a N-dimethylaminopropyl-S-oxide- benzo[1,4]thiazin-6-ol derivative; the presence of sulfoxide and phenolic groups is deduced from the loss of oxygen in the interpreted fragmentations (ion at m/z 206 compared with m/z 222 ion) and the loss of CO in some cases (ions at m/z 136 and 138), respectively. The positions of the hydroxyl and alkyl chain cannot be known exactly from the spectrum but it is assumed that the initial arrangement of the parent compound is kept.

The spectra for BT MET ($C_{12}H_{17}N_2OS^+$, Fig. SM14) and BT NH2 ($C_{11}H_{15}N_2OS^+$, Fig. SM15) had scarce fragmentation but the elemental compositions, number of RDB, and the similarity of fragments and neutral losses with respect to BT SO allowed to provide structures similar to BT SO, which differ mainly in the composition of the alkylamine chain.

Several structures can be attributed to the fragmentations and molecular formula calculated for DHBT MET ($C_{12}H_{19}N_2O_3S^+$, Fig. SM16); among them, the most coherent with the previous structures is shown. It was identified as a 3,4-dihydro-N-(methylaminopropyl)-S-oxide-benzo[1,4]thiazinediol. The position of a hydroxyl group cannot be fixed with precision but the losses of H_2O (ions at m/z 162, 180 and 237) suggest the link of hydroxyl to the heterocyclic ring. In addition, the losses of CO (ions at m/z 132, 136, 162 and 180) and oxygen (see ions at m/z 237, 226 and 210) corroborate the presence of phenolic and sulfoxide groups, respectively.

Finally, the structure of the last degradation product, BZDIOL ($C_{11}H_{19}N_2O_3S^+$, Fig. SM17), was thought to correspond to an N-hydroxyaminobenzenediol in which the position of the substituents is not clear. The number of RDB calculated for its molecular formula and the observed fragment-

ions indicate the existence of a benzene ring, and the ion $C_5H_{12}N^+$ (m/z 86) suggest the whole preservation of the alkylamine chain of CP. The inclusion of a hydroxylamine group instead of considering a benzenetriol is based on the disputable fact that low and middle m/z ions seems to contain a relatively small number of oxygen atoms. As regards the positions of the hydroxyls in the aromatic ring, only one of them is unequivocally ascertained in agreement with the structure of the parent compound.

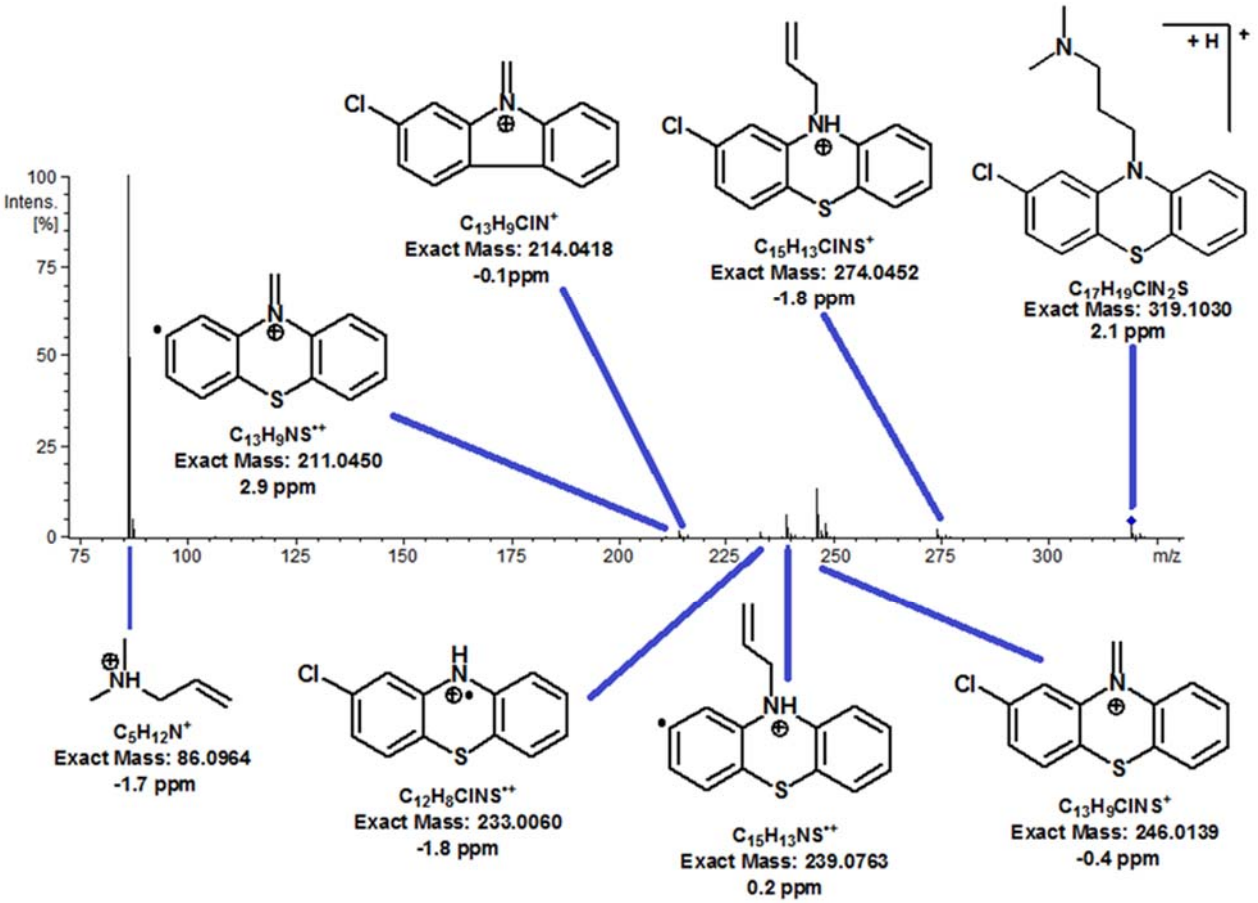

Figure SM1: MS/MS spectrum of CP. Collision energy: 32 eV. Exact mass and experimental error in its measurement

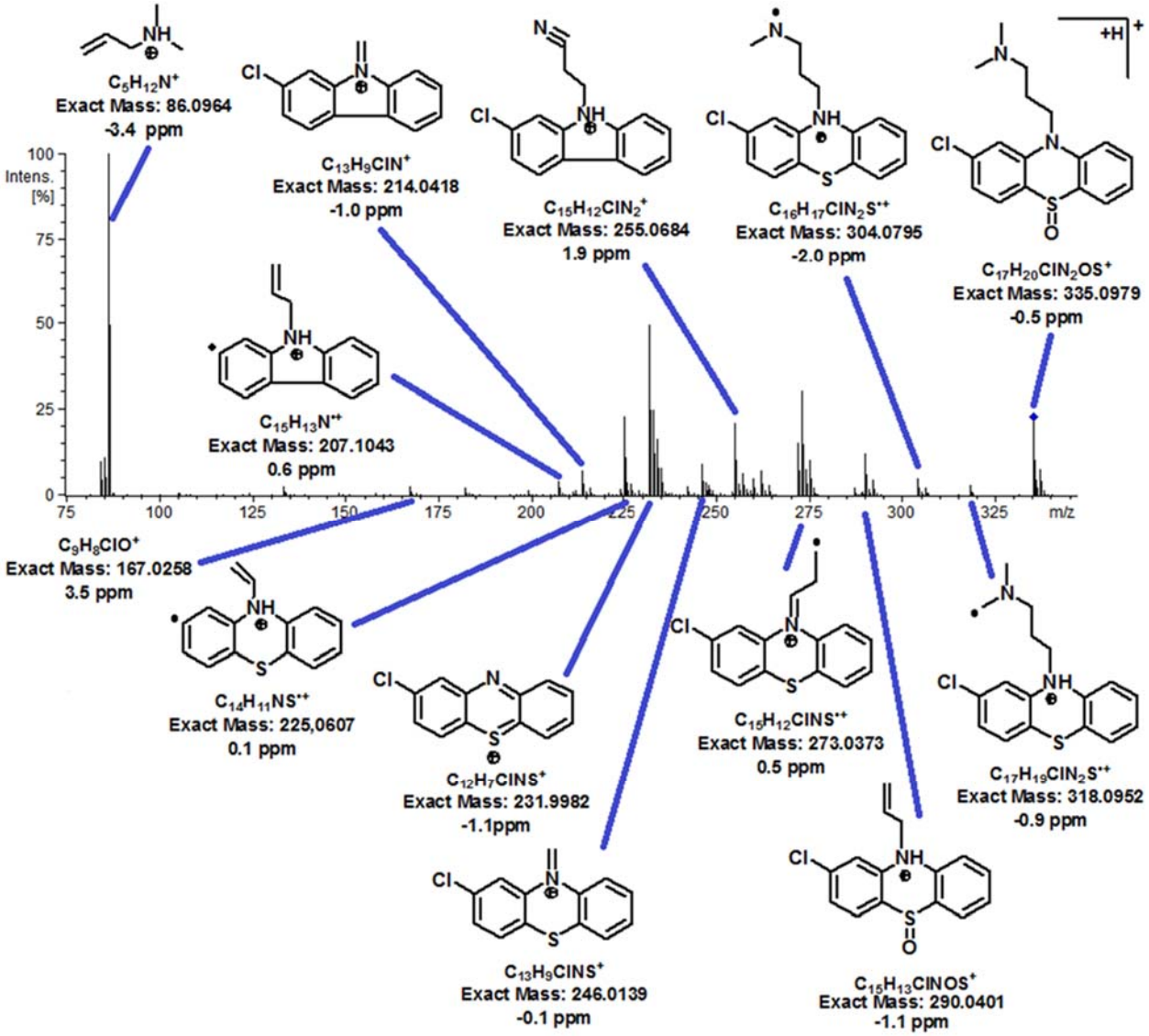

Figure SM2: MS/MS spectrum of CP SO. Collision energy: 38 eV. Exact mass and experimental error in its measurement.

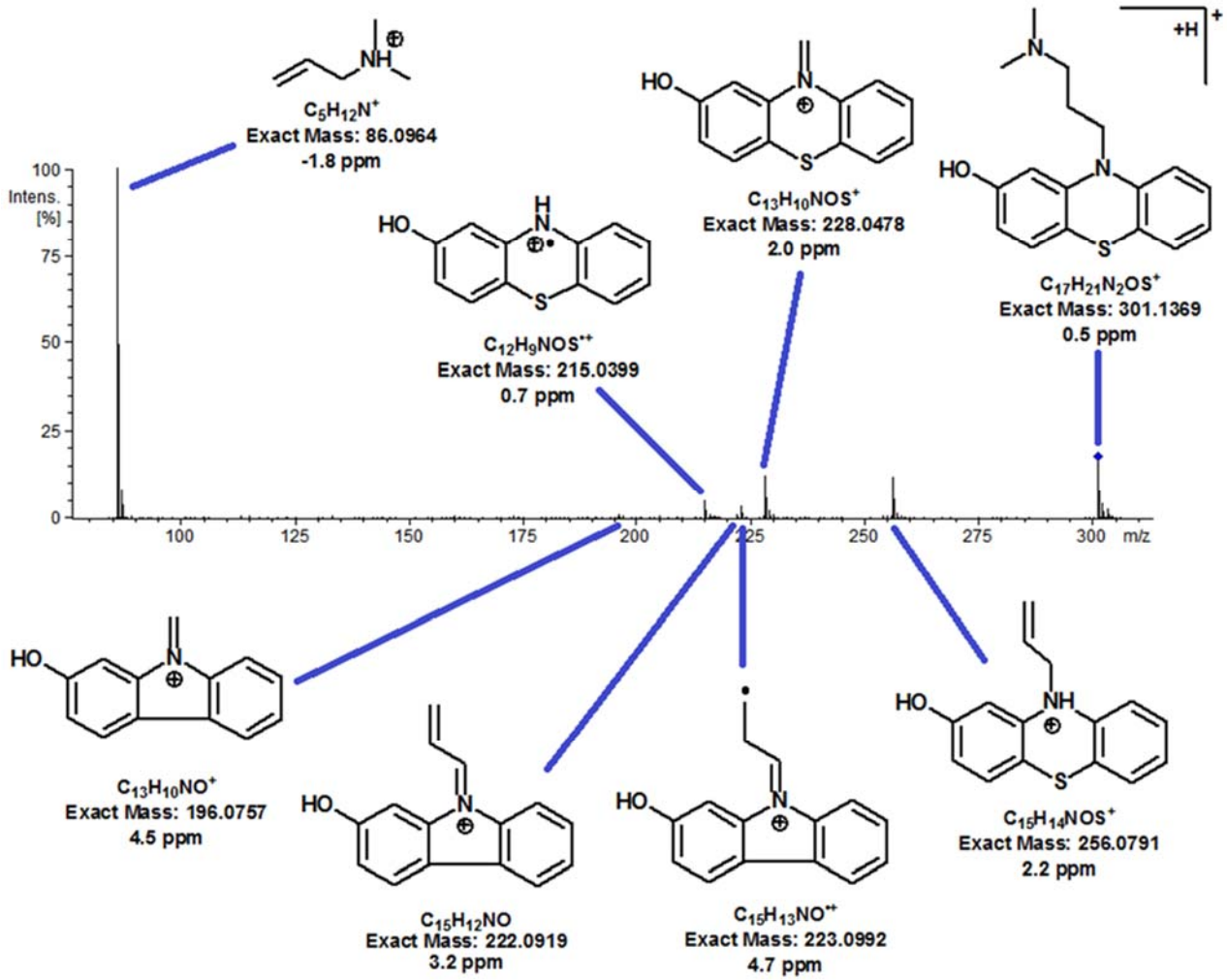

Figure SM3: MS/MS spectrum of 2HP. Collision energy: 27 eV. Exact mass and experimental error in its measurement.

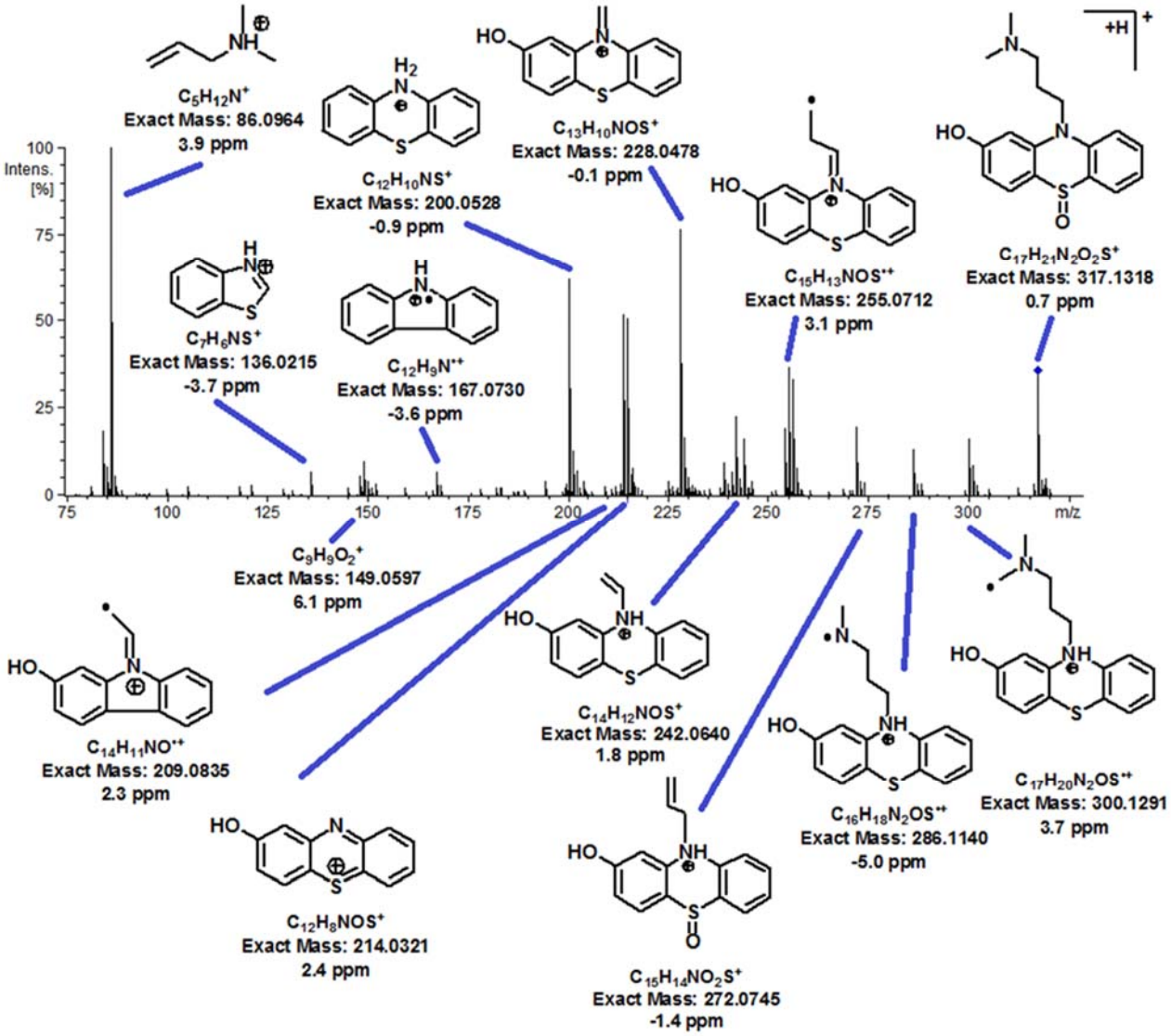

Figure SM4: MS/MS spectrum of 2HP SO. Collision energy: 35 eV. Exact mass and experimental error in its measurement.

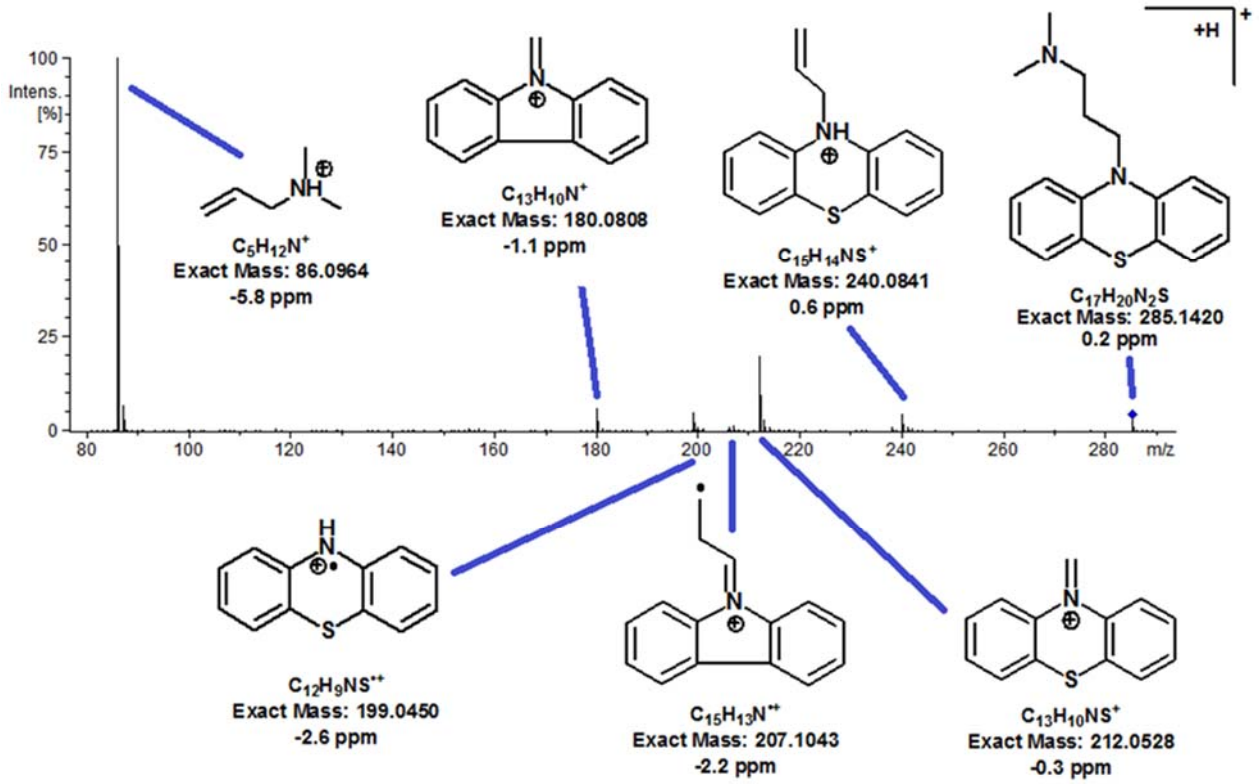

Figure SM5: MS/MS spectrum of PRO. Collision energy: 32 eV. Exact mass and experimental error in its measurement

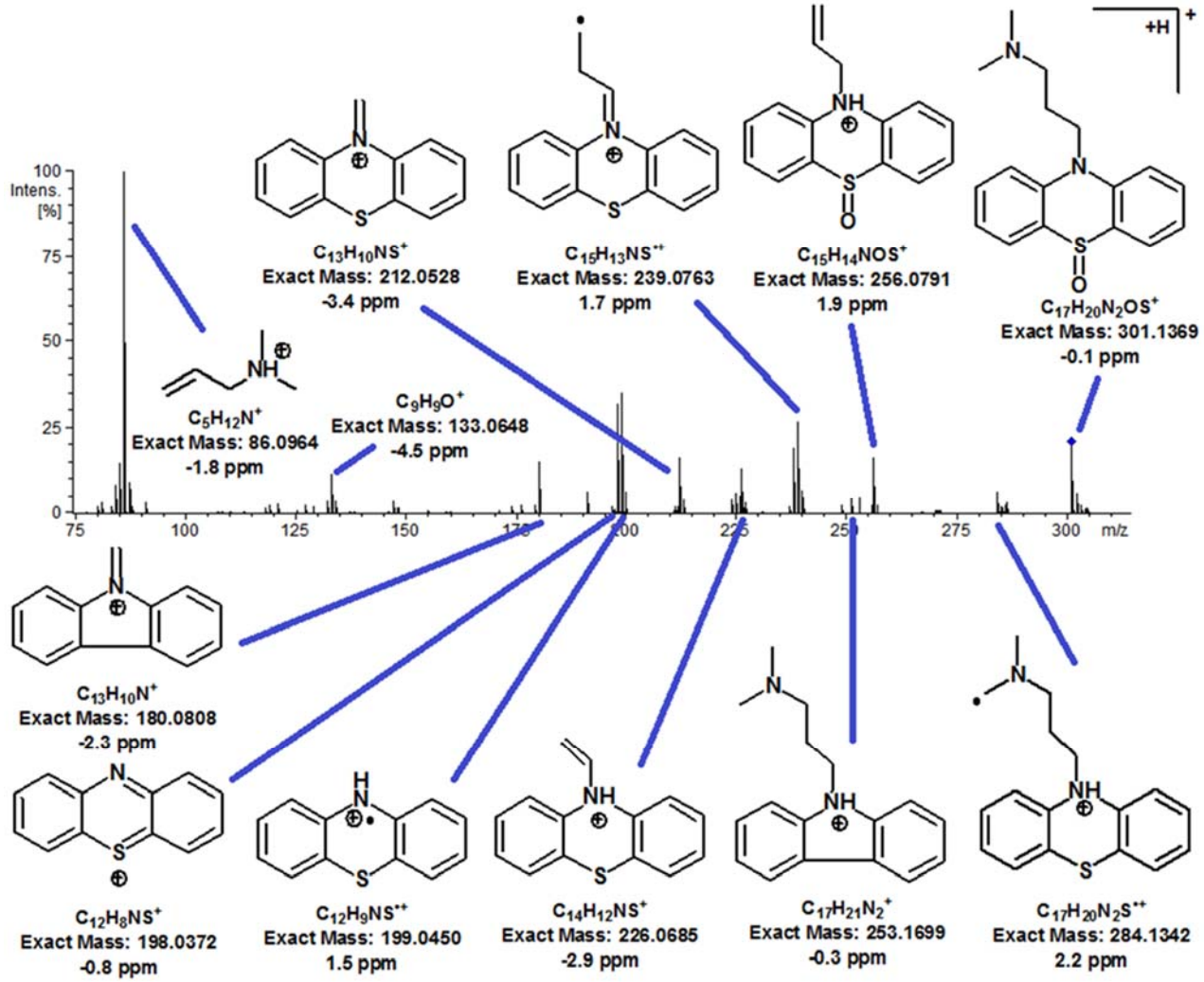

Figure SM6: MS/MS spectrum of PRO SO. Collision energy: 32 eV. Exact mass and experimental error in its measurement.

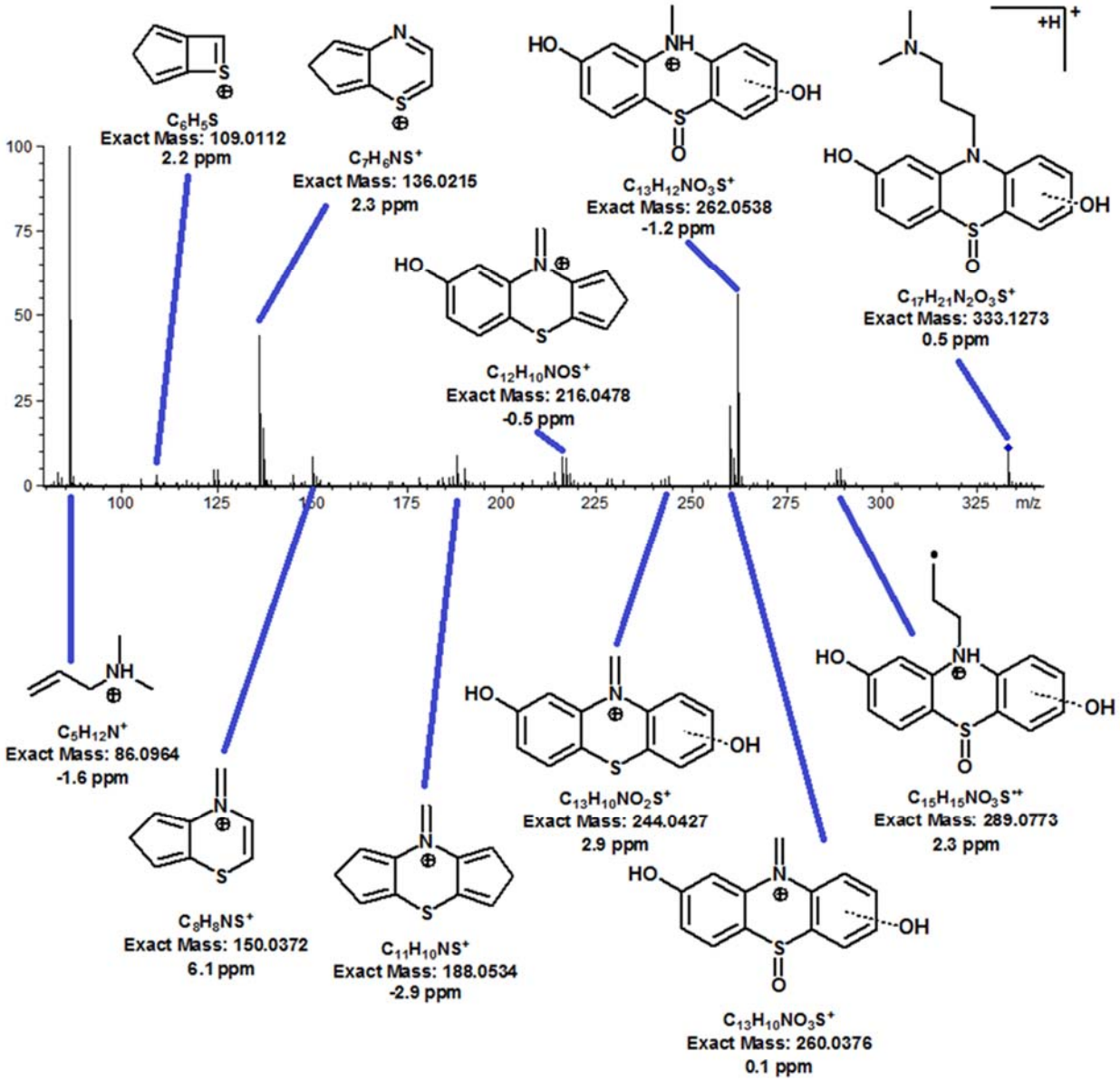

Figure SM7: MS/MS spectrum of DHP SO. Collision energy: 33 eV. Exact mass and experimental error in its measurement.

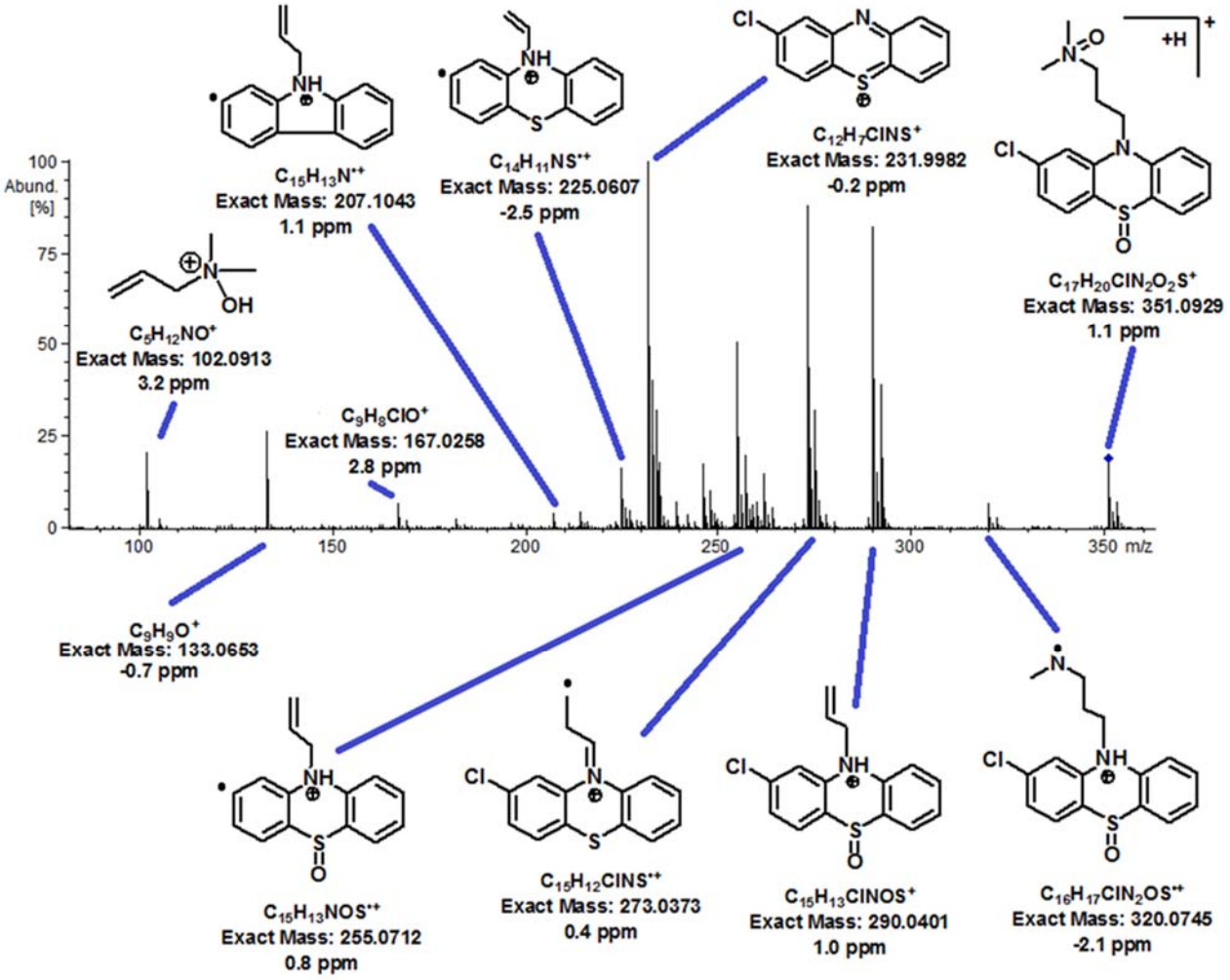

Figure SM8: MS/MS spectrum of CP SO NO. Collision energy: 35 eV. Exact mass and experimental error in its measurement.

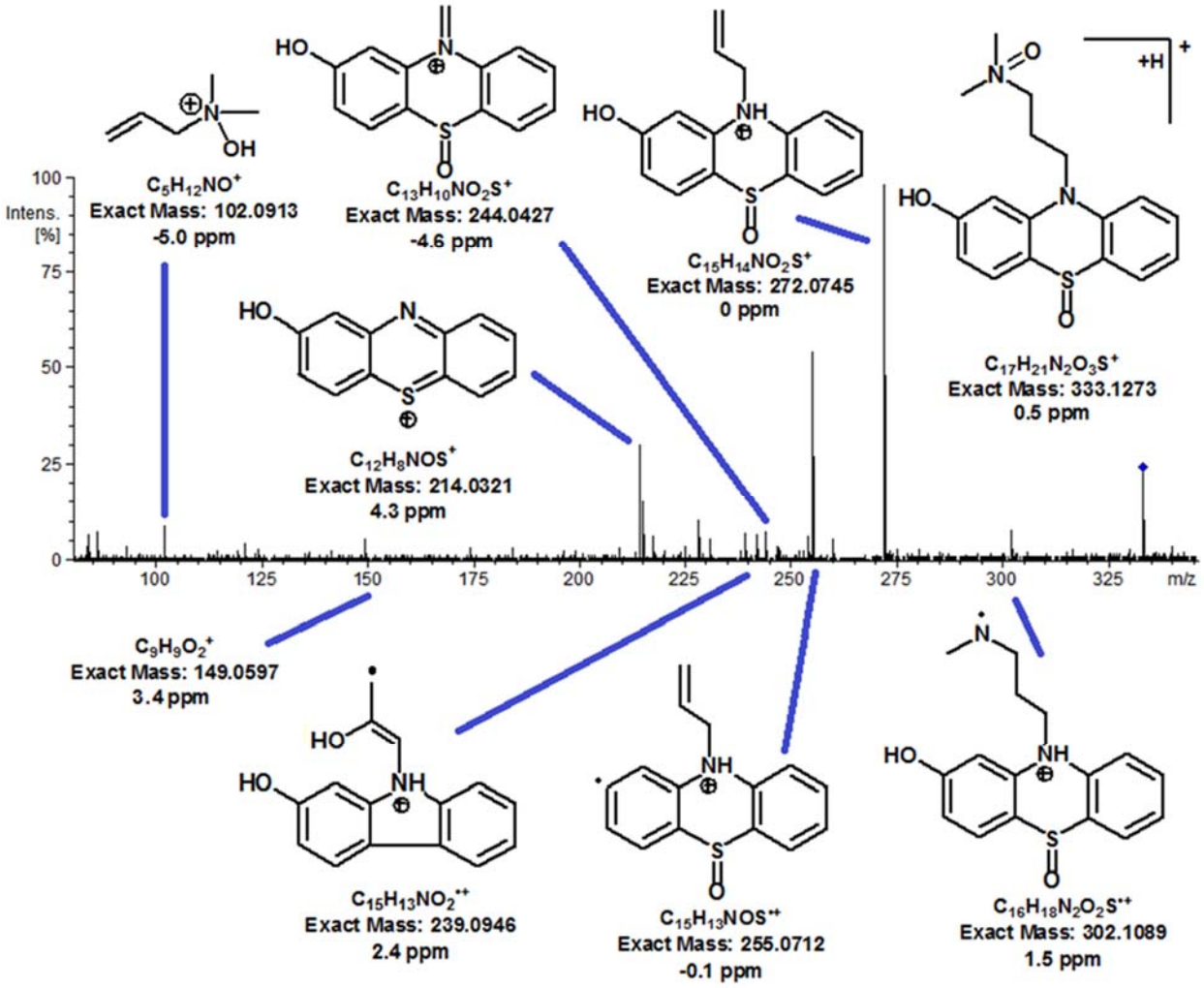

Figure SM9: MS/MS spectrum of 2HP SO NO. Collision energy: 30 eV. Exact mass and experimental error in its measurement.

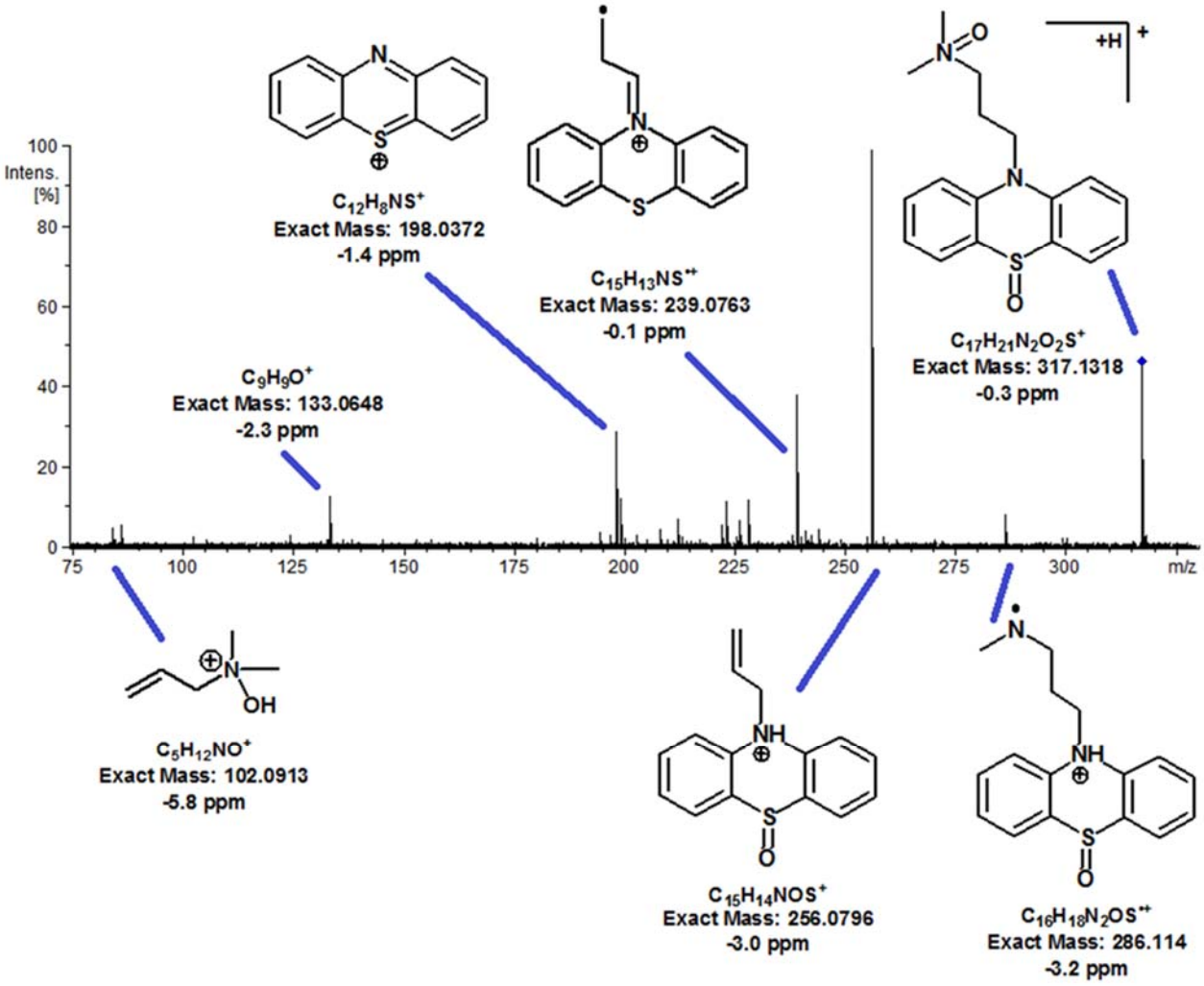

Figure SM10: MS/MS spectrum of PRO SO NO. Collision energy: 28 eV. Exact mass and experimental error in its measurement.

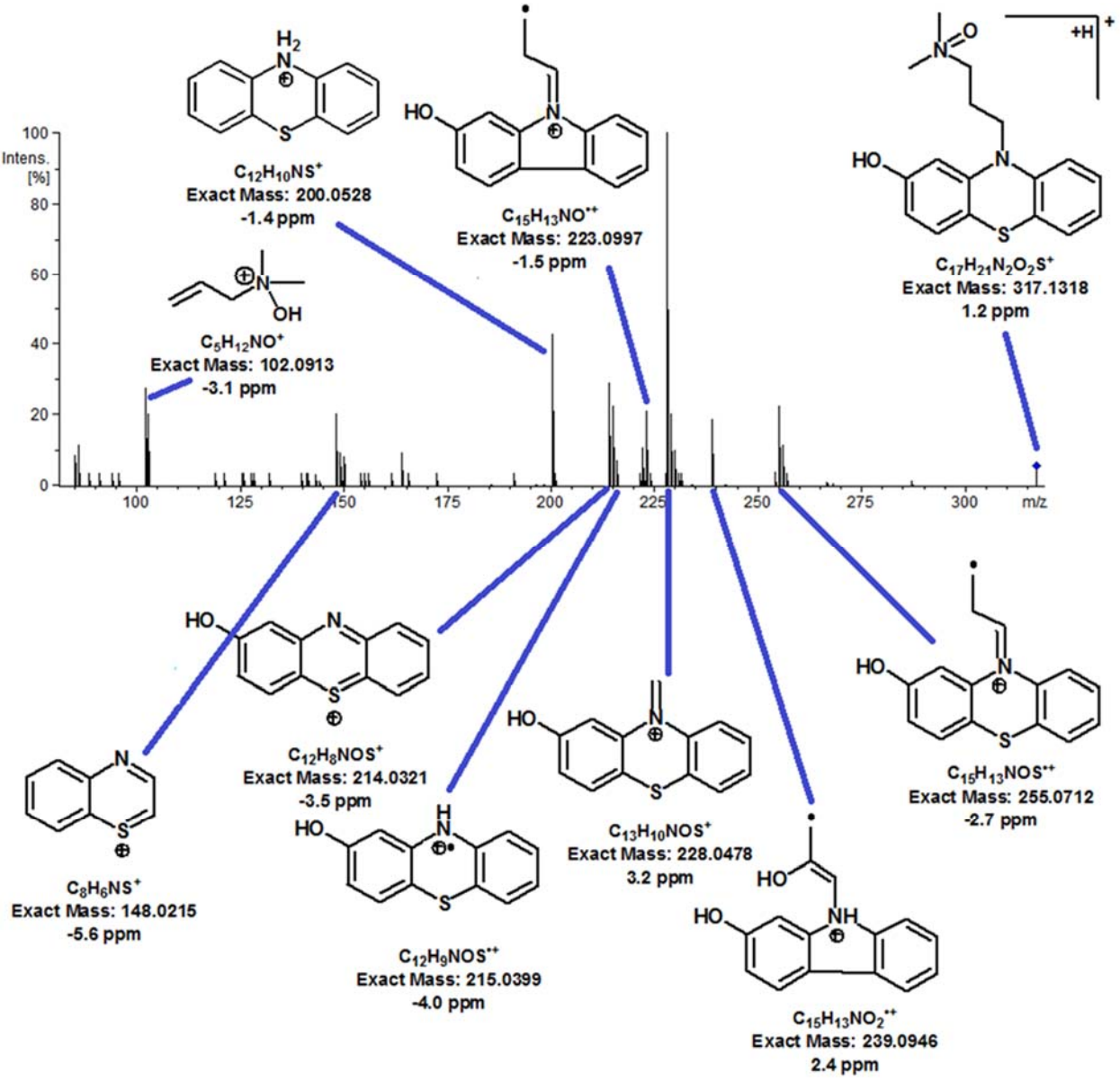

Figure SM11: MS/MS spectrum of 2HP NO. Collision energy: 32 eV. Exact mass and experimental error in its measurement

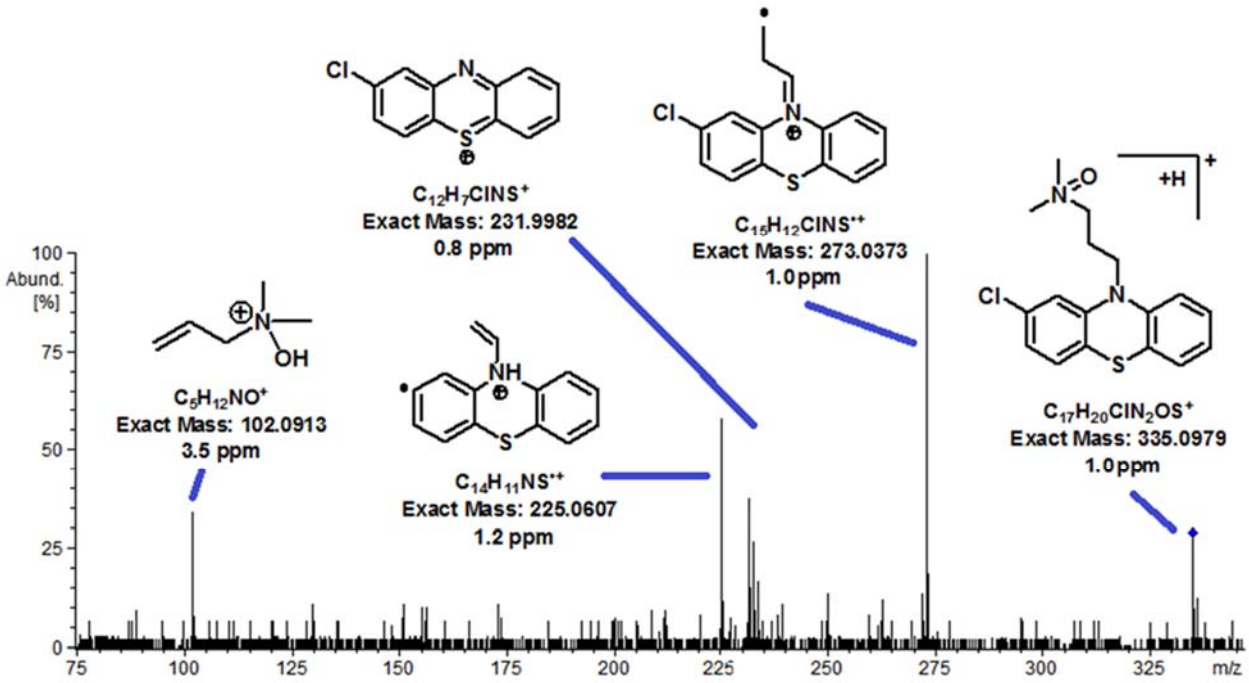

Figure SM12: MS/MS spectrum of CP NO. Collision energy: 33 eV. Exact mass and experimental error in its measurement.

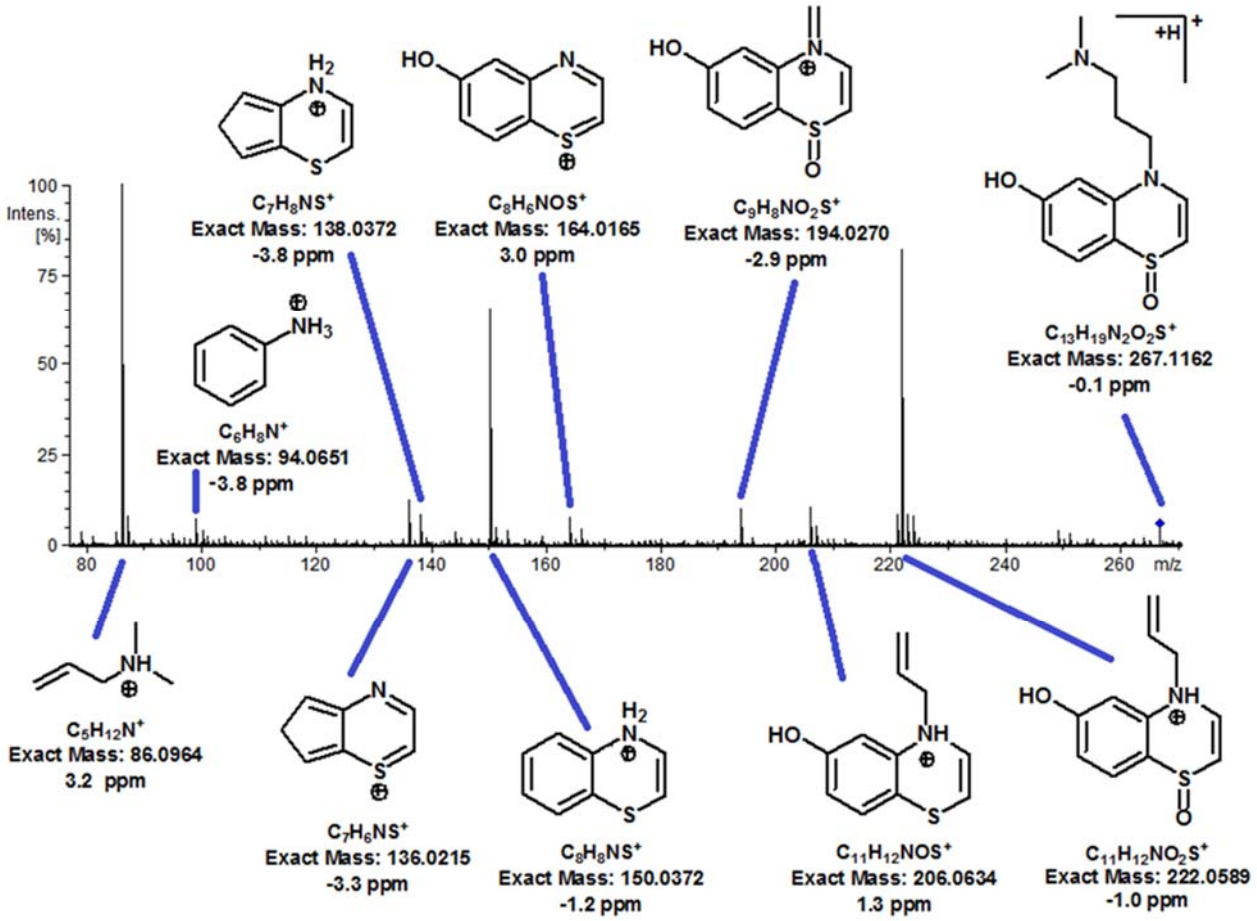

Figure SM13: MS/MS spectrum of BT SO. Collision energy: 25 eV. Exact mass and experimental error in its measurement.

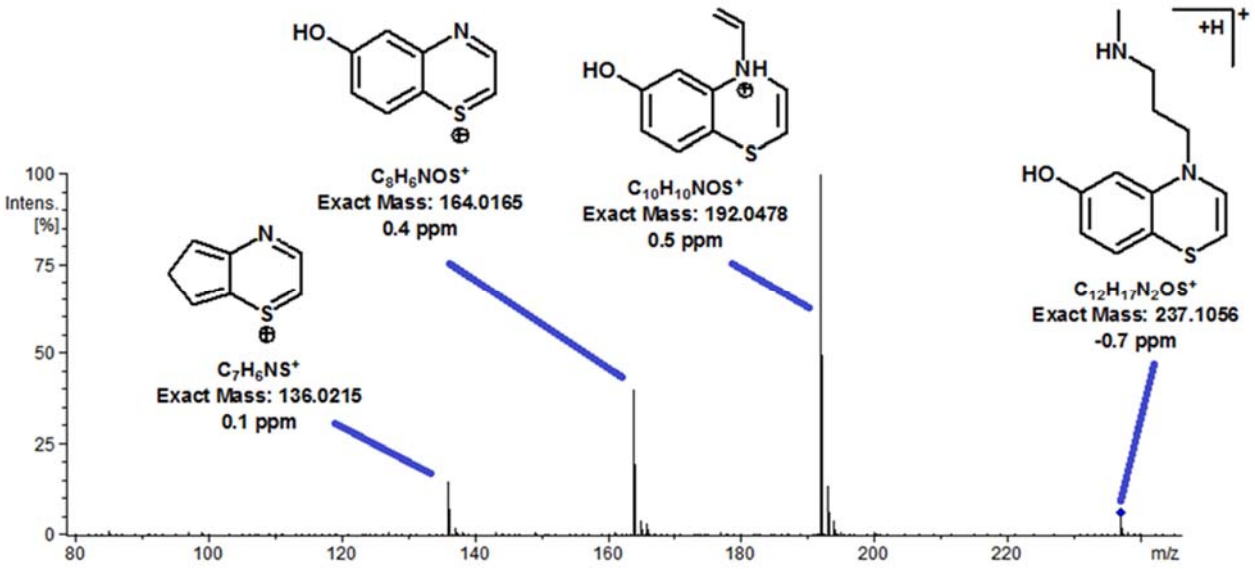

Figure SM14: MS/MS spectrum of BT MET. Collision energy: 25 eV. Exact mass and experimental error in its measurement.

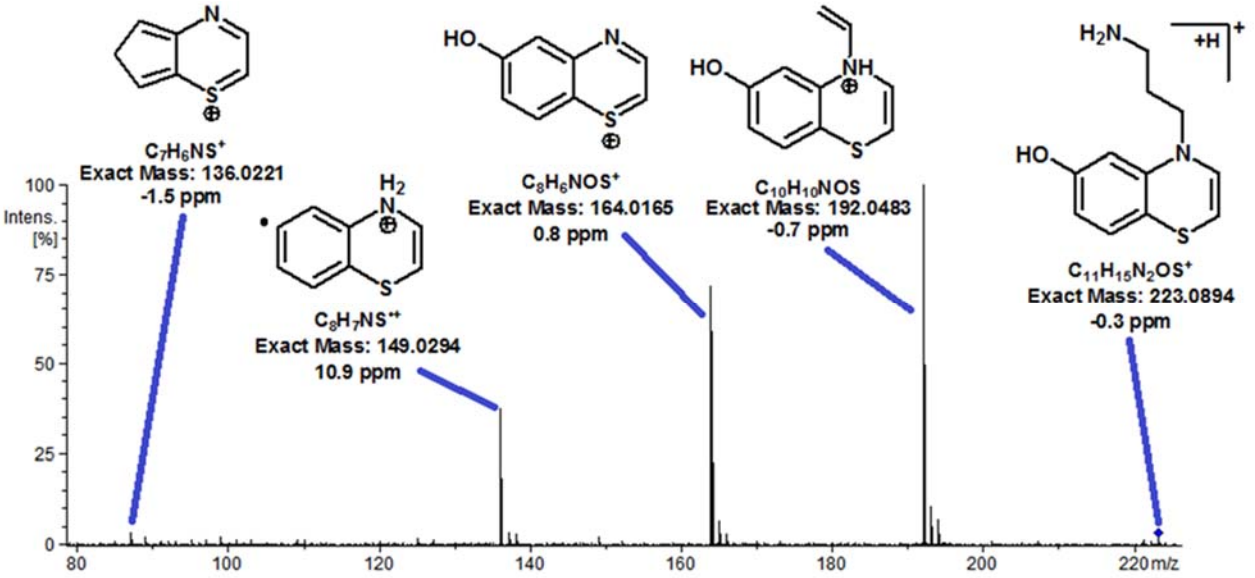

Figure SM15: MS/MS spectrum of BT NH2. Collision energy: 27 eV. Exact mass and experimental error in its measurement.

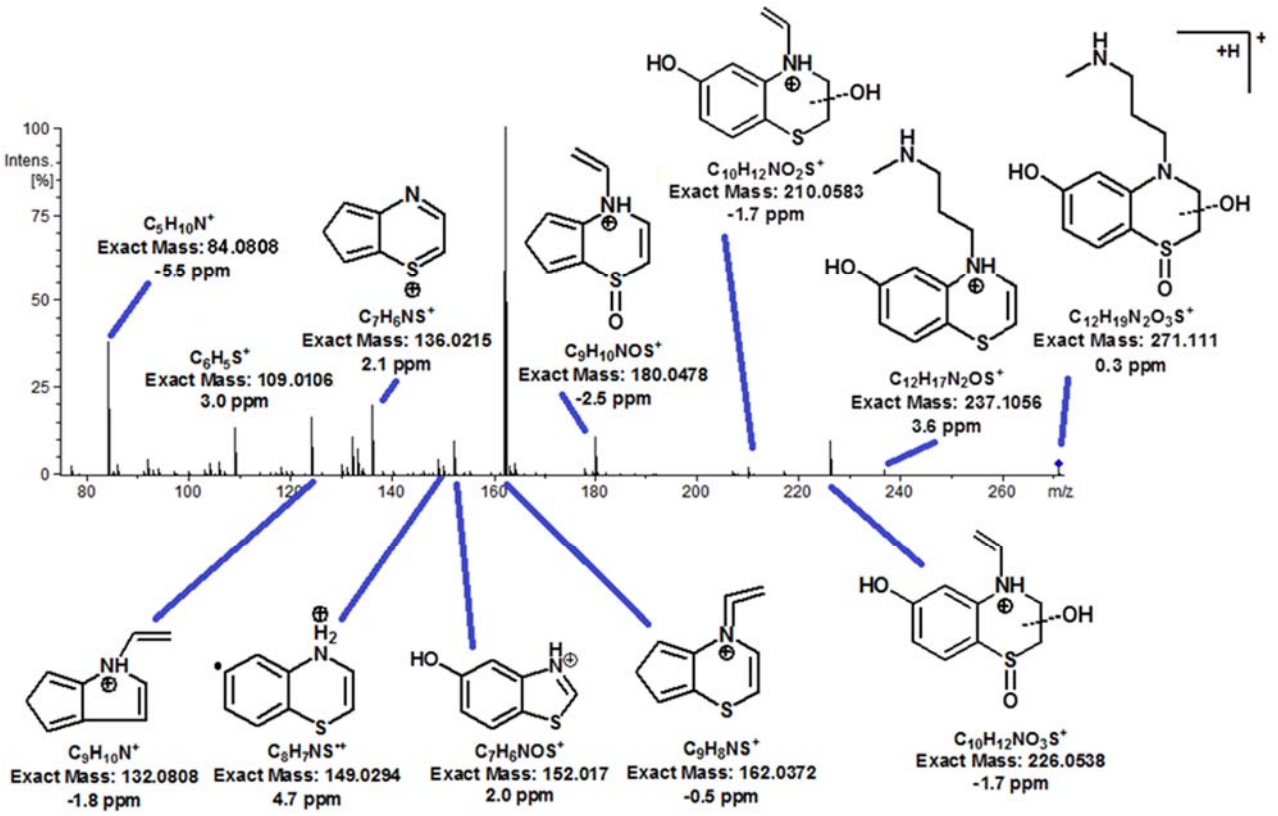

Figure SM16: MS/MS spectrum of DHBT MET. Collision energy: 28 eV. Exact mass and experimental error in its measurement.

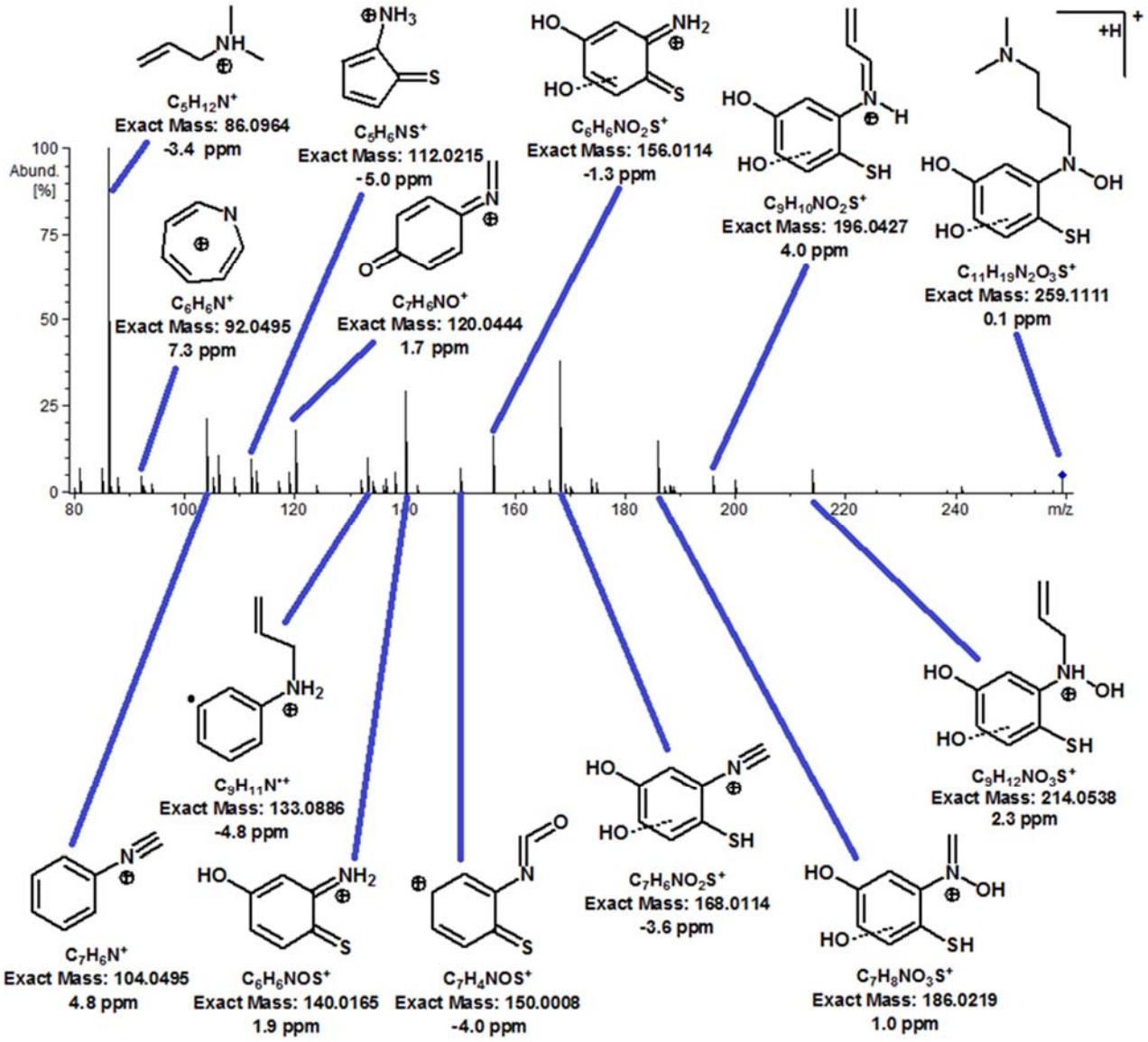

Figure SM17: MS/MS spectrum of BZDIOL. Collision energy: 32 eV. Exact mass and experimental error in its measurement.

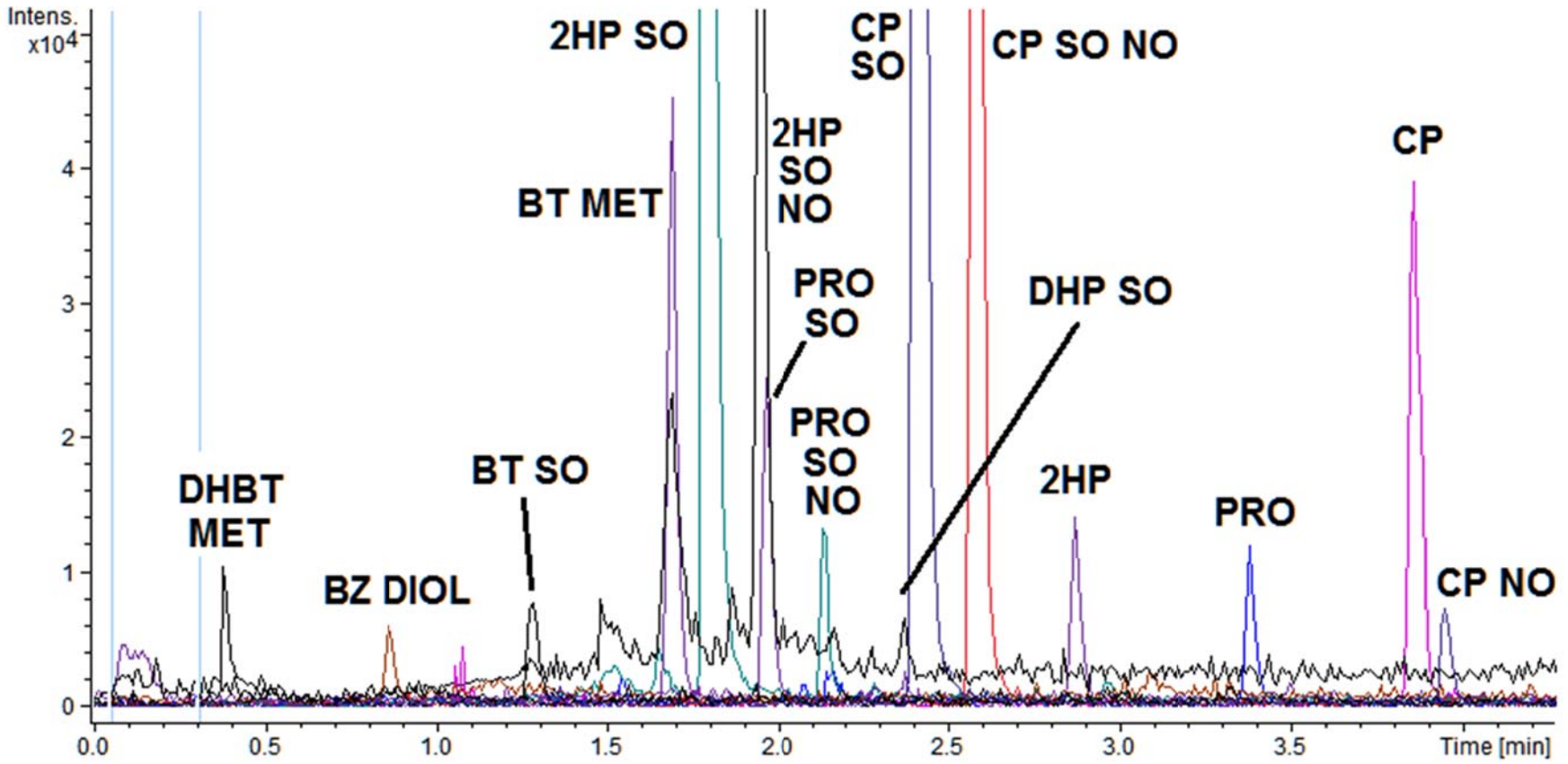

Figure (*): Chromatogram of an extract during the degradation study. Water spiked with chlorpromazine 8 weeks ago.

(*) not included in the published manuscript

3.3. *Occurrence of degradation products in river water.*

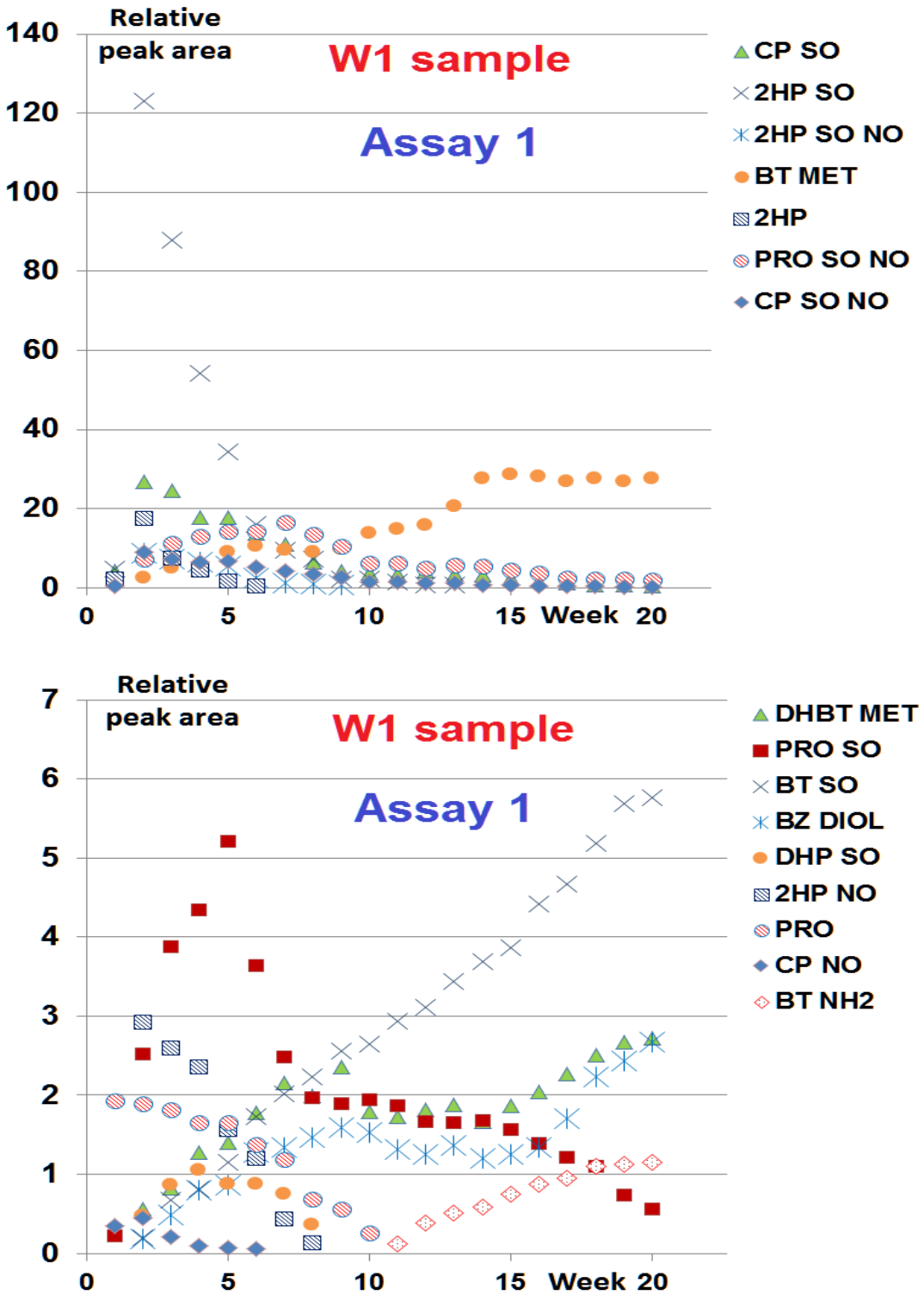

Figure: Variation of peak areas of the degradation products in the W1 sample (room conditions). Peak areas are referred to the initial peak area of CP in each experiment, to which a value of 100 was assigned. Assay 1.

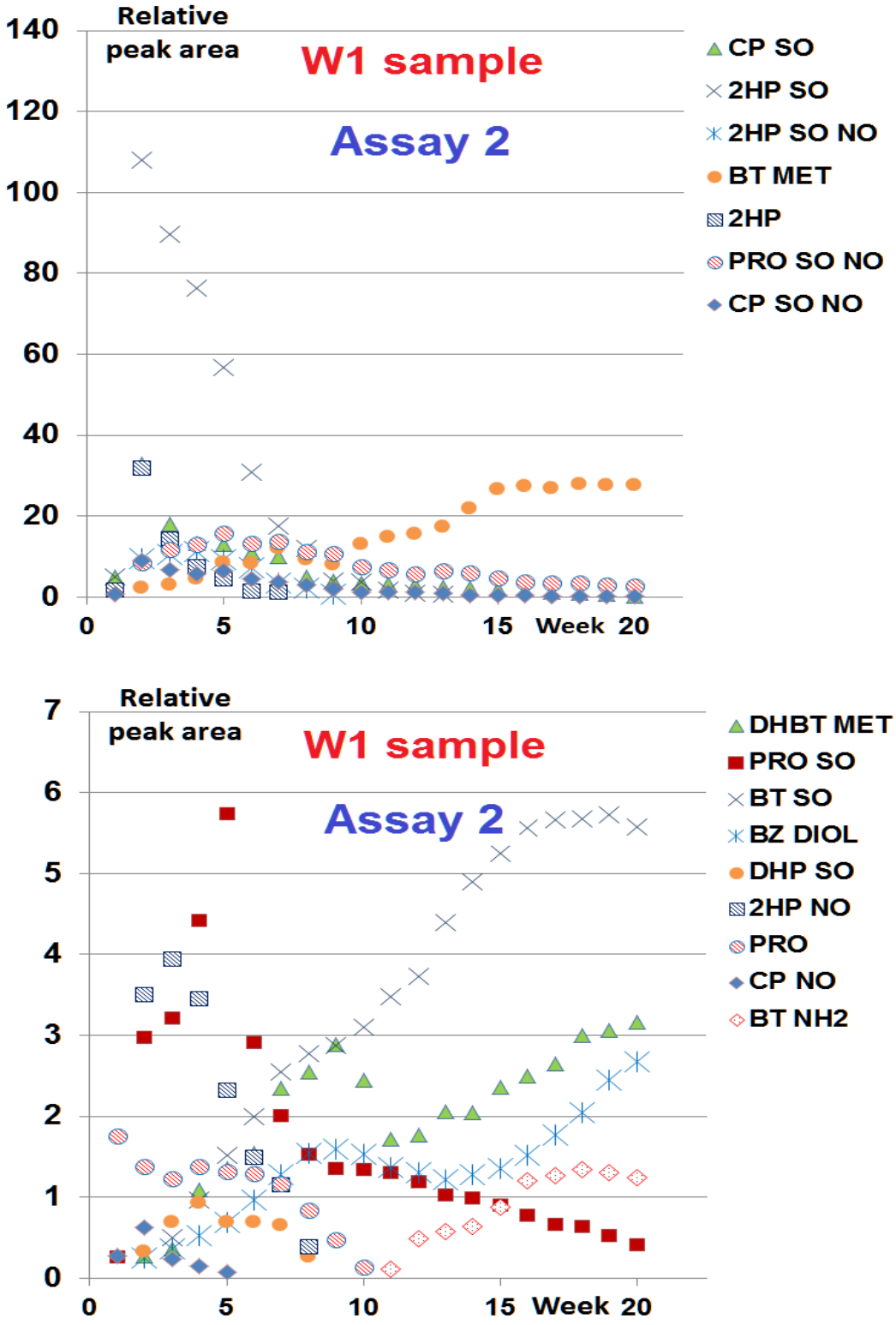

Figure: Variation of peak areas of the degradation products in the W1 sample (room conditions). Peak areas are referred to the initial peak area of CP in each experiment, to which a value of 100 was assigned. Assay 2.

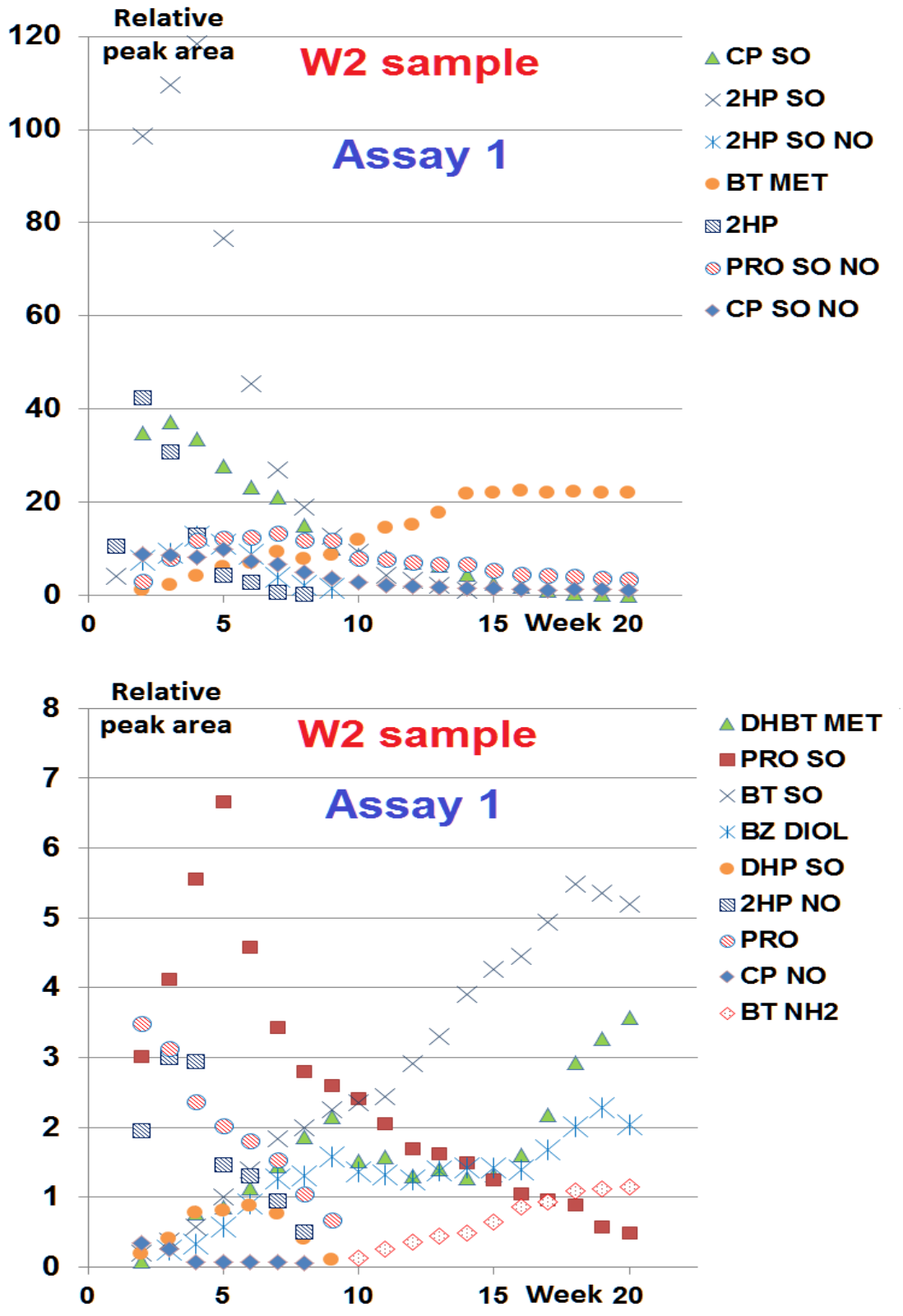

Figure: Variation of peak areas of the degradation products in the W2 sample (room conditions). Peak areas are referred to the initial peak area of CP in each experiment, to which a value of 100 was assigned. Assay 1.

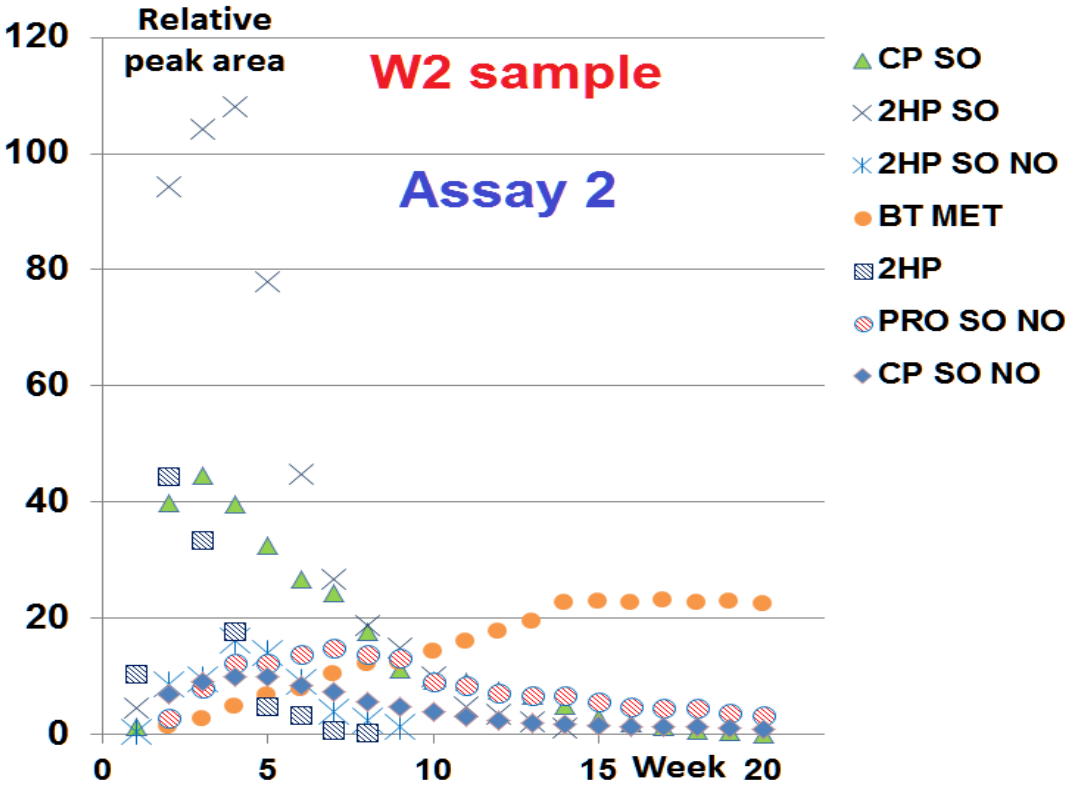

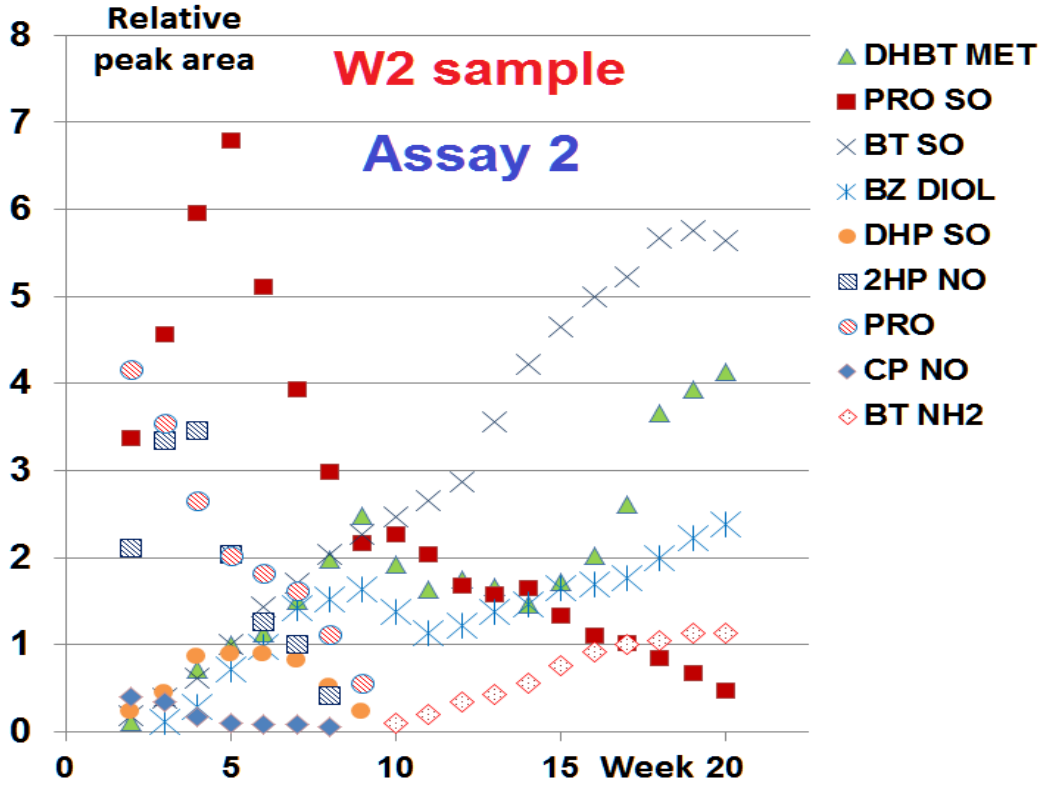

Figure: Variation of peak areas of the degradation products in the W2 sample (room conditions). Peak areas are referred to the initial peak area of CP in each experiment, to which a value of 100 was assigned. Assay 2.

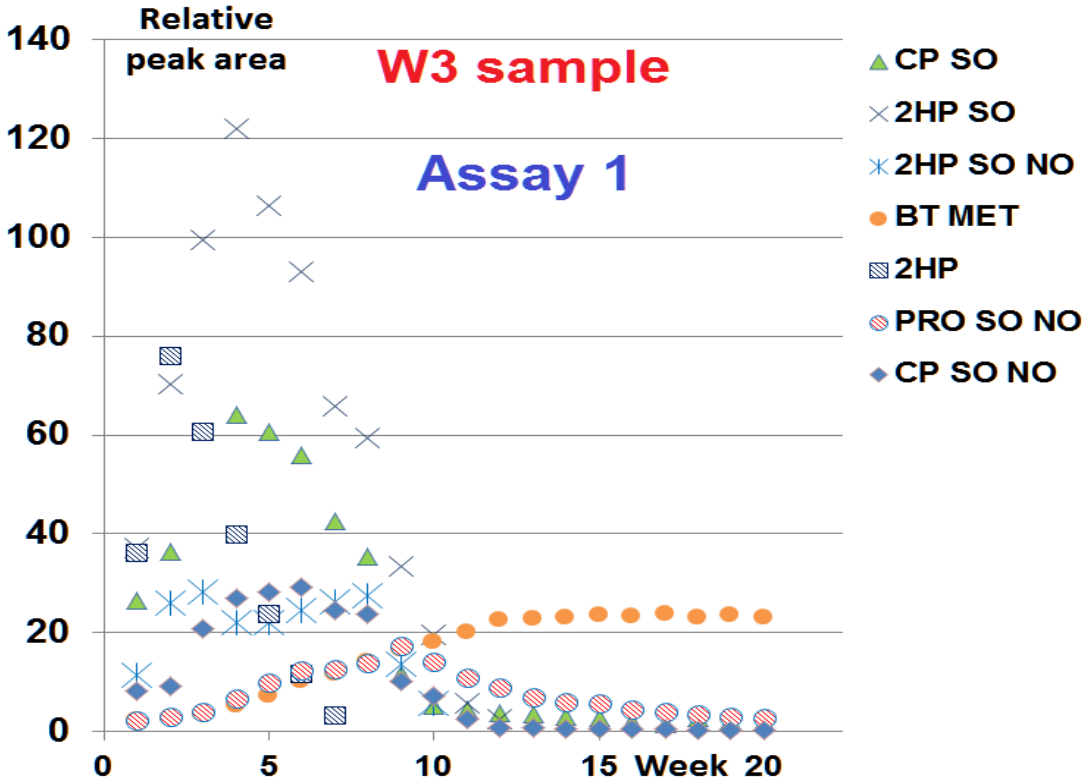

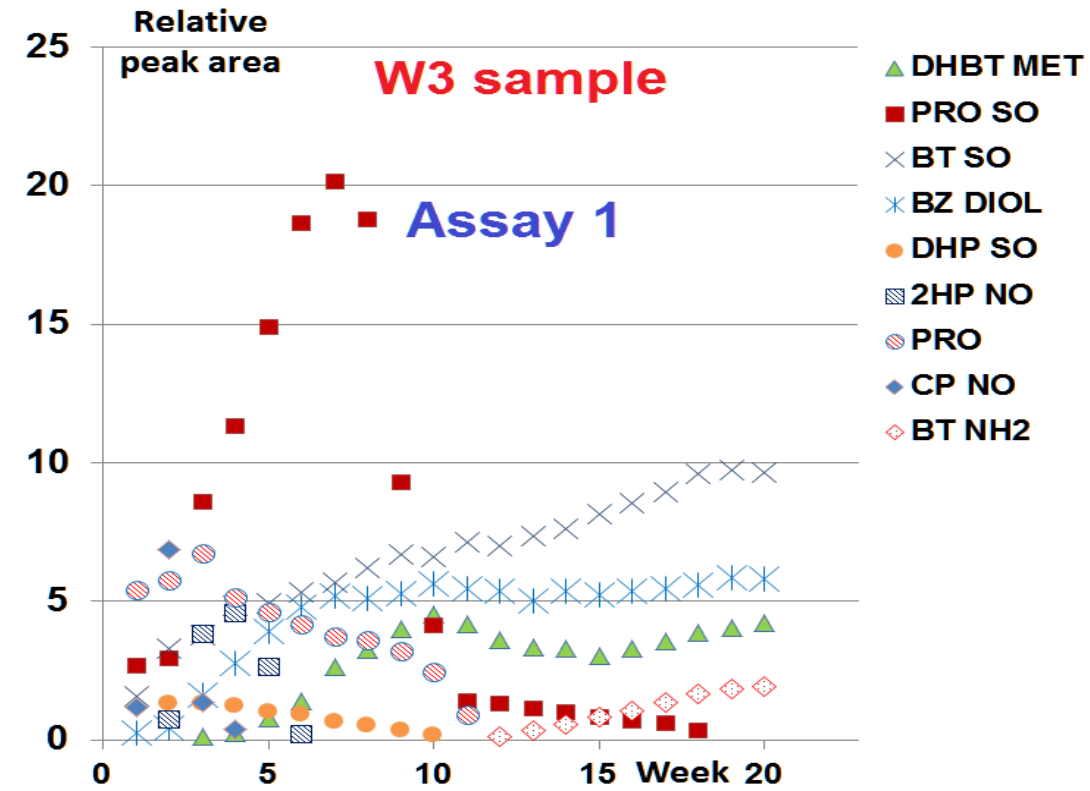

Figure: Variation of peak areas of the degradation products in the W3 sample (room conditions). Peak areas are referred to the initial peak area of CP in each experiment, to which a value of 100 was assigned. Assay 1.

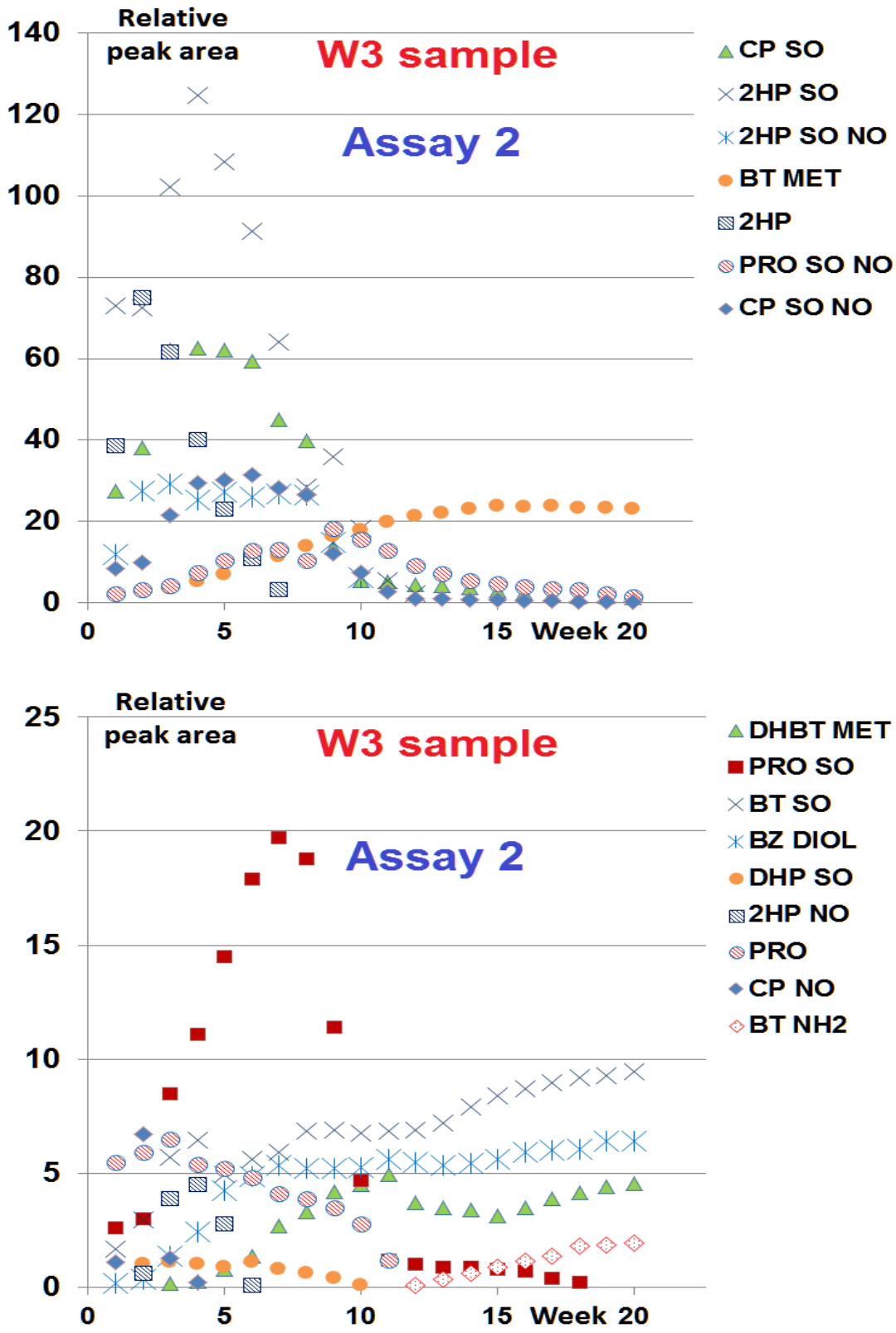

Figure: Variation of peak areas of the degradation products in the W3 sample (room conditions). Peak areas are referred to the initial peak area of CP in each experiment, to which a value of 100 was assigned. Assay 2.

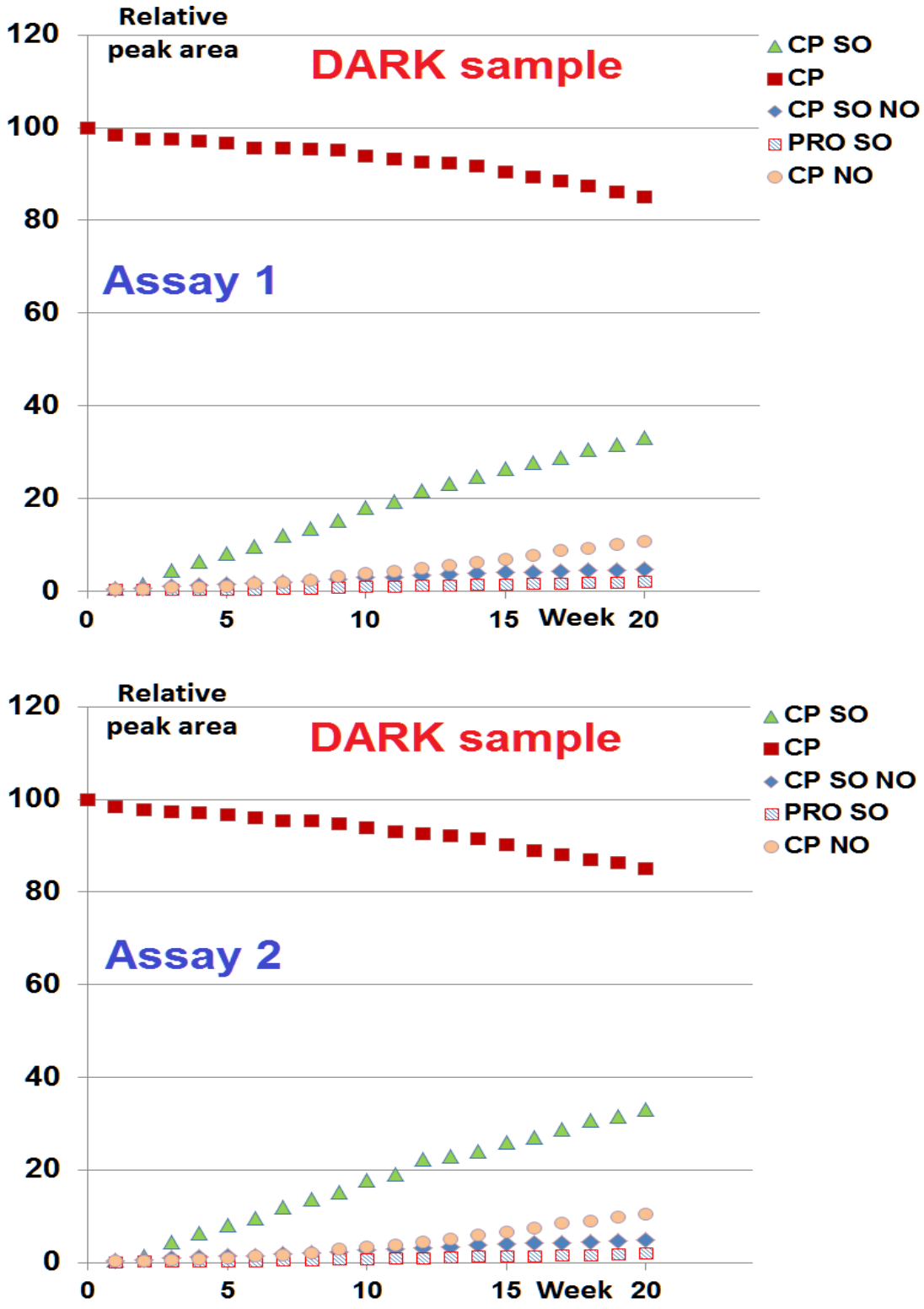

Figure: Variation of peak areas of the degradation products in the DARK sample (room conditions, protected from sunlight). Peak areas are referred to the initial peak area of CP in each experiment, to which a value of 100 was assigned. Assays 1 and 2.

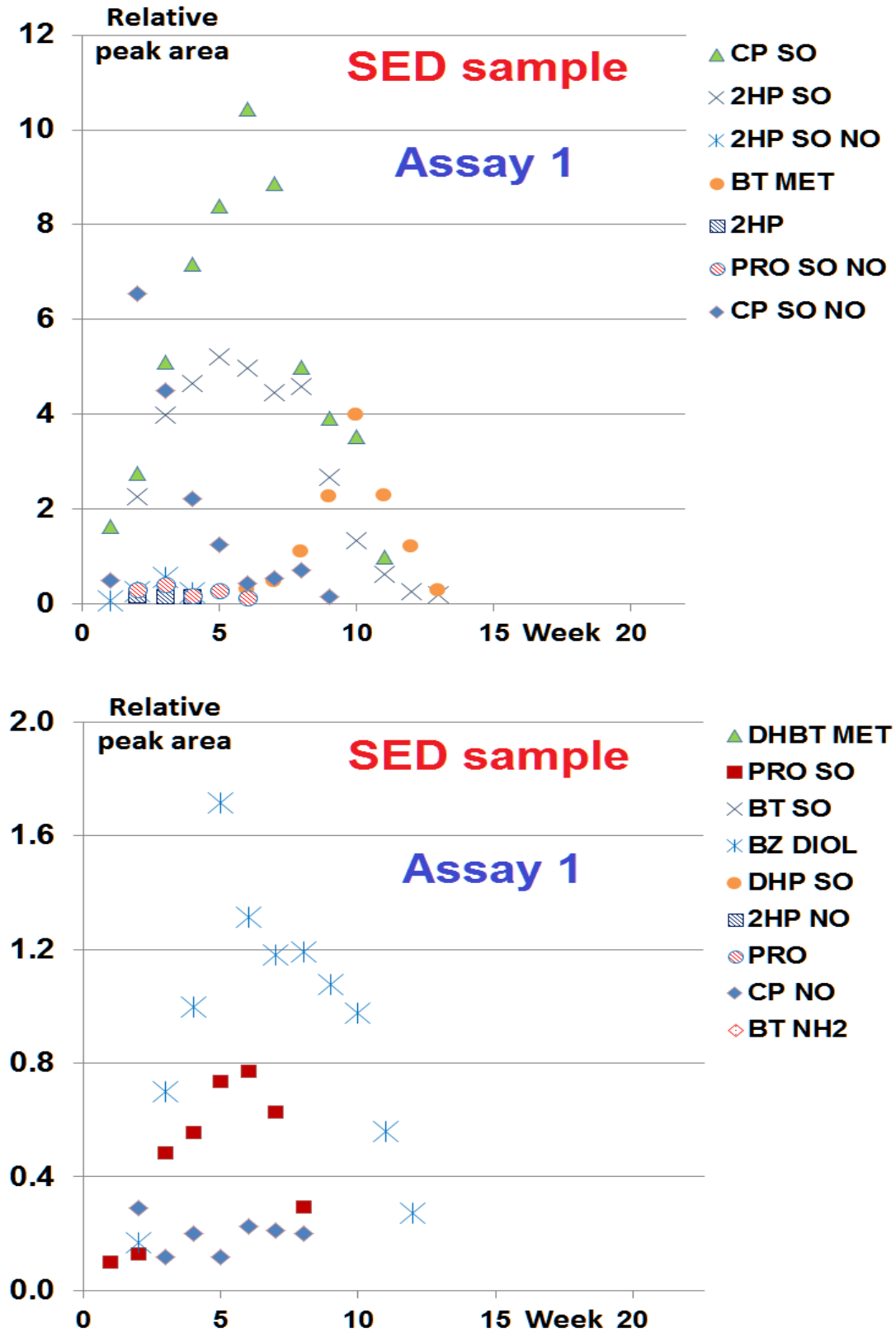

Figure: Variation of peak areas of the degradation products in the SED sample (room conditions, protected from sunlight). Peak areas are referred to a CP peak area average (average from W1 and W2 samples), to which a value of 100 was assigned. Assay 1.

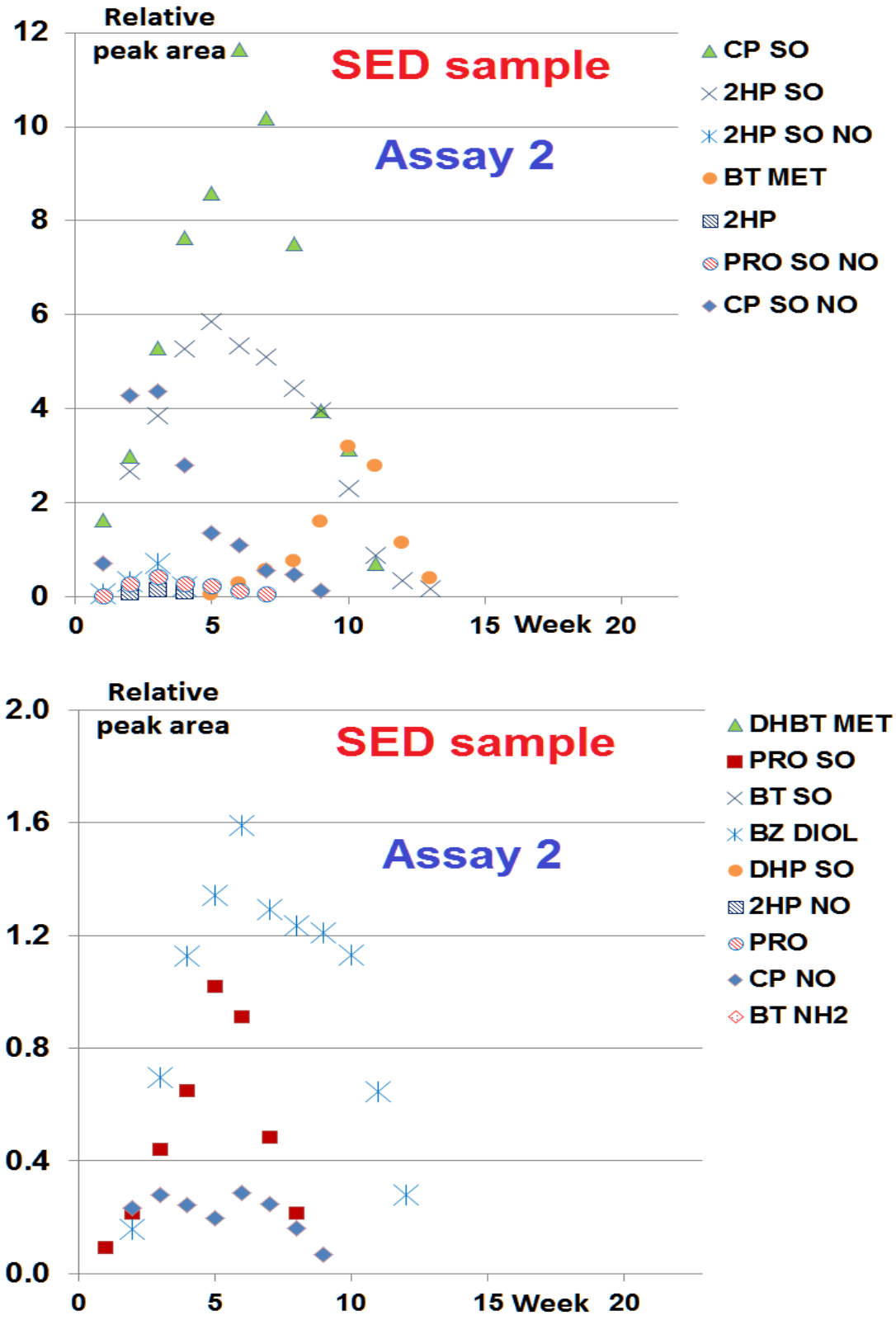

Figure: Variation of peak areas of the degradation products in the SED sample (room conditions, protected from sunlight). Peak areas are referred to a CP peak area average (average from W1 and W2 samples), to which a value of 100 was assigned. Assay 2.

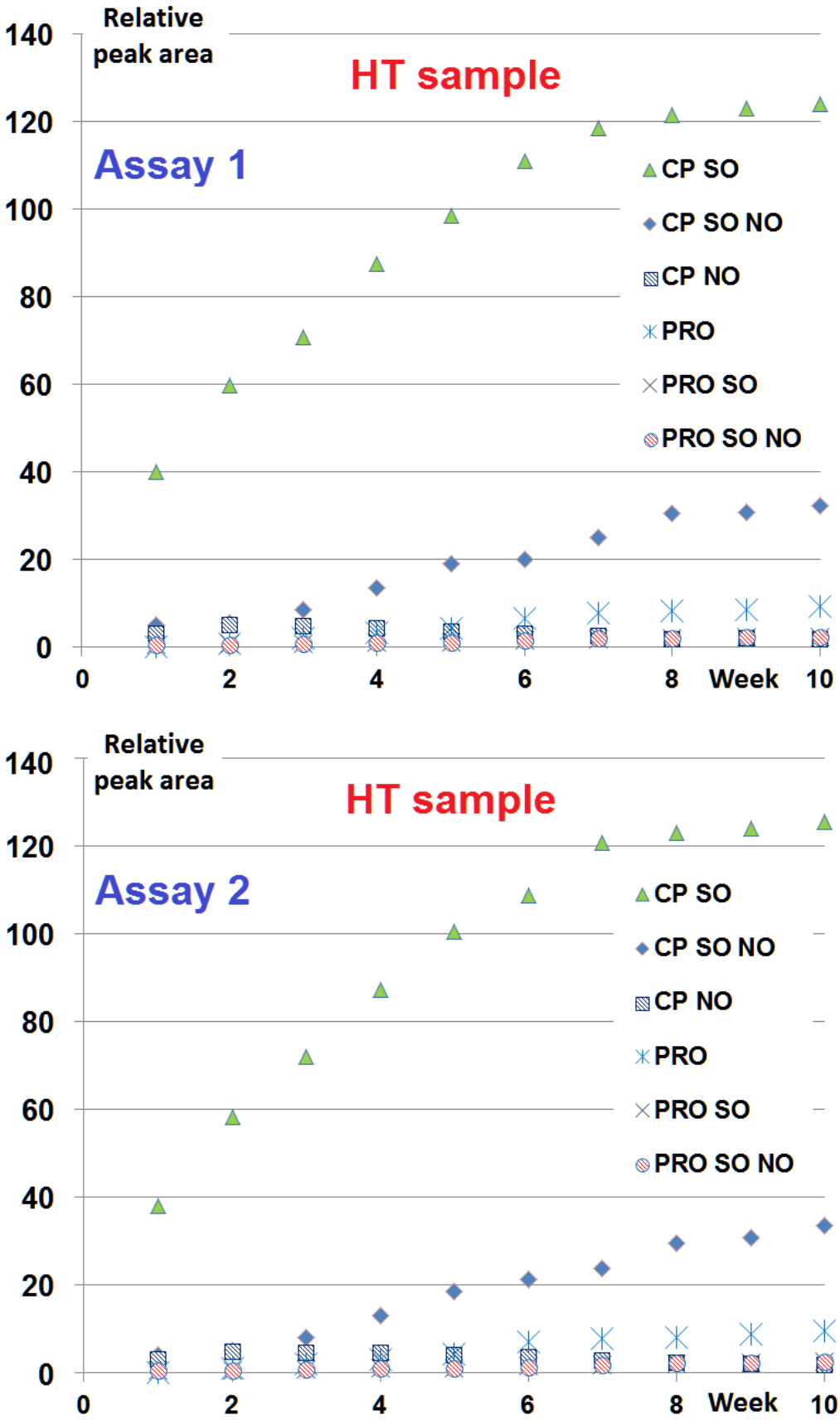

Figure: Variation of peak areas of the degradation products in the HT sample (70 °C, darkness). Peak areas are referred to the initial peak area of CP in each experiment, to which a value of 100 was assigned. Assays 1 and 2.

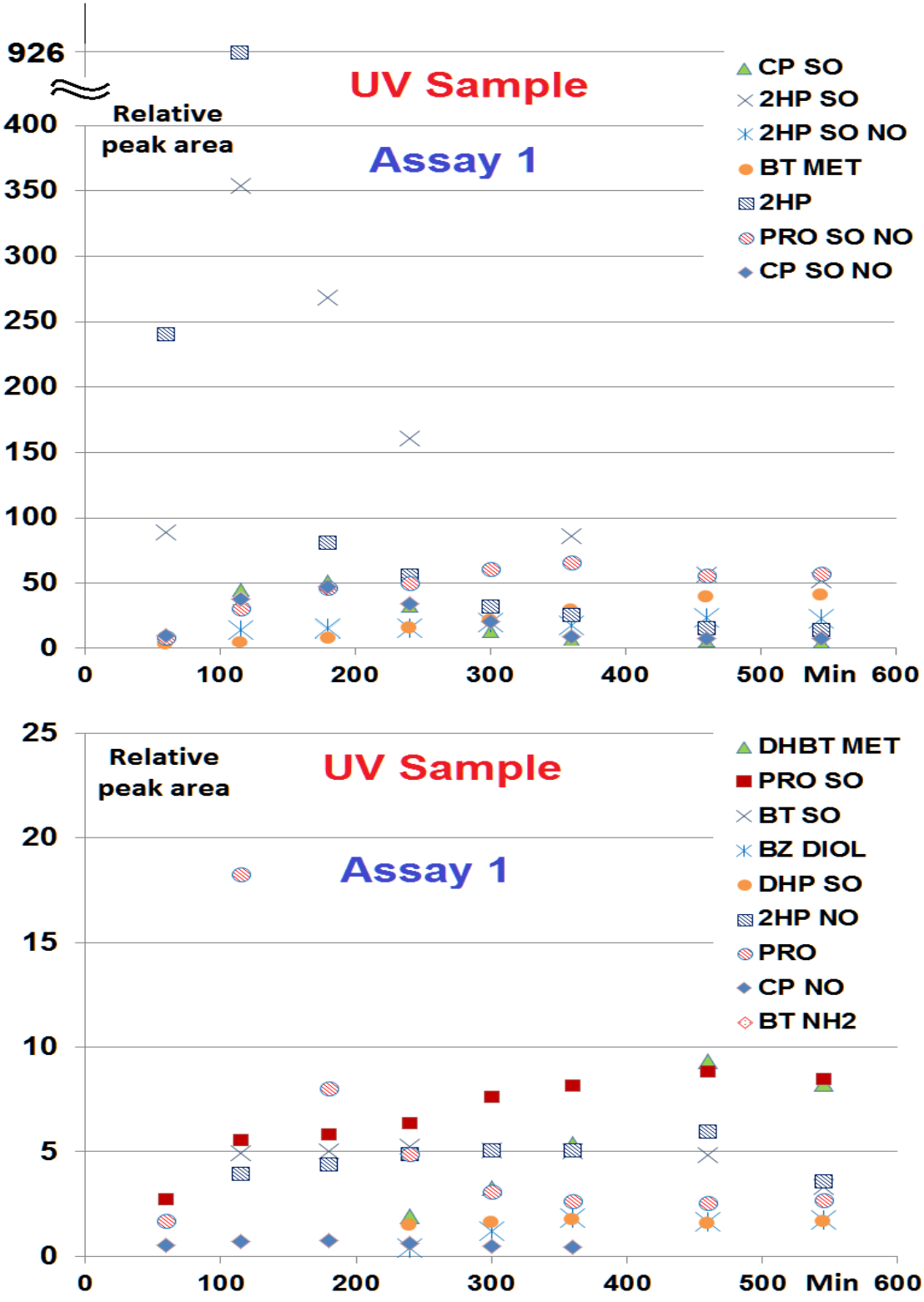

Figure: Variation of peak areas of the degradation products in the UV sample (quartz cuvette, sunlight irradiation). Peak areas are referred to the initial peak area of CP in each experiment, to which a value of 100 was assigned. Assay 1.

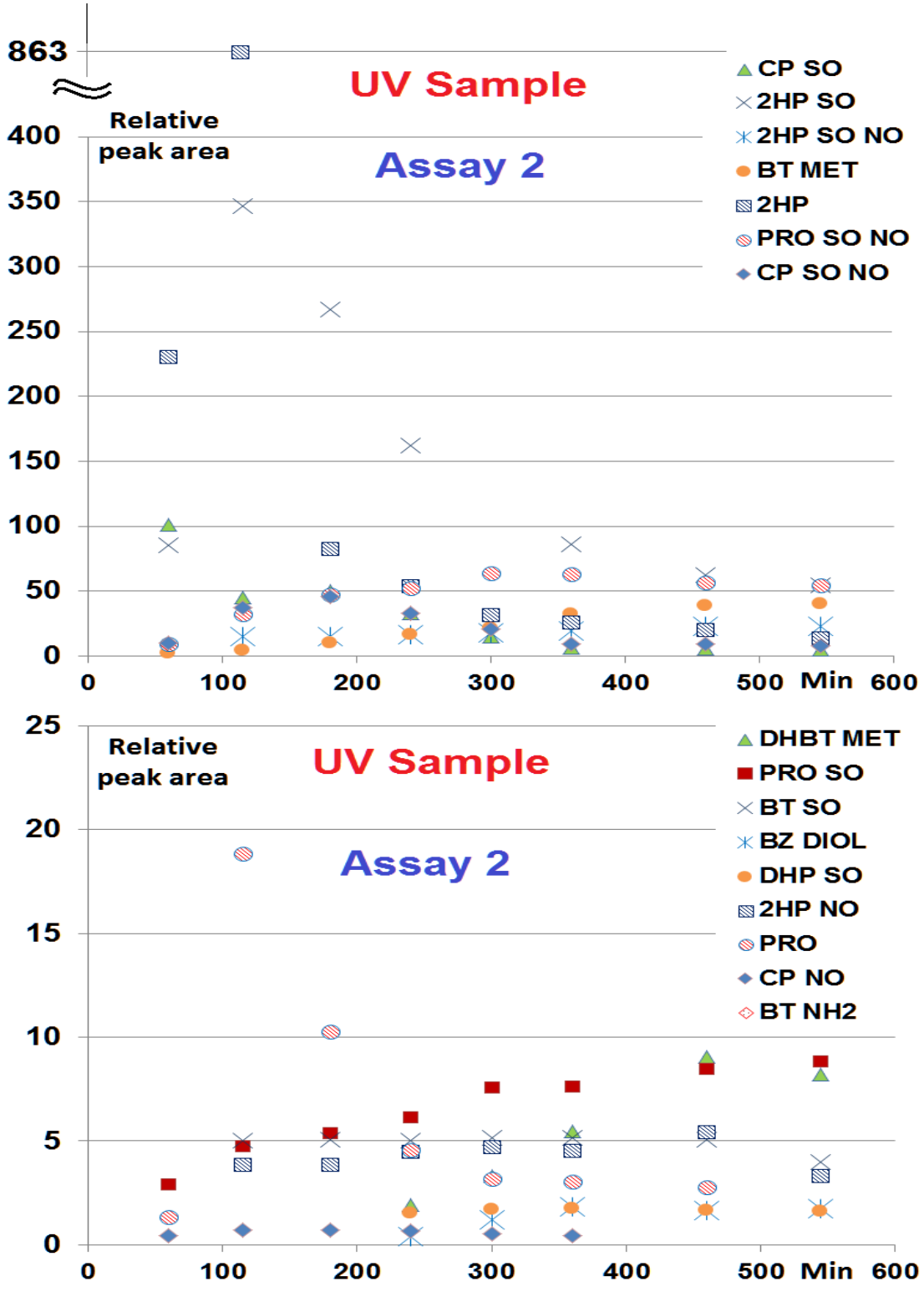

Figure: Variation of peak areas of the degradation products in the UV sample (quartz cuvette, sunlight irradiation). Peak areas are referred to the initial peak area of CP in each experiment, to which a value of 100 was assigned. Assay 2.

4.2. INDOMETACINA

JOURNAL OF ENVIRONMENTAL SCIENCES 51 (2017) 13–20

Available online at www.sciencedirect.com

ScienceDirect

www.elsevier.com/locate/jes

JES JOURNAL OF ENVIRONMENTAL SCIENCES www.jesc.ac.cn

Degradation of indomethacin in river water under stress and non-stress laboratory conditions: degradation products, long-term evolution and adsorption to sediment

Juan J. Jiménez[1,2,*], *María I. Sánchez*[3], *Rafael Pardo*[1], *Beatriz E. Muñoz*[3]

1. *Department of Analytical Chemistry, Faculty of Sciences, Campus Miguel Delibes, University of Valladolid, Paseo de Belén 7, 47011 Valladolid, Spain*
2. *I.U. CINQUIMA, Campus Miguel Delibes, University of Valladolid, Paseo de Belén 5, 47011 Valladolid, Spain*
3. *Department of Analytical Chemistry, School of Industrial Engineers, University of Valladolid, Francisco Mendizábal 1, 47014 Valladolid, Spain*

ARTICLE INFO

Article history:
Received 14 June 2016
Revised 25 August 2016
Accepted 1 September 2016
Available online 4 October 2016

Keywords:
Indomethacin
Degradation products
River water
Adsorption coefficients
High-resolution mass spectrometry

ABSTRACT

The pharmaceutical compound indomethacin is not totally removed in wastewater treatment plants, whose effluents flow into aquatic environments; concentrations in the 0.1–100 ng/L range are commonly found in surface waters, and its fate is unknown. Here, biological, photochemical and thermal degradation assays were conducted under stress and non-stress conditions to estimate its degradation rate in river water and establish its degradation products over time. The results revealed that direct sunlight irradiation promoted the complete degradation of indomethacin (2 μg/L) in less than 6 hr, but indomethacin was detected over a period of 4 months when water was kept under the natural day–night cycle and the exposure to sunlight was partially limited, as occurs inside a body of water. The biological degradation in water was negligible, while the hydrolysis at pH 7.8 was slow. Residues were monitored by ultra-pressure liquid chromatography/quadrupole time-of-flight/mass spectrometry after solid-phase extraction, and six degradation products were found; their structures were proposed based on the molecular formulae and fragmentation observed in high-resolution tandem mass spectra. 4-Chlorobenzoic and 2-acetamido-5-methoxybenzoic acids were the long-term transformation products, persisting for at least 30 weeks in water kept under non-stress conditions. Furthermore, the degradation in the presence of sediment was also monitored over time, with some differences being noted. The adsorption coefficients of indomethacin and degradation products on river sediment were calculated; long-term degradation products did not have significant adsorption to sediment.

Introduction

The presence of pharmaceutical compounds in the environment is a matter of increasing concern because they impact negatively on the environment. The effluents discharged from wastewater treatment plants (WWTPs) are the main introduction source of pharmaceuticals in surface waters. These compounds are found in the influents of the WWTPs mainly as a result of the inappropriate domestic disposal of unused medicinal products. Indomethacin (INDO) is a non-steroid

* *Corresponding author*. E-mail: jjimenez@qa.uva.es (Juan J. Jiménez).

http://dx.doi.org/10.1016/j.jes.2016.08.021
1001-0742/

anti-inflammatory drug detected in the primary influents that reach the WWTPs in concentrations, generally, of 20–100 ng/L, although concentrations of about 1 μg/L have also been reported (Sui et al., 2009; Radjenovic et al., 2009). Concentrations of about 10–20 ng/L have been found in depurated effluents (Zhou et al., 2009). In river water, INDO concentrations between 0.1 and 100 ng/L are frequent (Kim et al., 2009; Lewandowski et al., 2011; Yamamoto et al., 2009; Zhou et al., 2009). Concerning the efficiency of WWTPs at removing INDO, there are contradictory data; some authors have concluded that its removal in the global process is non-existent or slight (Radjenovic et al., 2009; Rosal et al., 2010; Sui et al., 2009; Tran et al., 2014), while other authors find that the removal rates are about 40%–100% (Huang et al., 2011; Matsuo et al., 2011; Zhou et al., 2009). Moreover, it has been stated that INDO infiltrates to subsurface waters (1 m depth) from surface waters, as has occurred for other pharmaceuticals (Lewandowski et al., 2011).

The frequent detection of INDO in surface waters and WWTP effluents discharged into rivers advises us not only to evaluate its persistence in the environment, but also to determine the possible transformation products in order to obtain an overall perspective and to assess possible risks, because the effects resulting from exposure to the parent pharmaceutical and the degradation products can be different (Celiz et al., 2009). So, INDO dissolved in different media has been subjected to degradation studies under stress conditions that indicate its photolability, and some degradation products generated in these conditions have been described (Temussi et al., 2011; Yamamoto et al., 2009), but there is no reliable information about its behavior in surface water and especially about its long-term fate in non-stress conditions.

In this context, river water spiked with INDO at trace levels was subjected to degradation studies in this work to ascertain the importance of the chemical, photochemical and biological processes in its degradation in surface water. In addition to assays under stress conditions, non-stress conditions were also applied to INDO in aqueous solution in order to simulate its behavior inside a body of water. Water aliquots were analyzed by ultra-pressure liquid chromatography/quadrupole time-of-flight/mass spectrometry, and the structures of the degradation products found were tentatively elucidated from the molecular formulae and fragmentation observed in high-resolution tandem mass spectra. The evolution of the degradation products was also monitored over time to estimate their occurrence, and a degradation pathway was outlined. In addition, the adsorption capacity of sediment for INDO and its degradation products was evaluated by calculating the corresponding adsorption coefficients.

1. Experimental

1.1. Materials and reagents

Water samples were collected from the rivers Pisuerga (pH value 7.8, chemical oxygen demand value 4.6 mg/L), in the urban area of the city of Valladolid, and Tuerto (pH value 7.4, chemical oxygen demand value 3.9 mg/L), in the rural area of the La Bañeza, province of León; chemical oxygen demand was determined by the potassium dichromate method. A sediment sample (total organic carbon 1.2%; clay 11%, silt 44%, sand 45%) was collected from the river Pisuerga. Total organic carbon was measured by a combustion method with a LECO CS-225 elemental analyzer (St. Joseph, MI, USA). Sediment particle size analysis was based on the Bouyoucos hydrometer method; soil aggregates were dispersed by chemical means.

Cellulose nitrate disks from Sartorius (Barcelona, Spain) were used: river water was filtered through 0.2 μm pore-size disks for the estimation of adsorption coefficients, through 3 μm pore-size disks to carry out biodegradation experiments, and through 0.45 μm pore-size disks for other degradation experiments.

Indomethacin (99% purity) was obtained from Sigma-Aldrich (St. Louis, MO, USA). LC–MS grade methanol, acetonitrile and formic acid were supplied by Panreac (Barcelona, Spain) and ultrapure water was obtained from a Milli-Q plus apparatus (Millipore, Milford, MA, USA). Analysis-grade sodium hydroxide, potassium dihydrogen phosphate and sodium azide were purchased from Panreac. EBH cartridges (60 mg) for solid-phase extraction (SPE) and PTFE disposable syringe filter units, 0.20 μm pore size, were obtained from Scharlab (Barcelona, Spain). Tryptone soya broth (TSB), a highly nutrient liquid culture medium for general purpose use, was purchased from Scharlab; its composition can be seen in the supplementary material (Appendix A Table S1). A vacuum centrifuge evaporator, Myvac model, was provided by Genevac (Ipswich, UK), a PK120 centrifuge by ALC (Winchester, VA, USA) and a Promax 2020 reciprocating platform shaker by Heidolph (Germany).

1.2. Biological degradation

1.2.1. Aerobic degradation

Biological degradation assays were carried out with water from the river Pisuerga (pH 7.8) which was spiked with INDO to achieve a concentration of 2 μg/L. A volume of 50 mL of river water was transferred into a 100 mL Erlenmeyer flask, which was then coated with aluminum foil to avoid exposure to sunlight but allowing the exchange of air with the atmosphere. An INDO control solution was similarly prepared in ultrapure water (pH 7.8 adjusted with NaOH) containing 0.02% (W/V) sodium azide as a biocide. Water blanks were prepared as well. Samples were run in parallel; flasks were shaken in a reciprocating shaker at a rotation speed of 130 r/min for 5 weeks, within a temperature range of 18–21°C. Aliquots of 5 mL were collected each week and subjected to analysis. Evaporation water losses were periodically restored by addition of water of the same type. All biological experiments were carried out in duplicate.

1.2.2. Anaerobic degradation

River water (pH 7.8) spiked at 2 μg/L was placed in 15 mL vials, completely filled to avoid the presence of air in the headspace. The vials were closed, protected from light by coating them with aluminum foil and kept in a temperature range of 18–21°C during experimentation. Control solutions with INDO in ultrapure water (pH 7.8 adjusted) containing 0.02% sodium azide, and the corresponding blanks, were also run in parallel. A batch of vials was assembled to withdraw weekly samples over a period of 5 weeks; a volume of 5 mL from each withdrawn vial was collected for analysis.

1.2.3. *Degradation in culture medium*

A 20/80 (V/V) mixture of TSB culture medium and river water was spiked with INDO at 2 μg/L, and 100 mL of the mixture was placed in a 250 mL glass container. A control solution in ultrapure water (pH 7.8 adjusted) containing 0.02% sodium azide and INDO, and a blank of the medium–water mixture, were also prepared and run in parallel. Closed vessels were heated at 35°C in darkness for 5 weeks. Aliquots of 10 mL were sampled weekly and filtered through 0.45 μm pore-size cellulose nitrate; 5 mL samples of filtrate were collected for analysis.

1.3. Photochemical and thermal degradation

River water (pH = 7.8) spiked with INDO (2 μg/L) was placed in a quartz cuvette, which was closed and placed on the outer edge of a window, south-facing, to allow its direct exposure to sunlight. The assay was performed in the city of Valladolid (latitude: 41°38′15″N, longitude: 4°44′17″W) in one day, in the month of January. Aliquots of 0.3 mL were withdrawn at regular time intervals and injected into the chromatographic system. Control samples of INDO in river water, protected from sunlight with aluminum foil, were prepared as well.

For thermal degradation, a volume of 100 mL of spiked river water (2 μg/L) was placed in a closed 250 mL glass flask. This was coated with aluminum foil and placed in an oven at 70 °C. Aliquots of 5 mL were collected hourly and subjected to analysis. All experiments were done in duplicate.

1.4. Non-stress degradation assays

A simple, although slow, approach was adopted in this work to simulate the concurrent natural process in a body of water. River water was placed in a transparent sodium calcium silicate glass container with air-tight seal, which was opened weekly to collect a sample aliquot and replace the air inside in contact with the water surface. The container was kept at laboratory temperature (18–21°C) under the natural day–night cycle and directly exposed to sunlight for 30 weeks, at which time the degradation assay was ended. In these conditions, the solar radiation must pass through the laboratory window glass and the glass of the container to reach the body of water; the glass absorbs UV radiation and the behavior of INDO in the glass container simulates, in a greater or lesser extent, that in a mass of water where the penetration of solar UV radiation is diminished with depth. The attenuation of the radiation was estimated by measurements of transmittance through the two types of glass (container and window), the UV–visible absorption spectra of the glasses were recorded; so, it was quantified that the percentages of radiation transmitted to the body of water were 40%, 1.3%, 0.02%, 8×10^{-4}% and 8×10^{-5}% at wavelengths of 350, 320, 310, 305 and 290 nm, respectively.

A volume of 2500 mL of river water placed in glass container was spiked with INDO to achieve an initial concentration of 2 μg/L in each degradation assay. Aliquots of 25 mL were collected periodically and subjected to SPE; extracts were injected in the chromatographic system to follow the degradation of INDO, identify degradation products and monitor them. Degradation experiments were carried out between the months of November and June with waters from the rivers Pisuerga (W1 sample) and Tuerto (W2 sample). Simultaneously, the degradation of the W1 sample was also studied in the presence of sediment by adding river sediment to the container in a sediment-to-solution ratio of 0.3 g/mL (SED sample), in the absence of sunlight by coating the container with aluminum foil (DARK sample), and in the presence of nutrients by adding culture medium at the percentage of 1% (BIO sample).

It was verified that the W1 and W2 river water samples were free of INDO residues. First, water blanks were subjected to analysis to test for the absence of the parent compound. Once the degradation products yielded in the stress assays were known, tests were also performed to verify that they were not present in the water extracts. Similarly, the absence of residues in the sediment sample was confirmed; to this aim, sediment was extracted with methanol by mechanical shaking and the extract was concentrated for analysis.

1.5. Study of adsorption to sediment

Experiments were conducted to investigate the adsorption capacity of the sediment for INDO and its degradation products. The adsorption coefficient (K_d) of INDO to sediment (sieved through a 0.5 mm mesh) was determined by using a batch approach. River water (100 mL) spiked with INDO was added to sediment (20 g) to achieve a sediment-to-solution ratio of 0.20 g/mL; INDO concentrations were 200, 400, 600, 800 and 1000 ng/L. River water contained 0.02% sodium azide as a biocide to minimize any possible microbial activity and pH (7.8) was controlled with phosphate buffer (0.02 mol/L). Control solutions without sediment were prepared as well. The flasks, protected from sunlight with aluminum foil, were manually shaken for 1 min and left standing at 20 ± 1°C for a period of 24 hr. Afterwards, an aliquot of 10 mL, previously centrifuged to remove solids, was collected to determine the INDO concentration at equilibrium. An adsorption isotherm was drawn in duplicate. The concentration adsorbed on the sediment was not directly measured.

Analytical standards are unavailable for most of the degradation products, however their K_d were estimated based on the assumption that there is a linear relationship between peak area and concentration for each compound. Experiments similar to the above-described were devised by spiking water with a solution containing the degradation products and an appropriate sediment-to-solution ratio. The decrease percentage of peak area in water was assumed to be the percentage of compound adsorbed onto sediment (A%), and K_d was calculated by Eq. (1), which is valid if the adsorption equation is linear (OECD, 2000). Peak areas of the adsorption experiments were compared with those of control solutions by a *t*-test ($n = 5$) to confirm the existence of significant differences before applying the equation.

$$\log K_d = \log\left(\frac{A\%/100}{1-A\%/100}\right) - \log R \quad (1)$$

1.6. Sample preparation

Except for the photochemical degradation study, river water aliquots were eluted through EBH cartridges previously conditioned by successive elution of methanol (6 mL) and

water (6 mL). The cartridges were washed with 3 mL of a water–methanol (80:20, V/V) mixture after sample elution. The stationary phase was dried with air for 3 min and the target compounds were eluted with methanol (4 mL) by gravity. Then, the extract was evaporated in 30 min by a vacuum centrifuge evaporator heated at 40 °C, and the dry residue was re-dissolved in 0.5 mL of methanol, which was filtered through a 0.20 μm pore-size PTFE filter for chromatographic analysis.

1.7. Determination by liquid chromatography – mass spectrometry

An Acquity ultra-pressure liquid chromatograph from Waters (Milford, MA, USA) coupled to a Maxis Impact quadrupole time-of-flight tandem mass spectrometer from Bruker Daltonics (Bremen, Germany) was used. Analyses were performed with electrospray ionization in negative mode. The chromatograph was fitted with a Waters BEH ODS column (50 mm × 2.1 mm, 1.7 μm particle size). The mobile phase flow rate was 0.5 mL/min and consisted of 0.1% formic acid in water (A) and 0.1% formic acid in acetonitrile (B); assays were performed under gradient conditions: from 20% B to 55% B in 4.5 min, and then 60% B in 1 min. Re-equilibration time was 1 min. Injection volume was 7 μL.

The operating parameters of the electrospray ionization source for the MS and MS/MS experiments were as follows: nebulizing gas pressure, 2 bar; end plate offset voltage, 1000 V; capillary voltage, 4500 V; drying gas temperature, 200°C; dry gas flow, 6 L/min. Nitrogen was used as drying and nebulizing gas. Mass calibration adjustments were performed by using a 10 mmol/L sodium formate solution in 2-propanol/water. MS/MS experiments based on collision-induced dissociation with nitrogen gas were performed. The quantitation of INDO was accomplished using linear calibration graphs based on the measurement of peak areas in the chromatograms extracted for the fragment-ion $[M–H–CO_2]^-$ generated in the electrospray source by MS experiments, with a mass range of ±0.01 Da. Similarly, peak areas of degradation products were integrated in the chromatograms extracted for the corresponding $[M–H]^-$ ions.

As regards the performance of the analytical method, the mean recovery of INDO (2 μg/L) was about 95% with a repeatability of 1.8% for W1 sample (n = 5). The repeatability in the determination of the degradation products varied from 1.6% to 5.5% (n = 5, Appendix A Table S2).

2. Results and discussion

2.1. Degradation of indomethacin

Fig. 1 shows the variation of the INDO concentration over time in biological and stress assays; data are the average of two independent experiments, and individual data are shown in Appendix A Tables S3 and S4. After 5 weeks, the degradation of INDO in river water was negligible under aerobic and anaerobic conditions at room temperature, but when a nutrient was added to river water and the mixture was incubated at 35°C, the concentration of INDO decreased by about 68%. A 1 week lag period was observed in this last experiment; if the initial concentration (time 0 weeks) was excluded, the variation of the remaining experimental concentrations with time could be fitted to a linear equation (R^2 = 0.98), from which a half-life of 3.70 weeks was calculated. On the other hand, heating at 70°C and UV radiation from the sunlight promoted faster degradation of INDO in river water; it could be detected for only 11 and 5 hr, respectively. Degradation data were fitted to a first-order kinetics equation with half-lives of 1.97 h (R^2 = 0.97) and 1.60 h (R^2 = 0.97) for the heating and direct irradiation assays, respectively. The UV radiation is the main factor that boosts the degradation of INDO.

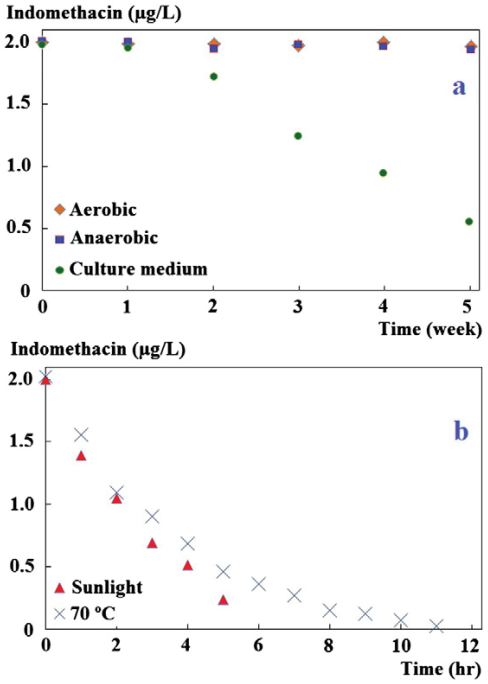

Fig. 1 – Degradation of indomethacin in river water according to biological (a) or stress (b) assays. Data are the mean of two experiments.

The evolution of the INDO concentration over weeks in the non-stress assays can be seen in Fig. 2 and Appendix A Table S5. INDO was detected for 16 and 15 weeks in water from the two rivers (W1 and W2 samples); the concentration decreased gradually until it was less than the detection limit achieved by the method, which was estimated to be about 10 ng/L. Experimental data were also well fitted to first-order kinetics; half-lives were 2.57 (R^2 = 0.97) and 2.47 weeks (R^2 = 0.94) for W1 and W2 samples, respectively. The degradation of INDO in river water at room temperature and in the absence of sunlight (DARK sample) was slower (half-life: 5.12 weeks, R^2 = 0.98), being detected throughout the 30 weeks of experimentation. These assays indicate that solar radiation is a notable factor in the behavior of INDO inside a body of water even though the transmission of UV radiation is attenuated. However, the photochemical reactions should not be the only

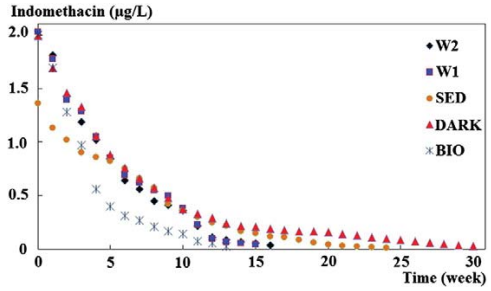

Fig. 2 – Degradation of indomethacin in river water under non-stress conditions. Data are the mean of two experiments.

factor considered because the degradation of INDO in darkness is not negligible.

INDO seems to be a non-biodegradable compound in unmodified river water. However, the degradation study over time in water whose nutrient content was enhanced (BIO sample) revealed that the degradation rate was slightly higher in comparison with that of the W1 sample. The half-life was now estimated to be 2.04 weeks (R^2 = 0.98, first-order kinetics). Otherwise, in the presence of aquatic sediment (SED sample) the half-life was higher, 3.39 weeks (R^2 = 0.96, first-order kinetics); INDO was found in the aqueous phase for 24 weeks. The measured initial concentrations in the SED sample were lower with regard to the previous assays, which suggested possible adsorption of INDO to sediment. This adsorption phenomenon could help protect INDO from sunlight exposure and increase its stability in water samples.

2.2. Detection and identification of degradation products

The presence of compounds related to degradation of INDO was established by the observation of new chromatographic peaks in the MS chromatograms, which were present neither in the previous chromatograms nor in blanks, and the gradual variation of their peak areas over time. In this way, six degradation products of INDO were found in the extracts. The $[M–H]^-$ ion of each degradation product, besides INDO, was isolated and fragmented by collision-induced dissociation to obtain structural information. MS/MS spectra (Appendix A Figs. S1–S7), discussion of the fragmentation patterns, interpretation of the fragment-ions and a brief explanation on the assignment of tentative structures to the degradation products can be found in the supplementary material. Table 1 shows the molecular formulae established and the identifications proposed for the compounds.

The compounds 5-methoxy-2-methyl-1H-indole-3-acetic acid (MMIA) and 4-chlorobenzoic acid (CBA) were unequivocally identified. They were the two basic constituent moieties of INDO. An unknown degradation product was identified as acid (DHINDO), a derivative of INDO hydroxylated at the C6 and C7 sites of the indole moiety, while the other unknown compound was thought to be 2-(4-chlorobenzamido)-5-methoxybenzoic acid (CMBA), which arose from the cleavage of the indole structure. The other two degradation products were identified as 5-methoxy-2-methyl-1H-indole-3-carbaldehyde (MMIC) and 2-acetamido-5-methoxybenzoic acid (AMBA) in agreement with two described photodegradation compounds (Temussi et al., 2011). Thus, a structure was ascribed to each compound considering spectral and bibliographic data.

2.3. Occurrence of degradation products in river water

The peak areas of the degradation products were monitored during the degradation studies; a value of 100 was assigned to the initial peak area of INDO (week 0) in each experiment, and all other peak areas were referred to this value. Fig. 3 illustrates the evolution of compounds in non-stress conditions. Data for all compounds and experiments are provided as Supplementary material. Four compounds were found in W1 and W2 samples (Appendix A Figs. S8 and S9), whose degradation conditions were intended to simulate the behavior of INDO inside a body of water; CBA, AMBA and MMIA were the major degradation products in the first 15 weeks, while CBA together with AMBA were the only compounds detected after 30 weeks. CBA was the most abundant degradation product in terms of peak area; its amount increased gradually until about the 10th week, and then decreased slowly. AMBA was a minor degradation product that seemed to persist over time. DHINDO was also a minor compound that reached its maximum occurrence at about the 9th–10th week; like MMIA, DHINDO was not detected after the 19th week. The evolution profile of the compounds was basically similar in waters from the two rivers (W1 and W2). The joint presence of CBA and

Table 1 – Retention times (RT), masses measured in the mass spectra for the $[M-H]^-$ ion, errors in the determination of exact masses, molecular formulae and number of rings and double bonds (rdb) of the corresponding structures for the detected degradation products.

RT (min)	Molecular formula	Exact mass (Da)	Measured mass (Da)	Error (ppm)	rdb	Compound	Abbreviation
0.89	$C_{10}H_{10}NO_4$	208.0615	208.0616	−0.5	6.5	2-acetamido-5-methoxybenzoic acid	AMBA
1.15	$C_{11}H_{10}NO_2$	188.0717	188.0724	−2.3	7.5	5-methoxy-2-methyl-1H-indole-3-carbaldehyde	MMIC
1.26	$C_{12}H_{12}NO_3$	218.0823	218.0824	−0.5	7.5	5-methoxy-2-methyl-1H-indole-3-acetic acid	MMIA
2.04	$C_7H_4ClO_2$	154.9905	154.9905	0.0	5.5	4-chlorobenzoic acid	CBA
2.82	$C_{19}H_{17}ClNO_6$	390.0750	390.0746	1.0	11.5	1-(4-chlorobenzoyl)-6,7-dihydro-6,7-dihydroxy-5-methoxy-2-methyl-1H-indole-3-acetic acid	DHINDO
3.80	$C_{15}H_{11}ClNO_4$	304.0382	304.0378	−1.3	10.5	2-(4-chlorobenzamido)-5-methoxybenzoic acid	CMBA
4.25	$C_{19}H_{15}ClNO_4$	356.0695	356.0696	−0.3	12.5	1-(4-chlorobenzoyl)-5-methoxy-2-methyl-1H-indole-3-acetic acid	INDO

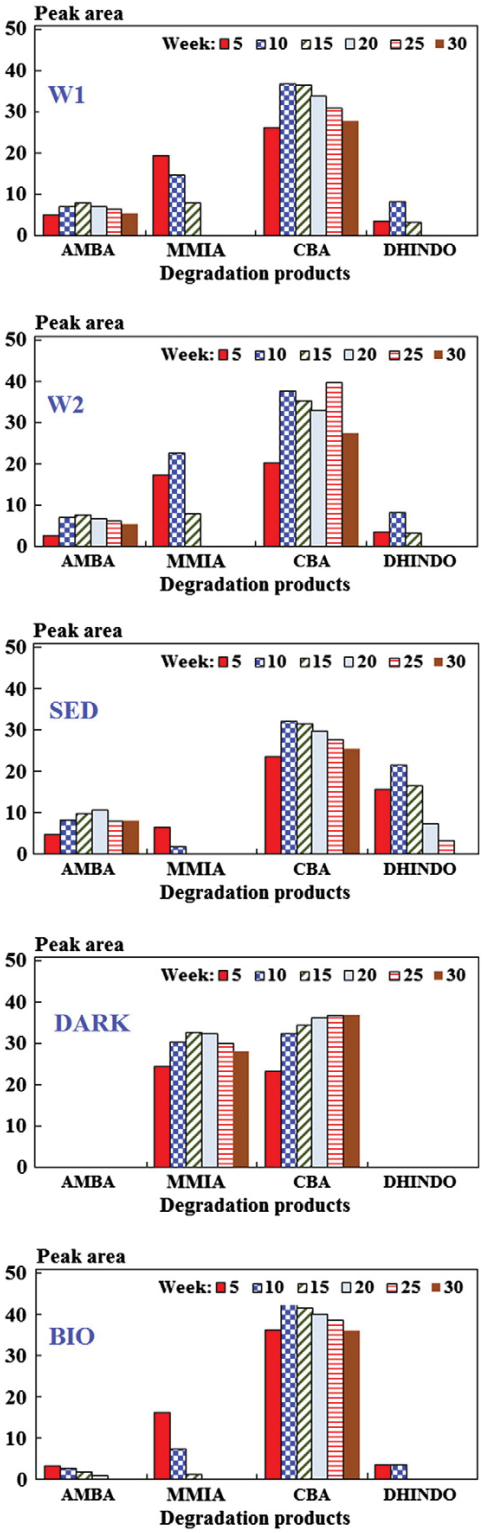

Fig. 3 – Variation of peak areas of the degradation products in river water under non-stress conditions. Mean of two experiments.

AMBA in surface water can constitute an indicator of the earlier presence of INDO in that body of water.

The evolution of the degradation products when the amount of nutrients in river water was increased to favor the growth of microorganisms (BIO sample) followed the pattern described for W1 and W2 samples, with the difference that the transformation rate of the compounds increased somewhat, as was previously stated for the degradation of INDO (Appendix A Fig. S10). Excepting CBA, all degradation products were detected during a smaller number of weeks; even AMBA was now fully degraded in 23 weeks.

Finally, the transformation products found in the SED sample (Appendix A Fig. S11) were the same as those in the W1 and W2 samples, although the evolution profile was clearly different. Regardless of the lower degradation rate of INDO, MMIA was detected only in extracts for 10 weeks, and its peak areas were lower in relation to assays without sediment. Moreover, DHINDO was present in higher relative amounts, which was attributed not only to the lower initial peak area of INDO, but also to the higher occurrence of DHINDO, whose formation was enhanced in the presence of sediment. Furthermore, the persistence of DHINDO also increased, being detected in water for 28 weeks. However, CBA and AMBA remained as the only compounds detected after 30 weeks.

As regards the origin of the degradation products, CBA and MMIA were the only degradation products detected in the stress assay at 70°C (Appendix A Fig. S12), the DARK sample (Appendix A Fig. S13), and the water sample incubated at 35°C with added culture medium (Appendix A Fig. S14). Their occurrence in the two first samples, in addition to W1 and W2, could be easily explained by chemical hydrolysis, while biochemical hydrolysis in the water containing nutrients could not be discarded. On the other hand, the peak areas of CBA and MMIA in the DARK sample after 30 weeks were not very different between them, in contrast to W1 and W2 samples, where the amount of MMIA was clearly lower than that of CBA at the end of the monitoring; this suggested that MMIA is a relatively stable compound in the absence of sunlight.

Five degradation products were yielded by photochemical reactions. They were found when river water was directly exposed to sunlight, without passing through the glass, which absorbs UV radiation (Appendix A Fig. S15). DHINDO was the predominant product in terms of peak area, which was two-fold higher than that of INDO after 6 hr of exposure (see Supplementary material). CBA and AMBA were also detected, but not MMIA. Two other photo-induced degradation products that resulted were MMIC and CMBA, which were not noted in the samples under non-stress conditions, likely as a consequence of the attenuation of the UV radiation. It is plausible that the amount of DHINDO could be higher in a body of water if the UV radiation was less attenuated with depth.

The described photodegradation compounds can be yielded by direct or indirect photolysis; data to differentiate and discuss the two photolysis mechanisms in the degradation of INDO are not available. In direct photolysis, the molecule of INDO in the excited state (after absorbing a photon) would be unstable and would break down. In indirect photolysis, the radiation is

absorbed for one or more chemical species in the water solution (for instance, the dissolved organic matter), which could then decompose INDO by direct reaction with it or through new chemical species derived from those excited compounds.

2.4. Distribution between water and sediment. Adsorption coefficients

Fig. 4 shows the adsorption isotherm obtained for INDO in the batch experiments; the resulting K_d and K_{oc} (organic carbon normalized adsorption coefficient) values were 1.79 and 149 kg/L (RSD 5.0%, n = 10), respectively. The K_d value was comparable to that already described in the literature (Yamamoto et al., 2009). Adsorption coefficients were also calculated for the degradation products from the experimental adsorption percentages; the K_d and K_{oc} values and the sediment-to-water ratios used are given in Table 2. The adsorption coefficient of INDO was also calculated by this method and was found to be similar to the previous value. CBA, and particularly AMBA and DHINDO, had a lower capacity for adsorption than INDO. In fact, the low adsorption percentages (<10%) of the latter two degradation compounds resulted in a worse precision (28%) in the determination performed for DHINDO, and only a rough estimate of K_d for AMBA. On the other hand, the adsorption coefficients of MMIA and MMIC were relatively high, about 18-fold higher than that of INDO, which was consistent with the low peak areas observed for MMIA in the SED sample. After checking the structures of the compounds, the notable capacity for adsorption of MMIA and MMIC to sediment would be related to the presence of a N–H bond in the indole moiety, because higher adsorption coefficients have been reported in amine compounds (Yamamoto et al., 2009). It should be noted that the water–sediment interaction is not simple and that the adsorption coefficients were estimated for only a sample of water and sediment; consequently, the data provided in this work should be considered preliminary.

2.5. Degradation pathway

A main degradation pathway of INDO in river water was outlined (Fig. 5). First, the amide group of INDO is hydrolyzed to give its two constituent moieties: MMIA and CBA, whose presence would be expected (Krzek and Starek, 2001). Simultaneously, INDO undergoes a secondary degradation reaction in which the diol derivative DHINDO is formed through a photochemical reaction; it is thought that DHINDO could undergo a similar hydrolysis reaction, but its corresponding indole moiety was not found in this work.

It has been reported that AMBA arises from INDO through a photodegradation process involving the non-prominent intermediate MMIC (Temussi et al., 2011), however it seems quite possible that MMIA is transformed into AMBA by photo-induced reactions as well. In fact, the amount of MMIA remained high and relatively constant in the DARK sample, as already noted above. In order to verify the conversion of MMIA in AMBA, an INDO aliquot was subjected to hydrolysis by heating at 70°C to yield CBA and MMIA, and then was placed in a quartz cuvette for direct exposure to sunlight. It was observed that MMIA was completely removed in about 4 hr, that MMIC was very abundant after 2 hr, decreasing quickly afterwards, and that AMBA was effectively a photoproduct arising from MMIA (Appendix A Fig. S16); the CBA amount remained virtually constant in this assay. Finally, there were no data to ascertain the fate of CMBA, however it is reasonable to hypothesize its transformation to CBA by hydrolysis.

Table 2 – K_d and K_{oc} mean values (RSDs in parenthesis) calculated for the degradation products. Mean adsorption percentages (A%) onto sediment and experimental sediment to water ratios (R), n = 5.

Compound	K_d (kg/L)	K_{oc} (kg/L)	A%	R (kg/L)	Experimental t-value*
AMBA	<0.10	<8.7(–)	<5	0.507	0.6
MMIC	35	2938 (6.0%)	54.0	0.0333	10.8
MMIA	33	2756 (6.7%)	52.2	0.0331	18.2
CBA	1.1	89 (8.6%)	30.5	0.409	10.1
DHINDO	0.15	12.3 (28%)	7.0	0.509	2.57
CMBA	1.8	150 (8.1)	27.4	0.210	15.2
INDO	1.8	150 (7.8%)	27.0	0.206	16.9

* Critical t-value: 2.3; –: without data.

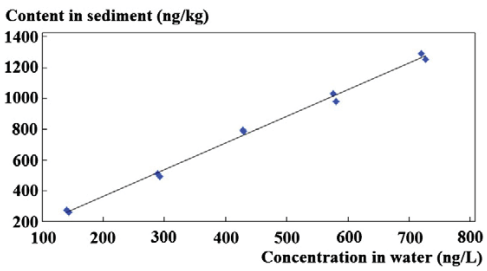

Fig. 4 – Adsorption isotherm of indomethacin (n = 2).

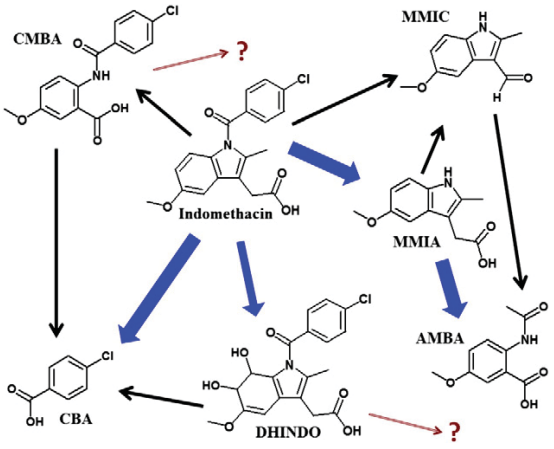

Fig. 5 – Degradation pathway of indomethacin in river water. Bold lines denote the possible predominance of the transformation process.

3. Conclusions

The hydrolysis of indomethacin into its two constituent moieties and the photochemical reactions undergone by the indole moiety were the main degradation pathways in river water. A relatively slow biological degradation took place only in the presence of high contents of nutrients. The degradation rate decreased notably when photochemical stress was avoided. The capability of the chemical and photochemical stress assays to properly predict the degradation products of indomethacin, or their relative amounts, inside a body of water was limited.

Four degradation products were found in river water under non-stress conditions and two of them, 4-chlorobenzoic acid and 2-acetamido-5-methoxy benzoic acid, were the only and persistent degradation products detected after 30 weeks. The half-life of indomethacin in river water under these conditions was estimated to be about 2.5 weeks. Two new degradation compounds of indomethacin were reported: acid and 2-(4-chlorobenzamido)-5-methoxybenzoic acid.

Indomethacin was partially adsorbed onto sediment and a degradation product, 5-methoxy-2-methyl-1H-indole-3-acetic acid, showed higher adsorption capacity. The degradation rate in contact with sediment was slower, likely as consequence of the protection supplied by the sediment against sunlight irradiation.

Acknowledgments

The authors would like to acknowledge the support given by the Laboratorio de Técnicas Instrumentales of the University of Valladolid to perform the experimental work.

Appendix A. Supplementary data

Supplementary data to this article can be found online at http://dx.doi.org/10.1016/j.jes.2016.08.021.

REFERENCES

Celiz, M.D., Tso, J., Aga, D.S., 2009. Pharmaceutical metabolites in the environment: analytical challenges and ecological risks. Environ. Toxicol. Chem. 28 (12), 2473–2484.

Huang, Q., Yu, Y., Tang, C., Zhang, K., Cui, J., Peng, X., 2011. Occurrence and behavior of non-steroidal anti-inflammatory drugs and lipid regulators in wastewater and urban river water of the Pearl River Delta, South China. J. Environ. Monit. 13 (4), 855–863.

Kim, J.W., Jang, H.S., Kim, J.G., et al., 2009. Occurrence of pharmaceutical and personal care products (PPCPs) in surface water from Mankyung river, South Korea. J. Health Sci. 55 (2), 249–258.

Krzek, J., Starek, M., 2001. Simultaneous densitometric determination of indomethacin and its degradation products, 4-chlorobenzoic acid and 5-methoxy-2-methyl-3-indoleacetic acid, in pharmaceutical preparations. J. AOAC Int. 84 (6), 1703–1707.

Lewandowski, J., Putschew, A., Schwesig, D., Neumann, C., Radke, M., 2011. Fate of organic micropollutants in the hyporheic zone of a eutrophic lowland stream: results of a preliminary field study. Sci. Total Environ. 409 (10), 1824–1835.

Matsuo, H., Sakamoto, H., Arizono, K., Shinohara, R., 2011. Behavior of pharmaceuticals in waste water treatment plant in Japan. Bull. Environ. Contam. Toxicol. 87 (1), 31–35.

OECD guideline for the testing of chemicals No 106, 2000. Adsorption - Desorption Using a Batch Equilibrium Method. p. 8.

Radjenovic, J., Petrovic, M., Barcelo, D., 2009. Fate and distribution of pharmaceuticals in wastewater and sewage sludge of the conventional activated sludge and advanced membrane bioreactor treatment. Water Res. 43 (3), 831–841.

Rosal, R., Rodrıguez, A., Perdigon-Melon, J.A., Petre, A., et al., 2010. Occurrence of emerging pollutants in urban wastewater and their removal through biological treatment followed by ozonation. Water Res. 44 (2), 575–588.

Sui, Q., Huang, J., Deng, S., Yu, G., 2009. Rapid determination of pharmaceuticals from multiple therapeutic classes in wastewater by solid-phase extraction and ultra-performance liquid chromatography tandem mass spectrometry. Chin. Sci. Bull. 54, 4633–4643.

Temussi, F., Cermola, F., DellaGreca, M., Iesce, M.R., Passananti, M., Previtera, L., Zarrelli, A., 2011. Determination of photostability and photodegradation products of indomethacin in aqueous media. J. Pharm. Biomed. Anal. 56 (4), 678–683.

Tran, N.H., Urase, T., Ta, T.T., 2014. A preliminary study on the occurrence of pharmaceutically active compounds in hospital wastewater and surface water in Hanoi, Vietnam. Clean Soil Air Water 42 (3), 267–275.

Yamamoto, H., Nakamura, Y., Moriguchi, S., et al., 2009. Persistence and partitioning of eight selected pharmaceuticals in the aquatic environment: laboratory photolysis, biodegradation, and sorption experiments. Water Res. 43 (2), 351–362.

Zhou, J.L., Zhang, Z.L., Banks, E., Grover, D., Jiangm, J.Q., 2009. Pharmaceutical residues in wastewater treatment works effluents and their impact on receiving river water. J. Hazard. Mater. 166 (2–3), 655–661.

Supplementary data

Degradation of indomethacin in river water under stress and non-stress laboratory conditions: degradation products, long-term evolution and adsorption to sediment.

Journal of Environmental Sciences, 2016

Contents

(*) not included in the published manuscript

1.1. Material and reagents

Table S1: Composition of the culture medium in agreement with the technical data sheet from the supplier.

Compound:	g/L
Peptone from casein	17.0
Soya peptone	3.0
Sodium chloride	5.0
Dipotassium phosphate	2.5
D(+) Glucose	2.5
pH	7.3±0.2

1.7. Determination by liquid chromatography – mass spectrometry

Table S2: Repeatabilities (expressed as RSDs) achieved in the determination of indomethacin degradation products in a river water sample by the applied analytical method (n=5). See section 3.2 for compound identification.

Sample Volume:	5 mL	25 mL
	RSD (%)	RSD (%)
AMBA	2.2	1.8
MMIC	1.9	3.1
MMIA	2.4	3.7
CBA	5.5	4.3
DHINDO	1.6	2.3
INDO	2.1	1.4

2.1. Degradation of indomethacin

Table S3: Biological degradation of indomethacin in river water under aerobic and anaerobic conditions, and in a mixture with culture medium. Individual data of each assay.

	Anaerobic Concentration ($\mu g \cdot L^{-1}$)		Aerobic Concentration ($\mu g \cdot L^{-1}$)		Culture medium Concentration ($\mu g \cdot L^{-1}$)	
Time (week)	Assay 1	Assay 1	Assay 2	Assay 2	Assay 2	Assay 2
0	2.02	2.01	2.02	1.99	1.98	1.99
1	1.98	2.03	2.00	1.98	1.94	1.96
2	1.95	1.94	1.96	2.02	1.72	1.68
3	2.00	1.98	1.99	1.97	1.14	1.21
4	1.97	1.98	2.04	1.98	0.91	0.78
5	1.95	1.96	1.97	1.99	0.57	0.52
R^2	--	--	--	--	0.97	0.99
$t_{1/2}$ (week)	--	--	--	--	3.75	3.62

R^2: Coefficient of regression of the linear fitting after excluding the first point (week 0).
$t_{1/2}$: Half-life time estimated from the linear fitting equation.
-- : without data.

Table S4: Degradation of indomethacin in river water at high temperature (70 °C) without sunlight irradiation, and in quartz cuvettes under sunlight irradiation. Individual data of each assay.

	High temperature Concentration ($\mu g \cdot L^{-1}$)		Sunlight Concentration ($\mu g \cdot L^{-1}$)	
Time (h)	Assay 1	Assay 1	Assay 2	Assay 2
0	2.03	2.02	2.01	1.98
1	1.54	1.57	1.38	1.40
2	1.11	1.08	1.08	1.02
3	0.92	0.89	0.70	0.69
4	0.70	0.67	0.51	0.52
5	0.45	0.47	0.23	0.25
6	0.37	0.35	--	--
7	0.25	0.29	--	--
8	0.16	0.14	--	--
9	0.12	0.13	--	--
10	0.061	0.083	--	--
11	0.025	0.030	--	--
R^2	0.97	0.97	0.97	0.98
$t_{1/2}$ (h)	1.74	1.83	1.57	1.63

R^2: Coefficient of regression of the fitting; kinetics of first-order reactions.
$t_{1/2}$: Half-life time.
-- : not detected.

Table S5: Degradation of indomethacin in river water under non-stress conditions: W1, W2, DARK, SED and BIO samples. Individual data of each assay.

	W1 Concentration ($\mu g \cdot L^{-1}$)		W2 Concentration ($\mu g \cdot L^{-1}$)		DARK Concentration ($\mu g \cdot L^{-1}$)		SED Concentration ($\mu g \cdot L^{-1}$)		BIO Concentration ($\mu g \cdot L^{-1}$)	
Week	Assay 1	Assay 2	Assay 1	Assay 2	Assay 1	Assay 2	Assay 1	Assay 2	Assay 1	Assay 2
0	2.04	2.00	2.03	2.02	1.99	1.99	1.34	1.37	2.00	2.00
1	1.82	1.81	1.81	1.72	1.68	1.69	1.14	1.12	1.76	1.62
2	1.34	1.44	1.69	1.54	1.48	1.50	1.02	1.01	1.32	1.23
3	1.25	1.14	1.32	1.25	1.31	1.34	0.91	0.89	0.95	0.98
4	1.08	0.96	1.06	1.04	1.05	1.07	0.87	0.85	0.54	0.57
5	0.82	0.85	0.86	0.84	0.87	0.89	0.83	0.81	0.38	0.42
6	0.68	0.60	0.66	0.71	0.75	0.76	0.74	0.75	0.29	0.33
7	0.58	0.84	0.62	0.61	0.66	0.66	0.65	0.66	0.26	0.27
8	0.46	0.44	0.54	0.56	0.56	0.57	0.56	0.58	0.20	0.21
9	0.42	0.39	0.52	0.48	0.48	0.47	0.42	0.41	0.17	0.16
10	0.37	0.35	0.41	0.38	0.37	0.37	0.36	0.35	0.14	0.13
11	0.23	0.20	0.24	0.21	0.32	0.33	0.29	0.30	0.090	0.060
12	0.12	0.098	0.090	0.11	0.29	0.29	0.24	0.26	0.048	0.058
13	0.10	0.080	0.071	0.069	0.24	0.23	0.21	0.22	0.023	0.024
14	0.072	0.071	0.058	0.051	0.22	0.22	0.17	0.17	--	--
15	0.055	0.052	0.041	0.044	0.20	0.21	0.14	0.15	--	--
16	0.040	0.038	--	--	0.19	0.19	0.12	0.12	--	--
17	--	--	--	--	0.18	0.18	0.11	0.11	--	--
18	--	--	--	--	0.17	0.17	0.085	0.084	--	--
19	--	--	--	--	0.17	0.16	0.065	0.059	--	--
20	--	--	--	--	0.16	0.15	0.044	0.043	--	--
21	--	--	--	--	0.14	0.14	0.032	0.032	--	--
22	--	--	--	--	0.13	0.13	0.024	0.023	--	--
23	--	--	--	--	0.11	0.11	0.015	0.016	--	--
24	--	--	--	--	0.10	0.10	0.011	0.012	--	--
25	--	--	--	--	0.089	0.091	--	--	--	--
26	--	--	--	--	0.080	0.070	--	--	--	--
27	--	--	--	--	0.066	0.062	--	--	--	--
28	--	--	--	--	0.049	0.046	--	--	--	--
29	--	--	--	--	0.037	0.039	--	--	--	--
30	--	--	--	--	0.027	0.029	--	--	--	--
R^2	0.97	0.97	0.93	0.94	0.97	0.98	0.96	0.96	0.97	0.98
$t_{1/2}$ (weeks)	2.59	2.54	2.45	2.47	5.14	5.10	3.37	3.39	2.03	2.02

R^2: Coefficient of regression of the fitting; kinetics of first-order reactions.

$t_{1/2}$: Half-life time.

-- : not detected.

2.2. Detection and Identification of degradation products

MS spectra of indomethacin and some related compounds showed the loss of CO_2, typical from the carboxylic compounds, as well as the $[M-H]^-$ ion and some minor adducts (abundance<0.3%) with components of the mobile phase. The additional loss of a methyl group yielded fragment-ions in those degradation products that kept the indoleacetic acid structure.

The $[M-H]^-$ ion of each degradation product, besides of indomethacin, was isolated and fragmented by collision with nitrogen gas at a given collision energy to generate MS/MS spectra. The molecular formulae of the ions considered as correct were generally those whose experimental error in the exact mass measurement was lower in the list of possible formulae supplied by the software. The molecular formulae of each fragment and the corresponding composition differences with respect to the precursor ion were established. The losses of CH_3 were common in the MS/MS spectra and they were mainly attributed to the cleavage of the CH_3-cycle bond in the C2 carbon atom of the indole ring of the indomethacin and related compounds, providing a methyl radical and the subsequent radical ion; they were also ascribed to the cleavage of the CH_3-O bond in the methoxy group linked to the C5 atom in the indole ring, which resulted in the formation of a conjugated carbonyl in the ring. The breakdown of the pyrrole ring was only seen in the MS/MS spectrum of indomethacin (Fig. S1) while the loss of CO from the chlorobenzoyl structure was observed in indomethacin and DHINDO. The loss of CO_2 was the only fragmentation in the MS/MS spectrum of CBA.

The structures of MMIA (Fig. S2) and CBA (Fig. S3) were unequivocally assigned to the two basic moieties of indomethacin; their origin in water is due to the hydrolysis of the parent compound and they are decomposition products commonly found in pharmaceutical formulations (Krzek and Starek, 2001). The MS/MS spectrum of DHINDO (Fig. S4) showed the loss of water together with other cleavages, which suggested that it was presumably a dihydroxylated compound in which the hydroxyl groups are reasonably bonded to the C6 and C7 carbon atoms in the indole moiety; this assumption is coherent with the number of rings and double bonds and the structures elucidated for the fragment-ions in its spectrum.

The structures of MMIC (Fig. S6) and AMBA (Fig. S7) had already been described in a study about the photodegradation of indomethacin (Temussi et al., 2011). As regards the identification of MMIC, its MS/MS spectrum only supplied two ions: the $[M-H]^-$ and $[M-H-CH_3]^-$ ones. However, it is quite possible that the proposed structure corresponds to that previously characterized due to the importance of the photolysis reactions in which the indomethacin residues are involved.

Finally, CMBA (Fig. S5) is thought to be similar to AMBA by replacing the acetyl substituent linked to the nitrogen atom for a chlorobenzoyl substituent. The fragmentation observed in the spectrum suggested that the methoxy and carboxyl groups were bonded to the benzene ring, in addition to the breakdown of the pyrrole ring.

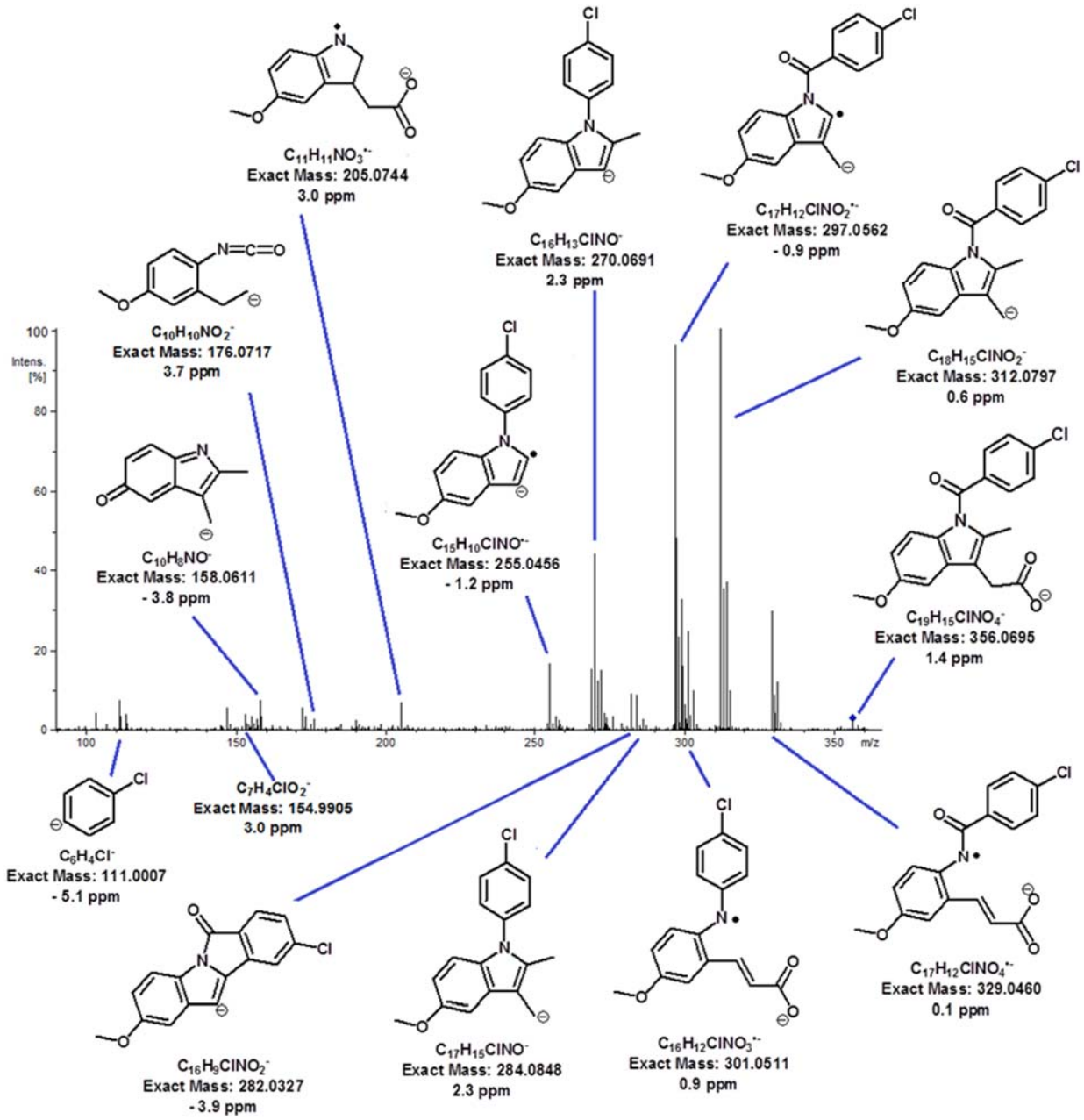

Fig. S1: MS/MS spectrum of indomethacin (INDO). Collision energy: 20 eV. Exact mass and experimental error in the measurement.

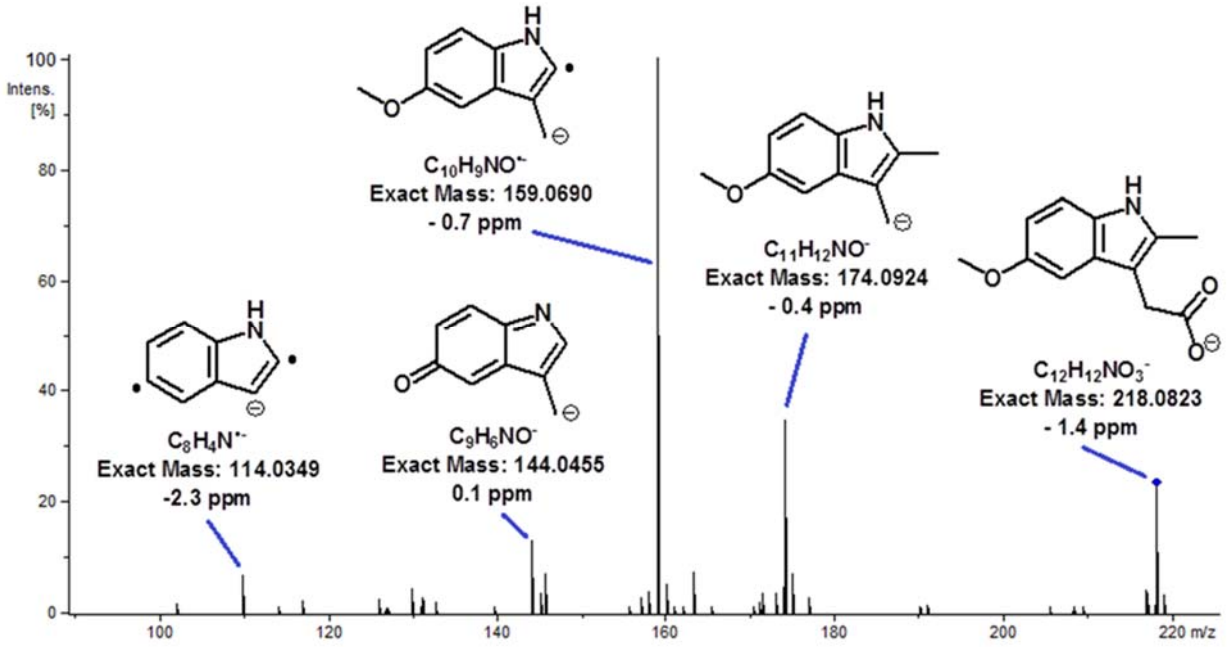

Fig. S2: MS/MS spectrum of 5-metoxhy-2-methyl-1H-indole-3-acetic acid (MMIA). Collision energy: 13 eV. Exact mass and experimental error in the measurement.

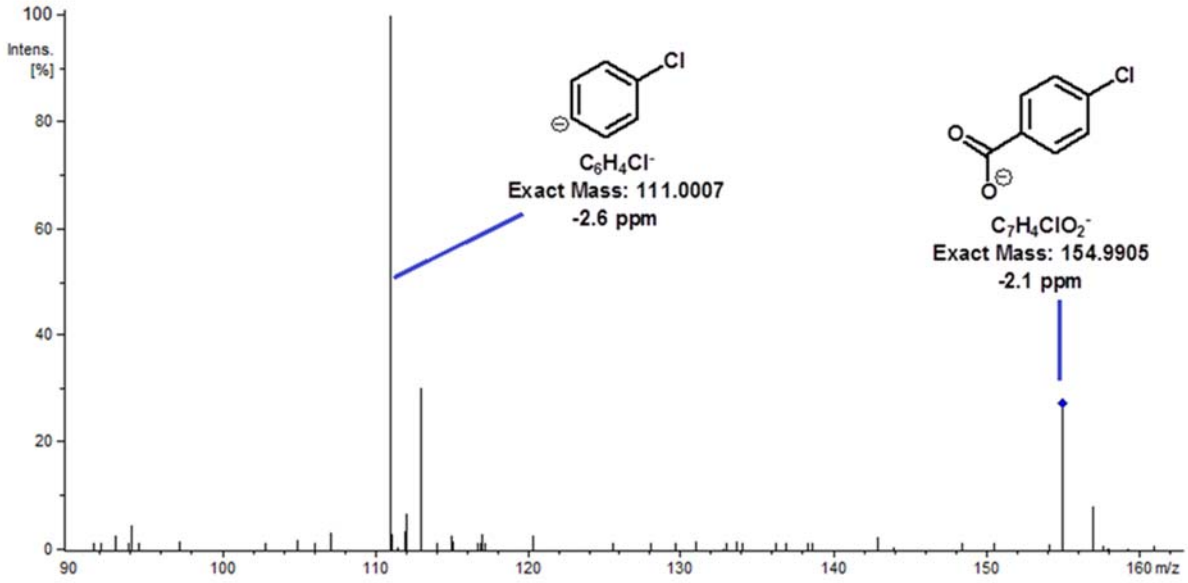

Fig. S3: MS/MS spectrum of 4-chlorobenzoic acid (CBA). Collision energy: 17 eV. Exact mass and experimental error in the measurement.

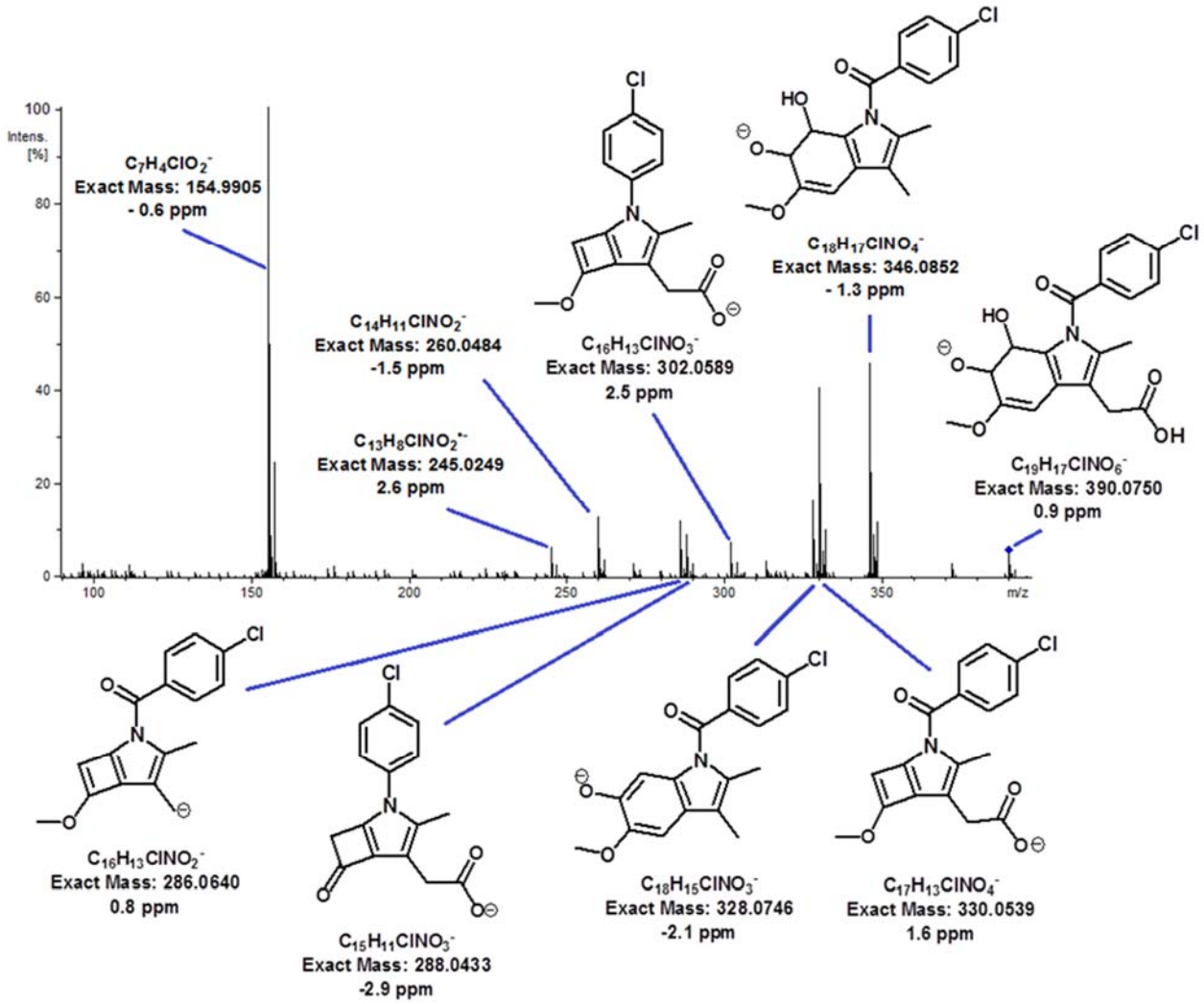

Fig. S4: MS/MS spectrum of 1-(4-chlorobenzoyl)-6,7-dihydro-6,7-dihydroxy-5-methoxy-2-methyl-1H-indole-3-acetic acid (DHINDO). Collision energy: 17 eV. Exact mass and experimental error in the measurement.

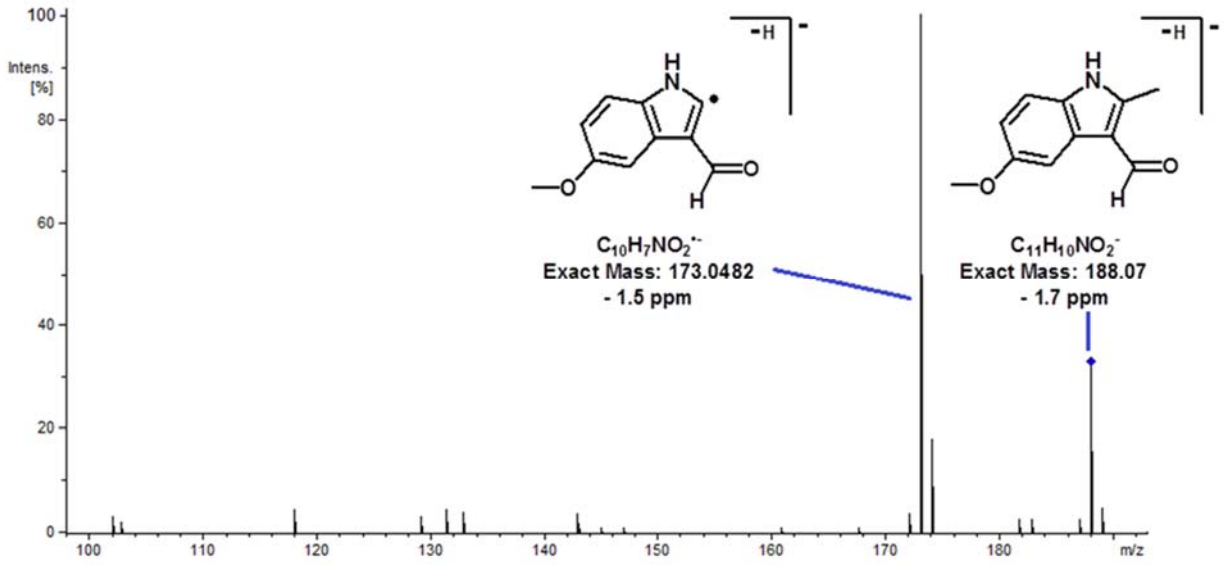

Fig. S5: MS/MS spectrum of 5-metoxhy-2-methyl-1H-indole-3-carbaldehyde (MMIC). Collision energy: 13 eV. Exact mass and experimental error in the measurement.

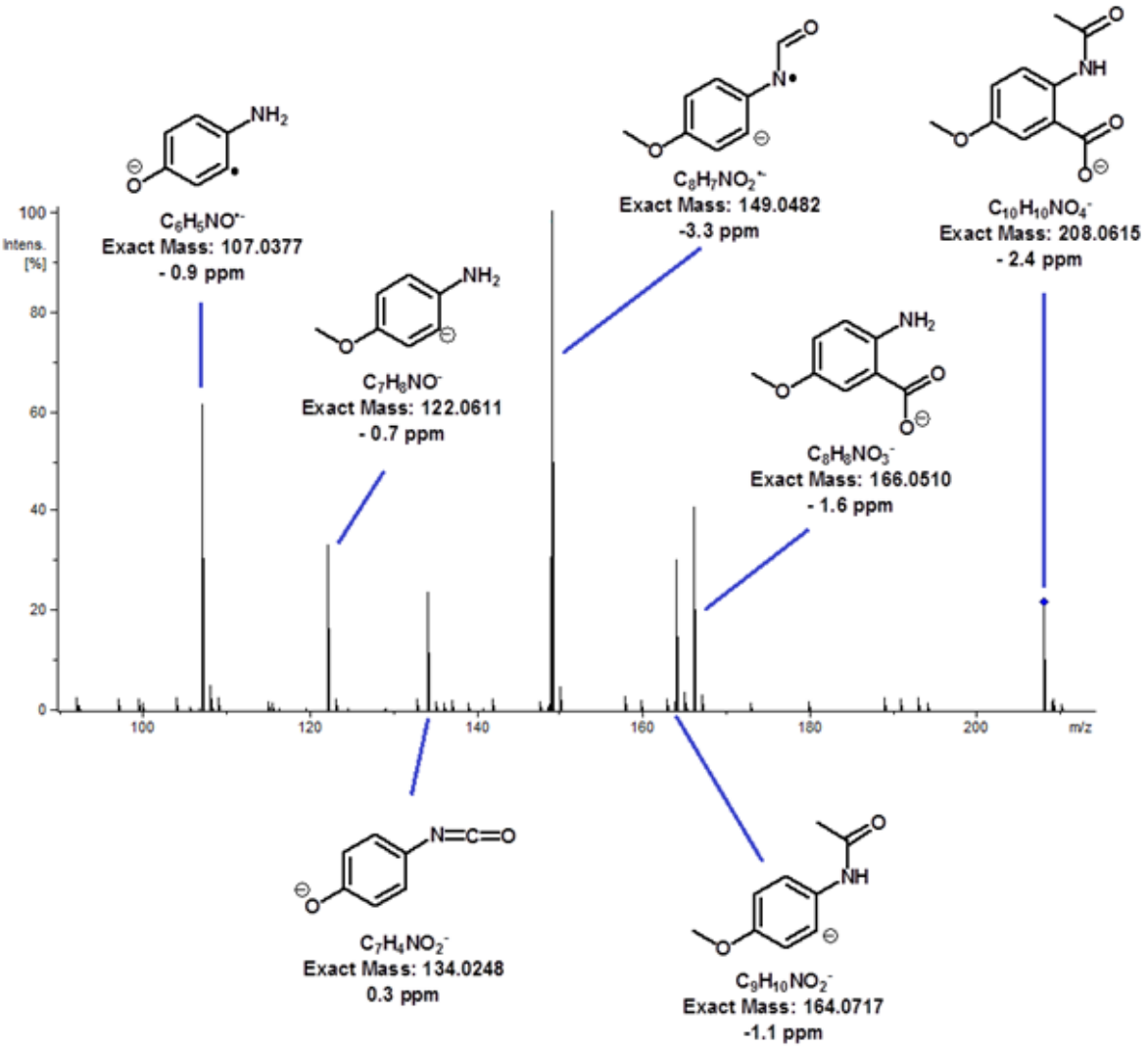

Fig. S6: MS/MS spectrum of 2-acetamido-5-methoxybenzoic acid (AMBA). Collision energy: 17 eV. Exact mass and experimental error in the measurement.

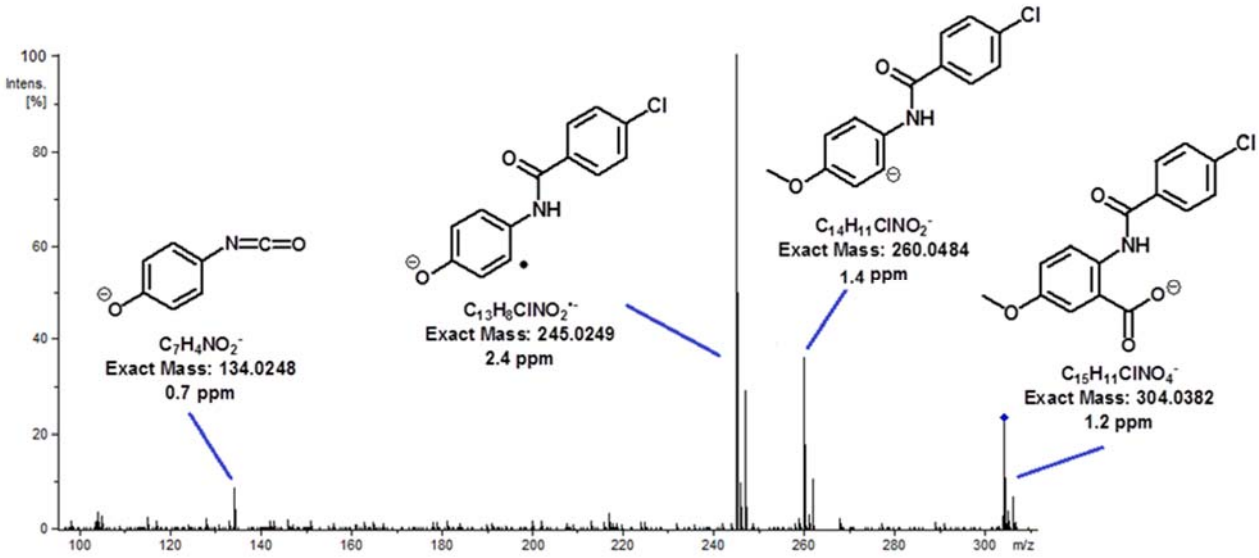

Fig. S7: MS/MS spectrum of 2-(4-chlorobenzamido)-5-methoxybenzoic acid (CMBA). Collision energy: 18 eV. Exact mass and experimental error in the measurement.

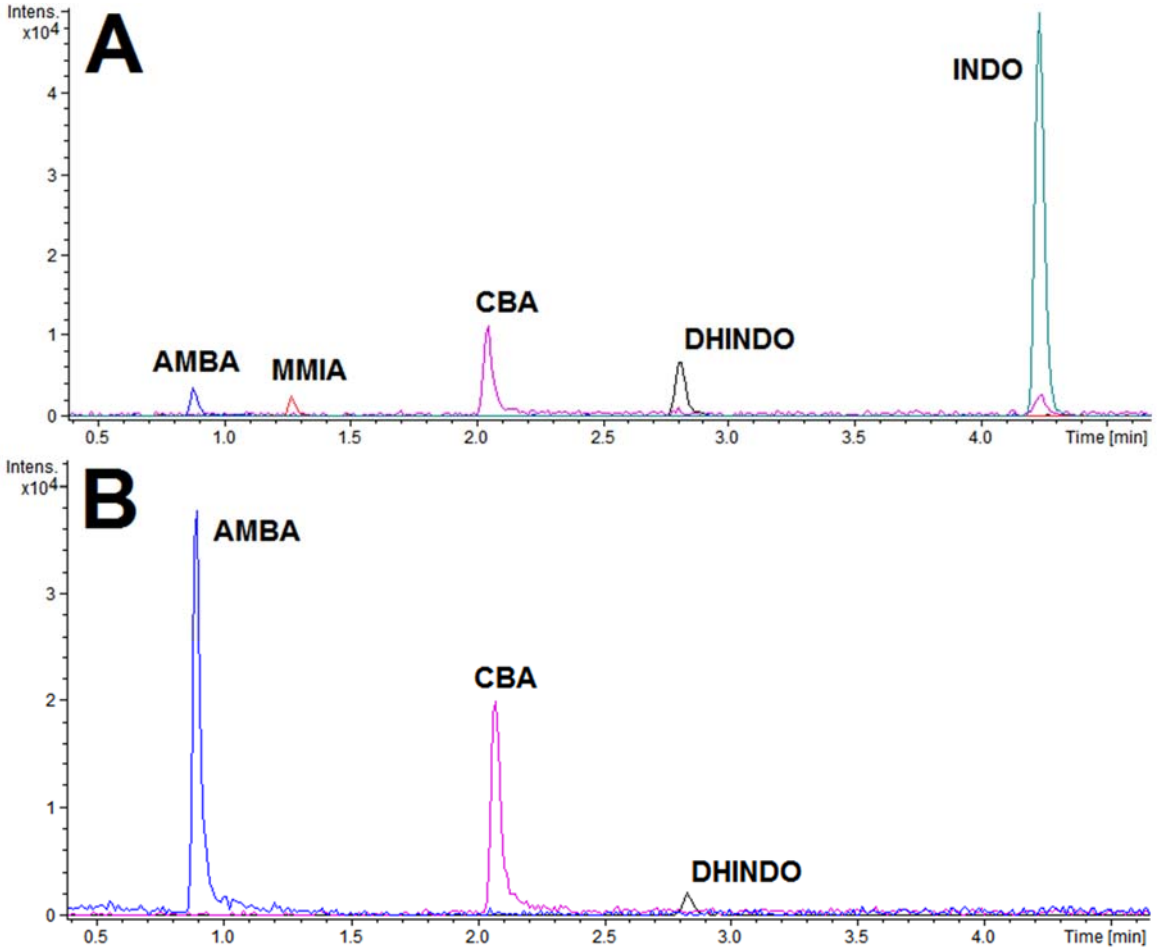

Figure(*): Extracted ion chromatograms ($[M-H]^-$ ± 0.01 Da for all compounds except for indomethacin, $[M-H-CO_2]^-$ ± 0.01 Da) of extracts obtained during the degradation study.

a) After 4 weeks
b) After 21 weeks

(*) not included in the published manuscript

2.3. *Occurrence of degradation products in river water*

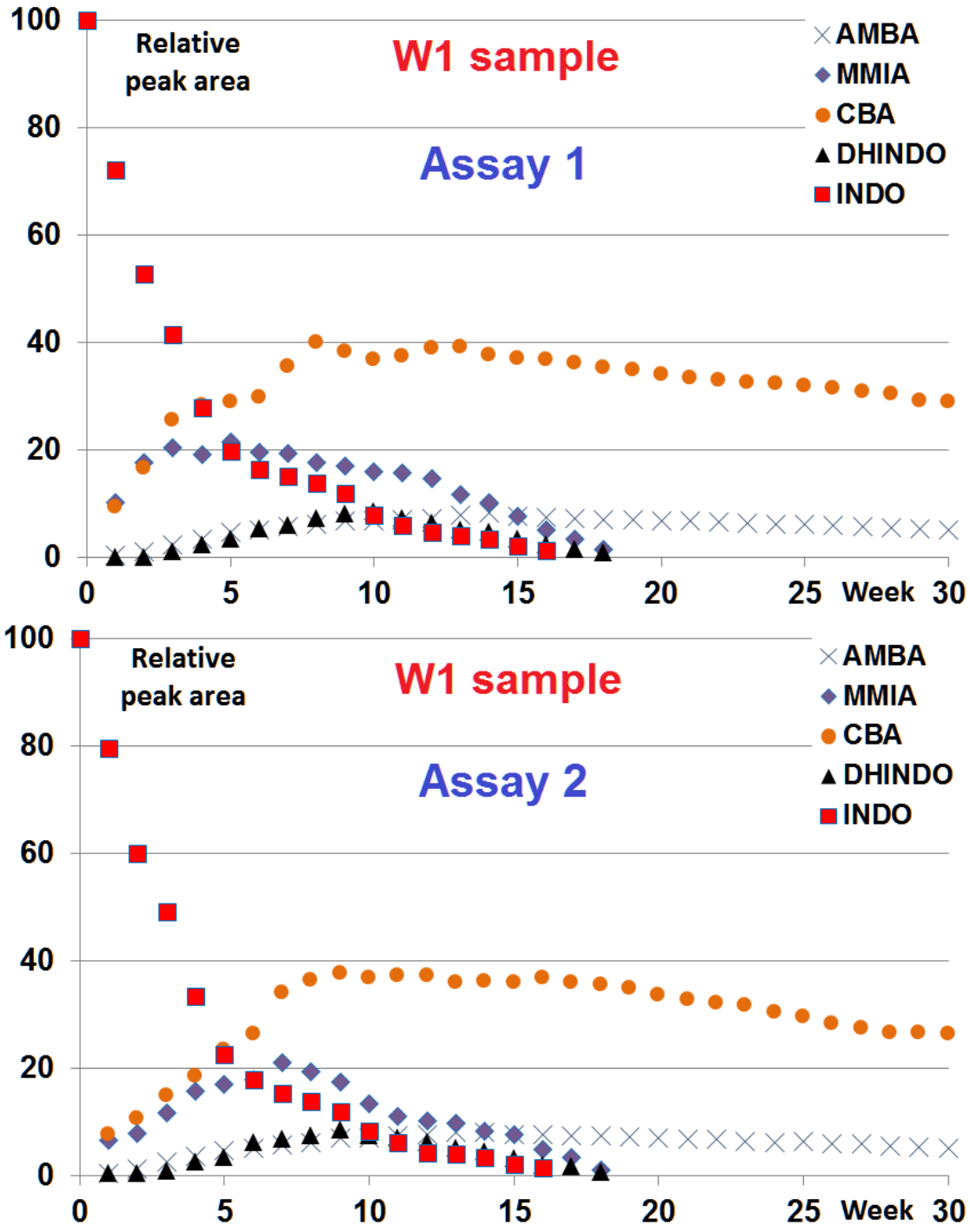

Fig. S8: Variation of peak areas of the degradation products in the W1 sample (room conditions). Peak areas are referred to the initial peak area of INDO in each experiment, to which a value of 100 was assigned. Assays 1 and 2.

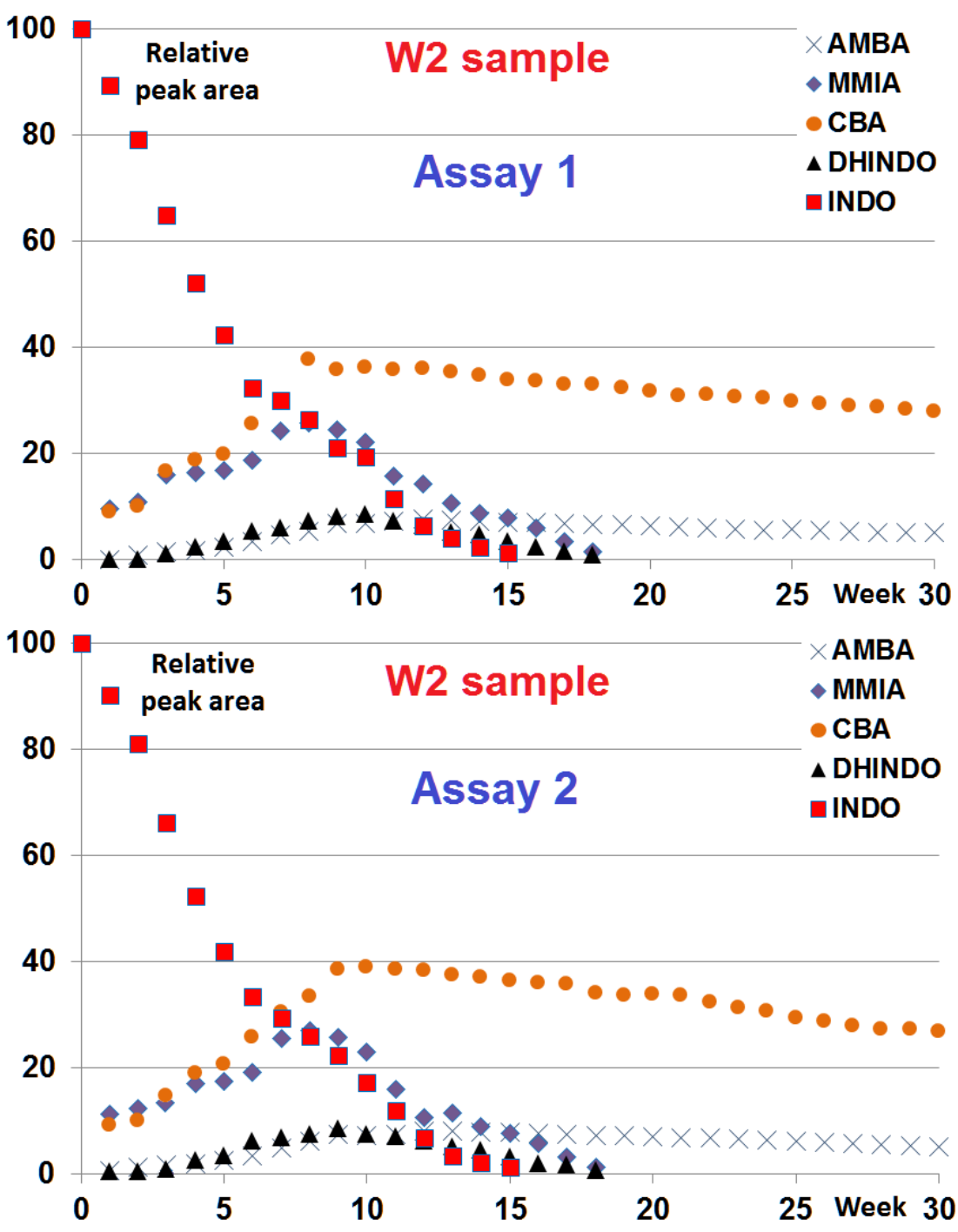

Fig. S9: Variation of peak areas of the degradation products in the W2 sample (room conditions). Peak areas are referred to the initial peak area of INDO in each experiment, to which a value of 100 was assigned. Assays 1 and 2.

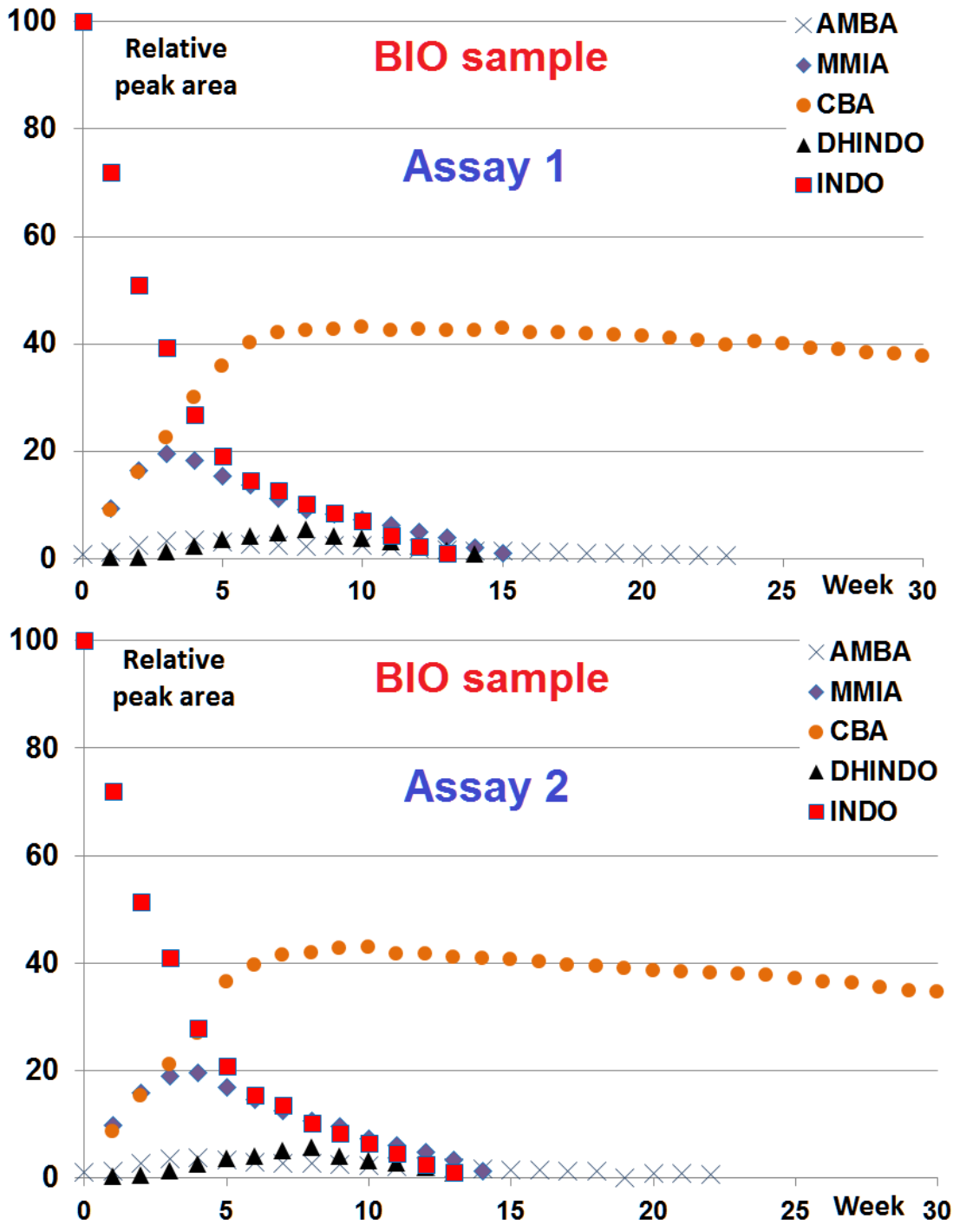

Fig. S10: Variation of peak areas of the degradation products in the BIO sample (room conditions). Peak areas are referred to the initial peak area of INDO in each experiment, to which a value of 100 was assigned. Assays 1 and 2.

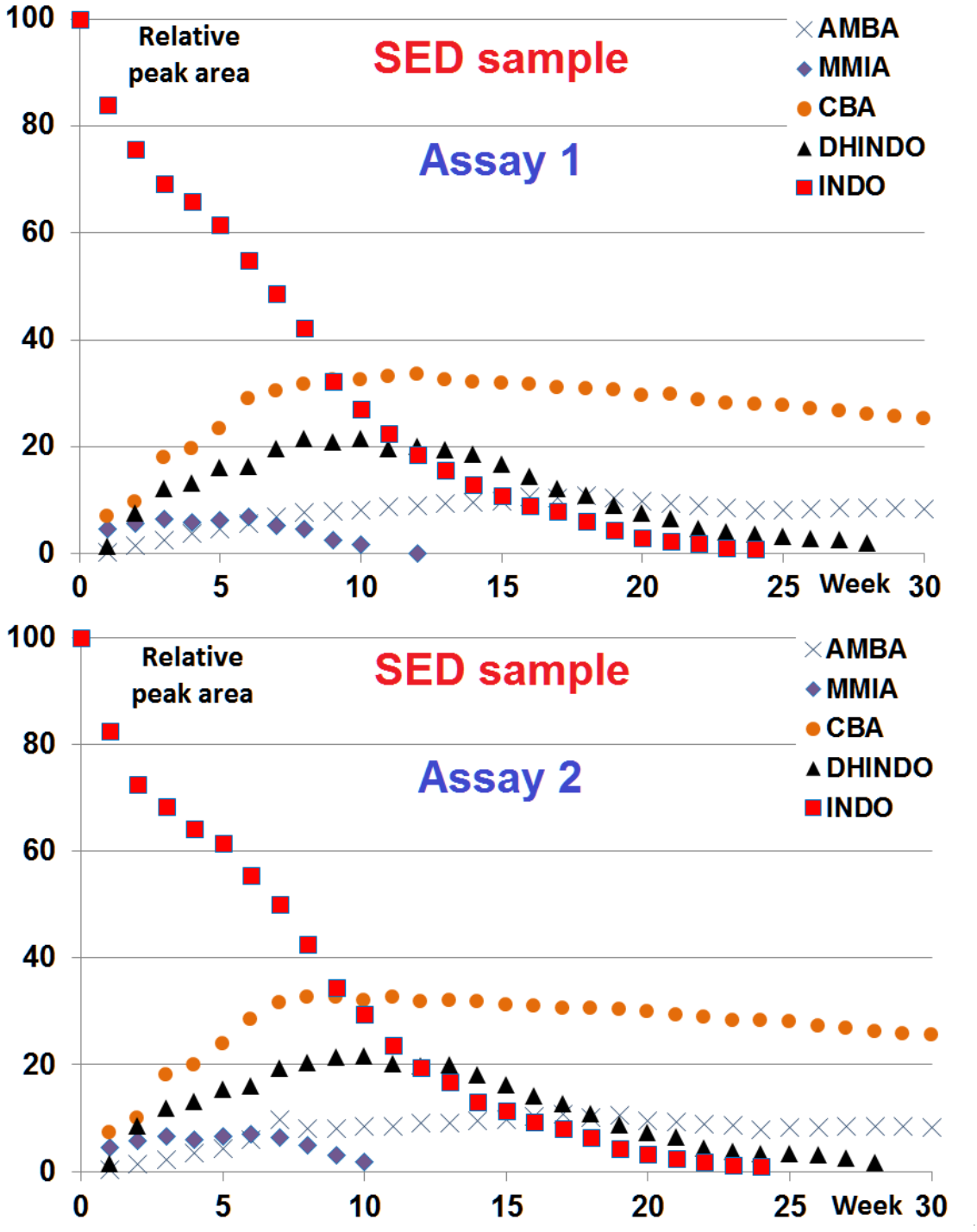

Fig. S11: Variation of peak areas of the degradation products in the SED sample (room conditions). Peak areas are referred to the initial peak area of INDO in each experiment, to which a value of 100 was assigned. Assays 1 and 2.

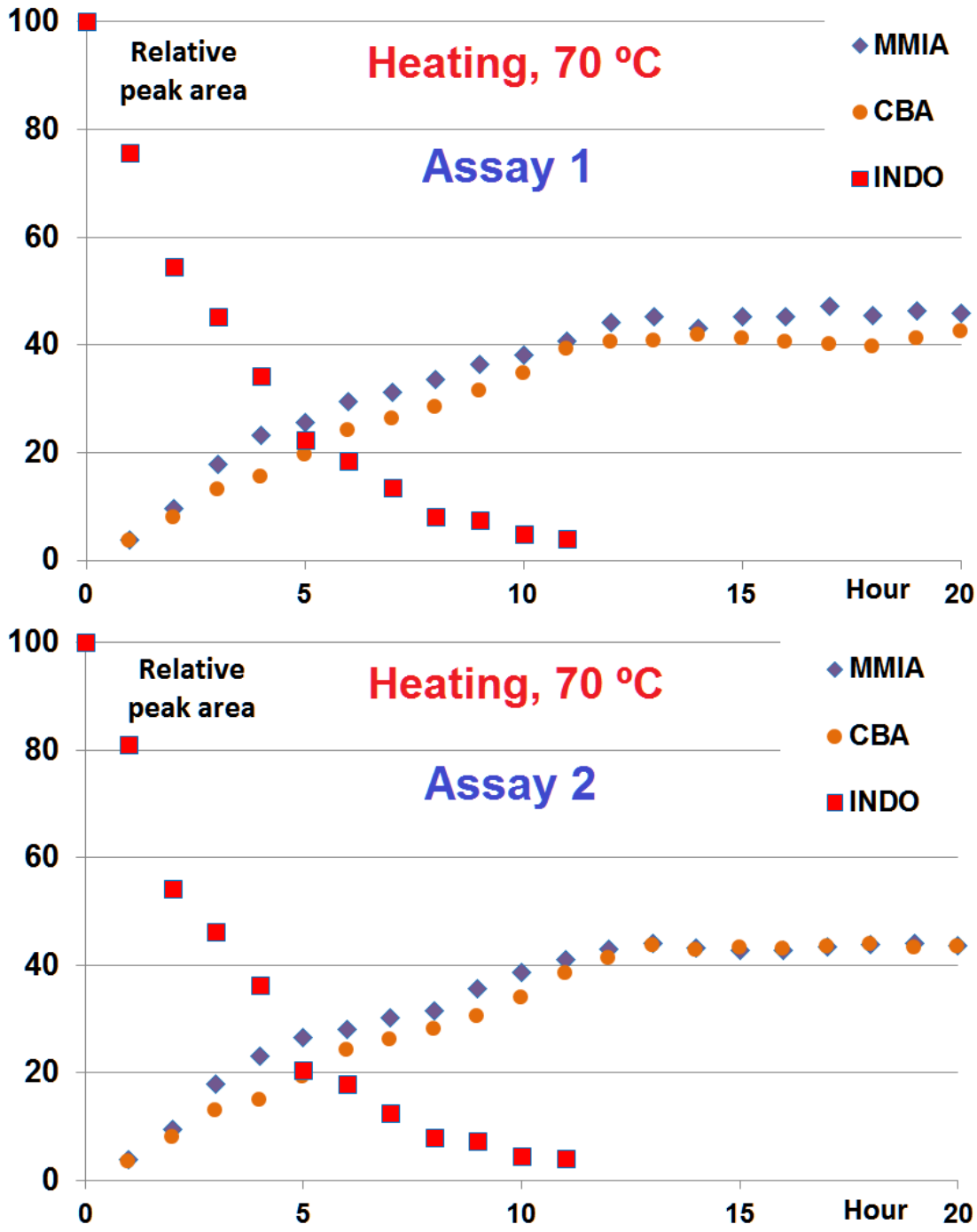

Fig. S12: Variation of peak areas of the degradation products in sample kept at 70 °C. Peak areas are referred to the initial peak area of INDO in each experiment, to which a value of 100 was assigned. Assays 1 and 2

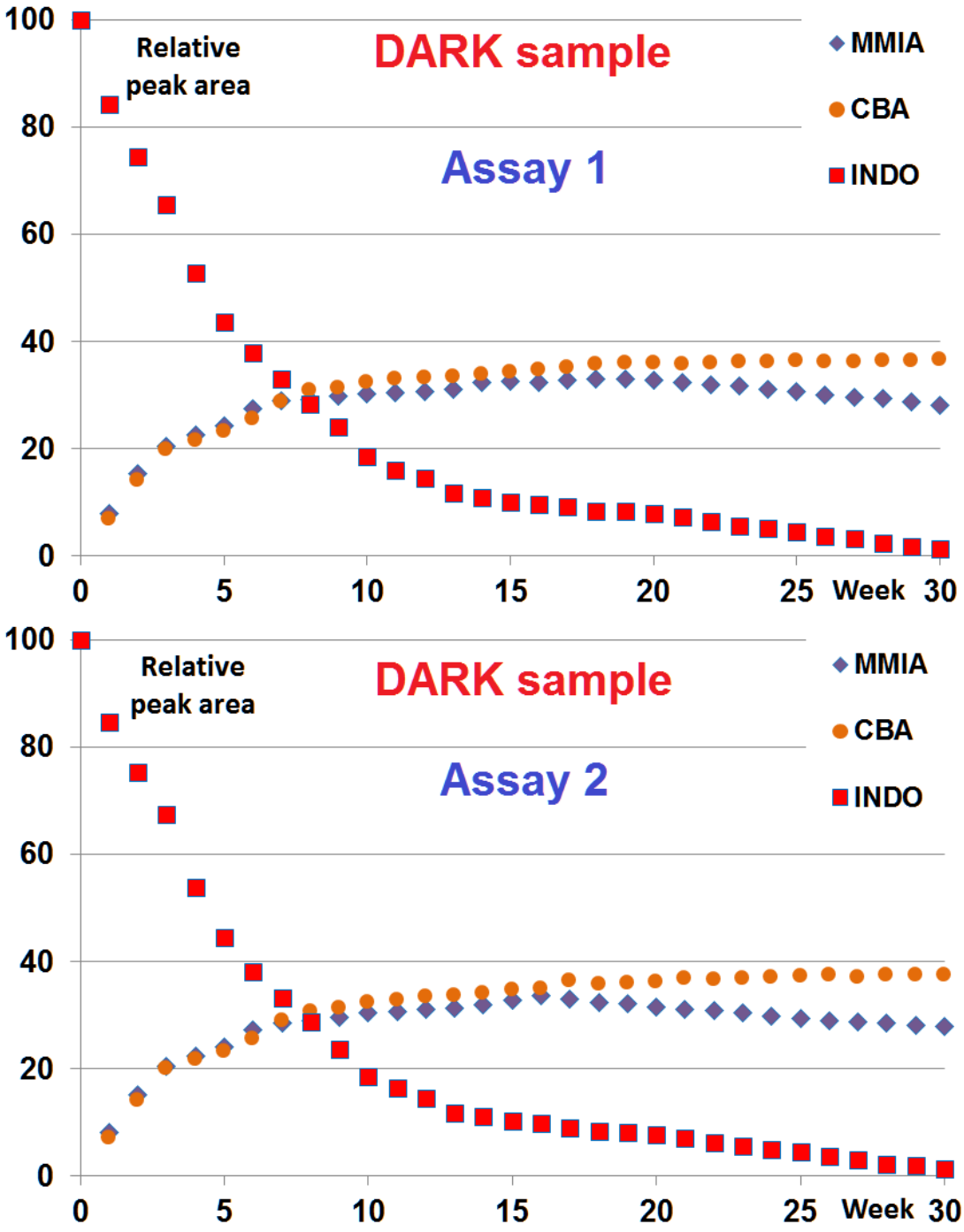

Fig. S13: Variation of peak areas of the degradation products in the DARK sample (room conditions). Peak areas are referred to the initial peak area of INDO in each experiment, to which a value of 100 was assigned. Assays 1 and 2.

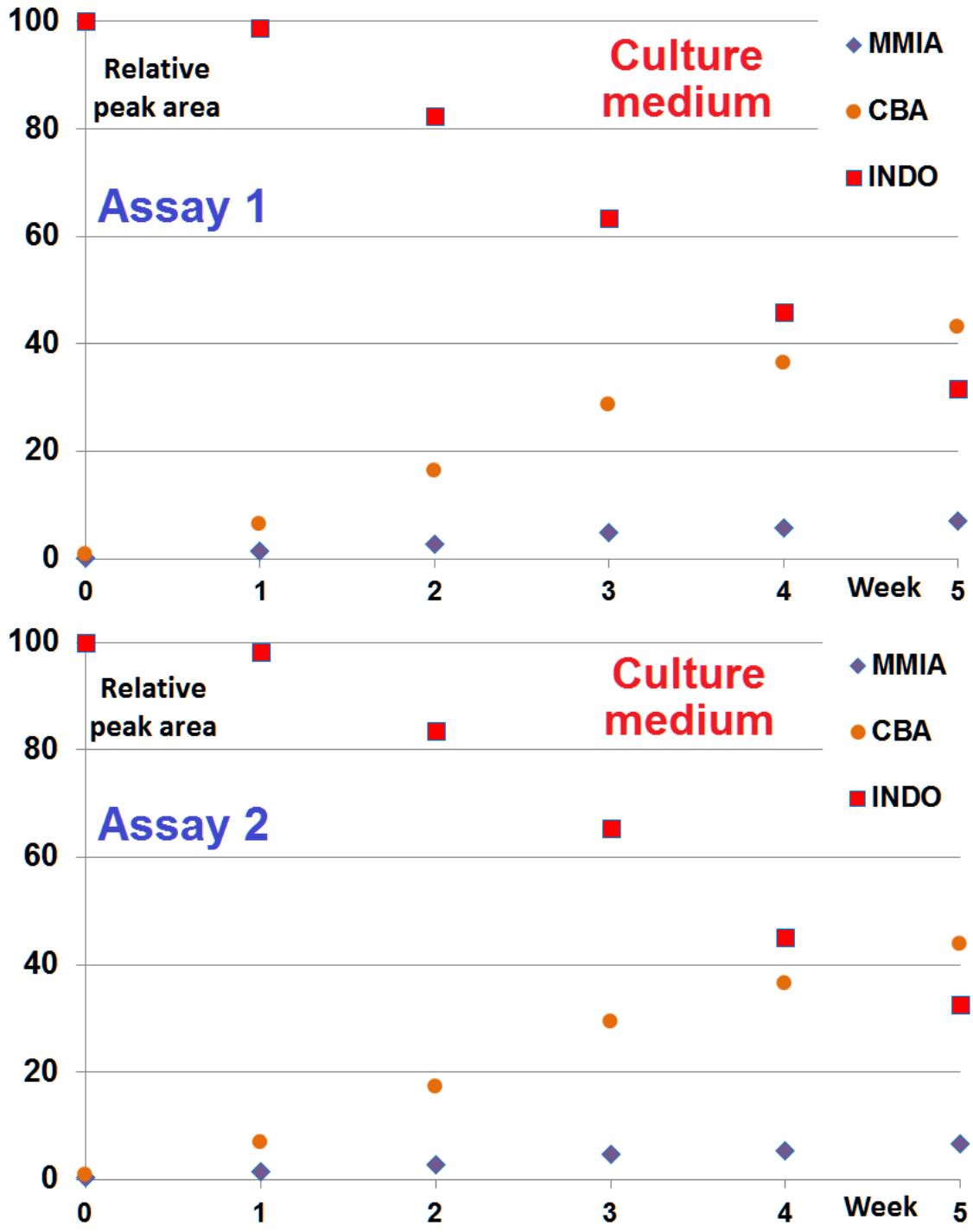

Fig. S14: Variation of peak areas of the degradation products in sample subjected to biological degradation in presence of culture medium. Peak areas are referred to the initial peak area of INDO in each experiment, to which a value of 100 was assigned. Assays 1 and 2.

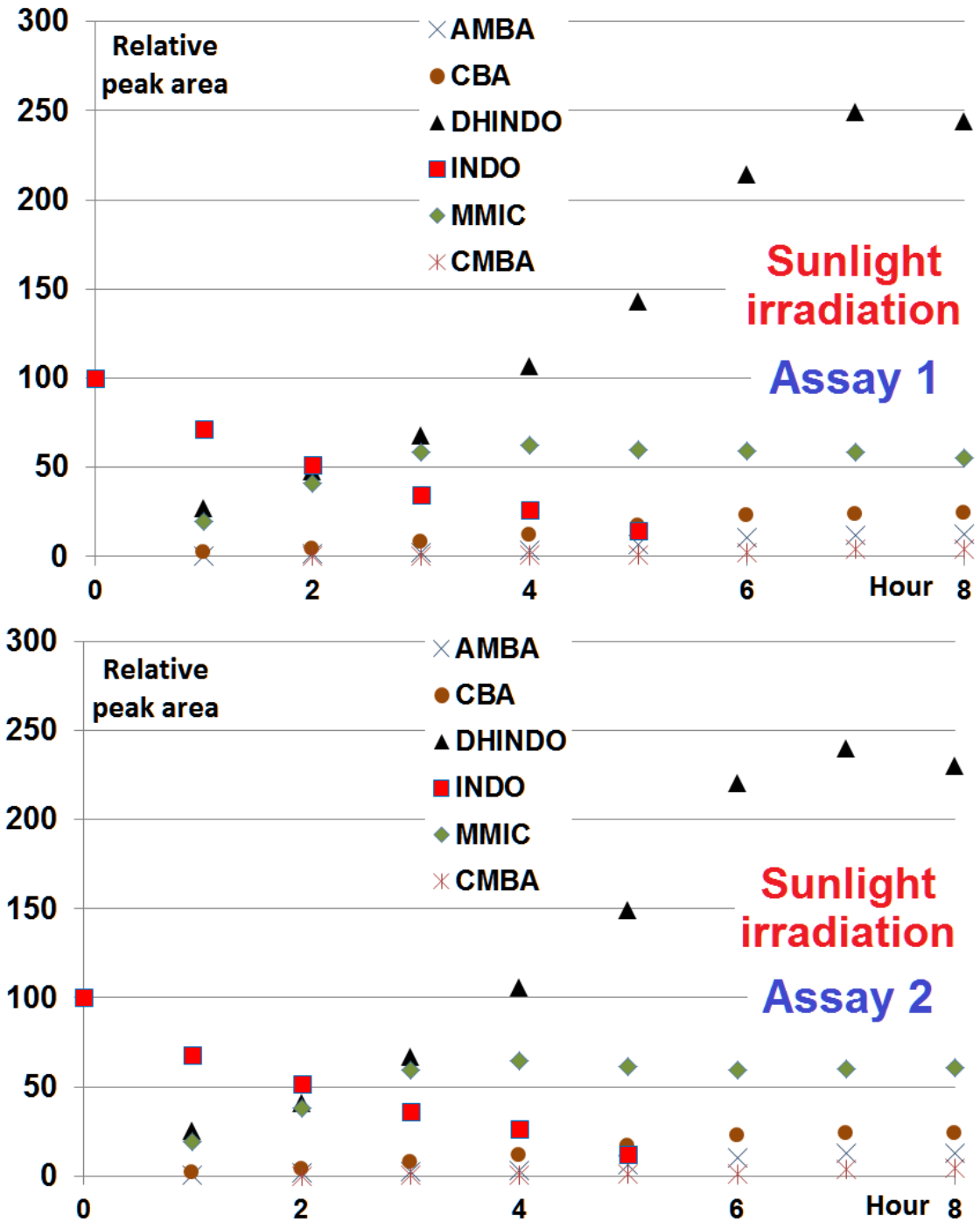

Fig. S15: Variation of peak areas of the degradation products in sample subjected to sunlight irradiation (quartz cuvette). Peak areas are referred to the initial peak area of INDO in each experiment, to which a value of 100 was assigned. Assays 1 and 2.

2.5. *Degradation pathway*

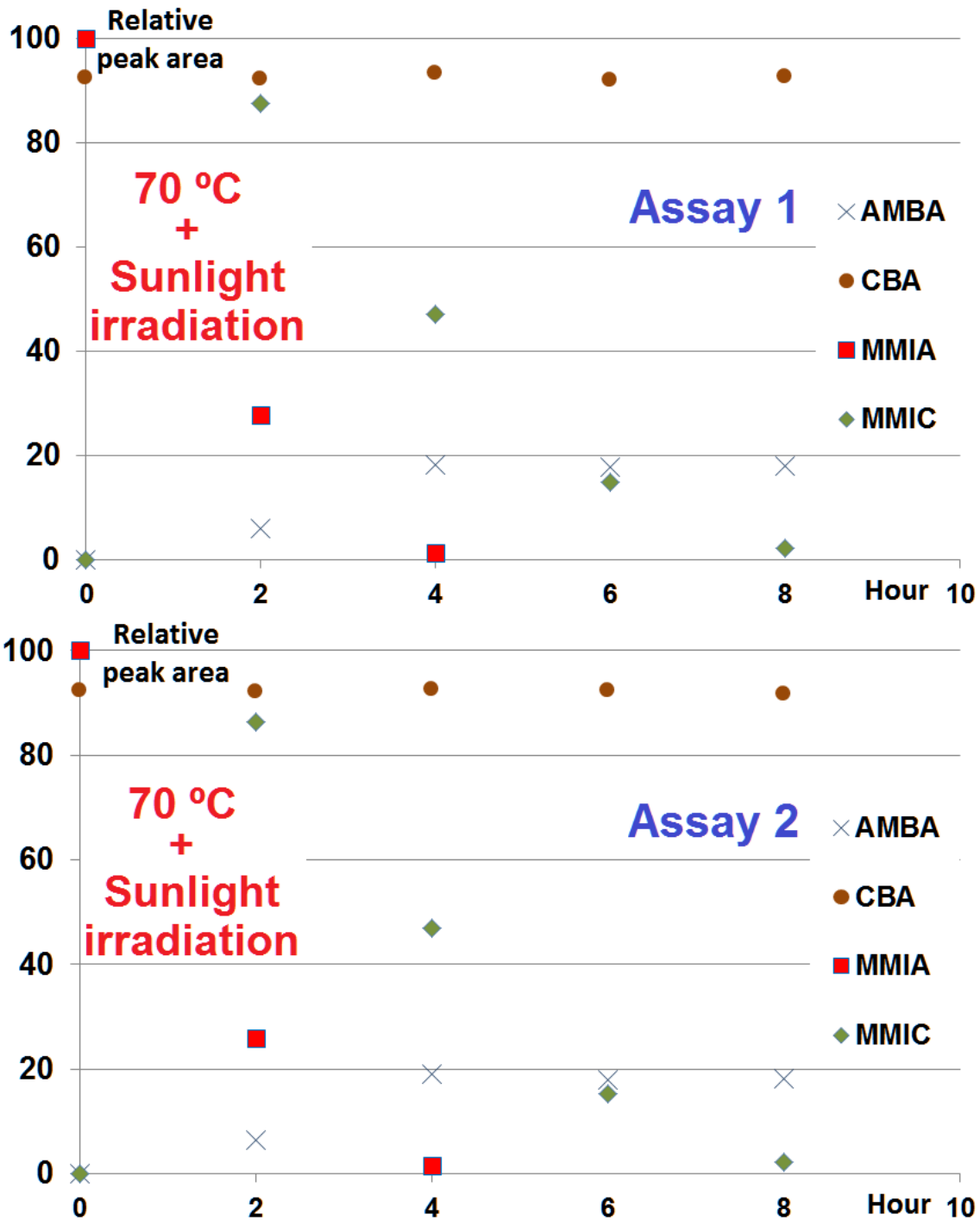

Fig. S16: Variation of peak areas of MMIA and CBA (yielded by heating at 70 °C for 24 h) when exposed to sunlight irradiation (quartz cuvette). Peak areas are referred to the initial peak area of MMIA in each experiment, to which a value of 100 was assigned. Assays 1 and 2.

2.6. Prediction of ecotoxicity.

The possible toxicity of indomethacin and its degradation products at three ecotoxicological endpoints has been estimated by the TEST software (Toxicological Estimation Software Tool), version 4.2, developed by the US Environmental Protection Agency.

Table S6: Predicted 50% lethal concentrations (LC_{50}, μM) and 50% growth inhibition concentrations (IGC_{50}, μM) of indomethacin and degradation products for different tests.

	Daphnia magna LC_{50} (48 hr)	*Tetrahymena pyriformis* IGC_{50}	Fathead minnow LC_{50} (96 hr)
AMBA	794	1862	331
MMIC	51	214	34
MMIA	95	339	34
CBA	661	1585	407
DHINDO	144	144	0.2
CMBA	52	52	3.5
Indomethacin	19	14	1.1

Indomethacin seems more toxic for fathead minnow than *Daphnia magna* and *Tetrahymena pyriformis.* As regards the degradation products, these seem less toxic than the parent compound, with the exception of DHINDO for fathead minnow, which is five-fold more toxic than indomethacin.

4.3. ALPRAZOLAM

Research article

Drug Testing and Analysis

Received: 3 September 2016 Revised: 8 December 2016 Accepted: 13 December 2016 Published online in Wiley Online Library: 10 February 2017

(www.drugtestinganalysis.com) DOI 10.1002/dta.2148

Persistence of alprazolam in river water according to forced and non-forced degradation assays: adsorption to sediment and long-term degradation products

Juan J. Jiménez,[a,b]* María I. Sánchez,[c] Beatriz E. Muñoz[c] and Rafael Pardo[a]

Alprazolam is a pharmaceutical compound that it is detected in surface waters. Some degradation studies in aqueous solutions and pharmaceutical products are available, but there is no reliable information about its stability in river water. Here, assays have been conducted under forced biological, photochemical, and thermal conditions, and under non-forced conditions, to estimate the fate of alprazolam in river water and know its degradation products. The forced assays indicated that the biological and photochemical degradation of alprazolam was negligible; heating at 70°C for a long time barely affected it. The degradation of alprazolam in river water at 100 μg/L was about 5% after 36 weeks, keeping the water under a natural day-night cycle at room temperature and limiting partially the exposure to sunlight as happens inside a body of water; no change in concentration was observed when the monitoring was performed at 2 μg/L. The results suggest the persistence of alprazolam in surface water and a possible accumulation over time. Residues were monitored by ultra-pressure liquid chromatography/quadrupole time-of-flight/mass spectrometry after solid-phase extraction; nine degradation products were found and the structures for most of them were proposed from the molecular formulae and fragmentation observed in high-resolution tandem mass spectra. (5-chloro-2-(3-methyl-4H-1,2,4-triazol-4-yl)phenyl)(phenyl)methanol was the main long-term transformation product in conditions that simulate those in a mass of water. The degradation rate in presence of sediment was equally very low under non-forced conditions; adsorption coefficients of alprazolam and major degradation products were calculated. Copyright © 2016 John Wiley & Sons, Ltd.

Keywords: alprazolam; river water; degradation products; high-resolution mass spectrometry; adsorption coefficient

Introduction

The benzodiazepine alprazolam is a widely prescribed anxiolytic drug; therapeutic doses are lower than 4 mg per day. Commonly, alprazolam is detected in river water at very low concentrations, in the 1–20 ng/L range, regardless of the season of the year.[1–6] The effluents discharged from waste-water treatment plants (WWTPs) are the main introduction source of pharmaceuticals in surface water, which can reach the WWTPs as a consequence of discharges of industrial or hospital waste waters, the inappropriate disposal of unused domestic medicinal products, or the excretion of the pharmaceuticals taken by patients. About 20% of alprazolam is excreted without metabolization in humans.[7]

Alprazolam has been detected in the primary influent that reaches the WWTPs at concentrations in the low ng/L range: 8 and 27 ng/L. The depurated effluents contained concentrations of 5 and 20 ng/L, respectively.[3,5] The efficiency of the WWTPs to remove alprazolam has also been estimated: removal rates of 30–35% were calculated.[3,5] Concentrations of alprazolam of about 1–10 ng/g have been reported in sewage sludge[8,9] while concentrations higher than 100 ng/L have been measured in sewage water from prisons.[7] Likewise, the same as happens for other pharmaceuticals, it has been pointed out that the occurrence of alprazolam is higher in sites downstream from WWTPs where the pattern of contaminants in surface water is similar to that in effluent.[1,3,5] Alprazolam has been detected in tap water, too.[3,5]

The behaviour of alprazolam in aqueous solution has been studied in some works in order to test the stability of some pharmaceutical preparations. Thus, it has been stated that alprazolam is insensitive to acidic or alkaline hydrolysis and that its photodegradation increases as the pH decreases; some degradation products have been found under the assayed stress conditions, too.[10–12]

The frequent detection of pharmaceuticals in surface waters is a matter of increasing concern. Therefore, it is advisable not only to evaluate their persistence but also to know their transformation products for a better understanding of possible risks; the effects caused by exposure to the transformation products are generally different to those of the parent compound.[13,14]

* Correspondence to: Juan J. Jiménez, Department of Analytical Chemistry (UIC090), Faculty of Sciences, Campus Miguel Delibes, University of Valladolid, Paseo de Belén 7, 47011-Valladolid, Spain. E-mail: jjimenez@qa.uva.es

a Department of Analytical Chemistry (UIC090), Faculty of Sciences, Campus Miguel Delibes, University of Valladolid, Paseo de Belén 7, 47011 Valladolid, Spain

b I.U. CINQUIMA, Campus Miguel Delibes, University of Valladolid, Paseo de Belén 5, 47011 Valladolid, Spain

c Department of Analytical Chemistry, School of Industrial Engineers, University of Valladolid, Francisco Mendizábal 1, 47014 Valladolid, Spain

Drug Testing and Analysis

In this context, river water spiked with alprazolam has been subjected to forced degradation studies in this work to ascertain the importance of the chemical, photochemical, and biological processes in its degradation on surface water. Moreover, non-forced degradation assays have been devised to obtain information about its long-term fate in river water. To this aim, river water containing alprazolam was placed in a glass container and exposed to sunlight for several months at laboratory conditions; since the glass partially absorbs the UV radiation, the behaviour of alprazolam is thus comparable to that in a mass of water where the penetration of solar UV radiation is diminished with depth. The non-forced degradation has also been monitored in presence of river sediment to take into account the possible influence of the last. Water aliquots were analyzed by ultra-pressure liquid chromatography/quadrupole time-of-flight/mass spectrometry and the structures of the found degradation products were tentatively elucidated from the molecular formulae and fragmentation observed in high-resolution tandem mass spectra. In addition, the adsorption capacity to sediment of alprazolam and some degradation products has been evaluated by calculating the corresponding adsorption coefficients.

Experimental

Water samples, reagents, and materials

Water samples were collected from the rivers Pisuerga (pH value 7.8, chemical oxygen demand value 4.6 mg/L), in the urban area of the city of Valladolid, and Tuerto (pH value 7.4, chemical oxygen demand value 3.9 mg/L), in the rural area of the La Bañeza, province of León. A sediment sample (total organic carbon 1.2%; clay 11%, silt 44%, sand 45%) was collected from the river Pisuerga. River water was filtered through cellulose nitrate disks (Sartorius, Barcelona, Spain): 0.2 μm pore-size disks for the estimation of adsorption coefficients, 3 μm pore-size disks to carry out biodegradation experiments and 0.45 μm pore-size disks for other degradation experiments.

Alprazolam (99% purity) was purchased from Sigma-Aldrich (St Louis, MO, USA). Methanol, acetonitrile, sodium hydroxide, potassium dihydrogen phosphate, and sodium azide were supplied by Panreac (Barcelona, Spain) and ultrapure water was obtained from a Milli-Q plus apparatus (Millipore, Milford, MA, USA). A lamp equipped with an 8 W UV tube, 29200 model, was obtained from Camag (Muttenz, Switzerland). Tryptone soya broth (TSB), a highly nutrient liquid culture medium for general purpose use, was purchased from Scharlab (Barcelona, Spain) and Oasis HLB cartridges (60 mg) for solid-phase extraction (SPE) were supplied by Waters (Milford, MA, USA).

Biological degradation

Aerobic degradation

Biological degradation assays were done with water from the river Pisuerga (pH 7.8) which was spiked with alprazolam to achieve a concentration of 2 or 100 μg/L. A volume of 50 mL of river water was transferred into a 100 mL Erlenmeyer flask, which was then coated with aluminum foil, including its opening, to avoid the exposure to sunlight but allowing the exchange of air with the atmosphere. An alprazolam control solution was similarly prepared in ultrapure water (pH 7.8 adjusted with NaOH) containing 0.02% (*w/v*) sodium azide as a biocide. Water blanks were prepared, too. Samples were run in parallel; flasks were shaken in a Promax 2020 reciprocating shaker (Schwabach, Heidolph, Germany) at a rotation speed of 130 rpm for 5 weeks, within a temperature range of 18–21°C. Aliquots of 2 mL were collected each week and subjected to the analytical method. Evaporation water losses were periodically restored by addition of water of the same type. All biological experiments were done in duplicate.

Anaerobic degradation

River water (pH 7.8) spiked at 2–100 μg/L was placed in 15 mL vials, completely filled to avoid the presence of air in the headspace. Vials were closed, protected from light by coating them with aluminium foil and kept in a temperature range of 18–21°C during experimentation. Control solutions with alprazolam in ultrapure water (pH 7.8 adjusted) containing 0.02% sodium azide, and the corresponding blanks, were also run in parallel. A batch of vials was assembled to withdraw weekly samples during 5 weeks; a volume of 2 mL of each withdrawn vial was collected for analysis.

Degradation in culture medium

A 20/80 (*v/v*) mixture of TSB culture medium and river water was spiked (2 or 100 μg/L) and a volume of 100 mL of mixture was placed in a 250 mL glass container. A control solution in ultrapure water (pH 7.8 adjusted) containing 0.02% sodium azide and alprazolam, and a blank of the medium-water mixture, were also prepared and run in parallel. Closed vessels were heated at 35°C in darkness for 5 weeks. Aliquots of 4 mL were sampled weekly and filtered through 0.45 μm pore-size cellulose nitrate; 2 mL of filtrate were collected for analysis.

Thermal and photochemical degradation

A volume of 100 mL of river water (pH = 7.8) spiked with alprazolam (2 or 100 μg/L) was placed in a closed 250 mL glass flask. This was coated with aluminium foil and placed in an oven at 70°C. A water blank was heated, too. Aliquots of 2 mL were collected at four and eight weeks and subjected to the analytical method.

River water was placed in quartz cuvettes for photochemical degradation. Closed cuvettes were irradiated at 254 nm with a lamp, or exposed directly to sunlight placing them on the outer edge of a window, south-facing; assay was done in the city of Valladolid (latitude: 41° 38′ 15″N, longitude: 4° 44′ 17″W), in the months of March–April. Water aliquots were withdrawn after four and eight weeks and injected in the chromatographic system. Control samples of alprazolam in river water, protected from radiation with aluminium foil, and a blank were also prepared. All experiments were done in duplicate.

Non-forced degradation assays

A simple approach was adopted to simulate the concurrent natural process in a body of water. River water was placed in a transparent and sodium calcium silicate glass container with air-tight seal, which was shaken and opened weekly to replace the air inside in contact with the water surface. The container was kept at laboratory temperature (18–21°C) under the natural day-night cycle and directly exposed to sunlight for 36 weeks, at which time the degradation assay was ended. In these conditions the solar radiation must pass through the laboratory window glass and the container glass to reach the body of water; glass absorbs UV radiation and the behaviour of alprazolam in the container simulates that in a mass of water where the penetration of solar UV radiation is diminished with depth. The

Drug Testing and Analysis

attenuation of the radiation was estimated by measurements of transmittance through the two types of glass (container and window); so, it was quantified that the percentages of radiation transmitted to the body of water were 40%, 1.3%, 0.02%, 8 10^{-4}%, and 8 10^{-5}% at wavelengths of 350, 320, 310, 305, and 290 nm, respectively.

A volume of 2500 mL of river water placed in glass container was spiked with alprazolam to achieve an initial concentration of 2 or 100 μg/L in each degradation assay; aliquots of 25 mL were collected periodically and subjected to SPE before analysis by the chromatographic system to follow the degradation of alprazolam, look for degradation products. And monitor them. Degradation experiments were done between the months of March and November with waters from the rivers Pisuerga (W1 sample) and Tuerto (W2 sample). Simultaneously, the degradation of W1 sample was also studied in presence of sediment by adding river sediment to the container in a sediment to solution ratio of 0.10 g/mL (SED sample).

It was verified that W1 and W2 river water samples were free of alprazolam residues. First, water blanks were subjected to the analytical method to test the absence of the parent compound. Once known the degradation products yielded in the forced assays it was also tested that they were not present in the water extracts. Similarly, the absence of residues in the sediment sample was confirmed; thus, a portion of sediment was extracted with methanol by mechanical shaking and the extract was concentrated for analysis.

Study of adsorption to sediment

Experiments to investigate the capacity of adsorption of alprazolam and major degradation products were conducted. The adsorption coefficient (K_d) of alprazolam into sediment (sieved through a 0.5 mm mesh) was determined by using a batch approach. Spiked river water (100 mL) was added to sediment (11 g) to achieve a sediment to solution ratio of 0.11 g/mL; alprazolam concentrations were 40, 80, 120, 160, and 200 ng/L. River water contained 0.02% sodium azide as a biocide to minimize a possible microbial activity and pH (7.8) was controlled with phosphate buffer (0.02 M). Control solutions without sediment were prepared, too. The flasks, protected from sunlight with aluminium foil, were manually shaken for 1 min and left standing at 20 ± 1°C for a period of 24 h. Afterwards an aliquot was centrifuged to remove solids, and 20 mL were collected to determine the alprazolam concentration in equilibrium. An adsorption isotherm was drawn in duplicate. The concentration adsorbed on the sediment was not directly measured.

Analytical standards are unavailable for the degradation products, however an estimation of their K_d was carried out on the assumption that there is a linear relationship between peak area and concentration for each compound; degraded solutions of alprazolam were used to this aim. Experiments similar to the above-described were devised by spiking water with a solution containing the degradation products and selecting an appropriate sediment to solution ratio. So, the decrease percentage of peak area in water was supposed to be the percentage of compound adsorbed onto sediment (A%) and K_d was calculated by Eqn (1), which is valid if adsorption equation is linear.[15] Peak areas of the adsorption experiments were compared with those of control solutions by a t-test ($n = 5$) to confirm the existence of differences before applying the equation.

$$\log K_d = \log\left[\frac{A\%/100}{1-(A\%/100)}\right] - \log R \quad (1)$$

Sample preparation

Except for the photochemical degradation assays, river water aliquots were eluted through Oasis HLB cartridges previously conditioned by successive elution of methanol (6 mL) and water (6 mL). Cartridges were washed with 3 mL of a water–methanol (80:20, *v/v*) mixture after sample elution. The stationary phase was dried with air for 3 min and the extract was eluted with methanol (4 mL) by gravity. Then, the extract was evaporated in 30 min by a Myvac vacuum centrifuge evaporator (Genevac, Ipswich, UK) heated at 40°C and the dry residue was collected in 0.5 mL of methanol, which was filtered through a 0.20 μm pore-size PTFE filter for chromatographic analysis.

Determination by liquid chromatography – mass spectrometry

An Acquity ultra-pressure liquid chromatograph from Waters coupled to a Maxis Impact quadrupole time-of-flight tandem mass spectrometer from Bruker Daltonics (Bremen, Germany) was used. Analyses were done with electrospray ionization in positive mode. The chromatograph was fitted with a Waters BEH ODS column (50 mm × 2.1 mm, 1.7 μm particle size). Mobile phase flow rate was 0.5 mL/min and it consisted of 0.1% formic acid in water (A) and 0.1% formic acid in acetonitrile (B); assays were done in gradient conditions: from 10% B to 44% B in 4.5 min, and then 60% B in 1 min. Re-equilibration time was 1 min. Injection volume was 5 μL.

The operation parameters of the electrospray ionization source for the mass spectrometry (MS) and tandem mass spectrometry (MS/MS) experiments were as follows: nebulizing gas pressure, 0.4 bar; end plate offset voltage, −2500 V; capillary voltage, −3500 V; drying gas temperature, 200°C; dry gas flow, 8 L/min. Nitrogen was used as drying and nebulizing gas. Mass calibration adjustments were performed by using a 10 mM sodium formate solution in 2-propanol/water. MS/MS experiments based on collision induced dissociation with nitrogen gas were performed.

In these conditions, the maximum variation of the retention times was within the range of ±0.02 min and the repeatability of the alprazolam peak area (2 μg/L) was lower than 0.8% ($n = 5$), expressed as relative standard deviation. The quantitation of alprazolam was done by linear calibration graphs based on the measurement of peak areas in the chromatograms extracted for the ion $[M + H]^+$ generated in the electrospray source by MS experiments, with a mass range of ±0.01 Da; similarly, peak areas of degradation products were integrated in the chromatograms extracted for the corresponding $[M + H]^+$ ions. The calibration graphs drawn with standards of alprazolam dissolved in methanol were linear in the concentration range comprised between 0.5 and 20 μg/L. The fitting of the linear regression had a coefficient of determination R^2 of, at least, 0.997. An ANOVA was done to verify the linearity of the fitting ($n = 3$), evaluating the lack of fit: the experimental F-value (0.03) was lower than the critical F-value (2.96, $p = 0.05$) which indicated that there was not lack of fit. The limits of detection and quantification were estimated on the basis of a signal-to-noise ratio of 3 or 10, they resulted to be about 0.20 and 0.50 μg/L, respectively. As regards the performance of the analytical method, mean recoveries of alprazolam in W1 sample volumes of 2 or 25 mL were about 97% with repeatabilities close to 3.0% and 1.4% ($n = 5$) for 2 and 100 μg/L, respectively. A dilution of the extracts was required to quantify alprazolam in the assays at high concentrations.

Drug Testing and Analysis

Results and discussion

Degradation of alprazolam

Table 1 resumes the results of the degradation assays. Individual concentration data of the different assays are supplied as supplementary material. An independent samples t-test (p = 0.05) was used to compare the concentrations measured at the beginning and end of the assays (n = 5), after checking the homogeneity of the variances which resulted to be homogeneous. Alprazolam was found to be basically resistant to biological degradation in river water at the two assayed concentrations, no significant differences were observed in the aerobic and anaerobic assays carried out on unaltered river water. Only a very small decay in concentration was observed in the experiments at 100 μg/L after 5 weeks in the presence of a culture medium, about 3.6% in relation to the initial concentration. In this case, the t-test only evinced significant difference between the initial and final concentrations in one of the two experiments carried out with the culture medium (Tables S1–S3).

Table 1. Initial and final mean concentrations (n = 5) of alprazolam in the different degradation assays, and time at which the final concentration was measured

Degradation	Assay	Initial concentration	Final concentration	Elapsed time
		(μg/L)	(μg/L)	(weeks)
Aerobic	1	2.04	2.02	5
	2	2.01	2.01	5
Aerobic	1	101.6	102.0	5
	2	101.0	99.6	5
Anaerobic	1	1.99	1.99	5
	2	2.01	1.99	5
Anaerobic	1	102.0	100.2	5
	2	100.6	100.0	5
Culture medium	1	2.00	2.02	5
	2	2.01	2.00	5
Culture medium	1	99.8	95.2**	5
	2	99.2	96.6	5
Photochemical, sunlight	1	2.00	1.99	8
	2	2.01	2.00	8
Photochemical, sunlight	1	100.8	100.8	8
	2	99.0	98.2	8
Photochemical, UV lamp	1	1.98	2.00	8
	2	2.01	1.98	8
Photochemical, UV lamp	1	100.8	99.6	8
	2	100.2	98.6	8
Thermal	1	1.99	1.97	8
	2	2.00	1.99	8
Thermal	1	100.0	96.8**	8
	2	99.8	96.8**	8
Non-forced, W1	1	1.98	1.97	36
	2	2.01	1.99	36
Non-forced, W1	1	100.8	95.6**	36
	2	99.6	94.8**	36
Non-forced, W2	1	2.01	1.99	36
	2	1.99	2.00	36
Non-forced, W2	1	99.0	94.2**	36
	2	100.2	95.4**	36
Non-forced, SED	1	1.43	1.41	36
	2	1.44	1.43	36
Non-forced, SED	1	70.2	67.0**	36
	2	69.8	66.6**	36

**Significant difference (p = 0.05).

As regards the photochemical degradation, the exposure of alprazolam in river water to sunlight or radiation arisen from a lamp (centred at 254 nm), for 8 weeks in both cases, did not modify its initial concentration (2 or 100 μg/L) which suggests that alprazolam is not amenable to photochemical degradation in surface water with slightly alkaline pH. On the contrary, significant differences (p = 0.05) in concentration were found in the thermal degradation assays on water spiked at 100 μg/L, although the decrease of initial concentration was scarce, about 3.1% after keeping at 70°C the alprazolam solution in river water. No significant differences were noted at the low concentration, 2 μg/L, either (Tables 1 and S4-S6). The influence of the chemical reactions in aqueous medium at alkaline pH seems to be a factor more important than the photochemical reactions in the long-term fate of alprazolam in river water.

Degradation assays of alprazolam under non-forced conditions were devised, too; they were done with water samples from two rivers. When waters were spiked with 2 μg/L the concentration of alprazolam was not modified during the experimentation period, 36 weeks, while some degradation was observed in the assays at 100 μg/L as it was confirmed by a t-test (Tables S7 and S8). Therefore, in this last case, the decrease of alprazolam concentration after 36 weeks was estimated to be about 5.0% and 4.8% in W1 and W2 samples, respectively. Assays in presence of aquatic sediment were also carried out to know its possible influence in the degradation; the concentrations measured were now lower and revealed that alprazolam has a certain capacity of adsorption onto sediment. In low concentration assays, the initial concentration did not differ with respect to the final concentration as it happened previously. Alprazolam at 100 μg/L was degraded in an amount similar to the above-mentioned assays without sediment, a 4.6% for the two water samples (Table S9); there were significant differences between the initial and final concentrations by applying a t-test (p = 0.05). It is also remarkable that a smelly odor began to be perceived in the glass containers with sediment after a few weeks, which denoted a possible growth of microorganisms in presence of sediment and the subsequent biodegradation process of the organic matter; alprazolam was not affected by this biodegradation process.

The results of these experiments suggest that alprazolam is an extremely persistent drug inside a body of water. Alprazolam seems to be a non-biodegradable compound in presence of the nutrients and conditions commonly existing in a river and, furthermore, it is minimally affected by the UV radiation that could reach the mass of water. Only the chemical reactions in aqueous solution alter it but their reaction rate is very slow at environmental temperatures, which is coherent with the previously reported stability against hydrolysis reactions[10]; the influence of these chemical reactions in aqueous solution can be noticed, exclusively, in the very long-term.

Alprazolam is a relatively stable benzodiazepine in comparison with other pharmaceutical drugs, and human metabolites, of the same family according to the results of some forced assays reported on several aqueous matrixes. Thus, the half-life of alprazolam in solution was notably higher than those of diazepam, oxazepam, nordiazepam, temazepam, and mainly midazolam and lorazepam, when they were irradiated with simulated sunlight,[16–19] which is coherent with the stability observed for alprazolam in the

photodegradation assays carried out in this work. In the same way, although the different assays are not totally comparable, it can be stated that the acidic or alkaline hydrolysis of lorazepam, oxazepam, diazepam and bromazepam is easier than for alprazolam[12,20–25]; conversely, midazolam and clonazepam seem to be more resistant to hydrolysis than alprazolam.[20,26,27] Regarding the biological degradation, it has been reported that diazepam is not biotransformed by bacterio-plankton either in river water or in bacterial liquid cultures from amended soil[28,29]; temazepam was also stable in the bacterial culture while ozaxepam underwent a partial biotransformation, about 40%.[29] There were no previous data for alprazolam.

Alprazolam is consumed at relatively low dosages and small concentrations (lower than 0.5 μg/L) are detected in surface waters; however, its persistence in them can favour a progressive accumulation over time. The concentration levels currently found are not harmful to *Daphnia magna* and *Ceriodaphnia dubia,*[30] and in agreement with the TEST software (Toxicity Estimation Software Tool) developed by the US Environmental Protection Agency, there is no risk for cyprinids such as the fathead minnow. The TEST software predicts the toxicity of an organic compound for an ecotoxicological endpoint by using quantitative structure activity relationships (QSARs) methodologies, and for fathead minnow it foresees a 50% lethal concentration (in 96 h) of 60 μg/L, away from the alprazolam concentrations detected nowadays.

Finally, as it was already stated, significant differences in the concentration of alprazolam were never seen at the lowest assayed concentration, 2 μg/L. This fact was attributed to the minimum concentration differences that very likely take place as consequence of the low degradation rate of alprazolam, and to the worse repeatability of the analytical method at low concentration.

Identification of degradation products

Nine degradation products were found during the experimentation. The presence of compounds related to the degradation of alprazolam was established by the observation of new chromatographic peaks in the MS chromatograms, which were not present in blanks. The $[M + H]^+$ ion of each degradation product, besides of alprazolam, was isolated and fragmented by collision-induced dissociation to obtain structural information and propose tentative structures from the interpretation of the fragment-ions in MS/MS spectra. Table 2 shows the established molecular formulae, the proposed identifications and the abbreviations of the compounds.

The fragmentation patterns of the degradation products in the MS/MS spectra were similar to that of alprazolam ($C_{17}H_{14}ClN_4^+$); in general terms, they involved the cleavage of the seven-membered ring of the benzodiazepine, which is not very stable, to yield ions with a triazoloquinoleine or indole structure. Moreover, it was frequent the loss of HCN or other nitrogen compounds, which affected the triazolo substituent.

Three compounds (DP327–1, DP327–2, DP327–3) showed a protonated molecular ion at *m/z* 327 ($C_{17}H_{16}ClN_4O^+$), this indicated the addition of H_2O to the alprazolam structure and the decrease of a unit in the number of rings and double bonds (RDBs). The structures and fragmentations of these compounds could be successfully explained after considering a nucleophilic addition reaction of H_2O to a double bond of the benzene rings of the alprazolam. The resonance contributors predict that the electrophilic carbons are placed in C2′ and C4′ sites (ortho and para positions) of the phenyl substituent and C10 carbon atom (ortho position) of the benzodiazepine group, therefore the hydroxyl should be preferentially linked to these sites. Figure 1 shows the corresponding MS/MS spectra. A more complete interpretation of the fragment-ions for all MS/MS spectra can be seen in supplementary material (Figures S1–S4).

DP327–1 and DP 327–2 had ions at m/z 309 and 282 that indicated the loss of H_2O and H_2O + HCN, respectively. The loss of water, and the number of RDBs of these ions, suggested the presence of a hydroxyl group in the precursor compound at a position prone to form a cyclic structure by elimination of H_2O. The interpretation of the oxygen-containing fragments at m/z 232 and 269 in the spectrum of DP327–1 lead to identify this

Table 2. Retention times (RT), accurate masses measured in the MS spectra for the $[M + H]^+$ ion, errors in the determination of the exact masses, molecular formulae and number of rings and double bonds (RDBs) of the corresponding structures for the detected degradation products

RT (min)	Molecular formula	Exact mass (Da)	Accurate mass (Da)	Error (ppm)	RDBs	Compound	Abbreviation
1.74	$C_{17}H_{16}ClN_4O$	327.1007	327.1005	0.6	11.5	9,10-Dihydro-8-chloro-10-hydroxy-1-methyl-6-phenyl-4H-[1,2,4] triazolo[4,3-a] [1,4]benzodiazepine	DP327–1
1.97	$C_{17}H_{16}ClN_4O$	327.1007	327.1005	0.6	11.5	8-Chloro-1-methyl-6-(5′-hydroxycyclohexa-1′,3′-dienyl)-4H-[1,2,4] triazolo[4,3-a] [1,4]benzodiazepine	DP327–2
2.30	$C_{17}H_{16}ClN_4O$	327.1007	327.1007	0.0	11.5	8-Chloro-1-methyl-6-(4′-hydroxycyclohexa-1′,5′-dienyl)-4H-[1,2,4] triazolo[4,3-a] [1,4]benzodiazepine	DP327–3
2.44	$C_{17}H_{14}ClN_4O$	325.0851	325.0850	0.3	12.5	Not identified	DP325–1
2.86	$C_{17}H_{14}ClN_4O$	325.0851	325.0852	-0.3	12.5	Chloro-1-methyl-x-hydroxy-6-phenyl-4H-[1,2,4]triazolo[4,3-a] [1,4] benzodiazepine	DP325–2
2.97	$C_{17}H_{14}ClN_4O$	325.0851	325.0851	0.0	12.5	8-Chloro-1-methyl-6-phenyl-4H-[1,2,4]triazolo[4,3-a] [1,4] benzodiazepine-4-ol	DP325–3
3.29	$C_{16}H_{15}ClN_3O$	300.0898	300.0900	-0.7	10.5	(5-chloro-2-(3-methyl-4H-1,2,4-triazol-4-yl)phenyl)(phenyl)methanol	DP300
3.78	$C_{16}H_{13}ClN_3O$	298.0742	298.0749	-2.0	11.5	5-chloro-2-(3-methyl-4H-1,2,4-triazol-4-yl)benzophenone	DP298
3.84	$C_{17}H_{14}ClN_4$	309.0902	309.0899	1.0	12.5	8-Chloro-1-methyl-6-phenyl-4H-[1,2,4]triazolo[4,3-a] [1,4] benzodiazepine (alprazolam)	Alprazolam
4.11	$C_{17}H_{14}ClN_4O$	325.0851	325.0853	-0.6	12.5	8-Chloro-1-methyl-6-(4′-hydroxy-phenyl)-4H-[1,2,4]triazolo[4,3-a] [1,4] benzodiazepine	DP325–4

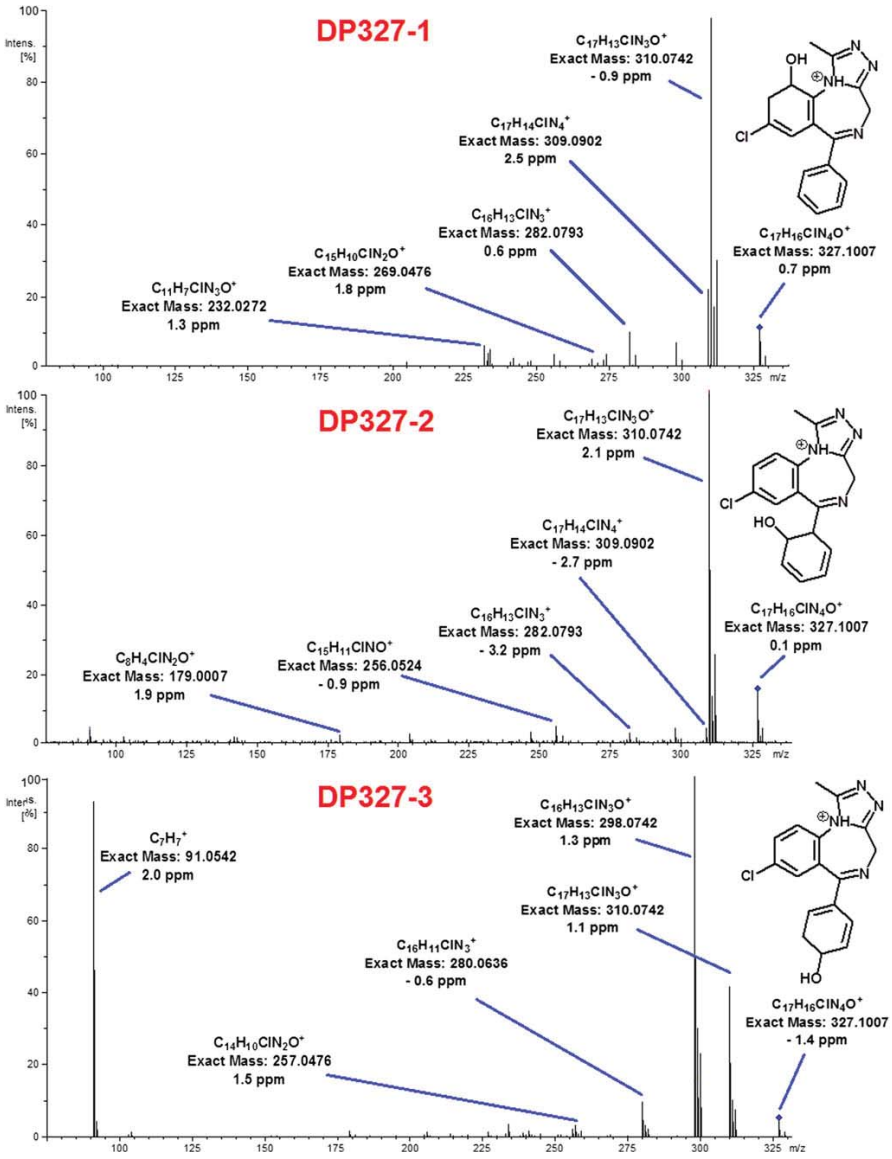

Figure 1. MS/MS spectra of DP327–1 (collision energy: 30 eV), DP327–2 (collision energy: 30 eV) and DP327–3 (collision energy: 35 eV). Exact mass and experimental error in the measurement. [Colour figure can be viewed at wileyonlinelibrary.com]

compound as that hydroxylated in C10 site while DP327–2 should correspond with that hydroxylated in C2′ position. The loss of H_2O was not recorded in any of the ions of the MS–MS spectrum of DP327–3, so it was thought that hydroxyl was bonded to the C4′ carbon atom in DP327–3.

The molecular formulae of the $[M + H]^+$ ion of other four degradation products resulted to be $C_{17}H_{14}ClN_4O^+$ (*m/z* 325), their spectra are shown in Figure 2. These compounds incorporated an oxygen atom in their structure and kept the number of RDBs with respect to alprazolam (Figures S5–S8). DP325–3 is proposed to be a benzodiazepine-4-ol, already described in the bibliography.[31] The radical-ion at *m/z* 308 was originated by the loss of a hydroxyl radical, loss not observed in the other three spectra. The ions at *m/z* 271 and 297 corroborated that the hydroxyl substituent was placed in the seven members ring.

As regards DP325–4, the ion at *m/z* 177 could correspond to the loss of C_6H_5OH from the ion *m/z* 271, whose formation could be similar to the formation of 255 in the alprazolam spectrum. Assuming that the hydroxylation takes place in the phenyl substituent of the benzodiazepine the ions at *m/z* 132 and 242 could not be explained if hydroxyl was bonded in position meta (C3′), and furthermore a loss of water had not been detected which suggested that hydroxyl was not placed in ortho position (C2′), either. So, it is plausible that DP325–4 is a 4′-hydroxyl derivative.

A well-defined structure for DP325–2 has not been ascertained. The interpretation of the structure of an oxygenated fragment-ion (*m/z* 154, $C_7H_5ClNO^+$) lead to the assumption that the

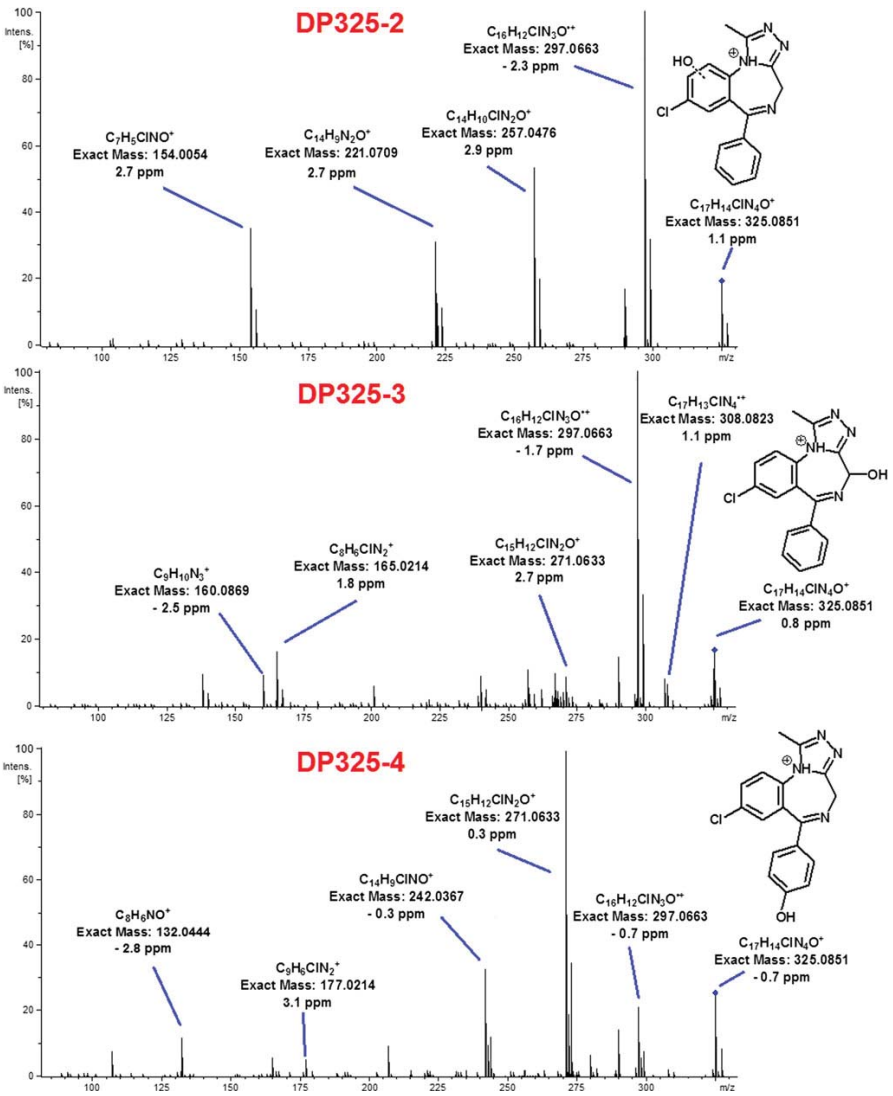

Figure 2. MS/MS spectra of DP325–2, DP325–3 and DP325–4. Collision energy in each spectrum: 40 eV. Exact mass and experimental error in the measurement. [Colour figure can be viewed at wileyonlinelibrary.com]

hydroxyl was bonded to the benzene ring of the benzodiazepine in the precursor compound, likely in C9 or C10 sites; the bond of hydroxyl to C7 carbon atom was discarded because a loss of H_2O was not seen in the MS/MS spectrum. Otherwise, a few ions were observed in the MS/MS spectrum of the last compound with protonated molecular ion at *m/z* 325 (DP325–1) which presumably contains also a phenolic moiety although a structure is not proposed.

DP300 ($C_{16}H_{15}ClN_3O^+$) and DP298 ($C_{16}H_{13}ClN_3O^+$) arise from the breakdown of the cyclic structure of the benzodiazepine, and the corresponding hydroxylation or formation of a ketone in the C6 carbon atom, respectively. Many fragment-ions were recorded in their MS/MS spectra and they support the attributed identifications (Figures S9 and S10). DP298 is a known transformation product of alprazolam.[10] A degradation product with a $[M + H]^+$ ion at *m/z* 300 had also been previously reported in the bibliography but it had not been completely identified.[18]

Occurrence of degradation products in photochemical and thermal degradation assays

No degradation products were found in the assays of biological degradation but some degradation products were found in the degradation assays at high temperature, mainly in the assays at 100 μg/L, and even in the photochemical assays for which no changes in alprazolam concentration were observed. Table 3 shows the peak areas of the degradation products after 4 and 8 weeks since the beginning of the assays: a value of 100 was assigned to the initial peak area of alprazolam (week 0) in each assay, and all other peak areas were referred to this value; data are the mean of two assays whose individual data can be seen in Table S10. Some chromatograms are presented in Figure S11.

The compounds DP327–1, DP327–2, DP327–3, DP325–1, DP325–4, and DP298 were found after heating the alprazolam solution at 70°C. The most abundant compounds at the high concentration

Table 3. Peak areas of the degradation products obtained in the forced and non-forced assays on river water samples spiked with alprazolam at 2 or 100 μg/L (river Pisuerga, W1; river Tuerto, W2; river Pisuerga in presence of sediment, SED). Peak areas are referred to the initial peak area of alprazolam in each experiment, to which a value of 100 was assigned. Data are the mean of two experiments

Assay:	Heat, 70°C		UV lamp		Sunlight		Non-forced								
Sample:	W1	W1	W1	W1	W1	W1	W1	W1	W1	W2	W2	W2	SED	SED	SED
Weeks:	4	8	4	8	4	8	12	24	36	12	24	36	12	24	36
2 μg/L															
DP300	--	--	--	--	--	--	0.39	0.92	1.31	0.40	0.95	1.26	0.30	0.77	1.22
DP327–1	--	0.38	--	--	--	--	--	--	0.28	--	--	0.25	--	--	0.28
DP327–2	--	--	--	--	--	--	--	--	--	--	--	--	--	--	--
DP327–3	--	0.38	--	--	--	--	--	0.20	0.36	--	0.23	0.45	--	--	0.33
DP325–1	--	--	--	--	--	--	--	--	--	--	--	--	--	--	--
DP325–2	--	--	--	--	--	--	--	--	--	--	--	--	--	--	--
DP325–3	--	--	--	--	--	--	--	--	--	--	--	--	--	--	--
DP325–4	--	--	--	--	--	--	--	--	--	--	--	--	--	--	--
DP298	0.21	0.65	--	--	--	--	--	--	--	--	--	--	--	--	--
100 μg/L															
DP300	--	--	0.06	0.14	0.02	0.05	0.42	0.97	1.41	0.44	0.92	1.34	0.37	0.85	1.30
DP327–1	0.20	0.42	--	0.03	--	--	0.09	0.22	0.33	0.08	0.19	0.29	0.07	0.18	0.28
DP327–2	0.07	0.13	--	0.02	--	--	0.06	0.10	0.19	0.03	0.09	0.18	0.04	0.10	0.16
DP327–3	0.18	0.37	--	0.02	--	--	0.14	0.28	0.37	0.10	0.29	0.44	0.08	0.21	0.31
DP325–1	0.06	0.15	--	0.02	--	--	0.02	0.07	0.10	0.03	0.09	0.11	0.07	0.09	0.06
DP325–2	--	--	--	--	--	--	--	0.02	0.03	--	0.01	0.02	--	0.01	0.01
DP325–3	--	--	--	--	--	--	--	0.02	0.04	--	0.02	0.05	--	--	0.02
DP325–4	0.03	0.09	--	--	--	--	0.02	0.07	0.11	0.03	0.05	0.10	0.03	0.05	0.07
DP298	0.29	0.71	--	0.02	--	0.01	--	0.02	0.05	--	0.02	0.06	--	--	0.02

--: not detected.

level were DP298, DP327–1, and DP327–3 with relative peak areas of 0.71, 0.42, and 0.37 after 8 weeks. The formation of the hydroxylcyclohexadiene derivatives DP327–1, DP327–2, and DP327–3 can be explained by a nucleophilic addition reaction of H_2O, as mentioned, while the formation of DP325–4 could be ascribed to a hydroxylation reaction of aromatic ring in alkaline aqueous solution, process known in organic chemistry. The origin of DP325–1, non-identified, is surely similar. As regards the formation of DP298, a benzophenone derivative, it had been claimed that it is a photodegradation product in water at acidic pH,[10,12,28] but it also arises from non-photochemical reactions at slight alkaline pH as shown in this work; the opening of the ring in benzodiazepine drugs is a phenomenon usually observed in extreme conditions and, moreover, a reversible equilibrium in which the ring is opened to form the benzophenone has been described for alprazolam in aqueous solution at acidic pH.[32] Very small amounts of DP298 were also found when river water (pH 7.8, 100 μg/L) spiked with alprazolam was directly exposed to radiation from the sun or the 254 nm lamp.

DP300, not observed in the assays at 70°C, resulted to be the prevalent degradation product in the photo-induced degradation assays. Furthermore, DP298, DP327–1, DP327–2, DP327–3, and DP325–1 were formed in minimum amounts under the irradiation with lamp; presumably, they are yielded by reactions involving radical species whose generation is favored by the UV radiation. In any case, after 8 weeks the amount of photodegradation products was clearly lower in relation to the thermal degradation products: the relative peak area of DP300 was 0.05 and 0.14 after irradiation with sunlight and lamp, respectively.

Occurrence of degradation products in non-forced conditions

The fate of alprazolam and its above-mentioned residues in river water was also monitored in conditions such that the penetration of UV radiation was hindered, which it is expected to happen in a body of water where the transmission of UV radiation is gradually attenuated when the depth increases. Table 3 shows the degradation products found, and their relative mean peak areas in two river water samples after 12, 24, and 36 weeks; individual data of each assay are given in Table S11. As it can be seen the occurrence of the different compounds increases with time.

The alcoholic compound DP300 was the most prominent degradation product after 36 weeks with relative peak areas of 1.41 and 1.34 for W1 and W2 samples spiked at 100 μg/L, respectively; this photochemical degradation product was curiously the main residue although the penetration of UV radiation had been limited. The incidence of DP327–1, DP327–2, and DP327–3, whose main formation is supposedly due to a chemical reaction in solution, was less notable with peak areas about 0.4, 0.3, and 0.19 for W1 and W2 samples, respectively. DP325–1, DP325–2, DP325–3, DP325–4, and DP298 were less abundant degradation products at the end of the monitoring. DP325–3 was detected only in these non-forced experiments at 100 μg/L. A chromatogram is shown in Figure S12.

The behaviour of alprazolam over time in presence of sediment resembled that without sediment; the amount proportions among the degradation products were essentially similar when the results of the assays with or without sediment were compared. Seemingly, peak areas were somewhat lower now regarding the assays only

with water (W1 sample), which is reasonable since the degradation products can also be adsorbed onto sediment.

It had been deduced from the forced assays that the influence of the photochemistry in the degradation of alprazolam was limited, emphasizing the importance of the non-photochemical reactions. In fact, thermal degradation products such as DP298, DP327–1, DP327–2, and DP 327–3 were the major ones in the corresponding forced assays. However, in the non-forced and long-term assays DP300 was the major transformation product and DP298 was minor. There is not a convincing explanation for this contradiction but a possible evolution of the degradation products should be taken into account, regardless of the greater or lesser capacity of the forced assays to predict the fate of a contaminant, too.

On the other hand, DP300, DP327–1, and DP327–3 were the only degradation products detected in extracts of experiments with water spiked at low concentration, and presumably, they are susceptible to being found in the analysis of real surface waters. Nevertheless, it must be stated that these degradation products will be hardly found in them according to the persistence of the parent compound and its commonly expected concentrations (in the order of ng/L).

Adsorption to sediment

Alprazolam has a certain capacity of adsorption on sediment; after spiking water at 2 or 100 μg/L its concentration in water decreased about 30% for a sediment to solution ratio of 0.1 g/mL. Figure 3 shows the adsorption isotherm obtained for alprazolam in the batch experiments, K_d and K_{oc} (organic carbon normalized adsorption coefficient) values resulted to be 4.44 and 370.1 Kg/L (RSD 5.4%, $n = 10$), respectively. The K_{oc} value is comparable for instance to those of microcontaminants such as 1,3-dichlorobenzene, 1,4-dichlorobenzene, linuron or prometryn.[33] Although only a sediment sample has been considered in this work it is possible that aquatic sediments could behave as a reservoir of alprazolam.

Adsorption coefficients were also calculated for the main degradation products (DP300, DP327–1, DP327–2, DP327–3), in addition to DP298, from the experimental adsorption percentages; K_d and K_{oc} values, and the used sediment to water ratios, can be consulted in Table 4. Adsorption coefficient of alprazolam was also calculated by this method, it was 4.23 Kg/L, similar to the previously estimated value. The capacity of adsorption of the five degradation products was lower, which is coherent with the presence of oxygen in their structures and the subsequent increase of water solubility.

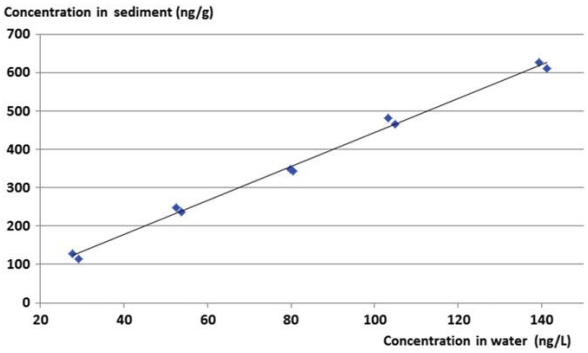

Figure 3. Adsorption isotherm of alprazolam ($n = 2$). [Colour figure can be viewed at wileyonlinelibrary.com]

Table 4. K_d and K_{oc} mean values (RSDs in parenthesis) calculated for the degradation products. Mean adsorption percentages (A%) onto sediment and experimental sediment to water ratios (R), $n = 5$

Compound	K_d (Kg/L)	K_{oc} (Kg/L)	A%	R (Kg/L)	Experimental t-value*
DP300	1.35	112.6 (6.0%)	41.3	0.521	31.8
DP327–1	2.93	244.2 (4.6%)	30.5	0.150	26.9
DP327–2	2.30	191.5 (4.6%)	25.6	0.150	42.3
DP327–3	3.13	261.0 (3.1%)	31.9	0.150	48.4
DP298	1.92	159.9 (5.8%)	36.8	0.303	46.6
Alprazolam	4.23	352.8 (3.2%)	34.3	0.123	41.2

*Critical t-value: 2.3.

Nevertheless, the K_d values of alprazolam and degradation products do not differ greatly among them; particularly, K_d value for DP300 was 1.35 Kg/L, the lowest one.

Conclusions

The concentration of alprazolam in surface water at slightly alkaline pH remains virtually constant over time, which suggests that alprazolam can be considered as a persistent organic pollutant in aquatic ecosystems. Some degradation products were yielded in low amount; the current concentration levels of the parent compound in surface water should make certainly difficult the detection of these degradation products by the methods usually applied to analyze water samples.

Alprazolam is a non-biodegradable compound in river water. It can undergo chemical and photochemical reactions. Tentative structures for 8 out of 9 detected degradation products are given from high-resolution mass spectrometry data. The capability of the forced degradation assays to properly predict the degradation products of alprazolam, and their relative amounts, inside a body of water is limited.

Alprazolam and their major degradation products can be partially adsorbed on aquatic sediment. The degradation rate of alprazolam at trace concentration in water kept in contact with sediment is insignificant, too. The occurrence of degradation products in this case is similar to that without sediment.

Acknowledgements

The authors would like to acknowledge the support given by the Laboratorio de Técnicas Instrumentales of the University of Valladolid to perform the experimental work.

References

[1] Y. Vystavna, F. Huneau, V. Grynenko, Y. Vergeles, H. Celle, N. Tapie, H. Budzinski, P. Le Coustumer. Pharmaceuticals in rivers of two regions with contrasted socio-economic conditions: occurrence, accumulation, and comparison for Ukraine and France. *Water Air Soil Pollut.* **2012**, *223*, 2111.

[2] A. Mendoza, M. López de Alda, S. González-Alonso, N. Mastroianni, D. Barceló, Y. Valcárcel. Occurrence of drugs of abuse and benzodiazepines in river waters from the Madrid Region (Central Spain). *Chemosphere.* **2014**, *95*, 247.

[3] S. Esteban, Y. Valcárcel, M. Catalá, M. González Castromil. Psychoactive pharmaceutical residues in the watersheds of Galicia. *Gac. Sanit.* **2012**, *26*, 457.

[4] A. Mendoza, J. L. Rodríguez-Gil, S. González-Alonso, N. Mastroianni, M. López de Alda, D. Barceló, Y. Valcárcel. Drugs of abuse and benzodiazepines in the Madrid Region (Central Spain): Seasonal variation in river waters, occurrence in tap water and potential environmental and human risk. *Environ. Int.* **2014**, *70*, 76.
[5] M. Wu, J. Xiang, C. Que, F. Chen, G. Xu. Occurrence and fate of psychiatric pharmaceuticals in the urban water system of Shanghai, China. *Chemosphere*. **2015**, *138*, 486.
[6] S. González Alonso, M. Catalá, R. R. Maroto, J. L. Gil, A. G. de Miguel, Y. Valcárcel. Pollution by psychoactive pharmaceuticals in the rivers of Madrid metropolitan area (Spain). *Environ. Int.* **2010**, *36*, 195.
[7] C. Postigo, M. López de Alda, D. Barceló. Evaluation of drugs of abuse use and trends in a prison through wastewater analysis. *Environ. Int.* **2011**, *37*, 49.
[8] N. Mastroianni, C. Postigo, M. Lopez de Alda, D. Barcelo. Ilicit and abused drugs in sewage sludge: Method optimization and occurrence. *J. Chromat. A.* **2013**, *1322*, 29.
[9] B. Subedi, S. Lee, H. B. Moon, K. Kannan. Psychoactive pharmaceuticals in sludge and their emission from wastewater treatment facilities in Korea. *Environ. Sci. Technol.* **2013**, *47*, 13321.
[10] C. Gallardo, R. Goldberg, N. S. Nudelman. Kinetic and mechanistic studies on the hydrolysis and photodegradation of diazepam and alprazolam. *J. Phys. Org. Chem.* **2005**, *18*, 156.
[11] N. S. Nudelman, C. Gallardo. Isolation and structural elucidation of degradation products of alprazolam: photostability studies of alprazolam tablets. *J. Pharm. Sci.* **2002**, *91*, 1274.
[12] N. S. Nudelman, C. Gallardo. Spectrofluorimetric assay for the photodegradation products of alprazolam. *J. Pharm. Biomed. Anal.* **2002**, *30*, 887.
[13] Y. Picó, D. Barceló. Transformation products of emerging contaminants in the environment and high-resolution mass spectrometry: a new horizon. *Anal. Bioanal. Chem.* **2015**, *407*, 6257.
[14] J. P. Sumpter. The challenge: Do pharmaceuticals present a risk to the environment, and what needs to be done to answer the question? *Environ. Toxicol. Chem.* **2014**, *33*, 1915.
[15] Adsorption - desorption using a batch equilibrium method, in *OECD Guideline for the Testing of Chemicals n° 106*, Organisation for Economic Co-operation and Development, Paris, **2000**, pp. 7–8.
[16] J. T. McMullan, E. Jones, B. Barnhart, K. Denninghoff, D. Spaite, E. Zaleski, R. Silbergleit. Degradation of benzodiazepines after 120 days of EMS deployment. *Prehosp. Emerg. Care*. **2014**, *18*, 368.
[17] I. Panderi, H. A. Archontaki, E. E. Gikas, M. Parisi. Kinetic investigation on the degradation of lorazepam in acidic aqueous solutions by high performance liquid chromatography. *J. Liq. Chromatogr. Relat. Technol.* **1998**, *12*, 1783.
[18] T. J. P. Smyth, V. R. Robledo, W. F. Smyth. Characterisation of oxazepam degradation products by high-performance liquid chromatography/electrospray ionisation mass spectrometry and electrospray ionisation quadrupole time-of-flight tandem mass spectrometry. *Rapid Commun. Mass Spectrom.* **2010**, *5*, 651.
[19] C. G. Cabrera, R. G. de Waisbaum, N. S. Nudelman. Kinetic and mechanistic studies on the hydrolysis and photodegradation of diazepam and alprazolam. *J. Phys. Org. Chem.* **2005**, *18*, 156.
[20] L. V. Allen, M. A. Erickson. Stability of alprazolam, chloroquine phosphate, cisapride, enalapril maleate, and hydralazine hydrochloride in extemporaneously compounded oral liquids. *Am. J. Health-Syst. Pharm.* **1998**, *55*, 1915.
[21] I. Panderi, H. Archontaki, E. Gikas, M. Parisi. Acidic hydrolysis of bromazepam studied by high performance liquid chromatography. Isolation and identification of its degradation products. *J. Pharm. Biomed. Anal.* **1998**, *17*, 327.
[22] C. M. Geiger, B. Sorensen, P. A. Whaley. Stability of midazolam in syrspend SF and syrspend SF cherry. *Int. J. Pharm. Compd.* **2013**, *17*, 344.
[23] L. V. Allen, M. A. Erickson. Stability of acetazolamide, allopurinol, azathioprine, clonazepam, and flucytosine in extemporaneously compounded oral liquids. *Am. J. Health-Syst. Pharm.* **1996**, *16*, 1944.
[24] A. D. Tappin, J. P. Loughnane, A. J. McCarthy, M. F. Fitzsimons. Bacterio-plankton transformation of diazepam and 2-amino-5-chlorobenzophenone in river waters. *Evnviron. Sci. Process. Impacts*. **2014**, *16*, 2227.
[25] C. H. Redshaw, M. P. Cooke, P. Martin, H. M. Talbot, S. McGrath, S. J. Rowland. Low biodegradability of fluoxetine HCl, diazepam and their human metabolites in sewage sludge-amended soil. *J. Soil. Sediment.* **2008**, *8*, 217.
[26] S. Vay, D. Huggett. Aquatic Toxicity of Oxazepam and Alprazolam on *Daphnia magna* and *Ceriodaphnia dubia*. Communication presented in *19th Texas National McNair Research Conference*, Denton, **2014**.
[27] N. S. Nudelman, C. Gallardo. Factors affecting the stability Alprazolam. Structural elucidation of the major degradants. *Vitae*. **1999**, *6*, 29.
[28] V. Calisto, M. R. M. Domingues, V. I. Esteve. Photodegradation of psychiatric pharmaceuticals in aquatic environments. Kinetics and photodegradation products. *Water Res.* **2011**, *45*, 6097.
[29] M. J. Cho, T. A. Scahill, J. B. Hester Jr. Kinetics and equilibrium of the reversible alprazolam ring-opening reaction. *J. Pharma Sci.* **1983**, *72*, 356.
[30] A. Delle-Site. Factors affecting sorption of organic compounds in natural sorbent water systems and sorption coefficients for selected pollutants. A review. *J. Phys. Chem. Ref. Data*. **2001**, *30*, 187.
[31] C. E. West, S. J. Rowland. Aqueous Phototransformation of Diazepam and Related Human Metabolites under Simulated Sunlight. *Environ. Sci. Technol.* **2012**, *46*, 4749.
[32] R. Andersin, K. Ovaskainen, S. Kaltia. Photochemical decomposition of midazolam. 3. Isolation and identification of products in aqueous solutions. *J. Pharm. Biomed. Anal.* **1994**, *12*, 165.
[33] M. A. Sousa, O. Lacina, P. Hradkova, J. Pulkrabova, V. J. P. Vilar, C. Goncalves, R. A. R. Boaventura, J. Hajslova, M. F. Alpendurada. Lorazepam photofate under photolysis and TiO2-assisted photocatalysis: Identification and evolution profiles of by-products formed during phototreatment of a WWTP effluent. *Water Res.* **2013**, *47*, 5584.

Supporting information

Additional Supporting Information may be found online in the supporting information tab for this article.

Supplementary data

Persistence of alprazolam in river water according to forced and non-forced degradation assays. Adsorption to sediment and long-term degradation products.

Drug Testing and Analysis, 2016

Supplementary material

Contents

(*) not included in the published manuscript

Table SM1: Concentrations of alprazolam (in $\mu g \cdot L^{-1}$) found in the biological degradation assays at 2 and 100 $\mu g \cdot L^{-1}$ under aerobic conditions. Two or five sample aliquots were taken each week. A t-test (p=0.05, n=5) was applied to check for differences between the initial and final mean concentrations of the assay.

2 $\mu g \cdot L^{-1}$												
	Assay 1						Assay 2					
Week:	**0**	**1**	**2**	**3**	**4**	**5**	**0**	**1**	**2**	**3**	**4**	**5**
Aliquot 1	2.04	2.00	2.03	2.01	2.02	2.01	2.01	2.01	1.99	2.02	2.02	2.03
Aliquot 2	2.08	2.05	2.04	1.99	2.01	2.03	2.00	2.03	2.01	2.02	2.00	2.01
Aliquot 3	2.05	--	--	--	--	2.03	1.98	--	--	--	--	2.00
Aliquot 4	2.02	--	--	--	--	2.04	2.03	--	--	--	--	2.01
Aliquot 5	2.03	--	--	--	--	2.01	2.01	--	--	--	--	2.02
Mean:	2.04					2.02	2.01					2.01
	Experimental t-value*: 1.7						Experimental t-value*: 0.8					
100 $\mu g \cdot L^{-1}$												
	Assay 1						Assay 2					
Week:	**0**	**1**	**2**	**3**	**4**	**5**	**0**	**1**	**2**	**3**	**4**	**5**
Aliquot 1	102	100	101	100	101	103	99	102	102	99	100	101
Aliquot 2	101	99	102	104	101	104	103	102	101	99	98	98
Aliquot 3	105	--	--	--	--	101	102	--	--	--	--	101
Aliquot 4	99	--	--	--	--	99	100	--	--	--	--	100
Aliquot 5	101	--	--	--	--	103	101	--	--	--	--	98
Mean:	101.6					102.0	101.0					99.6
	Experimental t-value*: 0.3						Experimental t-value*: 1.4					

--: without data

*Critical t-value: 2.3

Table SM2: Concentrations of alprazolam (in $\mu g \cdot L^{-1}$) found in the biological degradation assays at 2 and 100 $\mu g \cdot L^{-1}$ under anaerobic conditions. Two or five sample aliquots were taken each week. A t-test (p=0.05, n=5) was applied to check for differences between the initial and final mean concentrations of the assay.

2 $\mu g \cdot L^{-1}$												
	Assay 1						Assay 2					
Week:	**0**	**1**	**2**	**3**	**4**	**5**	**0**	**1**	**2**	**3**	**4**	**5**
Aliquot 1	1.99	2.02	2.01	2.00	1.99	1.98	2.01	2.05	2.02	2.01	1.99	2.00
Aliquot 2	2.01	2.00	2.01	1.98	2.00	1.97	2.02	2.02	2.03	2.00	2.02	1.99
Aliquot 3	2.02	--	--	--	--	2.01	2.01	--	--	--	--	2.01
Aliquot 4	1.98	--	--	--	--	1.99	2.00	--	--	--	--	1.98
Aliquot 5	1.97	--	--	--	--	2.01	2.01	--	--	--	--	1.99
Mean:	1.99					1.99	2.01					1.99
	Experimental t-value*: 0.1						Experimental t-value*: 1.7					

100 $\mu g \cdot L^{-1}$												
	Assay 1						Assay 2					
Week:	**0**	**1**	**2**	**3**	**4**	**5**	**0**	**1**	**2**	**3**	**4**	**5**
Aliquot 1	103	102	100	101	99	100	102	99	98	101	102	100
Aliquot 2	104	103	103	101	100	102	98	102	103	100	101	97
Aliquot 3	101	--	--	--	--	98	102	--	--	--	--	103
Aliquot 4	100	--	--	--	--	99	101	--	--	--	--	102
Aliquot 5	102	--	--	--	--	102	100	--	--	--	--	98
Mean:	102.0					100.2	100.6					100.0
	Experimental t-value*: 1.7						Experimental t-value*: 0.4					

--: without data

*Critical t-value: 2.3

Table SM3: Concentrations of alprazolam (in $\mu g \cdot L^{-1}$) found in the biological degradation assays at 2 and 100 $\mu g \cdot L^{-1}$ in presence of culture medium. Two or five sample aliquots were taken each week. A t-test (p=0.05, n=5) was applied to check for differences between the initial and final mean concentrations of the assay.

2 $\mu g \cdot L^{-1}$												
	Assay 1						Assay 2					
Week:	**0**	**1**	**2**	**3**	**4**	**5**	**0**	**1**	**2**	**3**	**4**	**5**
Aliquot 1	2.01	2.00	1.99	2.01	2.00	2.03	2.00	2.01	2.02	1.98	2.00	2.01
Aliquot 2	2.00	2.01	2.02	1.98	1.99	2.04	2.02	2.01	2.00	2.03	2.01	2.02
Aliquot 3	1.99	--	--	--	--	2.03	2.01	--	--	--	--	1.97
Aliquot 4	2.00	--	--	--	--	1.97	2.01	--	--	--	--	2.00
Aliquot 5	1.98	--	--	--	--	2.01	1.99	--	--	--	--	1.98
Mean:	2.00					2.02	2.01					2.00
	Experimental t-value*: 1.5						Experimental t-value*: 0.9					
100 $\mu g \cdot L^{-1}$												
	Assay 1						Assay 2					
Week:	**0**	**1**	**2**	**3**	**4**	**5**	**0**	**1**	**2**	**3**	**4**	**5**
Aliquot 1	102	101	97	98	96	95	97	98	95	94	95	96
Aliquot 2	98	99	98	96	94	94	100	101	99	98	96	98
Aliquot 3	99	--	--	--	--	100	99	--	--	--	--	99
Aliquot 4	102	--	--	--	--	93	100	--	--	--	--	93
Aliquot 5	98	--	--	--	--	94	100	--	--	--	--	97
Mean:	99.8					95.2	99.2					96.6
Experimental t-value*: 3.0							Experimental t-value*: 2.2					

--: without data

*Critical t-value: 2.3

Table SM4: Concentrations of alprazolam (in $\mu g \cdot L^{-1}$) found in the photochemical degradation assays, sunlight exposure, at 2 and 100 $\mu g \cdot L^{-1}$. Two or five sample aliquots were taken. A t-test (p=0.05, n=5) was applied to check for differences between the initial and final mean concentrations of the assay.

2 $\mu g \cdot L^{-1}$							
	Assay 1				Assay 2		
Week:	**0**	**4**	**8**		**0**	**4**	**8**
Aliquot 1	1.98	2.00	2.01		1.99	2.00	1.98
Aliquot 2	2.01	2.02	1.97		1.97	2.01	2.03
Aliquot 3	2.00	--	1.99		2.03	--	2.00
Aliquot 4	2.02	--	1.96		2.01	--	2.00
Aliquot 5	1.99	--	2.00		2.03	--	1.97
Mean:	2.00		1.99		2.01		2.00
	Experimental t-value*: 1.2				Experimental t-value*: 0.6		
100 $\mu g \cdot L^{-1}$							
	Assay 1				Assay 2		
Week:	**0**	**4**	**8**		**0**	**4**	**8**
Aliquot 1	102	103	100		101	101	98
Aliquot 2	102	104	103		100	99	97
Aliquot 3	100	--	97		98	--	98
Aliquot 4	101	--	102		97	--	101
Aliquot 5	99	--	102		99	--	97
Mean:	100.8		100.8		99.0		98.2
	Experimental t-value*: 0.1				Experimental t-value*: 1.1		

--: without data

*Critical t-value: 2.3

Table SM5: Concentrations of alprazolam (in $\mu g \cdot L^{-1}$) found in the photochemical degradation assays, 254 nm UV lamp, at 2 and 100 $\mu g \cdot L^{-1}$. Two or five sample aliquots were taken. A t-test (p=0.05, n=5) was applied to check for differences between the initial and final mean concentrations of the assay.

2 $\mu g \cdot L^{-1}$							
	Assay 1				Assay 2		
Week:	**0**	**4**	**8**		**0**	**4**	**8**
Aliquot 1	1.97	2.00	1.99		2.02	2.01	1.98
Aliquot 2	2.00	1.98	2.01		2.03	2.00	1.97
Aliquot 3	1.96	--	1.99		1.99	--	2.01
Aliquot 4	1.95	--	1.99		1.98	--	1.96
Aliquot 5	2.01	--	2.01		2.01	--	1.97
Mean:	1.98		2.00		2.01		1.98
	Experimental t-value*: 1.6				Experimental t-value*: 2.2		
100 $\mu g \cdot L^{-1}$							
	Assay 1				Assay 2		
Week:	**0**	**4**	**8**		**0**	**4**	**8**
Aliquot 1	100	102	100		100	98	99
Aliquot 2	101	99	99		102	100	101
Aliquot 3	100	--	100		99	--	98
Aliquot 4	101	--	101		98	--	97
Aliquot 5	102	--	98		102	--	98
Mean:	100.8		99.6		100.2		98.6
	Experimental t-value*: 1.9				Experimental t-value*: 1.5		

--: without data

*Critical t-value: 2.3

Table SM6: Concentrations of alprazolam (in µg·L^{-1}) found in the thermal degradation assays (70 °C) at 2 and 100 µg·L^{-1}. Two or five sample aliquots were taken. A t-test (p=0.05, n=5) was applied to check for differences between the initial and final mean concentrations of the assay.

2 µg·L^{-1}							
	Assay 1				Assay 2		
Week:	**0**	**4**	**8**		**0**	**4**	**8**
Aliquot 1	1.96	1.99	1.97		2.01	2.02	1.99
Aliquot 2	2.01	1.97	2.00		2.00	1.97	2.00
Aliquot 3	2.01	--	1.95		2.03	--	2.02
Aliquot 4	1.99	--	1.99		1.96	--	1.95
Aliquot 5	1.98	--	1.95		1.99	--	1.98
Mean:	1.99		1.97		2.00		2.00
	Experimental t-value*: 1.3				Experimental t-value*: 0.5		
100 µg·L^{-1}							
	Assay 1				Assay 2		
Week:	**0**	**4**	**8**		**0**	**4**	**8**
Aliquot 1	102	99	98		99	97	96
Aliquot 2	100	98	96		98	98	97
Aliquot 3	99	--	98		99	--	97
Aliquot 4	98	--	97		101	--	96
Aliquot 5	101	--	95		102	--	98
Mean:	100.0		96.8		99.8		96.8
	Experimental t-value*: 3.5				Experimental t-value*: 3.6		

--: without data

*Critical t-value: 2.3

Table SM7: Concentrations of alprazolam (in $\mu g \cdot L^{-1}$) found in the degradation assays over time on the W1 sample at 2 and 100 $\mu g \cdot L^{-1}$. Two or five sample aliquots were taken. A t-test (p=0.05, n=5) was applied to check for differences between the initial and final mean concentrations of the assay.

2 $\mu g \cdot L^{-1}$									
	Assay 1					Assay 2			
Week:	**0**	**12**	**24**	**36**		**0**	**12**	**24**	**36**
Aliquot 1	1.96	1.99	1.97	1.99		1.98	1.99	1.99	2.02
Aliquot 2	1.97	1.98	1.99	1.96		2.02	2.00	2.00	1.99
Aliquot 3	2.02	--	--	2.02		2.01	--	--	2.04
Aliquot 4	1.95	--	--	1.95		2.03	--	--	1.95
Aliquot 5	1.98	--	--	1.95		1.99	--	--	1.96
Mean:	1.98			1.97		2.01			1.99
	Experimental t-value*: 0.5					Experimental t-value*: 0.7			
100 $\mu g \cdot L^{-1}$									
	Assay 1					Assay 2			
Week:	**0**	**12**	**24**	**36**		**0**	**12**	**24**	**36**
Aliquot 1	103	100	98	96		102	101	98	96
Aliquot 2	99	99	98	98		100	99	97	95
Aliquot 3	101	--	--	94		100	--	--	94
Aliquot 4	103	--	--	95		97	--	--	94
Aliquot 5	98	--	--	95		99	--	--	95
Mean:	100.8			95.6		99.6			94.8
	Experimental t-value*: 4.2					Experimental t-value*: 5.4			

--: without data

*Critical t-value: 2.3

Table SM8: Concentrations of alprazolam (in $\mu g \cdot L^{-1}$) found in the degradation assays over time on the W2 sample at 2 and 100 $\mu g \cdot L^{-1}$. Two or five sample aliquots were taken. A t-test (p=0.05, n=5) was applied to check for differences between the initial and final mean concentrations of the assay.

2 $\mu g \cdot L^{-1}$									
	Assay 1					Assay 2			
Week:	**0**	**12**	**24**	**36**		**0**	**12**	**24**	**36**
Aliquot 1	2.02	2.01	2.01	1.98		1.97	1.99	1.97	2.01
Aliquot 2	2.03	2.00	2.01	1.99		1.96	2.01	1.99	2.03
Aliquot 3	1.99	--	--	2.01		2.00	--	--	1.97
Aliquot 4	2.01	--	--	1.98		2.01	--	--	2.00
Aliquot 5	1.98	--	--	1.97		1.99	--	--	1.99
Mean:	2.01			1.99		2.00			1.99
	Experimental t-value*: 1.7					Experimental t-value*: 1.0			
100 $\mu g \cdot L^{-1}$									
	Assay 1					Assay 2			
Week:	**0**	**12**	**24**	**36**		**0**	**12**	**24**	**36**
Aliquot 1	97	98	95	93		101	101	96	96
Aliquot 2	99	100	96	94		99	97	96	95
Aliquot 3	101	--	--	93		98	--	--	97
Aliquot 4	98	--	--	95		104	--	--	95
Aliquot 5	100	--	--	96		99	--	--	94
Mean:	99.0			94.2		100.2			95.4
	Experimental t-value*: 5.2					Experimental t-value*: 4.1			

--: without data

*Critical t-value: 2.3

Table SM9: Concentrations of alprazolam (in $\mu g \cdot L^{-1}$) found in the degradation assays over time on the SED sample at 2 and 100 $\mu g \cdot L^{-1}$. Two or five sample aliquots were taken. A t-test (p=0.05, n=5) was applied to check for differences between the initial and final mean concentrations of the assay.

2 $\mu g \cdot L^{-1}$									
	Assay 1					Assay 2			
Week:	**0**	**12**	**24**	**36**		**0**	**12**	**24**	**36**
Aliquot 1	1.42	1.43	1.42	1.42		1.43	1.45	1.45	1.45
Aliquot 2	1.45	1.44	1.44	1.40		1.45	1.43	1.47	1.42
Aliquot 3	1.43	--	--	1.41		1.43	--	--	1.41
Aliquot 4	1.42	--	--	1.44		1.41	--	--	1.45
Aliquot 5	1.44	--	--	1.40		1.46	--	--	1.42
Mean:	1.43			1.41		1.44			1.43
	Experimental t-value*: 1.9					Experimental t-value*: 0.5			
100 $\mu g \cdot L^{-1}$									
	Assay 1					Assay 2			
Week:	**0**	**12**	**24**	**36**		**0**	**12**	**24**	**36**
Aliquot 1	68	70	66	67		69	68	68	68
Aliquot 2	72	68	67	65		71	69	69	68
Aliquot 3	71	--	--	65		72	--	--	66
Aliquot 4	70	--	--	68		68	--	--	65
Aliquot 5	70	--	--	70		69	--	--	66
Mean:	70.2			67.0		69.8			66.6
	Experimental t-value*: 2.8					Experimental t-value*: 3.4			

--: without data

*Critical t-value: 2.3

Identification of degradation products

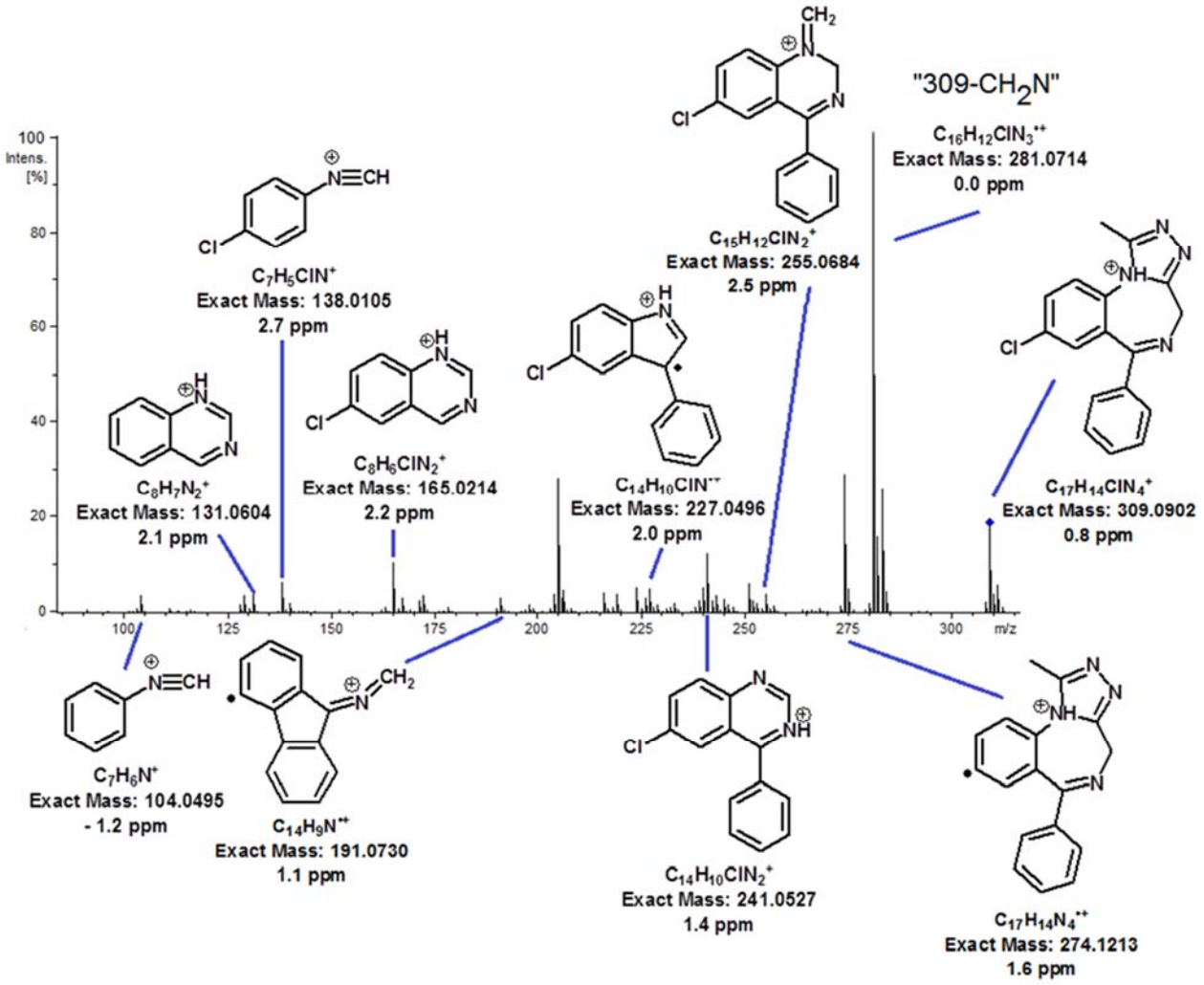

Figure SM1: MS/MS spectrum of alprazolam. Collision energy: 40 eV. Exact mass and experimental error in the measurement.

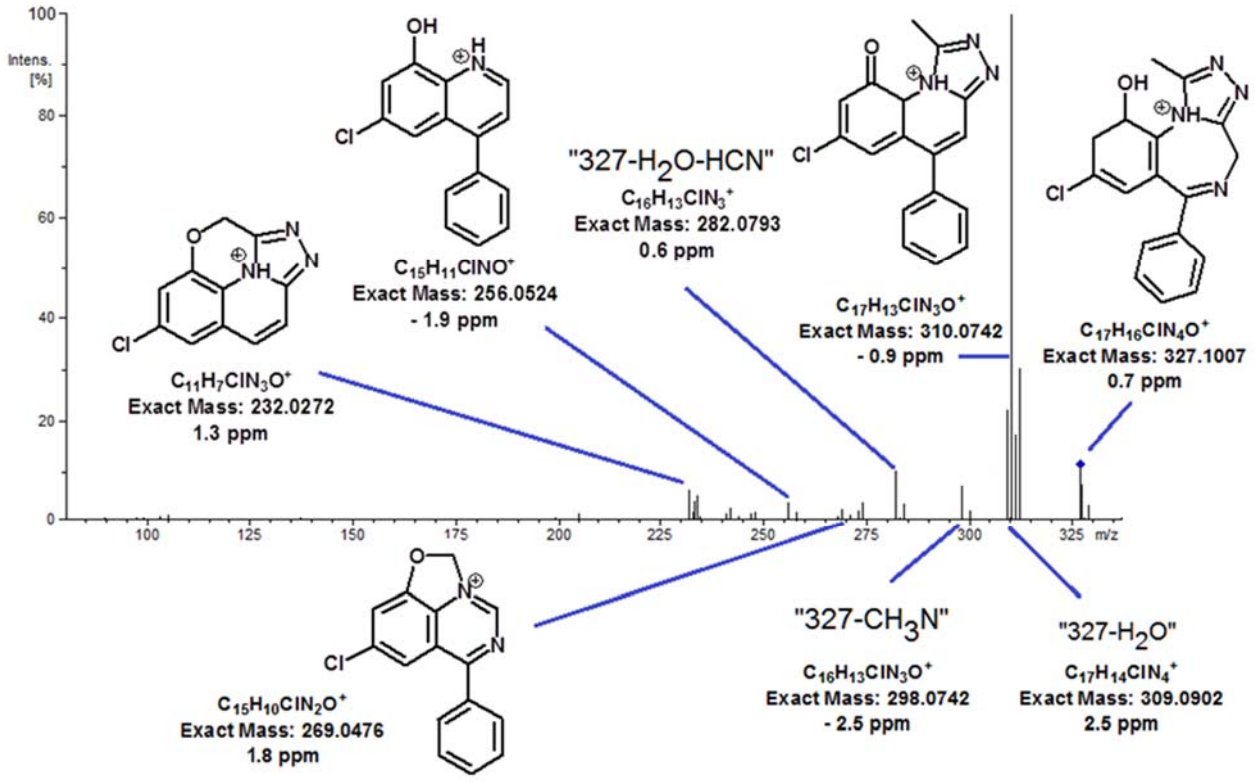

Figure SM2: MS/MS spectrum of DP327-1. Collision energy: 30 eV. Exact mass and experimental error in the measurement.

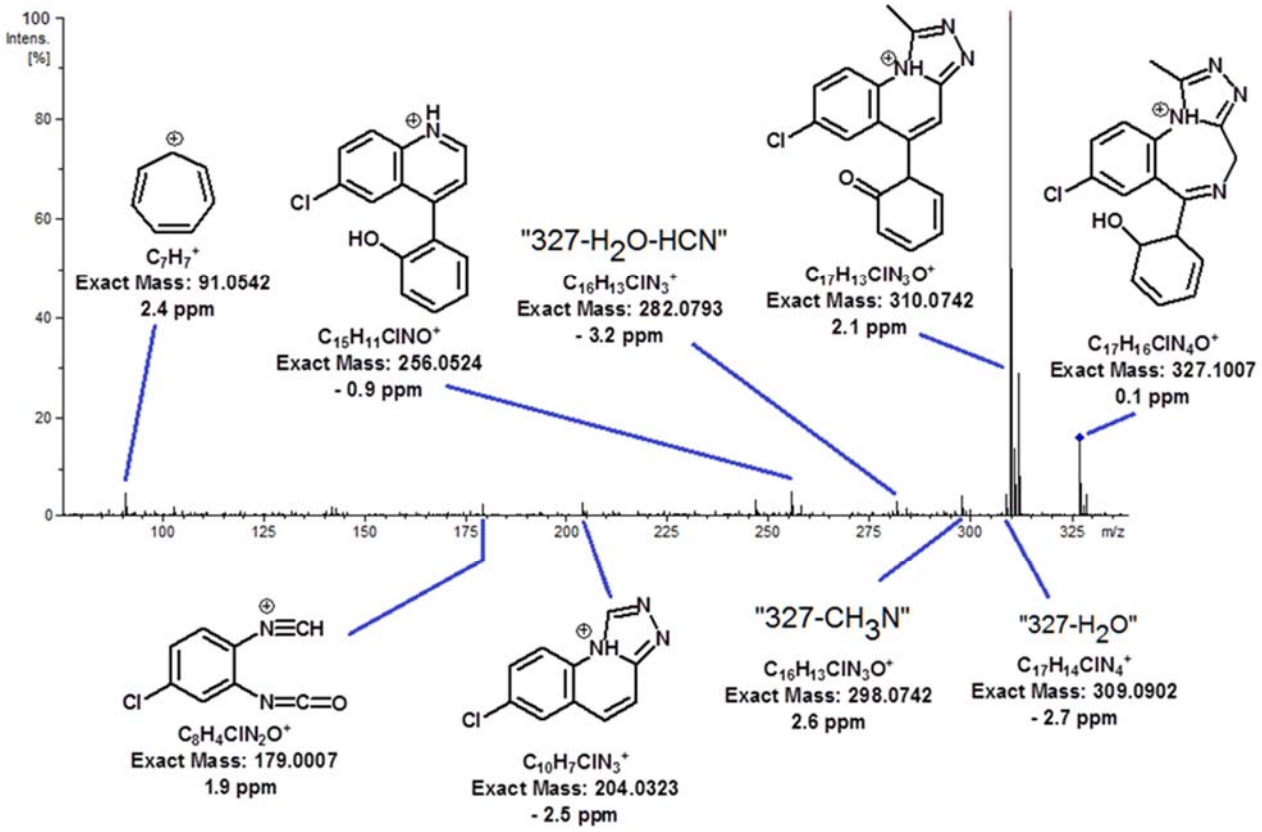

Figure SM3: MS/MS spectrum of DP327-2. Collision energy: 30 eV. Exact mass and experimental error in the measurement.

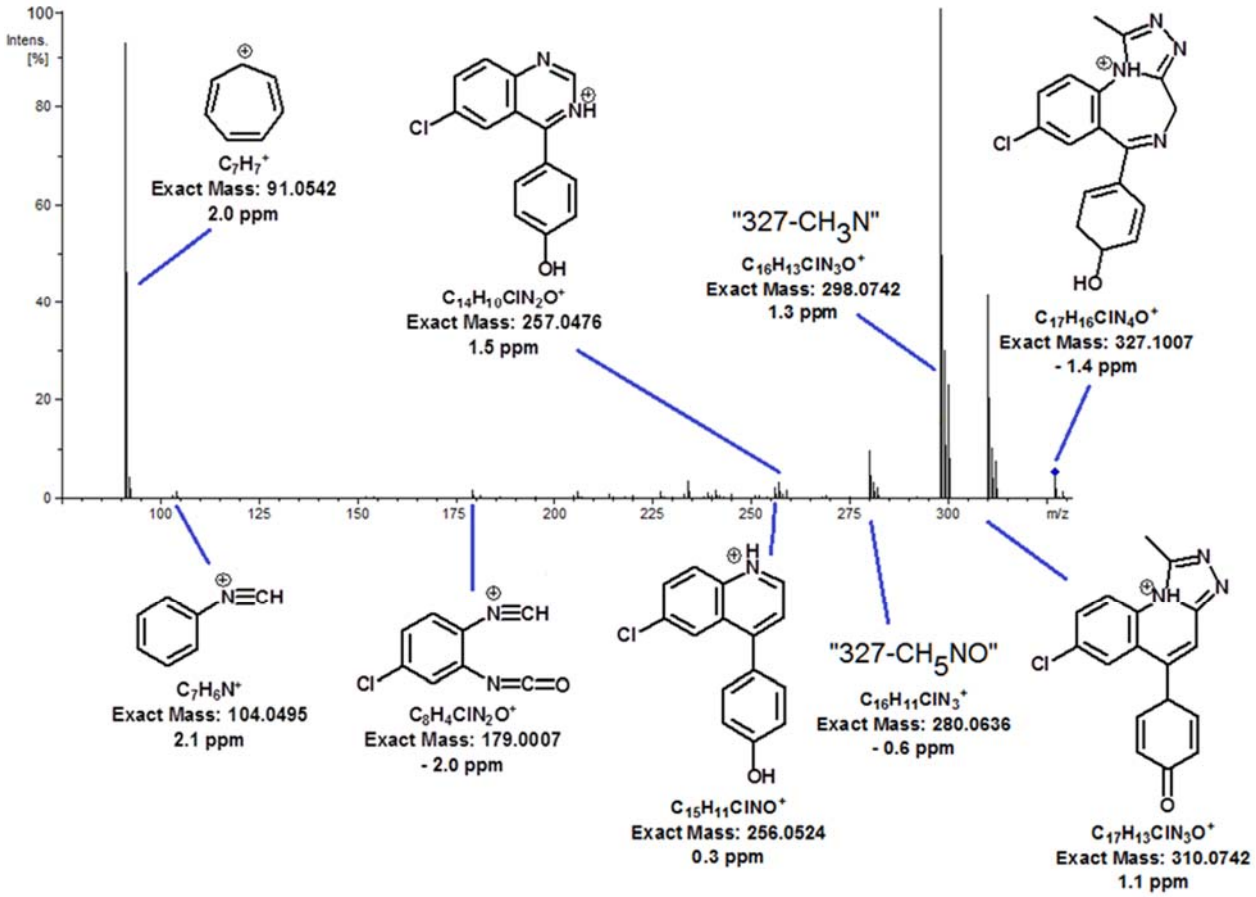

Figure SM4: MS/MS spectrum of DP327-3. Collision energy: 35 eV. Exact mass and experimental error in the measurement.

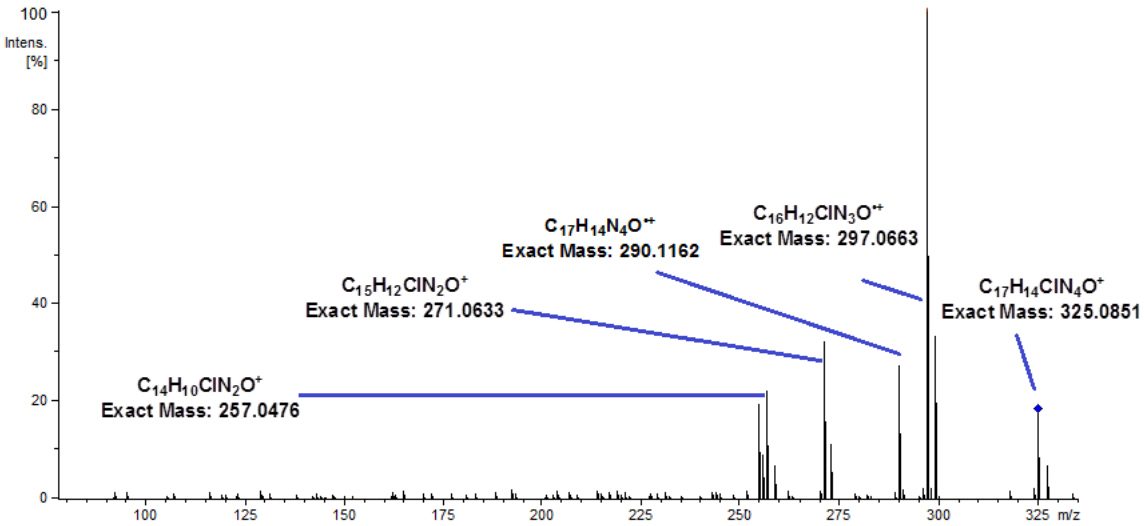

Figure SM5: MS/MS spectrum of DP325-1 (not identified). Collision energy: 40 eV. Molecular formulae attributed to the fragment-ions.

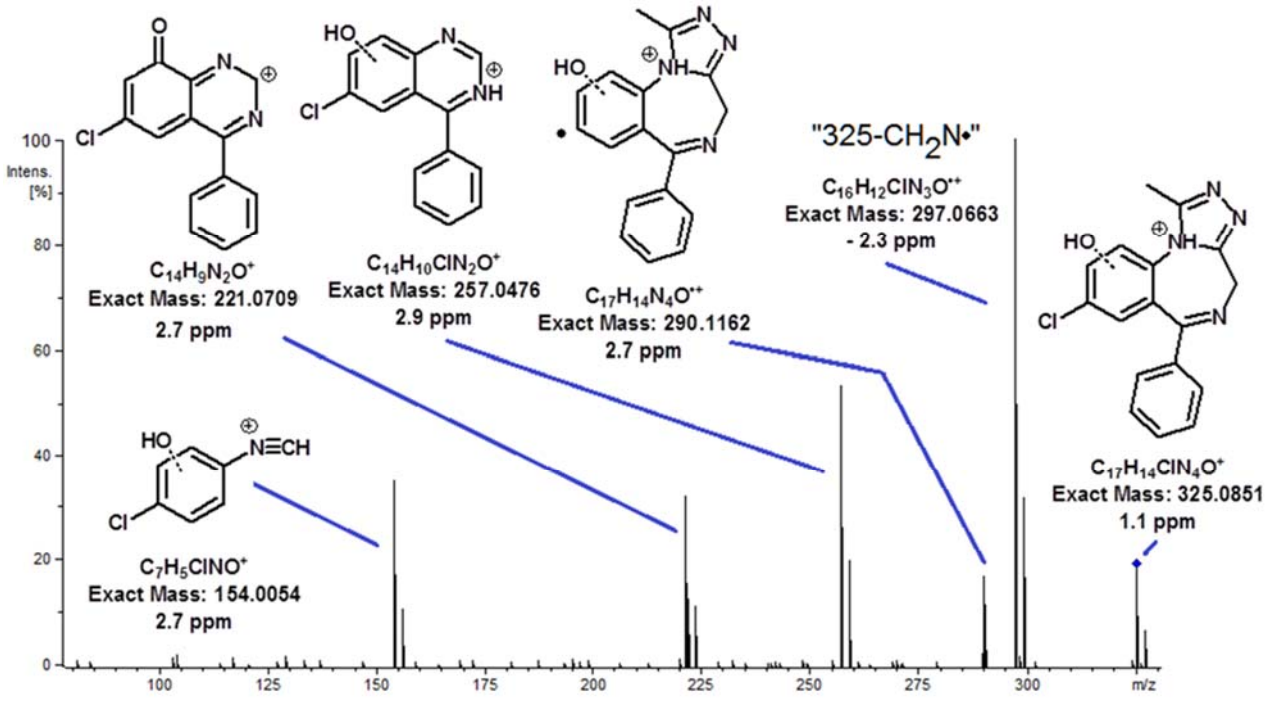

Figure SM6: MS/MS spectrum of DP325-2. Collision energy: 40 eV. Exact mass and experimental error in the measurement.

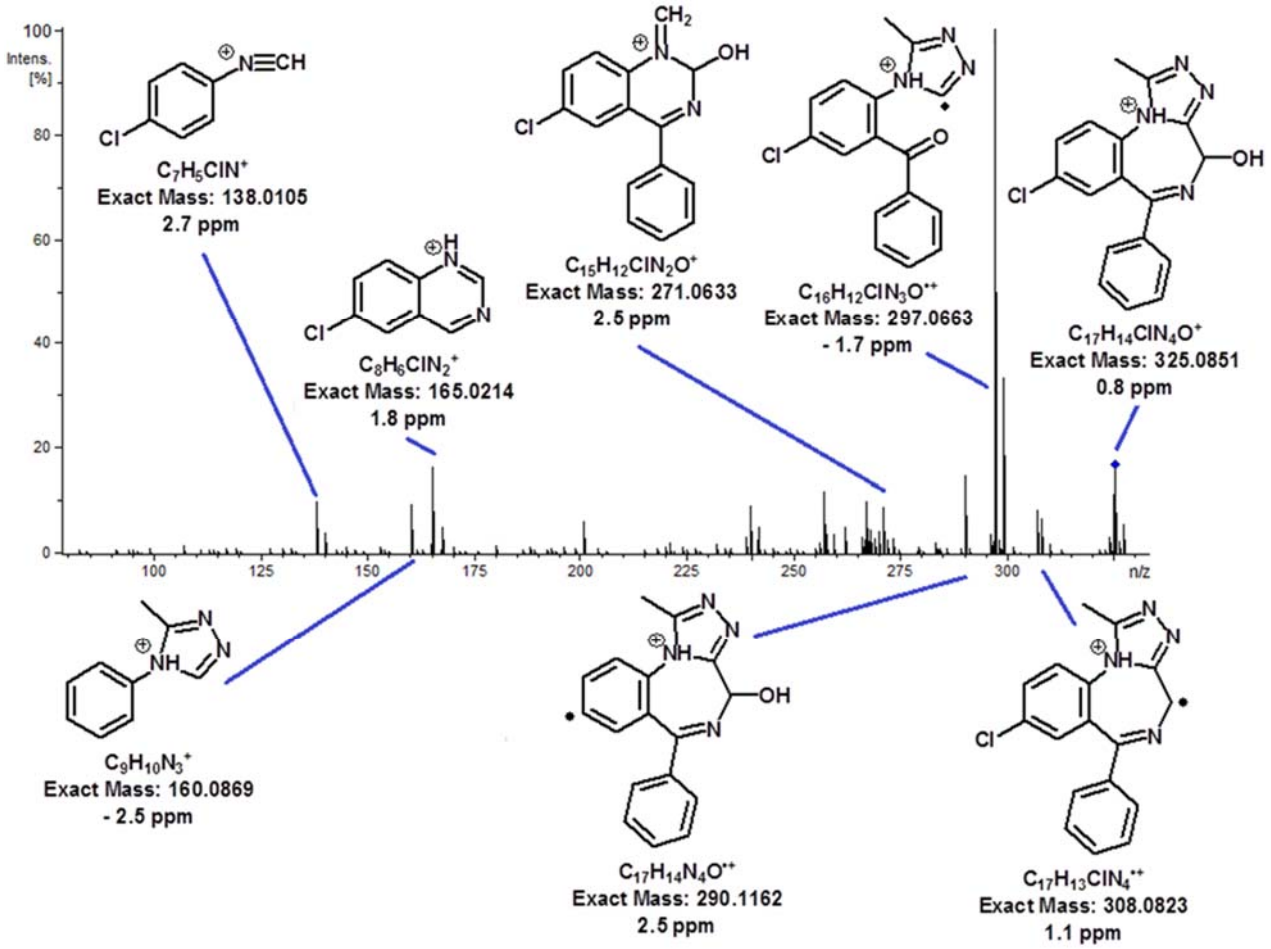

Figure SM7: MS/MS spectrum of DP325-3. Collision energy: 40 eV. Exact mass and experimental error in the measurement.

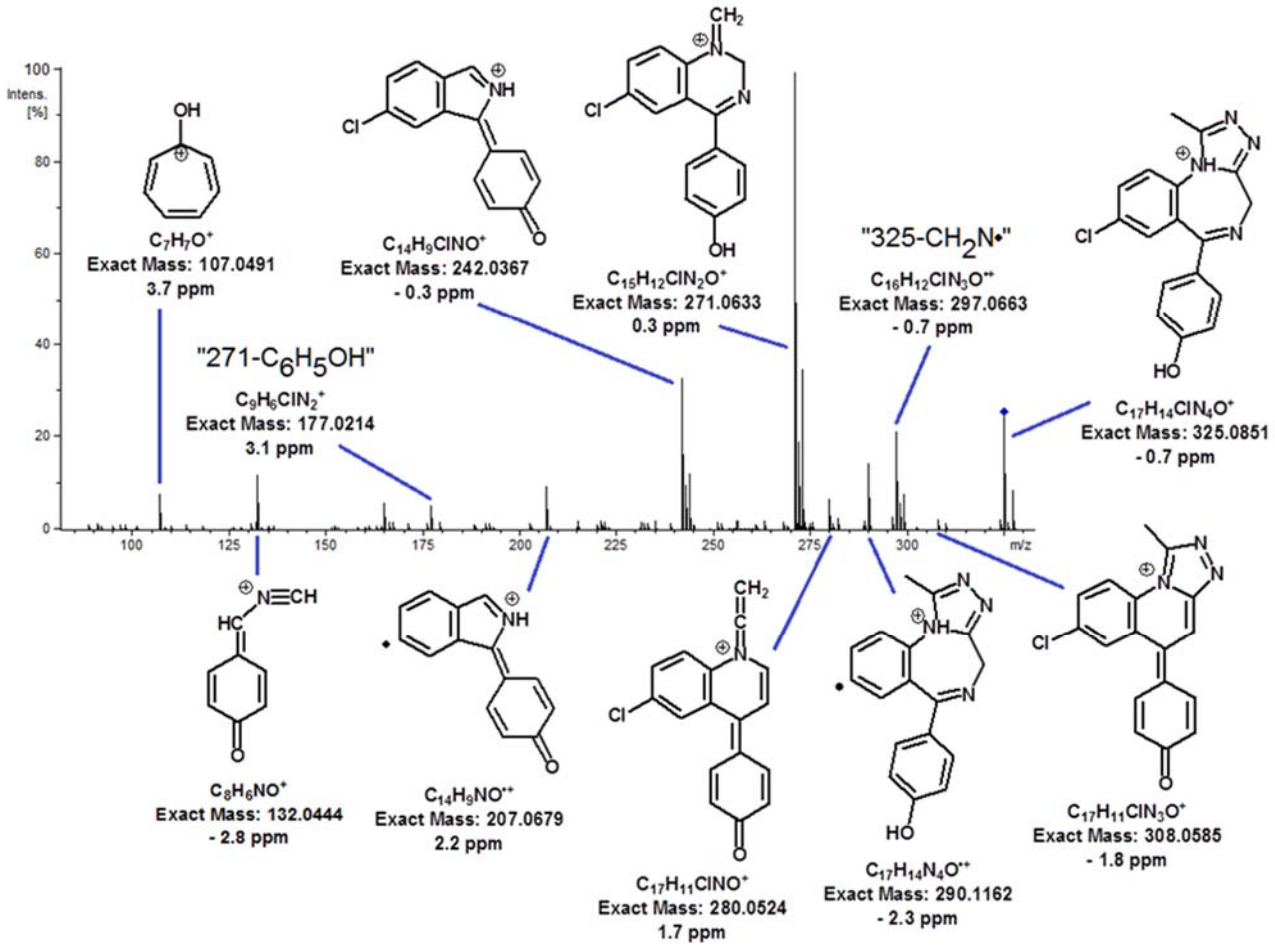

Figure SM8: MS/MS spectrum of DP325-4. Collision energy: 40 eV. Exact mass and experimental error in the measurement.

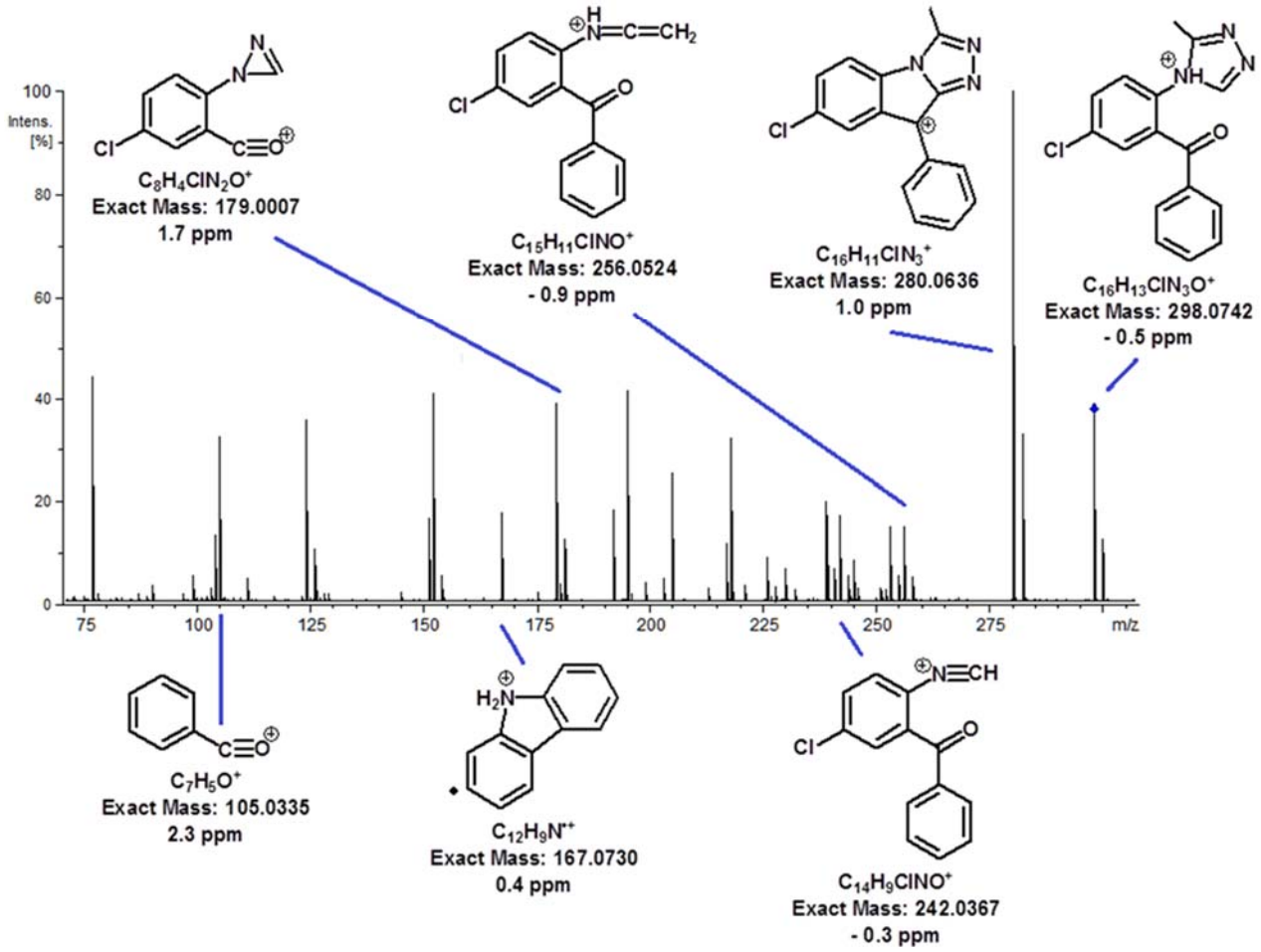

Figure SM9: MS/MS spectrum of DP298. Collision energy: 45 eV. Exact mass and experimental error in the measurement.

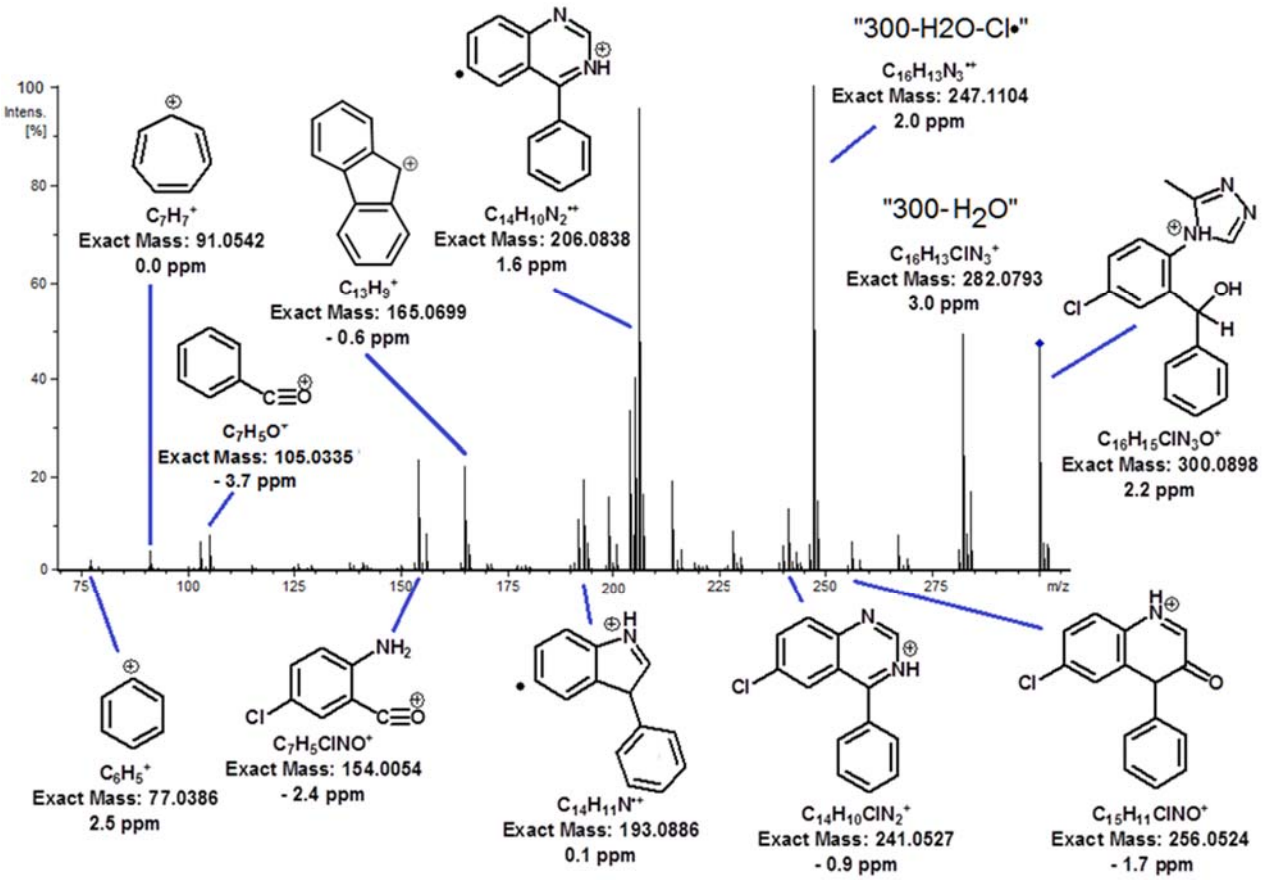

Figure SM10: MS/MS spectrum of DP300. Collision energy: 40 eV. Exact mass and experimental error in the measurement.

Occurrence of degradation products in photochemical and thermal degradation assays

Table SM10: Peak areas of the degradation products in the forced assays on a sample spiked with alprazolam at 2 or 100 $\mu g \cdot L^{-1}$. Peak areas are referred to the initial peak area of alprazolam in each experiment, to which a value of 100 was assigned. Mean values after the analysis of two aliquots.

	Heat, 70 ºC		UV lamp		Sunlight		Heat, 70 ºC		UV lamp		Sunlight	
Weeks:	**4**	**8**	**4**	**8**	**4**	**8**	**4**	**8**	**4**	**8**	**4**	**8**
	Assay 1, 2 $\mu g \cdot L^{-1}$						Assay 2, 2 $\mu g \cdot L^{-1}$					
DP300	--	--	--	--	--	--	--	--	--	--	--	--
DP327-1	--	0.36	--	--	--	--	--	0.39	--	--	--	--
DP327-2	--	--	--	--	--	--	--	--	--	--	--	--
DP327-3	--	0.37	--	--	--	--	--	0.39	--	--	--	--
DP325-1	--	--	--	--	--	--	--	--	--	--	--	--
DP325-2	--	--	--	--	--	--	--	--	--	--	--	--
DP325-3	--	--	--	--	--	--	--	--	--	--	--	--
DP325-4	--	--	--	--	--	--	--	--	--	--	--	--
DP298	0.21	0.64	--	--	--	--	0.21	0.66	--	--	--	--
	Assay 1, 100 $\mu g \cdot L^{-1}$						Assay 2, 100 $\mu g \cdot L^{-1}$					
DP300	--	--	0.05	0.13	0.02	0.05	--	--	0.06	0.14	0.02	0.05
DP327-1	0.20	0.43	--	0.03	--	--	0.20	0.41	--	0.04	--	--
DP327-2	0.07	0.12	--	0.02	--	--	0.07	0.13	--	0.02	--	--
DP327-3	0.17	0.37	--	0.02	--	--	0.19	0.37	--	0.02	--	--
DP325-1	0.07	0.15	--	0.02	--	--	0.06	0.14	--	0.02	--	--
DP325-2	--	--	--	--	--	--	--	--	--	--	--	--
DP325-3	--	--	--	--	--	--	--	--	--	--	--	--
DP325-4	0.03	0.09	--	--	--	--	0.03	0.09	--	--	--	--
DP298	0.30	0.70	--	0.02	--	0.01	0.28	0.72	--	0.02	--	0.01

-- : not detected

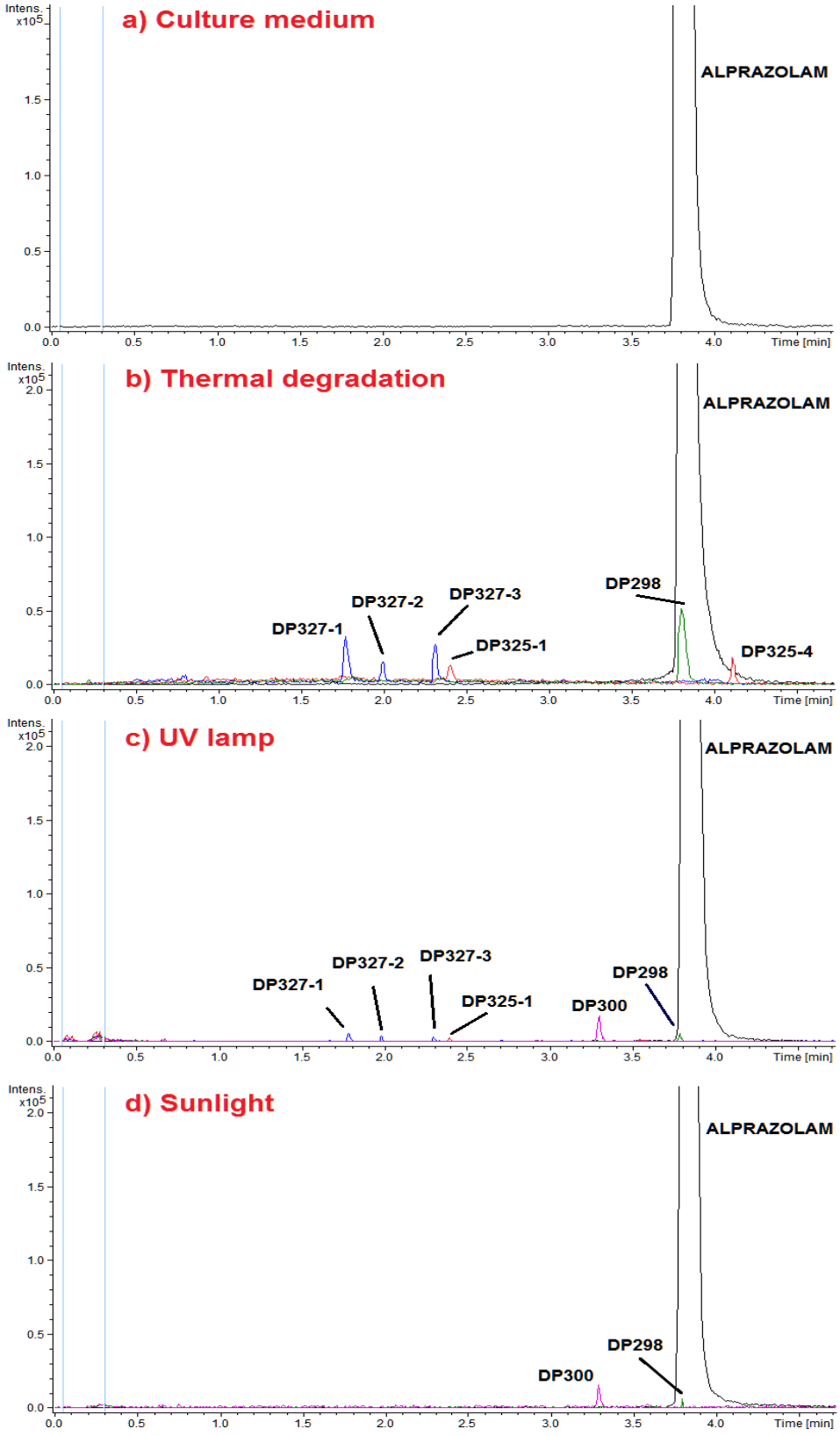

Figure SM11: Superposition of extracted ion chromatograms ([M+H]+ ± 0.01 for all compounds) obtained in different degradation assays for a water sample spiked with 100 µg·L^{-1}.

a) In presence of culture medium, after 5 weeks.
b) Thermal degradation, after 8 weeks.
c) Photochemical degradation (UV lamp), after 8 weeks.
d) Photochemical degradation (sunlight), after 8 weeks

Table SM11: Peak areas of the degradation products in the non-forced assays on river water samples spiked with alprazolam at 2 or 100 µg·L^{-1} (river Pisuerga, W1; river Tuerto, W2; river Pisuerga in presence of sediment, SED). Peak areas are referred to the initial peak area of alprazolam in each experiment, to which a value of 100 was assigned. Mean values after the analysis of two aliquots.

Sample:	W1	W1	W1	W2	W2	W2	SED	SED	SED	W1	W1	W1	W2	W2	W2	SED	SED	SED
Weeks:	**12**	**24**	**36**	**12**	**24**	**36**	**12**	**24**	**36**	**12**	**24**	**36**	**12**	**24**	**36**	**12**	**24**	**36**
	Assay 1, 2 µg·L^{-1}									Assay 2, 2 µg·L^{-1}								
DP300	0.40	0.94	1.36	0.40	0.96	1.26	0.29	0.76	1.25	0.38	0.90	1.27	0.4	0.94	1.26	0.30	0.78	1.20
DP327-1	--	--	0.27	--	--	0.27	--	--	0.28	--	--	0.29	--	--	0.25	--	--	0.28
Dp327-2	--	--	--	--	--	--	--	--	--	--	--	--	--	--	--	--	--	--
DP327-3	--	0.19	0.37	--	0.22	0.45	--	--	0.32	--	0.20	0.36	--	0.23	0.45	--	--	0.34
DP325-1	--	--	--	--	--	--	--	--	--	--	--	--	--	--	--	--	--	--
DP325-2	--	--	--	--	--	--	--	--	--	--	--	--	--	--	--	--	--	--
DP325-3	--	--	--	--	--	--	--	--	--	--	--	--	--	--	--	--	--	--
DP325-4	--	--	--	--	--	--	--	--	--	--	--	--	--	--	--	--	--	--
DP298	--	--	--	--	--	--	--	--	--	--	--	--	--	--	--	--	--	--
	Assay 1, 100 µg·L^{-1}									Assay 2, 100 µg·L^{-1}								
DP300	0.42	1.01	1.44	0.44	0.93	1.33	0.38	0.88	1.29	0.42	0.94	1.38	0.44	0.94	1.36	0.37	0.84	1.32
DP327-1	0.09	0.22	0.33	0.08	0.19	0.29	0.06	0.19	0.27	0.09	0.22	0.33	0.08	0.19	0.28	0.08	0.19	0.27
Dp327-2	0.06	0.11	0.18	0.03	0.09	0.17	0.04	0.10	0.16	0.06	0.09	0.20	0.03	0.09	0.19	0.04	0.10	0.16
DP327-3	0.14	0.30	0.37	0.11	0.29	0.44	0.09	0.23	0.30	0.15	0.27	0.37	0.09	0.30	0.43	0.07	0.20	0.33
DP325-1	0.02	0.07	0.09	0.03	0.10	0.11	0.06	0.08	0.09	0.02	0.07	0.11	0.03	0.09	0.11	0.06	0.07	0.09
DP325-2	--	0.02	0.05	--	0.01	0.04	--	0.01	0.02	--	0.03	0.04	--	0.01	0.03	--	0.01	0.02
DP325-3	--	0.02	0.04	--	0.02	0.05	--	--	0.02	--	0.02	0.04	--	0.02	0.05	--	--	0.02
DP325-4	0.02	0.06	0.11	0.03	0.05	0.10	0.03	0.05	0.07	0.02	0.08	0.12	0.03	0.06	0.11	0.02	0.06	0.07
DP298	--	0.02	0.06	--	0.02	0.06	--	--	0.02	--	0.02	0.05	---	0.02	0.06	--	--	0.02

-- : not detected

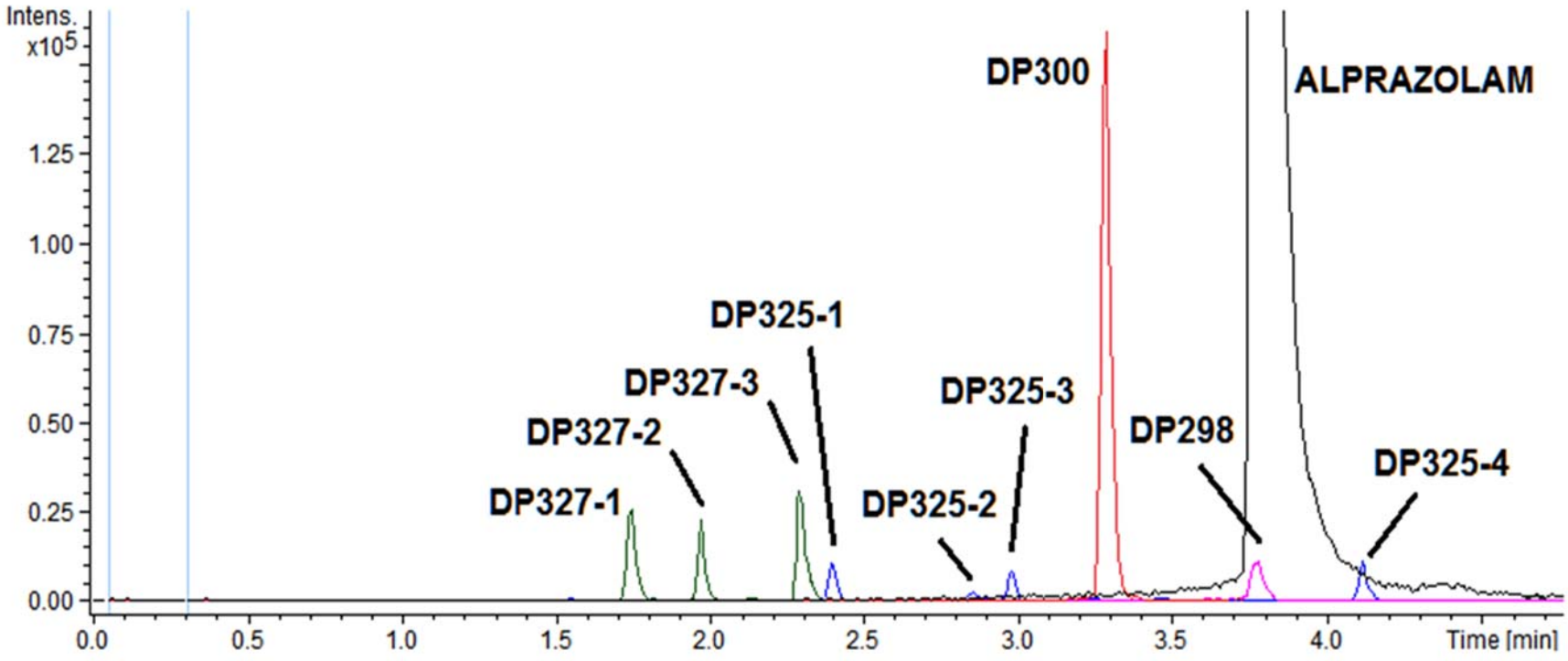

Figure SM12: Superposition of extracted ion chromatograms ($[M+H]^+$ ± 0.01 for all compounds) for a water sample spiked with 100 $\mu g \cdot L^{-1}$, after 36 weeks under non-forced conditions.

Prediction of ecotoxicity

In order to estimate the toxicity of alprazolam and its degradation products with a well-defined structure, the TEST software (Toxicological Estimation Software Tool), version 4.2, was applied.

Table SM12: Predicted 50% lethal concentrations (LC_{50}, μM) and 50% growth inhibition concentrations (IGC_{50}, μM) of alprazolam and degradation products for different tests.

	Daphnia magna LC_{50} (48 hr)	*Tetrahymena pyriformis* IGC_{50}	Fathead minnow LC_{50} (96 hr)
DP300	50	32	1.4
DP327-1	17	19	0.5
DP327-2	19	16	0.3
DP327-3	23	10	0.3
DP325-3	21	23	0.6
DP325-4	7.2	9	0.2
DP298	22	15	5.8
Alprazolam	8.9	14	0.2

Several degradation products showed predicted toxicities similar to that of alprazolam for the three ecotoxicological endpoints. DP300, the most prominent long-term degradation product in non-forced conditions, was about six or seven-fold less toxic than the parent compound for *Daphnia magna* and fathead minnow.

4.4. CELECOXIB

Journal of Hazardous Materials 342 (2018) 252–259

Contents lists available at ScienceDirect

Journal of Hazardous Materials

journal homepage: www.elsevier.com/locate/jhazmat

Photochemical, thermal, biological and long-term degradation of celecoxib in river water. Degradation products and adsorption to sediment

Juan J. Jiménez[a,b,*], Rafael Pardo[a], María I. Sánchez[c], Beatriz E. Muñoz[c]

[a] *Department of Analytical Chemistry (UIC090), Faculty of Sciences, Campus Miguel Delibes, University of Valladolid, Paseo de Belén 7, 47011, Valladolid, Spain*
[b] *I.U. CINQUIMA, Campus Miguel Delibes, University of Valladolid, Paseo de Belén 5, 47011, Valladolid, Spain*
[c] *Department of Analytical Chemistry, School of Industrial Engineers, University of Valladolid, Francisco Mendizábal 1, 47014, Valladolid, Spain*

HIGHLIGHTS

- Celecoxib is a persistent drug in surface water.
- The solar radiation promotes its slow degradation.
- 11 degradation products tentatively identified from high-resolution MS/MS spectra.
- Sulfonic, carboxylic and hydroxylated derivatives are the main degradation products.
- Celecoxib can be partially adsorbed onto aquatic sediment.

GRAPHICAL ABSTRACT

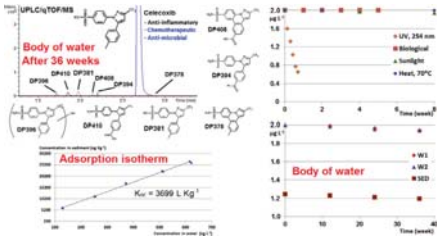

ARTICLE INFO

Article history:
Received 27 May 2017
Received in revised form 11 August 2017
Accepted 14 August 2017
Available online 19 August 2017

Keywords:
Celecoxib
Degradation products
River water
Adsorption equilibrium constants
High-resolution mass spectrometry

ABSTRACT

Celecoxib is an anti-inflammatory drug with antibacterial activity whose fate in surface water is unknown. Thus, some assays have been conducted under forced biological, photochemical and thermal conditions, and non-forced conditions, to establish its persistence and degradation products in river water. The results suggest that celecoxib dissolved in river water is not biologically degraded while it is minimally altered after its exposure to sunlight or high temperature (70 °C). Only the irradiation at 254 nm promotes its complete degradation. Celecoxib is degraded about 3%, in 36 weeks, when water was kept at room temperature and the exposure to sunlight was partially limited as it happens inside a body of water. Residues were monitored by ultra-pressure liquid chromatography/quadrupole time-of-flight/mass spectrometry after solid-phase extraction; eleven degradation products were detected and the structures of nine of them were unequivocally proposed from the molecular formulae and fragmentation observed in high-resolution tandem mass spectra. The long-term transformation products under non-forced conditions were 4-[5-(4-methylphenyl)-3-(trifluoromethyl)-1H-pyrazol-1-yl]benzenesulfonic acid, 4-[1-(4-sulfoaminephenyl)-3-(trifluoromethyl)-1H-pyrazol-5-yl]benzoic acid and a hydroxylated derivative. The degradation over time in presence of sediment was monitored, being slightly higher, about 4%. The adsorption equilibrium constants of celecoxib and degradation products on river sediment were estimated.

* Corresponding author at: Department of Analytical Chemistry (UIC090), Faculty of Sciences, Campus Miguel Delibes, University of Valladolid, Paseo de Belén 7, 47011, Valladolid, Spain.
E-mail address: jjimenez@qa.uva.es (J.J. Jiménez).

http://dx.doi.org/10.1016/j.jhazmat.2017.08.037
0304-3894/

1. Introduction

Trace concentrations of pharmaceuticals have been reported in surface waters in the last twenty years. The raw sewages and the effluents discharged from wastewater treatment plants (WWTPs) are the main source of introduction of these compounds in the environment. Therefore, several laboratory assays have been conducted to foresee the fate of many pharmaceuticals in water.

Celecoxib is a selective inhibitor of the inducible form of the enzyme cyclooxygenase; its prescription is approved to treat some painful musculoskeletal diseases. Regardless of the anti-inflammatory activity, it has been proven that celecoxib exhibits certain anti-microbial activity [1,2] in addition to chemotherapeutic properties against some cancers [3]. Celecoxib is extensively metabolized in humans and five phase I and phase II metabolites have been reported [4–8].

As regards its occurrence in aquatic ecosystems only a manuscript has considered the monitoring of celecoxib in water samples. After sampling the inlet and outlet streams of a WWTP in different months, authors concluded that the depuration treatment was ineffective to remove celecoxib; the maximum concentration in the effluents was 49 ng L^{-1}. Furthermore, a degradation product, celecoxib carboxylic acid, was identified with the help of a metabolite database [9].

Since celecoxib could have potentially harmful effects on the aquatic ecosystems it is convenient obtain information about its fate in surface water. In this context, river water spiked with celecoxib at low concentration has been subjected to photochemical, thermal and biological degradation assays to know the stability of the drug. Moreover, some degradation assays have been devised in order to know its long-term fate; to this aim, river water containing celecoxib was placed in a glass container and exposed to sunlight for several months at room conditions; as the glass absorbs UV radiation, the behavior of celecoxib can be so similar to that in a body of water where the penetration of solar UV radiation is diminished with depth. Water samples were analyzed by ultra-pressure liquid chromatography/quadrupole time-of-flight/mass spectrometry; eleven degradation products were detected and their structures were tentatively proposed from the molecular formulae and fragmentation observed in high-resolution tandem mass spectra. The evolution of the degradation products was also monitored through time to estimate their occurrence and the toxicities of some of them were predicted for three ecotoxicological endpoints, comparing them with those of celecoxib. In addition, as a certain capacity of adsorption of celecoxib on sediment was observed, an adsorption isotherm is presented while the adsorption equilibrium constants of the degradation products were also evaluated on the assumption that peak areas vary linearly with concentration.

2. Experimental

2.1. Water samples, reagents and materials

Water samples were collected from the rivers Pisuerga (pH value 7.8, chemical oxygen demand value 4.6 mg L^{-1}), in the urban area of the city of Valladolid, and Tuerto (pH value 7.4, chemical oxygen demand value 3.9 mg L^{-1}), in the rural area of the La Bañeza, province of León. A sediment sample (total organic carbon 1.2%; clay 11%, silt 44%, sand 45%) was collected from the river Pisuerga. River water was filtered through cellulose nitrate disks (Sartorius, Barcelona, Spain): 0.2 μm pore-size disks for the estimation of adsorption equilibrium constants, 3 μm pore-size disks to carry out biodegradation experiments and 0.45 μm pore-size disks for other degradation experiments.

Celecoxib (99% purity) was purchased from Sigma-Aldrich (St. Louis, MO, USA). Methanol, acetonitrile, sodium hydroxide, potassium dihydrogen phosphate and sodium azide were supplied by Panreac (Barcelona, Spain) and ultrapure water was obtained from a Milli-Q plus apparatus (Millipore, Milford, MA, USA). A lamp equipped with an 8W UV tube, 29200 model, was obtained from Camag (Muttenz, Switzerland). Tryptone soya broth (TSB), a highly nutrient liquid culture medium for general purpose use, and EBH cartridges (60 mg) for solid-phase extraction (SPE) were supplied by Scharlab (Barcelona, Spain).

2.2. Biological degradation

2.2.1. Aerobic degradation

Biological degradation assays were done with water from the river Pisuerga (pH 7.8) which was spiked with celecoxib to achieve a concentration of 2 or 100 μg L^{-1}. A volume of 50 mL of river water was transferred into a 100 mL Erlenmeyer flask, which was then coated with aluminum foil, including its opening, to avoid the exposure to sunlight but allowing the exchange of air with the atmosphere. A celecoxib control solution was similarly prepared in ultrapure water (pH 7.8 adjusted with NaOH) containing 0.02% (w/v) sodium azide as a biocide. Water blanks were prepared, too. Samples were run in parallel; flasks were shaken in a Promax 2020 reciprocating shaker (Heidolph, Germany) at a rotation speed of 130 rpm for 5 weeks, within a temperature range of 18–21 °C. Aliquots of 2 mL were collected each week and subjected to the analytical method. Evaporation water losses were periodically restored by addition of water of the same type. All biological experiments were done in duplicate.

2.2.2. Anaerobic degradation

River water (pH 7.8) spiked at 2–100 μg L^{-1} was placed in 15 mL vials, completely filled to avoid the presence of air in the headspace. Vials were closed, protected from light by coating them with aluminum foil and kept in a temperature range of 18–21 °C during experimentation. Control solutions in ultrapure water (pH 7.8 adjusted) containing 0.02% sodium azide, and the corresponding blanks, were also run in parallel. A batch of vials was assembled to withdraw weekly samples during 5 weeks; a volume of 2 mL of each withdrawn vial was collected for analysis.

2.2.3. Degradation in culture medium

A 20/80 (v/v) mixture of TSB culture medium and river water was spiked (2 or 100 μg L^{-1}) and a volume of 100 mL of mixture was placed in a 250 mL glass container. A control solution in ultrapure water (pH 7.8 adjusted) containing 0.02% sodium azide and celecoxib, and a blank of the medium-water mixture, were also prepared and run in parallel. Closed vessels were heated at 35 °C in darkness for 5 weeks. Aliquots of 4 mL were sampled weekly and filtered through 0.45 μm pore-size cellulose nitrate; 2 mL of filtrate were collected for analysis.

2.3. Thermal and photochemical degradation

A volume of 100 mL of river water (pH = 7.8) spiked with celecoxib (2 or 100 μg L^{-1}) was placed in a closed 250 mL glass flask. This was coated with aluminum foil and placed in an oven at 70 °C. A water blank was heated, too. Aliquots of 2 mL were collected at four and eight weeks and subjected to the analytical method.

River water was placed in quartz cuvettes for photochemical degradation. Closed cuvettes were irradiated at 254 nm with a lamp, or exposed directly to sunlight placing them on the outer edge of a window, south-facing; assay was done in the city of Valladolid (latitude: 41° 38′ 15″N, longitude: 4° 44′ 17″W), in the months of May–June. Water aliquots were collected at regular intervals of

time and injected in the chromatographic system. Control samples of celecoxib in river water, protected from radiation with aluminum foil, and a blank were also prepared. All experiments were done in duplicate.

2.4. Non-forced degradation assays

A simple approach was adopted to simulate the concurrent natural process in a body of water. River water was placed in a transparent glass container with air-tight seal, which was shaken and opened weekly to replace the air inside in contact with the water surface. The container was kept at laboratory temperature (18–21 °C) under the natural day-night cycle and directly exposed to sunlight for 36 weeks, at which time the degradation assay was ended. In these conditions the solar radiation must pass through the laboratory window glass and the container glass to reach the body of water; glass absorbs UV radiation and the behavior of celecoxib in the container simulates that in a mass of water where the penetration of solar UV radiation is diminished with depth. The attenuation of the radiation was estimated by measurements of transmittance through the two types of glass (container and window); so, it was quantified that the percentages of radiation transmitted to the body of water were 40%, 1.3%, 0.02%, 8 10^{-4}% and 8 10^{-5}% at wavelengths of 350, 320, 310, 305 and 290 nm, respectively.

A volume of 2500 mL of river water placed in glass container was spiked with celecoxib to achieve an initial concentration of 2 or 100 μg L^{-1} in each degradation assay; aliquots of 25 mL were collected periodically and subjected to SPE before analysis by the chromatographic system to follow the degradation, look for degradation products and monitor them. Degradation experiments were done between the months of March and November with waters from the rivers Pisuerga (W1 sample) and Tuerto (W2 sample). Furthermore, the degradation of W1 sample was studied in presence of sediment by adding river sediment to the container in a sediment to solution ratio of 0.013 g mL^{-1} (SED sample). Blank samples were prepared, as well.

It was verified that W1 and W2 river water samples were free of celecoxib residues. First, water blanks were subjected to the analytical method to test the absence of the parent compound. Once known the degradation products yielded in the forced assays it was also tested that they were not present in the water extracts. Similarly, the absence of residues in the sediment sample was confirmed by the extraction of a portion of sediment with methanol by mechanical shaking; the extract was concentrated for analysis.

2.5. Study of adsorption to sediment

Experiments to investigate the capacity of adsorption of celecoxib and degradation products were done. The adsorption equilibrium constant (K_d) of celecoxib into sediment (sieved through a 0.5 mm mesh) was determined by using a batch approach. Spiked river water (100 mL) was added to sediment (1.3 g) to achieve a sediment to solution ratio of 0.013 g mL^{-1}; celecoxib concentrations were 200, 400, 600, 800 and 1000 ng L^{-1}. River water contained 0.02% sodium azide as a biocide to minimize a possible microbial activity and pH (7.8) was controlled with phosphate buffer (0.02 M). Control solutions without sediment were prepared, too. The flasks, protected from sunlight with aluminum foil, were manually shaken for 1 min and left standing at 20 ± 1 °C for a period of 24 h. Afterwards, an aliquot was centrifuged to remove solids, and 20 mL were collected to determine the celecoxib concentration in equilibrium. An adsorption isotherm was drawn in duplicate. The concentration adsorbed on the sediment was not directly measured.

Analytical standards are unavailable for the degradation products, however an estimation of their K_d was carried out on the assumption that there is a linear relationship between peak area and concentration for each compound; degraded solutions of celecoxib were used to this aim. Experiments similar to the above-described were devised by spiking water with a solution containing the degradation products and selecting an appropriate sediment to solution ratio. So, the decrease percentage of peak area in water was supposed to be the percentage of compound adsorbed onto sediment (A%) and K_d was calculated by Eq. (1), which is valid if adsorption equation is linear [10]. Peak areas of the adsorption experiments were compared with those of control solutions by a *t*-test (n = 5) to confirm the existence of differences before applying the equation.

$$K_d = \frac{A\%}{R(100 - A\%)} \quad (1)$$

2.6. Sample preparation

Except for the photochemical degradation assays, river water aliquots were eluted through EBH cartridges previously conditioned by successive elution of methanol (6 mL) and water (6 mL). Cartridges were washed with 3 mL of a water-methanol (80:20, v/v) mixture after the sample elution. The stationary phase was dried with air for 3 min and the extract was eluted with methanol (4 mL) by gravity. Then, the extract was evaporated in 30 min by a Myvac vacuum centrifuge evaporator (Genevac, Ipswich, UK) heated at 40 °C and the dry residue was collected in 0.5 mL of methanol, which was filtered through a 0.20 μm pore-size PTFE filter for chromatographic analysis.

2.7. Determination by liquid chromatography–mass spectrometry

An Acquity ultra-pressure liquid chromatograph from Waters coupled to a Maxis Impact quadrupole time-of-flight tandem mass spectrometer from Bruker Daltonics (Bremen, Germany) was used. Analyses were done with electrospray ionization in negative mode. The chromatograph was fitted with a Waters BEH ODS column (50 mm x 2.1 mm, 1.7 μm particle size). Mobile phase flow rate was 0.5 mL min^{-1} and it consisted of 0.1% formic acid in water (A) and 0.1% formic acid in acetonitrile (B); assays were done in gradient conditions: from 25% B to 80% B in 4.5 min, and then 90% B in 1 min. Re-equilibration time was 1 min. Injection volume was 7 μL.

The operation parameters of the electrospray ionization source for the MS and MS/MS experiments were as follows: nebulizing gas pressure, 2 bar; end plate offset voltage, 1000 V; capillary voltage, 4000 V; drying gas temperature, 200 °C; dry gas flow, 6 L min^{-1}. Nitrogen was used as drying and nebulizing gas. Mass calibration adjustments were performed by using a 10 mM sodium formate solution in 2-propanol/water. MS/MS experiments based on collision induced dissociation with nitrogen gas were performed. The quantitation of celecoxib was done by linear calibration graphs based on the measurement of peak areas in the chromatograms extracted for the ion $[M-H]^-$ generated in the electrospray source by MS experiments, with a mass range of ±0.01 Da. Similarly, peak areas of degradation products were integrated in the chromatograms extracted for the corresponding $[M-H]^-$ ions. As regards the performance of the analytical method, mean recoveries of celecoxib in W1 sample volumes of 2 or 25 mL were about 96% with repeatabilities close to 1.6% and 1.2% (n = 5) for 2 and 100 μg L^{-1}, respectively. A dilution of the extracts was required to quantify celecoxib in the assays at high concentration.

Table 1
Initial and final mean concentrations (n = 5) of celecoxib in the different degradation assays; time at which the final concentration was measured.

Degradation	Assay	Initial concentration ($\mu g\,L^{-1}$)	Final concentration ($\mu g\,L^{-1}$)	Elapsed time (weeks)
Aerobic	1	2.00	1.99	5
	2	1.98	1.99	5
Aerobic	1	101.4	100.2	5
	2	99.2	99.2	5
Anaerobic	1	2.01	1.99	5
	2	2.00	2.00	5
Anaerobic	1	100.8	100.0	5
	2	99.4	99.2	5
Culture	1	2.01	2.01	5
medium	2	2.00	2.00	5
Culture	1	100.8	100.0	5
medium	2	100.4	99.8	5
Photochemical,	1	2.01	1.95**	8
sunlight	2	2.00	1.93**	8
Photochemical,	1	101.4	97.8**	8
sunlight	2	100.0	96.4**	8
Photochemical, UV	1	2.00	Not detected	1
lamp	2	2.00	Not detected	1
Thermal	1	2.00	1.99	8
	2	2.01	2.00	8
Thermal	1	100.6	99.2	8
	2	100.0	98.8	8
Non-forced, W1	1	2.00	1.94**	36
	2	2.01	1.94**	36
Non-forced, W1	1	100.8	97.6**	36
	2	100.2	97.0**	36
Non-forced, W2	1	2.00	1.95**	36
	2	2.00	1.94**	36
Non-forced, W2	1	100.4	97.4**	36
	2	99.6	96.6**	36
Non-forced, SED	1	1.26	1.21**	36
	2	1.23	1.18**	36
Non-forced, SED	1	60.2	57.8**	36
	2	61.2	58.6**	36

** Significant difference ($p < 0.05$).

3. Results and discussion

3.1. Degradation of celecoxib

Table 1 resumes the results of the degradation assays. The results of each individual assay are supplied as supplementary material (Appendix A). An independent samples *t*-test ($p = 0.05$) was used to compare the concentrations measured at the beginning and end of the assays ($n = 5$), after checking the homogeneity of the variances which resulted to be homogeneous. Celecoxib was found to be resistant to biological degradation in river water at the two assayed concentrations, 2 and 100 $\mu g\,L^{-1}$, even when a culture medium was added to river water in order to favor the growth of the microorganisms (Tables A1–A3). There were also no significant differences in concentration when a solution of celecoxib was heated at 70 °C for 8 weeks; however, a slight decay was observed in the assays carried out at 100 $\mu g\,L^{-1}$, about 1.3% with respect to the initial concentration (Table A4), which suggests that celecoxib is minimally affected by the possible chemical reactions in river water.

Regarding the photochemical degradation, the exposure of celecoxib in solution to sunlight for 8 weeks decreased significantly its initial concentration, about 3.3% and 3.6% for the low and high concentration levels (Table A5), respectively, while the exposure of celecoxib in river water to UV radiation from the lamp (centered at 254 nm) promoted a fast degradation; it was detected only during 5 days. The degradation followed a first-order kinetics with half-lives of 2.72 days ($R^2 = 0.98$) and 2.81 days ($R^2 = 0.99$) after two assays at 2 $\mu g\,L^{-1}$ (Table A6). These results indicate that celecoxib can undergo a slow photochemical degradation in surface water at slightly alkaline pH.

The degradation of celecoxib over time under non-forced conditions was monitored, too. Therefore, the decrease of celecoxib concentration after 36 weeks was estimated to be about 3.2% and 3.0% in W1 and W2 samples, respectively. Assays in presence of aquatic sediment were also devised to know its possible influence in the degradation; in this case, the degradation percentage was somewhat higher in comparison to the assays without sediment, about 4.2%. There were significant differences ($p = 0.05$) between the initial and final concentrations of the non-forced assays after applying a *t*-test (Tables A7–A9). On the other hand, the concentrations of celecoxib measured in water when the experimentation was done in presence of sediment diminished, which suggested a possible adsorption to sediment.

It must be pointed out that a smelly odor began to be perceived in the blank sample with sediment after a few weeks, which denoted a possible growth of microorganisms and the subsequent biodegradation process of the organic matter. However, this biodegradation process was not observed in the containers with celecoxib likely due to the anti-microbial activity described for this pharmaceutical.

The results of these laboratory assays suggest that celecoxib is a persistent drug in surface water. It seems to be a non-biodegradable compound and the chemical reactions in aqueous medium at a slightly alkaline pH and environmental temperature do not affect it perceptibly. Only the photochemical reactions seem to alter it but their reaction rate is very low inside a body of water.

3.2. Detection and identification of degradation products

Eleven degradation products were found during the experimentation. The presence of compounds related to the degradation of celecoxib was established by the observation of new chromatographic peaks in the MS chromatograms, which were not present in blanks. The $[M-H]^-$ ion of each degradation product, besides of

celecoxib, was isolated and fragmented by collision induced dissociation to obtain structural information and propose tentative structures from the interpretation of the fragment-ions in MS/MS spectra. Table 2 shows the established molecular formulae, the proposed identifications and the abbreviations of the compounds. A brief discussion about the assignation of structures to each compound is supplied as supplementary material. High-resolution tandem mass spectra can be seen in Figs. A1–A12.

In summary, some degradation products arose from the oxidation of the terminal methyl to aldehyde (DP394) or carboxylic acid (DP410) groups, moreover a hydroxylated derivative (DP396, not unequivocally identified) was detected; the position of the hydroxyl substituent could not be assigned from the fragmentation data. DP381 was thought to be the corresponding sulfonic acid from the celecoxib, in which the amine group had been replaced by a hydroxyl. The structure of DP395 was that of DP381 after the oxidation of the terminal methyl to aldehyde.

Several phenanthridines were observed after the exposure of celecoxib to radiation, two hydrogen atoms close to each other were removed to form a new six-membered cycle by the bond of the corresponding carbon atoms. Thus, DP378 derived directly from celecoxib; DP392 and DP408 were those whose terminal methyl was oxidized to aldehyde or carboxylic acid, respectively. The structure of DP424 was not completely elucidated but it seems to be a dihydroxylated derivative from DP392. DP409 kept the phenanthridine core and showed two frequent transformations: the oxidation of the methyl to carboxylic acid and the conversion of the sulfonamide group to sulfonic acid. Finally, the sulfonaminephenyl group was substituted for a carboxylic acid in DP269. Most of these degradation products had not been described till now; only DP410 (celecoxib carboxylic acid) and DP 381 (celecoxib sulfonic acid) had been previously described as degradation products yielded in metabolic processes of the living organisms [4,6,7].

3.3. Occurrence of degradation products in biological and forced degradation assays

Table 3 shows the peak areas of the degradation products after 4 and 8 weeks since the beginning of the assays: a value of 100 was assigned to the initial peak area of celecoxib (week 0) in each assay, and all other peak areas were referred to this value. Celecoxib was not degraded biologically but trace amounts (0.02) of DP381 were detected in the assays with culture medium at 100 $\mu g\,L^{-1}$ (Table A10).

Three degradation products were found in the degradation assays at high temperature and concentration. DP394 was the most abundant compound after 8 weeks with a relative peak area of 0.70; DP396 and DP381 were found in amounts of 0.13 and 0.07, respectively. As well, some degradation products were found when celecoxib was exposed to sunlight for 8 weeks; DP381 was the main degradation product with a relative peak area about 0.5–0.6, moreover it was the only celecoxib related compound detected in the forced degradation assay at low concentration. At high concentration, smaller amounts of DP394, DP410 and DP378 were detected under the influence of the solar radiation, too (Table A10).

The exposure of river water to UV radiation arisen from a lamp degraded completely the celecoxib, at 2 $\mu g\,L^{-1}$, in a week. Many degradation products were observed; among them DP381 and DP378 were the most abundant (Figs. A13 and A14). The compounds DP424 and DP269 were prominent, too. The occurrence of the degradation products decreased at the end of this study (5 days).

Table 2
Retention times (RT), accurate masses measured in the MS spectra for the $[M-H]^-$ ion, errors in the determination of the exact masses, molecular formulae and number of rings and double bonds (RDBs) of the corresponding structures for the detected degradation products.

RT (min)	Molecular formula	Exact mass (Da)	Accurate mass (Da)	Error (ppm)	RDBs	Compound	Abbreviation
1.45	$C_{17}H_8F_3N_2O_5S$	409.0113	409.0120	−1.7	13.5	2-trifluoromethyl-9-sulfo-H-pyrazolo[1,5-f]phenanthridine-6-carboxylic acid	DP409
1.48	$C_{17}H_{10}F_3N_2O_4S$	395.0319	395.0317	0.5	12.5	4-[5-(4-formylphenyl)-3-(trifluoromethyl)-1H-pyrazol-1-yl]benzenesulfonic acid	DP395
1.52	$C_{17}H_9F_3N_3O_5$	424.0220	424.0215	1.2	13.5	x,x-dihydroxy-2-trifluoromethyl-6-formyl-H-pyrazolo[1,5-f]phenanthridine-9-sulfonamide	DP424
1.70	$C_{12}H_8F_3N_2O_2$	269.0543	269.0546	−1.1	8.5	3-(trifluoromethyl)-5-*p*-tolyl-1H-pyrazole-1-carboxylic acid	DP269
1.72	$C_{17}H_{13}F_3N_3O_3S$	396.0635	396.0625	2.5	11.5	Hydroxylated celecoxib[a]	DP396
1.86	$C_{17}H_{11}F_3N_3O_4S$	410.0434	410.0428	1.5	12.5	4-[1-(4-sulfoaminephenyl)-3-(trifluoromethyl)-1H-pyrazol-5-yl]benzoic acid	DP410
1.96	$C_{17}H_{12}F_3N_3O_3S$	381.0526	381.0523	0.8	11.5	4-[5-(4-methylphenyl)-3-(trifluoromethyl)-1H-pyrazol-1-yl]benzenesulfonic acid	DP381
2.15	$C_{17}H_9F_3N_3O_4S$	408.0271	408.0269	0.5	13.5	2-trifluoromethyl-9-sulfonamine-H-pyrazolo[1,5-f]phenanthridine-6-carboxylic acid	DP408
2.20	$C_{17}H_{11}F_3N_3O_3S$	394.0476	394.0477	−0.3	12.5	4-[5-(4-formylphenyl)-3-(trifluoromethyl)-1H-pyrazol-1-yl]benzenesulfonamide	DP394
2.40	$C_{17}H_9F_3N_3O_3S$	392.0322	392.0330	−2.0	13.5	2-trifluoromethyl-6-formyl-H-pyrazolo[1,5-f]phenanthridine-9-sulfonamide	DP392
2.72	$C_{17}H_{13}F_3N_3O_2S$	380.0686	380.0688	−0.5	11.5	4-[5-(4-methylphenyl)-3-(trifluoromethyl)-1H-pyrazol-1-yl]benzenesulfonamide	Celecoxib
2.88	$C_{17}H_{11}F_3N_3O_2S$	378.0530	378.0525	1.3	12.5	2-trifluoromethyl-6-metyl-H-pyrazolo[1,5-f]phenanthridine-9-sulfonamide	DP378

[a] likely 4-[5-(4-(hydroxymethyl)-phenyl)-3-(trifluoromethyl)-1H-pyrazol-1-yl]benzenesulfonamide, x-hydroxy-4-[5-(4-methylphenyl)-3-(trifluoromethyl)-1H-pyrazol-1-yl]benzenesulfonamide or 4-[5-(x-hydroxy-4-methylphenyl)-3-(trifluoromethyl)-1H-pyrazol-1-yl]benzenesulfonamide.

Table 3
Peak areas of the degradation products obtained in forced and non-forced assays on river water samples spiked with celecoxib at 2 or 100 μg L^{-1} (river Pisuerga, W1; river Tuerto, W2; river Pisuerga in presence of sediment, SED). Peak areas are referred to the initial peak area of celecoxib in each experiment, to which a value of 100 was assigned. Data are the mean of two experiments.

Assay:		Heat, 70 °C		Sunlight		Non-forced								
Sample:		W1	W1	W1	W1	W1	W1	W1	W2	W2	W2	SED	SED	SED
Weeks:		4	8	4	8	12	24	36	12	24	36	12	24	36
DP396	2 μg L^{-1}	–	–	–	–	–	–	0.39	–	–	0.41	–	–	–
DP410	2 μg L^{-1}	–	–	–	–	–	0.36	0.63	–	0.37	0.65	–	–	0.99
DP381	2 μg L^{-1}	–	–	0.23	0.56	–	0.36	0.74	–	0.35	0.71	–	2.25	4.93
DP408	2 μg L^{-1}	–	–	–	–	–	–	–	–	–	–	–	–	–
DP394	2 μg L^{-1}	–	–	–	–	–	–	–	–	–	–	–	–	–
DP378	2 μg L^{-1}	–	–	–	–	–	–	–	–	–	–	–	–	–
DP396	100 μg L^{-1}	0.06	0.13	–	–	0.04	0.21	0.39	0.03	0.23	0.43	–	0.14	0.23
DP410	100 μg L^{-1}	–	–	–	0.02	0.12	0.39	0.66	0.11	0.38	0.67	0.05	0.59	1.08
DP381	100 μg L^{-1}	0.04	0.07	0.29	0.60	0.12	0.42	0.79	0.15	0.39	0.75	0.48	2.25	5.05
DP408	100 μg L^{-1}	–	–	–	–	–	–	0.05	–	–	0.04	–	–	0.02
DP394	100 μg L^{-1}	0.33	0.70	0.06	0.12	–	0.01	0.05	–	0.01	0.05	–	–	0.01
DP378	100 μg L^{-1}	–	–	–	0.01	–	–	0.01	–	–	0.01	–	–	–

–: not detected.

3.4. Occurrence of degradation products in non-forced conditions

Table 3 also shows the degradation products detected in river water at 12, 24 and 36 weeks after limiting the transmission of UV radiation, which simulates the attenuation of UV radiation that happens in a body of water. Data are the mean of two assays whose results can be seen in Table A11. The occurrence of the degradation compounds increased with time. Three compounds (DP396, DP410 and DP381) were observed in the assays at low concentration after 36 weeks; consequently, it is expected that they can be found in the analysis of real water samples. DP410 and DP381 were present in relative amounts about 0.64 and 0.73, respectively, while the amount of DP396 was about 0.40. The relative amounts of these three compounds were similar in the assays carried out at high concentration, where other three degradation products (DP408, DP394, DP378) were detected; they were minor compounds detected in amounts of 0.05 or lower.

DP381 was the main degradation product when the assay was done in presence of sediment, followed by DP410; they were found in relative amounts of about 5 and 1, respectively, higher than those found when the assay was done with water only. The addition of sediment promoted a faster degradation of the celecoxib and its transformation in DP381 and DP410. DP396, DP378, DP408 and DP394 were only detected in the assay at 100 μg L^{-1}; their relative amounts were now lower, which could be explained by an adsorption onto sediment or a minor generation.

As regards the origin of these degradation products, DP396 was supposed to arise from chemical reactions in solution according to the assays done under forced conditions; it was the only degradation product not detected when celecoxib in solution was exposed to the radiation from the lamp. DP381 was mainly formed by photochemical reactions while DP410 arose exclusively from photochemical process; the occurrence of DP381 in wastewater had been previously reported [9]. All other compounds were also observed in extracts from waters subjected to radiation although the major origin of DP394 seems to be a chemical reaction in aqueous solution. A degradation pathway of celecoxib in river water is outlined in Fig. 1.

The toxicity of the major degradation products with a well-defined structure to three ecotoxicological endpoints has been predicted by the TEST software (version 4.1) from the US Environmental Protection Agency, which applies quantitative structure activity relationships (QSARs) methodologies. DP381 and DP410 had a similar or scantly lower toxicity in comparison to celecoxib for *Daphnia magna* and fathead minnow according to the estimated 50% lethal concentrations (Table 4). The phenanthridines DP408 and DP378 were two and six-fold more toxic than celecoxib, respectively, for *Daphnia magna* while their toxicity was similar to that of celecoxib for fathead minnow; for these same endpoints, the toxicity of DP394 was about two-fold higher. On the other hand, the non-observed effect concentration on *Daphnia magna* has been experimentally measured for celecoxib, it was 62 μg L^{-1} [11]. Growth inhibition concentrations instead of lethal concentrations were estimated for *Tetrahymena pyriformis*; in this case the predicted toxicity values for celecoxib and related compounds did not differ almost from one another.

Table 4
Predicted 50% lethal concentrations (LC_{50}, μM) and 50% growth inhibition concentrations (IGC_{50}, μM) for celecoxib and degradation products detected under non-forced conditions.

	Daphnia magna LC_{50} (48 h)	*Tetrahymena pyriformis* IGC_{50}	Fathead minnow LC_{50} (96 h)
Celecoxib	1.8	11.8	0.5
DP410	1.9	14.8	0.5
DP381	6.0	8.7	0.8
DP408	0.9	14.8	0.7
DP394	0.8	7.8	0.2
DP378	0.3	6.9	0.5

3.5. Adsorption to sediment

Fig. 2 shows the adsorption isotherm obtained for celecoxib in the batch experiments; K_d (adsorption equilibrium constant) and K_{oc} (organic carbon normalized adsorption equilibrium constant) values resulted to be 44.4 and 3699 L kg^{-1} (RSD 3.8%, n = 10), respectively. K_{oc} relates K_d to the content of organic carbon of the sediment sample and it was calculated by Eq. (2), where OC% is the percentage of organic carbon in the sediment sample (1.2%). The K_{oc} value is similar to that of compounds such as 1,2,4-trichlorobenzene or 3,5-dichlorophenol [12]. Only a sediment sample has been considered in the experimentation but it is clear that celecoxib has a certain capacity of adsorption onto sediment, which should be taken into account to foresee its distribution in the environment.

$$K_{oc} = K_d \frac{100}{OC\%} \quad (2)$$

Adsorption equilibrium constants were also calculated for most of the degradation products from the experimental adsorption percentages; K_d and K_{oc} values, and the used sediment to water ratios,

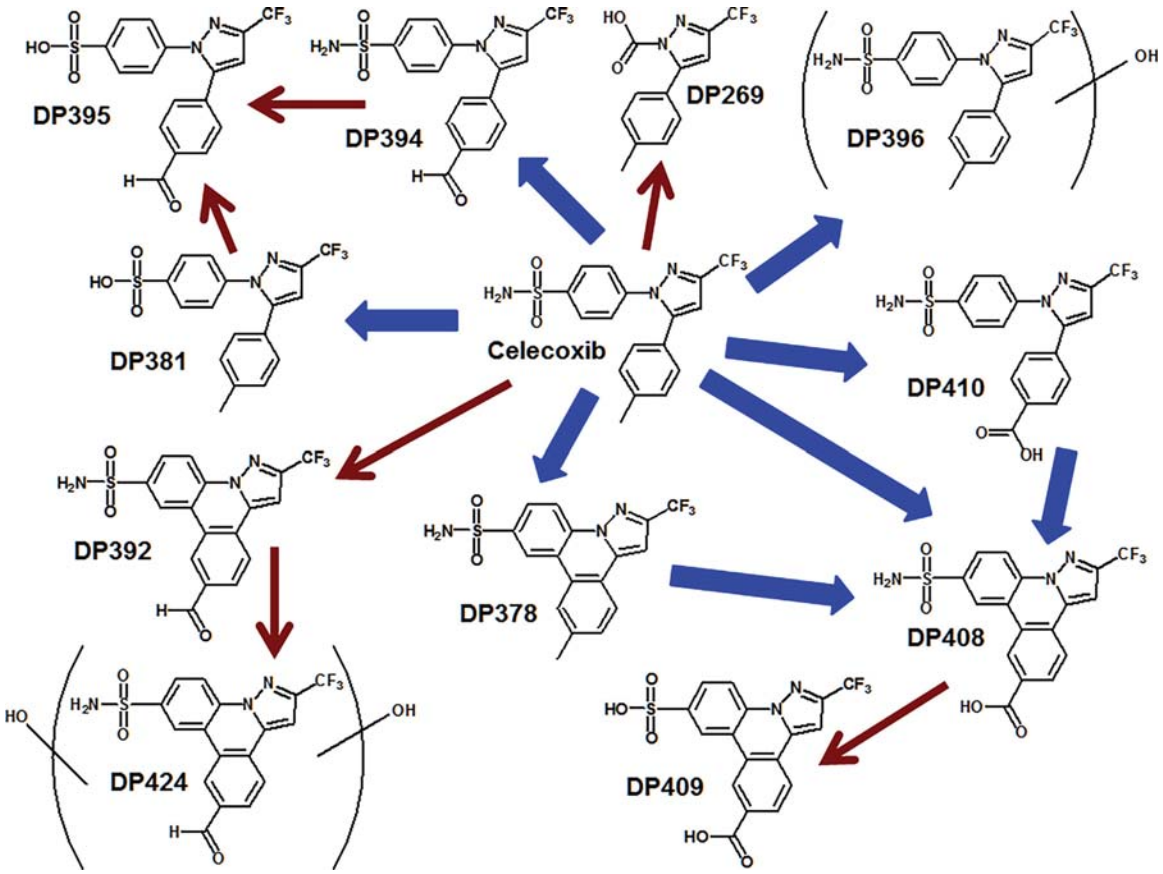

Fig. 1. Degradation pathway of celecoxib in river water. Thick lines denote the possible transformation process over time. Thin lines are related to the degradation under UV lamp.

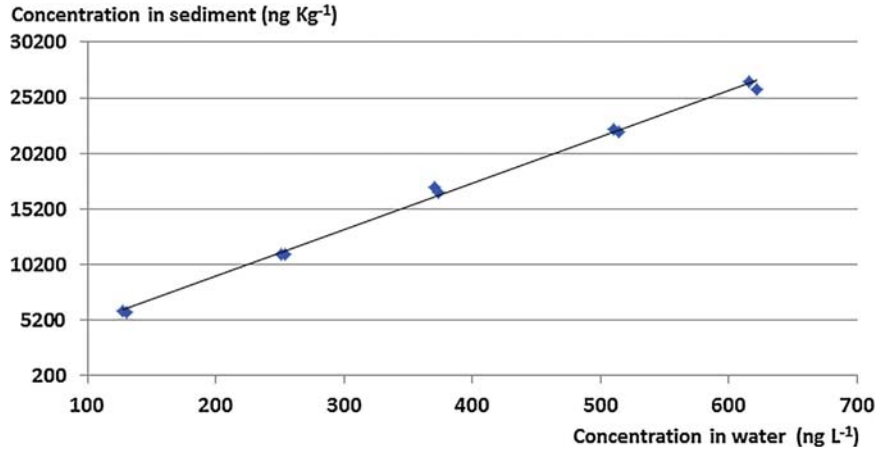

Fig. 2. Adsorption isotherm of celecoxib (n = 2).

can be seen in Table 5. The coefficient of adsorption of celecoxib was also calculated by this method and it resulted to be 45.0 L kg^{-1}, similar to the previously estimated value. The K_d values of the degradation products were lower and, in general, they did not differ much from the celecoxib value; they varied from 17.6 to 43.2 L kg^{-1}. It was inferred from the data that the formation of a phenanthridine did not modify greatly the adsorption capacity of the compound while the conversion of the sulfonamine and methyl groups into sulfonic and carboxylic acids, respectively, decreased the adsorption capacity.

Table 5
K_d and K_{oc} mean values (RSDs in parenthesis) calculated for the degradation products. Mean adsorption percentages (A%) onto sediment and experimental sediment to water ratios (R), n = 5.

Compound	K_d (L kg^{-1})	K_{oc} (L kg^{-1})	A%	R (kg L^{-1})	Experimental t-value[a]
DP395	17.6	1467 (8.9%)	27.4	0.022	27.4
DP424	23.9	1994 (8.9%)	33.8	0.021	18.4
DP269	34.8	2901 (7.0%)	42.6	0.021	29.2
DP396	37.6	3130 (9.4%)	43.9	0.021	16.1
DP410	29.4	2449 (7.4%)	38.6	0.021	17.0
DP381	30.2	2516 (6.8%)	39.2	0.021	26.8
DP408	26.8	2231 (8.3%)	36.5	0.022	29.2
DP394	33.5	2790 (6.7%)	41.1	0.021	20.1
DP392	29.6	2466 (10.4%)	38.8	0.022	18.0
DP378	43.2	3600 (5.3%)	48.0	0.021	26.6
Celecoxib	45.0	3748 (7.2%)	37.4	0.013	30.0

[a] Critical t-value: 2.3.

4. Conclusions

Celecoxib is a relatively persistent drug in river water under environmental conditions. The photochemical reactions are more important than the chemical reactions in aqueous solution, at a pH value of 7.8, to foresee its degradation in surface water. The biological degradation is negligible.

Tentative structures for 9 out of 11 detected degradation products are proposed from high-resolution mass spectrometry data. A hydroxylated derivative, celecoxib carboxylic acid and celecoxib sulfonic acid are the main degradation products over time. They are susceptible to being detected in the analysis of real samples. The ecotoxicities predicted for the elucidated chemical structures are basically similar, in general terms, to those of celecoxib.

The presence of an aquatic sediment increases slightly the degradation rate of celecoxib in river water and favors its transformation to celecoxib carboxylic acid and celecoxib sulfonic acid. Celecoxib and their degradation products can be partially adsorbed on aquatic sediment. The presence of celecoxib seems to affect the biodegradation process that occurs naturally in a sediment.

Acknowledgments

The authors would like to acknowledge the support given by the Laboratorio de Técnicas Instrumentales of the University of Valladolid to perform the experimental work.

This research did not receive any specific grant from funding agencies in the public, commercial, or not-for-profit sectors.

Appendix A. Supplementary data

Supplementary data associated with this article can be found, in the online version, at http://dx.doi.org/10.1016/j.jhazmat.2017.08.037.

References

[1] K. Kaur, V. Kumar, G. Kumar, Trifluoromethylpyrazoles as anti-inflammatory and antibacterial agents: a review, J. Fluor. Chem. 178 (2015) 306–326.
[2] S. Thangamani, W. Younisand, M.N. Seleem, Repurposing celecoxib as a topical antimicrobial agent, Front. Microbiol. 6 (2015), http://dx.doi.org/10.3389/fmicb.2015.00750.
[3] F.S. Garcia Praça, M.V. Lopes Badra, M. Guimaraes, M.B. Riemma, Celecoxib determination in different layers of skin by a newly developed and validated HPLC-UV method, Biomed. Chromatogr. 25 (2011) 1237–1244.
[4] J.Y. Zhang, Y.F. Wang, C. Dudkowski, D.C. Yang, M. Chang, J. Yuan, S.K. Paulson, A.P. Breau, Characterization of metabolites of celecoxib in rabbits by liquid chromatography/tandem mass spectrometry, J. Mass Spectrom. 35 (2000) 1259–1270.
[5] S.K. Paulson, J.D. Hribar, N.W.K. Liu, E. Hajdu, R.H.J.R. Bible, A. Piergies, A. Karim, Metabolism and excretion of [(14)C]celecoxib in healthy male volunteers, Drug Metab. Dispos. 28 (2000) 308–314.
[6] Y. Ma, S. Gao, M. Hu, Quantitation of celecoxib and four of its metabolites in rat blood by UPLC-MS/MS clarifies their blood distribution patterns and provides more accurate pharmacokinetics profiles, J. Chromatogr. B 1001 (2015) 202–211.
[7] H.A. Oh, D. Kim, S.H. Lee, B.H. Jung, Simultaneous quantitative determination of celecoxib and its two metabolites using liquid chromatography–tandem mass spectrometry in alternating polarity switching mode, J. Pharm. Biomed. Anal. 107 (2015) 32–39.
[8] A.M. Kalle, A. Rizvi, Inhibition of bacterial multidrug resistance by celecoxib, a cyclooxygenase-2 inhibitor, Antimicrob. Agents Chemother. 55 (2011) 439–442.
[9] S. Triñanes, M.C. Casais, M.C. Mejuto, R. Cela, Selective determination of COXIBs in environmental water samples by mixed-mode solid phase extraction and liquid chromatography quadrupole time-of-flight mass spectrometry, J. Chromatogr. A 1420 (2015) 35–45.
[10] OECD Guideline for the Testing of Chemicals No 106, Adsorption–Desorption Using a Batch Equilibrium Method, 2000, pp. 8.
[11] L.A. Constantine, D.B. Huggett, A comparison of the chronic effects of human pharmaceuticals on two cladocerans, *Daphnia magna* and *Ceriodaphnia dubia*, Chemosphere 80 (2010) 1069–1074.
[12] A. Delle-Site, Factors affecting sorption of organic compounds in natural sorbent water systems and sorption coefficients for selected pollutants. A review, J. Phys. Chem. Ref. Data 30 (2001) 187–439.

Supplementary data

Photochemical, thermal, biological and long-term degradation of celecoxib in river water. Degradation products and adsorption to sediment.

Journal of Hazardous Materials, 2017

Contents

Table A1: Concentrations of celecoxib (in µg·L^{-1}) found in the biological degradation assays at 2 and 100 µg·L^{-1} under aerobic conditions. Two or five sample aliquots were taken each week. A t-test (p=0.05, n=5) was applied to check for differences between the initial and final mean concentrations of the assay.

2 µg·L^{-1}												
	Assay 1						Assay 2					
Week:	**0**	**1**	**2**	**3**	**4**	**5**	**0**	**1**	**2**	**3**	**4**	**5**
Aliquot 1	1.99	2.03	2.00	1.99	1.98	2.01	1.98	1.98	2.00	1.99	2.01	1.98
Aliquot 2	2.02	1.99	2.02	2.02	1.99	1.99	1.99	2.00	2.01	1.97	1.99	2.00
Aliquot 3	1.97	--	--	--	--	1.97	2.00	--	--	--	--	1.99
Aliquot 4	2.00	--	--	--	--	1.98	1.97	--	--	--	--	1.97
Aliquot 5	2.01	--	--	--	--	2.02	1.98	--	--	--	--	2.00
Mean:	2.00					1.99	1.98					1.99
	Experimental t-value*: 0.3						Experimental t-value*: 0.5					

100 µg·L^{-1}												
	Assay 1						Assay 2					
Week:	**0**	**1**	**2**	**3**	**4**	**5**	**0**	**1**	**2**	**3**	**4**	**5**
Aliquot 1	102	100	98	100	99	101	98	101	102	100	98	100
Aliquot 2	101	98	102	99	100	99	100	99	102	100	97	100
Aliquot 3	99	--	--	--	--	102	101	--	--	--	--	98
Aliquot 4	103	--	--	--	--	100	99	--	--	--	--	97
Aliquot 5	102	--	--	--	--	99	98	--	--	--	--	101
Mean:	101.4					100.2	99.2					99.2
	Experimental t-value*: 1.1						Experimental t-value*: 0.1					

--: without data

*Critical t-value: 2.3

Table A2: Concentrations of celecoxib (in $\mu g \cdot L^{-1}$) found in the biological degradation assays at 2 and 100 $\mu g \cdot L^{-1}$ under anaerobic conditions. Two or five sample aliquots were taken each week. A t-test (p=0.05, n=5) was applied to check for differences between the initial and final mean concentrations of the assay

2 $\mu g \cdot L^{-1}$												
	Assay 1						Assay 2					
Week:	**0**	**1**	**2**	**3**	**4**	**5**	**0**	**1**	**2**	**3**	**4**	**5**
Aliquot 1	2.02	2.03	1.98	1.99	2.01	2.00	2.01	1.99	2.00	2.01	2.01	2.02
Aliquot 2	2.03	2.00	2.00	1.99	1.98	1.99	1.99	2.01	2.02	2.03	2.01	2.00
Aliquot 3	1.99	--	--	--	--	1.99	2.01	--	--	--	--	1.99
Aliquot 4	1.99	--	--	--	--	2.01	1.98	--	--	--	--	1.99
Aliquot 5	2.00	--	--	--	--	1.97	1.99	--	--	--	--	2.02
Mean:	2.01					1.99	2.00					2.00
	Experimental t-value*: 0.2						Experimental t-value*: 1.7					
100 $\mu g \cdot L^{-1}$												
	Assay 1						Assay 2					
Week:	**0**	**1**	**2**	**3**	**4**	**5**	**0**	**1**	**2**	**3**	**4**	**5**
Aliquot 1	101	100	102	99	101	99	98	97	99	100	98	99
Aliquot 2	99	103	99	102	97	102	100	101	102	99	99	102
Aliquot 3	102	--	--	--	--	101	101	--	--	--	--	98
Aliquot 4	102	--	--	--	--	100	99	--	--	--	--	98
Aliquot 5	100	--	--	--	--	98	99	--	--	--	--	99
Mean:	100.8					100.0	99.4					99.2
	Experimental t-value*: 0.8						Experimental t-value*: 0.2					

--: without data

*Critical t-value: 2.3

Table A3: Concentrations of celecoxib (in $\mu g \cdot L^{-1}$) found in the biological degradation assays at 2 and 100 $\mu g \cdot L^{-1}$ in presence of culture medium. Two or five sample aliquots were taken each week. A t-test (p=0.05, n=5) was applied to check for differences between the initial and final mean concentrations of the assay.

2 $\mu g \cdot L^{-1}$												
	Assay 1						Assay 2					
Week:	**0**	**1**	**2**	**3**	**4**	**5**	**0**	**1**	**2**	**3**	**4**	**5**
Aliquot 1	2.01	1.99	1.98	2.00	2.01	2.02	1.98	1.98	2.02	2.03	1.99	2.03
Aliquot 2	2.03	2.00	1.99	2.01	2.02	1.99	1.99	2.01	2.00	1.97	2.00	2.01
Aliquot 3	1.99	--	--	--	--	2.04	2.01	--	--	--	--	1.98
Aliquot 4	2.01	--	--	--	--	2.00	2.02	--	--	--	--	2.02
Aliquot 5	2.01	--	--	--	--	2.00	2.01	--	--	--	--	1.98
Mean:	2.01					2.01	2.00					2.00
	Experimental t-value*: 0.5						Experimental t-value*: 0.4					
100 $\mu g \cdot L^{-1}$												
	Assay 1						Assay 2					
Week:	**0**	**1**	**2**	**3**	**4**	**5**	**0**	**1**	**2**	**3**	**4**	**5**
Aliquot 1	101	100	101	99	99	102	102	100	99	100	101	103
Aliquot 2	102	100	101	99	100	99	100	99	102	101	99	97
Aliquot 3	100	--	--	--	--	103	101	--	--	--	--	102
Aliquot 4	102	--	--	--	--	98	99	--	--	--	--	98
Aliquot 5	99	--	--	--	--	98	100	--	--	--	--	99
Mean:	100.8					100.0	100.4					99.8
Experimental t-value*: 0.7							Experimental t-value*: 0.5					

--: without data

*Critical t-value: 2.3

Table A4: Concentrations of celecoxib (in $\mu g \cdot L^{-1}$) found in the thermal degradation assays (70 °C) at 2 and 100 $\mu g \cdot L^{-1}$. Two or five sample aliquots were taken. A t-test (p=0.05, n=5) was applied to check for differences between the initial and final mean concentrations of the assay.

2 $\mu g \cdot L^{-1}$							
	Assay 1				Assay 2		
Week:	**0**	**4**	**8**		**0**	**4**	**8**
Aliquot 1	1.99	1.99	2.00		2.01	2.00	1.99
Aliquot 2	1.98	2.01	2.01		2.01	2.00	2.00
Aliquot 3	2.01	--	1.99		2.03	--	2.01
Aliquot 4	2.01	--	1.98		2.00	--	2.00
Aliquot 5	2.00	--	1.96		2.00	--	1.99
Mean:	2.00		1.99		2.01		2.00
	Experimental t-value*: 0.2				Experimental t-value*: 1.8		
100 $\mu g \cdot L^{-1}$							
	Assay 1				Assay 2		
Week:	**0**	**4**	**8**		**0**	**4**	**8**
Aliquot 1	101	100	99		100	99	98
Aliquot 2	100	100	98		99	98	97
Aliquot 3	102	--	100		100	--	100
Aliquot 4	100	--	101		101	--	99
Aliquot 5	100	--	98		100	--	100
Mean:	100.6		99.2		100.0		98.8
	Experimental t-value*: 2.0				Experimental t-value*: 1.8		

--: without data

*Critical t-value: 2.3

Table A5: Concentrations of celecoxib (in $\mu g \cdot L^{-1}$) found in the photochemical degradation assays (sunlight exposure) at 2 and 100 $\mu g \cdot L^{-1}$. Two or five sample aliquots were taken. A t-test (p=0.05, n=5) was applied to check for differences between the initial and final mean concentrations of the assay.

2 $\mu g \cdot L^{-1}$							
	Assay 1				Assay 2		
Week:	**0**	**4**	**8**		**0**	**4**	**8**
Aliquot 1	2.01	1.98	1.96		2.00	1.98	1.92
Aliquot 2	2.01	1.96	1.93		2.00	1.96	1.95
Aliquot 3	2.03	--	1.96		1.99	--	1.92
Aliquot 4	2.00	--	1.94		2.00	--	1.93
Aliquot 5	2.01	--	1.94		1.99	--	1.92
Mean:	2.01		1.95		2.00		1.93
	Experimental t-value*: 8.5				Experimental t-value*: 10.7		
100 $\mu g \cdot L^{-1}$							
	Assay 1				Assay 2		
Week:	**0**	**4**	**8**		**0**	**4**	**8**
Aliquot 1	102	99	97		99	98	98
Aliquot 2	100	98	98		101	99	96
Aliquot 3	101	--	97		102	--	97
Aliquot 4	104	--	98		99	--	96
Aliquot 5	100	--	99		99	--	95
Mean:	101.4		97.8		100.0		96.4
	Experimental t-value*: 4.3				Experimental t-value*: 4.4		

--: without data

*Critical t-value: 2.3

Table A6: Photochemical degradation (UV lamp) of celecoxib in river water. Mean value and individual data of each assay.

	Concentrations ($\mu g \cdot L^{-1}$)		
Day	Assay 1	Assay 2	Mean
0	2.00	2.02	2.01
1	1.57	1.63	1.60
2	1.34	1.30	1.32
3	1.11	0.95	1.03
4	0.76	0.78	0.77
5	0.62	0.68	0.65
R^2	0.98	0.99	0.99
$t_{1/2}$ (days)	2.72	2.81	2.77

R^2: Coefficient of regression of the fitting; kinetics of first-order reactions.

$t_{1/2}$: half-life time.

Table A7: Concentrations of celecoxib (in $\mu g \cdot L^{-1}$) found in the degradation assays over time on W1 sample at 2 and 100 $\mu g \cdot L^{-1}$. Two or five sample aliquots were taken. A t-test (p=0.05, n=5) was applied to check for differences between the initial and final mean concentrations of the assay.

2 $\mu g \cdot L^{-1}$									
	Assay 1					Assay 2			
Week:	**0**	**12**	**24**	**36**		**0**	**12**	**24**	**36**
Aliquot 1	2.01	2.00	1.97	1.94		2.00	2.01	1.97	1.95
Aliquot 2	2.00	1.98	1.96	1.93		2.01	1.99	1.96	1.94
Aliquot 3	1.98	--	--	1.95		2.01	--	--	1.93
Aliquot 4	1.98	--	--	1.94		2.00	--	--	1.96
Aliquot 5	2.02	--	--	1.93		2.02	--	--	1.93
Mean:	2.00			1.94		2.01			1.94
	Experimental t-value*: 6.8					Experimental t-value*: 9.5			
100 $\mu g \cdot L^{-1}$									
	Assay 1					Assay 2			
Week:	**0**	**12**	**24**	**36**		**0**	**12**	**24**	**36**
Aliquot 1	100	99	99	98		99	100	97	96
Aliquot 2	101	100	98	99		101	99	96	97
Aliquot 3	100	--	--	97		100	--	--	97
Aliquot 4	101	--	--	96		100	--	--	98
Aliquot 5	102	--	--	98		101	--	--	97
Mean:	100.8			97.6		100.2			97.0
	Experimental t-value*: 5.1					Experimental t-value*: 6.5			

--: without data

*Critical t-value: 2.3

Table A8: Concentrations of celecoxib (in $\mu g \cdot L^{-1}$) found in the degradation assays over time on W2 sample at 2 and 100 $\mu g \cdot L^{-1}$. Two or five sample aliquots were taken. A t-test (p=0.05, n=5) was applied to check for differences between the initial and final mean concentrations of the assay.

2 $\mu g \cdot L^{-1}$									
	Assay 1					Assay 2			
Week:	**0**	**12**	**24**	**36**		**0**	**12**	**24**	**36**
Aliquot 1	1.99	1.98	1.96	1.94		2.00	1.97	1.96	1.95
Aliquot 2	2.01	1.99	1.96	1.95		2.01	1.99	1.95	1.93
Aliquot 3	2.00	--	--	1.96		2.00	--	--	1.92
Aliquot 4	2.01	--	--	1.95		2.01	--	--	1.95
Aliquot 5	2.01	--	--	1.94		2.00	--	--	1.94
Mean:	2.00			1.95		2.00			1.94
	Experimental t-value*: 10.2					Experimental t-value*: 10.4			
100 $\mu g \cdot L^{-1}$									
	Assay 1					Assay 2			
Week:	**0**	**12**	**24**	**36**		**0**	**12**	**24**	**36**
Aliquot 1	102	101	99	98		98	98	96	97
Aliquot 2	101	99	98	98		100	98	97	98
Aliquot 3	100	--	--	97		101	--	--	96
Aliquot 4	99	--	--	98		99	--	--	96
Aliquot 5	100	--	--	96		100	--	--	96
Mean:	100.4			97.4		99.6			96.6
	Experimental t-value*: 4.6					Experimental t-value*: 4.6			

--: without data

*Critical t-value: 2.3

Table A9: Concentrations of celecoxib (in $\mu g \cdot L^{-1}$) found in the degradation assays over time on SED sample at 2 and 100 $\mu g \cdot L^{-1}$. Two or five sample aliquots were taken. A t-test (p=0.05, n=5) was applied to check for differences between the initial and final mean concentrations of the assay.

2 $\mu g \cdot L^{-1}$									
	Assay 1					Assay 2			
Week:	**0**	**12**	**24**	**36**		**0**	**12**	**24**	**36**
Aliquot 1	1.25	1.26	1.22	1.20		1.23	1.20	1.19	1.17
Aliquot 2	1.27	1.24	1.23	1.22		1.23	1.22	1.19	1.19
Aliquot 3	1.29	--	--	1.21		1.23	--	--	1.16
Aliquot 4	1.24	--	--	1.20		1.22	--	--	1.18
Aliquot 5	1.26	--	--	1.21		1.24	--	--	1.19
Mean:	1.26			1.21		1.23			1.18
	Experimental t-value*: 5.8					Experimental t-value*: 7.8			
100 $\mu g \cdot L^{-1}$									
	Assay 1					Assay 2			
Week:	**0**	**12**	**24**	**36**		**0**	**12**	**24**	**36**
Aliquot 1	60	60	59	58		62	61	60	59
Aliquot 2	59	60	58	59		63	62	59	58
Aliquot 3	62	--	--	57		60	--	--	61
Aliquot 4	59	--	--	57		60	--	--	57
Aliquot 5	61	--	--	58		61	--	--	58
Mean:	60.2			57.8		61.2			58.6
	Experimental t-value*: 3.5					Experimental t-value*: 2.9			

--: without data

*Critical t-value: 2.3

3.2 Detection and Identification of degradation products

The fragmentations of celecoxib and their degradation products observed in the MS/MS spectra were relatively simple. Most of the fragment-ions could be explained by the typical fragmentation patterns of some functional groups. Thus, the MS/MS spectrum of celecoxib ($C_{17}H_{13}F_3N_3O_2S$) showed the loss of SO_2 (from the benzenesulfamide group), N_2 and HCCH (from the pyrazole ring), HF and CF_3 radical; these losses were commonly combined to yield the corresponding fragment-ion.

The structure of DP381 ($C_{17}H_{12}F_3N_2O_3S$) kept the number of rings and double bonds (RDBs) with respect to celecoxib, an oxygen atom was incorporated and fifteen units of mass (NH) were lost. DP381 was tentatively identified as the sulfonic derivative of celecoxib. The losses of SO_2 and CO_2 in the spectrum of DP410 ($C_{17}H_{11}F_3N_3O_4S$) suggested the presence of a sulfonamide group and a carboxylic acid, respectively, in its structure; it was identified as a carboxylic derivative of celecoxib (a [(4-carboxyphenyl)-pyrazolyl] benzenesulfonamide), a known degradation product yielded in the metabolic processes of the living organisms [4, 6, 7]. Other compound (DP394, $C_{17}H_{11}F_3N_3O_3S$) kept the three nitrogen atoms in its structure and the loss of SO_2 was seen in the MS/MS spectrum which suggested the presence of the sulfonamide substituent; a fragment at m/z 302 was assigned to the joint loss of SO_2 and CO, and the presence of an aldehyde group was assumed from the loss of CO. It was thought that DP394 was a [(4-formylphenyl)pyrazolyl]benzenesulfonamide derivative, in which the methyl group of the celecoxib had been less oxidized in relation to DP410. Similarly, the loss of SO_2 was observed in the spectrum of DP395 ($C_{17}H_{10}F_3N_2O_4S$) and a fragment-ion at m/z 263 was attributed to the loss of SO_2, two molecules of HF and CO; DP395 was identified as a [(4-formylphenyl)pyrazolyl]benzenesulfonic acid in agreement also with the estimated elemental composition.

A few fragment-ions were recorded in the spectrum of DP396 ($C_{17}H_{13}F_3N_3O_3S$) whose molecular formula incorporated an oxygen atom with regard to that of celecoxib; the ion-fragment at m/z 302 indicated the loss of SO_2 and H_2CO. Undoubtedly, a hydroxyl substituent was present in the structure of DP396 but its position has not been elucidated in this work. There are two possibilities for this compound: one of them involves the hydroxylation in the terminal methyl group to yield a known metabolic oxidation product [4, 6, 7] and the other implies the hydroxylation of an aromatic ring. As regards DP269, its molecular formula ($C_{12}H_8F_3N_2O_2$) indicated the losses of five carbon atoms and a nitrogen atom related to the parent compound; furthermore, CO_2 was removed in some ions of its MS/MS spectrum. DP269 is proposed to be 3-(trifluoromethyl)-5-p-tolyl-1H-pyrazole-1-carboxylic acid.

The molecular formula of DP378 ($C_{17}H_{11}F_3N_3O_2S$) showed the loss of two hydrogen atoms with respect to celecoxib, the number of RDBs was increased in a unit and the fragmentations in the spectrum were similar to those of celecoxib, too. It was identified as a phenanthridine-9-sulfonamide derivative; two hydrogen atoms close to each other were removed to form a new six-

membered cycle by the bond of the corresponding carbon atoms. The phenanthridine core was also observed in the degradation products commented below.

DP 408 ($C_{17}H_9F_3N_3O_4S$) was identified as a sulfonamine-pyrazolophenanthridine-carboxylic acid, similar to above-described degradation product DP410. The loss of a NH_2 radical to yield a radical ion was observed in the spectrum in addition to the losses of SO_2 and CO_2 among other simple molecules. The MS/MS spectrum obtained for DP392 ($C_{17}H_9F_3N_3O_3S$) was very simple, with low-abundance ions. However, the molecular formula and number of RDBs suggested that it was a 6-formyl-pyrazolophenanthridine-sulfonamide derivative, similar to DP394. A well-defined structure is not proposed for DP424 ($C_{17}H_9F_3N_3O_5$), its molecular formula contained two oxygen atoms more than the structure of DP392 while the number of RDBs was the same; the fragmentations found in the spectrum suggested the losses of SO_2, CO_2, HF and H_2O; it is assumed that DP424 is a compound similar to DP392 but dihydroxylated in the benzene rings. The photochemical origin of this degradation product in water leads to think that the hydroxyl substituents could be placed in meta position with regard to the sulfonamide and aldehyde groups because the free hydroxyl radicals behave as strong electrophilic compounds and the order of reactivity is similar to that found in an electrophilic aromatic substitution; in this case the hydroxylation should be favored in meta position with respect to the sulfonamide and aldehyde groups.

Finally, the MS/MS spectrum of DP409 ($C_{17}H_8F_3N_2O_5S$) showed fragment-ions that were explained by the loss of CO_2, SO_2 and OH radical, among other small molecules, which indicated the presence of sulfonic and carboxylic acids in its structure. These data together with the estimated elemental composition and number of RDBs prompted to identify DP409 as a 9-sulfo-pyrazolophenanthridine-carboxylic acid. Curiously, this is the only detected degradation product in which two frequent transformations coexist: the oxidation of the terminal methyl to carboxylic acid and the conversion of the sulfonamide group to sulfonic acid.

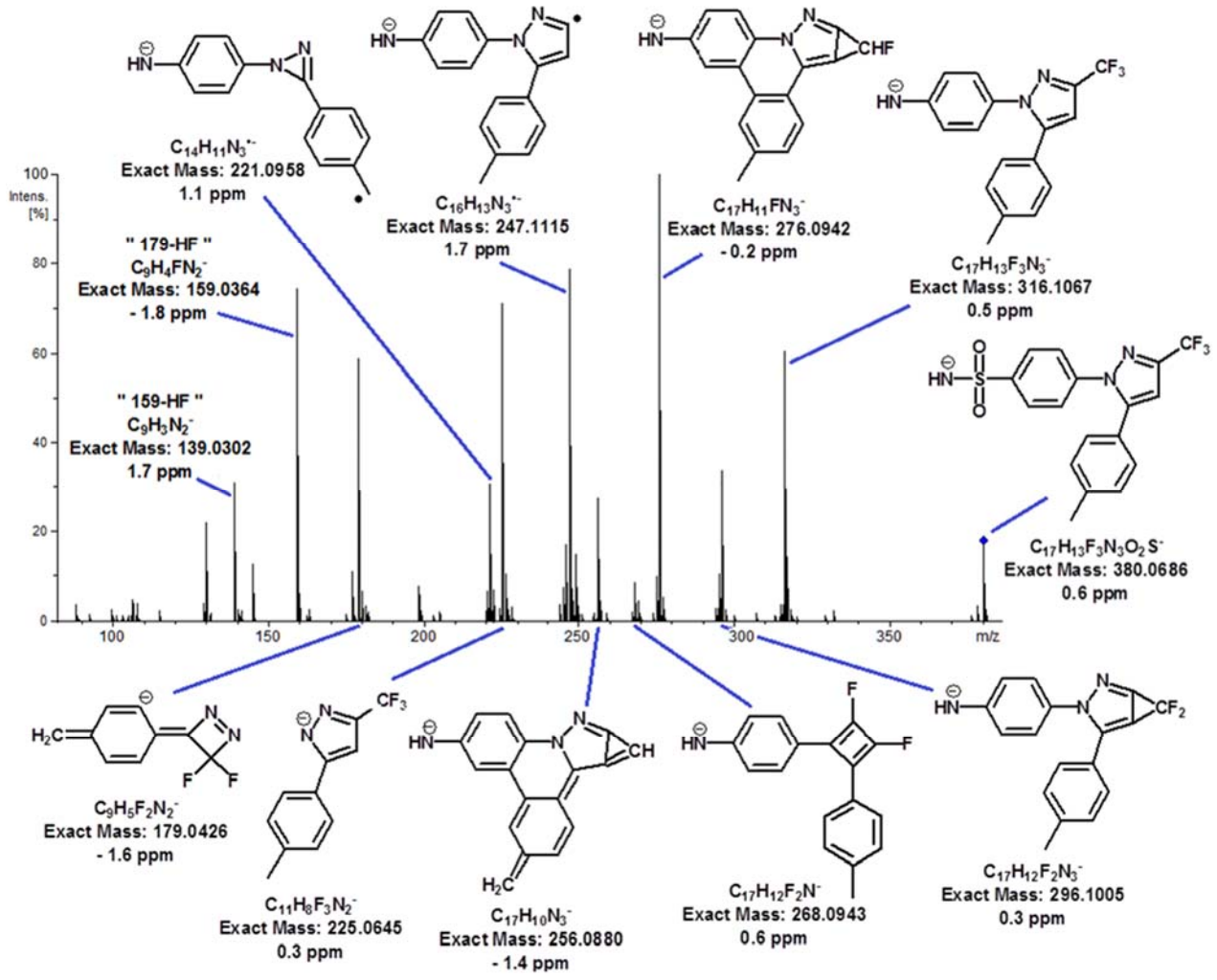

Figure A1: MS/MS spectrum of celecoxib. Collision energy: 40 eV. Exact mass and experimental error in the measurement.

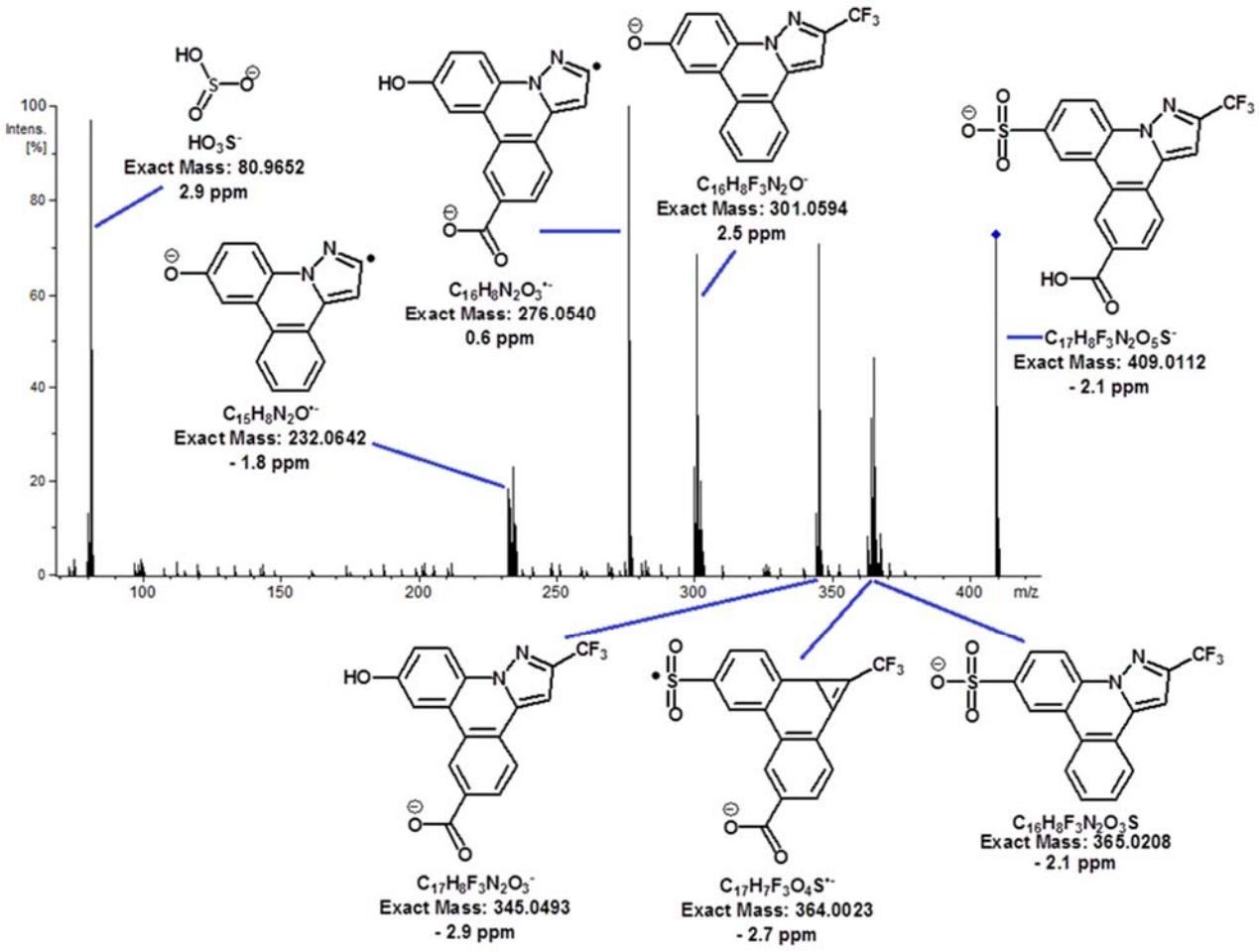

Figure A2: MS/MS spectrum of DP409. Collision energy: 44 eV. Exact mass and experimental error in the measurement.

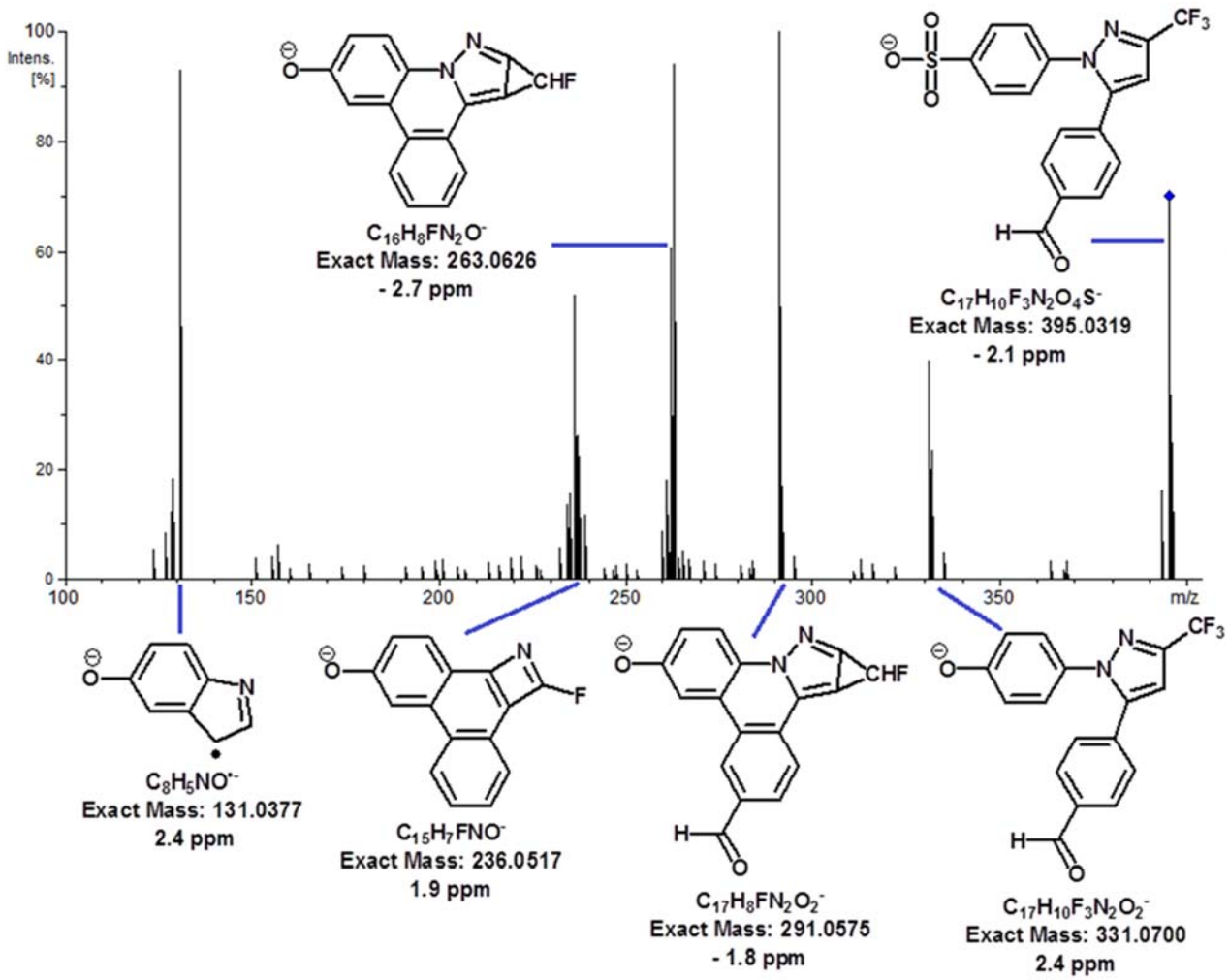

Figure A3: MS/MS spectrum of DP395. Collision energy: 45 eV. Exact mass and experimental error in the measurement.

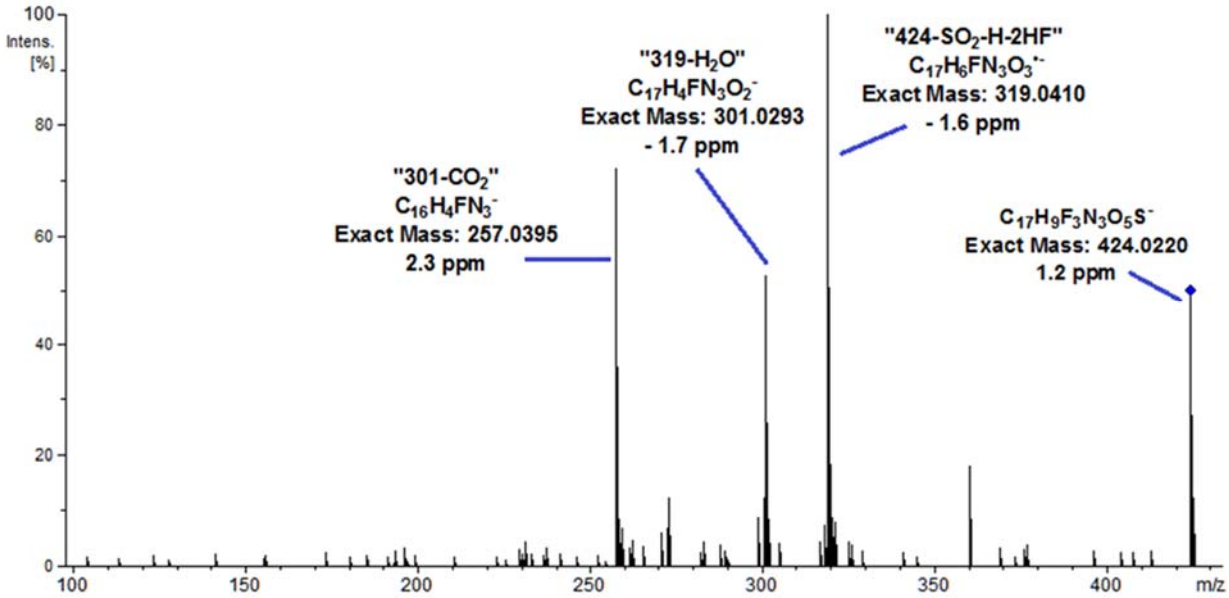

Figure A4: MS/MS spectrum of DP424. Collision energy: 28 eV. Exact mass and experimental error in the measurement.

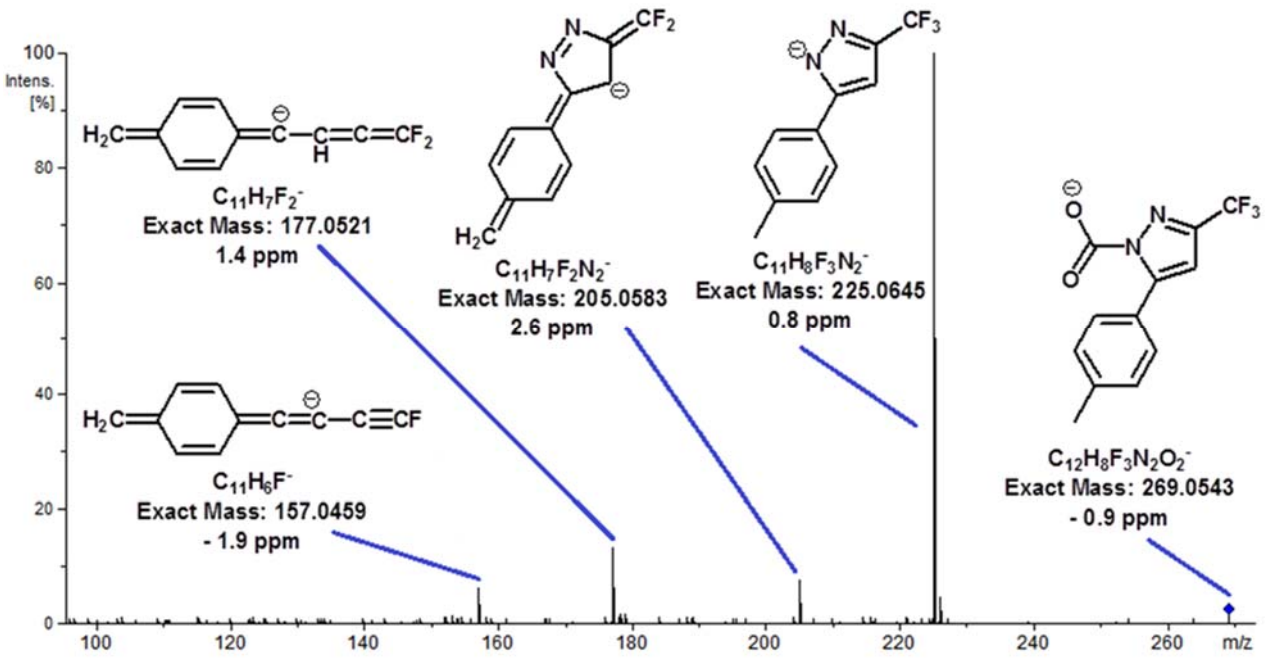

Figure A5: MS/MS spectrum of DP269. Collision energy: 22 eV. Molecular formulae attributed to the fragment-ions.

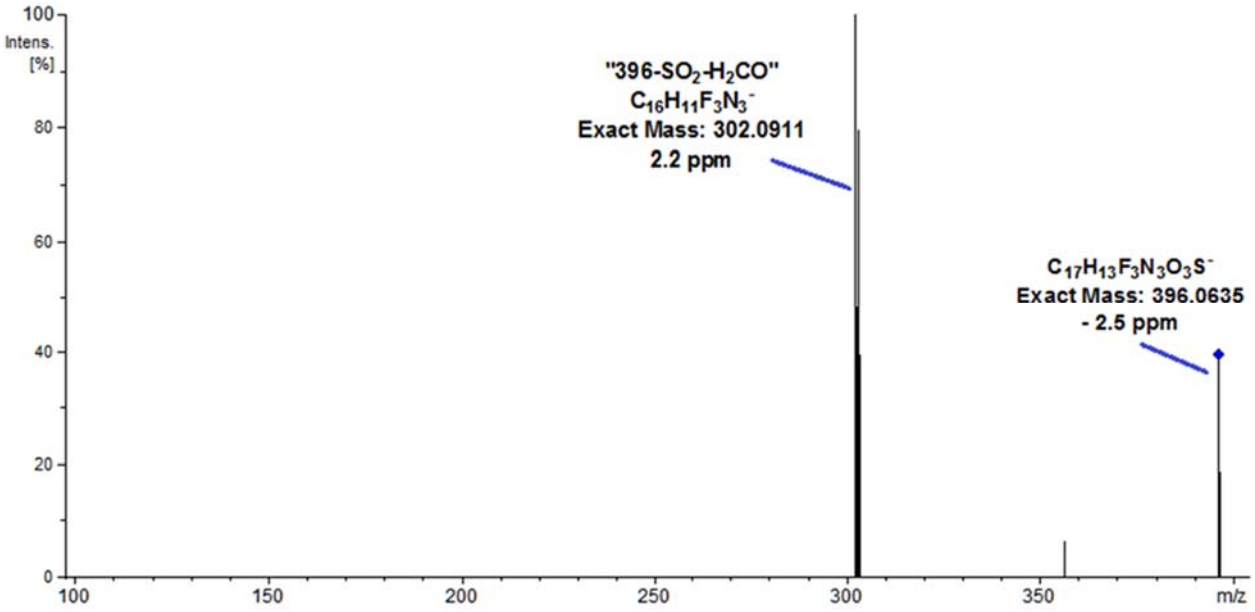

Figure A6: MS/MS spectrum of DP396. Collision energy: 30 eV. Exact mass and experimental error in the measurement.

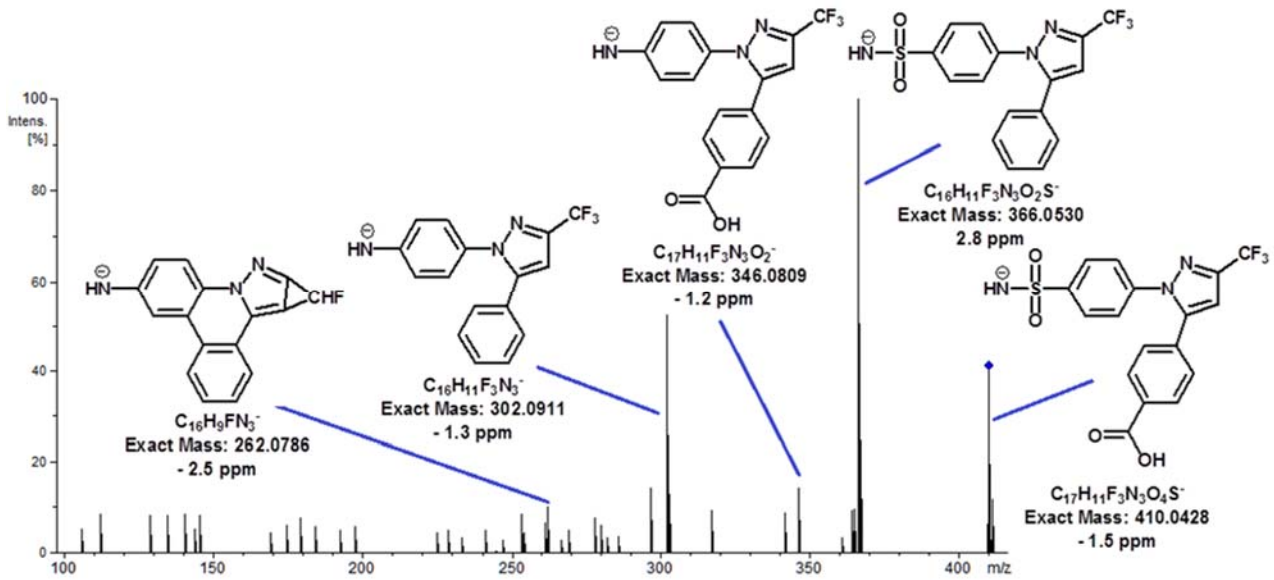

Figure A7: MS/MS spectrum of DP410. Collision energy: 22 eV. Exact mass and experimental error in the measurement.

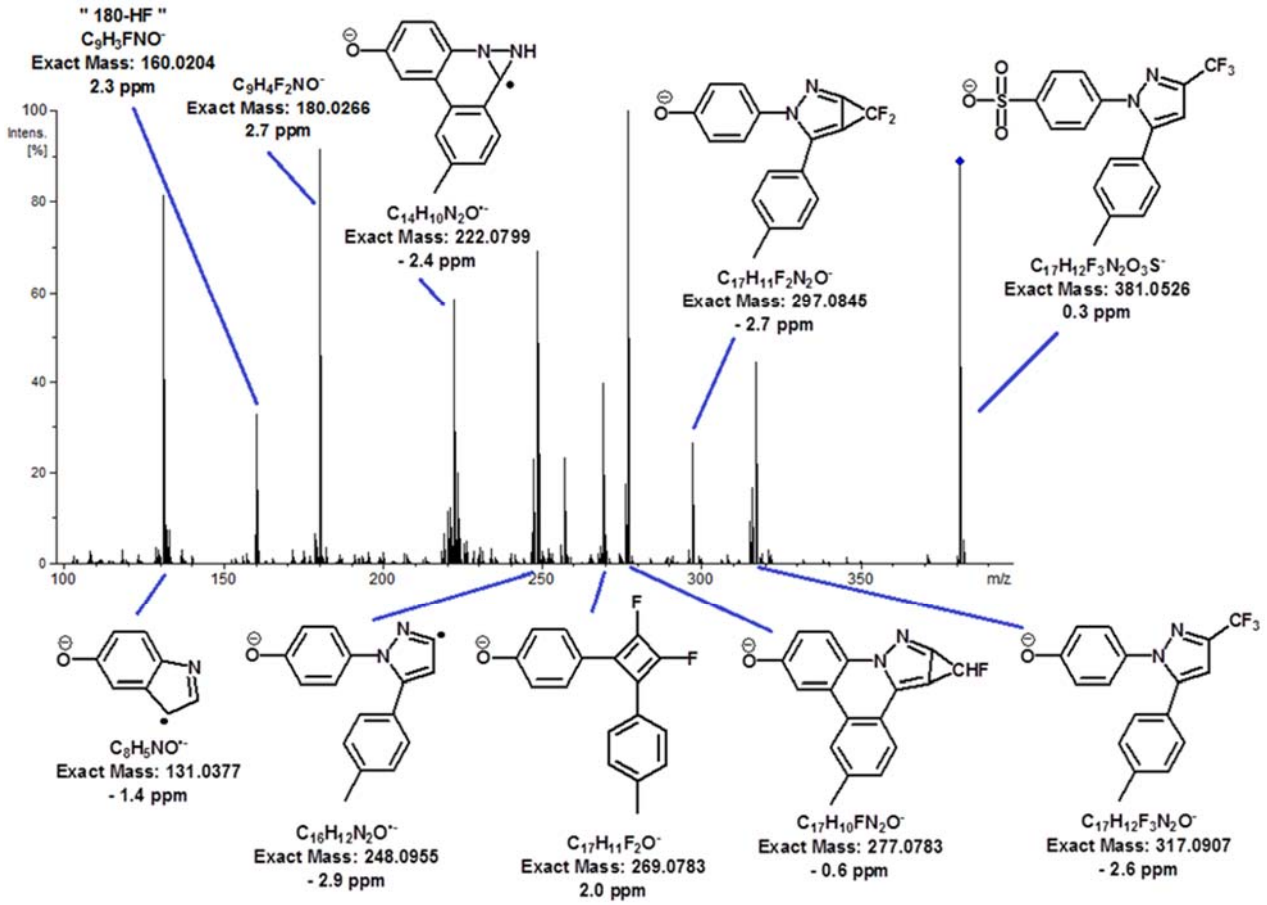

Figure A8: MS/MS spectrum of DP381. Collision energy: 48 eV. Exact mass and experimental error in the measurement.

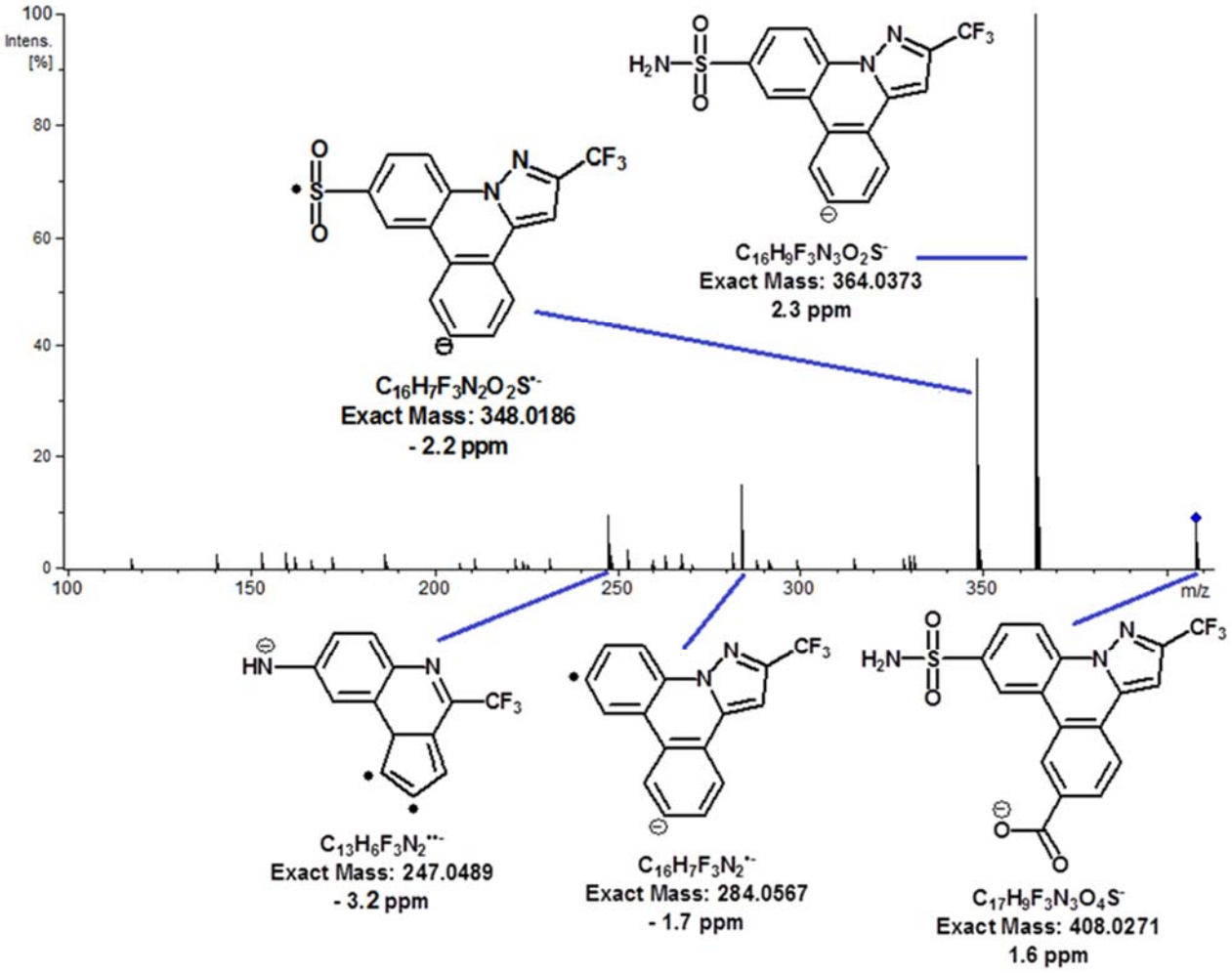

Figure A9: MS/MS spectrum of DP408. Collision energy: 32 eV. Exact mass and experimental error in the measurement.

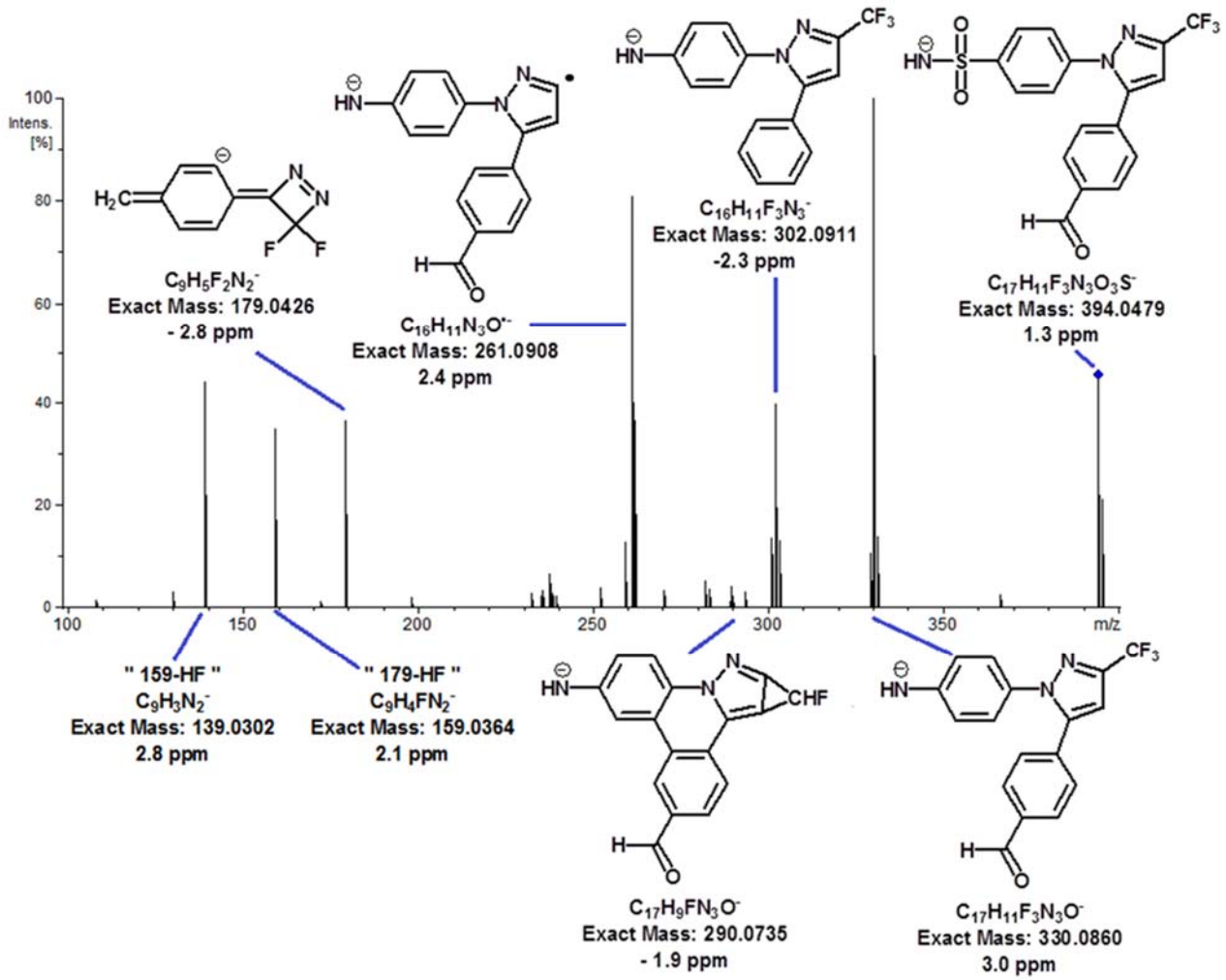

Figure A10: MS/MS spectrum of DP394. Collision energy: 30 eV. Exact mass and experimental error in the measurement.

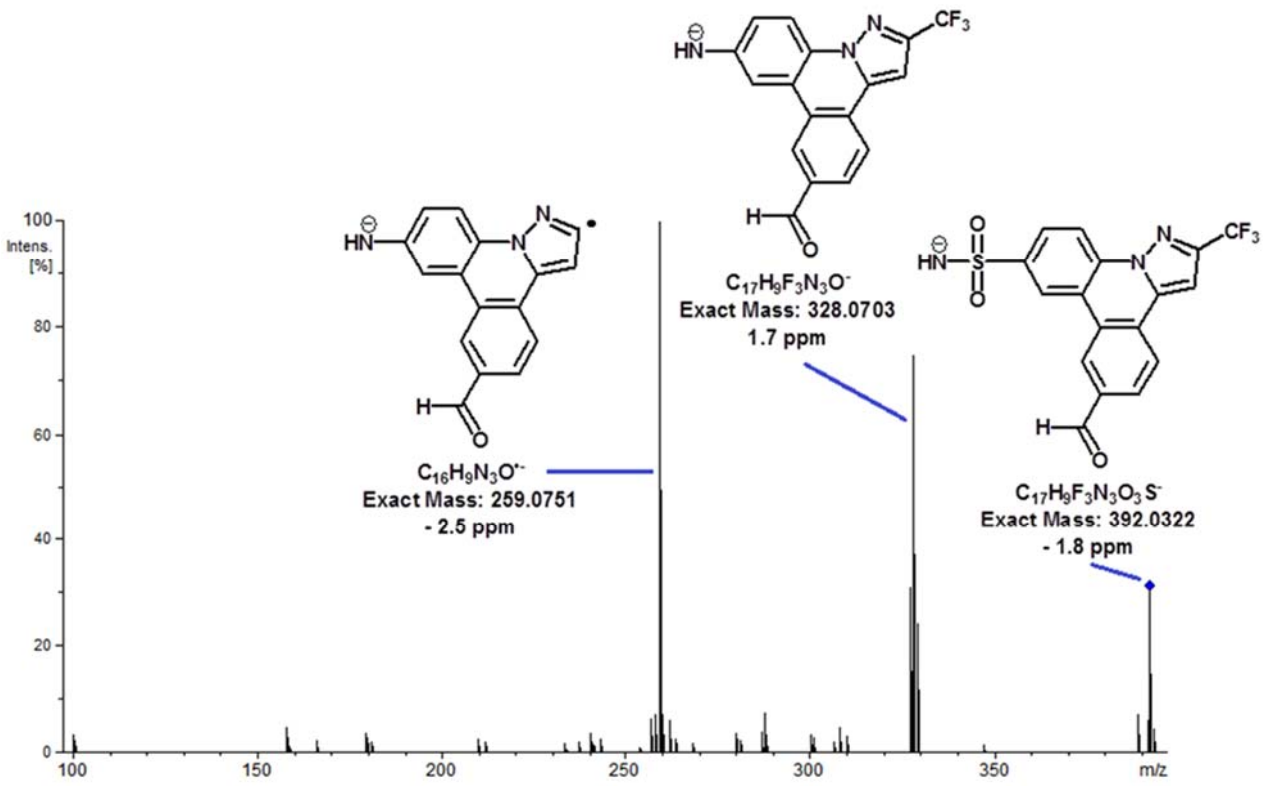

Figure A11: MS/MS spectrum of DP392. Collision energy: 35 eV. Exact mass and experimental error in the measurement.

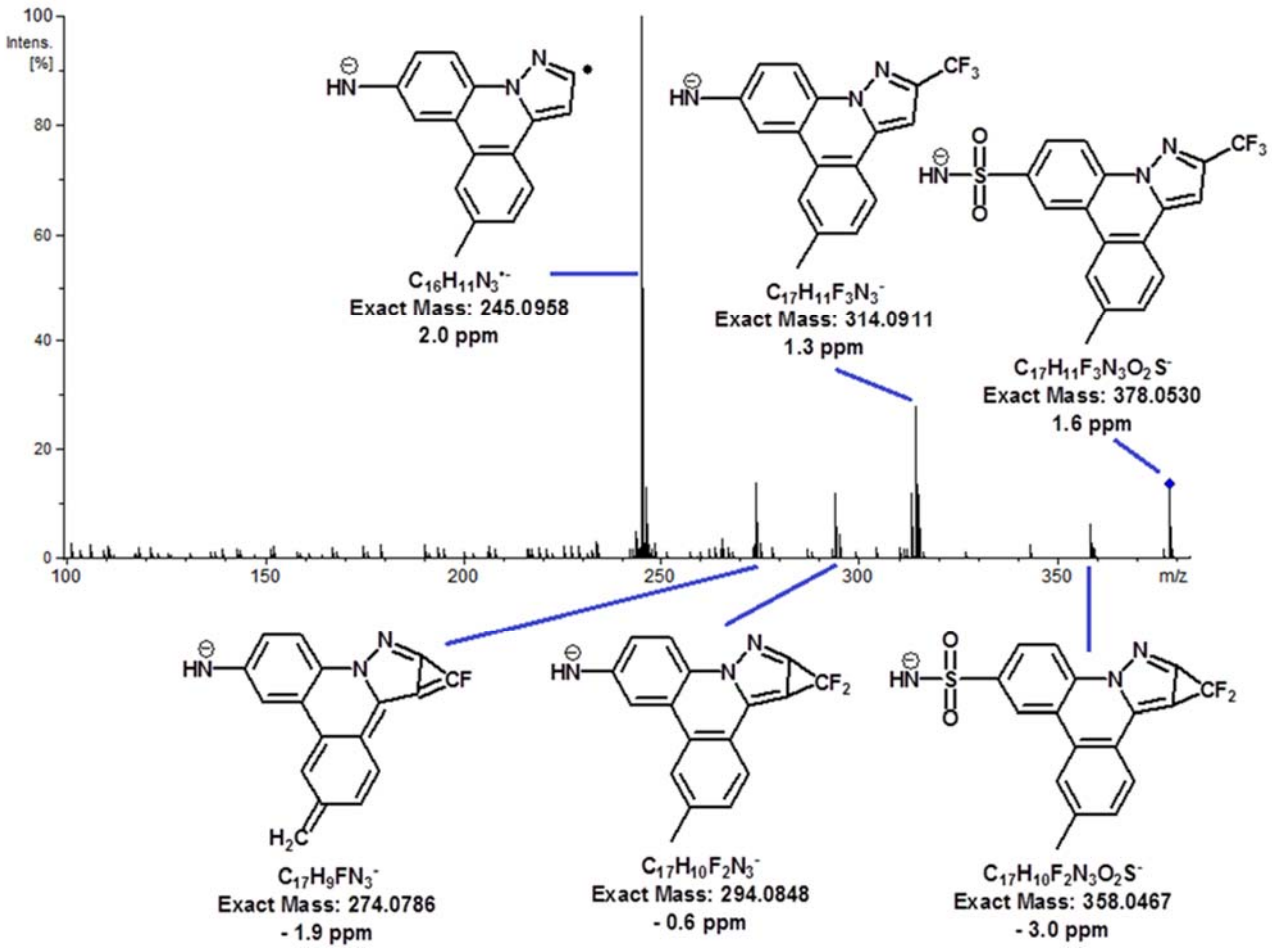

Figure A12: MS/MS spectrum of DP378. Collision energy: 40 eV. Exact mass and experimental error in the measurement.

3.3. Occurrence of degradation products in photochemical and thermal degradation assays

Table A10: Peak areas of the degradation products in the forced assays on a sample spiked with celecoxib at 2 or 100 $\mu g \cdot L^{-1}$. Peak areas are referred to the initial peak area of celecoxib in each experiment, to which a value of 100 was assigned. Mean values after the analysis of two aliquots.

	Sunlight		Heat, 70 °C		Culture medium	Sunlight		Heat, 70 °C		Culture medium
Weeks:	**4**	**8**	**4**	**8**	**5**	**4**	**8**	**4**	**8**	**5**
	Assay 1, 2 $\mu g \cdot L^{-1}$					Assay 2, 2 $\mu g \cdot L^{-1}$				
DP396	--	--	--	--	--	--	--	--	--	--
DP410	--	--	--	--	--	--	--	--	--	--
DP381	0.21	0.51	--	--	--	0.25	0.60	--	--	--
DP408	--	--	--	--	--	--	--	--	--	--
DP394	--	--	--	--	--	--	--	--	--	--
DP378	--	--	--	--	--	--	--	--	--	--
	Assay 1, 100 $\mu g \cdot L^{-1}$					Assay 2, 100 $\mu g \cdot L^{-1}$				
DP396	--	--	0.05	0.12	--	--	--	0.07	0.13	--
DP410	--	0.02	--	--	--	--	0.02	--	--	--
DP381	0.30	0.58	0.04	0.07	0.02	0.28	0.61	0.03	0.07	0.02
DP408	--	--	--	--	--	--	--	--	--	--
DP394	0.05	0.11	0.34	0.71	--	0.06	0.12	0.31	0.69	--
DP378	--	0.01	--	--	--	--	0.01	--	--	--

-- : not detected

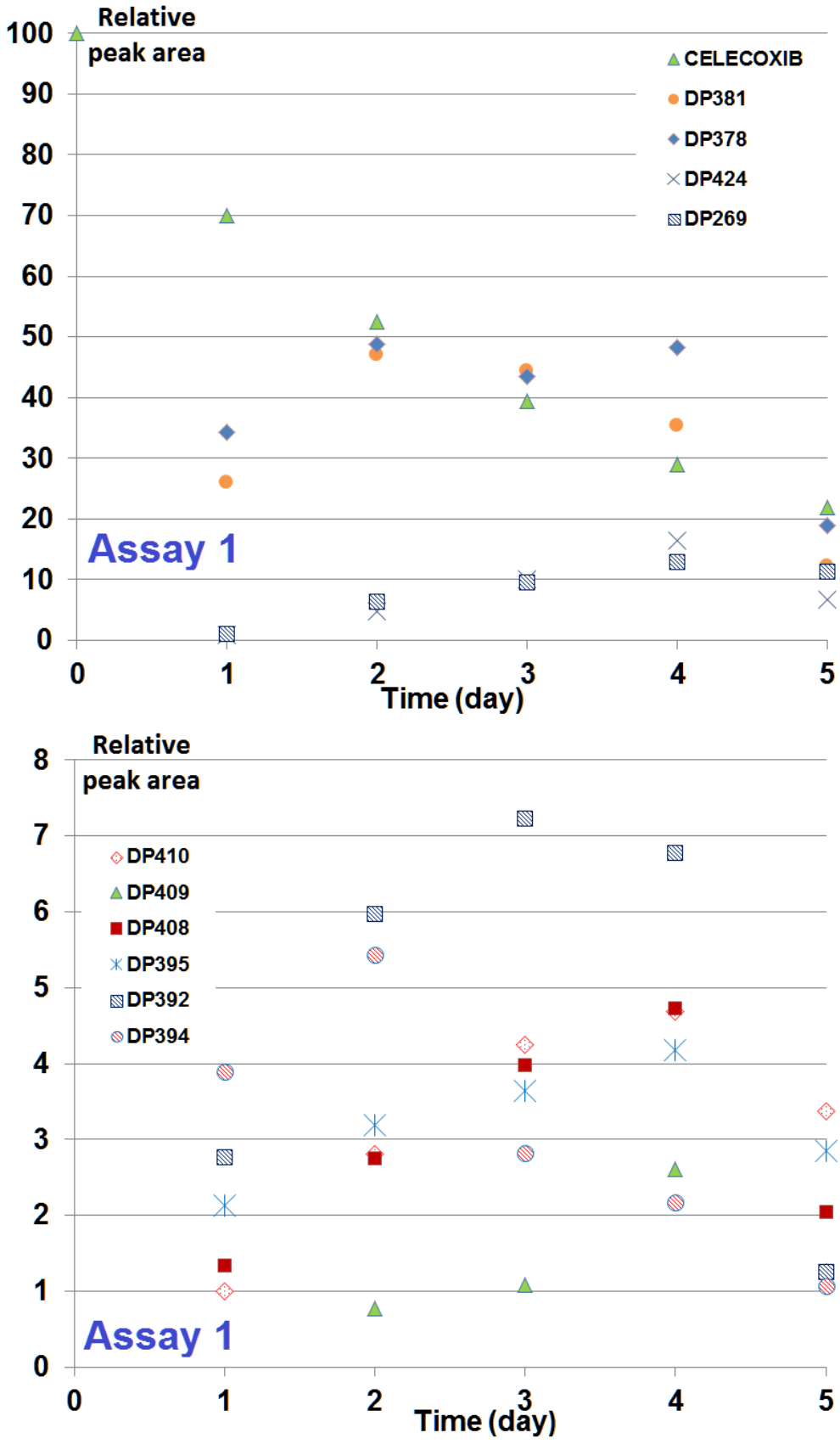

Figure A13: Variation of peak areas of the degradation products in the sample subjected to photochemical degradation (UV lamp). Peak areas are referred to the initial peak area of celecoxib in each experiment, to which a value of 100 was assigned. Assay 1.

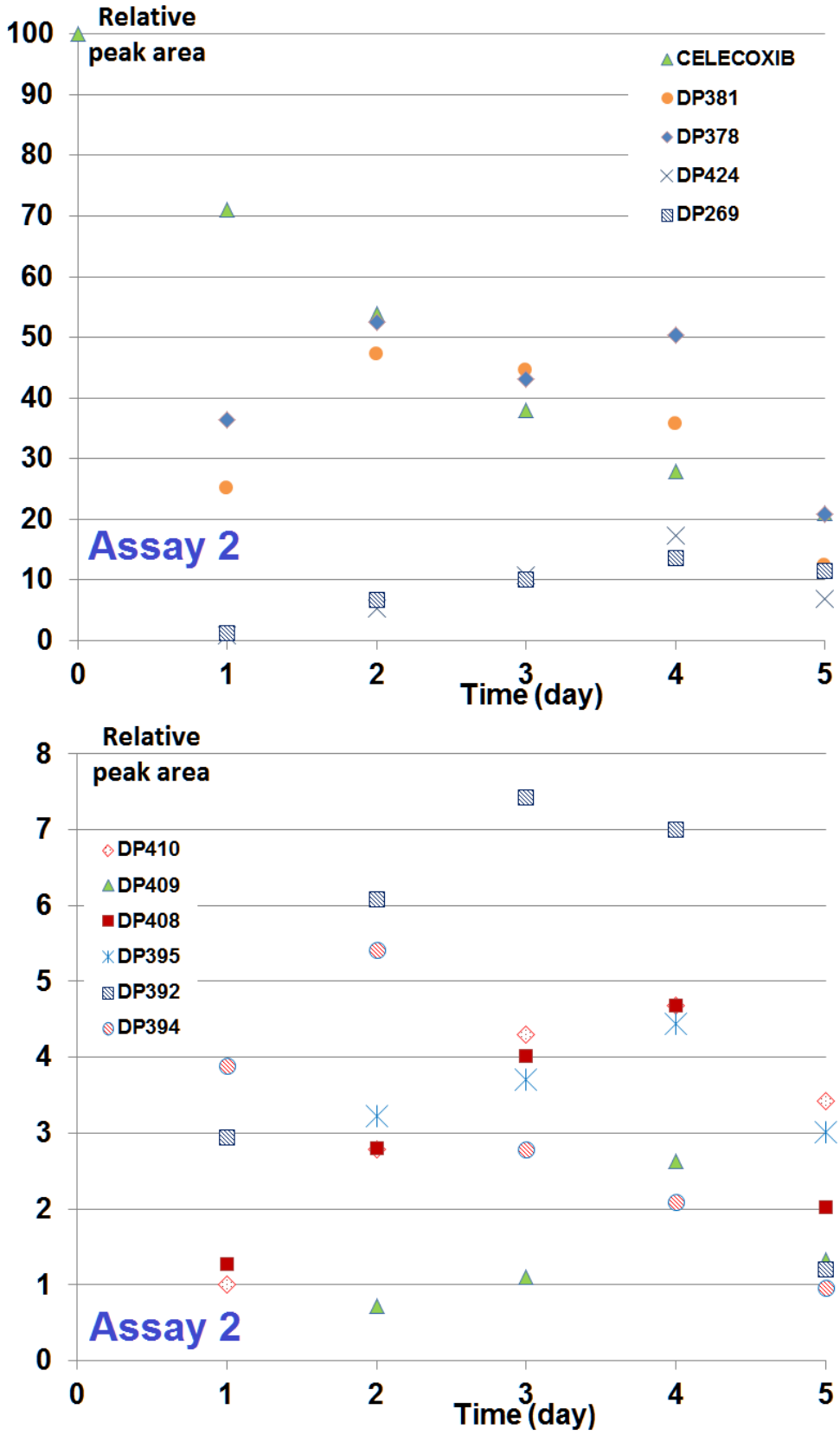

Figure A14: Variation of peak areas of the degradation products in the sample subjected to photochemical degradation (UV lamp). Peak areas are referred to the initial peak area of celecoxib in each experiment, to which a value of 100 was assigned. Assay 2.

Table A11: Peak areas of the degradation products in the non-forced assays on river water samples spiked with celecoxib at 2 or 100 μg·L^{-1} (river Pisuerga, W1; river Tuerto, W2; river Pisuerga in presence of sediment, SED). Peak areas are referred to the initial peak area of celecoxib in each experiment, to which a value of 100 was assigned. Mean values after the analysis of two aliquots.

Sample:	W1	W1	W1	W2	W2	W2	SED	SED	SED	W1	W1	W1	W2	W2	W2	SED	SED	SED
Weeks:	**12**	**24**	**36**	**12**	**24**	**36**	**12**	**24**	**36**	**12**	**24**	**36**	**12**	**24**	**36**	**12**	**24**	**36**
	Assay 1, 2 μg·L^{-1}									Assay 2, 2 μg·L^{-1}								
DP396	--	--	0.41	--	--	0.42	--	--	--	--	--	0.37	--	--	0.40	--	--	--
DP410	--	0.31	0.64	--	0.34	0.68	--	--	1.01	--	0.40	0.62	--	0.39	0.62	--	--	0.96
DP381	--	0.35	0.72	--	0.36	0.71	--	2.10	4.83	--	0.36	0.75	--	0.33	0.70	--	2.40	5.00
DP408	--	--	--	--	--	--	--	--	--	--	--	--	--	--	--	--	--	--
DP394	--	--	--	--	--	--	--	--	--	--	--	--	--	--	--	--	--	--
DP378	--	--	--	--	--	--	--	--	--	--	--	--	--	--	--	--	--	--
	Assay 1, 100 μg·L^{-1}									Assay 2, 100 μg·L^{-1}								
DP396	0.04	0.20	0.38	0.03	0.22	0.42	--	0.12	0.21	0.04	0.22	0.39	0.03	0.24	0.43	--	0.15	0.24
DP410	0.12	0.38	0.67	0.10	0.37	0.69	0.03	0.62	1.11	0.11	0.40	0.64	0.12	0.39	0.65	0.06	0.55	1.05
DP381	0.12	0.42	0.78	0.15	0.37	0.75	0.52	2.20	5.00	0.11	0.41	0.79	0.15	0.41	0.74	0.43	2.30	5.10
DP408	--	--	0.05	--	--	0.04	--	--	0.02	--	--	0.05	--	--	0.03	--	--	0.01
DP394	--	0.01	0.04	--	0.01	0.05	--	--	0.01	--	0.01	0.05	--	0.01	0.04	--	--	0.01
DP378	--	--	0.01	--	--	0.01	--	--	--	--	--	0.01	--	--	0.01	--	--	--

-- : not detected

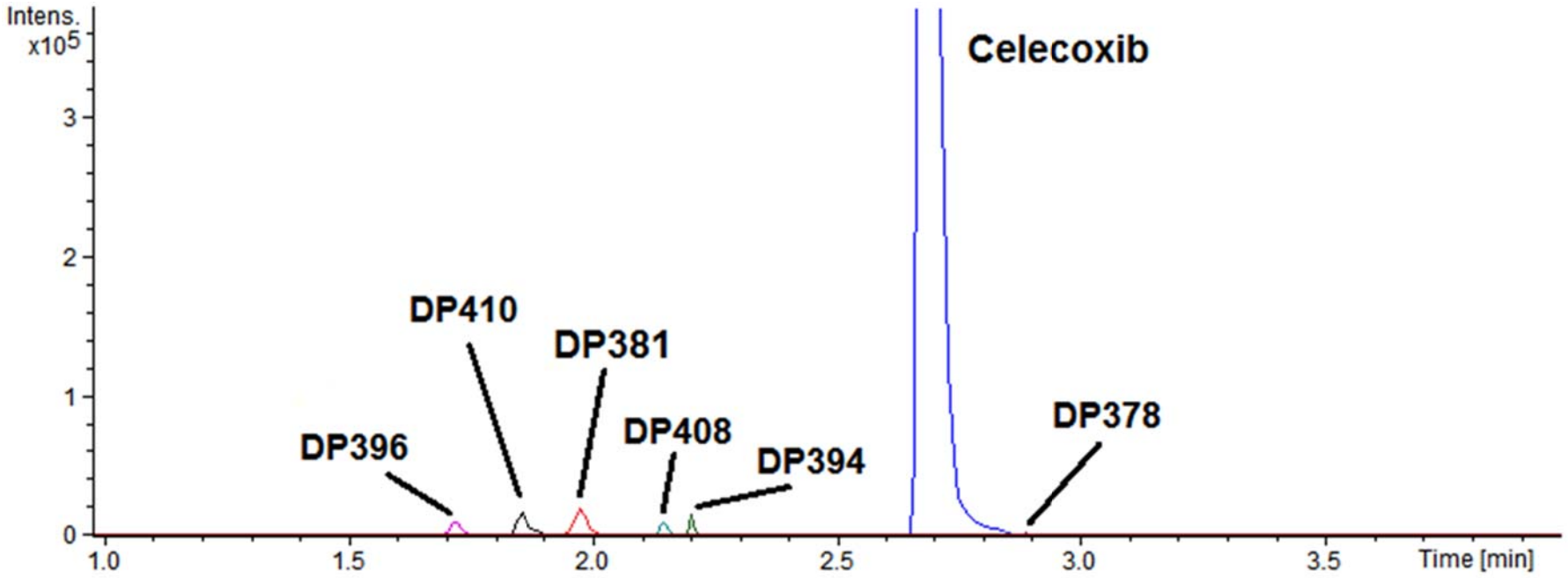

Figure A15: Superposition of extracted ion chromatograms ($[M+H]^-$ ± 0.01 for all compounds) for a water sample spiked with 100 µg L^{-1}, after 36 weeks under non-forced conditions.

4.5. TENOXICAM, PIROXICAM Y MELOXICAM

Chemosphere 191 (2018) 903–910

Contents lists available at ScienceDirect

Chemosphere

journal homepage: www.elsevier.com/locate/chemosphere

Forced and long-term degradation assays of tenoxicam, piroxicam and meloxicam in river water. Degradation products and adsorption to sediment

Juan J. Jiménez [a, b, *], Beatriz E. Muñoz [c], María I. Sánchez [c], Rafael Pardo [a]

[a] Department of Analytical Chemistry, Faculty of Sciences, Campus Miguel Delibes, University of Valladolid, Paseo de Belén 7, 47011, Valladolid, Spain
[b] I.U. CINQUIMA, Campus Miguel Delibes, University of Valladolid, Paseo de Belén 5, 47011, Valladolid, Spain
[c] Department of Analytical Chemistry, School of Industrial Engineers, University of Valladolid, Francisco Mendizábal 1, 47014, Valladolid, Spain

HIGHLIGHTS

- Tenoxicam, piroxicam and meloxicam are not persistent in river water.
- The degradation rate increases in this order: meloxicam, piroxicam, tenoxicam.
- Sunlight promotes their degradation and yields many degradation products.
- Most degradation products arise from the breakdown and oxidation of their moieties.
- The three oxicams have certain capacity of adsorption on a river sediment.

GRAPHICAL ABSTRACT

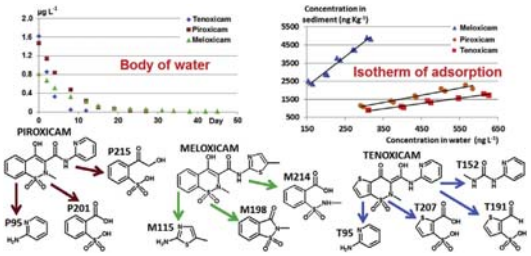

ARTICLE INFO

Article history:
Received 11 August 2017
Received in revised form
6 October 2017
Accepted 9 October 2017
Available online 25 October 2017

Handling Editor: I. Cousins

Keywords:
Oxicams
Degradation products
River water
Adsorption coefficients
High-resolution mass spectrometry

ABSTRACT

The fate of the pharmaceutical drugs tenoxicam, piroxicam and meloxicam in river water is evaluated here for first time. So, biological, photochemical and thermal degradation assays have been conducted to estimate their degradation rates and know their degradation products. Results indicated that the direct sunlight irradiation, without any protection, promoted a fast degradation of the oxicams while the chemical reactions in solution were less important. The biological degradation in water was negligible except for tenoxicam in whose case its influence was scarce. When the exposition of river water to sunlight was partially limited and kept under the natural day-night cycle, as occurs inside a body of water, tenoxicam, piroxicam and meloxicam (at 2 μg L^{-1}) were detected during a period of 15, 27 and 45 days, respectively. Residues were monitored by ultra-pressure liquid chromatography/quadrupole time-of-flight/mass spectrometry after solid-phase extraction and several degradation products were found (10 for tenoxicam, 9 for piroxicam and 7 for meloxicam) and monitored over time. Their structures were proposed from the molecular formulae and fragmentation observed in high-resolution tandem mass spectra; the nature of the transformation products found in the long-term resulted to be very variable for each oxicam. Furthermore, the degradation in presence of river sediment was also monitored over time, with some differences being noted; the adsorption coefficients of the compounds on sediment were

* Corresponding author. Department of Analytical Chemistry, Faculty of Sciences, Campus Miguel Delibes, University of Valladolid, Paseo de Belén 7, 47011, Valladolid, Spain.
E-mail address: jjimenez@qa.uva.es (J.J. Jiménez).

https://doi.org/10.1016/j.chemosphere.2017.10.056

calculated, meloxicam exhibited a higher sorption capacity. The ecotoxicity of the different compounds in aquatic ecosystems was predicted, too.

1. Introduction

The presence of pharmaceutical drugs in surface waters and sewage, which is the main introduction source of these drugs in the environment, has been revealed in many publications since the beginning of the 21st century. So, the stability of some drugs in aqueous medium has been studied to foresee their degradation and persistence in surface water. Among these microcontaminants are tenoxicam, piroxicam and meloxicam, which are non-steroid anti-inflammatory drugs prescribed for the treatment of painful musculoskeletal disorders. There is much information in the scientific bibliography about their pharmacokinetics but very few manuscripts have considered their possible occurrence in surface water. In this way, piroxicam has been detected in average concentrations of 103 and 15 ng L^{-1} in effluent wastewaters and surface waters (Petre et al., 2016), and in concentrations lower than 32 ng L^{-1} for 5 out of 17 samples collected in the Danube basin river (Chitescu et al., 2015). In other work, meloxicam was detected in the influent of a wastewater treatment plant at a concentration of 1.8 μg L^{-1} but it was not detected in the effluent (Zhao et al., 2014). There are no data for tenoxicam.

The behavior of piroxicam and meloxicam in aqueous solution has been assessed in some works in order to test their stability in pharmaceutical preparations. Thus, it has been stated that meloxicam is stable in water at room temperature for at least 7 days (Ingrao et al., 2013) and that both compounds are insensitive to alkaline hydrolysis under reflux while they are decomposed at acidic pH (Bandarkar and Vavia, 2009; Suntornsuk et al., 2005). In other work it is remarked that piroxicam and meloxicam in water-acetonitrile solution are labile compounds under hydrolytic, oxidative and photoneutral conditions besides describing some degradation products (Modhave et al., 2011). Various degradation products arisen from biological processes are known for tenoxicam, piroxicam and meloxicam; they are found in plasma, urine and feces of human or animal origin and, mainly, they are hydroxylated derivatives of the three oxicams (Aberg et al., 2009; Dell et al., 1984; Grude et al., 2009; Marland et al., 1999; McKinney et al., 2004; Milligan, 1992; Ródenas et al., 1998; Wasfi et al., 2001). A microbial transformation of meloxicam by fungi isolated from soil has been reported, too (Prasad et al., 2009).

Reliable information about the fate of the three oxicams in surface water and especially about their long-term fate in non-forced conditions is not available. In this context, river water spiked individually with each oxicam at trace level was subjected to degradation studies in this work to ascertain the importance of the chemical, photochemical and biological processes in their degradation in surface water. Moreover, their behavior in a body of water over time under non-forced conditions has also been simulated. Water aliquots were analyzed by ultra-pressure liquid chromatography/quadrupole time-of-flight/mass spectrometry, and the structures of the degradation products found have been tentatively elucidated from the molecular formulae and fragmentation observed in high-resolution tandem mass spectra. The evolution of the degradation products was also monitored over time to estimate their occurrence and propose a degradation pathway. In addition, the adsorption capacity of the oxicams on a sediment was evaluated by calculating the corresponding adsorption coefficients and ecotoxicities were predicted.

2. Experimental

2.1. Material and reagents

Water samples were collected from the rivers Pisuerga (pH value 7.8, chemical oxygen demand value 4.6 mg L^{-1}), in the urban area of the city of Valladolid, and Tuerto (pH value 7.4, chemical oxygen demand value 3.9 mg L^{-1}), in the rural area of the La Bañeza, province of León. A sediment sample (total organic carbon 1.2%; clay 11%, silt 44%, sand 45%) was collected from the river Pisuerga. Cellulose nitrate disks from Sartorius (Barcelona, Spain) were used: river water was filtered through 0.2 μm pore-size disks for the estimation of adsorption coefficients, through 3 μm pore-size disks to carry out biodegradation experiments, and through 0.45 μm pore-size disks for other degradation experiments.

Tenoxicam, piroxicam and meloxicam (99% purity) were obtained from Sigma-Aldrich (St. Louis, MO, USA). LC-MS grade methanol, acetonitrile and formic acid were supplied by Panreac (Barcelona, Spain) and ultrapure water was obtained from a Milli-Q plus apparatus (Millipore, Milford, MA, USA). Analysis-grade sodium hydroxide, potassium dihydrogen phosphate and sodium azide were purchased from Panreac. Oasis HLB cartridges (60 mg) for solid-phase extraction were purchased from Waters (Milford, MA, USA) and PTFE disposable syringe filter units, 0.20 μm pore size, were obtained from Scharlab (Barcelona, Spain). A vacuum centrifuge evaporator, Myvac model, was provided by Genevac (Ipswich, UK), a PK120 centrifuge by ALC (Winchester, VA, USA) and a Promax 2020 reciprocating platform shaker by Heidolph (Germany).

2.2. Biological degradation

2.2.1. Aerobic degradation

Biological degradation assays were carried out individually for each compound with water from the river Pisuerga (pH 7.8) which was spiked to achieve a concentration of 2 μg L^{-1} for each analyte. A volume of 50 mL of river water was transferred into a 100 mL Erlenmeyer flask, which was then coated with aluminum foil to avoid exposure to sunlight but allowing the exchange of air with the atmosphere. An analyte control solution was similarly prepared in ultrapure water (pH 7.8 adjusted with NaOH) containing 0.02% (*W/V*) sodium azide as a biocide. Water blanks were prepared as well. Samples were run in parallel; flasks were shaken in a reciprocating shaker at a rotation speed of 130 r min^{-1} for 5 weeks, within a temperature range of 18–21 °C. Aliquots (5 mL) were collected each week and subjected to analysis. Evaporation water losses were periodically restored by addition of water of the same type. All biological experiments were carried out in duplicate.

2.2.2. Anaerobic degradation

River water (pH 7.8) spiked at 2 μg L^{-1} was placed in 15 mL vials, completely filled to avoid the presence of air in the headspace. The vials were closed, protected from light by coating them with aluminum foil and kept in a temperature range of 18–21 °C. Control solutions with analyte in ultrapure water (pH 7.8 adjusted) containing 0.02% sodium azide, and the corresponding blanks, were

also run in parallel. A batch of vials was assembled to withdraw weekly samples over a period of 5 weeks; a volume of 5 mL from each withdrawn vial was collected for analysis.

2.3. Photochemical and thermal degradation

River water (pH 7.8) spiked individually with each oxicam (2 μg L^{-1}) was placed in a quartz cuvette, which was closed and placed on the outer edge of a window, south-facing, to allow its direct exposure to sunlight. The assay was performed in the city of Valladolid (latitude: 41°38′15″N, longitude: 4°44′17″W), in the month of May. Aliquots (0.25 mL) were withdrawn at regular time intervals and injected into the chromatographic system. Control samples, protected from sunlight with aluminum foil, were prepared as well.

For thermal degradation, a volume of 50 mL of individually spiked river water (2 μg L^{-1}) was placed in a closed 100 mL glass bottle. This was coated with aluminum foil and placed in an oven at 70 °C. Aliquots were collected periodically for its analysis. All experiments were done in duplicate.

2.4. Non-forced degradation assays

A simple approach was adopted to simulate the concurrent natural process in a body of water. River water was placed in a transparent glass container with air-tight seal, which was opened weekly to collect a sample aliquot and replace the air inside in contact with the water surface. The container was kept at laboratory temperature (18–21 °C) under the natural day-night cycle and directly exposed to sunlight for several days. In these conditions, the solar radiation must pass through the laboratory window glass and the container glass to reach the body of water; the glass absorbs UV radiation and the behavior of the oxicams in the glass container simulates, in a greater or lesser extent, that in a body of water where the penetration of solar UV radiation is diminished with depth. The attenuation of the radiation was estimated by measurements of transmittance through the two types of glass (container and window), the UV–visible absorption spectra of the glasses were recorded; so, it was quantified that the percentages of radiation transmitted to the body of water were 40%, 1.3%, 0.02%, 8×10^{-4}% and 8×10^{-5}% at wavelengths of 350, 320, 310, 305 and 290 nm, respectively.

Volumes of 2500 mL of river water placed in glass containers were spiked individually to achieve an initial concentration of 2 μg L^{-1} in each degradation assay. Aliquots of 25 mL were collected periodically and subjected to SPE; extracts were injected in the chromatographic system to follow the degradation, identify degradation products and monitor them. Degradation experiments were carried out in the months of June and July with waters from the rivers Pisuerga (W1 sample) and Tuerto (W2 sample). Simultaneously, the degradation in the W1 sample was also studied in presence of sediment by adding river sediment to the container in a sediment-to-solution ratio of 0.10 g mL^{-1} (SED sample).

It was verified that W1 and W2 river water samples were free of oxicam residues. First, water blanks were subjected to analysis to test for the absence of the parent compounds. Once the degradation products were known, tests were also performed to verify that they were not present in the water extracts. Similarly, the absence of residues in the sediment sample was confirmed; to this aim, sediment was extracted with methanol by mechanical shaking and the extract was concentrated for analysis.

2.5. Study of adsorption to sediment

Experiments were conducted to investigate the adsorption capacity of the sediment for tenoxicam, piroxicam and meloxicam. The adsorption coefficient (K_d) of the three compounds to sediment (sieved through 0.5 mm mesh) was determined by using a batch approach. River water (100 mL) spiked with the compounds was added to sediment (10 g) to achieve a sediment-to-solution ratio of 0.10 g mL^{-1}; oxicam concentrations were 400, 500, 600, 700 and 800 ng L^{-1}. River water contained 0.02% sodium azide as a biocide to minimize any possible microbial activity and pH (7.8) was controlled with phosphate buffer (0.02 M). Control solutions without sediment were prepared as well. The flasks, protected from sunlight with aluminum foil, were manually shaken for 1 min and left standing at 20 ± 1 °C for a period of 24 h. Afterwards, an aliquot of 20 mL, previously centrifuged to remove solids, was collected to determine the oxicam concentration at equilibrium. Adsorption isotherms were drawn in duplicate. The concentration adsorbed on the sediment was not directly measured.

2.6. Sample preparation

Except for the photochemical and thermal degradation studies, river water aliquots were eluted through Oasis cartridges previously conditioned by successive elution of methanol (6 mL) and water (6 mL). The cartridges were washed with water (3 mL) after sample elution. The stationary phase was dried with air for 3 min and the compounds were eluted with methanol (4 mL) by gravity. Then, the extract was evaporated in 30 min by a vacuum centrifuge evaporator heated at 40 °C, and the dry residue was re-dissolved in 0.5 mL of methanol, which was filtered through a 0.20 μm pore-size PTFE filter for chromatographic analysis.

2.7. Determination by liquid chromatography – mass spectrometry

An Acquity ultra-pressure liquid chromatograph from Waters coupled to a Maxis Impact quadrupole time-of-flight tandem mass spectrometer from Bruker Daltonics (Bremen, Germany) was used. Analyses were performed with electrospray ionization in positive and negative modes. The chromatograph was fitted with a Waters BEH ODS column (50 mm × 2.1 mm, 1.7 μm particle size). The mobile phase flow rate was 0.5 mL min^{-1} and consisted of 0.1% formic acid in water (A) and 0.1% formic acid in acetonitrile (B). Assays were performed under gradient conditions, from 0% B to 2% B in 1 min, then 28% B in 3.5 min for tenoxicam; from 0.5% B to 10% B in 2.5 min, then 44% B in 2 min for piroxicam; from 0.5% B to 18% B in 2.5 min, then 46% B in 2 min for meloxicam. The injection volume was 5 and 7 μL in positive and negative mode, respectively.

The operating parameters of the electrospray ionization source for the MS and MS/MS experiments in positive and negative (in parenthesis) modes were as follows: nebulizing gas pressure, 0.4 (2) bar; end plate offset voltage, −2500 (1000) V; capillary voltage, −3500 (2900) V; drying gas temperature, 200 (200) °C; dry gas flow, 8 (6) L min^{-1}. Nitrogen was used as drying and nebulizing gas. Mass calibration adjustments were performed by using a 10 mmol L^{-1} sodium formate solution in 2-propanol/water. MS/MS experiments based on collision-induced dissociation with nitrogen gas were performed. The quantitation of the analytes was accomplished using linear calibration graphs based on the measurement of peak areas in the chromatograms extracted for the ion $[M+H]^+$ generated in the electrospray source by MS experiments, with a mass range of ±0.001 Da. Similarly, peak areas of degradation products were integrated in the chromatograms extracted for the corresponding $[M+H]^+$ or $[M-H]^-$ ions.

As regards the sample preparation method, the mean recoveries of the oxicams (2 μg L^{-1}) were about 90–92% with repeatabilities in the range 4.1–4.5% (RSDs, n = 5). Solutions with the degraded parent compounds were used to estimate the performance of the

method in the monitoring of the degradation products; the recoveries varied widely between 37 and 79% whiles the RSDs were comprised between 4.5 and 14.1%, n = 5 (Table SM1).

3. Results and discussion

3.1. Degradation of oxicams

Fig. 1 shows the variation of the oxicam concentrations over time in the high temperature and photochemical assays; data are the average of two independent experiments whose results are shown in Tables SM2-SM3 presented as supplementary material. Tenoxicam, piroxicam and meloxicam were gradually broken down in water river at 70 °C; concentration data over time were fitted to first-order kinetics equations with half-lives of 2.75 (R^2 = 0.92), 28.24 (R^2 = 0.95) and 73.76 (R^2 = 0.93) d, respectively. Tenoxicam was only detected for 5 d. The degradation rate was faster when the oxicams were exposed directly to the UV radiation from the sunlight; concentration data were also fitted to first-order kinetics, with half-lives of 188.63 (R^2 = 0.99), 528.58 (R^2 = 0.94) and 649.51 (R^2 = 0.93) min for tenoxicam, piroxicam and meloxicam, respectively. After 5 weeks, the degradation of piroxicam and meloxicam in river water resulted to be negligible under aerobic and anaerobic conditions at room temperature, while tenoxicam showed certain degradation: its concentration decreased by 8.7 and 2.7% in aerobic and anaerobic conditions, respectively. The results of the individual assays can be seen in Tables SM4-SM6.

It is deduced from these assays that the UV radiation promote a fast degradation of oxicams in river water and that the chemical reactions in aqueous medium, at pH 7.8, can also affect to the stability of the oxicams although its reaction rate at environmental temperature could be rather slow. The biological processes only degrade minimally to tenoxicam. In fact, tenoxicam presents the lowest persistence in the three degradation studies; piroxicam and meloxicam show a relatively similar behavior, mainly under the sunlight assays. As regards these observations, it should be noted that the chemical structure of tenoxicam differs in greater extension from those of piroxicam and meloxicam, which are more similar to each other because both only differ in a substituent: a pyridyl or a thiazolyl group.

The evolution of the oxicam concentrations over days in the long-term assays can be seen in Tables SM7-SM9. Fig. 2 resumes the results for W1 and SED samples. Tenoxicam, piroxicam and meloxicam were detected for 15, 27 and 45 d in the W1 and W2 samples, respectively. The concentrations decreased gradually until they were lesser than the corresponding detection limits achieved by the method, which were estimated to be about 10 ng L^{-1}. The degradation in presence of sediment (SED sample) followed in general terms the same pattern than in its absence but the degradation of tenoxicam was slightly favored by the sediment particles while the persistence of piroxicam and meloxicam was somewhat enhanced. Experimental data were also well fitted to first-order kinetics; half-lives for tenoxicam were 1.95 (R^2 = 0.997), 1.95 (R^2 = 0.996) and 1.82 (R^2 = 0.96) d for W1, W2 and SED samples, respectively. For piroxicam and meloxicam half-lives were 3.62 (R^2 = 0.99) and 6.22 (R^2 = 0.99) d for W1 sample, 3.64 (R^2 = 0.996) and 6.26 (R^2 = 0.99) d for W2 sample, and 3.75 (R^2 = 0.99) and 6.99 (R^2 = 0.99) d for SED sample, respectively. As in the forced assays tenoxicam is the least stable compound and meloxicam is the most stable. On the other hand, the measured initial concentrations in the SED samples were lower with regard to the previous assays, which suggested a possible adsorption of the oxicams to sediment.

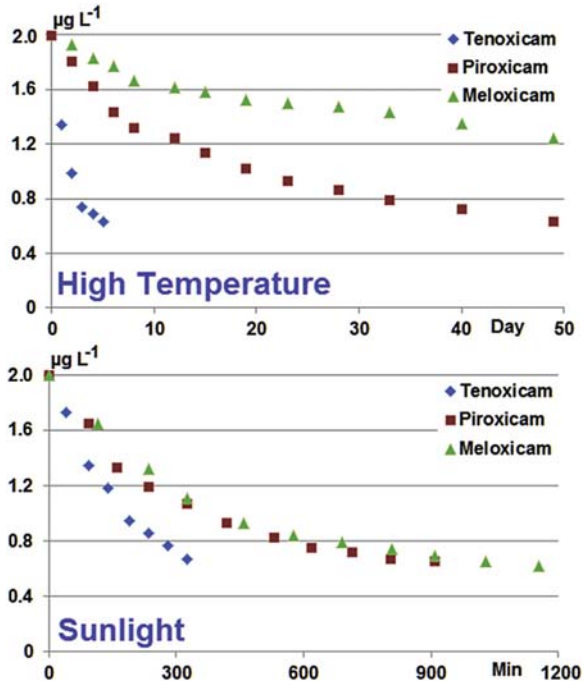

Fig. 1. Degradation of oxicams in river water according to assays under forced conditions. Data are the mean of two experiments.

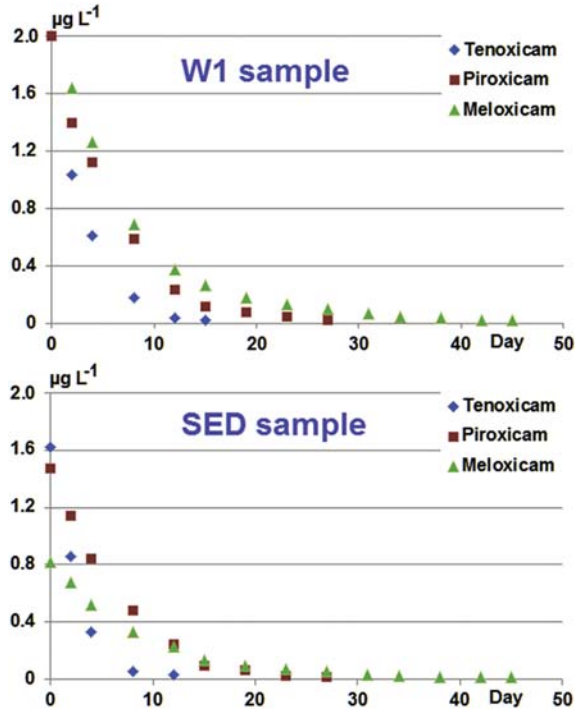

Fig. 2. Degradation of oxicams in W1 river water under non-forced conditions. Data are the mean of two experiments.

Table 1
Retention times (RT), masses measured in the mass spectra for the $[M+H]^+$ ion (positive mode; POS) or the $[M-H]^-$ ion (negative mode; NEG), errors in the determination of exact masses, molecular formulae and number of rings and double bonds (rdb) of the corresponding structures for the detected degradation products.

Mode	RT (min)	Molecular formula	Exact mass (Da)	Measured mass (Da)	Error (ppm)	rdb	Compound	Abbreviation
POS	0.42	$C_5H_7N_2^+$	95.0604	95.0603	1.1	3.5	2-aminopyridine	T95
POS	0.64	$C_6H_8N_3O^+$	138.0662	138.0662	0.0	4.5	1-(2-pyridyl)urea	T138
POS	0.66	$C_7H_7N_2O_3^+$	167.0451	167.0450	0.6	5.5	(2-pyridylcarbamoyl)formic acid	T167
NEG	1.33	$C_5H_3O_5S_2^-$	206.9427	206.9423	1.9	4.5	3-sulfotiophene-2-carboxylic acid	T207
POS	1.39	$C_7H_{10}N_3O^+$	152.0818	152.0821	−2.0	4.5	1-methyl-3-(2-pyridyl)urea	T152
POS	1.62	$C_8H_8N_3O^+$	162.0662	162.0665	−1.9	6.5	1,2-2H-1-(2-pyridyl)-imidazole-5-one	T162
POS	1.75	$C_7H_9N_2O_2^+$	153.0659	153.0660	−0.7	4.5	2-hydroxy-*N*-(2-pyridyl)acetamide	T153
NEG	1.92	$C_5H_3O_4S_2^-$	190.9478	190.9476	1.1	4.5	2-formyltiophene-3-sulfonic acid	T191
NEG	2.22	$C_6H_5O_4S_2^-$	204.9635	204.9632	1.5	4.5	2-propionyltiophene-3-sulfonic acid	T205
POS	2.70	$C_8H_{10}N_3O_2^+$	180.0768	180.0767	0.6	5.5	*N*-methyl-N'-pyridin-2-yl-oxalamide *N*-methyl-N'-(2-pyridyl)oxalamide	T180
POS	4.18	$C_{13}H_{12}N_3O_4S_2^+$	338.0264	338.0269	−1.5	9.5	4-hydroxy-2-methyl-*N*-(2-pyridyl)-2H-1-thieno[2,3-e][1,2]thiazine-3-carboxamide 1,1-dioxide	Tenoxicam
POS	0.29	$C_5H_7N_2^+$	95.0694	95.0606	−2.1	3.5	2-aminopyridine	P95
NEG	0.44	$C_7H_5O_5S^-$	200.9863	200.9865	−1.0	5.5	2-sulfobenzoic acid	P201
POS	0.35	$C_8H_8N_3O^+$	162.0662	162.0666	−2.4	6.5	1,2-2H-1-(2-pyridyl)-imidazole-5-one	P162
POS	0.45	$C_7H_9N_2O_2^+$	153.0659	153.0662	−2.0	4.5	2-hydroxy-*N*-(2-pyridyl)acetamide	P153
POS	0.51	$C_7H_{10}N_3^+$	136.0869	136.0870	−0.8	4.5	*N*-methyl-*N*'-(2-pyridyl)formamidine	P136
NEG	0.67	$C_7H_5O_4S^-$	184.9914	188.9915	−0.5	5.5	2-formyl-benzenesulfonic acid	P185
NEG	0.73	$C_8H_7O_5S^-$	215.0020	215.0021	−0.5	5.5	2-(2-hydroxyacetyl)benzenesulfonic acid	P215
POS	0.92	$C_8H_{10}N_3O_2^+$	180.0768	180.0769	−0.6	5.5	*N*-methyl-N'-pyridin-2-yl-oxalamide *N*-methyl-N'-(2-pyridyl)oxalamide	P180
NEG	1.72	$C_8H_8NO_4S^-$	214.0180	214.0184	−1.9	5.5	2-((*N*-methylamine)sulfonyl)benzoic acid	P214
POS	3.99	$C_{15}H_{14}N_3O_4S^+$	332.0700	332.0705	−1.5	10.5	4-Hydroxy-2-methyl-*N*-(2-pyridyl)-2H-1,2-benzothiazin-3-caboxamide 1,1-dioxide	Piroxicam
NEG	0.35	$C_7H_5O_4S^-$	184.9914	184.9915	−0.5	5.5	2-formyl-benzenesulfonic acid	M185
POS	0.87	$C_4H_7N_2S^+$	115.0324	115.0326	−1.7	2.5	5-methylthiazol-2-amine	M115
NEG	0.88	$C_8H_8NO_4S^-$	214.0180	214.0185	−2.3	5.5	2-((*N*-methylamine)sulfonyl)benzoic acid	M214
POS	1.58	$C_5H_8N_3OS^+$	158.0383	158.0381	1.3	3.5	1-(5-methyl-2-thiazolyl)urea	M158
POS	1.71	$C_6H_7N_2O_3S^+$	187.0172	187.0175	−1.6	4.5	((5-methyl-2-thiazolyl)carbamoyl)formic acid	M187
POS	2.68	$C_8H_8NO_3S^+$	198.0221	198.0219	−1.0	5.5	2-methylbenzoisothiazol-3-one 1,1-dioxide	M198
POS	2.88	$C_7H_{10}N_3O_2S^+$	200.0488	200.0491	−1.5	4.5	*N*-methyl-N'-(5-methylthiophen-2-yl)oxalamide	M200
POS	4.29	$C_{14}H_{14}N_3O_4S_2^+$	352.0420	352.0422	−0.6	9.5	4-hydroxy-2-methyl-*N*-(5-methyl-1,3-thiazol-2-yl)-2H-1,2-benzothiazine-3-carboxamide 1,1-dioxide	Meloxicam

3.2. Detection and identification of degradation products

The presence of degradation products of the oxicams was established by the observation of new chromatographic peaks in the MS chromatograms, which were present neither in the previous chromatograms nor in blanks, and the gradual variation of their peak areas over time. In this way, ten, nine and seven degradation products of tenoxicam, piroxicam and meloxicam, respectively, were found in the extracts analyzed by electrospray ionization in positive and negative mode. The $[M+H]^+$ or $[M-H]^-$ ion of each degradation product, and the parent compounds, was isolated and fragmented by collision-induced dissociation to obtain structural information. MS/MS spectra (Figs. SM1-SM24), a brief discussion of the fragmentation patterns, and the interpretation of the fragment-ions can be found in the supplementary material. Table 1 shows the molecular formulae established, the identifications proposed for the compounds and the abbreviations used in the manuscript.

In summary form, it can be stated that the three oxicams are constituted by two basic moieties. These moieties are a thiazolamine or pyridylamine group, and a benzothiazine or thienothiazine group, and these moieties are combined together one to another. In this way, the found degradation products derived from these basic moieties and some of them were the same for different oxicams. In general terms, the degradation products from the benzothiazine or thienothiazine groups were benzoic or benzenesulfonic acid derivatives commonly detected in negative electrospray ionization, while those arisen from the benzothiazine or thienothiazine groups had a more varied nature but always containing an aminopyridyl or aminothiazolyl substituent that facilitated its monitoring by positive electrospray ionization. Only the compounds P95, P180, M115, M187 and M198 had been previously noted as degradation products of piroxicam and meloxicam in a study under various forced conditions (Modhave et al., 2011).

3.3. Occurrence of degradation products in forced and over time degradation assays

A few degradation products were found in the assays carried out at 70 °C (see Figs. SM25-SM27); they were T95, T152, T207 and T191 for tenoxicam, P95 for piroxicam, and M115, M198 and M214 for meloxicam. The degradation products belonged to the two main moieties of the oxicams, excepting piroxicam and they were found in relatively small amounts. Fig. 3 shows the evolution of the detected compounds when river water was irradiated with sunlight without any limitation, in each assay a value of 100 was assigned to the initial peak area in mode positive electrospray ionization for the corresponding oxicam (hour 0), and all other peak areas were referred to this value; data are the mean of two assays whose individual data can be seen in Figs. SM28-30. Nine, eight and four degradation products were found for tenoxicam, piroxicam and meloxicam, respectively, in amounts much higher in comparison with the assays at 70 °C.

Peak areas of the degradation products were also monitored for W1 water sample in the degradation study over time to simulate the behavior of the oxicams inside a body of water (Fig. 4, Figs. SM31-33). T95, T138, T152, T162, T167, T180, T191 and T207 were the degradation products of tenoxicam detected in W1 sample. T138, a pyridylurea derivative, was only detected under non-forced conditions while the oxidation photoproducts T153 and T205 were not seen in these assays. As happened for the other

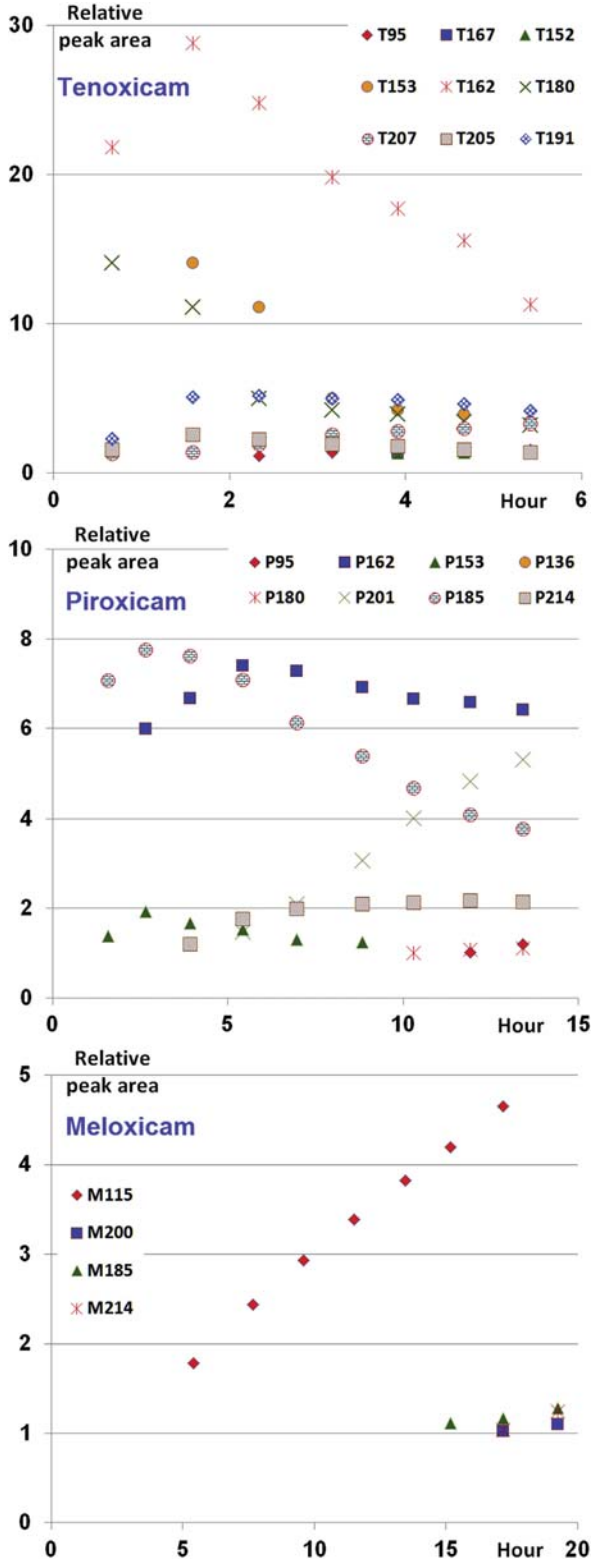

Fig. 3. Variation of peak areas of the degradation products in river water under solar irradiation without any limitation. Data are the mean of two experiments.

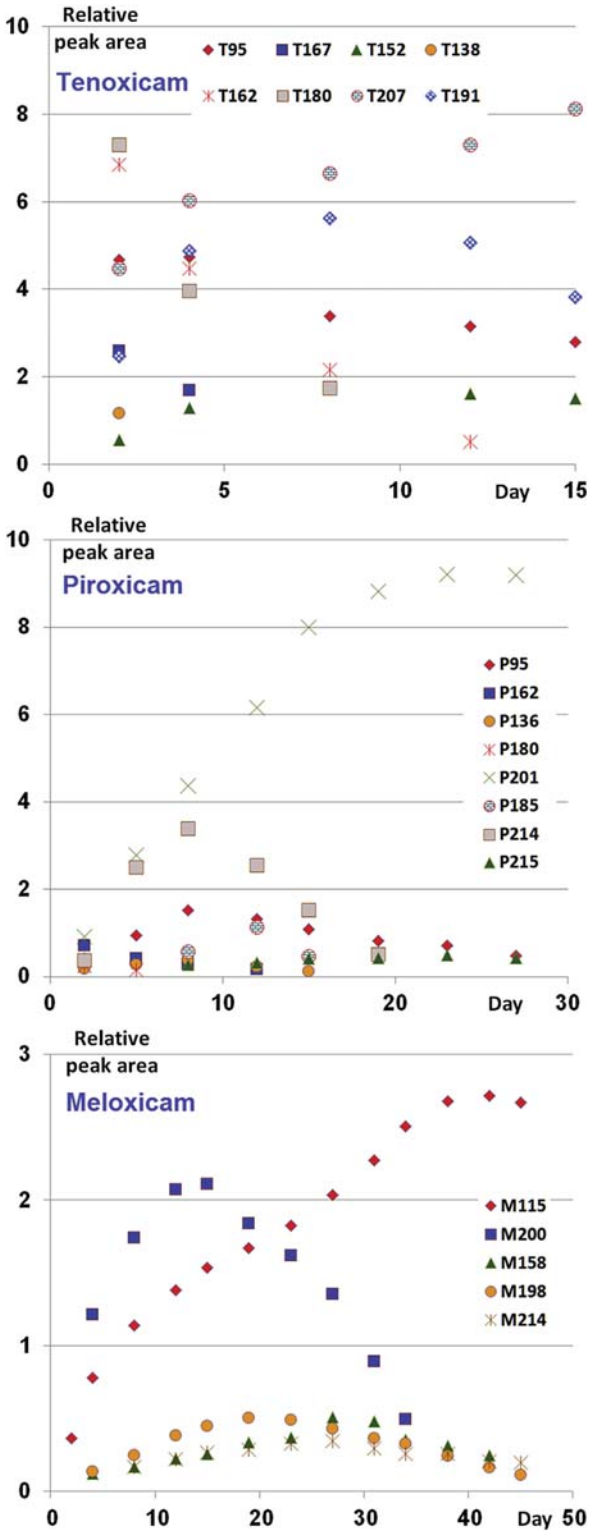

Fig. 4. Variation of peak areas of the degradation products in W1 river water over time under non-forced conditions. Data are the mean of two experiments.

oxicams, all degradation products observed in the assays at 70 °C were detected in the long-term degradation, too. According to the results, the compounds T95, T152, T191 and T207 are, presumably, more likely to be found in the analysis of real surface waters when tenoxicam has been completely degraded.

Other eight compounds were found in the degradation of piroxicam over time, they were P95, P136, P153, P162, P180, P185, P201 and P214. P215 was only detected in the non-forced study while P153 was only seen in the photochemical degradation. P201 was the major degradation product after 27 days in terms of peak area, and perhaps it could be easily detected in surface waters; P95 and P215 were also detected but in very low amount with regards to P201. Finally, M115, M158, M198, M200 and M214 were the degradation products recorded during the degradation of meloxicam. In this case, M158 was exclusively detected in the non-forced assay while M185 was detected only in the photochemical degradation assay. M115 was the main degradation product in terms of peak area.

The evolution of the degradation compounds in W1 sample was also monitored in presence of sediment (SED sample, Figs. SM34-36). The same degradation products were observed in SED sample, and their evolution with time followed the evolution profile observed for W1 sample, with the difference that the peak area values were different although the relative amounts among the different compounds were similar, in general terms, to those recorded without sediment. On the other hand, no degradation products were detected in the biological assays.

Fig. 5 shows a degradation pathway for the three oxicams in river water and outlines a possible photochemical reaction mechanism because the photo-induced reactions are the main reason of the degradation of the oxicams in water. It must be remarked that the transformation compounds resulted from the hydrolysis of the parent compounds and the oxidation to acids or alcohols. Although there are structural similarities among the three oxicams it is not possible propose a completely common degradation pathway and some observed transformations are not easily explainable. For

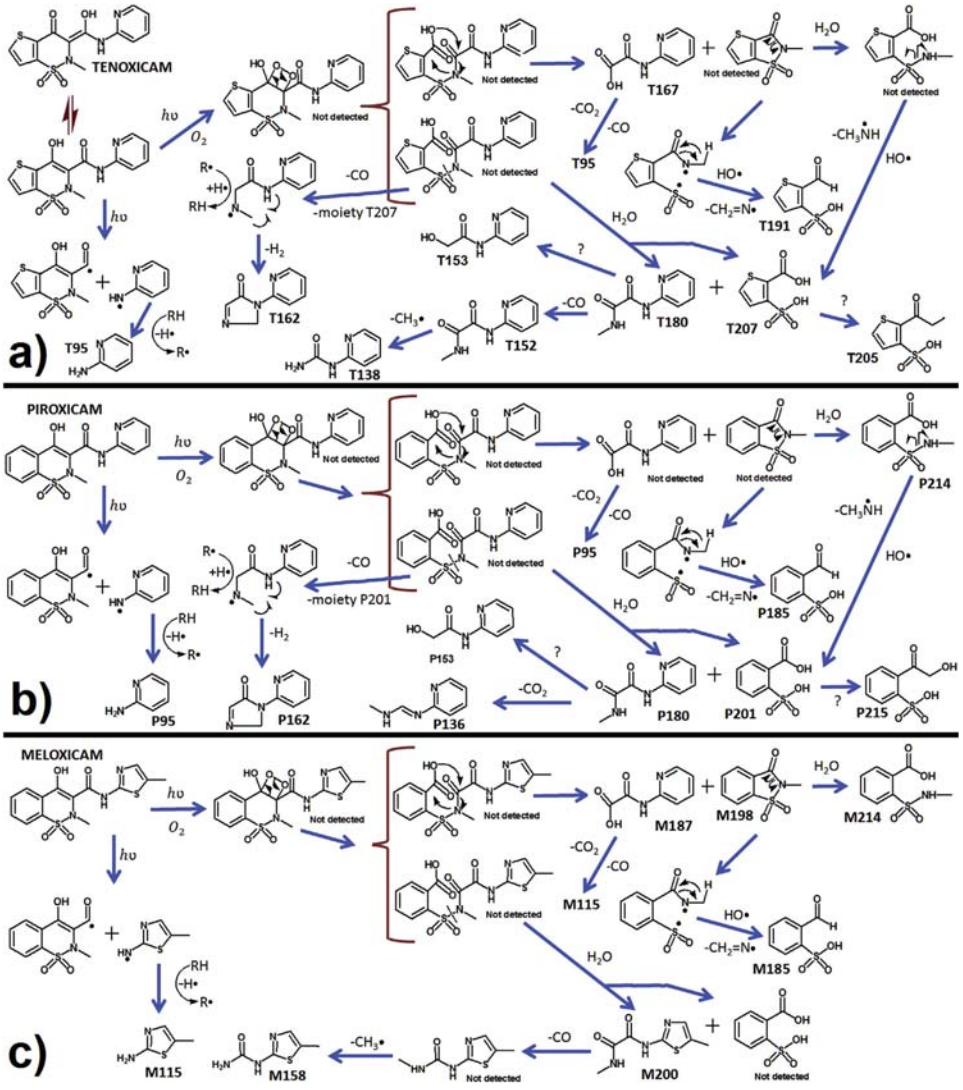

Fig. 5. Degradation pathway of tenoxicam (a), piroxicam (b) and meloxicam (c) in river water.

instance, a degradation product for piroxicam similar to M198 would be expected in agreement with the likeness of the structures of meloxicam and piroxicam, but it had not been detected. On the contrary, P214, the same compound than M214, has been detected, and M214 is supposed to arise from M198 throughout a hydrolysis reaction. .

3.4. Prediction of ecotoxicity

The toxicity of the oxicams and degradation products has been predicted for three ecotoxicological endpoints by the TEST software (version 4.1) from the US Environmental Protection Agency, which applies quantitative structure activity relationships (QSARs) methodologies. Data are presented in Table SM10. As regards the parent compounds, tenoxicam seems more toxic than piroxicam and meloxicam for the three endpoints and the three drugs seem more toxic to fathead minnow than *Daphnia magna* and *Tetrahymena pyriformis*. Their degradation products are, in general terms, less toxic for the three endpoints. Only T95/P95, P136 and M200 had a toxicity towards *Daphnia magna* scantly lower but comparable to that of the drugs; M198 was about two-fold more toxic than meloxicam for *Tetrahymena pyriformis*. On the other hand, *Tetrahymena pyriformis* is theoretically the ecological endpoint less affected by the presence of oxicams and their degradation products.

3.5. Distribution between water and sediment. Adsorption coefficients

Fig. SM37 shows the adsorption isotherms obtained for tenoxicam, piroxicam and meloxicam in the batch experiments. The K_d estimated values were 2.83, 3.82 and 15.31 L kg^{-1}, respectively, which corresponds to K_{oc} (organic carbon normalized adsorption coefficient) values of 236 (3.9%), 318 (5.2%) and 1276 L kg^{-1} (5.3%), respectively; the RSDs of the experiments (n = 10) are shown in parenthesis. The K_{oc} values of tenoxicam and piroxicam were comparable for instance to those of microcontaminants such as alachlor, 4-chlorophenol or chlorbromuron, while the K_{oc} value of meloxicam was similar to that of biphenyl or malathion in agreement with data published in the bibliography (Delle-Site, 2001). The water-sediment interaction is complex and only a sample of water and sediment has been considered to estimate the adsorption coefficients, however meloxicam seems to have a higher sorption capacity than tenoxicam and piroxicam.

4. Conclusions

Tenoxicam is the oxicam most affected by the chemical, photochemical and biochemical processes in river water in comparison with piroxicam and meloxicam. Meloxicam is the most persistent oxicam while the behavior of piroxicam is more similar to that of meloxicam, perhaps as consequence of the great similarity between their structures. The three drugs do not appear to be persistent in surface water in the medium-term.

Many degradation products have been characterized and identified; some of them could be detected in real water samples when the parent compounds have been degraded completely. There is not an absolute concordance between the degradation products found in the forced and non-forced assays for the three oxicams. Degradation products are mainly yielded from photochemical reactions.

The presence of sediment in water modifies very slightly the half-life of the oxicams during the degradation over time. The nature of the degradation products and their relative amounts in the assays with sediment seem similar to those obtained without sediment. Sorption coefficients of the oxicams to a sediment have been evaluated.

Acknowledgment

The authors would like to acknowledge the support given by the Laboratorio de Técnicas Instrumentales of the University of Valladolid to perform the experimental work.

Appendix A. Supplementary data

Supplementary data related to this article can be found at https://doi.org/10.1016/j.chemosphere.2017.10.056.

References

Aberg, A.T., Olsson, C., Bondesson, U., Hedeland, M., 2009. A mass spectrometric study on meloxicam metabolism in horses and the fungus *Cunninghamella elegans*, and the relevance of this microbial system as a model of drug metabolism in the horse. J. Mass. Spectrom. 44, 1026–1037.

Bandarkar, F.S., Vavia, P.R., 2009. A Stability Indicating HPLC Method for the determination of meloxicam in bulk and commercial formulations. Trop. J. Pharm. Res. 8, 257–264.

Chitescu, C.L., Kaklamanos, G., Nicolau, A.I., Stolker, A.A.M., 2015. High sensitive multiresidue analysis of pharmaceuticals and antifungals in surfacewater using U-HPLC-Q-Exactive Orbitrap HRMS. Application to the Danube river basin on the Romanian territory. Sci. Total Environ. 532, 501–511.

Dell, D., Joly, R., Meister, W., Arnold, W., Partos, C., Guldimann, B., 1984. Determination of tenoxicam, and the isolation, identification and determination of Ro17-6661, its major metabolite, in human urine. J. Chromat. 31, 483–492.

Delle-Site, A., 2001. Factors affecting sorption of organic compounds in natural sorbent water systems and sorption coefficients for selected pollutants. A review. J. Phys. Chem. Ref. Data 30, 187–439.

Grude, P., Guittard, J., Garcia, C., Daoulas, I., Thoulon, F., Ebner, T., 2009. Excretion mass balance evaluation, metabolite profile analysis and metabolite identification in plasma and excreta after oral administration of [14C]-meloxicam to the male cat: preliminary study. J. Vet. Pharmacol. Ther. 33, 396–407.

Ingrao, J.C., Johnson, R., Tor, E., Gu, Y., Litman, M., Turner, P.V., 2013. Aqueous stability and oral pharmacokinetics of meloxicam and carprofen in male C57BL/6 mice. J. Am. Assoc. Lab. Anim. Sci. 52, 553–559.

Marland, A., Sarkar, P., Leavitt, R., 1999. The elimination profiles of tenoxicam and hydroxytenoxicam in equine urine and serum after a 200-mg oral dose. J. Anal. Toxicol. 23, 237–241.

McKinney, A.R., Suann, C.J., Leeuse, A.M.S., 2004. The detection of piroxicam, tenoxicam and their metabolites in equine urine by electrospray ionization ion trap mass spectrometry. Rapid Commun. Mass Spectrom. 18, 2338–2342.

Milligan, P.A., 1992. Determination of piroxicam and its major metabolites in the plasma, urine and bile of humans by high-performance liquid chromatography. J. Chromat. 516, 121–128.

Modhave, D.T., Handa, T., Shah, R.P., Singh, S., 2011. Successful characterization of degradation products of drugs unsing LC-MS tools: application to piroxicam and meloxicam. Anal. Methods 3, 2864–2872.

Petre, J., Galaon, T., Iancu, V.I., Cruceru, L., Niculescu, M., 2016. Simultaneous liquid chromatography- tandem mass spectrometry determination of some pharmaceuticals and antimicrobial disinfectant agents in surface water and in urban wastewater. J. Environ. Prot. Ecol. 17, 119–126.

Prasad, G.S., Girisham, S., Reddy, S.M., 2009. Biotransformation of meloxicam by *Aspergillus fumigatus* and *Fusarium moniliforme* isolated from soil. Natl. Acad. Sci. Lett. (India) 32, 157–161.

Ródenas, V., García, M.S., Sánchez-Pedreño, C., Albero, M.I., 1998. Simultaneous determination of piroxicam and its major metabolite 5 '-hydroxypiroxicam in human plasma by derivative spectrophotometry. Analyst 123, 1749–1752.

Suntornsuk, L., Bunavitayakij, P., Pitayatienan, P., 2005. Spectrophotometric method for the simultaneous determination of piroxicam and 2-aminopyridine. Indian J. Chem. Sect. A Inorg. Bio-inorg. Phys. Theor. Anal. Chem. 44, 737–740.

Wasfi, I.A., Al Ali, W.A., Agha, B.A., Kamel, A.M., Al Biriki, N.A., Al Neaimi, K.M., 2001. The pharmacokinetics and metabolism of meloxicam in camels after intravenous administration. J. Vet. Pharmacol. Ther. 35, 155–162.

Zhao, L., Liang, N., Lun, X., Chen, X., Hou, X., 2014. LC-QTOF-MS method for the analysis of residual pharmaceuticals in wastewater: application to a comparative multiresidue trace analysis between spring and winter water. Anal. Methods 6, 6956–6962.

Supplementary data

Forced and long-term degradation assays of tenoxicam, piroxicam and meloxicam in river water. Degradation products and adsorption to sediment.

Chemosphere, 2017

Contents

2.7. Determination by liquid chromatography – mass spectrometry

Table SM1: Recoveries and repeatabilities (expressed as RSDs) achieved in the determination of oxicams and degradation products on the W1 river water sample by the solid phase extraction method (n=5). See section 3.2 for compound identification.

Compound	Recovery (%)	RSD (%)
T95	47	9.6
T138	46	8.9
T167	46	8.9
T207	43	5.6
T152	44	9.0
T162	72	5.5
T153	48	10.6
T191	50	5.2
T205	51	6.0
T180	63	5.6
Tenoxicam	90	4.5
P95	51	7.7
P201	37	14.1
P162	68	6.6
P153	50	9.3
P136	60	7.3
P185	37	6.9
P215	41	7.4
P180	61	4.9
P214	63	5.4
Piroxicam	92	4.1
M185	40	8.7
M115	66	4.8
M214	69	5.3
M158	56	5.6
M187	52	5.0
M198	79	3.7
M200	72	5.6
Meloxicam	92	4.2

Table SM2: Thermal degradation at 70°C of tenoxicam, piroxicam and meloxicam on river water spiked with 2 $\mu g \cdot L^{-1}$. Individual data of each assay.

Tenoxicam				Piroxicam				Meloxicam			
Assay 1		Assay 2		Assay 1		Assay 2		Assay 1		Assay 2	
Day	Concent. ($\mu g \cdot L^{-1}$)	**Day**	Concent. ($\mu g \cdot L^{-1}$)	**Day**	Concent. ($\mu g \cdot L^{-1}$)	**Day**	Concent. ($\mu g \cdot L^{-1}$)	**Day**	Concent. ($\mu g \cdot L^{-1}$)	**Day**	Concent. ($\mu g \cdot L^{-1}$)
0	2.01	**0**	2.02	**0**	2.00	**0**	1.99	**0**	2.01	**0**	2.00
1	1.35	**1**	1.34	**2**	1.81	**2**	1.80	**2**	1.93	**2**	1.92
2	0.98	**2**	0.99	**4**	1.61	**4**	1.64	**4**	1.83	**4**	1.82
3	0.75	**3**	0.73	**6**	1.41	**6**	1.45	**6**	1.77	**6**	1.77
4	0.68	**4**	0.69	**8**	1.34	**8**	1.29	**8**	1.67	**8**	1.65
5	0.64	**5**	0.62	**12**	1.23	**12**	1.25	**12**	1.62	**12**	1.60
				15	1.14	**15**	1.13	**15**	1.59	**15**	1.57
				19	1.02	**19**	1.02	**19**	1.55	**19**	1.50
				23	0.92	**23**	0.94	**23**	1.51	**23**	1.48
				28	0.88	**28**	0.85	**28**	1.49	**28**	1.46
				33	0.77	**33**	0.81	**33**	1.45	**33**	1.42
				40	0.72	**40**	0.73	**40**	1.38	**40**	1.32
				49	0.64	**49**	0.62	**49**	1.24	**49**	1.25
R^2	0.92	R^2	0.92	R^2	0.94	R^2	0.95	R^2	0.93	R^2	0.92
$t_{1/2}$ (days)	2.78	$t_{1/2}$ (days)	2.73	$t_{1/2}$ (days)	28.30	$t_{1/2}$ (days)	28.18	$t_{1/2}$ (days)	74.99	$t_{1/2}$ (days)	72.53

R^2: Coefficient of regression of the fitting; kinetics of first-order reactions.

$t_{1/2}$: half-life time.

Table SM3: Photochemical degradation under sunlight of tenoxicam, piroxicam and meloxicam on river water spiked with 2 $\mu g \cdot L^{-1}$. Individual data of each assay.

Tenoxicam				Piroxicam				Meloxicam			
Assay 1		Assay 2		Assay 1		Assay 2		Assay 1		Assay 2	
Minute	Concent. ($\mu g \cdot L^{-1}$)	**Minute**	Concent. ($\mu g \cdot L^{-1}$)	**Minute**	Concent. ($\mu g \cdot L^{-1}$)	**Minute**	Concent. ($\mu g \cdot L^{-1}$)	**Minute**	Concent. ($\mu g \cdot L^{-1}$)	**Minute**	Concent. ($\mu g \cdot L^{-1}$)
0	2.01	**0**	2.00	**0**	2.00	**0**	1.99	**0**	2.00	**0**	1.99
40	1.74	**40**	1.72	**95**	1.64	**95**	1.65	**115**	1.67	**115**	1.62
95	1.36	**95**	1.34	**160**	1.31	**160**	1.35	**235**	1.35	**235**	1.30
140	1.19	**140**	1.17	**235**	1.21	**235**	1.18	**325**	1.12	**325**	1.10
190	0.94	**190**	0.96	**325**	1.06	**325**	1.07	**460**	0.94	**460**	0.92
235	0.87	**235**	0.84	**418**	0.94	**418**	0.92	**575**	0.84	**575**	0.84
280	0.75	**280**	0.78	**530**	0.82	**530**	0.82	**690**	0.80	**690**	0.78
325	0.66	**325**	0.68	**618**	0.75	**618**	0.75	**807**	0.74	**807**	0.74
				715	0.72	**715**	0.71	**910**	0.70	**910**	0.69
				805	0.68	**805**	0.66	**1030**	0.65	**1030**	0.65
				910	0.66	**910**	0.64	**1155**	0.62	**1155**	0.62
R^2	0.991	R^2	0.987	R^2	0.933	R^2	0.942	R^2	0.929	R^2	0.922
$t_{1/2}$ (min)	185.33	$t_{1/2}$ (min)	192.00	$t_{1/2}$ (min)	536.60	$t_{1/2}$ (min)	520.75	$t_{1/2}$ (min)	643.14	$t_{1/2}$ (min)	656.12

R^2: Coefficient of regression of the fitting; kinetics of first-order reactions.
$t_{1/2}$: half-life time.

Table SM4: Concentrations (in $\mu g \cdot L^{-1}$) of tenoxicam found in the biological degradation assays at 2 $\mu g \cdot L^{-1}$, under aerobic and anaerobic conditions. Two or five sample aliquots were taken each week. A t-test (p=0.05, n=5) was applied to check for differences between the initial and final mean concentrations of the assay.

Aerobic conditions												
	Assay 1						Assay 2					
Week:	**0**	**1**	**2**	**3**	**4**	**5**	**0**	**1**	**2**	**3**	**4**	**5**
Aliquot 1	2.00	1.96	1.92	1.89	1.84	1.81	2.01	1.97	1.95	1.90	1.85	1.82
Aliquot 2	2.01	1.98	1.94	1.88	1.85	1.83	2.02	1.95	1.93	1.91	1.88	1.84
Aliquot 3	2.02	--	--	--	--	1.85	2.02	--	--	--	--	1.85
Aliquot 4	2.00	--	--	--	--	1.83	2.00	--	--	--	--	1.86
Aliquot 5	1.99	--	--	--	--	1.82	2.01	--	--	--	--	1.83
Mean:	2.00					1.83	2.01					1.84
	Experimental t-value*: 21.0						Experimental t-value*: 21.5					
Anaerobic conditions												
	Assay 1						Assay 2					
Week:	**0**	**1**	**2**	**3**	**4**	**5**	**0**	**1**	**2**	**3**	**4**	**5**
Aliquot 1	2.01	2.00	1.98	1.97	1.96	1.94	2.01	1.99	1.99	1.98	1.96	1.95
Aliquot 2	2.00	1.99	1.98	1.96	1.97	1.96	2.01	1.98	1.98	1.97	1.97	1.96
Aliquot 3	2.00	--	--	--	--	1.95	1.99	--	--	--	--	1.96
Aliquot 4	1.98	--	--	--	--	1.93	2.00	--	--	--	--	1.95
Aliquot 5	1.98	--	--	--	--	1.94	2.02	--	--	--	--	1.93
Mean:	1.99					1.94	2.01					1.95
Experimental t-value*: 6.4							Experimental t-value*: 7.5					

--: without data

*Critical t-value: 2.3

Table SM5: Concentrations (in $\mu g \cdot L^{-1}$) of piroxicam found in the biological degradation assays at 2 $\mu g \cdot L^{-1}$, under aerobic and anaerobic conditions. Two or five sample aliquots were taken each week. A t-test (p=0.05, n=5) was applied to check for differences between the initial and final mean concentrations of the assay.

Aerobic conditions												
	Assay 1						Assay 2					
Week:	**0**	**1**	**2**	**3**	**4**	**5**	**0**	**1**	**2**	**3**	**4**	**5**
Aliquot 1	2.00	1.99	1.99	2.01	2.02	2.01	2.02	2.00	1.99	2.01	2.00	2.00
Aliquot 2	2.00	2.00	2.01	2.01	2.00	1.99	1.99	2.00	2.01	2.00	1.99	2.01
Aliquot 3	2.01	--	--	--	--	2.01	2.01	--	--	--	--	1.98
Aliquot 4	2.00	--	--	--	--	2.01	2.01	--	--	--	--	2.01
Aliquot 5	1.99	--	--	--	--	2.00	2.02	--	--	--	--	2.00
Mean:	2.00					2.00	2.01					2.00
	Experimental t-value*: 0.8						Experimental t-value*: 1.3					
Anaerobic conditions												
	Assay 1						Assay 2					
Week:	**0**	**1**	**2**	**3**	**4**	**5**	**0**	**1**	**2**	**3**	**4**	**5**
Aliquot 1	2.02	2.00	1.98	2.00	1.99	1.99	1.99	1.99	2.00	2.01	1.99	1.97
Aliquot 2	2.01	2.00	2.01	2.02	1.98	1.98	2.01	2.00	2.01	1.98	2.00	2.00
Aliquot 3	1.99	--	--	--	--	1.99	1.98	--	--	--	--	2.00
Aliquot 4	1.99	--	--	--	--	2.00	1.99	--	--	--	--	1.99
Aliquot 5	2.01	--	--	--	--	2.01	1.98	--	--	--	--	1.98
Mean:	2.00					1.99	1.99					1.99
	Experimental t-value*: 1.9						Experimental t-value*: 0.3					

--: without data

*Critical t-value: 2.3

Table SM6: Concentrations (in $\mu g \cdot L^{-1}$) of meloxicam found in the biological degradation assays at 2 $\mu g \cdot L^{-1}$, under aerobic and anaerobic conditions. Two or five sample aliquots were taken each week. A t-test (p=0.05, n=5) was applied to check for differences between the initial and final mean concentrations of the assay.

Aerobic conditions												
	Assay 1						Assay 2					
Week:	**0**	**1**	**2**	**3**	**4**	**5**	**0**	**1**	**2**	**3**	**4**	**5**
Aliquot 1	2.03	2.01	2.00	2.00	2.01	2.02	2.01	2.02	2.00	2.00	2.01	2.01
Aliquot 2	2.02	2.00	2.01	2.03	2.01	2.00	2.01	2.03	2.02	2.02	2.01	2.03
Aliquot 3	2.01	--	--	--	--	2.02	2.03	--	--	--	--	2.00
Aliquot 4	2.00	--	--	--	--	2.01	2.02	--	--	--	--	2.00
Aliquot 5	2.01	--	--	--	--	2.00	2.02	--	--	--	--	2.01
Mean:	2.01					2.01	2.02					2.01
	Experimental t-value*: 0.6						Experimental t-value*: 1.2					
Anaerobic conditions												
	Assay 1						Assay 2					
Week:	**0**	**1**	**2**	**3**	**4**	**5**	**0**	**1**	**2**	**3**	**4**	**5**
Aliquot 1	1.99	2.00	2.01	1.99	2.00	2.00	2.00	2.01	1.98	1.99	2.01	2.01
Aliquot 2	1.98	1.99	1.98	2.00	2.00	2.01	1.99	2.00	2.02	2.00	1.99	2.01
Aliquot 3	1.99	--	--	--	--	1.99	2.01	--	--	--	--	1.99
Aliquot 4	2.00	--	--	--	--	1.99	2.01	--	--	--	--	1.98
Aliquot 5	2.00	--	--	--	--	2.01	2.01	--	--	--	--	1.99
Mean:	1.99					2.00	2.00					2.00
Experimental t-value*: 1.4							Experimental t-value*: 1.1					

--: without data

*Critical t-value: 2.3

Table SM7: Degradation of tenoxicam on river water samples spiked with 2 $\mu g \cdot L^{-1}$ under non-forced conditions (river Pisuerga, W1; river Tuerto, W2; river Pisuerga in presence of sediment, SED). Individual data of each assay.

W1 sample				W2 sample				SED sample			
Assay 1		Assay 2		Assay 1		Assay 2		Assay 1		Assay 2	
Day	Concent. ($\mu g \cdot L^{-1}$)	**Day**	Concent. ($\mu g \cdot L^{-1}$)	**Day**	Concent. ($\mu g \cdot L^{-1}$)	**Day**	Concent. ($\mu g \cdot L^{-1}$)	**Day**	Concent. ($\mu g \cdot L^{-1}$)	**Day**	Concent. ($\mu g \cdot L^{-1}$)
0	1.99	**0**	2.02	**0**	2.00	**0**	2.01	**0**	1.62	**0**	1.63
2	1.02	**2**	1.05	**2**	1.03	**2**	1.04	**2**	0.84	**2**	0.87
4	0.61	**4**	0.61	**4**	0.61	**4**	0.59	**4**	0.34	**4**	0.32
8	0.17	**8**	0.18	**8**	0.18	**8**	0.19	**8**	0.054	**8**	0.047
12	0.030	**12**	0.038	**12**	0.031	**12**	0.037	**12**	0.032	**12**	0.031
15	0.019	**15**	0.014	**15**	0.015	**15**	0.017	**15**	--	**15**	--
R^2	0.99	R^2	0.998	R^2	0.99	R^2	0.996	R^2	0.96	R^2	0.95
$t_{1/2}$ (days)	1.97	$t_{1/2}$ (days)	1.92	$t_{1/2}$ (days)	1.91	$t_{1/2}$ (days)	1.98	$t_{1/2}$ (days)	1.84	$t_{1/2}$ (days)	1.80

R^2: Coefficient of regression of the fitting; kinetics of first-order reactions.
$t_{1/2}$: half-life time.
--: non detected

Table SM8: Degradation of piroxicam on river water samples spiked with 2 $\mu g \cdot L^{-1}$ under non-forced conditions (river Pisuerga, W1; river Tuerto, W2; river Pisuerga in presence of sediment, SED). Individual data of each assay.

W1 sample				W2 sample				SED sample			
Assay 1		Assay 2		Assay 1		Assay 2		Assay 1		Assay 2	
Day	Concent. ($\mu g \cdot L^{-1}$)	**Day**	Concent. ($\mu g \cdot L^{-1}$)	**Day**	Concent. ($\mu g \cdot L^{-1}$)	**Day**	Concent. ($\mu g \cdot L^{-1}$)	**Day**	Concent. ($\mu g \cdot L^{-1}$)	**Day**	Concent. ($\mu g \cdot L^{-1}$)
0	2.01	**0**	2.01	**0**	2.00	**0**	2.00	**0**	1.44	**0**	1.47
2	1.42	**2**	1.37	**2**	1.39	**2**	1.46	**2**	1.04	**2**	1.14
4	1.10	**4**	1.14	**4**	1.13	**4**	1.11	**4**	0.81	**4**	0.84
8	0.58	**8**	0.59	**8**	0.61	**8**	0.58	**8**	0.42	**8**	0.48
12	0.23	**12**	0.24	**12**	0.25	**12**	0.22	**12**	0.19	**12**	0.24
15	0.11	**15**	0.12	**15**	0.11	**15**	0.13	**15**	0.071	**15**	0.094
19	0.068	**19**	0.074	**19**	0.081	**19**	0.077	**19**	0.052	**19**	0.062
23	0.042	**23**	0.042	**23**	0.040	**23**	0.033	**23**	0.028	**23**	0.025
27	0.015	**27**	0.019	**27**	0.018	**27**	0.020	**27**	0.021	**27**	0.018
R^2	0.99	R^2	0.995	R^2	0.99	R^2	0.996	R^2	0.98	R^2	0.99
$t_{1/2}$ (days)	3.55	$t_{1/2}$ (days)	3.67	$t_{1/2}$ (days)	3.64	$t_{1/2}$ (days)	3.63	$t_{1/2}$ (days)	3.81	$t_{1/2}$ (days)	3.70

R^2: Coefficient of regression of the fitting; kinetics of first-order reactions.

$t_{1/2}$: half-life time.

Table SM9: Degradation of meloxicam on river water samples spiked with 2 $\mu g \cdot L^{-1}$ under non-forced conditions (river Pisuerga, W1; river Tuerto, W2; river Pisuerga in presence of sediment, SED). Individual data of each assay.

W1 sample				W2 sample				SED sample			
Assay 1		Assay 2		Assay 1		Assay 2		Assay 1		Assay 2	
Day	Concent. ($\mu g \cdot L^{-1}$)	**Day**	Concent. ($\mu g \cdot L^{-1}$)	**Day**	Concent. ($\mu g \cdot L^{-1}$)	**Day**	Concent. ($\mu g \cdot L^{-1}$)	**Day**	Concent. ($\mu g \cdot L^{-1}$)	**Day**	Concent. ($\mu g \cdot L^{-1}$)
0	2.01	**0**	2.02	**0**	2.00	**0**	2.00	**0**	0.82	**0**	0.81
2	1.63	**2**	1.64	**2**	1.66	**2**	1.64	**2**	0.67	**2**	0.69
4	1.25	**4**	1.27	**4**	1.31	**4**	1.26	**4**	0.52	**4**	0.51
8	0.64	**8**	0.73	**8**	0.80	**8**	0.82	**8**	0.28	**8**	0.38
12	0.37	**12**	0.38	**12**	0.50	**12**	0.60	**12**	0.24	**12**	0.21
15	0.26	**15**	0.27	**15**	0.31	**15**	0.30	**15**	0.13	**15**	0.14
19	0.18	**19**	0.17	**19**	0.18	**19**	0.19	**19**	0.080	**19**	0.10
23	0.14	**23**	0.12	**23**	0.14	**23**	0.13	**23**	0.061	**23**	0.082
27	0.11	**27**	0.090	**27**	0.11	**27**	0.10	**27**	0.041	**27**	0.064
31	0.07	**31**	0.062	**31**	0.078	**31**	0.080	**31**	0.032	**31**	0.035
34	0.040	**34**	0.051	**34**	0.051	**34**	0.050	**34**	0.021	**34**	0.024
38	0.035	**38**	0.039	**38**	0.038	**38**	0.039	**38**	0.016	**38**	0.018
42	0.024	**42**	0.023	**42**	0.031	**42**	0.033	**42**	0.014	**42**	0.016
45	0.017	**45**	0.021	**45**	0.019	**45**	0.018	**45**	0.013	**45**	0.013
R^2	0.99	R^2	0.98	R^2	0.99	R^2	0.99	R^2	0.98	R^2	0.99
$t_{1/2}$ (days)	6.17	$t_{1/2}$ (days)	6.25	$t_{1/2}$ (days)	6.28	$t_{1/2}$ (days)	6.25	$t_{1/2}$ (days)	6.61	$t_{1/2}$ (days)	6.76

R^2: Coefficient of regression of the fitting; kinetics of first-order reactions.
$t_{1/2}$: half-life time.

3.2 Detection and Identification of degradation products

3.2.1. Tenoxicam

The MS/MS spectrum of tenoxicam in positive mode was characterized by fragment-ions arisen from the thienothiazine and N-(2-pyridyl) formamide groups (Fig. SM1); the degradation products of tenoxicam were related to these two constituent moieties, too. Those degradation products detected by electrospray ionization in positive mode contained a pyridyl substituent in their structure, and basically they were different derivatives from 2-pyridylformamide; this was the case for compounds such as T138, T167, T152, T162, T153 and T180 (Figs. SM2-SM7). T95 (Fig. SM8) was identified as 2-aminopyridine, the simpler degradation product from tenoxicam. The fragmentations observed in the MS-MS spectra of these degradation products were relatively simple and they were attributed to the loss of small molecules such as NCO, alkylamines, CO_2 and H_2CO.

As regards the fragmentation recorded in negative electrospray ionization it was verified, for the three oxicams, that the fragment-ions yielded by collision-induced dissociation in the MS/MS spectra were also observed in the corresponding MS spectra. Three degradation products (T207, T191 and T205) were observed in the analysis of the samples spiked with tenoxicam by negative electrospray ionization; they were structurally related with the tiophenesulfonic acid, which arised from the thienothiazine moiety of the tenoxicam (Figs. SM9-SM11). The compound T167 was detected in negative mode, too.

The MS and MS/MS spectra of tenoxicam, piroxicam and meloxicam in negative mode were characterized by the losses of simple neutral molecules; thus, it was common the presence of fragment-ions yielded by loss of CO_2 and SO_2 in addition to other such as CO and H_2CO.

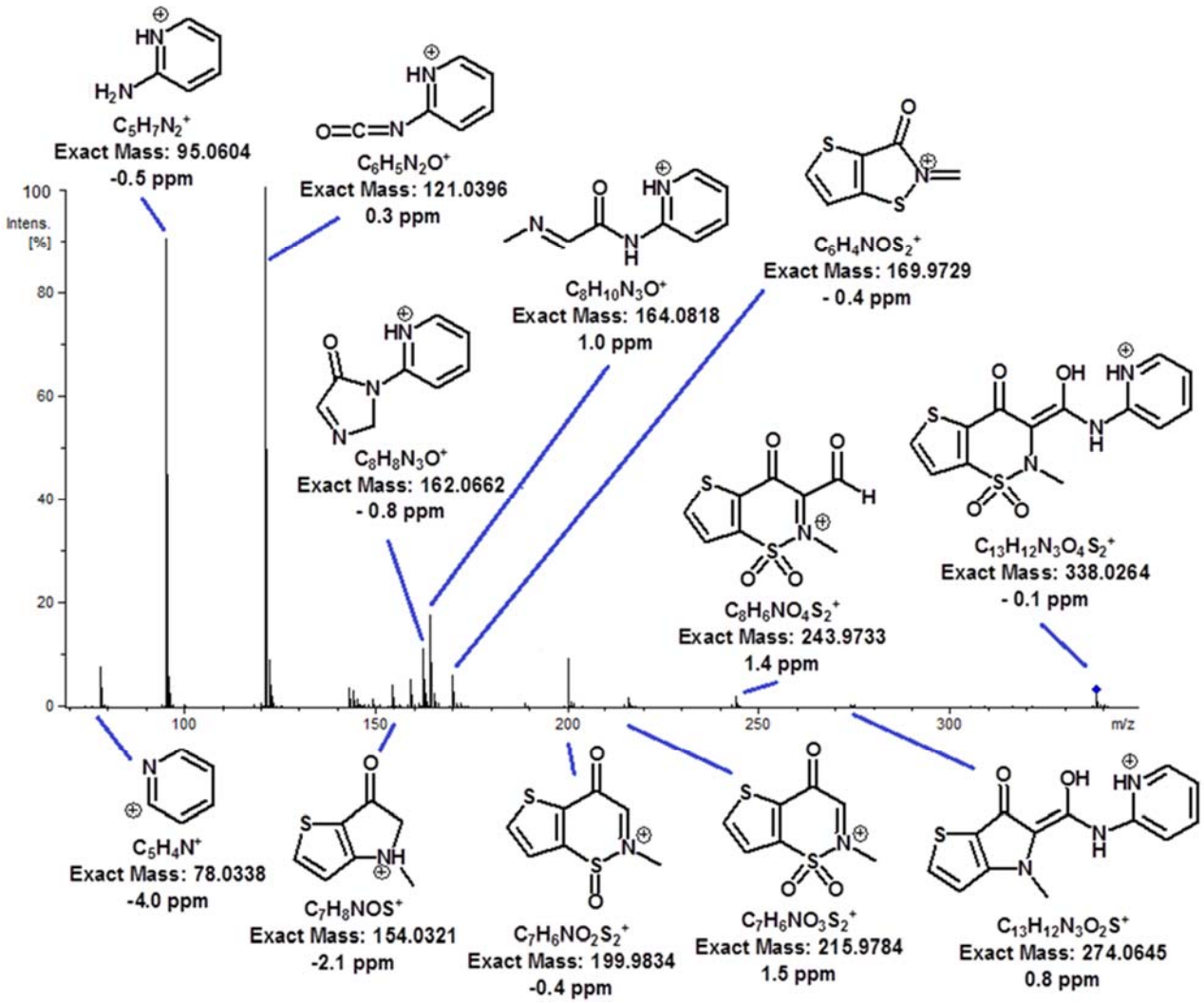

Figure SM1: MS/MS spectrum of tenoxicam. Positive mode. Collision energy: 30 eV. Exact mass and experimental error in the measurement.

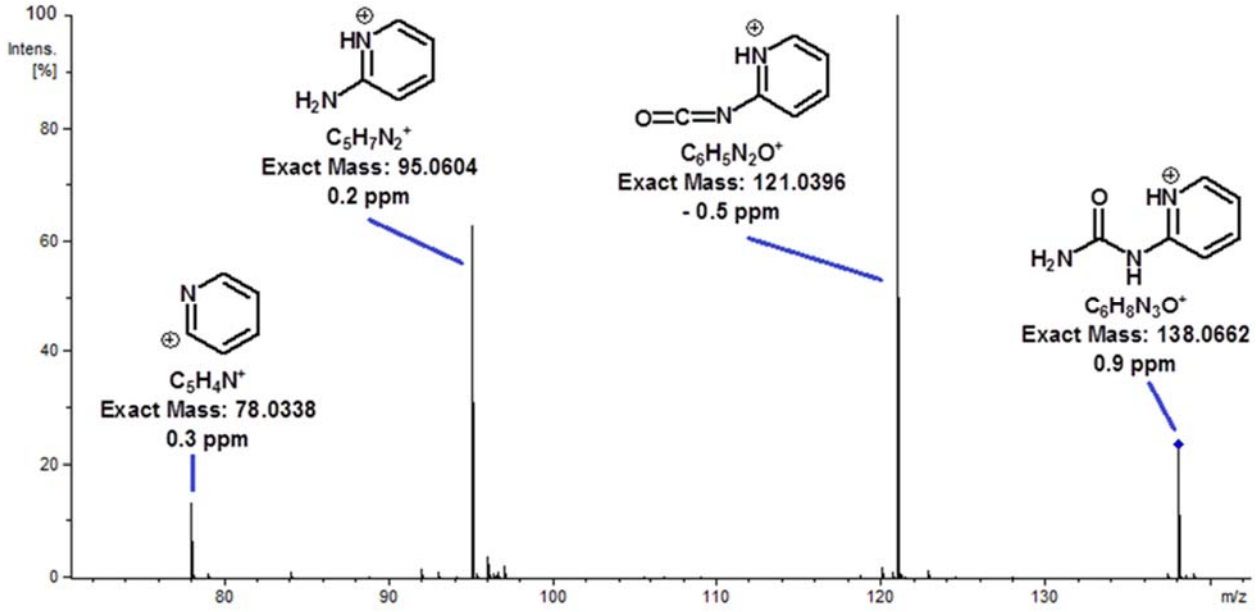

Figure SM2: MS/MS spectrum of the degradation product T138. Positive mode. Collision energy: 18 eV. Exact mass and experimental error in the measurement.

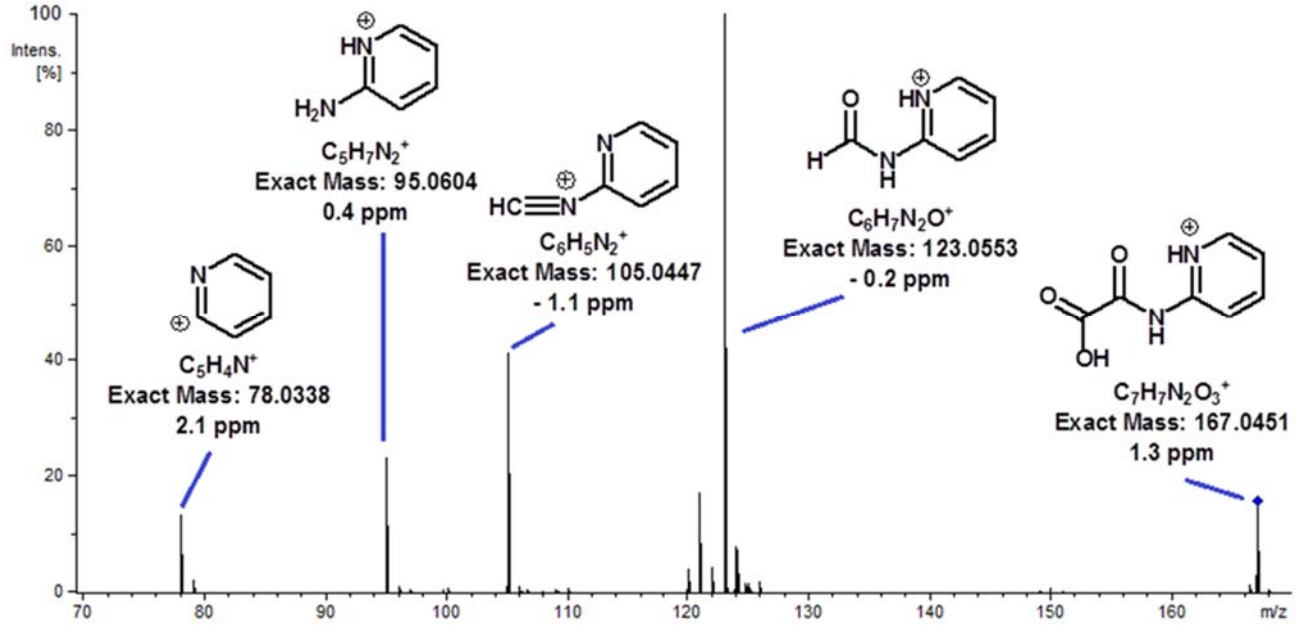

Figure SM3: MS/MS spectrum of the degradation product T167. Positive mode. Collision energy: 15 eV. Exact mass and experimental in the measurement.

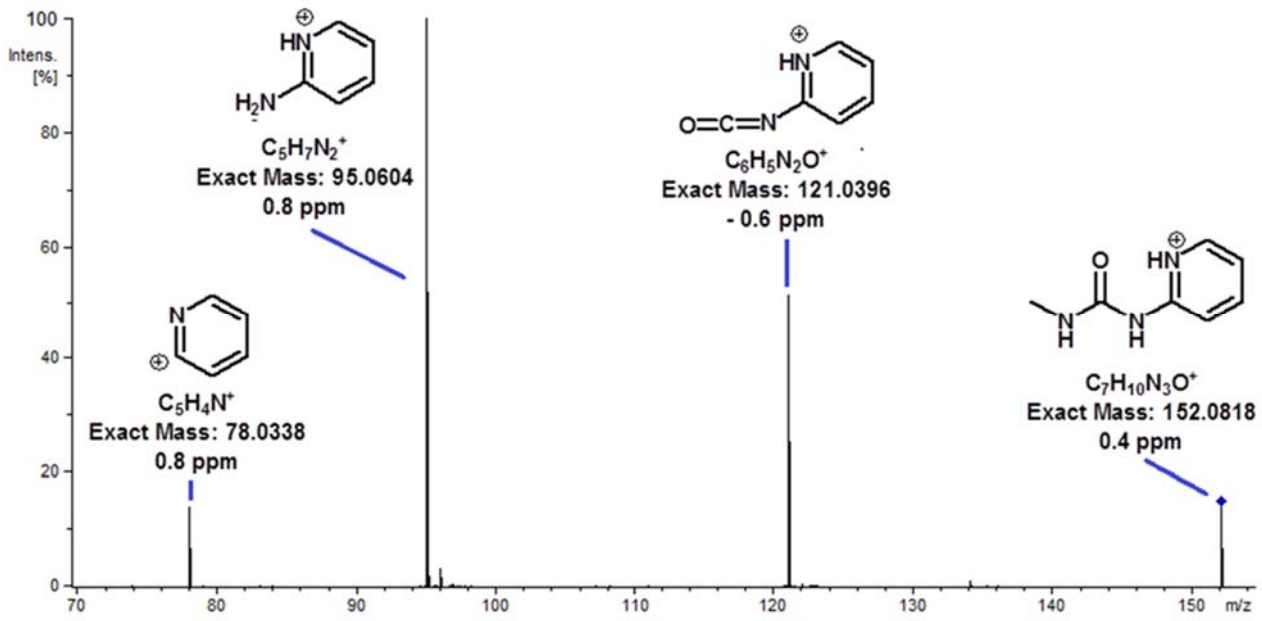

Figure SM4: MS/MS spectrum of the degradation product T152. Positive mode. Collision energy: 20 eV. Exact mass and experimental in the measurement.

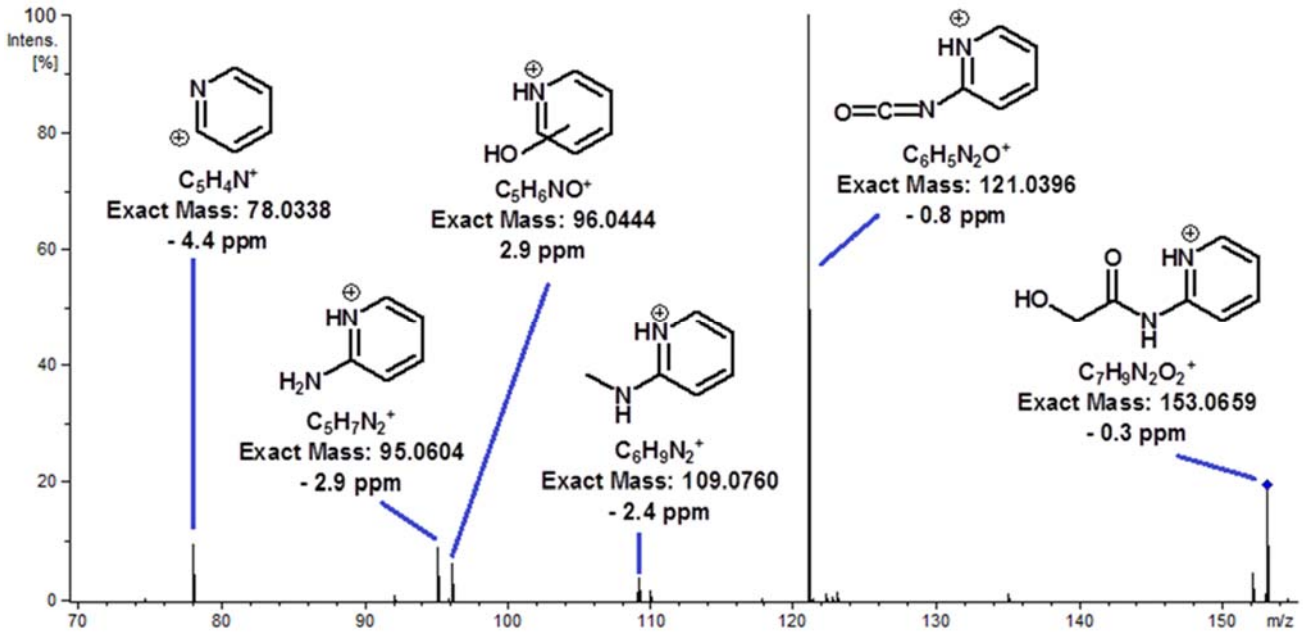

Figure SM5: MS/MS spectrum of the degradation product T153. Positive mode. Collision energy: 20 eV. Exact mass and experimental in the measurement.

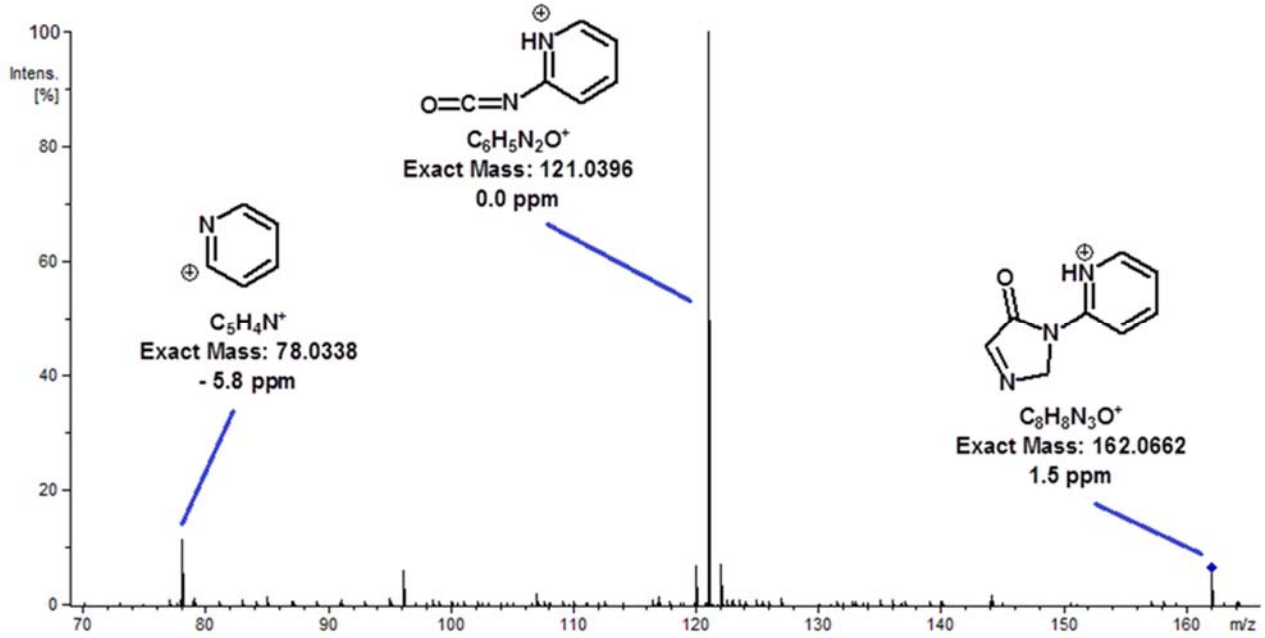

Figure SM6: MS/MS spectrum of the degradation product T162. Positive mode. Collision energy: 20 eV. Exact mass and experimental in the measurement.

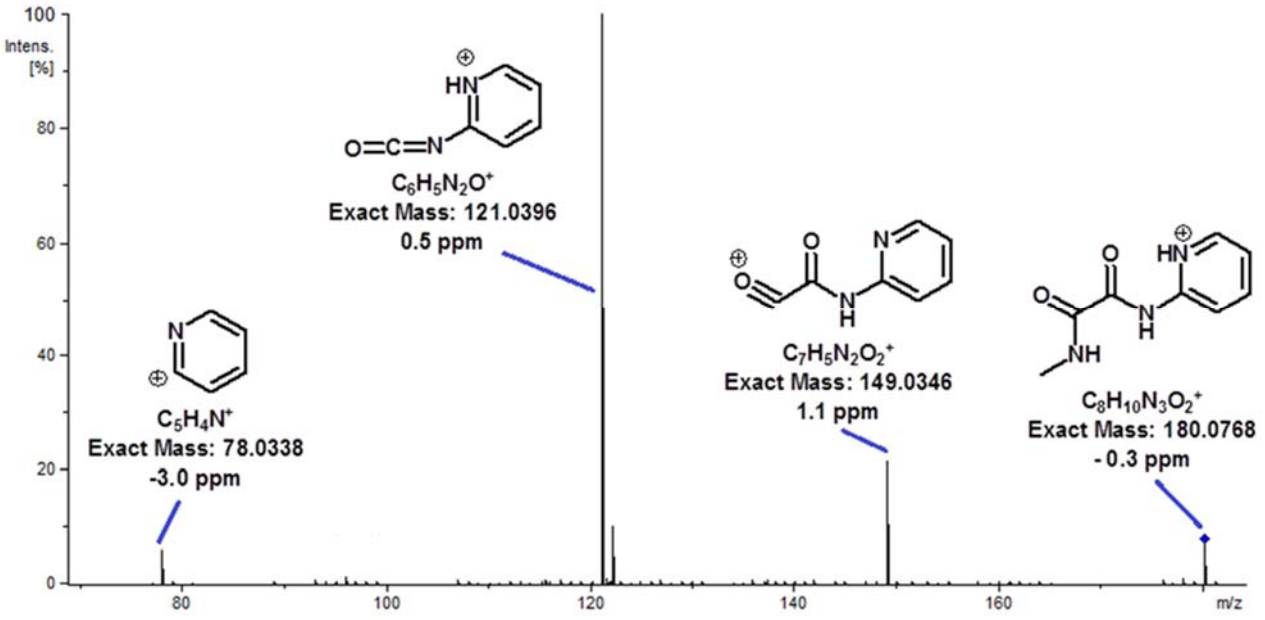

Figure SM7: MS/MS spectrum of the degradation product T180. Positive mode. Collision energy: 20 eV. Exact mass and experimental in the measurement.

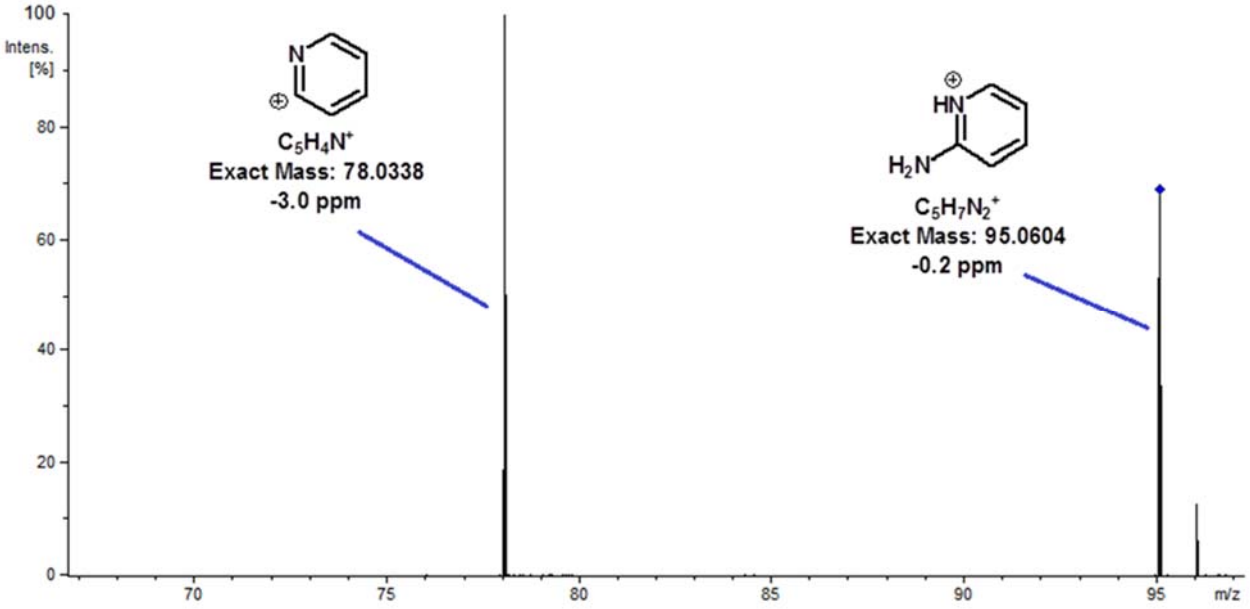

Figure SM8: MS/MS spectrum of the degradation product T95. Positive mode. Collision energy: 22 eV. Exact mass and experimental in the measurement.

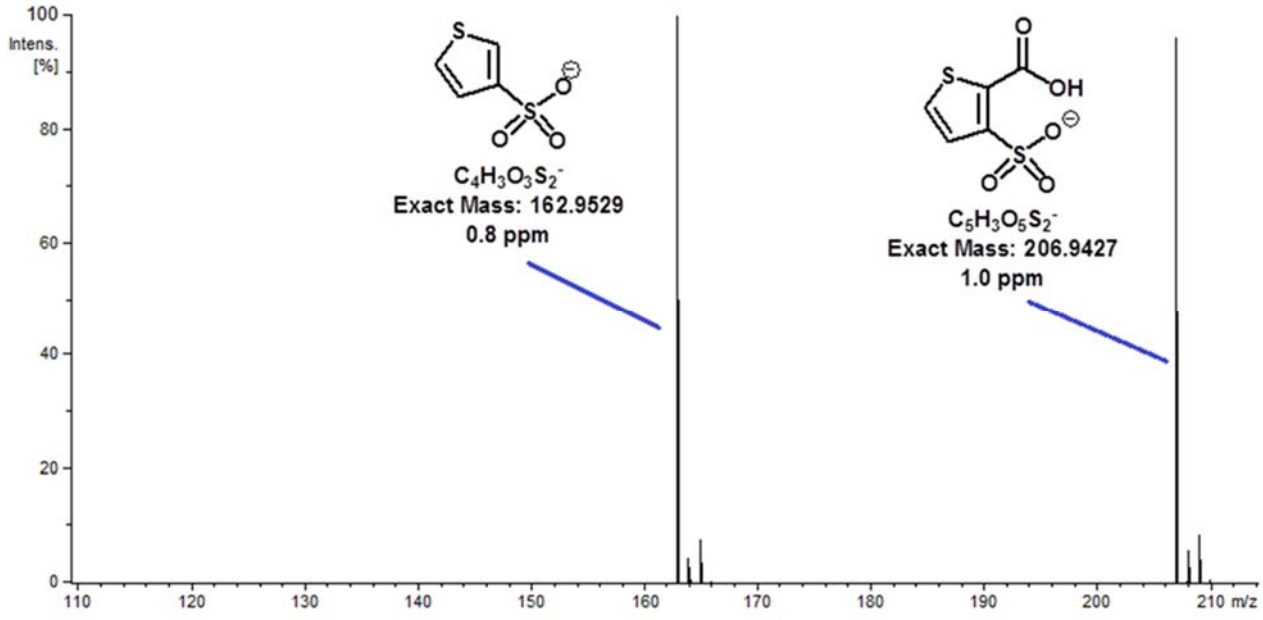

Figure SM9: MS spectrum of the degradation product T207. Negative mode. Exact mass and experimental error in the measurement.

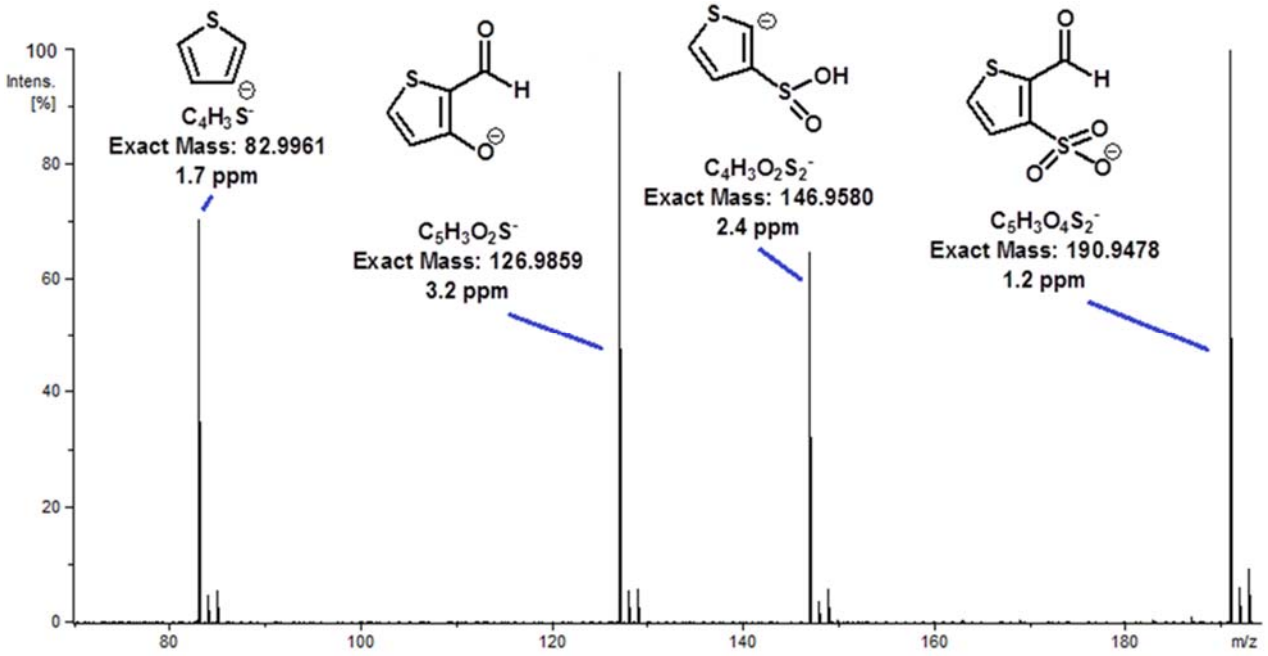

Figure SM10: MS spectrum of the degradation product T191. Negative mode. Exact mass and experimental error in the measurement.

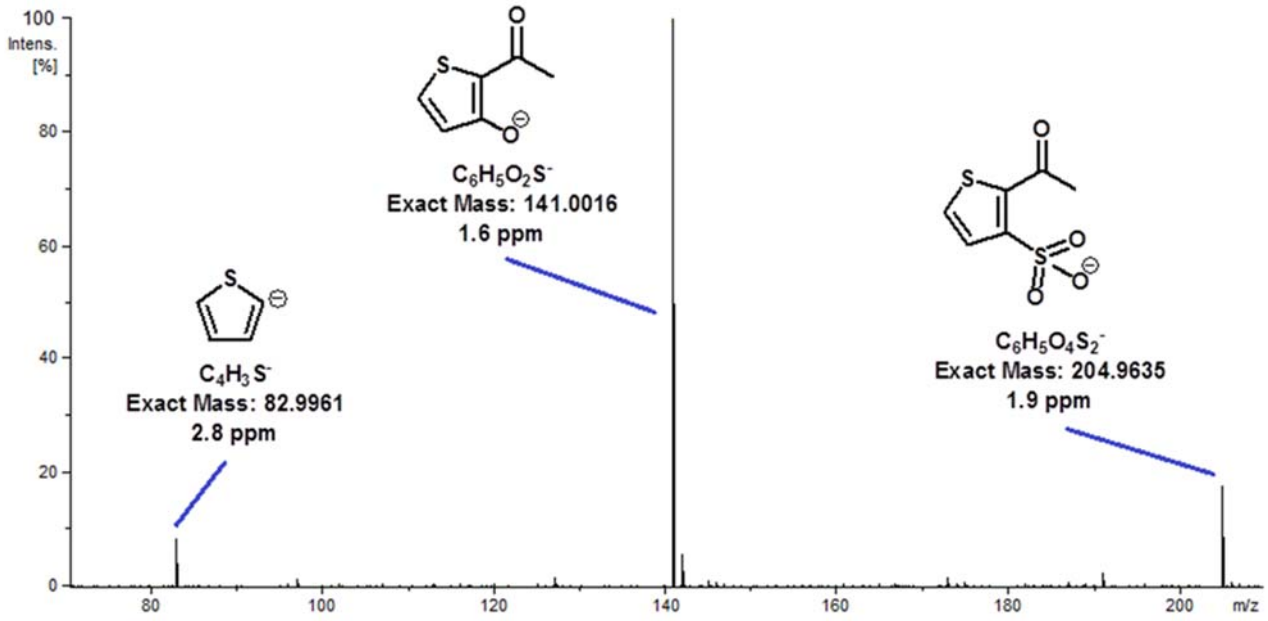

Figure SM11: MS spectrum of the degradation product T205. Negative mode. Exact mass and experimental error in the measurement.

3.2.2. Piroxicam

Nine degradation products were seen in the degradation assays for piroxicam whose MS/MS spectrum by positive ionization electrospray is shown in Fig. SM12, it had several fragmentations that involved the breakdown of the carboxamide group. Five degradation compounds were ascertained in positive mode. As it happened for tenoxicam they were those compounds containing a pyridyl substituent; in fact, some of the degradation products of piroxicam (P95, P162, P153 and P180) are the same as in the case of tenoxicam because both drugs have a great structural similarity. A formamidine derivative, labeled as P136, was only seen in the piroxicam assays (Fig. SM13). The loss of alkylamines was frequent in their MS/MS spectra.

Four degradation products were observed in negative mode; they were benzene derivatives from the benzothiazine moiety of the piroxicam and all of them kept the SO_2 group in their structures. These degradations products (P201, P185, P215 and P214) were relatively simple compounds as it can be seen in the spectra shown in Figs. SM14-SM17). The acquirement of structural information by MS/MS experimentation was required for P215 since it was not observed fragmentation in its MS spectrum unlike what happened for the other degradation compounds in negative mode.

The compounds P95 and P180 had been previously reported in the bibliography as degradation products of piroxicam in water subjected to stress conditions [D.T. Modhave, T. Handa, R.P. Shah, S. Singh, Successful characterization of degradation products of drugs unsing LC-MS tools: Application to piroxicam and meloxicam, Anal. Methods 3 (2011) 2864-2872]; other degradation products described in that work had not been found in the experimentation presented here

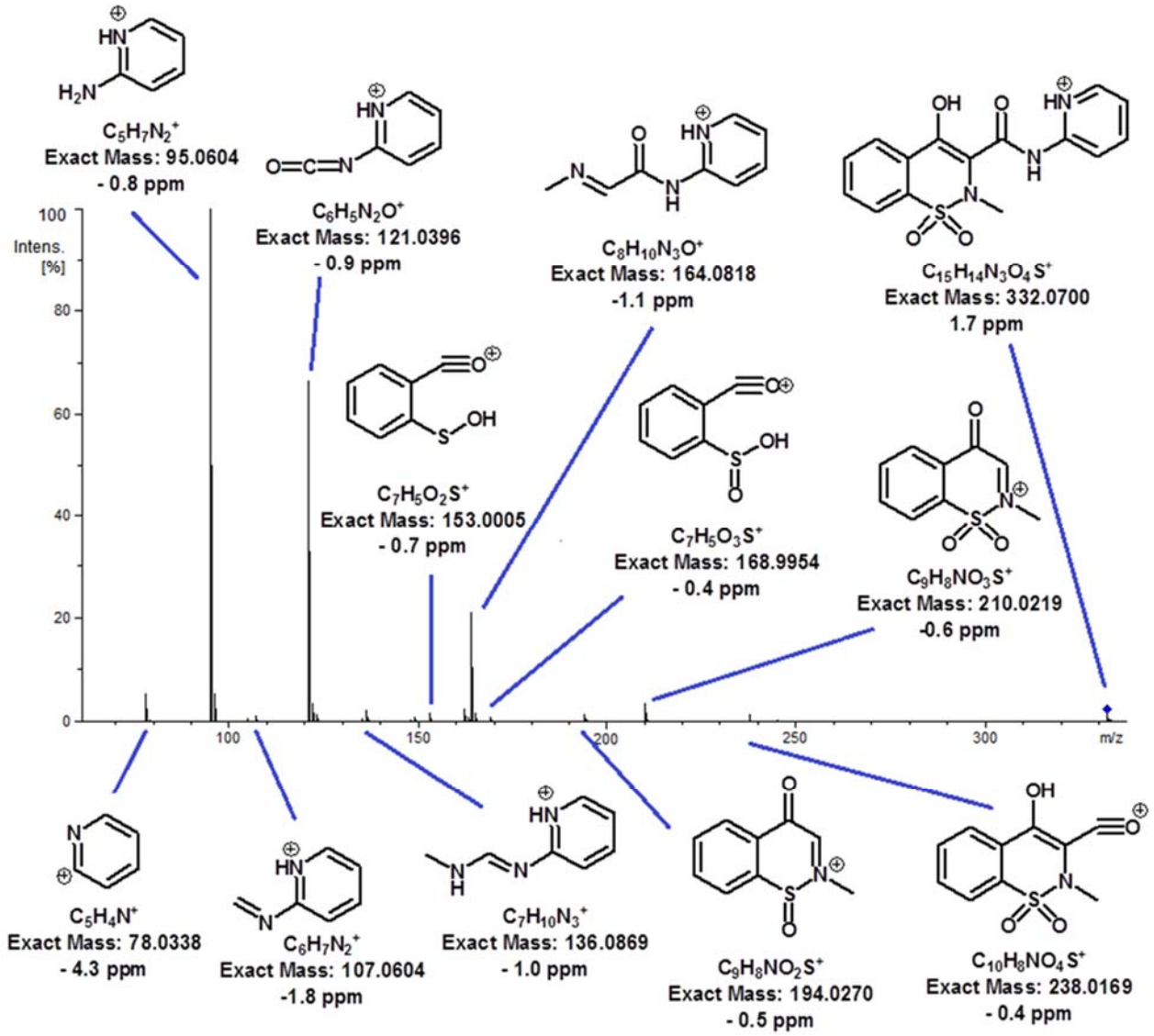

Fig. SM12: MS/MS spectrum of piroxicam. Positive mode. Collision energy: 30 eV. Exact mass and experimental in the measurement.

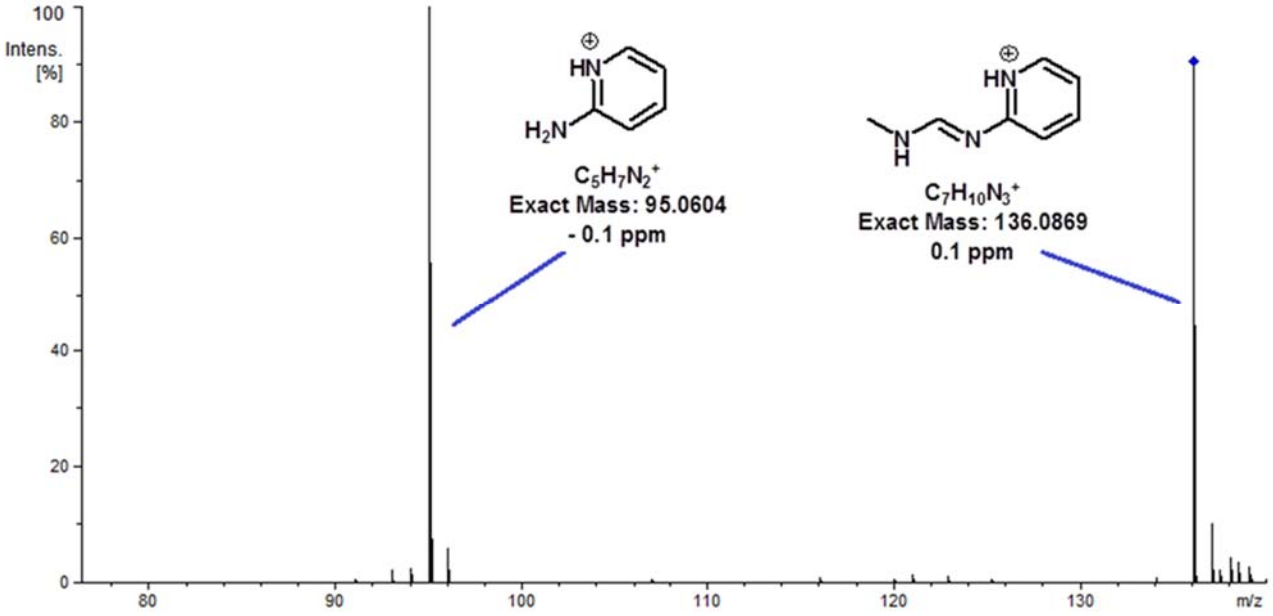

Fig. SM13: MS/MS spectrum of the degradation product P136. Positive mode. Collision energy: 14 eV. Exact mass and experimental in the measurement.

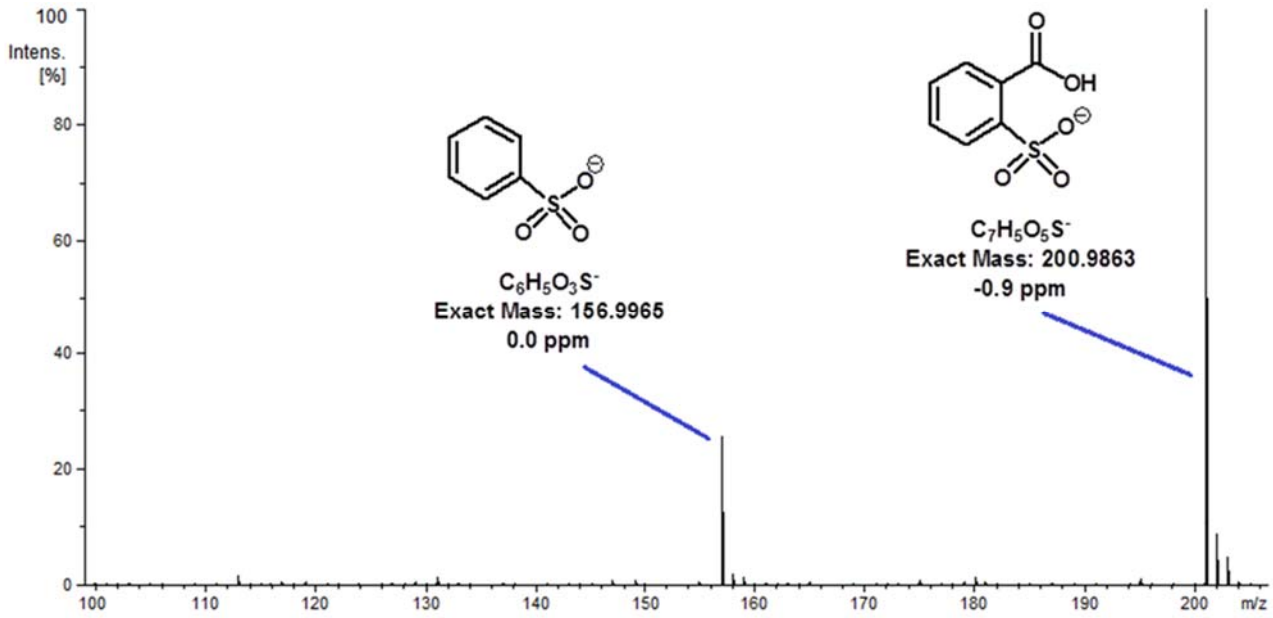

Fig. SM14: MS spectrum of the degradation product P201. Negative mode. Exact mass and experimental error in the measurement.

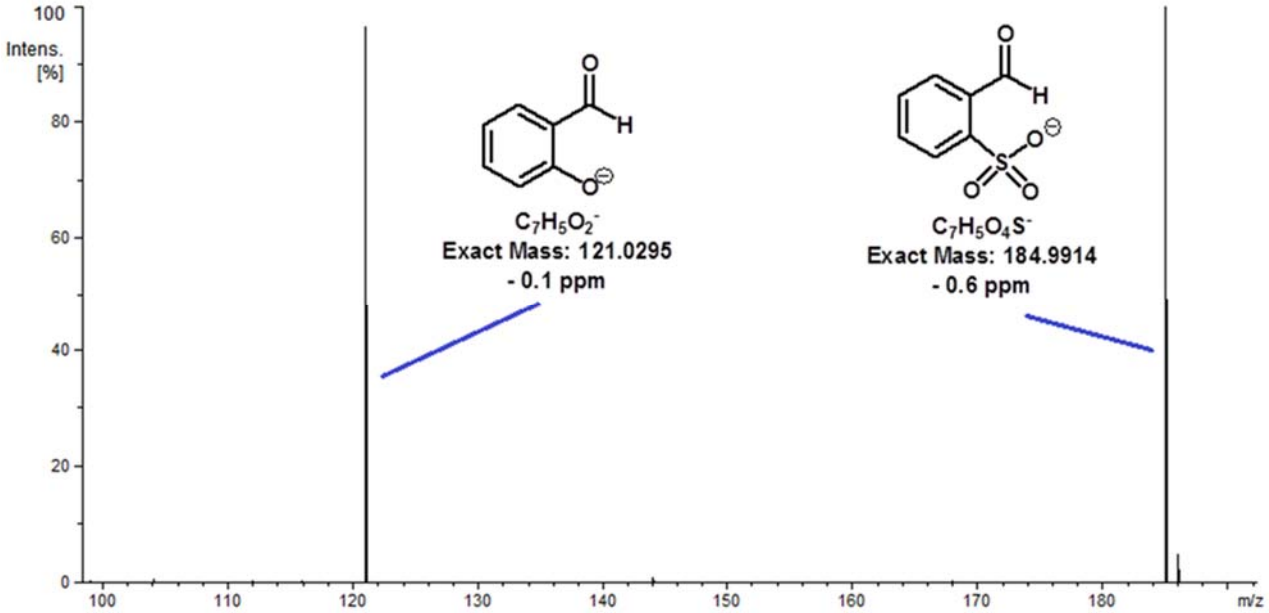

Fig. SM15: MS spectrum of the degradation product P185. Negative mode. Exact mass and experimental error in the measurement.

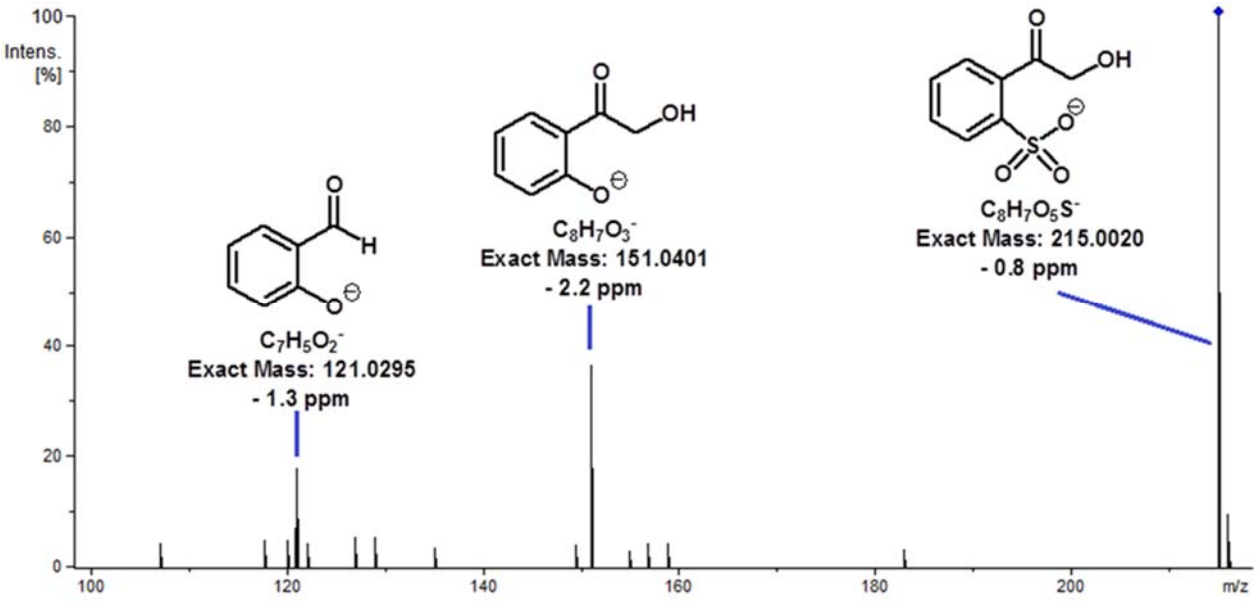

Fig. SM16: MS/MS spectrum of the degradation product P215. Negative mode. Collision energy: 16 eV. Exact mass and experimental in the measurement.

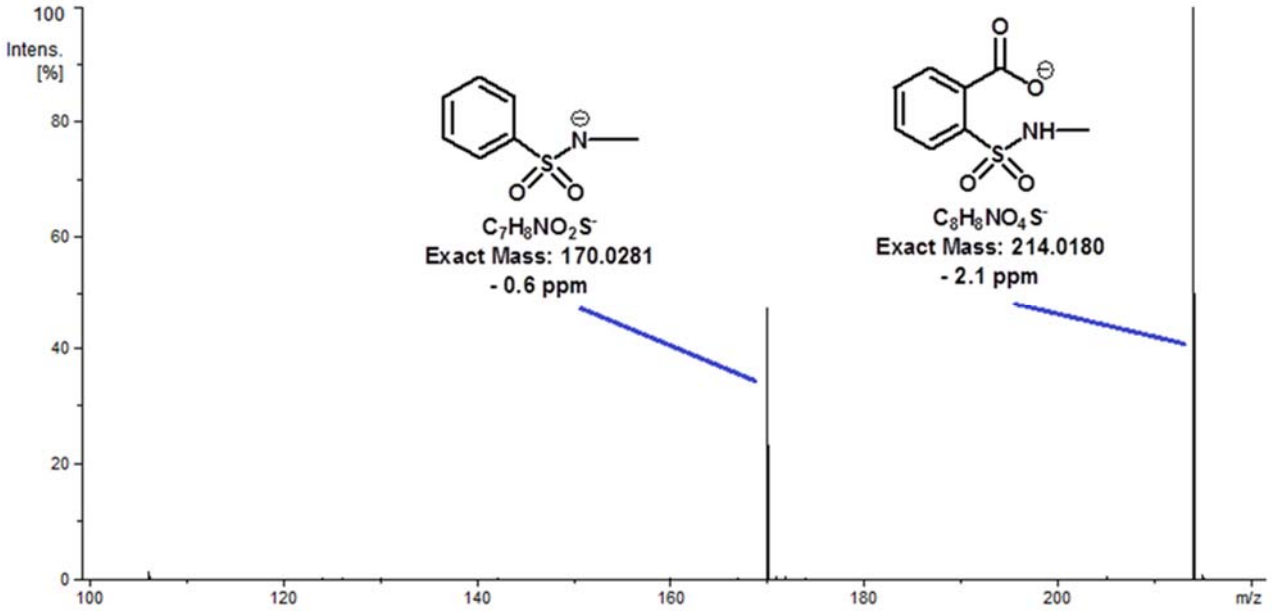

Fig. SM17: MS spectrum of the degradation product P214. Negative mode. Exact mass and experimental error in the measurement.

3.2.3. Meloxicam

Fig. SM18 shows the MS/MS spectrum of meloxicam in positive mode which show fragmentations arisen from its two basic moieties (benzothiazine and thiazolamine groups) according to the interpretation carried out from the high-resolution mass spectrometry data, although the ions containing the thiazolamine group are the predominant. Seven degradation products were elucidated.

Five degradation products were detected by positive electrospray ionization, one of them, M198 (Fig. SM19), derived from the benzothiazine moiety and the other four compounds, M115, M158, M187 and M200 (Figs. SM20-SM23) from the methylthiazolamine. Only two degradation compounds were seen in negative mode; they were related to the benzenesulfonic acid and one of them, M185, was detected and identified in the assays done with piroxicam, too. The spectrum of the other compound, M214, is presented in Fig. SM24. The neutral losses observed in the positive and negative mode spectra were simple as for the above-described compounds.

The degradation products M115, M187 and M198 had already been described previously by Modhave et al. [D.T. Modhave, T. Handa, R.P. Shah, S. Singh, Successful characterization of degradation products of drugs unsing LC-MS tools: Application to piroxicam and meloxicam, Anal. Methods 3 (2011) 2864-2872].

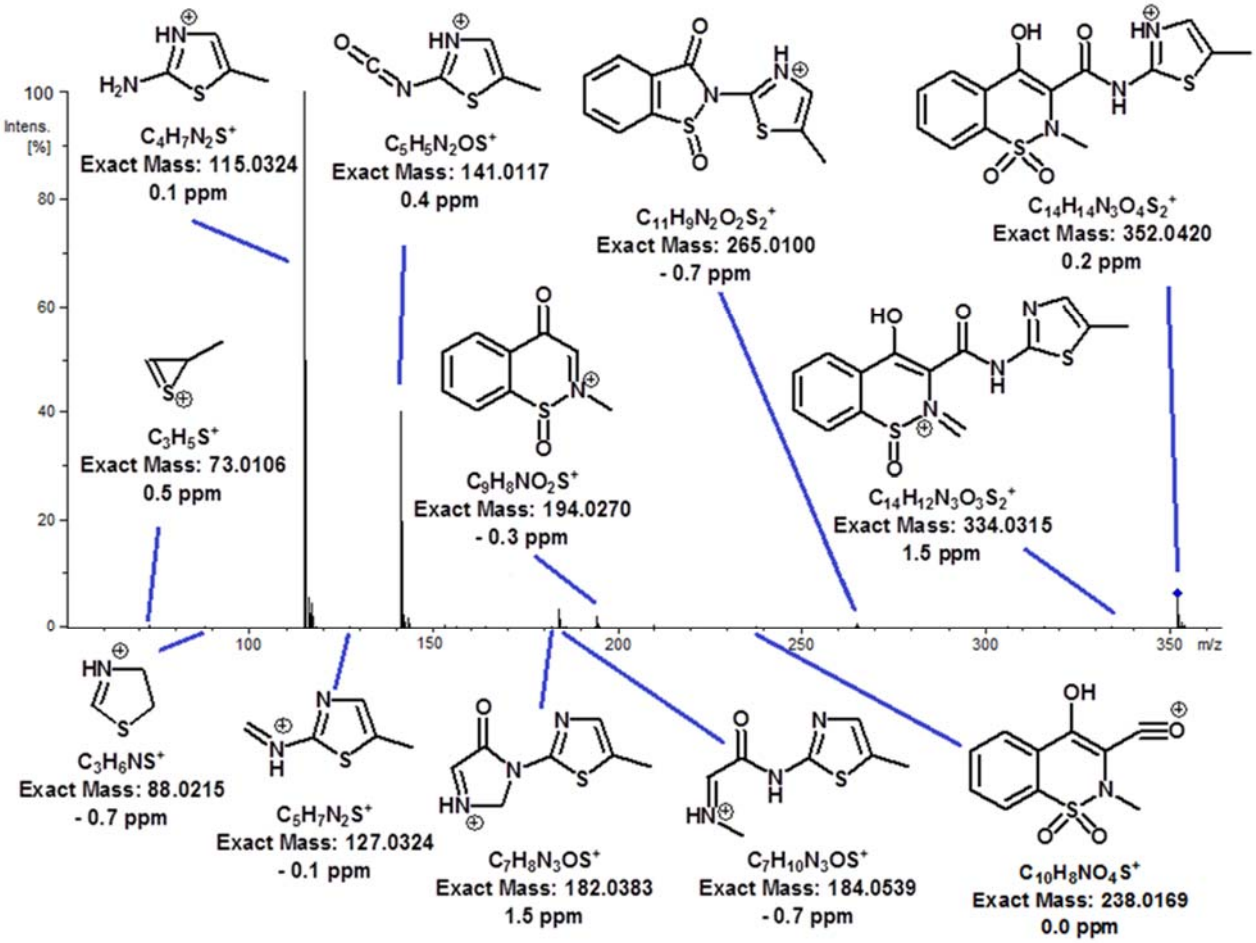

Fig. SM18: MS/MS spectrum of meloxicam. Positive mode. Collision energy: 25 eV. Exact mass and experimental in the measurement.

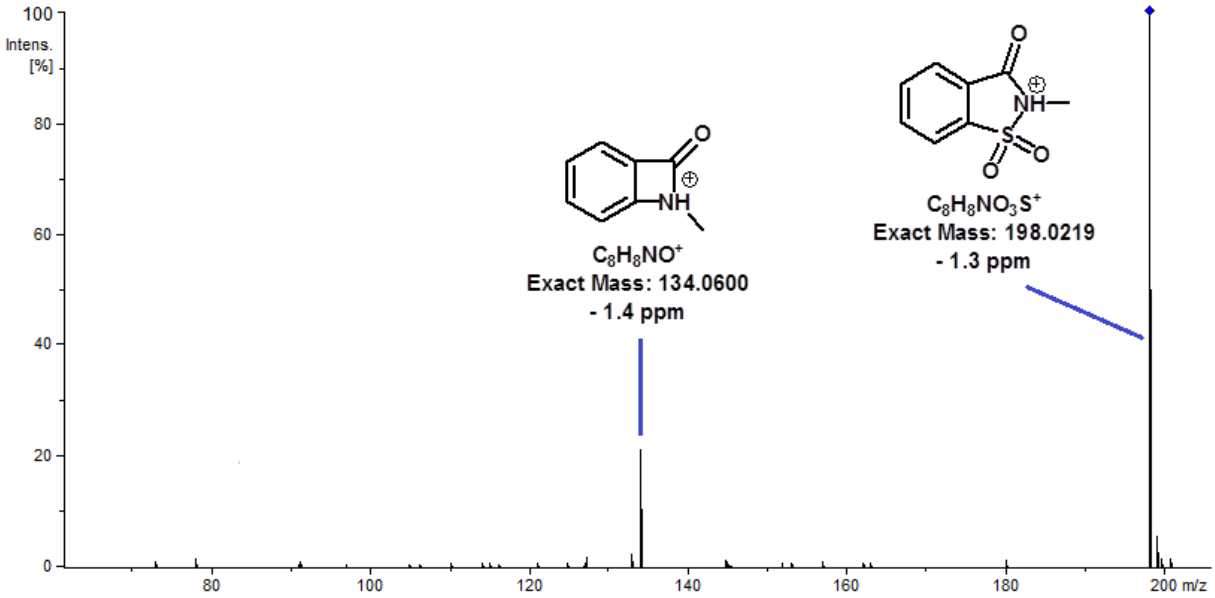

Fig. SM19: MS/MS spectrum of the degradation product M198. Positive mode. Collision energy: 15 eV. Exact mass and experimental in the measurement.

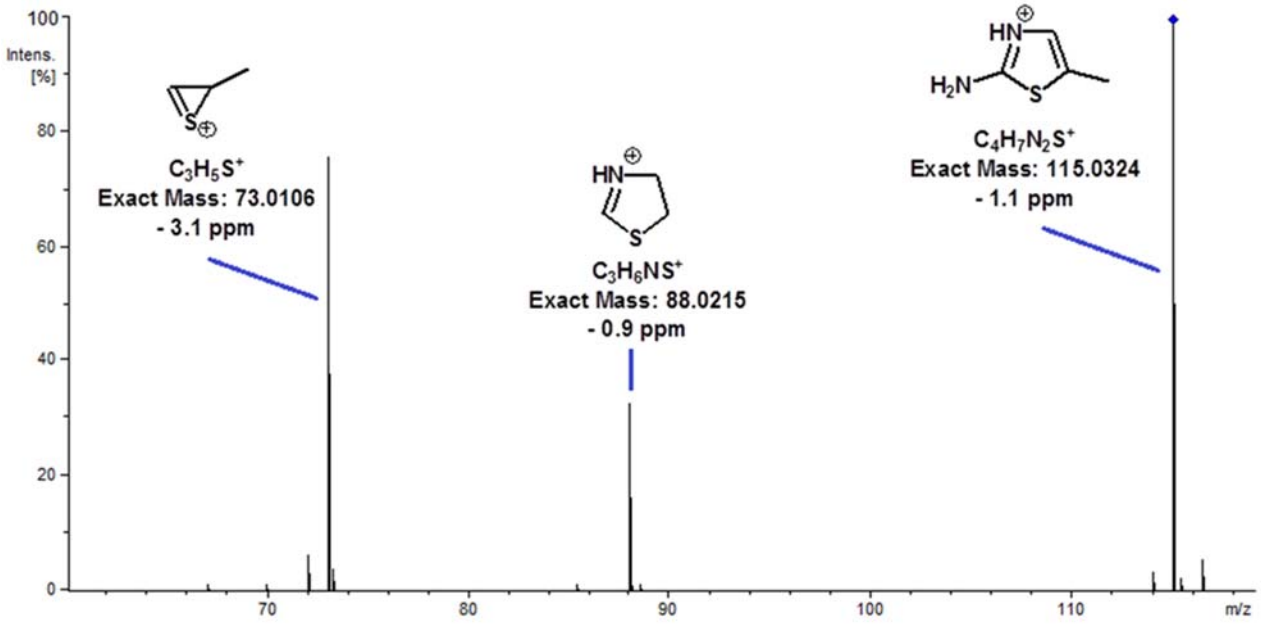

Fig. SM20: MS/MS spectrum of the degradation product M115. Positive mode. Collision energy: 28 eV. Exact mass and experimental in the measurement.

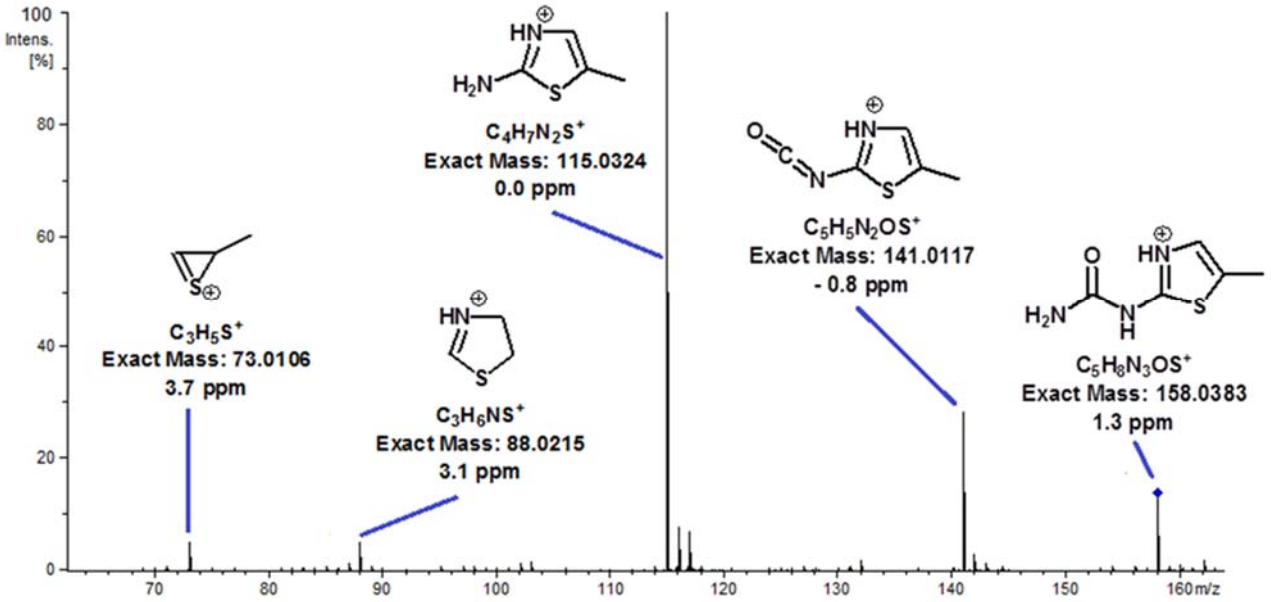

Fig. SM21: MS/MS spectrum of the degradation product M158. Positive mode. Collision energy: 20 eV. Exact mass and experimental in the measurement.

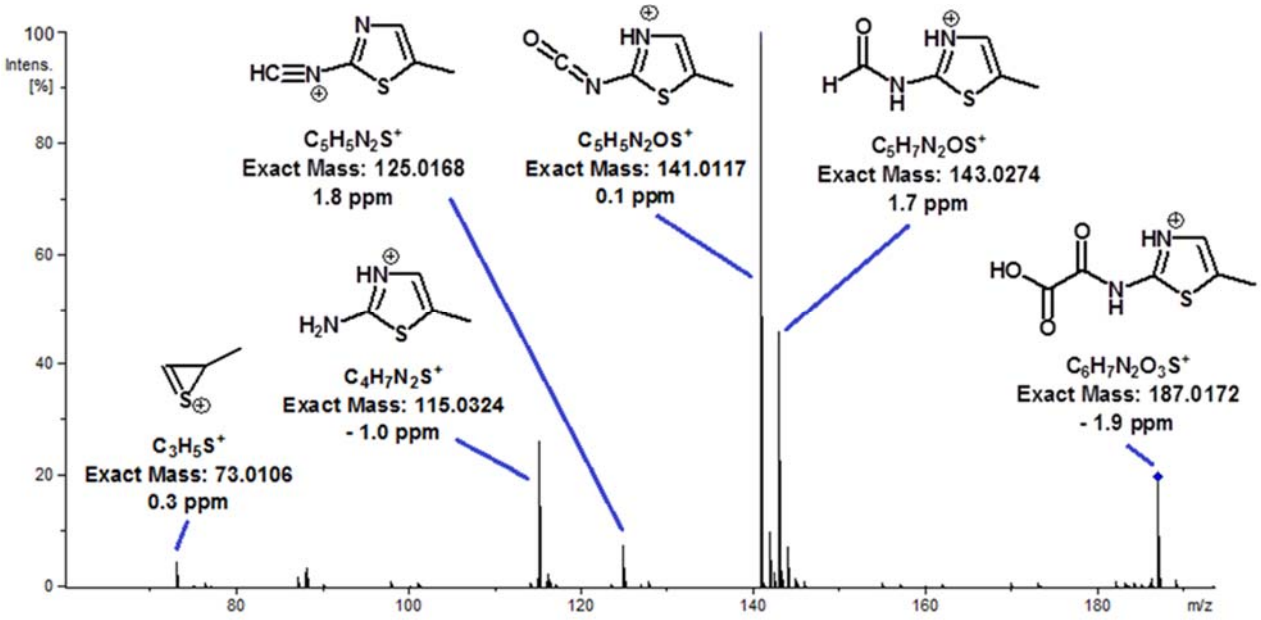

Fig. SM22: MS/MS spectrum of the degradation product M187. Positive mode. Collision energy: 20 eV. Exact mass and experimental in the measurement.

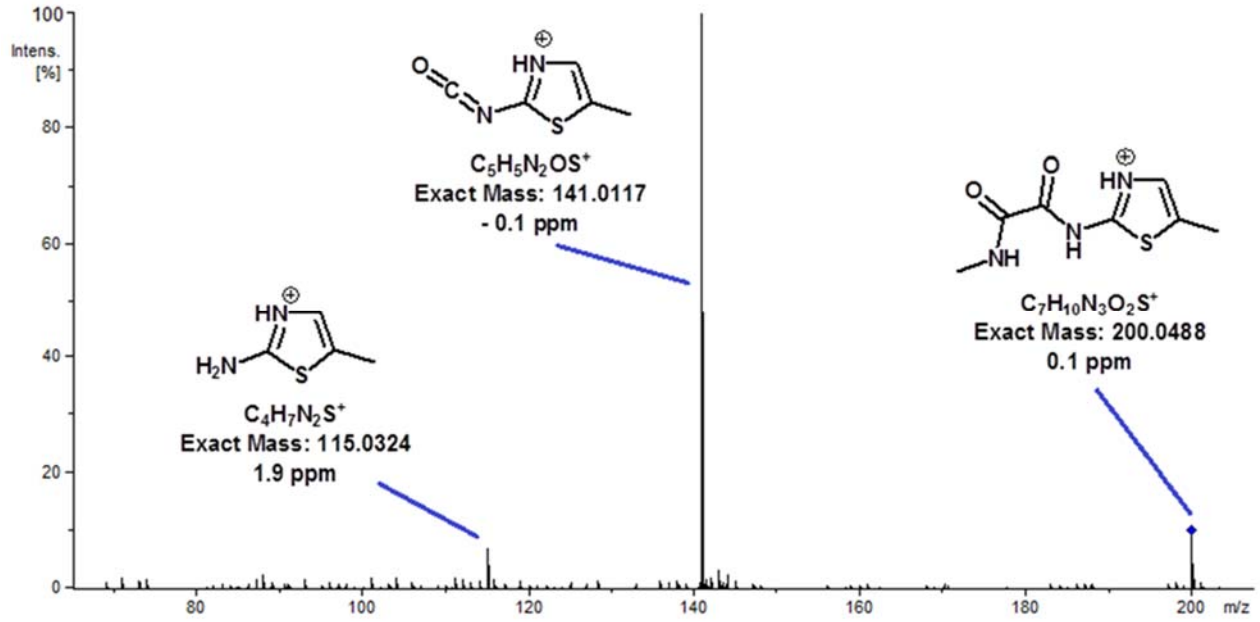

Fig. SM23: MS/MS spectrum of the degradation product M200. Positive mode. Collision energy :20 eV. Exact mass and experimental in the measurement.

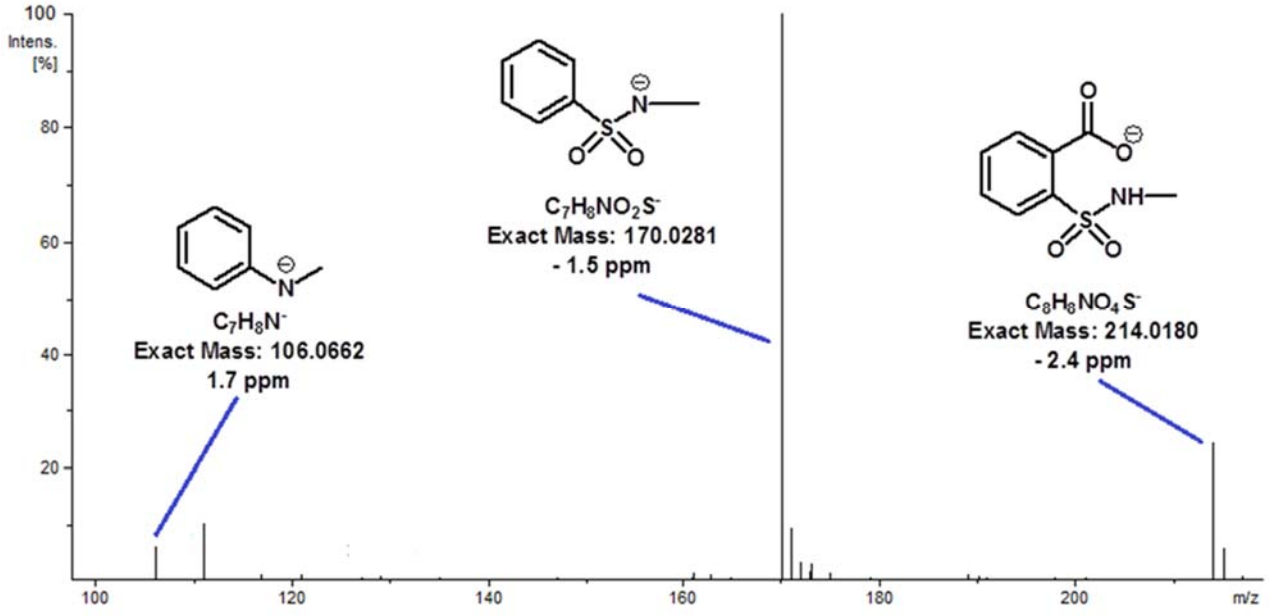

Fig. SM24: MS spectrum of the degradation product M214. Negative mode. Exact mass and experimental error in the measurement.

3.3. Occurrence of degradation products in forced and over time degradation assays.

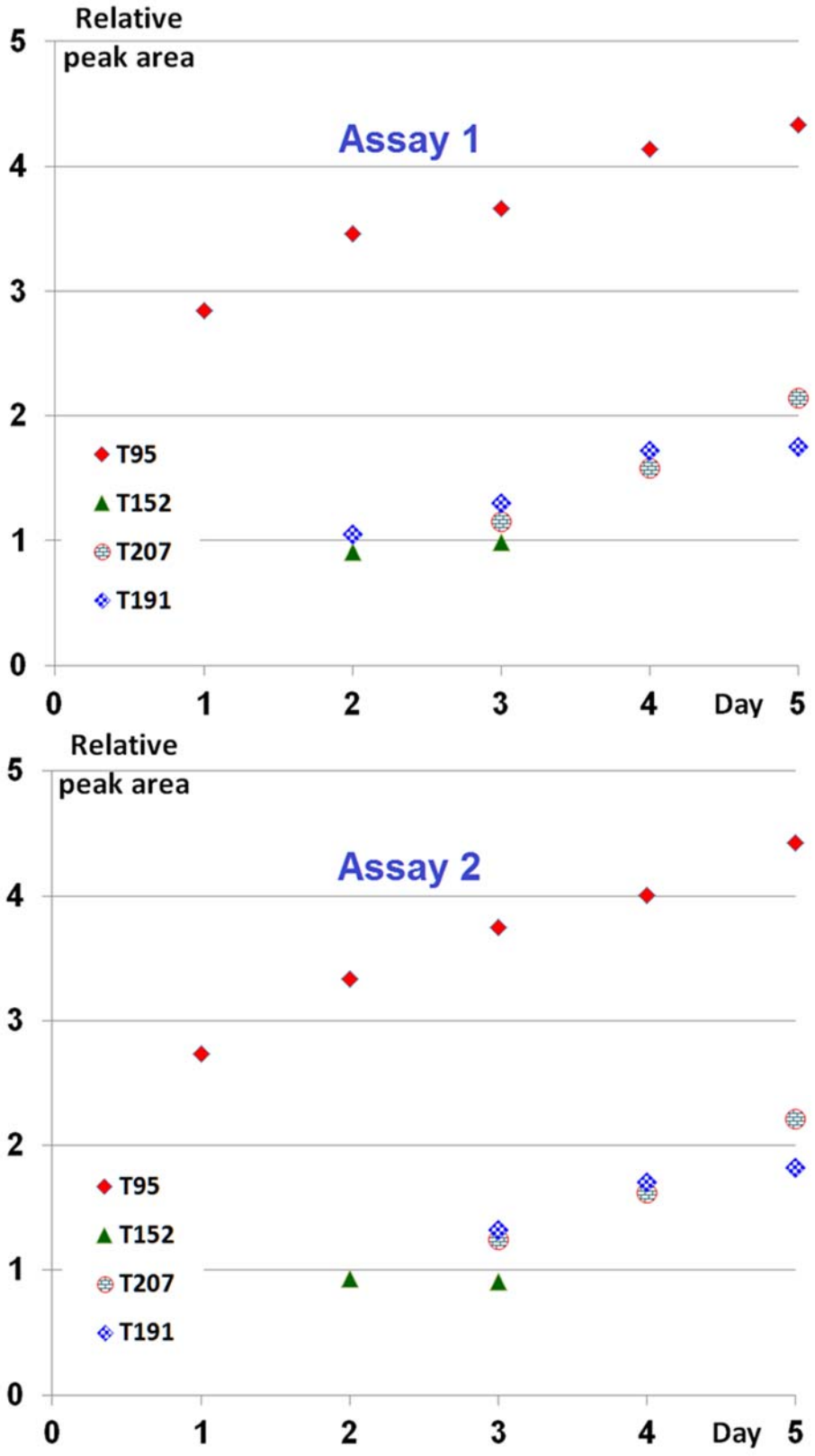

Fig. SM25: Peak areas of the degradation products of tenoxicam in the forced degradation assays at high temperature. Peak areas are referred to the initial peak area (positive mode) of tenoxicam in each experiment, to which a value of 100 was assigned.

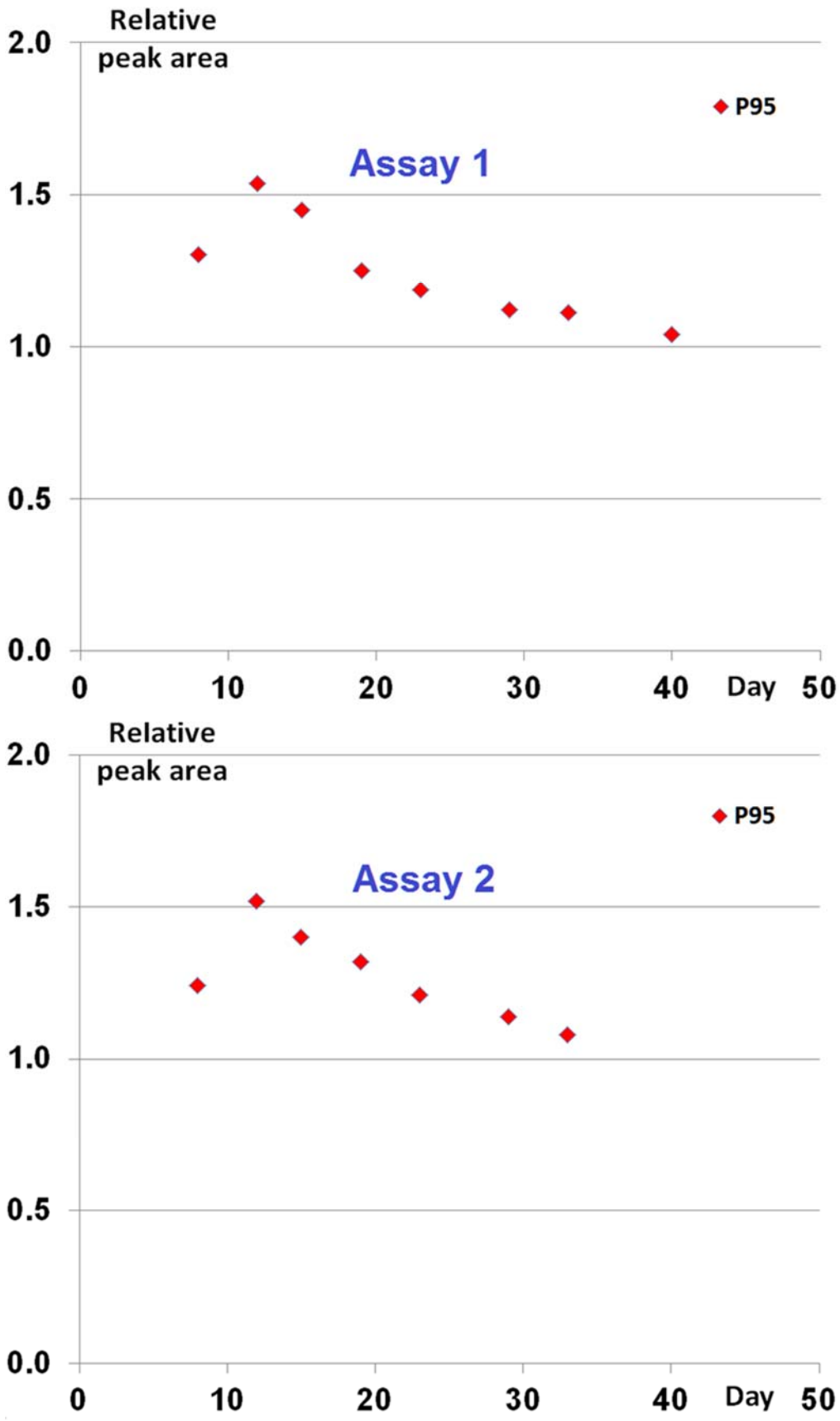

Fig. SM26: Peak areas of the degradation products of piroxicam in the forced degradation assays at high temperature. Peak areas are referred to the initial peak area of piroxicam (positive mode) in each experiment, to which a value of 100 was assigned.

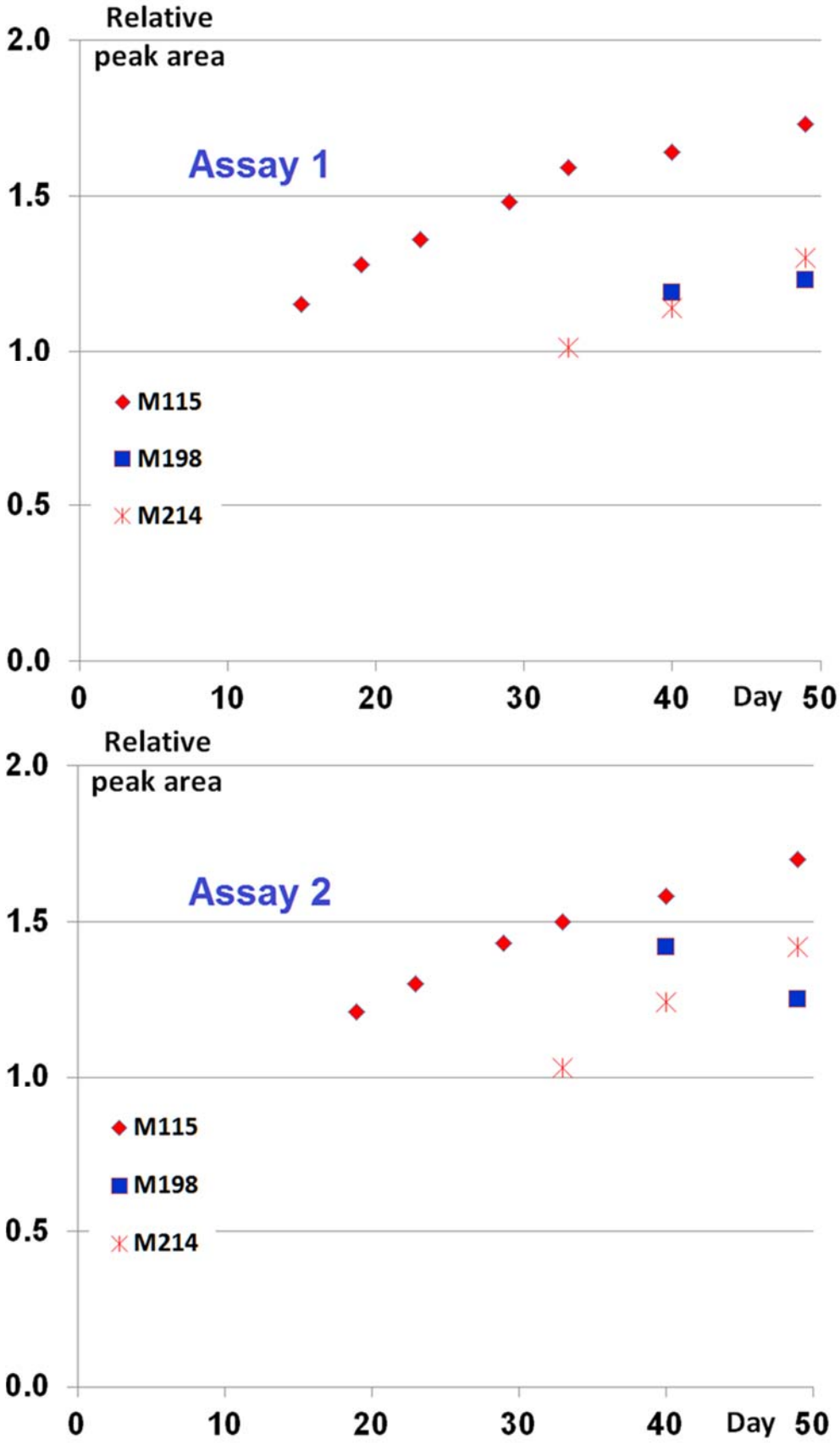

Fig. SM27: Peak areas of the degradation products of meloxicam in the forced degradation assays at high temperature. Peak areas are referred to the initial peak area of meloxicam (positive mode) in each experiment, to which a value of 100 was assigned.

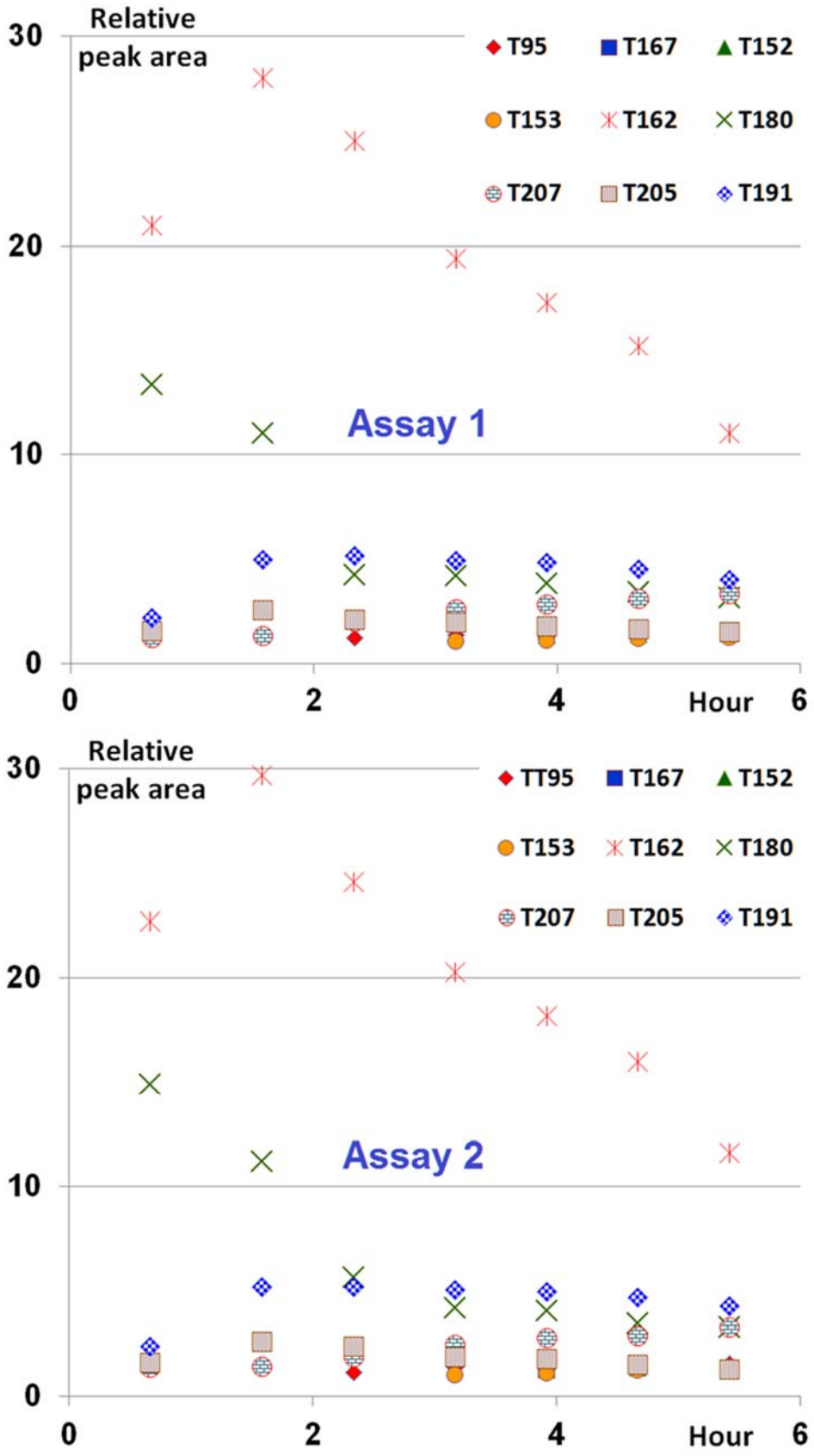

Fig. SM28: Peak areas of the degradation products of tenoxicam in the forced degradation assays under solar irradiation. Peak areas are referred to the initial peak area of tenoxicam (positive mode) in each experiment, to which a value of 100 was assigned.

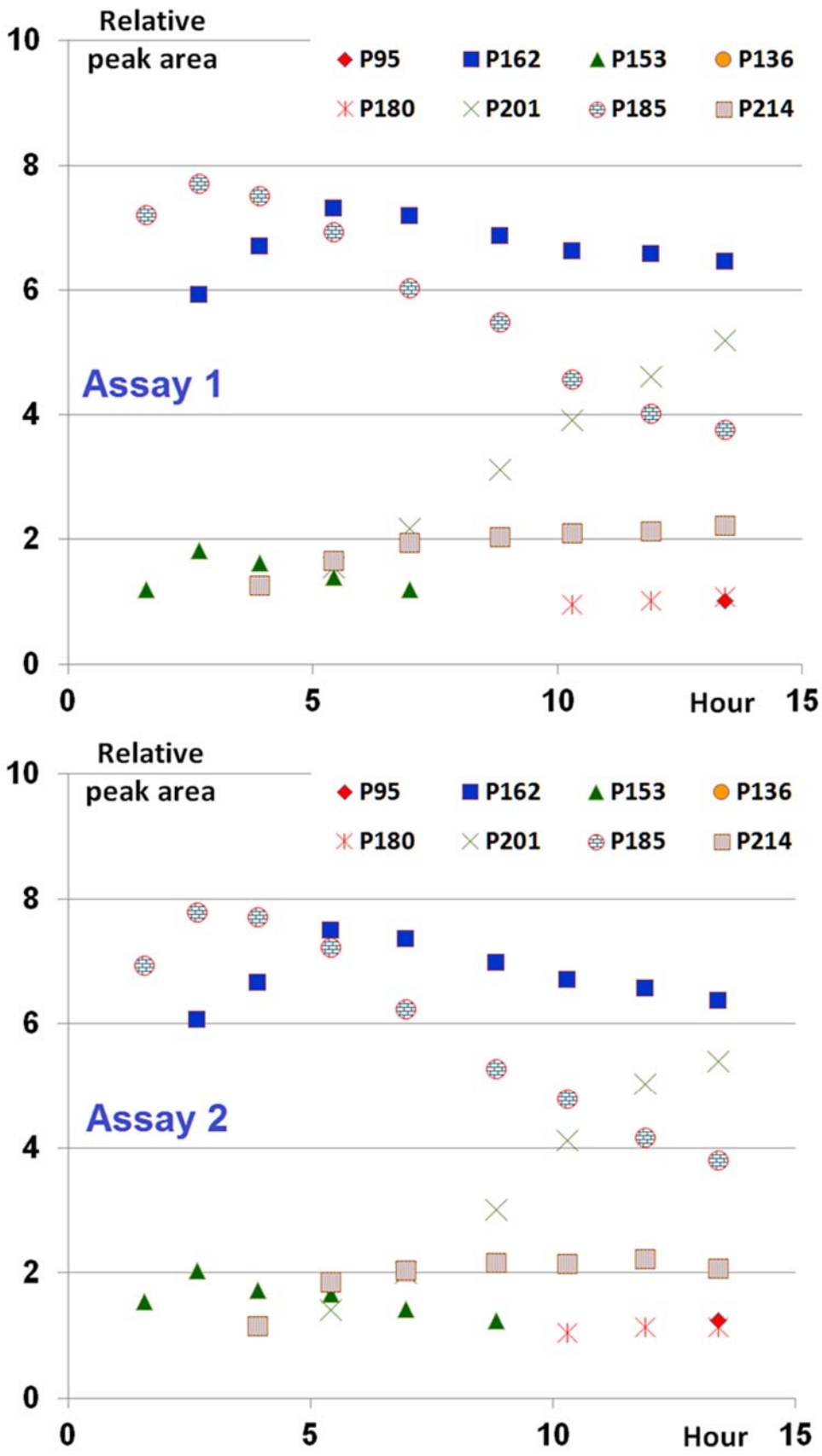

Fig. SM29: Peak areas of the degradation products of piroxicam in the forced degradation assays under solar irradiation. Peak areas are referred to the initial peak area of piroxicam (positive mode) in each experiment, to which a value of 100 was assigned.

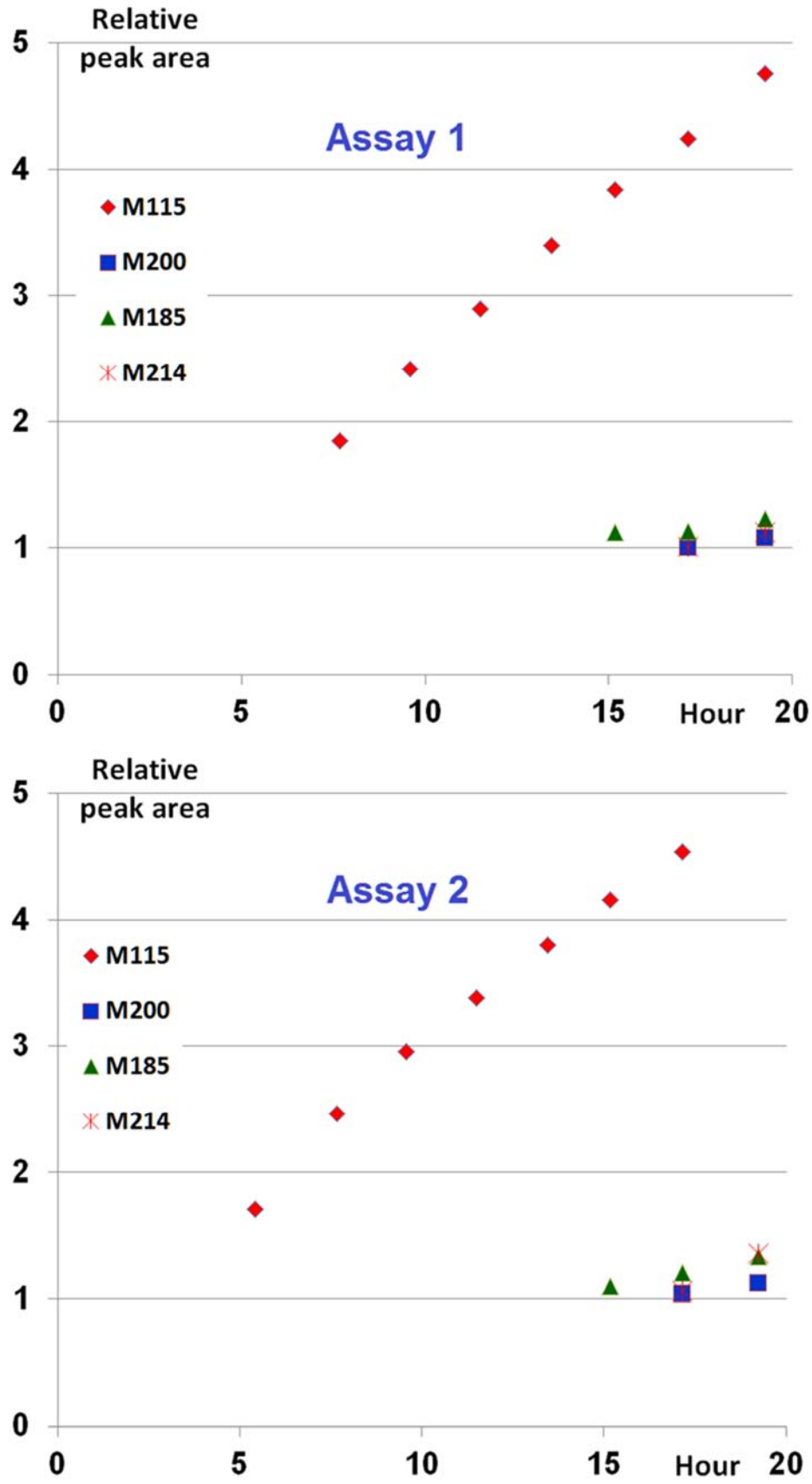

Fig. SM30: Peak areas of the degradation products of meloxicam in the forced degradation assays under solar irradiation. Peak areas are referred to the initial peak area of meloxicam (positive mode) in each experiment, to which a value of 100 was assigned.

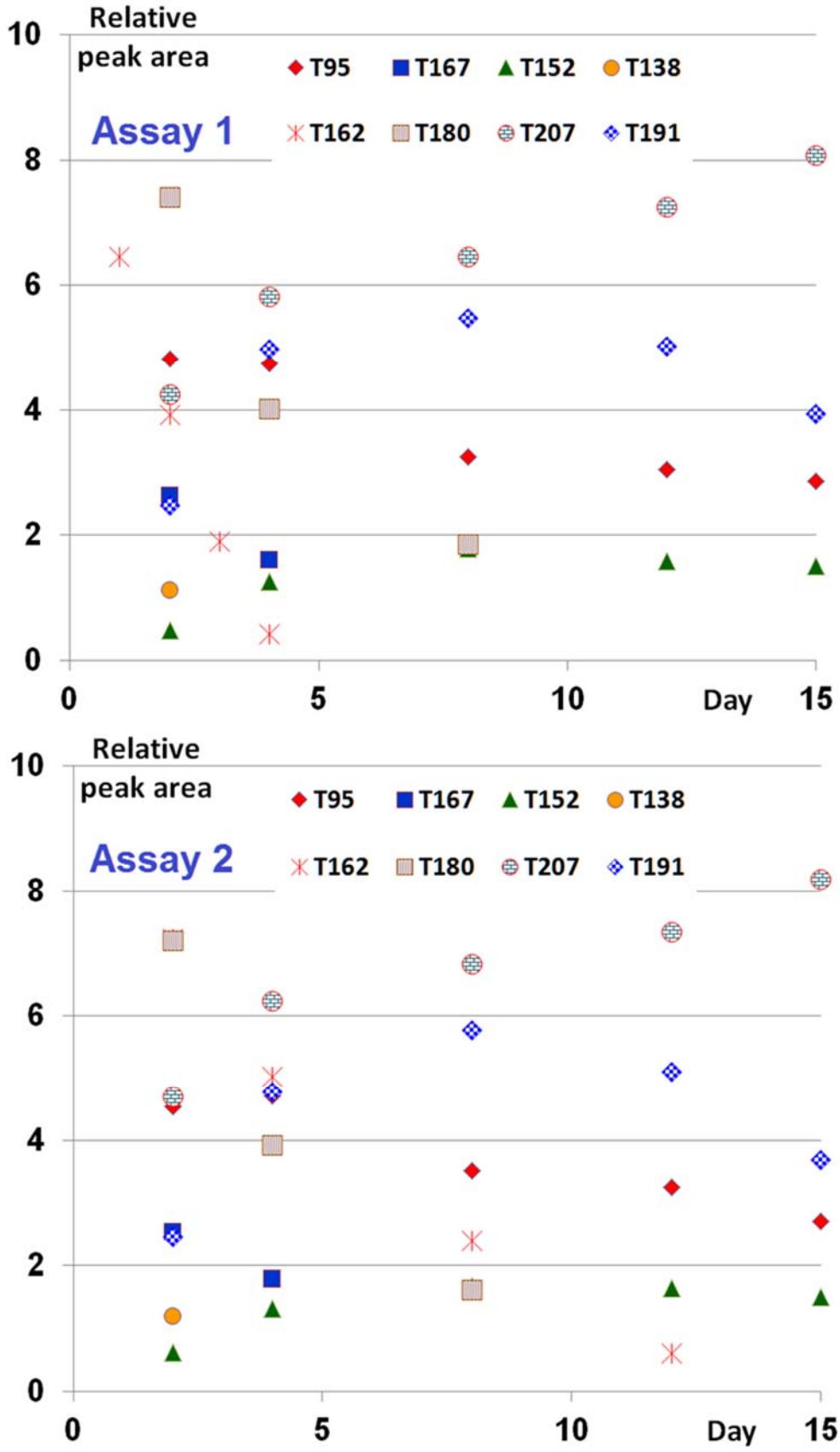

Fig. SM31: Peak areas of the degradation products in the non-forced assays on W1 river water sample spiked with tenoxicam .Peak areas are referred to the initial peak area of tenoxicam (positive mode) in each experiment, to which a value of 100 was assigned.

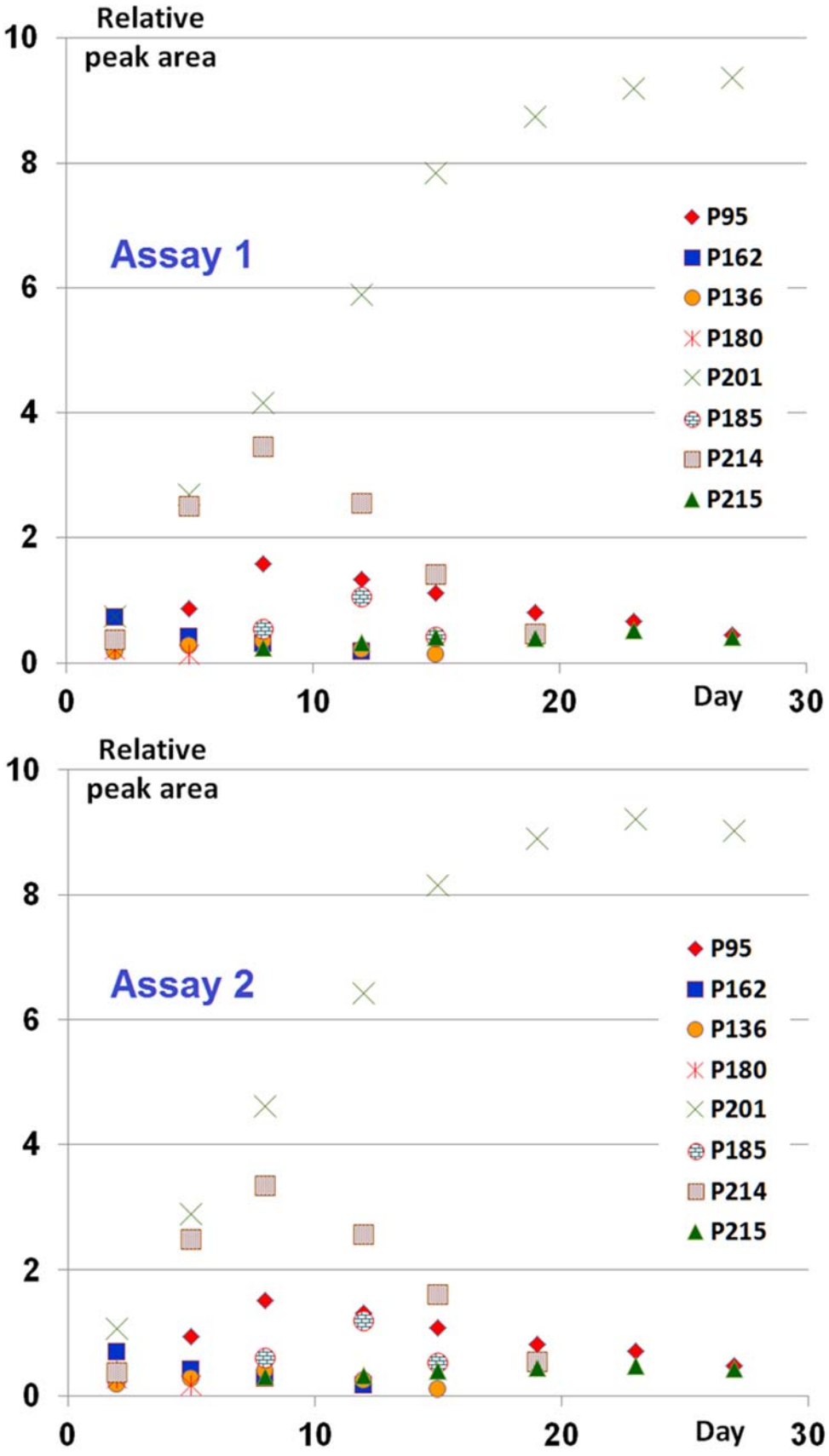

Fig. SM32: Peak areas of the degradation products in the non-forced assays on W1 river water sample spiked with piroxicam. Peak areas are referred to the initial peak area of piroxicam (positive mode) in each experiment, to which a value of 100 was assigned.

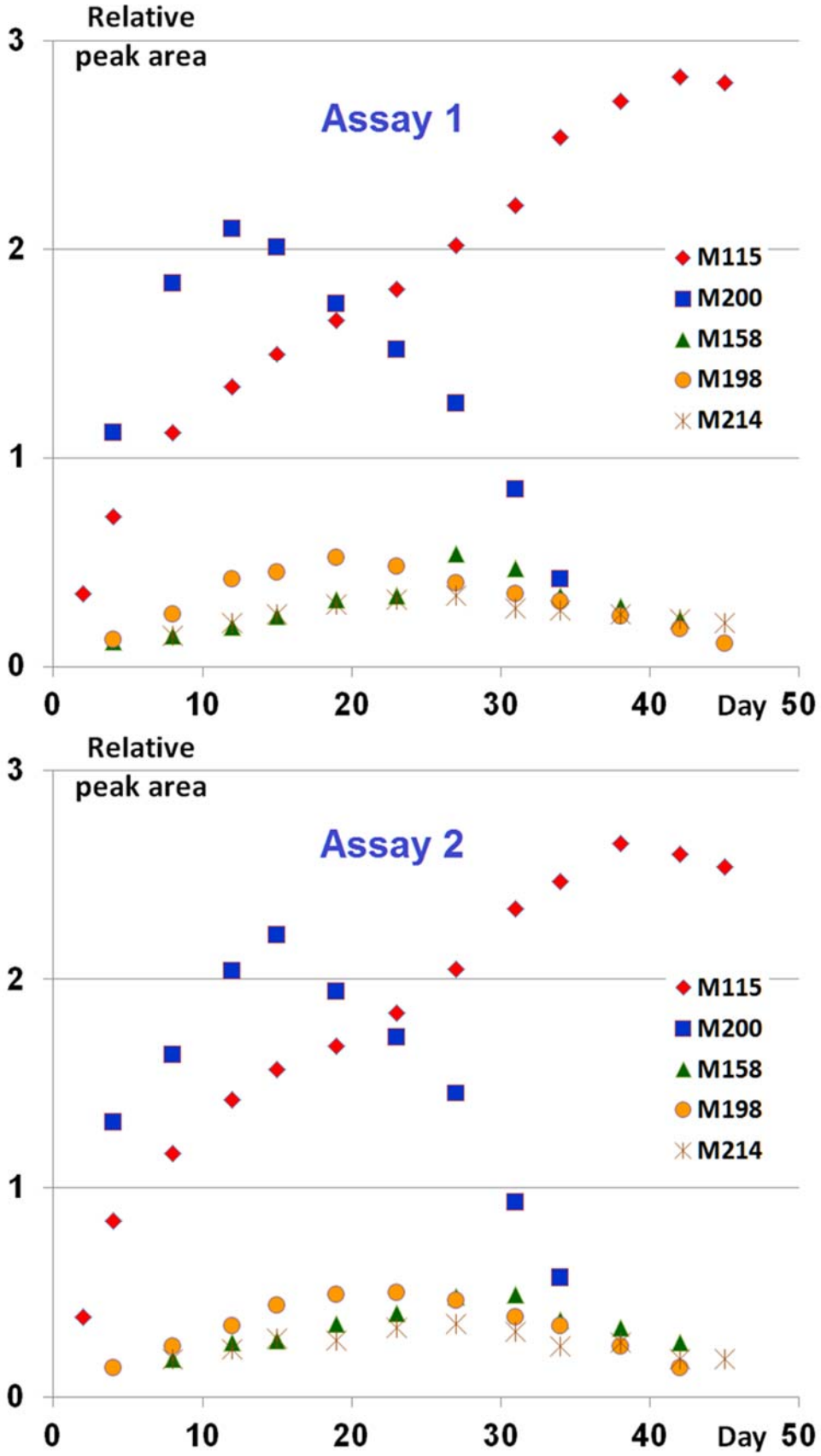

Fig. SM33: Peak areas of the degradation products in the non-forced assays on W1 river water sample spiked with meloxicam. Peak areas are referred to the initial peak area of meloxicam (positive mode) in each experiment, to which a value of 100 was assigned.

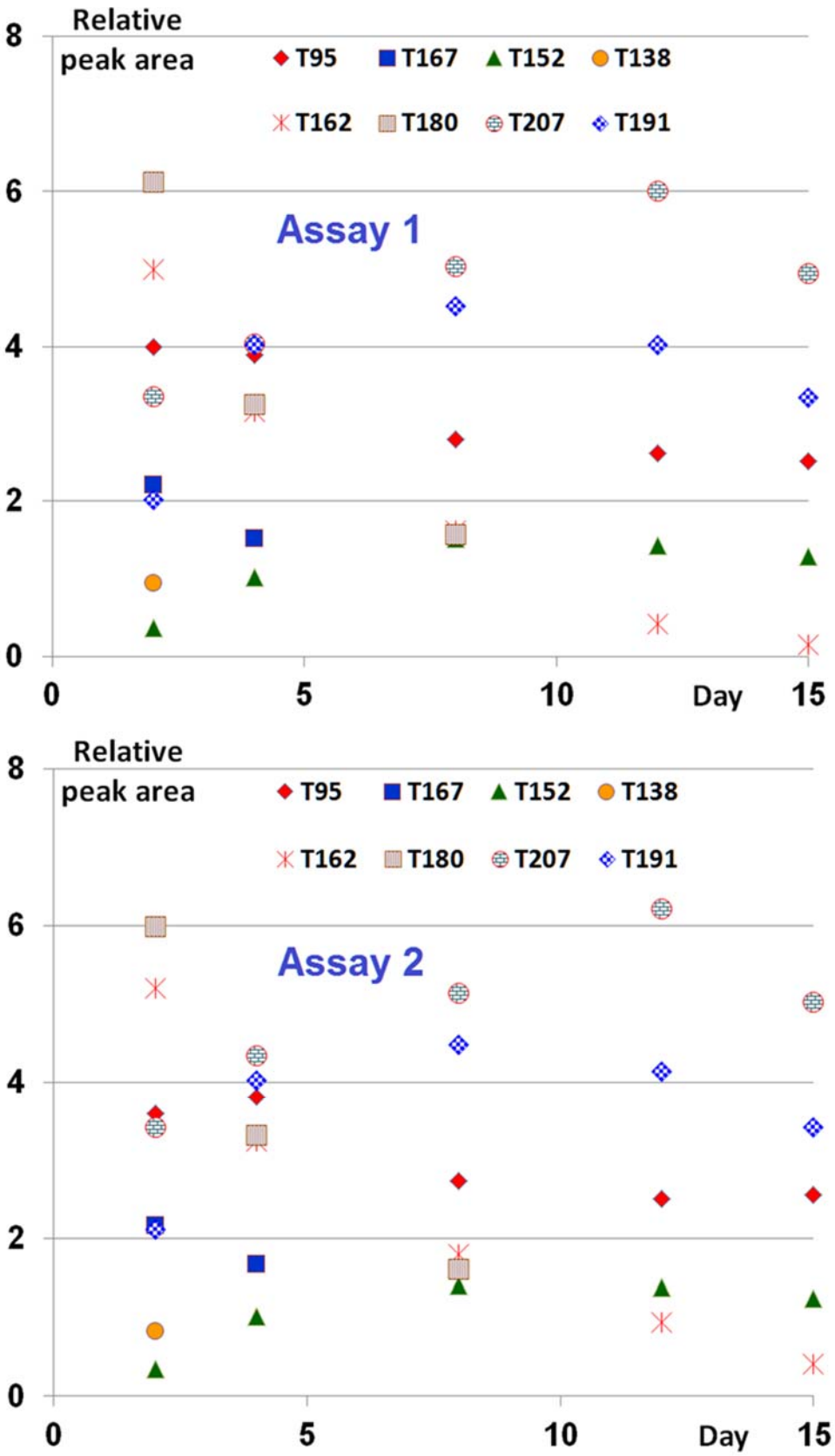

Fig. SM34: Peak areas of the degradation products in the non-forced assays on river water sample spiked with tenoxicam in presence of sediment (SED sample). Peak areas are referred to the initial peak area of tenoxicam (positive mode) in each experiment, to which a value of 100 was assigned.

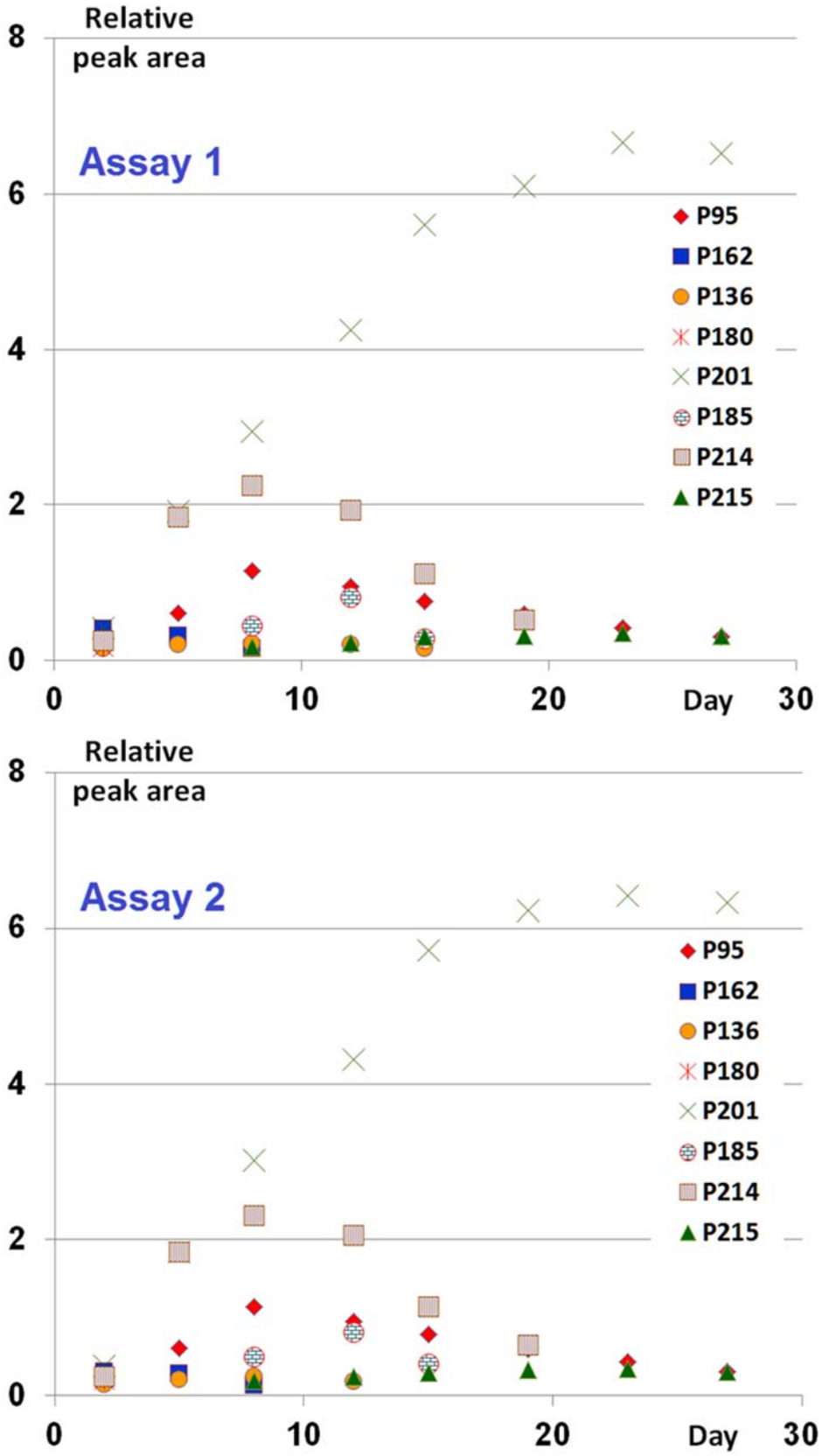

Fig. SM35: Peak areas of the degradation products in the non-forced assays on W1 river water sample spiked with piroxicam in presence of sediment (SED sample).Peak areas are referred to the initial peak area of piroxicam (positive mode) in each experiment, to which a value of 100 was assigned.

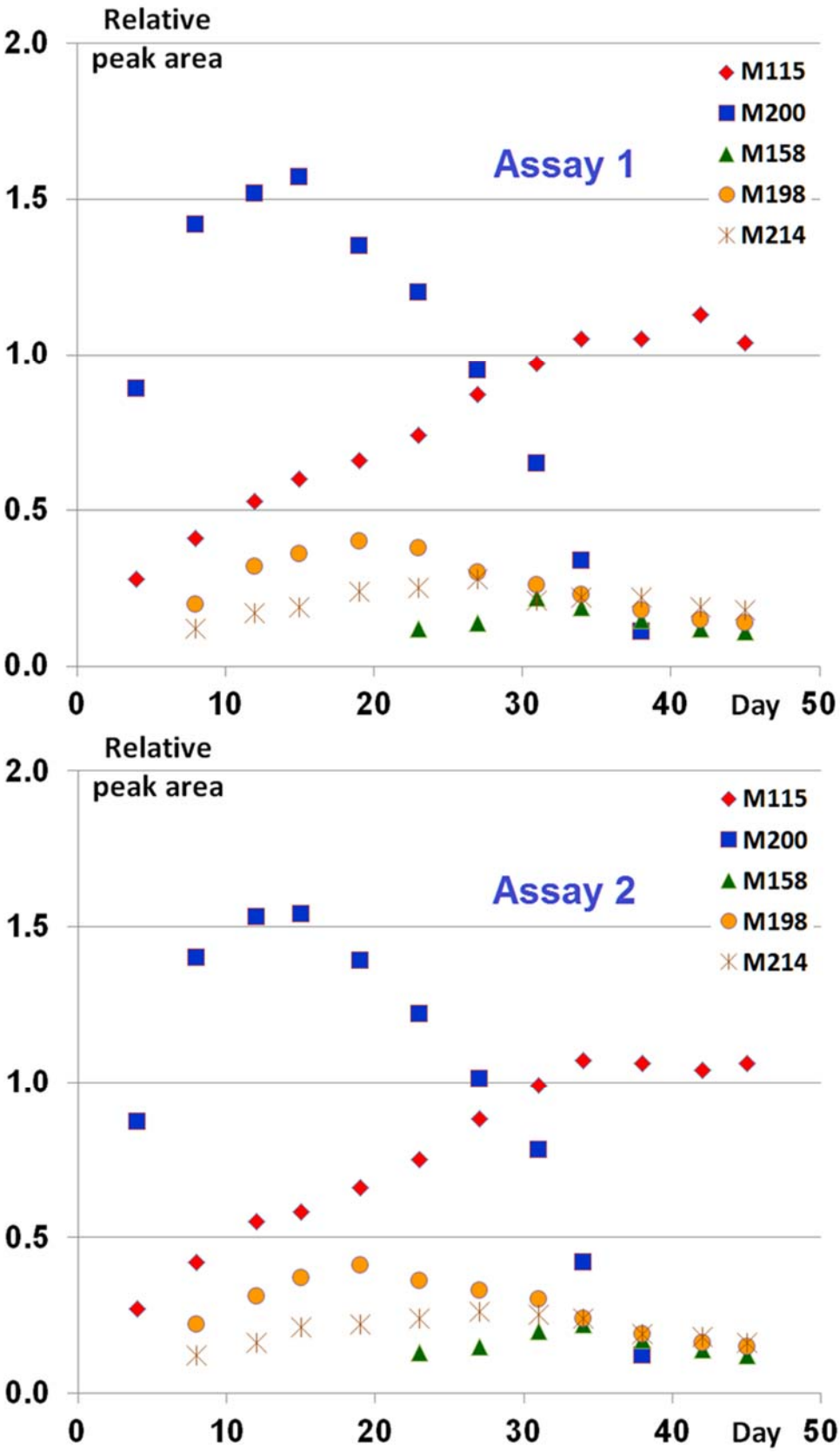

Fig. SM36: Peak areas of the degradation products in the non-forced assays on W1 river water sample spiked with meloxicam in presence of sediment (SED sample).Peak areas are referred to the initial peak area of meloxicam (positive mode) in each experiment, to which a value of 100 was assigned.

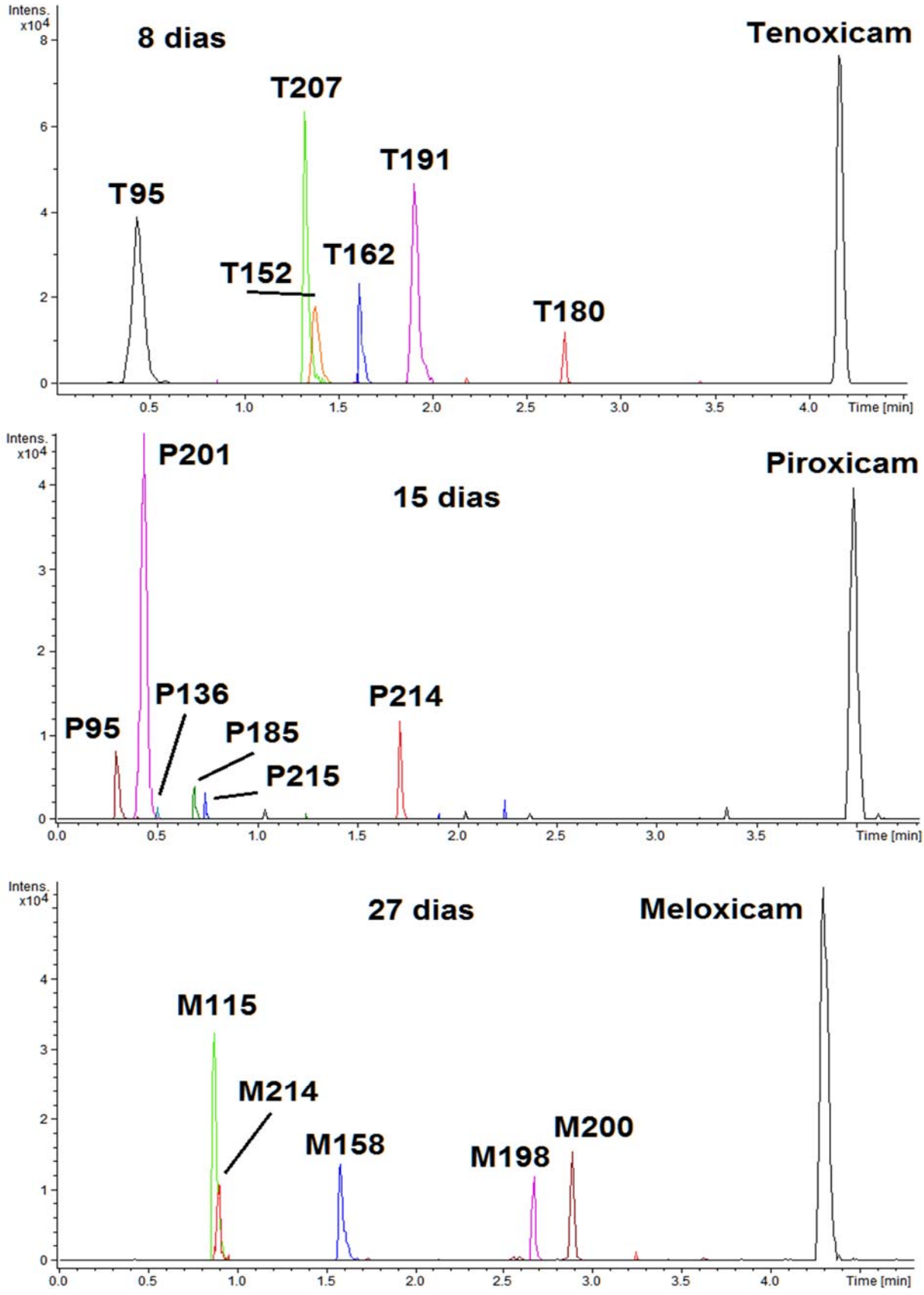

Figure (*): Superposition of extracted ion chromatograms ($[M+H]^+$ ± 0.01 for all compounds) for a water sample spiked with 2 µg L^{-1}, under non-forced conditions

3.4. Prediction of ecotoxicity.

Table SM10: Predicted 50% lethal concentrations (LC_{50}, μM) and 50% growth inhibition concentrations (IGC_{50}, μM) of oxicams and degradation products for different tests.

	Daphnia magna LC_{50} (48 hr)	*Tetrahymena pyriformis* IGC_{50}	Fathead minnow LC_{50} (96 hr)
T95	68	6761	3715
T138	240	5248	4571
T167	631	9120	1202
T207	1698	1175	501
T152	479	4571	1202
T162	562	4074	389
T153	398	8318	2188
T191	741	759	240
T205	575	724	126
T180	617	5754	1148
Tenoxicam	11	55	1
P95	68	6761	3715
P201	355	1906	617
P162	562	4074	389
P153	398	8318	2188
P136	49	8318	912
P185	219	1479	186
P215	832	1318	468
P180	617	5754	1148
P214	98	1259	589
Piroxicam	23	1175	2
M185	219	1479	186
M115	324	3801	4365
M214	978	1259	589
M158	389	2188	4571
M187	468	5623	1514
M198	448	468	214
M200	135	6607	2042
Meloxicam	29	933	2

3.5. Distribution between water and sediment. Adsorption coefficients.

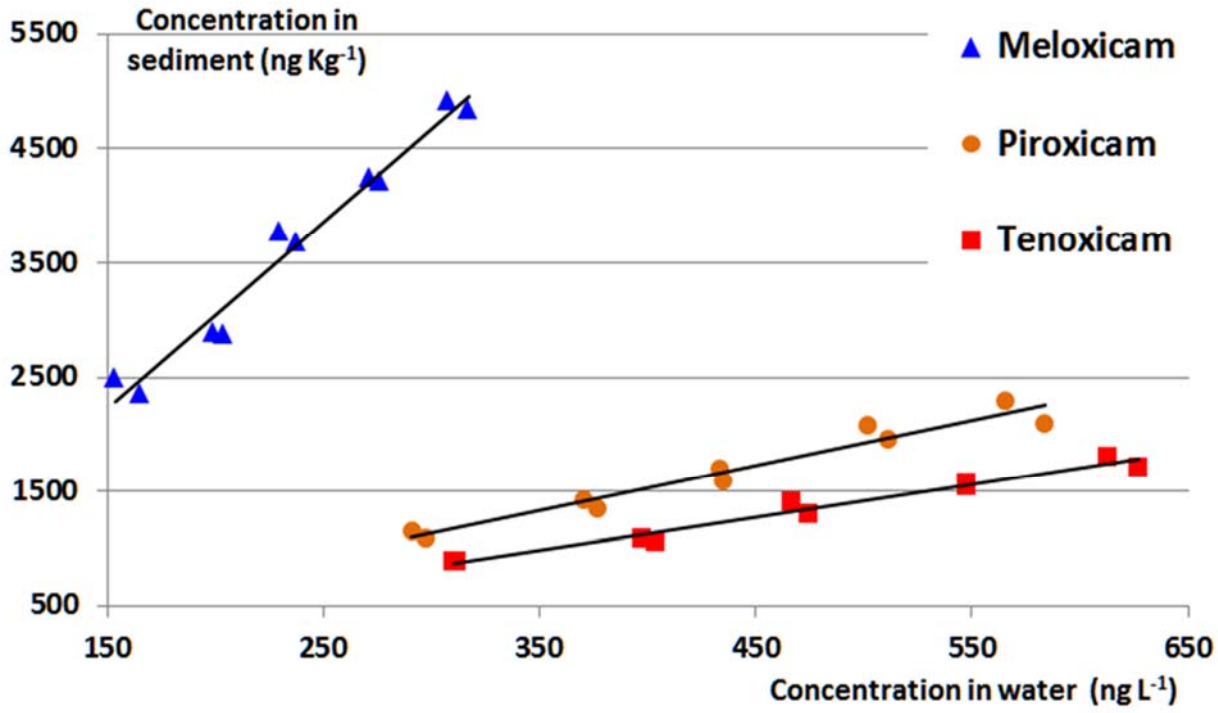

Fig. SM37: Adsorption isotherms of tenoxicam, piroxicam and meloxicam (n = 2).

5. RECUPERACIÓN Y PRECISIÓN, PRODUCTOS DE DEGRADACIÓN

Asumiendo que los productos de degradación mayoritarios encontrados en los ensayos de degradación bajo condiciones no forzadas son aquellos que probablemente pueden ser detectados en el análisis de muestras reales de agua superficial se han calculado sus tasas de recuperación y precisión, mediante el método de análisis ensayado para la determinación de drogas a nivel de trazas, con el fin de verificar si se pueden monitorizar conjuntamente con el principio activo. Para ello se ha dopado 1 L de muestra de agua de río con una disolución que contenía los productos de degradación y se ha realizado la extracción en fase sólida con el cartucho seleccionado para el compuesto precursor.

Dado que no se dispone de patrones analíticos para la mayoría de los productos de degradación identificados se ha planificado la estrategia que ahora se comenta para calcular las tasas de recuperación. Alícuotas de agua dopadas con las drogas a elevada concentración (1 $mg \cdot L^{-1}$) fueron sometidas a los ensayos de degradación para generar los productos de transformación y se usaron después para dopar el agua de río, libre de analitos, con el fin de calcular las recuperaciones. Así, la concentración nominal de droga en el agua dopada para hacer las extracciones era del orden de 1-2 $\mu g \cdot L^{-1}$, entendiendo la concentración nominal como la concentración del principio activo sin degradar.

Es necesario disponer de una disolución de referencia conteniendo los analitos para calcular las tasas de recuperación después de la preparación de muestra. En esta experimentación esta disolución fue preparada por dilución de la disolución con productos de degradación usada para dopar las muestras de agua; la dilución se hacía con metanol de modo que se obtuvieran concentraciones (o áreas de pico) iguales a aquellas que se obtendrían en los extractos de muestras si la recuperaciones fueran del 100%. Evidentemente, las concentraciones de los productos de degradación no son conocidas pero las áreas de pico medidas proporcionan una indicación de su cantidad en estas disoluciones.

Tabla 26: Recuperaciones (REC) obtenidas para los productos de degradación mayoritarios (n=5). Se indica también el tipo de cartucho y modo de ionización utilizados así como el área de pico del compuesto en la disolución de referencia.

Precursor	Producto de degradación	Modo de ionización	Área de pico (disolución de referencia)	REC (%)	RSD (%)
Clorpromazina (Oasis HLB)	2HP	Positivo	119770	112	6.1
	CP SO	Positivo	127082	94	5.3
	PRO SO NO	Positivo	55418	82	4.4
	2HP SO	Positivo	82472	101	11
	2HP SO NO	Positivo	83468	90	6.2
	PRO SO	Positivo	10532	148	22
	CP SO NO	Positivo	171485	64	4.0
	BZ DIOL	Positivo	16728	114	8.3
	DHBT MET	Positivo	6881	125	25
	BT SO	Positivo	3748	105	4.0
	BT MET	Positivo	26756	73	11
Indometacina (EBH)	MMIA	Negativo	39099	86	8.1
	CBA	Negativo	115351	76	3.9
	AMBA	Negativo	12866	80	7.2
	DHINDO	Negativo	14243	90	7.6
Alprazolam (Oasis HLB)	DP300	Positivo	21592	83	6.5
	DP327-1	Positivo	8811	78	10
	DP327-3	Positivo	9360	81	7.2
Celecoxib (EBH)	DP381	Negativo	15749	82	6.2
	DP410	Negativo	17163	81	7.3
	DP396	Negativo	8655	84	6.6
Tenoxicam (Oasis HLB)	T95	Positivo	40089	53	8.8
	T152	Positivo	47582	41	10
	T191	Negativo	57516	57	6.6
	T207	Negativo	98367	51	6.7
Piroxicam (Oasis HLB)	P201	Negativo	114388	40	11
	P214	Negativo	29752	69	5.9
	P215	Negativo	31163	43	6.4
	P95	Positivo	32047	57	7.1
Meloxicam (Oasis HLB)	M115	Positivo	57487	69	5.1
	M198	Positivo	39875	77	4.2
	M214	Positivo	34420	62	4.7
	M200	Positivo	42511	68	5.0
	M158	Positivo	28754	61	4.8

En la Tabla 26 se observa que las recuperaciones y precisiones de los productos de degradación varían ampliamente. Las recuperaciones medias para los productos de degradación de la clorpromazina usando cartuchos Oasis HLB varían entre el 64 y el 148% mientras que la desviación típica relativa está comprendida en el rango comprendido entre 4.4 y 25%, sin que sea posible, en principio, establecer una relación entre la naturaleza del producto de degradación (algunos de ellos de elevada polaridad) y los resultados de recuperación y precisión obtenidos.

Las recuperaciones medias de los productos de degradación de la indometacina (cartuchos EBH), alprazolam (cartuchos Oasis HLB) y celecoxib (cartuchos EBH) variaban entre los rangos 76-90%, 78-83% y 81-84%, con precisiones del orden de 3.9-8.1%, 6.5-10% y 6.2-7.3%, respectivamente. Los resultados obtenidos para estos productos de degradación son, en líneas generales, similares a los de sus correspondientes compuestos precursores.

Finalmente, se observa en la Tabla 26 que las tasas de recuperación medias de los productos de degradación de los oxicanes son relativamente bajas, variando entre el 41 y 57 % para tenoxicam, entre el 40 y 69% para piroxicam y entre el 61 y 77 % para meloxicam, con desviaciones típicas del orden de 6.6-10 %, 5.9-11% y 4.2-5.1 % respectivamente. En este caso los productos de degradación son moléculas relativamente pequeñas y presentan una polaridad elevada, y en consecuencia su solubilidad en agua debería ser elevada también, todo lo cual podría justificar los resultados obtenidos.

Pensando en la posibilidad de monitorizar estos compuestos en aguas superficiales mediante el procedimiento de análisis descrito se podría afirmar que esto es perfectamente factible para los productos derivados del alprazolam, celecoxib, indometacina y clorpromazina.

El seguimiento de los compuestos de degradación de tenoxicam, piroxicam y meloxicam en agua de río mediante el método empleado para estos sería menos recomendable en función de las tasas de recuperación estimadas. La detección de los compuestos en los cromatogramas podría ser posible pero la determinación de la cantidad presente, en términos de concentración o de forma relativa frente al precursor, tendría un carácter semicuantitativo más que cuantitativo.

6. ROBUSTEZ, PRODUCTOS DE DEGRADACIÓN

Se ha estudiado la posibilidad de determinar los productos de degradación mediante el método de preparación de muestra aplicado a las drogas de las cuales provienen, y al igual que para éstas se ha considerado también la robustez del método en lo que atañe a la determinación de los productos de degradación. De esto modo, se planteó y llevó a cabo un diseño de experimentos similar al descrito en la sección 3 del capítulo “Resultados y Discusión” para estudiar la influencia de los mismos cuatro factores: pH de la muestra de agua, volumen de elución con metanol, volumen de la disolución de lavado y tiempo de evaporación del extracto para tener en cuenta su posible inestabilidad térmica.

El experimento se ha hecho para los productos de degradación mayoritarios y los resultados se resumen en la Tabla 27.

Si se comparan los efectos en valor absoluto se puede comprobar que el efecto de cada factor es siempre menor que el efecto crítico por lo que se puede afirmar que la determinación de los productos de degradación es robusta para un nivel de significación p=0.05.

Tabla 27: Resultados del diseño de experimentos para evaluar la robustez del método de análisis de productos de degradación.

Precursor	Producto de degradación	E_c	E (pH)	E (V metanol)	E (V lavado)	E (tiempo evaporación)
Clorpromazina (Oasis HLB)	2HP	9192	4434	-5147	-2923	2466
	CP SO	62356	-430	24860	-13	39284
	PRO SO NO	4347	-2320	-617	-1099	-3815
	2HP SO	4568	-2015	-2459	1746	362
	2HP SO NO	25845	315	-9047	-4479	-5529
	PRO SO	36190	13337	13799	7835	11845
	CP SO NO	8219	-3053	3339	-1344	-1421
	BZ DIOL	3213	-20	-371	756	618
	DHBT MET	5876	849	188	533	-1821
	BT SO	412	-105	-55	-40	-104
	BT MET	9922	-492	-4492	1993	-4811
Indometacina (EBH)	MMIA	25500	2571	2350	-12292	-1971
	CBA	76572	6961	6073	-32863	4211
	AMBA	5023	-397	690	-2656	770
	DHINDO	12285	-397	1632	-3782	144
Alprazolam (Oasis HLB)	DP300	3903	2400	-515	2088	779
	DP327-1	1479	-1046	-621	1031	-155
	DP327-3	18035	5425	-1661	13237	2330
Celecoxib (EBH)	DP381	1023	294	275	-385	851
	DP410	1771	185	-736	-284	-94
	DP396	1506	585	158	-117	-452
Tenoxicam (Oasis HLB)	T95	9026	595	1456	-1664	-2132
	T152	5936	-127	673	-854	-736
	T191	4174	-833	635	812	1238
	T207	6516	1192	1415	204	1218
Piroxicam (Oasis HLB)	P201	8951	-2597	-1796	3830	1687
	P214	7187	-192	-747	875	572
	P215	4481	1547	1859	396	-2756
	P95	3648	1434	791	3086	397
Meloxicam (Oasis HLB)	M115	6905	-218	387	-378	-1751
	M198	6200	953	1680	2308	-1576
	M214	7735	849	-2888	-2276	-1611
	M200	5507	-1138	459	-2788	402
	M158	4699	-250	-1258	309	2797

CONCLUSIONES

- Los cartuchos de extracción Oasis HLB y EBH de 60 mg proporcionan recuperaciones similares (p=0.05) para la determinación de alprazolam, clorpromazina, indometacina, celecoxib y piroxicam en agua de río, mientras que para la extracción de tenoxicam y meloxicam es preferible el uso de cartuchos Oasis HLB.

- Después de seleccionar un tipo de cartucho para cada compuesto, las recuperaciones medias en agua de río dopada a nivel de trazas son superiores al 70 %, excepto para la clorpromazina, con repetividades del orden del 6.0-11 %. Los límites de detección son inferiores a 1 $ng \cdot L^{-1}$.

- Los productos de degradación mayoritarios pueden ser monitorizados conjuntamente con la droga precursora mediante el mismo procedimiento de preparación de muestra, si bien las recuperaciones de los compuestos derivados de los oxicanes son relativamente bajas. La repetitividad del análisis de algunos productos de degradación de la clorpromazina es escasa en comparación con la de los demás compuestos.

- Se ha comprobado la robustez del método de análisis de principios activos y residuos detectados para cuatro parámetros de operación mediante un diseño de experimentos Plackett-Burman que incluía factores simulados. Los parámetros de operación considerados son el pH de la muestra de agua, el volumen de metanol usado para eluir el cartucho, el volumen de disolución de lavado de los cartuchos y el tiempo de evaporación del extracto.

- La radiación solar promueve la degradación fotoquímica de clorpromazina, tenoxicam, piroxicam, meloxicam e indometacina en agua de río. El celecoxib es también degradado por la luz solar pero muy lentamente. La atenuación de la radiación solar con la profundidad que tiene lugar en una masa de agua disminuye considerablemente la velocidad de degradación de estos compuestos.

- Las reacciones químicas en agua de río a pH ligeramente alcalino afectan muy escasamente a las siete drogas estudiadas. Sin embargo, son la causa principal de la degradación del alprazolam. Son también relevantes en la transformación de la indometacina, y en menor medida, de los tres oxicanes.

- La degradación biológica, tanto en condiciones aeróbicas como anaeróbicas, y sin adición de nutrientes, de alprazolam, celecoxib, indometacina, piroxicam y meloxicam en agua de río no es significativa, mientras que tenoxicam muestra cierta degradación tanto en condiciones aeróbicas como anaeróbicas.

- En condiciones no forzadas las concentraciones de alprazolam y celecoxib en agua de río disminuyen menos de un 5% (4.9 y 3.1%, respectivamente) en un plazo de 36 semanas, y pueden ser considerados como microcontaminantes persistentes en aguas superficiales bajo condiciones

medioambientales. La vida media estimada en agua de río no sometida a condiciones forzadas del tenoxicam, clorpromazina, piroxicam, meloxicam e indometacina es del orden de 1.9, 3.2, 3.6, 6.2 y 35.3 días, respectivamente.

- En presencia de sedimento la velocidad de degradación de alprazolam, tenoxicam, piroxicam y meloxicam en agua de río es básicamente similar a aquella en agua sin presencia de sedimento, siendo ligeramente mayor la velocidad de degradación para indometacina (vida media, 23.7 días) y celecoxib (degradación, 4.2 % en 36 semanas).

- La clorpromazina no se detecta en agua en contacto con un sedimento acuático (0.03 kg/L) debido a su elevadísimo coeficiente de adsorción (41632 L/kg). Las otras seis drogas presentan una cierta capacidad de adsorción sobre el sedimento; celecoxib es el más adsorbido (44.4 L/kg), seguido del meloxicam (15.3 L/kg), alprazolam (4.4 L/kg), piroxicam (3.8 L/kg) y tenoxicam (2.8 L/kg); la indometacina es el compuesto menos retenido (1.8 L/kg).

- Se han detectado varios productos de degradación en los ensayos de degradación en condiciones forzadas y no forzadas, proponiéndose las estructuras de la mayoría de ellos a partir de las fórmulas moleculares y fragmentaciones observadas en los espectros de masas en tándem obtenidos en un equipo de alta resolución; 16 productos de degradación para la clorpromazina, 6 para la indometacina, 9 para el alprazolam y piroxicam, 10 para el tenoxicam, 7 para el meloxicam y 11 para el celecoxib.

- Los productos de degradación se originan, en líneas generales, mediante reacciones de oxidación de grupos funcionales, hidroxilación de anillos aromáticos, apertura de estructuras cíclicas e hidrólisis. En el caso de la clorpromazina existen también procesos de descloración y en el caso del alprazolam hay reacciones de adición de agua a estructuras cíclicas aromáticas.

- En condiciones no forzadas similares a las que se podrían encontrar en una masa de agua los productos de degradación mayoritarios del celecoxib son celecoxib sulfónico, celecoxib ácido y un derivado hidroxilado mientras que para el alprazolam éstos son básicamente un triazolfenil-fenilmetanol, dihidro-hidroxifenil-benzodiacepina e hidroxiciclohexadien-benzodiacepina.

- Los productos de degradación a largo plazo de la clorpromazina son derivados del benzo[1,4]tiazinol; de la indometacina son los correspondientes ácidos clorobenzoico y acetamido-metoxibenzoico; para el caso de los oxicanes, derivan de la aminopiridina para tenoxicam y piroxicam y de metiltiazolamina para meloxicam, o bien de los ácidos tiofensulfónico para el primero y bencenosulfónico para los otros dos. Estos productos de transformación podrían usarse como indicadores de la presencia de los compuestos padre después de su degradación total.

- Los productos de degradación presentan en general una menor capacidad de adsorción sobre un sedimento acuático con respecto a sus precursores. Únicamente aquellos compuestos con una amina libre en su estructura tienen coeficientes de adsorción ligeramente mayores.

REFERENCIAS

[1] R. Carson. Silent Spring. Houghton Mifflin Harcourt. Boston, USA (1962).

[2] S. Jensen, A. G. Johnels, M. Olsson, G. Otterlind. DDT and PCB in marine animals from Swedish waters. *Nature Vol. 224 (1969) p. 247*.

[3] J. J. Rook. Formation of haloforms during chlorination of natural water. *Water Treat. Exam. 23 (1974) 234-236.*

[4] Directiva 2013/39/UE del Parlamento Europeo y del Consejo de 12 de agosto de 2013 por la que se modifican las Directivas 2000/60/CE y 2008/105/CE en cuanto a las sustancias prioritarias en el ámbito de la política de aguas. L226/1 – L226/17. (Bruselas, 24.8.2013).

[5] D. Barceló, M. López de Alda, M. Petrović, S. Lacorte, B. Piña, A. Ginebreda. Los contaminantes emergentes en los sistemas de saneamiento y sus efectos ambientales. II Jornadas Técniques de Gestió d'EDAR (Barcelona, 2005).

[6] A. W. Garrison, J. D. Pope, F. R. Allen. GC/MS Analysis of organic compounds in domestic wastewaters. In: Identification and Analysis of Organic Pollutants in Water (Keith CH, ed). Ann Arbor, Ml: Ann Arbor Science Publishers, (1976) 517-556.

[7] C. Hignite, D. L. Azarnoff. Drugs and drug metabolites as environmental contaminants: Chlorophenoxyisobutyrate and salicylic acid in sewage water effluent. *Life Sci. 20 (1977) 337-341.*

[8] C.D. Watts, M. Crathorne, M. Fielding, C.P. Steel, in: G. Angeletti, A. Bjorseth (Eds.), Analysis of Organic Micropollutants in Water, Reidel, Dordrecht (1983) p. 120.

[9] A. Waggott, in: W.J. Cooper (Ed.), Chemical Water Reuse, Vol. 2, Ann Arbor Sci. Publ., Ann Arbor, MI (1981) p. 55.

[10] M.L. Richardson, J.M. Bowron. The fate of pharmaceutical chemicals in the aquatic environment. *J. Pharm. Pharmacol. 37 (1985) 1-12.*

[11] C. G. Daughton, A. T. Ternes. Pharmaceuticals and personal care products in the environment: Agents of subtle change? *Environ. Health Perspect. 107 (1999) 907-938.*

[12] T. A. Ternes. Occurrence of drugs in German sewage treatment plants and rivers. *Water Res. 32 (1998) 3245–3260.*

[13] M. A. Mottaleb, W. C. Brumley. Environmental analytical chemistry of pharmaceutical and personal care products: The separations focus turns to polar analytes. *Trends Chromatogr. 2 (2006) 11-29.*

[14] T. Kosjek, E. Heath, A. Krbavcic. Determination of non-steroidal anti-inflammatory drug (NSAIDs) residues in water samples. *Environ. Int. 31 (2005) 679–685.*

[15] L. J. Zhou, G. G. Ying, S. Liu, J. L. Zhao, F. Chen, R. Q. Zhang, F. Q. Peng, Q. Q. Zhang. Simultaneous determination of human and veterinary antibiotics in various environmental matrices by rapid resolution liquid chromatography–electrospray ionization tandem mass spectrometry. *J. Chromatogr. A 1244 (2012) 123–138.*

[16] S. L. Rice, S. Mitra. Microwave-assisted solvent extraction of solid matrices and subsequent detection of pharmaceuticals and personal care products (PPCPs) using gas chromatography–mass spectrometry. *Anal. Chim. Acta 589 (2007) 125–132.*

[17] B. Tiwari, B. Sellamuthu, Y. Ouarda, P. Drogui, R. D. Tyagi, G. Buelna. Review on fate and mechanism of removal of pharmaceutical pollutants from wastewater using biological approach. *Bioresour. Technol. 224 (2017) 1–12.*

[18] E. J. Routledge, D. Sheahan, C. Desbrow, G. C. Brighty, M. Waldock, J. P. Sumpter. Identification of estrogenic chemicals in STW effluent. 2. In vivo responses in trout and roach. *Environ. Sci. Technol. 32 (1998) 1559-1565.*

[19] C. Lacey, S. Basha, A. Morrissey, J. M. Tobin. Occurrence of pharmaceutical compounds in wastewater process streams in Dublin, Ireland. *Environ. Monit. Assess. 184 (2012) 1049–1062.*

[20] Informe de la Comisión al Parlamento Europeo y al Consejo sobre el resultado de la revisión del anexo X de la Directiva 2000/60/CE del Parlamento Europeo y del Consejo, en relación con las sustancias prioritarias en el ámbito de la política de aguas (Bruselas 31.1.2012).

[21] Decisión de ejecución (UE) 2018/840 de la Comisión de 5 de junio de 2018, publicado en el Diario Oficial de la Comunidad de fecha 7-6-2018, L141/9 – L141/12.

[22] J. Hollender, S. G. Zimmermann, S. Koepke, M. Krauss, C. S. McArdell, C. Ort, H. Singer, U. Von Gunten, H. Siegrist. Elimination of organic micropollutants in a municipal wastewater treatment plant upgraded with a full-scale post-ozonation followed by sand filtration**.** *Environ. Sci. Technol. 43 (2009) 7862–7869.*

[23] J. P. Bound, N. Voulvoulis. Predicted and measured concentrations for selected pharmaceuticals in UK rivers: Implications for risk assessment**.** *Water Res. 40 (2006) 2885-2892.*

[24] B. W. Brooks, C. K. Chambliss, J. K. Stanley, A. Ramirez, K. E. Banks, R. D. Johnson, R. J. Lewis. Determination of select antidepressants in fish from an effluent-dominated stream. *Environ. Toxicol. Chem. 24 (2) (2005) 464–469.*

[25] S. Chu, C. D. Metcalfe. Analysis of paroxetine, fluoxetine and norfluoxetine in fish tissues using pressurized liquid extraction, mixed mode solid phase extraction cleanup and liquid chromatography–tandem mass spectrometry. *J. Chromatogr. A 1163 (1–2) (2007) 112–118.*

[26] R. Aznar, B. Albero, R. A. Pérez, C. Sánchez-Brunete, E. Miguel, J. L. Tadeo. Analysis of emerging organic contaminants in poultry manure by gas chromatography–tandem mass spectrometry. *J. Sep. Sci. 41 (2018) 940–947.*

[27] J. Hou, W. Wan, D. Mao, C. Wang, Q. Mu, S. Qin, Y. Luo. Occurrence and distribution of sulfonamides, tetracyclines, quinolones, macrolides, and nitrofurans in livestock manure and amended soils of Northern China. *Environ. Sci. Pollut. Res. 22 (2015) 4545–4554.*

[28] M. Pan, L. M. Chu. Occurrence of antibiotics and antibiotic resistance genes in soils from wastewater irrigation areas in the Pearl River Delta region, southern China. *Sci. Total Environ. 624 (2018) 145-152.*

[29] M. Pan, C. K. C. Wong, and L. M. Chu. Distribution of antibiotics in wastewater-irrigated soils and their accumulation in vegetable crops in the Pearl River Delta, Southern China. *J. Agric. Food Chem. 62 (2014) 11062−11069.*

[30] M. C. Bastos, D. R. dos Santos, E. Aubertheau, J. A. M. D. Lima, T. Le Guet, L. Caner, L. Mondamert, J. Labanowski. Antibiotics and microbial resistance in Brazilian soils under manure application. *Land Degrad. Dev. 29 (8) (2018) 2472-2484.*

[31] T. Kivits, H. P. Broers, H. Beeltje, M. van Vliet, J. Griffioen. Presence and fate of veterinary antibiotics in age-dated groundwater in areas with intensive livestock farming. *Environ. Pollut. 241 (2018) 988-998.*

[32] B. Albero, C. Sánchez-Brunete, E. Miguel, J. L. Tadeo. Application of matrix solid-phase dispersion followed by GC–MS/MS to the analysis of emerging contaminants in vegetables. *Food Chem. 217 (2017) 660-667.*

[33] K. Kumar, S. C. Gupta, S. K. Baidoo, Y. Chander, and C. J. Rosen. Antibiotic uptake by plants from soil fertilized with animal manure. *J. Environ. Qual. 34 (2005) 2082–2085.*

[34] C. S. Holling, J. L. Bailey, B. Vanden Heuvel, C. A. Kinney. Uptake of human pharmaceuticals and personal care products by cabbage (Brassica campestris) from fortified and biosolids-amended soils. *J. Environ. Monit. 14 (2012) 3029–3036.*

[35] X. Wu, L. K. Dodgen, J. L. Conkle, J. Gan. Plant uptake of pharmaceutical and personal care products from recycled water and biosolids: a review. *Sci. Total Environ. 536 (2015) 655–666.*

[36] D. H. Kang, S. Gupta, C. Rosen, V. Fritz, A. Singh, Y. Chander, H. Murray, C. Rohwer. Antibiotic uptake by vegetable crops from manure-applied soils. *J. Agric. Food Chem. 61 (2013) 9992−10001.*

[37] D. Fatta, A. Nikolaou, A. Achilleos, S. Meric. Analytical methods for tracing pharmaceutical residues in water and wastewater. *TrAC, Trends Anal. Chem. 26 (2007) 515-533.*

[38] M. Carballa, F. Omil, J. M. Lema, M. Llompart, C. García-Jares, I. Rodríguez, M. Gómez, T. Ternes. Behavior of pharmaceuticals, cosmetics and hormones in a sewage treatment plant. *Water Res. 38 (2004) 2918–2926.*

[39] J.L. Zhou, Z.L. Zhang, E. Banks, D. Grover, J.Q. Jiang. Pharmaceutical residues in wastewater treatment works effluents and their impact on receiving river water. *J. Hazard. Mater. 166 (2009) 655–661.*

[40] N. H. Tran, K. Y.-H. Gin. Occurrence and removal of pharmaceuticals, hormones, personal care products, and endocrine disrupters in a full-scale water reclamation plant. *Sci. Total Environ. 599–600 (2017) 1503–1516.*

[41] L. Patrolecco, S. Capri, Nicoletta Ademollo. Occurrence of selected pharmaceuticals in the principal sewage treatment plants in Rome (Italy) and in the receiving surface waters. *Environ. Sci. Pollut. Res. 22 (2015) 5864‑5876.*

[42] P. Paíga, L. H. M. L. M. Santos, S. Ramos, S. Jorge, J. G. Silva, C. Delerue-Matos. Presence of pharmaceuticals in the Lis river (Portugal): Sources, fate and seasonal variation. *Sci. Total Environ. 573 (2016) 164–177.*

[43] N. Nakada, T. Tanishima, H. Shinohara, K. Kiri, H. Takada. Pharmaceutical chemicals and endocrine disrupters in municipal wastewater in Tokyo and their removal during activated sludge treatment. *Water Res. 40 (2006) 3297-3303.*

[44] D. Bendz, N. A. Paxeus, T. R. Ginn, F. J. Loge. Occurrence and fate of pharmaceutically active compounds in the environment, a case study: Höje river in Sweden. *J. Hazard. Mater. 122 (2005) 195–204.*

[45] B. Kasprzyk-Hordern, R. M. Dinsdale, A. J. Guwy. Multiresidue methods for the analysis of pharmaceuticals, personal care products and illicit drugs in surface water and wastewater by solid-phase extraction and ultra-performance liquid chromatography–electrospray tandem mass spectrometry. *Anal. Bioanal. Chem. 391 (2008) 1293–1308.*

[46] B. Petrie, J. Youdan, R. Barden, B. Kasprzyk-Hordern. Multi-residue analysis of 90 emerging contaminants in liquid and solid environmental matrices by ultra-high-performance liquid chromatography tandem mass spectrometry. *J. Chromatogr. A 1431 (2016) 64–78.*

[47] R. Rosal, A. Rodríguez, J. A. Perdigón-Melón, A. Petre, E. García-Calvo, M. J. Gómez, A. Agüera, A. R. Fernández-Alba. Occurrence of emerging pollutants in urban wastewater and their removal through biological treatment followed by ozonation. *Water Res. 44 (2010) 578 -588.*

[48] J. T. Yu, Edward J. Bouwer, M. Coelhan. Occurrence and biodegradability studies of selected pharmaceuticals and personal care products in sewage effluent**.** *Agric. Water Manag. (2006) 72–80*

[49] M. G. Pintado-Herrera, E. González-Mazo, P. A. Lara-Martín. Environmentally friendly analysis of emerging contaminants by pressurized hot water extraction-stir bar sorptive extraction-derivatization and gas chromatography-mass spectrometry. *Anal. Bioanal. Chem. (2013) 405: 401-411.*

[50] C. I. Kosma, D. A. Lambropoulou, T. A. Albanis. Investigation of PPCPs in wastewater treatment plants in Greece: Occurrence, removal and environmental risk assessment. *Sci. Total Environ. 466–467 (2014) 421–438.*

[51] O. Golovko, V. Kumar, G. Fedorova, T. Randak, R. Grabic. Seasonal changes in antibiotics, antidepressants/psychiatric drugs, antihistamines and lipid regulators in a wastewater treatment plant. *Chemosphere 111 (2014) 418–426.*

[52] S. Mohapatra, C.-H. Huang, Suparna Mukherji, L. P. Padhye. Occurrence and fate of pharmaceuticals in WWTPs in India and comparison with a similar study in the United States. *Chemosphere 159 (2016) 526-535.*

[53] S. A. Snyder, P. Westerhoff, Y. Yoon, D. L. Sedlak. Pharmaceuticals, personal care products, and endocrine disruptors in water: implications for the water industry*. Environ. Eng. Sci. 20 (2003) 449–469.*

[54] M. J. Benotti, R. A. Trenholm, B. J. Vanderford, J. C. Holady, B. D. Stanford, S. A. Snyder. Pharmaceuticals and endocrine disrupting compounds in U.S. drinking water**.** *Environ. Sci. Technol. 43 (2009) 597–603.*

[55] P. H. Roberts, K. V. Thomas. The occurrence of selected pharmaceuticals in wastewater effluent and surface waters of the lower Tyne catchment. *Sci. Total Environ. 356 (2006) 143– 153.*

[56] P. Guerra, M. Kim, A. Shah, M. Alaee, S.A. Smyth. Occurrence and fate of antibiotic, analgesic/anti-inflammatory, and antifungal compounds in five wastewater treatment processes. *Sci. Total Environ. 473–474 (2014) 235–243.*

[57] Bryan W. Brooks, Duane B. Huggett (Editors). Human Pharmaceuticals in the Environment. Current and Future Perspectives. Springer 2012.

[58] Y. Yu, L. Wu, A. C. Chang. Seasonal variation of endocrine disrupting compounds, pharmaceuticals and personal care products in wastewater treatment plants. *Sci. Total Environ. 442 (2013) 310–316.*

[59] S. D. Kim, J. Cho, I. S. Kim, B. J. Vanderford, S. A. Snyder. Occurrence and removal of pharmaceuticals and endocrine disruptors in South Korean surface, drinking, and waste waters. *Water Res. 41 (2007) 1013–1021.*

[60] S. Suarez, J. M. Lema, F. Omil. Pre-treatment of hospital wastewater by coagulation–flocculation and flotation. *Bioresour. Technol. 100 (2009) 2138-2146.*

[61] Y. Yang, Y. S. Ok, K.-H. Kim, E. E. Kwon, Y. F. Tsang. Occurrences and removal of pharmaceuticals and personal care productos (PPCPs) in drinking water and water/sewage treatment plants: A review. *Sci. Total Environ. 596-597 (2017) 303-320.*

[62] K. Kimura, H. Hara, Y. Watanabe. Elimination of selected acidic pharmaceuticals from municipal wastewater by an activated sludge system and membrane bioreactors. *Environ. Sci. Technol. 41 (2007) 3708-3714.*

[63] M. Clara, N. Kreuzinger, B. Strenn, O. Gans, H. Kroiss. The solids retention times - a suitable design parameter to evaluate the capacity of wastewater treatment plants to remove micropollutants. *Water Res. 39 (2005) 97-106.*

[64] M. Petrović, S. González, D. Barceló. Analysis and removal of emerging contaminants in wastewater and drinking water. *TrAC, Trends Anal. Chem. 22 (2003) 685 – 696.*

[65] M. D. Celiz, S. Pérez, D. Barceló, and D. S. Aga. Trace analysis of polar pharmaceuticals in wastewater by LC–MS–MS: Comparison of membrane bioreactor and activated sludge systems. *J. Chromatogr. Sci. 47 (2009) 19-25.*

[66] M. Bernhard, J. Müller, T.P. Knepper. Biodegradation of persistent polar pollutants in wastewater: comparison of an optimised lab-scale membrane bioreactor and activated sludge treatment. *Water Res. 40 (2006), 3419–3428*.

[67] J. Radjenovic, M. Petrović, D. Barceló. Fate and distribution of pharmaceuticals in wastewater and sewage sludge of the conventional activated sludge (CAS) and advanced membrane bioreactor (MBR) treatment. *Water Res. 43 (2009) 831-841.*

[68] A. Joss, E. Keller, A. C. Alder, A. Göbel, C.S. McArdell, T. Ternes, H. Siegrist. Removal of pharmaceuticals and fragrances in biological wastewater treatment. *Water Res. 39 (2005) 3139-3152.*

[69] S. A. Snyder, E. C. Wert, H. Lei, P. Westerhoff, Y. Yoon. Removal of EDCs and pharmaceuticals in drinking and reuse treatment processes. AWWA Research Foundation, IWA Publishing, London. (2007).

[70] T. Wintgens, T. Melin, A. Schiller, S. Khan, M. Muston, D. Bixio, C. Thoeye. The role of membrane processes in municipal wastewater reclamation and reuse. *Desalination 178 (2005) 1-11.*

[71] M. Boshir Ahmed, J. L. Zhou, H. Hao Ngo, W. Guo, N. S. Thomaidis , J. Xu. Progress in the biological and chemical treatment technologies for emerging contaminant removal from wastewater: A critical review. *Journal Hazard. Mater. 323 (2017) 274–298.*

[72] M. Pera-Titus, V. García-Molina, M. A. Baños, J. Giménez, S. Esplugas. Degradation of chlorophenols by means of advanced oxidation processes: a general review. *Appl. Catal., B 47 (2004) 219–256.*

[73] I. Oller, S. Malato, J.A. Sánchez-Pérez. Combination of Advanced Oxidation Processes and biological treatments for wastewater decontamination—A review. *Sci. Total Environ. 409 (2011) 4141–4166.*

[74] B. A. Wols, C. H. M. Hofman-Caris. Review of photochemical reaction constants of organic micropollutants required for UV advanced oxidation processes in water. *Water Res. 46 (2012) 2815-2827.*

[75] L. Feng, E. D. van Hullebusch, M. A. Rodrigo, G. Esposito, M. A. Oturan. Removal of residual anti-inflammatory and analgesic pharmaceuticals from aqueous systems by electrochemical advanced oxidation processes. A review. *Chem. Eng. J. 228 (2013) 944–964.*

[76] L. Mansouri, S. Jellali, H. Akrout. Recent advances on advanced oxidation process for sustainable water management. *Environ. Sci. Pollut. Res. 26 (2019) 18939-18941.*

[77] M. Marce, O. Palacios, A. Bartolomé, J. Caixach, S. Baig, S. Esplugas. Application of Ozone on Activated Sludge: Micropollutant Removal and Sludge Quality. *Ozone: Sci. Eng. 39:5 (2017) 319-332.*

[78] A. Pal, P. Mahamallik, S. Saha, A. Majumdar. Degradation of tetracycline antibiotics by advanced oxidation processes: application of MnO_2 nanomaterials. *Nat. Resour. Eng. 2:1 (2017) 32-42.*

[79] K.O. K'oreje, L. Vergeynst, D. Ombaka, P. De Wispelaere, M. Okoth, H. Van Langenhove, K. Demeestere. Occurrence patterns of pharmaceutical residues in wastewater, surface water and groundwater of Nairobi and Kisumu city, Kenya. *Chemosphere 149 (2016) 238-244.*

[80] Q. Yan, Y.-X. Zhang, J. Kang, X.-M. Gan, P. Xu-Y, J.-S. Guo, X. Gao. A preliminary study on the occurrence of pharmaceutically active compounds in the river basins and their removal in two conventional drinking water treatment plants in Chongqing, China. *CSAWAC 43 (6) (2015) 787-966.*

[81] J. A. Rivera-Jaimes, C. Postigo, R. M. Melgoza-Alemán, J. Aceña, D. Barceló, M. López de Alda. Study of pharmaceuticals in surface and wastewater from Cuernavaca, Morelos, Mexico: Occurrence and environmental risk assessment. *Sci. Total Environ. 613–614 (2018) 1263–1274.*

[82] E. Carmona, V. Andreu, Y. Picó. Occurrence of acidic pharmaceuticals and personal care products in Turia River Basin: From waste to drinking water. *Sci. Total Environ. 484 (2014) 53–63.*

[83] A. Chiffre, F. Degiorgi, A. Buleté, L. Spinner, P.-M. Badot. Occurrence of pharmaceuticals in WWTP effluents and their impact in a karstic rural catchment of Eastern France. *Environ. Sci. Pollut. Res. 23 (2016) 25427–25441.*

[84] A. Togola, H. Budzinski. Multi-residue analysis of pharmaceutical compounds in aqueous samples. *J. Chromatogr. A 1177 (2008) 150–158.*

[85] N. Nakada, K. Komori, Y. Suzuki, C. Konishi, I. Houwa and H. Tanaka. Occurrence of 70 pharmaceutical and personal care products in Tone River basin in Japan. *Water Sci. Technol. 56 (2007) 133-140.*

[86] V. Osorio, S. Pérez, A. Ginebreda, D. Barceló. Pharmaceuticals on a sewage impacted section of a Mediterranean River (Llobregat River, NE Spain) and their relationship with hydrological conditions. *Environ. Sci. Pollut. Res. 19 (2012) 1013–1025.*

[87] S. Matongo, G. Birungi, B. Moodley, P. Ndungu. Pharmaceutical residues in water and sediment of Msunduzi River, KwaZulu-Natal, South Africa. *Chemosphere 134 (2015) 133–140.*

[88] A. L. Spongberg, J. D. Witter, J. Acuña, J. Vargas, M. Murillo, G. Umaña, E. Gómez, G. Pérez. Reconnaissance of selected PPCP compounds in Costa Rican surface waters. *Water Res. 45 (2011) 6709-6717.*

[89] E. Archer, B. Petrie, B. Kasprzyk-Hordern, G. M. Wolfaardt. The fate of pharmaceuticals and personal care products (PPCPs), endocrine disrupting contaminants (EDCs), metabolites and illicit drugs in a WWTW and environmental waters. *Chemosphere 174 (2017) 437-446.*

[90] G. Dai, B. Wang, J. Huang, R. Dong, S. Deng, G. Yu. Occurrence and source apportionment of pharmaceuticals and personal care products in the Beiyun River of Beijing, China. *Chemosphere 119 (2015) 1033‑1039.*

[91] Y. Valcárcel, S. González Alonso, J. L. Rodríguez-Gil, A. Castaño, J. C. Montero, J. J. Criado-Alvarez, I. J. Mirón, M. Catalá. Y. Valcárcel, S. González Alonso, J. L. Rodríguez-Gil, A. Castaño, J. C. Montero, J. J. Criado-Álvarez, I. J. Mirón, M. Catalá. Seasonal variation of pharmaceutically active compounds in surface (Tagus River) and tap water (Central Spain). *Environ. Sci. Pollut. Res. 20 (2013) 1396-1412.*

[92] C. L. Chitescu, G. Kaklamanos, A. I. Nicolau, A. A. M. (Linda) Stolker. High sensitive multiresidue analysis of pharmaceuticals and antifungals in surfacewater using U-HPLC-Q-Exactive Orbitrap HRMS. Application to the Danube river basin on the Romanian territory. *Sci. Total Environ. 532 (2015) 501–511.*

[93] A. Szymonik, J. Lach, K. Malinska. Fate and removal of pharmaceuticals and illegal drugs present in drinking water and wastewater. *Ecol. Chem. Eng. S 24 (1) (2017) 65-85.*

[94] P. Vázquez-Roig, V. Andreu, M. Onghena, C. Blasco, Y. Picó. Assessment of the occurrence and distribution of pharmaceuticals in a Mediterranean wetland (L'Albufera, Valencia, Spain) by LC-MS/MS. *Anal. Bioanal. Chem. 400 (2011) 1287–1301.*

[95] R. Mirzaei, M. Yunesian, S. Nasseri, M. Gholami, E. Jalilzadeh, S. Shoeibi, A. Mesdaghinia. Occurrence and fate of most prescribed antibiotics in different water environments of Tehran, Iran. *Sci. Total Environ. 619–620 (2018) 446–459.*

[96] A. Honjo Ide, R. Arimura Osawa, L. Oliveira Marcante, J. da Costa Pereira, J. C. Rodrigues de Azevedo. Occurrence of Pharmaceutical Products, Female Sex Hormones and Caffeine in a Subtropical Region in Brazil. *CSAWAC 45 (9) (2017)*.

[97] A. Daneshvar, J. Svanfelt, L. Kronberg, M. Prévost, G. A. Weyhenmeyer. Seasonal variations in the occurrence and fate of basic and neutral pharmaceuticals in a Swedish river–lake system. *Chemosphere 80 (2010) 301–309.*

[98] Y. M. Awad, S. C. Kim, S. A. M. Abd El-Azeem, K. H. Kim, K. R. Kim, K. Kim, C. Jeon, S. Soo Lee, Y. Sik Ok. Veterinary antibiotics contamination in water, sediment, and soil near a swine manure composting facility. *Environ. Earth Sci. 71 (2014) 1433–1440.*

[99] B. P. Gumbi, B. Moodley, G. Birungi, P. G. Ndungu. Assessment of nonsteroidal anti-inflammatory drugs by ultrasonic-assisted extraction and GC-MS in Mgeni and Msunduzi river sediments, KwaZulu-Natal, South Africa. *Environ. Sci. Pollut. Res. 24 (2017) 20015–20028.*

[100] J. Wilkinson, P. S. Hooda, J. Barker, S. Barton, J. Swinden. Occurrence, fate and transformation of emerging contaminants in water: An overarching review of the field. *Environ. Pollut. 231 (2017) 954-970.*

[101] Drug Stability for Pharmaceutical Scientists. Thorsteinn Loftsson (Ed). Academic Press, Oxford, 2014.

[102] A Basic Introduction to Pollutant Fate and Tranpsort: An Integrated Approach with Chemistry, Modeling, Risk Assessment, and Environmental Legislation. F.M. Dunnivant, E. Anders, Wiley Interscience. Hoboken, New Jersey, 2006.

[103] Emerging Contaminants in River Ecosystems. Occurrence and Effects Under Multiple Stress Conditions. p.10. M. Petrović, S. Sabater, A. Elosegi, D. Barceló (Eds.). Springer, 2016.

[104] J. Wilkinson, P.S. Hooda, J. Barker, S. Barton, J.Swinden. Occurrence, fate and transformation of emerging contaminants in water: An overarching review of the field. *Environ. Pollut. 231 (2017) 954-970.*

[105] R.M. Baena, E. González, P.A. Lara. Degradation kinetics of pharmaceuticals and personal care products in surface waters: photolysis vs biodegradation. *Sci. Total Environ. 590–591 (2017) 643–654*.

[106] M. Blessy, R.D. Patel, P.N. Prajapati, Y.K. Agrawal. Development of forced degradation and stability indicating studies of drugs—A Review. *J. Pharm. Anal. 4 (2014) 159–165*.

[107] T. Rawat, I.P. Pandey. Forced degradation studies for drug substances and drug products-Scientific and regulatory considerations*. J. Pharm. Sci. Res. 7 (2015) 238–241*.

[108] K. Kowabata, K. Sugihara, S. Sainoh, S. Kitamura. Photodegradation of pharmaceuticals in the aquatic environment by sunlight and UV-A, -B and -C irradiation. *J. Toxicol. Sci. 38 (2013) 215–223.*

[109] S. D. Richardson. Water Analysis: Emerging Contaminants and Current Issues. *Anal. Chem. 79 (2007) 4295.*

[110] P. Paíga, A. Lolic, F. Hellebuyck, L. H.M.L.M. Santos, M. Correia, C. Delerue-Matos. Development of a SPE–UHPLC–MS/MS methodology for the determination of non-steroidal anti-inflammatory and analgesic pharmaceuticals in seawater. *J. Pharm. Biomed. Anal. 106 (2015) 61–70.*

[111] M. Ibáñez, C. Guerrero, J. V. Sancho, F. Hernández. Screening of antibiotics in surface and wastewater samples by ultra-high-pressure liquid chromatography coupled to hybrid quadrupole time-of-flight mass spectrometry. *J. Chromatogr. A 1216 (2009) 2529–2539.*

[112] A. L. Batt, M. S. Kostich, J. M. Lazorchak. Analysis of ecologically relevant pharmaceuticals in wastewater and surface water using selective solid-phase extraction and UPLC-MS/MS**.** *Anal. Chem. 80 (2008),* 5021–5030.

[113] M. Gros, S. Rodríguez-Mozaz, D. Barceló. Fast and comprehensive multi-residue analysis of a broad range of human and veterinary pharmaceuticals and some of their metabolites in surface and treated waters by ultra-high-performance liquid chromatography coupled to quadrupole-linear ion trap tandem mass spectrometry. *J. Chromatogr. A 1248 (2012) 104-121.*

[114] M. Petrović, M. Gros, D. Barceló. Multi-residue analysis of pharmaceuticals in wastewater by ultra-performance liquid chromatography-quadrupole-time-of-flight mass spectrometry. *J. Chromatogr. A 1124 (2006) 68-81.*

[115] J. Sadkowska, M. Caban, M. Chmielewski, P. Stepnowski, J. Kumirska. Environmental aspects of using gas chromatography for determination of pharmaceutical residues in samples characterized by different composition of the matrix. *Arch. Environ. Prot. 43 (3) (2017) 3–9.*

[116] W. W. Buchberger. Review. Current approaches to trace analysis of pharmaceuticals and personal care products in the environment. *J. Chromatogr. A 1218 (2011) 603–618.*

[117] L. Araujo, J. Wild, N. Villa, N. Camargo, D. Cubillan, A. Prieto. Determination of anti-inflammatory drugs in water samples, by in situ derivatization, solid phase microextraction and gas chromatography–mass spectrometry. *Talanta 75 (2008) 111–115.*

[118] S. Weigel, R. Kallenborn, H. Huhnerfuss. Simultaneous solid-phase extraction of acidic, neutral and basic pharmaceuticals from aqueous samples at ambient (neutral) pH and their determination by gas chromatography–mass spectrometry. *J. Chromatogr. A 1023 (2004) 183–195.*

[119] S. S. Verenitch, C. J. Lowe, A. Mazumder. Determination of acidic drugs and caffeine in municipal wastewaters and receiving waters by gas chromatography–ion trap tandem mass spectrometry. *J. Chromatog. A 1116 (2006) 193–203.*

[120] C. D. Metcalfe, B. G. Koenig, D. T. Bennie, M. Servos, T. A. Ternes, R. Hirsch. Occurrence of neutral and acidic drugs in the effluents of Canadian sewage treatment plants. *Environ. Toxicol. Chem.. 22 (12) (2003) 2872–2880.*

[121] V. Koutsouba, Th. Heberer, B. Fuhrmann, K. Schmidt-Baumler, D. Tsipi, A. Hiskia. Determination of polar pharmaceuticals in sewage water of Greece by gas chromatography–mass spectrometry. *Chemosphere 51 (2003) 69-75.*

[122] F. Sacher, F.T. Lange, H.J. Brauch, I. Blankenhorn. Pharmaceuticals in groundwaters Analytical methods and results of a monitoring program in Baden-Wurttemberg, Germany. *J. Chromatog. A 938 (2001) 199–201.*

[123] W.C. Lin, H.C. Chen, W.H. Ding. Determination of pharmaceutical residues in waters by solid-phase extraction and large-volume on-line derivatization with gas chromatography–mass spectrometry. *J. Chromatogr. A 1065 (2005) 279–285.*

[124] H. B. Lee, T. E. Peart, M. L. Svoboda. Determination of endocrine-disrupting phenols, acidic pharmaceuticals, and personal-care products in sewage by solid-phase extraction and gas chromatography–mass spectrometry. *J. Chromatogr. A 1094 (2005) 122–129.*

[125] A. Sebök, A. Vasanits-Zsigrai, Gy. Palkó, Gy. Záray, I. Molnár-Perl. Identification and quantification of ibuprofen, naproxen, ketoprofen and diclofenac present in waste-waters, as their trimethylsilyl derivatives, by gas chromatography mass spectrometry. *Talanta 76 (2008) 642 ‑650.*

[126] O.A.H. Jones, N. Voulvoulis, J.N. Lester. The occurrence and removal of selected pharmaceutical compounds in a sewage treatment works utilising activated sludge treatment. *Environ. Pollut. 145 (2007) 738-744.*

[127] A. Togola, H. Budzinski. Analytical development for analysis of pharmaceuticals in water samples by SPE and GC–MS. *Anal. Bioanal. Chem. 388 (2007) 627–635.*

[128] S. Aydin, M. E. Aydin, F. Beduk, A. Tekinay, H. Kilic. Analysis of diclofenac in water samples using in situ derivatization-vortex-assisted liquid-liquid microextraction with gas chromatography-mass spectrometry. *Acta Pharm. 68 (2018) 313–324.*

[129] I. Rodríguez, J.B. Quintana, J. Carpinteiro, A.M. Carro, R.A. Lorenzo, R. Cela. Determination of acidic drugs in sewage water by gas chromatography–mass spectrometry as tert.-butyldimethylsilyl derivatives. *J. Chromatogr. A 985 (2003) 265–274.*

[130] R. López-Serna, D. Marín-de-Jesús, R. Irusta-Mata, P. A. García-Encina, R. Lebrero, M. Fdez-Polanco, R. Muñoz. Multiresidue analytical method for pharmaceuticals and personal care products in sewage and sewage sludge by online direct immersion SPME on-fiber derivatization–GCMS. *Talanta 186 (2018) 506–512.*

[131] M. Moeder, S. Schrader, M. Winkler, P. Popp. Solid-ph ase microextraction–gas chromatography–mass spectrometry of biologically active substances in water samples. *J. Chromatogr. A 873 (2000) 95–106.*

[132] B. P. Gumbi, B. Moodley, G. Birungi, P. G. Ndungu. Detection and quantification of acidic drug residues in South African surface water using gas chromatography-mass spectrometry. *Chemosphere 168 (2017) 1042-1050.*

[133] J. Kumirska, A. Plenis, P. Łukaszewicz, M. Caban, N. Migowska, A. Białk-Bielińska, M. Czerwicka, P. Stepnowski. Chemometric optimization of derivatization reactions prior to gas chromatography–mass spectrometry analysis. *J. Chromatogr. A 1296 (2013) 164-178.*

[134] S. Öllers, H.P. Singer, P. Fassler, S.R. Müller. Simultaneous quantification of neutral and acidic pharmaceuticals and pesticides at the low-ng/l level in surface and waste water. *J. Chromatogr. A 911 (2001) 225-234.*

[135] C. Tixier H.P. Singer, S. Öllers, S.R. Müller. Occurrence and fate of carbamazepine, clofibric acid, diclofenac, ibuprofen, ketoprofen, and naproxen in surface waters. *Environ. Sci. Technol. 37 (2003) 1061-1068.*

[136] M. Wu, J. Xiang, C. Que, F. Chen, G. Xu. Occurrence and fate of psychiatric pharmaceuticals in the urban water system of Shanghai, China. *Chemosphere 138 (2015) 486–493.*

[137] S. S. Verenitch, C. J. Lowe, A. Mazumder. Determination of acidic drugs and caffeine in municipal wastewaters and receiving waters by gas chromatography–ion trap tandem mass spectrometry. *J. Chromatogr. A 1116 (2006) 193–203.*

[138] K. Choi, Y. Kim, J. Park, C. K. Park, M. Kim, H. S. Kim, P. Kim. Seasonal variations of several pharmaceutical residues in surface water and sewage treatment plants of Han River, Korea. *Sci. Total Environ. 405 (2008) 120-128.*

[139] A. L. Spongberg, J. D. Witter. Pharmaceutical compounds in the wastewater process stream in Northwest Ohio. *Sci. Total Environ. 397 (2008) 149-157.*

[140] N. M. Vieno, T. Tuhkanen, L. Kronberg. Analysis of neutral and basic pharmaceuticals in sewage treatment plants and in recipient rivers using solid phase extraction and liquid chromatography–tandem mass spectrometry detection. *J. Chromatogr. A 1134 (2006) 101–111.*

[141] P. Gao, Y. Ding, H. Li, I. Xagoraraki. Occurrence of pharmaceuticals in a municipal wastewater treatment plant: Mass balance and removal processes. *Chemosphere 88 (2012) 17–24.*

[142] M. Česen, M. Ahel, S. Terzić, D. J. Heath, E. Heath. The occurrence of contaminants of emerging concern in Slovenian and Croatian wastewaters and receiving Sava river. *Sci. Total Environ. 650 (2019) 2446–2453.*

[143] M. E. Lindsey, M. Meyer, E. M. Thurman. Analysis of Trace Levels of Sulfonamide and Tetracycline Antimicrobials in Groundwater and Surface Water Using Solid-Phase Extraction and Liquid Chromatography/Mass Spectrometry. *Anal. Chem. 73 (2001) 4640-4646.*

[144] O. Zuloaga, P. Navarro, E. Bizkarguenaga, A. Iparraguirre, A. Vallejo, M. Olivares, A. Prieto. Overview of extraction, clean-up and detection techniques for the determination of organic pollutants in sewage sludge: A review. *Anal. Chim. Acta 736 (2012) 7 – 29.*

[145] D. Lopes Cunha, F. Goytacazes de Araujo, M. Marques. Psychoactive drugs: occurrence in aquatic environment, analytical methods, and ecotoxicity—a review. *Environ. Sci. Pollut. Res. 24 (2017) 24076–24091.*

[146] M. Rabiet, A. Togola, F. Brissaud, J.-L. Seidel, H. Budzinski, F. Elbaz-Poulichet. Consequences of treated water recycling as regards pharmaceuticals and drugs in surface and ground waters of a medium-sized Mediterranean catchment. *Environ. Sci. Technol. 40 (2006) 5282-5288.*

[147] A. A. M. Stolker, W. Niesing, E. A. Hogendoorn, J. F. M. Versteegh, R. Fuchs, U. A. Th. Brinkman. Liquid chromatography with triple-quadrupole or quadruple-time of flight mass spectrometry for screening and confirmation of residues of pharmaceuticals in water. *Anal. Bioanal. Chem. 378 (2004) 955-963.*

[148] V. L. Borova, N. C. Maragou, P. Gago-Ferrero, C. Pistos, N. S. Thomaidis. Highly sensitive determination of 68 psychoactive pharmaceuticals, illicit drugs, and related human metabolites in wastewater by liquid chromatography–tandem mass spectrometry. *Anal. Bioanal. Chem. (2014) 406: 4273-4285.*

[149] M. E. Torres Padrón, C. Afonso-Olivares, Z. Sosa-Ferrera, J. J. Santana-Rodríguez. Microextraction techniques coupled to liquid chromatography with mass spectrometry for the determination of organic micropollutants in environmental water samples. *Molecules 19 (2014) 10320-10349.*

[150] V. K. Balakrishnan, K. A. Terry, J. Toito. Determination of sulfonamide antibiotics in wastewater: A comparison of solid phase microextraction and solid phase extraction methods. *J. Chromatogr. A 1131 (2006) 1–10.*

[151] E. L. McClure, C. S. Wong. Solid phase microextraction of macrolide, trimethoprim and sulfonamide antibiotics in wastewaters. *J. Chromatogr. A 1169 (2007) 53–62.*

[152] S. S. Lakade, F. Borrull, K. G. Furton, A. Kabir, N. Fontanals, R. M. Marcé. Comparative study of different fabric phase sorptive extraction sorbents to determine emerging contaminants from

environmental water using liquid chromatography–tandem mass spectrometry. *Talanta 144 (2015) 1342–1351.*

[153] D. Bratkowska, N. Fontanals, P.A.G. Cormack, F. Borrull, R.M. Marcé. Preparation of a polar monolithic stir bar based on methacrylic acid and divinylbenzene for the sorptive extraction of polar pharmaceuticals from complex water samples. *J. Chromatogr. A 1225 (2012) 1–7.*

[154] D. Bratkowska, R.M. Marcé, P. A. G. Cormack, F. Borrull, N. Fontanals. Development and application of a polar coating for stir bar sorptive extraction of emerging pollutants from environmental water samples. *Anal. Chim. Acta 706 (2011) 135–142.*

[155] N. Gilart, P.A.G. Cormack, R.M. Marcé, F. Borrull, N. Fontanals. Preparation of a polar monolithic coating for stir bar sorptive extraction of emerging contaminants from wastewaters*. J. Chromatogr. A 2013, 1295, 42–47.*

[156] F. Suazo, J. Vásquez, M. Ratamal, L. Ascar, A. Giordano. Pharmaceutical compounds determination in water samples: Comparison between solid phase extraction and stir bar sorptive extraction. *J. Chil. Chem. Soc. 62, (3) (2017) 3597-3601***.**

[157] J. Martín, W. Buchberger, E. Alonso, M. Himmelsbach, I. Aparicio. Comparison of different extraction methods for the determination of statin drugs in wastewater and river water by HPLC/Q-TOF-MS. *Talanta 85 (2011) 607–615.*

[158] A. Zgoła-Grześkowiak. Application of DLLME to isolation and concentration of non-steroidal anti-inflammatory drugs in environmental water samples. *Chromatographia 72 (2010) 671–678.*

[159] J. Cotton, Fanny Leroux, Simon Broudin, Marion Poirel, Bruno Corman, Christophe Junot, Céline Ducruix. Development and validation of a multiresidue method for the analysis of more than 500 pesticides and drugs in water based on on-line and liquid chromatography coupled to high resolution mass spectrometry. *Water Res. 104 (2016) 20-27.*

[160] Z. Márta, B. Bobályc, J. Fekete, B. Magda, T. Imre, P. T. Szabó.. Simultaneous determination of ten nonsteroidal anti-inflammatorydrugs from drinking water, surface water and wastewater using microUHPLC-MS/MS with on-line SPE system. *J. Pharm. Biomed. Anal. 160 (2018) 99–108.*

[161] N. F. Tetzner[a], M. Guedes Maniero, C. Rodrigues-Silva, S. Rath. On-line solid phase extraction-ultra high performance liquidchromatography-tandem mass spectrometry as a powerful techniquefor the determination of sulfonamide residues in soils. *J. Chromatogr. A 1452 (2016) 89–97.*

[162] M. Gros, M. Petrović, D. Barceló. Tracing pharmaceutical residues of different therapeutic classes in environmental waters by using liquid chromatography/quadrupole-linear ion trap mass spectrometry and automated library searching. *Anal. Chem. 81 (2009) 898–912.*

[163] J. B. Quintana, S. Weiss, T. Reemtsma. Pathways and metabolites of microbial degradation of selected acidic pharmaceutical and their occurrence in municipal wastewater treated by a membrane bioreactor. *Water Res. 39 (2005) 2654–2664.*

[164] T. Kosjek, E. Heath, M. Petrović, D. Barceló. Mass spectrometry for identifying pharmaceutical biotransformation products in the environment. TrAC, *Trends Anal. Chem. 26, No. 11 (2007) 1076-1085.*

[165] R. López-Serna, S. Pérez, A. Ginebreda, M. Petrović, D. Barceló. Fully automated determination of 74 pharmaceuticals in environmental and waste waters by online solid phase extraction–liquid chromatography-electrospray–tandem mass spectrometry. *Talanta 83 (2010) 410–424.*

[166] F. Hernández, T. Portolés, M. Ibáñez, M. C. Bustos-López, R. Díaz, A.M. Botero-Coy, C. L. Fuentes, G. Peñuela. Use of time-of-flight mass spectrometry for large screening of organic pollutants in surface waters and soils from a rice production area in Colombia. *Sci. Total Environ. 439 (2012) 249–259.*

[167] S. Terzic, I. Senta, M. Matosic, M. Ahel. Identification of biotransformation products of macrolide and fluoroquinolone antimicrobials in membrane bioreactor treatment by ultrahigh-performance liquid chromatography/quadrupole time-of-flight mass spectrometry. *Anal. Bioanal. Chem. 401 (2011) 353–363.*

[168] T. Kosjek, D. Zigon, B. Kralj, E. Heath. The use of quadrupole-time-of-flight mass spectrometer for the elucidation of diclofenac biotransformation products in wastewater. *J. Chromatogr. A 1215 (2008) 57–63*

[169] C. Boix, M. Ibáñez, J. V. Sancho, J.R. Parsons, P. de Voogt, F. Hernández. Biotransformation of pharmaceuticals in surface water and during waste water treatment: Identification and occurrence of transformation products. *J. Hazard. Mater. 302 (2016) 175–187.*

[170] J. B. Golubović, A. D. Protić, M. L. Zečević, B. M. Otašević. Quantitative structure retention relationship modeling in liquid chromatography method for separation of candesartan cilexetil and its degradation products. *Chemom. Intell. Lab. Syst. 140 (2015) 92–101.*

[171] T. Haddad, K. Kümmerer. Characterization of photo-transformation products of the antibiotic drug Ciprofloxacin with liquid chromatography–tandem mass spectrometry in

combination with accurate mass determination using an LTQ-Orbitrap. *Chemosphere 115 (2014) 40–46.*

[172] S. M. Baira, D. K. Sigalapalli, N. B. Bathini, Srinivas R., M.V.N Kumar Talluri. LC/QTOF/MS/MS characterization, molecular docking and *in silico* toxicity prediction studies on degradation products of anagliptin. *J. Pharm. Biomed. Anal. 159 (2018) 92-99.*

[173] T.C. Schmidt. Recent trends in water analysis triggering future monitoring of organic micropollutants. *Anal. Bioanal. Chem. 410 (2018) 3933–3941.*

[174] Y. Picó, D. Barceló. Transformation products of emerging contaminants in the environment and high-resolution mass spectrometry: a new horizon. *Anal. Bioanal. Chem. 407 (2015) 6257–6273.*

[175] E.J. Han, D.S. Lee. Significance of metabolites in the environmental risk assessment of pharmaceuticals consumed by human. *Sci. Total Environ. 592 (2017) 600–607.*

[176] L.H.M.L.M. Santosa A.N. Araújo, A.Fachini, A. Pena, C. Delerue-Matos, M.C.B.S.M. Montenegro. Ecotoxicological aspects related to the presence of pharmaceuticals in the aquatic environment. *J. Hazard. Mater. 175 (2010) 45–95*.

[177] S. Triñanes, M. C. Casais, M.C. Mejuto, R.Cela. Selective determination of COXIBs in environmental water samples by mixed-mode solid phase extraction and liquid chromatography quadrupole time-of-flight mass spectrometry. *J. Chromatogr. A 1420 (2015) 35-45.*

[178] B. Subedi, S. Lee, H. B. Moon, K. Kannan. Psychoactive pharmaceuticals in sludge and their emission from wastewater treatment facilities in Korea. *Environ. Sci. Technol. 47 (2013) 13321-13329.*

[179] Q. Sui, J. Huang, S. Deng, G. Yu. Rapid determination of pharmaceuticals from multiple therapeutic classes in wastewater by solid-phase extraction and ultra-performance liquid chromatography tandem mass spectrometry. *Chin. Sci. Bull. 54 (2009) 4633-4643.*

[180] J. Petre, T. Galaon, V. I. Iancu, I. Cruceru, M. Niculescu. Simultaneous liquid chromatography- tandem mass spectrometry determination of some pharmaceuticals and antimicrobial disinfectant agents in surface water and in urban wastewater. *J. Environ. Prot. Ecol. 17 (2016) 119-126.*

[181] L. Zhao, N. Liang, X. Lun, X. Chen, X. Hou. LC-QTOF-MS method for the analysis of residual pharmaceuticals in wastewater: application to a comparative multiresidue trace analysis between spring and winter water. *Anal. Methods 6 (2014) 6956-6962.*

[182] C. Trautwein, K. Kümmerer. Degradation of the tricyclic antipsychotic drug chlorpromazine under environmental conditions, identification of its main aquatic biotic and abiotic transformation products by LC-MS^n and their effects on environmental bacteria*. J. Chromatogr. B, 889-890 (2012) 24-38.*

[183] OECD guideline for the testing of chemicals No 106, 2000. Adsorption - Desorption Using a Batch Equilibrium Method, p. 8.

[184] Y. Vander Heyden, A. Nijhuis, J. Semeyers-Verbeke, B.G.M. Vandeginste, D.L. Massart. Guidance for robustness/ruggedness test in method validation. *J. Pharm. Biomed. Anal. 24 (2001) 723-753*.

[185] Y. Vander Heyden, D.L. Massart, in.: M.W.B. Hendriks, J.H. de Boer, A.K. Smilde (Eds.), Review of the use of robustness and ruggedness in analytical chemistry, Elsevier, Amsterdam, 1996, pp. 79-148.